



**UNITED STATES
NUCLEAR REGULATORY COMMISSION**
REGION II
245 PEACHTREE CENTER AVENUE NE, SUITE 1200
ATLANTA, GEORGIA 30303-1257

October 12, 2010

Mr. Jon A. Franke
Vice President, Crystal River Nuclear Plant
Crystal River Nuclear Plant (NA2C)
15760 W. Power Line Street
Crystal River, FL 34428-6708

**SUBJECT: CRYSTAL RIVER NUCLEAR PLANT - SPECIAL INSPECTION REPORT
05000302/2009007**

Dear Mr. Franke:

On September 2, 2010, the U.S. Nuclear Regulatory Commission (NRC) completed a Special Inspection at your Crystal River Unit 3 Nuclear Plant. The enclosed report documents the inspection results, which were discussed on September 2, 2010, with you and members of your staff in an exit meeting open for public observation at the Crystal River Nuclear Plant EOF/Training Center.

The purpose of this inspection was to examine activities associated with the delamination identified in the Unit 3 containment. The inspection was conducted in accordance with the Special Inspection charter issued by the Region II Administrator on October 13, 2009. As part of the inspection, the NRC examined your evaluation of extent of condition, your evaluation of root cause, and your planned corrective action for continued operability. The inspectors interviewed personnel and conducted plant walk downs, including visual examination of accessible portions of the outside and inside surfaces of the containment.

This inspection was conducted prior to the completion of your planned corrective actions. Follow-on inspections of your corrective actions to repair the containment and conduct post maintenance testing are being conducted in accordance with NRC inspection procedure IP 50001, Steam Generator Replacement Inspection.

In accordance with 10 CFR 2.390 of the NRC's "Rules of Practice," a copy of this letter, its enclosure, and your response (if any) will be available electronically for public inspection in the NRC Public Document Room or from the Publicly Available Records (PARS) component of

NRC's document system (ADAMS). ADAMS is accessible from the NRC Web site at <http://www.nrc.gov/reading-rm/adams.html> (the Public Electronic Reading Room).

Sincerely,

/RA/

Christopher G. Miller, Acting Director
Division of Reactor Safety

Docket No.: 50-302
License No.: DRP-72

Enclosures:

1. Inspection Report 05000302/2009007
W/Attachment: Supplemental Information
2. Special Inspection Charter
3. Crystal River Root Cause Report

cc w/encl.: (See page 3)

FPC

3

cc w/encl:

R. J. Duncan, II
Vice President
Nuclear Operations
Carolina Power & Light Company
Electronic Mail Distribution

Brian C. McCabe
Manager, Nuclear Regulatory Affairs
Progress Energy Carolinas, Inc.
Electronic Mail Distribution

James W. Holt
Plant General Manager
Crystal River Nuclear Plant (NA2C)
Electronic Mail Distribution

Stephen J. Cahill
Engineering Manager
Crystal River Nuclear Plant (NA2C)
Electronic Mail Distribution

R. Alexander Glenn
Associate General Counsel
(MAC - BT15A)
Florida Power Corporation
Electronic Mail Distribution

Christos Kamilaris
Director
Fleet Support Services
Carolina Power & Light Company
Electronic Mail Distribution

William A. Passetti
Chief
Florida Bureau of Radiation Control
Department of Health
Electronic Mail Distribution

Daniel R. Westcott
Supervisor
Licensing & Regulatory Programs
Crystal River Nuclear Plant (NA1B)
Electronic Mail Distribution

Joseph W. Donahue
Vice President
Nuclear Oversight
Carolina Power and Light Company
Electronic Mail Distribution

Jack E. Huegel
Manager, Nuclear Oversight
Crystal River Nuclear Plant
Electronic Mail Distribution

David T. Conley
Associate General Counsel
Legal Dept.
Progress Energy Service Company, LLC
Electronic Mail Distribution

Mark Rigsby
Manager, Support Services - Nuclear
Crystal River Nuclear Plant (NA2C)
Electronic Mail Distribution

Senior Resident Inspector
U.S. Nuclear Regulatory Commission
Crystal River Nuclear Generating Plant
U.S. NRC
6745 N Tallahassee Rd
Crystal River, FL 34428

Attorney General
Department of Legal Affairs
The Capitol PL-01
Tallahassee, FL 32399-1050

Ruben D. Almaguer
Director
Division of Emergency Preparedness
Department of Community Affairs
Electronic Mail Distribution

Chairman
Board of County Commissioners
Citrus County
110 N. Apopka Avenue
Inverness, FL 32650

Letter to Jon A. Franke from Christopher G. Miller dated October 12, 2010

SUBJECT: CRYSTAL RIVER NUCLEAR PLANT - SPECIAL INSPECTION REPORT
05000302/2009007

Distribution w/encl:

C. Evans, RII EICS

L. Douglas, RII EICS

OE Mail (email address if applicable)

RIDSNRRDIRS

PUBLIC

RidsNrrPMCystal River Resource

PUBLICLY AVAILABLE NON-PUBLICLY AVAILABLE SENSITIVE NON-SENSITIVE

ADAMS: Yes ACCESSION NUMBER: _____

SUNSI REVIEW COMPLETE

OFFICE	RII:DRS	RII:DRS	RII:DRS	RII:DRS	RII:DRS	RII:DRP	RII:DRS	Region 1
SIGNATURE	RA	RA	RA	RA	RA	RA	RA	RA
NAME	M. Franke	D.Rich	R, Carrion	F. Farzman	A. Masters	D. Naus	G. Thomas	L. Lake
DATE	10/9 /2010	10/6/2010	10/4/2010	10/6/2010	10/1/2010	10/1/2010	10/6/2010	10/5/2010
E-MAIL COPY?	YES NO	YES	YES N	YES	YES NO	YES NO	YES N	

OFFICIAL RECORD COPY DOCUMENT NAME: S:\DRS\ENG BRANCH 3\INPUTS\DRAFT REV 2 CRYSTAL RIVER
SPECIAL INSPECTION REPORT 2009007.DOCX

U. S. NUCLEAR REGULATORY COMMISSION

REGION II

Docket No: 50-302

License No: DRP 72

Report No: 05000302/2009007

Licensee: Progress Energy Company

Facility: Crystal River Unit 3

Location: 15760 West Power Line Street
Crystal River, Florida

Dates: October 13, 2009 through September 2, 2010

Inspectors: L. Lake, Senior Reactor Inspector and Inspection Team Leader
R. Carrion, Senior Reactor Inspector
F. Farzam, Senior Structural Engineer
A. Masters, Senior Construction Inspector
D. Naus, Consultant
G. Thomas, Structural Engineer

Approved by: M. Franke, Chief
Engineering Branch 3
Division of Reactor Safety

TABLE OF CONTENTS

EXECUTIVE SUMMARY	1
REPORT DETAILS	3
Introduction and Charter	3
Background	4
Section 1 – Description of Problem	6
Section 2 – Operability and Reportability	7
Section 3 – Structural Integrity	8
Section 4 – Adequacy of Maintenance and Inspection Programs	9
Section 5 – Extent of Condition and Root Cause	10
Section 6 – Corrective Actions	28
Section 7 – Safety Significance	29
Section 8 – Generic Issues	30
EXIT MEETING	31
Attachment 1, Supplemental Information	
Key Personnel	
Sequence of Events	
Documents Reviewed	
Acronyms Used	
Enclosure 2, Special Inspection Charter	
Enclosure 3, Root Cause Report	

EXECUTIVE SUMMARY
Crystal River, Unit 3
NRC Inspection Report 05000302/2009007

Crystal River shut down for a planned refueling outage on September 26, 2009. One of the major work activities planned for this outage was a steam generator replacement. In order to take the old steam generators out and put the new steam generators in, the licensee created a construction opening in the side of the containment building. On October 2, 2009, while creating this opening, workers saw that there was a gap, or separation, affecting the outer layer of concrete of the building wall. The gap or separation in the concrete has been commonly referred to as a delamination.

The discovery of the delamination did not represent an immediate safety concern because the plant was shut down. However, the discovery was important because the containment building is one of the three main barriers that protect public safety. The concrete delamination was not expected and had not been seen before during steam generator replacement activities at other nuclear plants. Because this issue involved possible adverse generic implications, because the structural integrity of the containment was not fully known and the concrete separation was not well understood, and because of the potential safety implications, Region II began a Special Inspection to better understand the issue. The inspection started on October 13, 2009, and was completed on September 2, 2010.

The Special Inspection Team (SIT) found that the delamination did not represent an increase in risk to the public. There were no radiological releases associated with the event, and no Technical Specification Safety Limits were approached or exceeded. The SIT found that the licensee's investigation was thorough and supported their conclusions on the delamination cause, extent of condition, and safety significance. The SIT did not identify immediate generic safety concerns associated with the delamination.

The licensee's investigation concluded that the delamination was caused during the creation of the opening in containment. As part of preparing the containment building for making the opening, tendons in the containment building wall were detensioned. The main cause of the delamination was attributed to the scope and sequence of this tendon detensioning. Tendon detensioning began after the plant was shut down in Operating Mode 5, when containment operability was not required.

The licensee found that the delamination was centered on the steam generator opening and formed the shape of an hour-glass. The delamination was limited to the containment bay between buttresses 3 and 4, and did not affect other bays of containment.

The licensee's repair plan to remove and replace the delaminated condition included: (1) additional detensioning of containment; (2) removal of delaminated concrete; (3) installation of reinforcement, including radial reinforcement through the delamination plane; (4) placing of new concrete; (5) retensioning containment; and (6) post-repair confirmatory system pressure testing. The licensee developed new finite element analysis models to predict stresses in the repaired containment wall under design basis loads. Using these and other supporting new analysis models, the licensee planned and implemented additional containment detensioning without causing further delamination. Subsequent to removal of the delaminated concrete, vertical cracks were observed along the vertical tendon lines in the concrete surface between

buttresses 3 and 4. Following an engineering evaluation, the licensee planned to excavate and fill in cracks above elevation (EI) 176'. The licensee's evaluation determined that cracks below 176 feet were acceptable as-is. The licensee's investigation also identified additional tight vertical cracks in other locations around the circumference of the containment wall. The licensee's evaluation of these vertical cracks remained ongoing at the conclusion of the Special Inspection.

Crystal River Unit 3 (CR3) is unique in that no other plants that have cut openings in their containments have experienced similar delamination. As discussed above, the root cause analysis determined that the delamination was caused by scope and sequence of this tendon detensioning in preparation for making the opening. The licensee developed new analytical methods to adequately identify the redistribution of stresses in the containment wall and identify an acceptable expanded detensioning scheme to perform the repair. The licensee has been communicating to other plants, through INPO and other industry organizations, lessons learned from this event.

REPORT DETAILS

INTRODUCTION AND CHARTER

In accordance with Management Directive 8.3, "NRC Incident Investigation Program," the deterministic and conditional risk criteria were used to evaluate the level of NRC response for this event.

Based on the deterministic criteria that this issue involved possible adverse generic implications, the event was evaluated for risk in accordance with Management Directive 8.3. Due to lack of information on the structural integrity of the concrete containment and how it would interact with the steel liner during a seismic event in its current condition, a risk analysis was not able to be performed at the time of the event. However, if the concrete containment reacted adversely with the steel liner during a seismic event, the Large Early Release Frequency (LERF) would be adversely affected and a Special Inspection would be warranted. Therefore, Region II has determined that the appropriate level of NRC response was to conduct a Special Inspection. Enclosure 2 of this report contains the Special Inspection Team (SIT) charter.

BACKGROUND

The purpose of this section is to provide information about the design of the Crystal River Unit 3 (CR3) containment structure (containment), the maintenance history of the structural integrity of the containment, and the condition of the containment leading up to the delamination discovered during the recent plant shutdown for refueling outage #16 (RFO 16). Included is information related to a delamination that was identified in the containment dome during the final stages of containment construction and before initial plant startup.

Crystal River Nuclear Generating Plant Unit 3 (CR3) is a pressurized water reactor. It has been in operation for over 30 years, with the current license due to expire December 3, 2016. Crystal River has submitted an application to the NRC to request a license renewal to extend the operation of the plant for another 20 years.

Design

In a pressurized water reactor plant there are three main barriers that protect the public from the radiation hazards associated with nuclear operations. One of those barriers is known as the containment, which houses the fuel, the reactor, and the reactor cooling system. The Crystal River containment structure is a steel lined post-tensioned cylindrical concrete structure of about 157 feet in height with an outside diameter of about 138 feet. The containment has 42-inch thick concrete walls and has a flat foundation mat and a shallow torispherical dome. Post-tensioning is achieved by utilizing an outer array of horizontal tendons immediately adjacent to an inner array of vertical tendons that are embedded in the walls about 15 inches from the outside surface. Tendons are also provided in the dome. In addition, steel rebar is embedded in the concrete walls at the outside surface and at other locations.

The containment is lined with a continuous 3/8-inch-thick carbon steel liner (that acts as a vapor barrier for leak-tightness and also as an inner form for the concrete). A series of equally spaced vertical steel angle irons are attached to the concrete side of the liner and serve as anchors and stiffeners. The dome is post-tensioned by 123 tendons that are arranged in a three-way (layer) configuration and are anchored to a ring girder. The containment walls include 282 horizontal and 144 vertical tendons that are anchored to 6 vertical buttresses equally spaced circumferentially around the containment. Each tendon consists of numerous small diameter wires, which are greased and housed inside a conduit. The conduit for each tendon is about five inches in diameter and is made of galvanized steel. The concrete has a minimum 28-day compressive strength of 5,000 pounds per square inch (psi).

Dome Delamination

On April 14, 1976, about two years after completion of concrete placement of the containment dome and one year after tensioning the tendons, electricians were attempting to secure drilled-in anchors to the top surface of the dome and certain anchors would not hold. Upon further investigation a delamination in the containment dome was discovered. The area of the delaminated concrete was approximately circular in shape with a 105-foot diameter. The approximate thickness of the delamination was 15 inches, with a maximum gap of approximately two inches between layers. No cracks appeared on the dome surface and, except for springiness when walking on the dome, there were no other indications of any problems.

Analysis of the dome delamination included engineering investigations that took into consideration all factors that were believed to be potentially contributory to the delaminated condition. Factors considered included: (1) properties of concrete and its constituents; (2) radial tension due to prestress; (3) compression-tension interaction; (4) thermal effects; (5) tendon alignment; (6) heavy construction loads; (7) coastal location; (8) location adjacent to fossil units; (9) construction methods; (10) impact loads; and (11) shrinkage effects. The dome investigation team concluded that a compression-tension interaction failure had occurred. The dome delamination was caused by the effects of radial tensile stresses combined with biaxial compressive stresses and lower-than-normal concrete tensile strength and aggregate strength. Tensile tests of the concrete indicated that the concrete had low resistance to crack propagation thus permitting local cracking to propagate. These factors and the conclusion were included as part of the 75 failure modes considered in Progress Energy's root cause investigation into the delamination identified during RFO 16. For more information on the root cause see Section 5 of this report.

The dome repair process included: removal of the delaminated dome cap; meridional, hoop, and radial reinforcement; and placement of a new dome cap. Instrumentation was installed to monitor the dome during tendon detensioning, retensioning and during a structural integrity test. The structural integrity test subjected the repaired containment to 115 percent of design pressure.

Maintenance history of the containment

The structural integrity of the containment structure was initially confirmed by the structural integrity test prior to the plant's initial startup. Baseline crack mapping of the outside surface of the containment wall was conducted at this time. Subsequent periodic inspections and tests were conducted to confirm containment integrity. This included dome monitoring, leak rate tests, and visual examinations.

Since 1976, the containment passed six integrated leak rate tests. The most recent integrated leak rate test was conducted in December 2005. These tests pressurized the containment to accident pressure to measure for leakage. They also included internal and external visual examinations.

Other periodic examinations and testing included:

Examination of containment surfaces – The containment was periodically visually examined in accordance with the requirements of Title 10 of the Code of Federal Regulations (CFR) Part 50.55a and Subsections IWL and IWE of American Society of Mechanical Engineers (ASME) Boiler and Pressure Vessel Code (Code). These examinations were conducted on a frequency of every 5 years and no unacceptable conditions were identified.

Tendon Testing – Tendon testing was performed in accordance with the requirements of 10 CFR Part 50.55a and Subsection IWL of the code. These tests required measurement of tendon lift-off force and visual examination of the tendons for grease leakage and tendon wire condition. Tendon testing was performed during the first 3 refueling outages and at a frequency of every 5 years (during outages). The 30th year testing was performed during refueling outage #15 between October and November

2007. Results of the examinations included minor anomalies and corrective action was taken. No unacceptable conditions were identified.

Metal Surfaces - Metal surfaces of the containment have been visually examined in accordance with the requirements of the requirements of 10 CFR Part 50.55a and Subsection IWE of the code. These visual examinations cover all accessible surfaces and require the documentation of any anomalies such as corrosion, cracking and bulges, in the containment liner. Bulges in the containment liner were identified by visual examination conducted in 1996 and have been monitored for acceptability in accordance with regulatory requirements. No unacceptable conditions have been identified.

The inspectors reviewed the containment building maintenance and test records, from 1976 to present, to determine whether the containment was monitored in accordance with regulatory requirements. No issues of significance were identified. Furthermore, the inspectors did not identify any potential signs in the test and maintenance history between 1976 and 2009 that a concrete separation occurred, before the wall delamination was discovered in October 2009.

1.0 Description of the Problem

Crystal River scheduled the replacement of the steam generators during the CR3 Refueling Outage 16. Replacing steam generators is a major activity and in preparation for the steam generator replacement the licensee planned to make a construction opening in the containment wall, approximately forty feet directly above the equipment hatch. This opening would facilitate removing the existing steam generators and the transport of the replacement steam generators into the Reactor Building. Cutting the opening in the containment included preparing the containment by detensioning tendons, then removing the concrete with high pressure water, a process known as hydrolazing, and cutting the containment liner plate.

The licensee began Refueling Outage 16 on September 25, 2009 with a reduction in power from Mode 1. The unit continued down in power through Modes 2, 3, 4, and 5 on September 26. Upon reaching Mode 5 at about 5:00 p.m. on September 26, tendon work activities began. Two vertical tendons (34V12 and 34V13) were detensioned simultaneously. These tendons were detensioned prior to cutting the button heads. From September 26 through October 1, eight additional vertical tendons and seventeen hoop tendons were detensioned by plasma cutting the button heads as part of the process to make the required construction opening. The licensee began the removal of concrete by hydrolazing (hydro-demolition) on September 30, 2009, as the first step in making the construction opening. This process was accomplished by using water under pressure (as great as 25000 psi) to "cut" the concrete. On October 3, during hydro-demolition work to expose the first layer of tendon sheaths, water from the work was observed leaking from the exterior surface of the containment at various locations below the elevation of the bottom of the construction opening. The leaking water was not limited to the construction opening, but was observed at the edges of the construction opening extending into undisturbed concrete for an indeterminate distance but at least as far as the post-tensioning buttresses (Buttresses #3 and #4). As the work continued, some of the

concrete rubble unexpectedly broke off into large pieces. Licensee personnel inspected the construction opening and discovered a concrete separation condition. It was located approximately in the cylindrical plane of the centerline of the hoop tendons, approximately nine to twelve inches from the exterior surface of the containment building. Approximately 30 inches of concrete remained in apparent good condition all the way to the liner plate. The hydro-demolition of the concrete continued through October 7, when the containment building liner was exposed and all concrete had been removed down to the liner.

The licensee assembled a technical analysis group dedicated to analyze the separation (called a delamination) to: (1) determine the extent of condition; (2) determine the root cause; (3) perform a design basis analysis; and (4) perform a repair alternatives analysis. Each area was enhanced by support from external consultants. These consultants included one with expertise in non-destructive testing of large concrete structures to help determine the extent of the delamination, and another recognized for its expertise in root cause analyses to determine the root cause for this event. The licensee also included a consultant with expertise in computer analysis and design basis calculations to participate on the team to review the effect of the delamination on the design bases and design margin of the containment structure. This effort was placed under the responsibility of the Containment Project Manager. The Containment Project Manager was also responsible for interfaces with INPO, NEI, the NRC, media, etc. as well as project controls dealing with scheduling, contract administration, and financial issues.

2.0 Operability and Reportability

a. Scope

The inspectors reviewed the licensee's Reportability Evaluation to determine whether the containment de-lamination was reportable in accordance with the CFR, specifically 10 CFR Part 50.72 and 10 CFR Part 50.73. The review included: (1) any operation or condition which was prohibited by the plants technical specifications; (2) any event or condition that resulted in the condition of the nuclear plant, including its principal safety barriers, being seriously degraded; and (3) any event or condition that could have prevented the fulfillment of the safety function of structures or systems that are needed to shutdown the reactor and maintain it in a safe condition, remove residual heat, control the release of radioactive material or mitigate the consequences of an accident.

b. Observations

The licensee determined that the extent of condition of the delamination was limited to the location of the steam generator replacement opening made in the containment between buttresses 3 and 4 to support the replacement of steam generators during RFO16. The licensee's root cause analysis determined that the delamination occurred during the creation of the steam generator replacement opening and was caused by the pattern and scope of the detensioning of tendons within the area of the opening. These activities were performed after the plant was shut down for RFO16 and when the plant was in Operating Mode 5. In accordance with Technical Specification (TS) 3.6.1, the containment is required to be operable in Operating Modes 1 through 4. The containment is not required to be operable to meet containment integrity requirements for Modes 5, 6, and NO Mode,

but is required to perform the key safety function of containment closure. All fuel had been transferred out of containment before the liner was opened.

Therefore, based on the above information, the inspectors concluded that none of the reporting criteria under 10 CFR Part 50.72 or Part 50.73 applied and this condition was not reportable to the NRC.

3.0 Structural Integrity

a. Scope

The SIT reviewed the licensee's program that implements regulatory requirements required to maintain the structural integrity of the containment. These requirements included the structural integrity test conducted prior to plant initial operation, containment leakage tests required by TS 5.6.2.20 and 10 CFR Part 50, Appendix J, Option B, the inspections required by 10 CFR Part 50.55a and the requirements of ASME Section XI, Article IWL. Inspectors also reviewed the root cause and repairs associated with the containment dome delamination identified in 1976.

b. Observations

The SIT reviewed the licensee's Structural Integrity Test report conducted prior to plant initial operation. The structural integrity test was conducted in accordance with the intent of NRC Regulatory Guide 1.18, Structural Acceptance Test for Concrete primary Reactor Containment. The inspectors also reviewed the procedure used by the licensee to conduct the Containment Integrated Leak Rate Tests (ILRT). The ILRT incorporated the methods and provisions of the total-time method using the provisions of BN-TOP-1 or the mass-point method as specified in ANSI/ANS-56.8-1987 or ANSI/ANS-56.8-1994. Six ILRTs have been conducted on the Crystal River Unit 3 containment building, including the pre-service ILRT in October 1976. The other required ILRTs were performed in June 1980, July 1983, November 1987, November 1991, and December 2005. The inspectors reviewed each of the referenced ILRT results to verify that the acceptance criteria were satisfied. The inspectors also interviewed the engineer responsible for the licensee's program to evaluate his knowledge of the program and its requirements. The inspector determined that each ILRT satisfied the acceptance criteria and that the program engineer was knowledgeable and well versed in the requirements of the ILRT program.

The SIT also reviewed Progress Energy Procedure NAP-02, Preparation and Control of CR3 Site Specific Special Process Specifications and Guidelines. NAP-02, Appendix 4, Attachment Q, Visual Examination of ASME Section XI, Subsection IWL Components, is used as the specification for performing visual examinations of the concrete portions of the containment building. Procedure SP-182, Reactor Building Structural Integrity Tendon Surveillance Program, is used as the procedure for conducting examinations of the tendons specified in ASME Section XI, Subsection IWL. Procedure NDEP-0620, VT-1 and VT-3 Visual Examination of ASME Section XI, Subsection IWE Components of Nuclear Power Plants, defines the methods and requirements for performing the examinations for the steel liner specified in ASME Section XI, Subsection IWE. Procedure NDEP-A, Nuclear NDE Program and Personnel Process, establishes the nuclear nondestructive

examination (NDE) program criteria and process for certification of NDE personnel, such as the inspectors performing the visual examinations (VT) for the IWL and IWE examinations specified in the ASME Section XI.

The SIT reviewed a sample of inspection results documentation for VT-1 and VT-3 examinations from various years. VT-3C and VT-1C reports were sampled and reviewed for the IWL visual inspections of the concrete associated with Refueling Outage 15 completed on December 3, 2007, which was completed and documented in connection with Work Order (WO) 681043-08. The Final Report for the 30th Year Containment IWL Inspection was reviewed to evaluate the adequacy of the tendon examinations conducted between October and November 2007. Visual examination (VT-3) reports were sampled and reviewed for the IWE visual inspections of the steel liner associated with the Refueling Outage 13, completed on August 21, 2003, and which was completed and documented in connection with WO 321405-01. Examiner qualifications were reviewed for inspectors that conducted visual examinations in connection with the Refueling Outage 15 IWL and IWE examinations.

Based on the review, the inspectors concluded that the structural integrity of the CR3 containment was maintained consistent with regulations and the requirements of ASME Code. No findings of significance were identified.

4.0 Adequacy of Maintenance and Inspection Programs

a. Scope

The SIT reviewed plant Maintenance Programs including plant administrative and implementing procedures associated with the plant's IWL and IWE programs. The IWL program requires visual examination of the containment concrete surface, and performing periodic testing of tendons. The IWE program also requires visual examination of the containment liner. In addition the SIT reviewed the results of these inspections, engineering evaluations, and related corrective actions.

The inspectors reviewed procedures and specifications for the in-service inspections (ISI) required by ASME Section XI, and reviewed the historical documentation regarding the dome delamination issue and associated repairs. The inspectors also reviewed a sample of ISI-related documentation, including various reports of results from examinations and examiner qualifications.

The SIT reviewed various licensee procedures, specifications, and documentation of inspection results to determine if surveillance programs for monitoring the concrete structure, tendons, and steel liner were in accordance with ASME Boiler and Pressure Vessel Code Section XI, Rules for ISI of Nuclear Power Plant Components. The inspectors reviewed Progress Energy Procedure NAP-02, Preparation and Control of CR3 Site Specific Special Process Specifications and Guidelines. The inspectors reviewed NAP-02, Appendix 4, Attachment Q, Visual Examination of ASME Section XI, Subsection IWL Components, which is used for performing visual examinations of the concrete portions of the containment building specified in ASME Section XI, Subsection IWL. Also reviewed was Procedure SP-182, Reactor Building Structural Integrity Tendon Surveillance Program, which is used as the procedure for conducting examinations of the tendons specified in ASME Section XI, Subsection IWL. The inspectors reviewed

Procedure NDEP-0620, VT-1 and VT-3 Visual Examination of ASME Section XI, Subsection IWE Components of Nuclear Power Plants, that defines the methods and requirements for performing the examinations for the steel liner specified in ASME Section XI, Subsection IWE, and reviewed Procedure NDEP-A, Nuclear NDE Program and Personnel Process, which establishes the nuclear NDE program criteria and process for certification of NDE personnel, such as the inspectors performing the visual examinations (VT) for the IWL and IWE examinations specified in the ASME Section XI.

The SIT reviewed a sampling of inspection results for scheduled VT-1 and VT-3 examinations. The inspectors reviewed Work Order 681043-08 that documented the VT-3C and VT-1C reports for the IWL visual inspections of the concrete associated with the Refueling Outage 15. The Final Report for the 30th Year Containment IWL Inspection of the tendon examinations conducted between October and November 2007 was also reviewed. VT-3 reports were sampled and reviewed for the IWE visual inspections of the steel liner conducted using WO 321405-01 during Refueling Outage 13, completed on August 21, 2003. Qualifications were reviewed for three inspectors who conducted IWL and IWE visual examinations during that Refueling Outage 15.

The inspectors verified the licensee was adequately examining, monitoring, and documenting ISI requirements in accordance with ASME Section XI. The inspectors verified that the NDE performance was adequate and personnel performing the examinations were appropriately qualified, trained, and performed examinations in accordance with documented procedures and specifications.

b. Observations

The inspectors verified that the rough and uneven surface condition of the dome has existed since the 1976 repair. The licensee has periodically completed numerous surface patches to attempt to address the surface spalls. Following additional reviews of the dome tendon stresses and monitoring, the uneven surface also appeared to be a result of concrete installation and finishing from the 1976 repair and not related to settlement of the dome or the concrete wall delamination issue.

The SIT concluded that the licensee's ISI program was adequate. No findings of significance were identified.

5.0 Extent of Condition and Root Cause

5.1 Extent of Condition

a. Scope

The SIT reviewed Progress Energy's (PE) determination of the extent of condition of the delamination, including results of the NDE and the testing of core bores taken from Bay 3-4, and other areas of the containment. The SIT also conducted a thorough review of the licensee's in-process information associated with the root cause analysis and the root cause report that determined the root cause is the scope and sequence of detensioning the tendons in preparation for making the Steam Generator Replacement (SGR) opening. The licensee's activities associated with its investigation into the extent of

the delamination and its effect on the containment was also reviewed by the SIT inspectors.

b. Observations

The licensee contracted CTLGroup to perform the non-destructive testing (NDT) in support of the analysis to determine the extent of the condition associated with the delamination. CTLGroup's main objective was to characterize the extent of the delamination around the opening, and assess whether similar delamination existed elsewhere within the wall structure. CTLGroup performed initial trial testing to evaluate suitability of several NDT techniques in detection of the delamination in the containment wall structure. A test procedure/program was developed for the selected test methods. Impulse Response (IR) was selected as the most suitable method for detecting a delamination consistent with the delamination in Bay 3-4. Documentation was provided related to quality control, safety training, qualification requirements, and equipment calibration.

The SIT reviewed the licensee's information on the NDT that was performed at all accessible areas, including nearly all of the exposed exterior containment building wall surface, portions of wall areas accessed inside adjacent buildings, and a portion of the containment dome. Bays 1-2, 2-3, and 6-1 were tested over the entire exterior surface of each bay. Bay 3-4 was tested from the top of the equipment hatch enclosure to ~7' below the ring girder with the exception of the SGR opening and panels within the inner boundary of the delamination (~4,100 ft²). Bay 4-5 was tested ~90% of the exterior surface (~5,200 ft²). Bay 5-6 was tested over ~80% of the exterior surface (~2,500 ft²). Portions of each bay were tested below the roof lines of the adjacent structures. The areas tested were limited by numerous factors such as, 1) high radiation and contamination areas, 2) physical restrictions due to plant equipment located near the walls or components attached to the walls, 3) areas in the fuel transfer area restricted by energized equipment and fuel transfer pool foreign material concerns. The expansive scope of this IR testing over the containment surface provided assurance that sufficient testing has been performed to detect delamination similar to what has been observed between Buttresses 3 and 4.

The SIT reviewed the CTLGroup project report that presented the test program and findings. IR data files with graphical imagery were provided to corroborate the IR Log Sheets that were used to document the IR results.

The SIT also reviewed concrete cores that were drilled to confirm the NDT results. Visual examination of core bored holes was performed using a boroscope. Cores were also taken to provide test specimens in support of the root cause analysis. Material test results were retained with the root cause investigation. ASME Section XI, IWL, visual examination of the affected areas was performed to identify non-conforming conditions observed since the last surveillance, which may have been caused by the delamination event.

The SIT reviewed licensee information in conjunction with NDT and core boroscope inspections performed on the dome, and the survey that was performed that replicated the dome surveillance established after the dome delamination event during construction. The dome survey was performed to identify if there were significant changes on the surface of the dome by comparing the current survey data to the final dome survey performed in

1981. A survey of accessible surfaces of the buttresses was performed to determine the relative position of the buttress corners. A survey was also performed inside containment.

Condition Assessment Results - IR and Confirmatory Core Bore Boroscope Examinations

The SIT reviewed the following licensee information on the methodology and results of the extent of condition analysis.

The IR test method employs a low strain transient impact, generated by a hammer, to send a stress wave into the concrete structure. The resulting bending behavior of the structure is analyzed to characterize the integrity of the structure. The IR analysis produces an average mobility, which is the principal parameter. Presence of significant voiding or an internally delaminated or unbounded layer will result in an increased average mobility value. On the other hand, a sound concrete element without distress will produce a relatively low average mobility value. The presence of delamination will effectively reduce the thickness of wall or slab responding to the impact, which results in a drastically increased average mobility value.

The IR method is utilized on a comparative basis, which allows the engineer to compare the difference in dynamic responses between test areas within the structure. The measured response data are correlated to condition via intrusive sampling such as core drilling or chipping. For those test areas that do not warrant intrusive sampling, as determined by the CTLGroup IR Team Leader/Senior Engineer, test results are evaluated and a technical basis for acceptance is provided. The basis for acceptance was reviewed and approved by the Progress Energy Civil Engineer.

Bay 3-4 was found to have large delamination with an hour glass shape centered at the SGR opening. The delamination was concluded to be within an area of approximately 80 ft by 60 ft, extending between the edges of the two buttresses in horizontal direction, and from top of the equipment hatch opening to approximately ten feet below the ring girder in the vertical direction. Average mobility values exceeded the potential damage threshold in the delaminated area. Based on core sampling and boroscope examination of core holes, the depth of delamination ranged from three to ten inches, with an average delamination depth between seven and eight inches from the exterior face. The delamination appeared to be in the plane of the hoop tendons. The extent of the delamination was confirmed by the core samples and boroscope examination.

The remaining five bays were found to have sound concrete, based on the IR test results. Significant delamination similar to that noted in Bay 3-4 was not found in the other areas of the containment wall structure. A small portion of the tested areas showed elevated average mobility values. Very isolated points had average mobility values slightly above the potential damage threshold. These areas required further investigation to determine the higher average mobility values, which include visual inspections, ground penetrating radar testing, hammer sounding, and core sampling. IR testing was also performed on selected areas of the dome, which is discussed later in this section.

The small portion of tested areas showing elevated average mobility values were evaluated on a case-by-case basis. A large number of elevated average mobility values were resolved due to a lack of a significant number of elevated values. Localized test locations with elevated average mobility values do not represent a condition similar to the

observed delamination in Bay 3-4. A conservative correction factor was applied to normalize the average mobility values used for a specified population of panels. The normalization value determination produced a correction factor of 1.77; however, a correction factor of 2.0 was applied conservatively. This produced elevated average mobility values that were evaluated as acceptable based on the actual normalization value. A number of elevated average mobility values were resolved by determining the proximity of the test location to tendons. A tendon having less cover than normal will produce a higher average mobility value. Test locations between two closely spaced tendons may produce higher values without the presence of a defect. Core boroscope inspections confirmed this condition. Variations in material properties, such as less-than-normal coarse aggregate in the concrete, can influence IR testing. In all cases, the case-by-case justification of acceptance was provided by CTLGroup and reviewed and approved by Progress Energy as documented in WO 1636782-03.

The very isolated points above the potential damage threshold required additional investigation to determine the condition. Three panels exhibited some type of isolated internal defect. Bay designated RBCN-0003B, below the equipment hatch, had an elevated average mobility value. Core Number 54, 2-inch diameter x 12-inches deep, was drilled near the highest mobility value. The boroscope inspection detected an indication but a determination could not be made. It was observed that this location appeared to contain less large aggregate than normal. This condition would cause elevated average mobility values. An additional core, 4-inch diameter x 12-inches deep, was drilled directly over the two-inch diameter core. After removing the core sample and performing the boroscope inspection, it was clear that there was a crack. The core bore confirmed that the IR test detected the existence of a crack. The area was excavated (WO 1686388), the depth of the core exposing rebar and the top surface of a tendon sheath. The concrete was removed to a diameter of approximately eight inches at which point the crack could no longer be seen. With the defect removed, it was believed that the relatively large area of high mobility as shown on the IR Mobility Plot, for an isolated condition, was attributed to the less-than-normal amount of large aggregate.

Panel W of Bay RBCN-0012 had an elevated average mobility value that required investigation. The bottom left corner of the panel exhibited an isolated internal defect. Core Number 85 was near the location but didn't reveal any indication of a crack. It was likely that this defect was a shallow spall similar to that of other panels that had experienced spalling around the perimeter of a panel at the edge of the feature strip surrounding the panels. (The feature strip is a ¾-inch deep by 4-inch wide horizontal and vertical recess located in the horizontal plane at the ten-foot placement joints and in the vertical plane at 20-foot intervals.) Concrete had fallen off in these areas or was removed for personnel safety concerns during the IR testing. The corner was sounded using a hammer and an isolated intact shallow spall was determined to be present with an area of slightly larger than one square foot. The shallow spall is to be removed by WO 1686388. Any unanticipated results found after the spall is removed will be addressed in a planned revision to this engineering change (EC).

The remaining defect was in RBCN-0011; Panel Q, in the upper right hand corner. Core Number 42 was drilled near the elevated average mobility value with no defect detected. The licensee was determined that another core would be necessary to characterize this suspect area after the area was sounded and nothing abnormal was detected. The IR Mobility Plot shows an area of elevated mobility with an area of approximately one

square foot. The core was worked under WO 1686388. The results from the boroscope inspection identified an anomaly approximately 8¾" deep. This anomaly was being investigated further and is assumed to be an isolated condition with no adverse structural affect, similar to that identified by IR at Core Number 54. Any unanticipated results found after the spall is removed were to be addressed by the licensee.

An area on the Reactor Building dome between Buttresses 3 and 4 was IR tested to assist with determining core bore locations to allow for examination of the dome after tendon detensioning. The core boroscope inspections assessed if changes occurred in the dome that would have been caused by tendon detensioning via EC 75218. These inspections also provided information regarding the condition of the interface between the original concrete and the repair material used to address the dome delamination that occurred in 1976. A total of seven cores were bored, two in the area of the dome that was not repaired after the dome delamination which occurred during construction and five in the repaired area. The mobility scale used for the walls in the six bays was not used due to the differences in various aspects such as thickness, orientation, materials, amount and configuration of tendons and reinforcement. Two relatively high average mobility values were identified in the repaired area. Cores were located at these locations to assess the condition. Boroscope inspection of each of the seven core locations did not detect evidence of cracking or delamination. The apparent bonding adhesive used in the repair could be seen and there was no appearance of a separation between the original concrete and the repair material. Although the core samples did separate upon removal when removed during boring operations, the licensee assumed that the boring process exerted forces at the interface of the original concrete and the repair material.

The scope of the dome IR testing expanded to the area of the dome between Buttresses 1 and 6 due to the planned tendon detensioning of vertical tendons between Buttresses 1 and 6 as part of EC 75218. The IR test data will be used to compare IR test results obtained after tendon detensioning, which was part of the testing section in EC 75218, the scope of which is not part of the Condition Assessment. Results from a core (Number 130) and boroscope inspection at a relatively high average mobility value indicate that an anomaly exists approximately seven inches deep in the repair area that has a step transition from the outer bounds of the delamination to the full excavation depth of approximately twelve inches. The licensee plans to investigate this anomaly further under NCR 388332. Any additional cores and boroscope results are planned to be incorporated into a revision to EC 75218. In addition to the IR testing and core bore drilling on the dome, a condition assessment was made on a depression in the concrete surface of the dome. This assessment was made in response to a NRC SIT request. The request asked if the depression is evidence of repeat delamination damage. The assessment concluded that the cracking was in the cosmetic patches used to smooth the surface during construction where a depression was present. The cosmetic patches were determined to have no correlation to the structural integrity of the Reactor Building dome. The licensee concluded that the thin concrete patches may be removed and not replaced without adversely affecting the operational function of the dome structure.

Reactor Building Containment Surveys

Surveys of the exterior and interior surfaces of the containment were performed at the request of the Containment Root Cause Team. An exterior survey of the containment dome and buttresses was performed to identify if there were significant changes to the

surface of the dome compared to the final dome survey performed in 1981. The dome survey data did not indicate the presence of a new delamination of the dome surface. The buttress survey was performed to determine the relative position of the buttress corners. The buttress survey data showed that the vertical alignment of the buttresses was within the vertical alignment tolerance provided by American Concrete Institute (ACI) 117-90. A survey was also performed inside containment. Its purpose was to duplicate a survey performed as part of an original structural integrity test (SIT) measurement data set. The dome and buttress survey data was used by the Root Cause Team to address multiple Failure Mode (FM) Analyses. The survey performed of the internal diameter of containment was not used in the FM analysis but was used in the finite element model developed by Performance Improvement International (PII).

SGR Opening - Top and Bottom Wall Crack Assessment

An assessment was performed on cracks that were documented in Quality Control (QC) inspection report dated December 7, 2009. NCR 370853 documented this condition and was tracking the repair of the identified condition. The assessment concluded that the cracks in the top and bottom of the SGR opening were not the result of the delamination event, based on observations made after the initial event. The SGR opening and the overall repair surface area are to be mapped for cracks in accordance with EC 75219. The licensee planned to incorporate the assessment of any cracks and determine the necessary repairs in EC 75220.

Condition Assessment Conclusion

Delamination similar to that noted between Buttresses 3 and 4 was not found in other areas of the containment wall structure or dome. IR testing with confirmatory core bores identified delamination only between Buttresses 3 and 4 above the equipment hatch, as accurately predicted by IR. The few isolated areas found with small defects are being repaired by the Containment Repair Team. The remaining condition assessment information has been accepted by the Containment Root Cause Team and is being used as input into the root cause analysis as the team deems necessary

5.2 Root Cause Analysis

a. Scope

Based on the scope, significance, and complexity of the issue, the licensee's overall Root Cause Investigation Team was broadly organized into four separate branches: Root Cause Analysis, Condition Assessment, Design Basis Analysis, and Repair Analysis. Each branch focused on a particular strategic area, with appropriate information sharing and cross-checking, such that each group's efforts fed into the common goals of: (1) understanding the cause of the event, (2) determining the extent of the problem, and (3) identifying the repairs necessary to satisfy the design basis requirements of the containment structure. The inspection review documented in this section is limited to the technical root cause analysis work performed by the licensee's Root Cause Analysis branch.

The SIT inspectors reviewed the licensee's problem investigation activities related to determining the technical root cause(s) of the containment wall delamination event and

corrective actions to prevent recurrence and/or propagation of the delamination. The inspectors reviewed the licensee's root cause analysis activities to determine whether the licensee's causal analysis activities were performed in accordance with applicable licensee procedures and standards. The objectives of the inspection were to determine: (1) whether the licensee's efforts and the determination of the technical root cause(s) and contributing causes were comprehensive and reasonable, and whether the time-line of its containment wall delamination event was reasonable. In addition, the SIT inspectors reviewed the licensee's responses to the SIT questions associated with the root cause analysis.

The inspectors reviewed documentation of all identified failure modes and contributing causes for significance. The inspectors also reviewed the licensee's new computer modeling approach and input material properties used to simulate the delamination in support of the root cause determination. The inspectors reviewed the corrective actions to prevent recurrence and for betterment identified in the licensee's root cause evaluation report to determine whether they addressed the causal factors. Note: The review and discussion documented by this inspection review relates specifically to the delamination failure.

The SIT review of the root cause analysis included 75 potential failure modes in the areas of: (1) Containment Design and Analysis; (2) Concrete Construction; (3) Use of Concrete Materials; (4) Concrete Shrinkage, Creep, and Settlement; (5) Chemically or Environmentally Induced Distress; (6) Concrete-Tendon-Liner Interactions; (7) Containment Cutting; (8) Operational Events; and (9) External Events. A total of 67 failure modes were refuted. The remaining eight FMs were combined to determine that the root cause was a combination of inadequate detensioning scope and detensioning sequence. The number and order of the detensioned tendons resulted in redistribution of stresses in the containment wall which led to the delamination. A much larger scope with a detailed sequence would be required to maintain acceptable tensile stress levels. The licensee determined that new modeling and evaluation techniques were required to successfully determine or predict margin to delamination.

b. Observations

Criterion XVI, "Corrective Action," of Appendix B of 10 CFR Part 50, "Quality Assurance Criteria for Nuclear Power Plants and Fuel Reprocessing Plants," requires that... "Measures shall be established to assure that conditions adverse to quality, such as failures, malfunctions, deficiencies, deviations, defective material and equipment, and non-conformances are promptly identified and corrected. In the case of significant conditions adverse to quality, the measures shall assure that the cause of the condition is determined and corrective action taken to preclude repetition. The identification of the significant condition adverse to quality, the cause of the condition, and the corrective action taken shall be documented and reported to appropriate levels of management." The delaminated condition of the CR3 containment wall was identified to be a significant condition adverse to quality and, therefore, this regulation required the licensee to perform and document a root cause evaluation to determine the cause(s) and implement corrective action(s) not only to correct the condition but also to prevent recurrence.

The CR3 reactor containment building provides the third and final fission product barrier against the uncontrolled release of radioactivity to the environment. The delamination

event of October 2009 during RFO16 resulted in a degraded condition of the containment wall that reduced its structural capability and could challenge the ability of the structure to perform its safety function of providing a leak-tight barrier against the release of radiation to the environment and the public in the event of a design basis accident. The licensee classified the unprecedented containment wall delamination event as a “Significant Adverse Condition” in accordance with its procedure CAP-NGGC-0200, “Corrective Action Program,” which implements the requirements of 10 CFR Part 50, Appendix B, Criterion XVI. Accordingly, the licensee initiated Nuclear Condition Report (NCR) Action Request 358724 (Assignment 1) and conducted a technical root cause evaluation (RCE) to determine cause and take corrective action(s) to prevent recurrence (CAPR).

The licensee conducted and documented a structured root cause evaluation of the “Significant Adverse Condition Investigation” of the delamination event in accordance with the guidance in its supplemental procedure CAP-NGGC-0205, Revision 11, “Significant Adverse Condition Investigations and Adverse Condition Investigations – Increased Rigor.” The resulting report of the investigation documented the technical root cause evaluation and identified the root cause(s) and the contributing causes, including a failure mode timeline, of the CR3 containment wall delamination event and corrective actions to prevent recurrence (CAPRs) and betterment actions.

In accordance with procedure CAP-NGGC-0205, the licensee convened a root cause review team that performed an informal review of specified elements of the containment wall delamination root cause investigation to ensure that the procedural and investigative process requirements were met and to improve the quality of the report to the “highest degree possible” prior to the Quality Review Board (QRB) review. The technical root cause report was reviewed and approved by the licensee’s QRB panel and the Plant Nuclear Safety Committee (PNSC). The inspectors observed the proceedings of the QRB and PNSC meetings for the root cause.

The licensee’s investigation team for the root cause analysis comprised of individuals from across the Progress Energy fleet, industry peers, and an external “subject matter expert” root cause contractor. The contractor with whom Progress Energy partnered for the root cause analysis was PII, a consulting firm specializing and experienced in structured root cause investigations. The PII team consisted of over 15 engineering professionals and analysts with expertise in root cause investigations, concrete materials, behavior and testing, containment structural analysis and design, and advanced finite element analyses and computer modeling. PII’s root cause evaluation work of the CR3 containment wall delamination event was performed under CR3’s 10 CFR 50 Appendix B Program.

Technical Root Cause Determination

During RFO16, the delamination gap was observed in the vertical plane of the horizontal tendons, approximately ten inches from the outer surface, of the CR3 containment wall. The delamination was first observed while concrete removal (by hydro demolition) was in progress for the creation of a 25 ft wide by 27 ft high construction opening in the 42-inch thick containment wall to facilitate the steam generator replacement (SGR). The SGR opening was centered on azimuth 150° between elevation (EI) 183 ft and EI 210 ft. The creation of the opening involved detensioning and removal of 17 horizontal (or hoop) tendons and 10 vertical tendons that traversed the foot print of the SGR construction opening. The licensee’s condition assessment of the delamination event, using the

impulse response non-destructive testing technique with confirmatory core boring and boroscopic examinations, determined that the extent of the delamination was limited to Bay 3-4 corresponding to an approximately 60 ft wide by 82 ft high hourglass-shaped area, which included the SGR construction opening, between Buttresses 3 and 4, extending from above the equipment hatch to approximately ten ft below the bottom of the ring girder. The tendon pattern at the SGR opening and the hourglass delaminated boundary is shown in Figure 5.2.1.

The root cause analysis team identified 75 FMs that could potentially cause or contribute to the delamination of Bay 3-4 of the CR3. These failure modes were binned into nine categories, as indicated below, and subsequently evaluated using a "Support/Refute" methodology to conclude whether or not it was supported as a causal factor.

1. Containment Design and Analysis
2. Concrete Construction
3. Use of Concrete Materials
4. Concrete Shrinkage, Creep, and Settlement
5. Chemically or Environmentally Induced Distress
6. Concrete-Tendon-Liner Interactions
7. Containment Cutting (SGR-related construction activities)
8. Operational Events
9. External Events

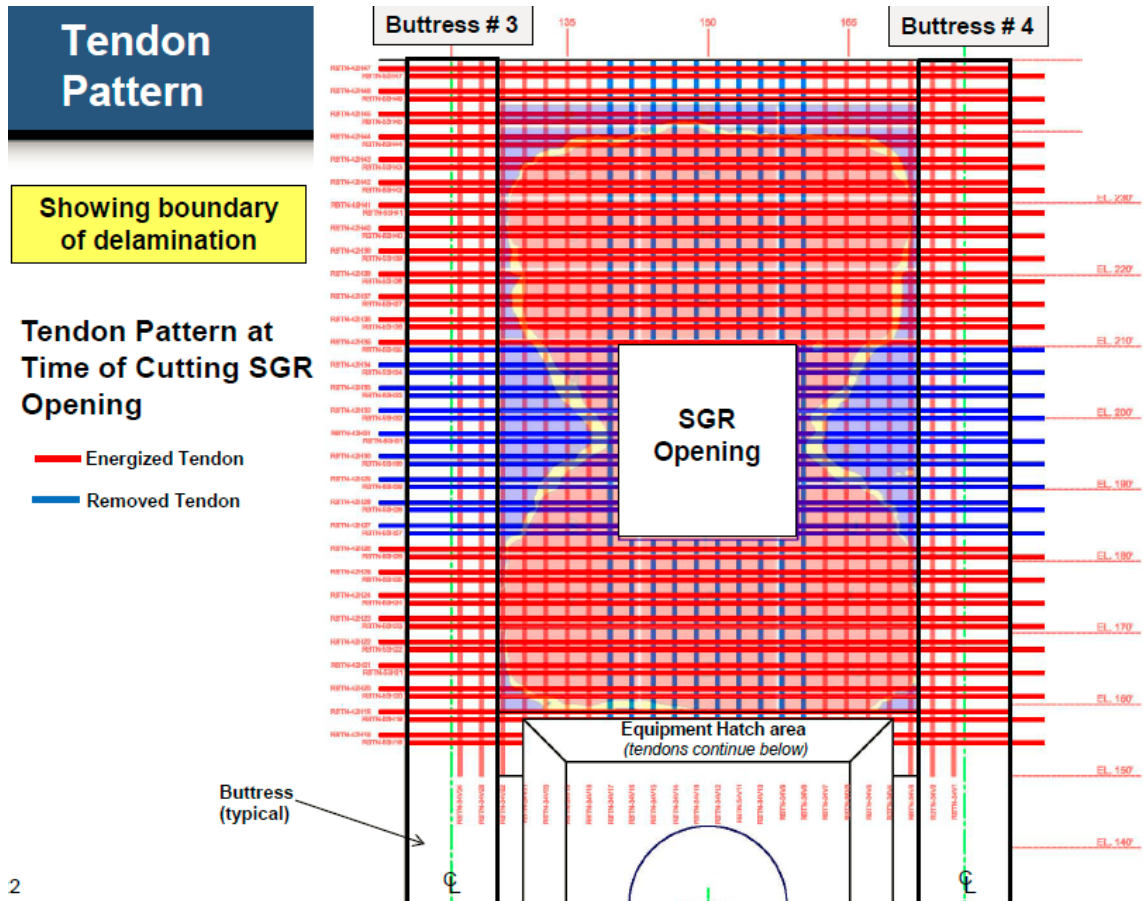


Figure 5.2.1 Tendon Pattern at SGR Opening and Delamination Profile

The support/refute methodology involved collection and analyses of information and evidence for each failure mode that allowed a conclusion to be drawn regarding its involvement (or lack of) in the event. The evidence used to inform the investigation included historical plant records of design, construction and operation of the CR3 containment, related industry operating experience, field observations and surveys, interviews of cognizant personnel, specialized technical literature, laboratory tests, and specialized analyses, including new state-of-the-art concrete fracture-based finite element computer models for simulation of the delamination event. These models allowed PII to start with information now known about how the CR3 containment structure behaves and work backwards in time to determine what factors contributed to the delamination event. The material property inputs (such as concrete elastic modulus, creep coefficient, tensile strength, fracture energy) used in the model were based on measured properties obtained following the delamination event.

The root cause team also reviewed and considered the operating experience and causal factors from the delamination events of the containment dome, all during original construction, at Turkey Point Unit 3 (June 1970), Crystal River Unit 3 (April 1976), and Kaiga Atomic Power Project Unit 2 (India, May 1994), as well as containment design data, from some of the other operating plants with similar post-tensioned containments that had successfully executed SGR construction openings. As each failure mode was

investigated, the resulting conclusions were reviewed within PII, by Progress Energy, and also by third party reviewers. The licensee, based on the evidence and modeling, refuted 67 of the 75 failure modes and determined that they did not contribute to this event. The remaining 8 supported failure modes (associated with Categories 1, 2, 3, and 7) were confirmed by the licensee as contributors. The failure modes that were supported as contributors to the delamination event are discussed below. The licensee's root cause analysis determined that the delamination was not caused by any one of these factors acting alone, but was the result of the combined interplay of these contributing factors acting together.

- FM 1.1 Excessive Vertical and Hoop Prestress / Compressive-Tensile Interaction: The CR3 containment design uses larger diameter (163-wire) prestressing tendons, which results in higher vertical and hoop compression stresses and higher peak stresses, when compared to the design of other 6-buttress containments. The hoop prestressing system at CR3 is designed to resist 1.5 times the design accident pressure, which is in the high end among post-tensioned containment designs. Although the high level of prestress did not alone cause the delamination, the licensee determined that it likely reduced the margin to delamination by augmenting inherent weakness in the potential delamination plane.
- FM 1.2 Excessive Radial Tensile Stresses/No Radial Reinforcement: The high as-designed vertical and hoop prestress translates to relatively higher radial tensile stresses in the outer concrete region. The CR3 design did not provide radial reinforcement in these locations at the elevations of the delamination, which is not uncommon for post-tensioned containments of this vintage. The licensee determined that the high level of radial tensile stress did not alone cause delamination but reduced the margin to delamination.
- FM 1.15 Inadequate Design Analysis Methods for Local Stress Concentrations: The presence of the tendon sleeves in the concrete creates local stress concentration effects adjacent to the sleeves under prestressing force, which result in high peak tensile stresses, especially around the hoop tendon sleeves, that potentially caused small localized cracks during original tendon tensioning. These small cracks are potential sites for delamination initiation and propagation during modification activities such as tendon detensioning and concrete removal for SGR openings. These stress concentrations were not explicitly considered in the original containment design. The licensee determined that the predicted radial tension in the original design using standard industry calculation tools, based on only hoop prestressing force, is smaller than the actual.
- FM 2.12 Inadequate Strength Properties: The test results of concrete cores from the delaminated Bay 3-4 show that the tensile strength is variable and occasionally low, primarily due to the soft aggregate used in the concrete. Even though the average strength properties met design criteria for CR3, the tensile strength and fracture energy of the concrete was not adequate for radial stresses produced during the activities of tendon detensioning and of cutting the opening for the SGR project. Therefore, the licensee determined that the lower-than-normal concrete tensile strength was a contributor to the delamination.

- FM 3.4 Inadequate Aggregate: The Florida (Brookville) calcareous limestone coarse aggregate used in the CR3 containment concrete was relatively soft, porous, and gap graded. This aggregate was not appreciably stronger than the hardened cement paste and allowed cracks to propagate directly through the aggregate. Typically, the aggregate provides a dense stable medium that helps arrest and slow the propagation of cracks. While its properties were sufficient to produce concrete of acceptable specifications and design requirements, the tensile strength, elastic modulus and ability to arrest cracks were lower than normally found at other nuclear containment structures. Thus, the licensee determined that the strength properties of the coarse aggregate contributed to the delamination at CR3.

It is noted that FMs 1.1, 1.2, 1.15, 2.12, and 3.4, discussed above, are inherent in the original containment design and construction, and the containment structure met the requirements for all design basis conditions.

- FM 7.3 and FM 7.4 Inadequate Scope and Sequence of Detensioning of Tendons (used for creation of SGR opening) (ROOT CAUSE): The number and order of detensioned tendons resulted in the redistribution of stresses in the containment wall. The redistributed stresses exceeded the tensile capacity (fracture energy) of the CR3 concrete and, therefore, this was the driver that caused the delamination. In an area as large as Bay 3-4 with large stress concentration effects on a detailed scale, it is probable that cracking began in isolated points of highest stress. As the stresses increased and shifted (due to the progression of growing number of tendons being detensioned), small cracks grew and joined until they eventually covered the entire delaminated area. Delamination occurs where radial tensile stress is high. Delamination occurs at sharp bends and points of reversal of curvature in the wall. The scope and sequence of detensioning tendons for the SGR created a bulge and curvature reversal in the wall and the stress created by the curvature of the bay wall precipitated the cracking and delamination of Bay 3-4. Figure 5.2.2 shows, to an exaggerated scale, the profile of radial displacements following original tendon tensioning, creep deformation, and progressive detensioning of tendons for the SGR opening.

It is noted that an expanded scope and sequence of tendon detensioning was developed in March 2010 for the delamination repair and it successfully detensioned the containment without delamination in any of the other bays.

- FM 7.5 Added Stress Due to Removing Concrete at the SGR Opening: The licensee found that although the evidence seems to indicate that much of the delamination occurred prior to large scale removal of concrete, the removal of concrete at the construction opening increased the stresses in the remaining concrete which contributed to the final extent of the delaminated condition.

The inspection team noted that several of the causal factors of the CR3 containment wall delamination, i.e., biaxial compression-tension interaction, such as high radial tension; stress concentrations; concrete tensile strength; and material properties of the coarse aggregates, were consistent contributors as in the CR3 containment dome delamination event of 1976.

Following the analysis of failure modes, the licensee determined the timing of the contribution of each causal failure mode to the wall delamination event in the Failure Modes Timeline, as shown in Figure 5.2.3. The licensee's root cause analysis and computer simulation determined that the large-scale delamination observed did not exist prior to the SGR opening operations but occurred during construction activities for creation of the SGR construction opening, while the unit was shut down. This determination was supported by the following evidence: (1) the condition assessment confirmed that the delamination was present only in Bay 3-4, the panel where the SGR opening operations were performed, and not in any of the other five bays; (2) the shape of the delaminated area of Bay 3-4 corresponds exactly to the region of detensioned horizontal and vertical tendons (see Figure 5.2.1), indicating that the detensioning process influenced the delamination process, which could not happen if the delamination occurred prior to the detensioning; and (3) traditional petrographic analyses did not detect the presence of pre-existing defects (general lack of significant carbonation and mineral growth on the fracture surface).

In summary, the delamination was determined to have been caused by the combination and interplay of (1) certain design features of the CR3 containment structure; (2) the type of concrete used (material characteristics) in the CR3 containment structure; and (3) the acts of de-tensioning and cutting of the CR3 containment structure for creating the SGR opening. Through state-of-the-art nonlinear fracture-based computer models that PII developed using CR3 specific forensic information that was available after the delamination had taken place, the licensee determined that none of the individual contributing factors, on its own, would have caused a delamination. Rather, the complex interplay between all the contributing causes led to the delamination, with the tendon detensioning being the driver.

The licensee stated that, of particular importance in this analysis is that typical industry containment structure analysis tools that were used to calculate the radial tension and assess the delamination potential, when creating containment openings in other similar projects, have consistently shown large margins for stress tolerance to delamination by using average tensile stress values. The licensee stated that its computer simulation, however, had shown that the CR3 containment structure had a lower margin of tolerance to delamination cracking than other plants which have used common industry calculations.

In conclusion, the licensee's root cause evaluation determined that the immediate technical root cause of the delamination event was the redistribution of stresses, as a result of the SGR containment opening activities, resulting in additional stress beyond original containment design. The condition exceeded the fracture capacity/tensile strength of the concrete resulting in cracking along the high stress plane connecting the horizontal tendons. As the cracks propagated and joined, delamination occurred over a wide area. Evaluation of the contributing failure modes identified only one practical technical root cause subject to licensee's control, and that was inadequate scope/sequence of tendon detensioning used in the SGR outage. The licensee stated that the fracture-based computer simulation effort and post-event research by its contractor highlighted the inability (or limitation) of standard industry accepted analysis tools to predict delamination.

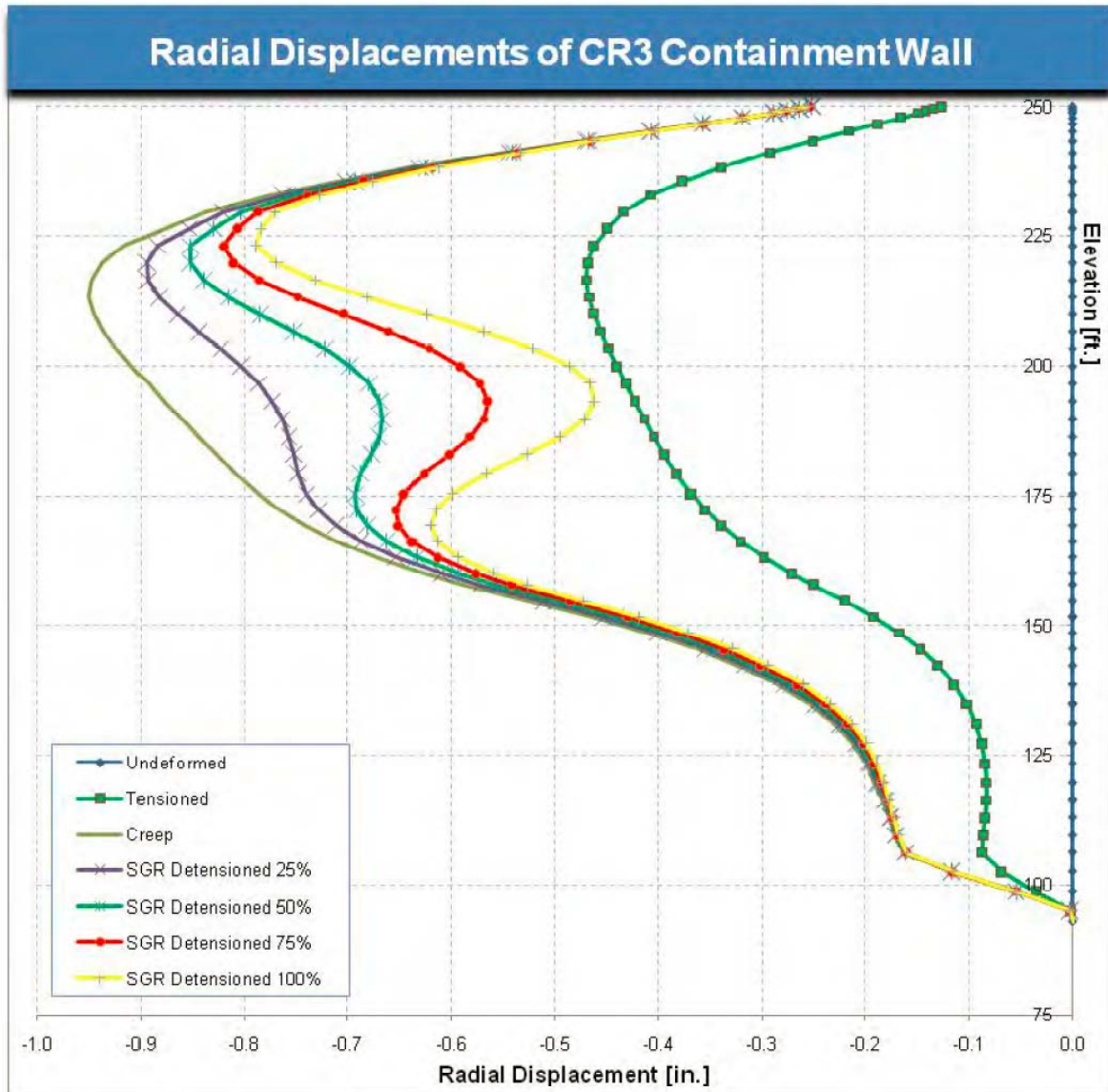


Figure 5.2.2 Bay 3-4 midline vertical profile of radial displacements during progressive SGR detensioning (Note that displacements are plotted to an exaggerated scale)

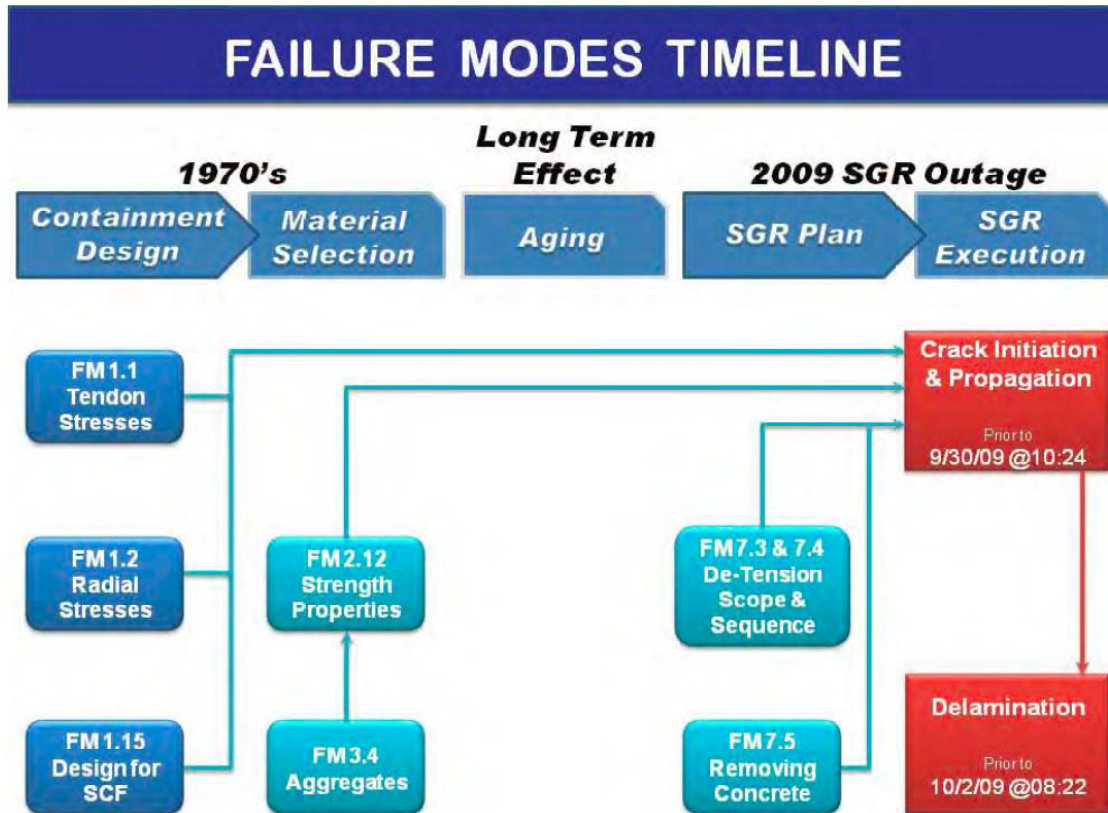


Figure 5.2.3 Failure Modes Timeline

Role of Prestressing Force in Vertical Tendons in Producing Radial Tensile Stresses and Stress Concentrations in the Plane of the Hoop Tendons

The licensee's root cause analysis report identified excessive radial tensile stress in the plane of the hoop tendons without radial reinforcement (FM 1.2) and peak tensile stress concentrations stresses in the concrete around the hoop tendon sleeve holes (FM 1.15) as contributing failure modes to the CR3 delamination event. These high radial tensile stresses and peak stress concentration effects, that are potential localized crack initiators around the periphery of the hoop tendon sleeves, are caused by the prestressing force in the hoop tendons, and apparently also the prestressing force in the vertical tendons, following initial tensioning. This was also physically indicated in the root cause investigation by the presence of small (approximately 5mm long) pre-existing cracks that were observed at the intersection of the fracture surface and tendon sleeves using phenolphthalein experiments on concrete specimens taken from the delaminated area. A paper by Acharya and Menon in Nuclear Engineering and Design (2003) highlights that significant local tensile stresses are developed at the periphery of the duct hole that can contribute to the problem of delamination, and that these localized effects are difficult to compute theoretically.

The common theoretical approach for calculating radial forces and stresses is a cylindrical shell analysis (such as in CR3 Calculation S09-0054, and reviewed in the paper in Nuclear Engineering and Design (2003) that gives an average radial tensile stress value in the

plane of the hoop tendons and is based on the prestressing force in the hoop tendons only. This approach does not account for stress concentration effects around the tendon ducts, nor does it include the effect of prestressing forces in the vertical tendons in producing radial tensile stresses/concentrations in the plane of the hoop tendons. The licensee observed that standard industry analysis of this type (that predict average radial tensile stresses due to hoop tendon forces only) cannot adequately predict the radial tensile stresses that would lead to delamination, such as that observed at CR3. Therefore, in support of the root cause determination, the licensee implemented a three-dimensional fracture-based computer analysis methodology in order to be able to adequately simulate the delamination observed at CR3.

From the CR3 root cause analysis report, it is noted that the standard industry analysis for hoop pre-stressing performed for CR3 predicted the average radial tensile stress in the vertical plane of the hoop tendons to be of the order of 31 psi. The PII computer model calculated actual combined stress conditions at a given location due to all the contributing factors, whether they be from horizontal tendons, vertical tendons, or stress concentrating factors. For the PII linear elastic analysis case assuming no concrete cracking, the tensile stress peaks at a very high value at the edge of the horizontal tendon hole, at the intersection with a vertical tendon, due to the vertical and horizontal tendons. It reaches 1630 psi at the hole and declines rapidly by a factor of two for approximately every inch away. More generally, tensile stress peaks at about 510 psi on the edge of a horizontal tendon hole away from the vertical tendons and declines by a factor of two for every inch away. Note that the 1630 psi peak stress is of such a large magnitude that it would likely exceed the tensile strength of all concrete materials and initiate a small localized crack.

The SIT inspectors questioned the licensee about whether the contribution of vertical tendon prestress was adequately considered. The licensee agreed that the vertical tendon prestressing contributed to the concrete radial tensile stresses and stated that the PII simulation of the delamination event was achieved based upon modeling the combined effect of the entire set of conditions which produced radial tensile stresses and stress concentrations in the plane of the hoop tendons, without a separate quantitative assessment of the contribution of each individual factor. The licensee stated that the purpose of the analysis was to draw overall root cause conclusions versus separating the contribution of the horizontal and vertical tendons.

The SIT inspectors conducted a review by comparing the peak radial tensile stresses from PII's uncracked analysis with the average predicted radial tensile stress from the standard industry analysis, along with some calculations. The results indicated that the prestressing force in the vertical tendons could have a more significant effect than the hoop tendons in producing radial tensile stresses in the vertical plane (delamination plane) of the hoop tendons and peak tensile stress concentrations around the hoop tendon holes. These peak stresses can drive the formation of small localized cracks around the hoop tendon holes during tendon tensioning that become potential sites for delamination initiation and propagation during later modification activities that involve tendon detensioning. The peak tensile stresses can also be influenced by the level of bond between the tendon sleeve and the adjacent concrete. Typical industry calculations consider only radial tensile stresses caused by prestress from the hoop tendons (Reference CR3 calculation S09-0054, and paper in Nuclear Engineering and Design (2003)).

Root Cause - Corrective Actions to Prevent Recurrence (CAPRs)

The repair option selected by the licensee to correct the delaminated condition for continued operability was to “remove and replace the delaminated concrete.” Although the delamination was limited to Bay 3-4, all six bays and the dome of the containment building are susceptible to a similar event. Therefore, CAPRs developed by the licensee’s root cause investigation considered the entire containment building. The selected repair of the containment building requires additional detensioning and subsequent retensioning of tendons, and will therefore subject the building to additional stress redistribution events. Corrective actions specified in the root cause investigation are designed to minimize the risk of delamination in any areas of the containment building, either during the repair process or during modifications involving tendon detensioning and retensioning in the future.

The CAPRs developed by the licensee’s root cause analysis were:

1. Perform a detailed analysis of the tendon detensioning plan in support of the containment repair effort. Modify the plan as necessary and ensure that the stresses show positive margin as validated using CR3 delamination data. This had already been completed at the time of completion of this inspection and the licensee was successful in performing the expanded detensioning without propagating the delamination and without causing additional delamination.
2. Perform a detailed analysis of the tendon re-tensioning plan in support of the containment repair effort. Modify the plan as necessary and ensure that the stresses show positive margin as validated using CR3 delamination data.
3. Establish programmatic controls to prevent de-tensioning more than one tendon/group without a validated detailed analysis using CR3 delamination experience.

The corrective action plan from the root cause analysis also included additional “betterment” corrective actions, considering life extension and aging characteristics, with an appropriate tracking plan:

- Monitor displacement of the containment walls during re-tensioning to confirm the building response relative to computer prediction.
- Monitor the containment wall with strain gauges and acoustic instruments during re-tensioning to ensure that responses are within established limits per the repair design documents.
- Perform a detailed analysis of the stress consequences of typical activities such as heating up and cooling down of containment during outages or solar heating of an entire bay. Ensure that there is no cumulative impact with time.
- Establish an inspection plan to periodically monitor the containment concrete condition to ensure that there are no unexpected changes. The inspection should use NDE, such as Impulse Response mapping of the area and selective core drilling, in areas identified as suspect by NDE.

- Establish a monitoring program that evaluates the response of the installed containment monitoring sensors to ensure the two types of concrete in Bay 3-4 are behaving consistently as an indication of good coupling/bonding.

In accordance with its corrective action procedures, the licensee had a designated action item to perform an effectiveness review after the CAPRs and designated corrective actions have been implemented and sufficient time has elapsed to determine if the action(s) taken were effective in preventing recurrence of the condition and effective in resolving the investigated problem. This effectiveness review was to be performed using the following criteria: (1) monitoring of the containment building during Refuel Outage 17 using installed instrumentation and NDE as described in the monitoring programs established as part of the root cause investigation, to demonstrate that there is no delamination of concrete in the repaired wall or other bays; and (2) verifying that the tendon surveillance program has been revised to include the appropriate limitation on detensioning multiple tendons and the program owner understands the limitations.

Concluding Observations on the Root Cause Evaluation

The NRC SIT inspectors determined that the licensee performed its root cause investigation of the CR3 containment delamination event in accordance with its standard implementing procedures, CAP-NGGC-0200 and CAP-NGGC-0205, for its corrective action program. The inspectors determined that the licensee's problem investigation activities related to determining the technical root cause and contributing causes of the CR3 containment wall delamination event were comprehensive and thorough.

The inspectors determined that the technical root cause and contributing causes, and failure mode timeline, identified by the licensee were reasonable, and adequately supported by appropriate evidence. The inspectors determined that the licensee's investigation results reasonably supported their conclusion that the technical root cause of the delamination was attributed to the scope/sequence of tendon detensioning used for the creation of the SGR construction opening, in combination with other contributing factors related to certain design features of the CR3 containment structure, the materials used in the containment concrete, and the activities related to the cutting of the SGR opening. The inspectors determined that the approach and inputs used in developing fracture-based computer models used to simulate the delamination were reasonable.

The inspectors also determined that the corrective actions developed/taken by the licensee to prevent recurrence and/or propagation of the containment wall delamination, as well as, other related betterment corrective actions developed from the root cause investigation were appropriate and addressed the causal factors.

The NRC inspectors noted that the contribution of the prestressing force in the vertical tendons in causing radial tensile stresses and stress concentrations in the delamination plane of the hoop tendons may be significant and may require research to determine its significance and impact, if any, in design of post-tensioned containments. This is important since vertical tendons are typically tensioned before hoop tendons during tendon detensioning. Typical industry calculations to assess radial tension are based on hoop prestressing force only. The PII modeling appropriately considered the combined effect of all contributing factors, including vertical tendons, in producing radial tension in the

delamination plane, but the relative significance of each individual contributing factor was not separated in the assessment.

The licensee presented their root cause to the NRC Special Inspection Team and staff of NRC Region II and Office of Nuclear Reactor Regulation during a meeting held at the CR3 site on June 14, 2010. Results of the root cause analysis were also presented to the NRC staff during a public meeting held on June 30, 2010 at NRC Headquarters in Rockville, MD. Information and data presented at the meetings were consistent with the NRC's independent review and on-site verification. The licensee's root cause analysis report was used for the inspection team's review for potential generic implications addressed in SIT Charter Item 8.

6.0 Corrective Actions

a. Scope

To repair the containment for continued operability, the licensee elected to remove and replace the delaminated part of the containment wall. The licensee performed design calculations in support of implementation of the selected repair such that the restored containment is in compliance with the plant's licensing design basis described in the FSAR. SIT inspectors conducted a review of selected evaluations relative to the licensee's new finite element analysis and evaluations of the interim and restored configuration of the containment under design basis loads and load combinations described in the FSAR.

b. Observations

The licensee reviewed several repair alternatives. Their review of repair options included consideration for restoration of design margin, extended life, and root cause findings. Some of the rejected repair options included use-as-is, anchorage only, cementitious grout, and epoxy resin. The final repair decision was to remove and replace the delaminated part of the containment wall. The licensee's repair plans included: (1) additional detensioning of containment; (2) removal of delaminated concrete; (3) installation of reinforcement, including radial reinforcement through the delamination plane; (4) placing of new concrete; (5) retensioning containment; and (6) post-repair confirmatory system pressure testing.

After the tendon detensioning and removal, the delaminated concrete was removed. Upon removal of the delamination, the licensee observed vertical cracking in the concrete surface between Buttresses 3 and 4. The cracks were evaluated for size and through-wall penetration. These vertical cracks essentially lined up with the location of the vertical tendons and in most cases went through-wall to the containment liner. The cracks were excavated and were filled in with new concrete. The licensee evaluated the cracks below El 176 and determined them to be acceptable as-is. The licensee also identified tight vertical cracks in other locations around the circumference of the containment. The evaluation of these was on-going at the conclusion of this inspection.

Plant Design Basis Analysis

The SIT inspectors also conducted a review of selected licensee's design basis analysis calculations and evaluations that were in progress and ongoing. The inspectors reviewed containment structural drawings and the applicable portions of the FSAR in order to determine the appropriateness of the design parameters used in these calculations. At the conclusion of this inspection, the licensee was continuing to develop the design basis calculations to bring the containment structure into compliance with the CR3 design basis as described in the FSAR, and to respond to questions that arose as the result of inspectors' review of licensee engineering calculations. The NRC continued to review the available calculations related to the structural modeling, loads and load combinations, design and analysis methodology, structural acceptance criteria, and design of reinforcing steel for the repair of the delaminated bay.

The SIT inspectors began a review of the licensee's evaluations to establish: (1) correlation between the new finite element analysis of the containment structure and the original design basis computer analysis; (2) calculations to demonstrate compliance with the structural acceptance criteria specified in the FSAR and the CR3 design code of record, ACI 318-63; and (3) the design of the required reinforcing steel for the repair of the delaminated bay, all of which to bring the containment structure into compliance with the CR3 design basis as described in the FSAR. The SIT identified errors in data used in calculation S10-0030. These errors were incorporated into the plant's corrective action program for further evaluation to ensure that they did not impact the final results of this calculation. The licensee was conducting additional evaluations on other calculations to determine the extent of this condition.

The NRC planned continued review of selected licensee engineering calculations related to the design basis of the containment structure and its ability to function under all applicable loading conditions. The continued review will be conducted as part of inspections under NRC Inspection Procedure (IP) 50001, "Steam Generator Replacement Inspection."

At the conclusion of the Special Inspection, the licensee had further detensioned the containment and had removed the delaminated concrete. The licensee's repair activities and design engineering evaluations remained ongoing.

7.0 Safety Significance

The licensee's root cause report determined that the delamination was caused by the scope and pattern of detensioning the tendons in preparation of cutting the construction opening for replacement of the steam generators. The inspectors found that the licensee's investigation was thorough and supported its conclusion that the delamination was caused by tendon detensioning. Therefore, the assessment of the safety significance related to the formation of the delamination was limited to the time period after the beginning of RFO16 and when the plant was shut down in Operating Mode 5.

The following information is from the plant operator logs.

- On September 25, 2009, at 7:03 p.m., the plant commenced power reduction for refueling outage 16.
- On September 26, 2009, at 4:51 p.m., the plant was shut down in Operating Mode 5.

- On September 26, 2009, at 4:58 p.m., authorization was given to begin work on tendon activities.
- On October 1, 2009, at 5:44 p.m., the plant was in Mode 6
- On October 9, 2009 the plant was in No Mode with all fuel removed from the reactor and placed temporarily in the spent fuel pool.

After reaching Mode 5 on September 26, 2009, two vertical tendons (34V12 and 34V13) were detensioned simultaneously. From September 26 through October 1, additional vertical tendons and 16 hoop tendons were detensioned as part of the process to make the required construction opening to support the steam generator replacement. Hydrolazing activities began on September 30, 2009. The hydrolazing activities continued through October 7. Work to create an opening in the containment steel liner began on October 15.

According to plant TS, the containment is not required to be operable to meet containment integrity requirements for Modes 5, 6, and "No Mode," but is required to perform the key pressure retaining safety function of containment closure. Because the containment liner was intact and functional until October 15, 2009, when the liner was opened, the containment was able to perform this function.

Based on the above time-line, and plant technical specifications, all activities associated with the work on the steam generator construction opening related to the delamination were conducted either when containment operability was not required or when all fuel had been transferred to the spent fuel pool. The inspectors determined that the delamination did not represent an increase in risk to the public.

No findings of significance were identified.

8.0 Generic Issues

The SIT did not identify immediate generic safety concerns.

The CR3 containment wall delamination was an unprecedented event. The SIT determined that some aspects of the issue may warrant consideration for further industry review and information sharing.

Some of the contributing causes (such as high radial tension without radial reinforcement, stress concentrations around the tendon sleeves, etc.) may be inherent in the containment designs of many post-tensioned plants, and therefore, licensees should be aware of the potential adverse effects of these conditions when evaluating potential containment modifications that involve detensioning of tendons. From the licensee's root cause analysis, it appears that standard industry analysis tools typically used for predicting radial tension may be limited in their ability to predict the potential for delamination failures for major modification activities, such as the creation of SGR construction openings that involve detensioning of tendons.

As contributing causes to the CR3 delamination event, the root cause analysis identified high radial tensile stresses in the delamination plane of the hoop tendons and peak tensile

stress concentrations around the hoop tendons sleeves. These high tensile stresses could initiate one or more small localized cracks around the hoop tendon sleeves during original tensioning (or subsequent retensioning, if performed) which then become potential sites for delamination initiation and propagation under additional drivers such as detensioning during later modification activities. The licensee's root cause analysis acknowledges that the prestressing force in the vertical tendons contributes to causing radial tensile stress and stress concentrations in the vertical plane of the hoop tendons, in addition to prestressing from the hoop tendons. The inspectors noted that this finding maybe a departure from a common belief that radial tension in the plane of the hoop tendons is caused by the prestressing force in the hoop tendons only. Typical industry calculations only consider radial tensile stresses caused by prestressing from the hoop tendons.

It appears that the contribution from the vertical tendons in producing radial tensile stress may be significant and possibly even more significant than the contribution from hoop tendons. Although the PII computer simulation included the combined effect of all conditions in producing radial tension that causes delamination, it did not provide a quantitative assessment of the relative contribution and significance of individual factors (primarily the prestressing force in hoop tendons and vertical tendons) in producing the high radial tensile stresses, which are potential local crack initiators. This issue may warrant further review to understand the role and relative significance of prestress in vertical tendons in causing local tensile stress around tendon conduit and address its impact, if any, on design of post-tensioned containments. Exploratory analytical research may be warranted to positively quantify the relative contributions and significance of the prestressing force in the vertical tendons and hoop tendons in producing radial tensile stresses and peak tensile stresses due to stress concentration effects, which could result in small local cracks at the tendon holes. This is important because the vertical tendons are typically tensioned before the hoop tendons. Any research in this area should also factor in the role of the bond between the tendon sleeves and adjacent concrete in producing tensile stress concentration effects.

Meetings, Including Exit

On September 2, 2010, the inspectors presented the inspection results to Mr. J. Franke and other members of the licensee staff in an exit meeting open for public observation at the Crystal River Nuclear Plant EOF/Training Center, 8200 West Venable Street, Crystal River, Florida.

SUPPLEMENTAL INFORMATION

KEY POINTS OF CONTACT

Licensee Personnel

B. Komara, National Inspection and Consultants (NIC)
Charles Williams, HNP Technical Services Superintendent
Craig Miller CR3 Lead Mechanical Engineer
Dennis Herrin CR3 Licensing
Don Dyksterhouse NPC Supervisor
Ed Avella CR3 Major Projects Manager
Emin Ortalan CR3 Design Engineering Supervisor
G. Pugh, Progress Energy
Garry Miller, Vice President, Progress Energy
Glenn Pugh CR3 Senior Civil/Structural Engineer
Howard Hill CR3 Contractor
J. Franke, Vice President, CR3
Joe Lese CR3 Lead Engineer
John Holliday CR3 Contractor
Martin Souther BNP Senior Engineer
Paul Fagan RNP Technical Services Superintendent
R. Pepin CR3 Mechanical Maintenance Superintendent
R. Portmann CR3 IWE/IWL Program Manager
R. Knott NPC Lead Engineer
R. Tyrie CR3 Operations Supervisor
S. Cahill, Engineering Manager, CR3
W. Rogers HNP Senior Engineer
W. Worthington CES Lead Engineer

LIST OF ITEMS OPENED, CLOSED, AND DISCUSSED

None

Sequence of Events Time Line

Plant Operations

9/25/2009 7:03:00 p.m., commenced power reduction for R16 planned outage per OP-209A.

9/26/2009 12:29:00 a.m., CR3 is in Mode 2.

9/26/2009 12:44:00 a.m., CR3 is in Mode 3.

9/26/2009 8:39:00 a.m., CR3 has entered Mode 4.

9/26/2009 4:51:00 p.m., CR3 has entered Mode 5.

9/26/2009 4:58:00 p.m., authorized to commence tendon work activities.

10/1/2009 5:44:31 p.m., Crystal River Unit 3 is in Mode 6.

Steam Generator Opening Activity Time Line

At approximately 5:00 p.m. on September 26, 2009, following entry into Mode 5, the tendon crews began detensioning and removing the tendons in the area of the construction opening. Vertical tendons 34V12 and 34V13 were detensioned first. These tendons were detensioned prior to cutting the button heads in case they needed to be reused. The button heads on the remaining tendons were plasma cut under full tension. Following 34V12 and 34V13, the crews started on vertical tendon 34V8 and progressed to 34V17 while simultaneously detensioning horizontal tendons 42H27 and 53H27 through 42H34 and 53H35. The horizontal tendons were detensioned from the bottom to the top. The detensioning and tendon removal was completed on October 1, 2009.

On September 30, 2009, the hydro-excavation crew performed a test demonstration on an 8 feet wide by 6 feet high area in the lower right corner of the construction opening. The depth of the concrete removal generally varied from 4-1/2 inches to 8 inches, and exposed some horizontal and vertical tendon sleeves.

Full scale hydro-excavation commenced at approximately 4:30 a.m. on October 1, 2009 and removed the outer layer of concrete down to the rebar by 1:00 p.m. that afternoon. Hydro-excavation restarted at about 4:00 a.m. on October 2, 2009, following removal of the rebar, but was stopped an hour later due to obstructions in the debris chute that caused water to spill onto the berm. During this period of hydro-excavation operation, workers identified a stream of water flowing from a crack below and to the right of the construction opening. A subsequent inspection of the construction opening revealed the presence of the separation (delamination).

LIST OF DOCUMENTS REVIEWED

GAI Report No. 1930, Crystal River Unit 3 Nuclear Generating Plant Reactor Containment Building Structural Integrity Test, dated December 7, 1976.

Crystal River Unit 3 Nuclear Power Plant Reactor Containment Building Integrated Leakage Rate Test Report, dated June 30, 1980

Crystal River Unit 3 Nuclear Power Plant Reactor Containment Building Integrated Leakage Rate Test Report, dated July 11, 1983

Crystal River Unit 3 Nuclear Power Plant Reactor Containment Building Integrated Leakage Rate Test Report, dated November 15, 1987

Crystal River Unit 3 Nuclear Power Plant Reactor Containment Building Integrated Leakage Rate Test Report, dated November 7, 1991

Progress Energy Crystal River Unit 3 Plant Operating Manual SP-178 Containment Leakage Test – Type “A” including Liner Plate. Revision 29C (used for 2005 ILRT)

Florida Power Letter 3F0301-05 to NRC, dated March 7, 2001; License Amendment Request #267, Revision 0; Revision to Improved Technical Specification 5.6.2.20, "Containment Leakage Rate Testing Program"

NRC Letter to Florida Power responding to Florida Power Letter 3F0301-05, issuing Amendment No. 197 to Facility Operating License No. DPR-72 for Crystal River Unit 3.

Analysis/Calculation S09-0045, Integrity Evaluation of Cracked Containment Shell for LODHR (Loss of Decay Heat Removal), Revision 0, dated October 6, 2009

Progress Energy Crystal River Unit 3 Plant Operating Manual SP-178 Containment Leakage Test – Type “A” including Liner Plate. Revision 30

Licensee Event Report (LER) 97-014, Report Date: July 11, 1997

Final Safety Analysis Report, Revision 31.3, Section 5.6.3, Initial Integrated Leak Rate Test.

Final Safety Analysis Report, Revision 31.3, Section 5.6.4, Operational Leak Rate Tests.

NAP-02, Preparation and Control of CR3 Site Specific Special Process Specifications and Guidelines

SP-182, Reactor Building Structural Integrity Tendon Surveillance Program

NDEP-0620, VT-1 and VT-3 Visual Examination of ASME Section XI, Subsection IWE Components of Nuclear Power Plants

NDEP-A, Nuclear NDE Program and Personnel Process

Work Order 1636782-03

Work Order 681043-08

Work Order 321405-01

Work Order 1686388

Final Report for the 30th Year Containment IWL Inspection, Dated 02/04/2009

AR 368389

NAP-02, Preparation and Control of CR3 Site Specific Special Process Specifications and Guidelines

SP-182, Reactor Building Structural Integrity Tendon Surveillance Program

NDEP-0620, VT-1 and VT-3 Visual Examination of ASME Section XI, Subsection IWE Components of Nuclear Power Plants

NDEP-A, Nuclear NDE Program and Personnel Process

Work Order 681043-08

Work Order 321405-01

Final Report for the 30th Year Containment IWL Inspection, Dated 02/04/2009

AR 370875

Calculation S10-0002, Revision 0; Finite Element Model Description

Calculation S10-0032, Revision 0; Containment Repair Project – Limiting Load Cases

Calculation S10-0014, Revision 0; Containment Repair Project - Finite Element Model Benchmarking

Calculation S10-0040, Revision 0; Containment Repair Project – Comparison of ANSYS Results to Kalinin's SIT Calculation and SIT measurements

Calculation S10-0012, Revision 1; Containment Repair Project – Stresses Around the SGR Opening due to Design Basis Load Cases

Calculation S10-0015, Revision 0; Containment Repair Project – Refined Containment Finite Element Model Evaluation

Calculation S10-0021, Revision 4; Containment Repair Project – Concrete Radial Reinforcement (Grouted Reinforcement Option)

Calculation S10-0030, Revision 0; Containment Repair Project – Reinforcement Design for Delaminated Containment Wall

Significant Adverse Condition Investigation Report, Action Request Number 358724 (Attachment 1) for Event Date 10/2/09, Revision 0 approved by PNSC on June 7, 2010. Attachment 1 of this is the report “Root Cause Assessment – Crystal River Unit 3 Containment Concrete Delamination,” dated June 7, 2010, by Performance Improvement International

Engineering Change Package EC 75218, “Reactor Building Delamination Repair Phase 2 – Detensioning Tendons,” Attachment Z40R2 - PII Evaluation of Detensioning Plan and Concrete Removal which includes Margin to Delamination Analysis of Proposed CR3 Detensioning Sequence Option 10F.

Crystal River Unit 3 Nuclear Generating Station, Reactor Building Dome Delamination Final Report, December 10, 1976, Prepared for Florida Power Corporation by Gilbert/Commonwealth Associates Inc., Reading, PA.

Progress Energy Nuclear Generation Group Standard Procedure CAP-NGGC-0205, Significant Adverse Conditions Investigations and Adverse Condition Investigations – Increased Rigor, Revision 11.

Progress Energy Nuclear Generation Group Standard Procedure CAP-NGGC-0200, Corrective Action Program, Revision 28.

Progress Energy CTL Group Project No. 059169, Nondestructive Evaluation of Delamination in a Containment Wall Structure, Crystal River Nuclear Plant Unit 3, January 22, 2010, Submitted by CTL Group, Skokie, IL

Calculation S09-0054, Rev. 0, Containment Repair Project – Radial Pressure at Hoop Tendons

Acharya, S., and Menon, D., Prediction of radial stresses due to prestressing in PSC shells, Nuclear Engineering and Design 225 (2003) 109-125, Elsevier.

LIST OF ACRONYMS USED

ACI	American Concrete Institute
AREVA	AREVA NP (formerly Framatome ANP) a supplier of nuclear services
ASME	American Society of Mechanical Engineers
ASTM	American Society for Testing Materials
CAP	Corrective Action Program
CAPR	Corrective Action to Prevent Recurrence
CFR	Code of Federal Regulations
CLB	Current Licensing Basis
CR3	Crystal River Unit 3
EC	Engineering Change
EFPY	Effective Full Power Years
EI	Elevation
EPRI	Electric Power Research Institute
FM	Failure Mode
FSAR	Final Safety Analysis Report
Ft	foot (feet)
ILRT	Integrated Leak Rate Test
INPO	Institute of Nuclear Power Operations
IP	Inspection Procedure
IR	Impulse Response
ISI	Inservice Inspection
LERF	Large Early Release Frequency
LLRT	Local Leak Rate Test
LR	License Renewal
NCR	Nuclear Condition Report
NDE	Non-Destructive Examination
NDT	Non-Destructive Testing
NEI	Nuclear Energy Institute
NRC	Nuclear Regulatory Commission
NUREG	Publications Prepared By The NRC Staff
OE	Operating Experience
PdM	Predictive Maintenance
PE	Progress Energy
PII	Performance Improvement International
PNSC	Plant Nuclear Safety Committee
Psi	pounds per square inch
PWR	Pressurized Water Reactor
QC	Quality Control
QRB	Quality Review Board
RAI	Request for Additional Information
RCE	Root Cause Evaluation
RCPB	Reactor Coolant Pressure Boundary
RCS	Reactor Coolant System
RFO	Refueling Outage
SGR	Steam Generator Replacement
SIT	Special Inspection Team and Structural Integrity Test
UT	Ultrasonic Examination
VT	Visual Examination
WO	Work Order

October 13, 2009

MEMORANDUM TO: Louis F. Lake, Team Leader
Special Inspection

FROM: Luis A. Reyes **/RA/**
Regional Administrator

SUBJECT: SPECIAL INSPECTION CHARTER TO EVALUATE CRYSTAL
RIVER CONTAINMENT BUILDING

You have been selected to lead a Special Inspection to assess the circumstances associated with a delamination discovered in the concrete of the containment building at Crystal River Unit 3. Your onsite inspection should begin on October 13, 2009. Robert Carrion, Senior Reactor Inspector, George Thomas of NRR, Anthony Masters, Senior Construction Inspector, and an independent Structural Engineering Contractor (TBD) will assist you in this inspection.

A. Basis

Recently, the plant was shut down for a planned refueling outage as well as to replace the steam generators inside containment. In order to move the steam generators into containment, workers began removing concrete to create the necessary opening. During that work, a small gap was found while making approximately a 25 foot x 25 foot concrete cut (liner is still intact). The gap is about one half inch wide and 10 inches inward from the outside edge of the concrete and located just at the layer of horizontal tendons. The Crystal River containment is about 42 inches thick, contains both horizontal and vertical tensioned steel tendons, and is lined with steel plate.

The licensee is evaluating the extent of the condition. The discovery of this gap in the concrete does not represent an immediate safety concern because the plant is shut down.

In accordance with Management Directive 8.3, "NRC Incident Investigation Program," deterministic and conditional risk criteria were used to evaluate the level of NRC response for this event.

Based on the deterministic criteria that this issue involved possible adverse generic implications, the event was evaluated for risk in accordance with Management Directive 8.3. Due to lack of information on the structural integrity of the concrete containment and how it would interact with the free-standing steel liner during a seismic event in its current condition, a risk analysis was not able to be performed at this time. However, if

CONTACT: Mark Franke, RII/DRS
404-562-6349

the concrete containment reacted adversely with the free-standing steel liner during a seismic event, LERF would be adversely affected and a Special Inspection would be warranted. Therefore, Region II has determined that the appropriate level of NRC response is to conduct a Special Inspection.

B. Scope

The inspection is expected to perform data gathering and fact-finding in order to address the following:

1. Develop a complete description of the problems and circumstances surrounding the gap in the containment building.
2. Verify that the licensee has appropriately evaluated Operability and Reportability.
3. Review structural integrity testing data of the containment.
4. Assess the adequacy of the licensee's maintenance and inspection programs related to this event.
5. Assess the licensee's activities related to the problem investigation (e.g., root cause analysis, extent of condition, etc).
6. Assess the licensee's corrective action/"fix" in addressing the containment delamination issue.
7. Collect data necessary to develop and assess the safety significance of any findings in accordance with IMC 0609, "Significance Determination Process."
8. Determine potential generic issues or any design and construction inadequacies and make recommendations for appropriate follow-up actions (e.g., Information Notices, Generic Letters, and Bulletins).

C. Guidance

Inspection Procedure 93812, "Special Inspection," provides additional guidance to be used during the conduct of the Special Inspection. Your duties will be as described in Inspection Procedure 93812. The inspection should emphasize fact-finding in its review of the circumstances surrounding the event. Safety or security concerns identified that are not directly related to the event should be reported to the Region II office for appropriate action.

Your team will report to the site, conduct an entrance, and begin inspection no later than October 13, 2009. In accordance with IP 93812, you should promptly recommend a change in inspection scope or escalation if information indicates that the assumptions utilized in the MD 8.3 risk analysis were not accurate. A report documenting the results of the inspection should be issued within 45 days of the completion of the inspection. A copy of the inspection report shall be forwarded to the Crystal River Unit 3 License Renewal Inspection Team. The report should address all applicable areas specified in Section 3.02 of Inspection Procedure 93812. At the completion of the inspection, you should provide recommendations for improving the Reactor Oversight Process baseline

inspection procedures and the Special Inspection process based on any lessons learned.

This charter may be modified should you develop significant new information that warrants review. Should you have any question concerning this charter, contact Mark Franke at (404) 562-6349.

Docket No.: 50-302
License No.: DPR-72

References:

Inspection Procedure 93812, Special Inspection
Management Directive 8.3, NRC Incident Investigation Program
Inspection Manual Chapter 0609, Significance Determination Process
Inspection Manual Chapter 0612, Power Reactor Inspection Reports

cc: R. Borchardt, EDO
B. Mallett, DEDR
L. Reyes, RII
V. McCree, RII
J. Munday, RII
M. Sykes, RII
L. Wert, RII
T. Boyce, NRR
F. Saba, NRR
K. Kennedy, RII
H. Christensen, RII
S. Ninh, RII
C. Fletcher, RII
M. Franke, RII
M. Khanna, NRR

PROGRESS ENERGY ROOT CAUSE REPORT

INSERT ROOT CAUSE REPORT



Performance Improvement International

ROOT CAUSE ASSESSMENT CRYSTAL RIVER UNIT 3 CONTAINMENT CONCRETE DELAMINATION



August 10, 2010

NON-PROPRIETARY VERSION

This report is a Root Cause Assessment (RCA) of the Crystal River Unit 3 containment concrete delamination identified on October 2, 2009. The assessment was performed by Performance Improvement International (PII) at the request of Progress Energy.

Chong Chiu, PhD, Team Leader
Marci Cooper, Assistant Team Leader
Patrick Berbon, PhD, Assistant Team Leader
Ray Waldo, PhD, Assistant Team Leader
Avi Mor, Dr. Eng.
Joe Amon, PE
Henric Larsson
Tyson Gustus
David Brevig
Gary Hughes, PhD
Mostafa S. Mostafa, PhD
David Dearth, PE
Jan Cervenka, PhD
Doug Marx
Luke Snell, PhD

Note: The information in this report should not be used as “design basis input” for any design basis analyses unless the specific information has been validated to have been obtained under an approved 10CFR50 Appendix B program.



INTRODUCTION

Issue:

Progress Energy Florida's (PEF) Crystal River Unit 3 (CR3) nuclear power plant discovered a delamination in one section of the reactor containment structure wall during the process of cutting a temporary opening in the containment to be used to replace the steam generators. PEF subsequently engaged Performance Improvement International (PII) to perform a comprehensive root cause assessment to identify the cause or causes of the delamination. This report provides the results of PII's root cause assessment both for the technical cause of the concrete delamination and for the Organizational and Programmatic (O&P) aspects of the project.

Report Structure:

This report is intended to be a single point reference document that includes the detailed information needed to understand the circumstances and conclusions associated with the containment wall delamination at CR3. The report has a pyramidal structure. The Executive Summary provides detailed summary and overall conclusions. [Section 1](#) provides a brief description of CR3 and the delamination event. The first step in the analysis process is to identify potential Failure Modes (FMs) to determine the overall scope of the issues to be investigated. A total of 75 potential FMs in nine general groups were identified to encompass the scope of possible contributors to the delamination event. This report provides a discussion of the eight confirmed failure modes grouped by topic area. [Sections 2](#) through [6](#) discuss the failure mode process and the individual Failure Modes that contributed to the delamination. The nature of the FMs is that they cover all aspects of the event so that a review of each FM correlates from issue to issue. The contributing FMs are organized into a failure mode timeline in [Section 7](#). This method of presentation assembles the contributors into a chronological analysis of the interactions and individual factors that created the conditions for the delamination to occur. Next, the computer simulations are presented which provides a visual display of the actual circumstances that led to the delamination. [Section 8](#) discusses the root cause of the event. [Section 9](#) provides recommendations to prevent recurrence of the issue. [Section 10](#) provides the O&P evaluation. [Attachment 1](#) provides a detailed discussion of the computer models used. [Attachment 2](#) describes the benchmarking done to validate the computer modeling results. The individual failure mode assessments are provided in [Attachment 6](#).

Note: All TOC elements are clickable links. Additional links to referenced locations can be found throughout the document.



EXECUTIVE SUMMARY

Through a complex process which involved deductive investigation of data and information that was available to PII after the delamination event at CR3, PII was able to create a state-of-the-art computer model. This model allowed PII to start with information now known about how the CR3 containment structure behaves and work backwards in time to determine what factors contributed to the delamination event. Using this process, PII has identified seven discrete factors that, working in conjunction, caused the delamination. These factors are: (1) tendon stresses; (2) radial stresses; (3) design for stress concentration factors; (4) concrete strength properties; (5) aggregates; (6) de-tensioning sequence and scope; and (7) removing concrete.

Considered alone, none of these individual contributing factors would have led to a delamination. For example, the type of concrete and aggregates used at CR3, while a contributing collective cause, would not alone have caused a delamination without the combined interplay of the other contributing factors acting in concert while the containment structure was being de-tensioned and while the Steam Generator Replacement (SGR) opening was created. Thus, it is important to understand both the specifics of each contributing factor as well as how all of those factors worked together.

Of particular importance in this analysis is that typical industry containment structure analysis tools have consistently shown large margins for stress tolerance when creating containment openings in other similar projects by using average tensile stress values. Other projects have typically included de-tensioning tendons around the containment opening so that the containment structure was in a state to accept replacement concrete after the major equipment movements in and out of containment were complete. PII's computer model, however, has shown that the CR3 containment structure had a lower margin of tolerance to cracking than other plants which have used common industry calculations. PII further determined that the de-tensioning of more tendons immediately around the containment opening in CR3 may have exacerbated the delamination event, a result that would not have been apparent from experiences with other Steam Generator Replacement (SGR) projects. Both of these examples demonstrate the complexity and the unique nature of PII's investigation into delamination.

PII has determined that the delamination did not exist prior to the work to create the containment opening by the SGR. Rather, the delamination appears to have been caused by the combination and interplay of (1) certain design features of the CR3 containment structure; (2) the type of concrete used in the CR3 containment structure; and (3) the acts of de-tensioning and cutting the containment structure. Through a state-of-the-art computer model that PII developed CR3 specific information, available to PII after the delamination had taken place, PII was able to determine that none of the individual contributing factors to the delamination, on its own, would have caused a delamination. Rather, the complex interplay between all the contributing causes led to the delamination as discussed in detail in this report.

In conclusion, PII has determined that the immediate cause of the delamination event was the redistribution of stresses as a result of the containment opening activities resulting in additional stress beyond original containment design. The condition exceeded the fracture capacity of the concrete and resulted in cracking along the high stress plane connecting the horizontal tendons. As the cracks propagated and joined, delamination occurred over a wide area. Evaluation of the contributing failure modes identified only one practical root cause subject to control and that was inadequate scope/sequence of tendon de-tensioning used in the SGR outage. The O&P

NON-PROPRIETARY VERSION

evaluation concluded that the inability of industry accepted tools to predict delamination was the programmatic root cause of the event. PII found that six methodology improvements were needed to accurately analyze the containment response.



TABLE OF CONTENTS

Note: All TOC elements are clickable links. Additional links to referenced locations can be found throughout the document.

INTRODUCTION	3
EXECUTIVE SUMMARY	4
1. PLANT DESCRIPTION AND HISTORY	8
GENERAL DESIGN:	8
PREVIOUS INDUSTRY OPERATING EXPERIENCE:	8
STEAM GENERATOR REPLACEMENT OUTAGE EVENT CHRONOLOGY:	8
2. FAILURE MODE PROCESS	144
INTRODUCTION:	14
3. GROUP 1: CONTAINMENT DESIGN	166
CONFIRMED FAILURE MODES:	166
SUMMARY:	166
DISCUSSION:	16
4. GROUP 2: CONCRETE CONSTRUCTION	26
CONFIRMED FAILURE MODES:	26
DISCUSSION:	26
5. GROUP 3: USE OF MATERIALS	277
CONFIRMED FAILURE MODES:	27
DISCUSSION:	27
6. GROUP 7: SGR ACTIVITIES	288
CONFIRMED FAILURE MODES:	28
DISCUSSION:	28
7. FAILURE MODE TIMELINE	30
SEQUENCE OF STEPS:	31
DETAILED COMPUTER SIMULATION:	31
WHOLE CONTAINMENT RADIAL DISPLACEMENT SIMULATION:	32
DETAILED LOCAL WALL RADIAL DISPLACEMENT RESPONSE:	39
SHEET DELAMINATION:	59
SCENARIO VALIDATION:	60
8. ROOT CAUSE AND CONTRIBUTING CAUSES	62
SUMMARY CONCLUSIONS:	62
FAILURE MODE EVALUATION:	62
FREQUENTLY ASKED QUESTIONS:	64
9. RECOMMENDATIONS TO PREVENT RECURRENCE	67
CORRECTIVE ACTIONS TO PREVENT RECURRENCE	67
A. RE-TENSIONING CONTAINMENT IN R 16	67
B. CAPTURING THE OPERATING EXPERIENCE	67
BETTERMENT ACTIONS	67

NON-PROPRIETARY VERSION

C. LIFE EXTENSION	67
D. DIFFERENTIAL AGING CHARACTERISTICS	68
10. ORGANIZATIONAL AND PROGRAMMATIC ROOT CAUSE	70
11. REFERENCES	73
ATTACHMENT 1: COMPUTER MODELING	74
ATTACHMENT 2: FLEXING OF CONTAINMENT WALLS	84
PURPOSE:	84
EXPECTED BUILDING RESPONSE:	84
CONCLUSION:	96
COMPARISON OF LASER SCANNING AND COMPUTER MODEL SIMULATION	92
ATTACHMENT 3: CONTAINMENT WALL INTERNAL RESPONSE	978
ATTACHMENT 4: SGR OPENING SEQUENCE	989
EVENT CHRONOLOGY:	989
ATTACHMENT 5: REVIEWER TABLE AND RESUMES	105
FAILURE MODE AUTHOR AND REVIEWER LIST:	1055
RESUMES OF PII PARTICIPANTS:	1077
ATTACHMENT 6: CONFIRMED AND REFUTED FAILURE MODE ASSESSMENTS	1478
1. CONTAINMENT DESIGN AND ANALYSIS	1478
2. CONCRETE CONSTRUCTION	147
3. USE OF CONCRETE MATERIALS	147
4. CONCRETE SHRINKAGE, CREEP, AND SETTLEMENT	148
5. CHEMICALLY OR ENVIRONMENTALLY INDUCED DISTRESS	148
6. CONCRETE-TENDON-LINER INTERACTIONS (DURING OPERATION)	1489
7. CONTAINMENT CUTTING	148
8. OPERATIONAL EVENTS	148
9. EXTERNAL EVENTS	1499



1. PLANT DESCRIPTION AND HISTORY

This discussion is limited to a brief summary of the plant and its history to ensure the reader understands the general flow of events. Detailed discussions of specific plant data are delayed until they are addressed in the analysis of each applicable topic.

General Design:

Prior to the current outage, Crystal River 3 was a 2609 thermal megawatt Babcock and Wilcox pressurized water reactor located in Crystal River, Florida. Gilbert Associates was the architect engineer for the plant. The plant went online for the first time on 3/13/1977.

Construction of the CR3 containment wall was completed in 1973. The dome concrete was placed from February to July, 1974. Post tensioning was completed in early 1975. The nominal inner radius is 65'-0" and thickness of 42". Horizontal tendons are arranged in pairs that are located at 39" intervals. Each tendon is housed in a 5.25" diameter conduit. The inner containment surface has an integral 3/8" steel liner. The containment building is generally a right circular cylinder but it contains six buttresses with six bays that form the containment walls between the buttresses.

Previous Industry Operating Experience:

In April, 1976, workmen identified a delamination of the concrete on the dome of CR3. The delaminated concrete was removed and additional radial reinforcing was grouted into the remaining 24" thickness of concrete. New concrete was placed, reinforced with meridional and hoop steel, and a nominal thickness of 12" new concrete was placed. The event investigation concluded, "...that radial stresses combined with biaxial compression to initiate laminar cracking in a concrete having lower than normal direct tensile capacity and limited crack arresting capability".

Prior to the CR3 dome delamination, on 6/17/70 Turkey Point Unit 3 also identified delamination of their containment dome during post tensioning after 2/3 of the tendons had been tensioned. This occurred three months after the last concrete was placed.

Additionally containment dome delamination occurred during construction of the Kaiga Atomic Power Project Unit 1 in 1994. The event occurred during the post-tensioning process after 1/3 of the tendons had been tensioned. It was accompanied by a collapse of the inner surface of the dome (Reference 6).

Steam Generator Replacement Outage Event Chronology:

On 9/26/09 the Crystal River steam generator replacement outage began. This included the creation of an access opening in the containment wall. The construction opening was a 27' by 25' rectangle running from elevation 183' to 210'. The centerline of the opening was coincident with the centerline of panel 34. Tendon cutting began on 9/26/09. The first two tendons (V12 and V13) were hydraulically de-tensioned. The remaining 25 tendons were de-tensioned by flame cutting under full tension (FM 7.6 evaluates this practice). A demonstration of hydro-lasing was conducted on 9/30/09. The final tendon was de-tensioned on 10/1/2009. Detailed information is available in Attachment 4. Figure 1.1 below shows the area of interest.



Figure 1.1 Photograph of the steam generator opening worksite.
Note the newly constructed rectangular opening above the existing circular equipment hatch.

The pictures of cracks between horizontal tendons taken on 9/30/09, the day before the final two tendons were de-tensioned, and before any significant concrete removal, provide a rough estimate for the onset of cracking in the Failure Mode Timeline.

On 10/2/09 plant personnel identified a delamination of the concrete about 10 inches into the 42 inch thick concrete containment wall in the plane of the horizontal tendon conduits. Shortly thereafter, process water was noted seeping out of the concrete about 20 feet away from the hydro-lasing work area (Figure 1.2). The appearance of water is the most compelling evidence that the delamination occurred during the last stages of the de-tensioning rather than as a result of concrete removal. For water to travel a significant distance inside the wall there must have been an extensive network of delamination which provided an estimate for its onset in the Failure Mode Timeline. Action Request (AR) 358724 was opened to address this event.



Figure 1.2 Photograph of water leakage from the containment wall (10/3/2009).

Figure 1.3 shows the extent of delamination visible on the edge surfaces of the SGR construction opening. Figure 1.4 is a sketch identifying the most important features of the containment wall construction.

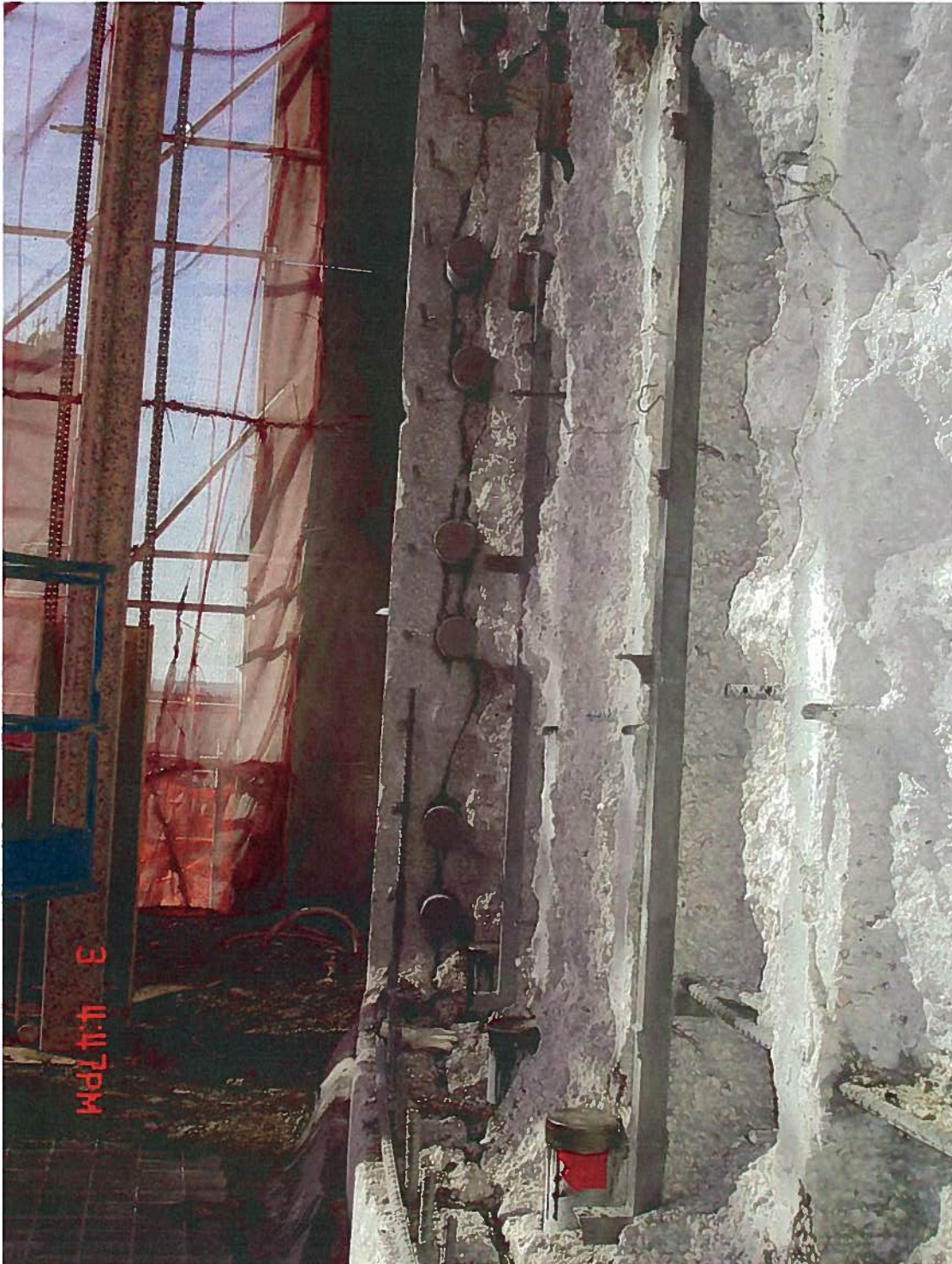


Figure 1.3 Photograph of delamination crack running from horizontal tendon to horizontal tendon, parallel to the wall surface, approximately 10 inches deep. (Photo taken after partial concrete demolition)

NON-PROPRIETARY VERSION

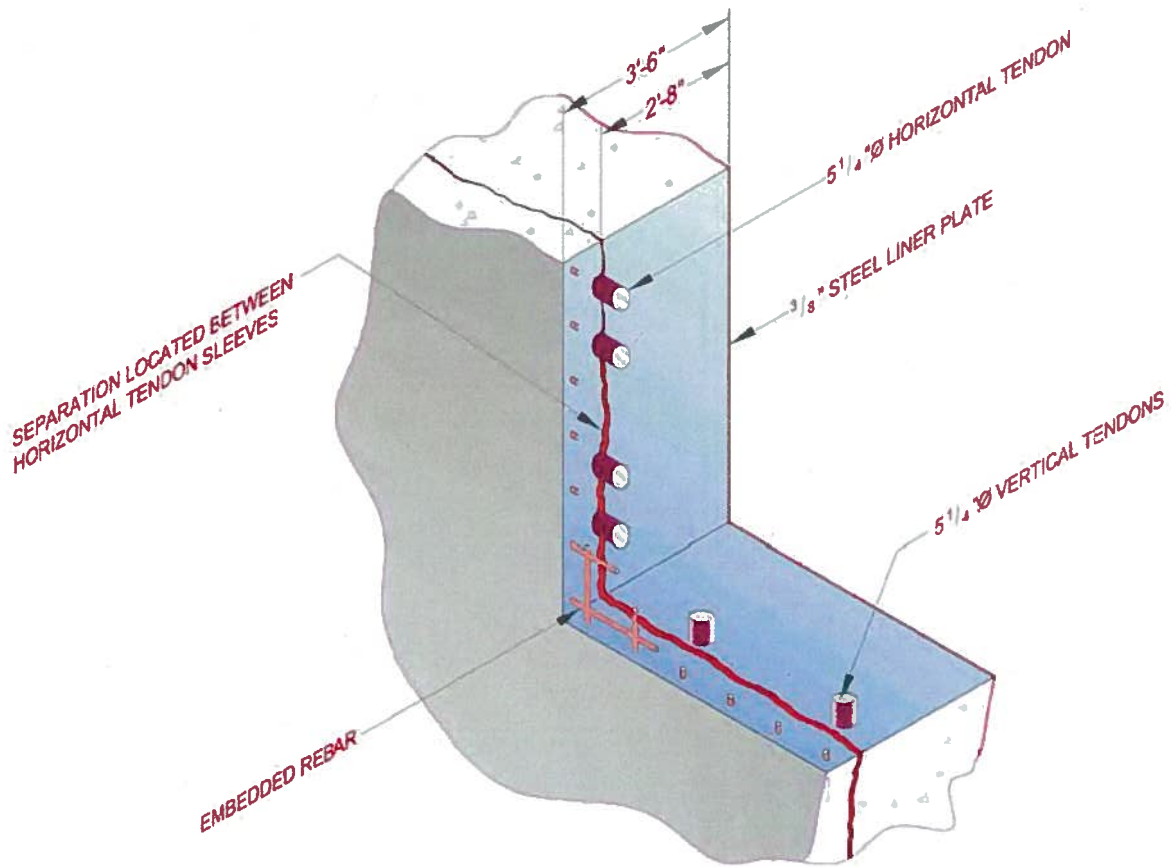


Figure 1.4 Sketch of the delamination cracking in the bay 34 wall.

With identification of the delamination, a detailed extent of condition assessment plan was developed. Impulse Response inspections and core drills have been performed at many locations around the containment with a good correlation between the two techniques. Delamination was only found in bay RBCN-0015 (containing the equipment hatch and steam generator replacement opening), also known as bay 34 because it lies between buttresses 3 and 4. Figure 1.5 shows a map of all six containment bays.

During the investigation and repair process other items were identified. Action Request (AR) 00359670 documents a surface separation in the containment concrete approximately 22 feet away from the SGR opening. AR 00368389 documents an isolated crack beneath the equipment hatch support area; however, this area was not impacted by the delamination event or its causes. AR 388332 identifies a crack in a core bore sample of the dome concrete at the interface of the original concrete and the concrete used to repair the dome delamination in 1976. The interface area was not impacted by the delamination event or its causes. Both of these isolated cracks are far removed from the area of high stress resulting from tendon de-tensioning, and they are physically separated from the delaminated concrete. The conditions were determined to be unrelated and will be dispositioned separately by the station.

NON-PROPRIETARY VERSION

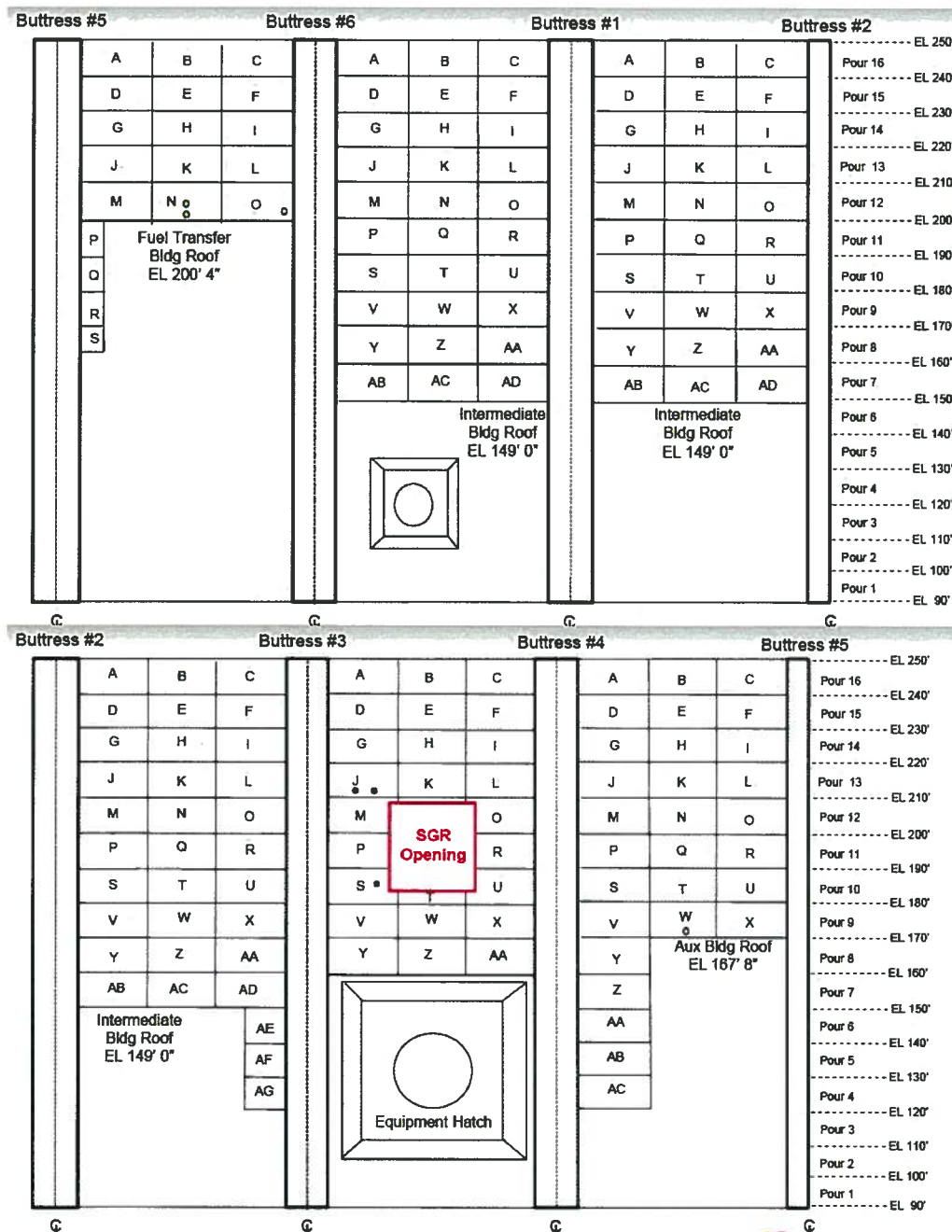


Figure 1.5 Sketch of the containment structure unfolded.

Figure 1.5 shows the details of each containment bay and the 10' by 20' panels in each bay.

Having discussed the history and plant conditions associated with Crystal River, Unit 3, the analysis then focused on the potential failure modes for the event.



2. FAILURE MODE PROCESS

Introduction:

At the start of the root cause evaluation, PII identified possible contributing factors and then systematically assessed the individual importance of each factor to the event. These possible contributors are called Failure Modes (FMs) and are organized into logical groupings. Each failure mode is investigated and the resulting conclusions are reviewed within PII, by the utility, and also by third party reviewers. A primary component in the analysis of each Failure Mode is the identification of information needed to either confirm or refute the Failure Mode as a contributor to the event. This information is then obtained and analyzed.

Nine groups containing 75 individual Failure Modes were identified as possible contributors for this event. The analysis sheets for each of the Failure Modes may be found in [Attachment 6](#). Of the 75 Failure Modes, 67 were refuted and did not contribute to this event, eight were confirmed as contributors. The eight Failure Modes that were not explicitly refuted are individually discussed in the next few sections of the report with one section for each group containing a confirmed Failure Mode. Attachment 6 of this report contains each of the 75 FMs evaluated. The entire Failure Mode file, including exhibits, is found in the appendices of this report.

Once the analysis of Failure Modes was complete, a Failure Modes Timeline was generated to identify when the issue arose and how it contributed to the event. This timeline is shown in [Figure 2.1](#).

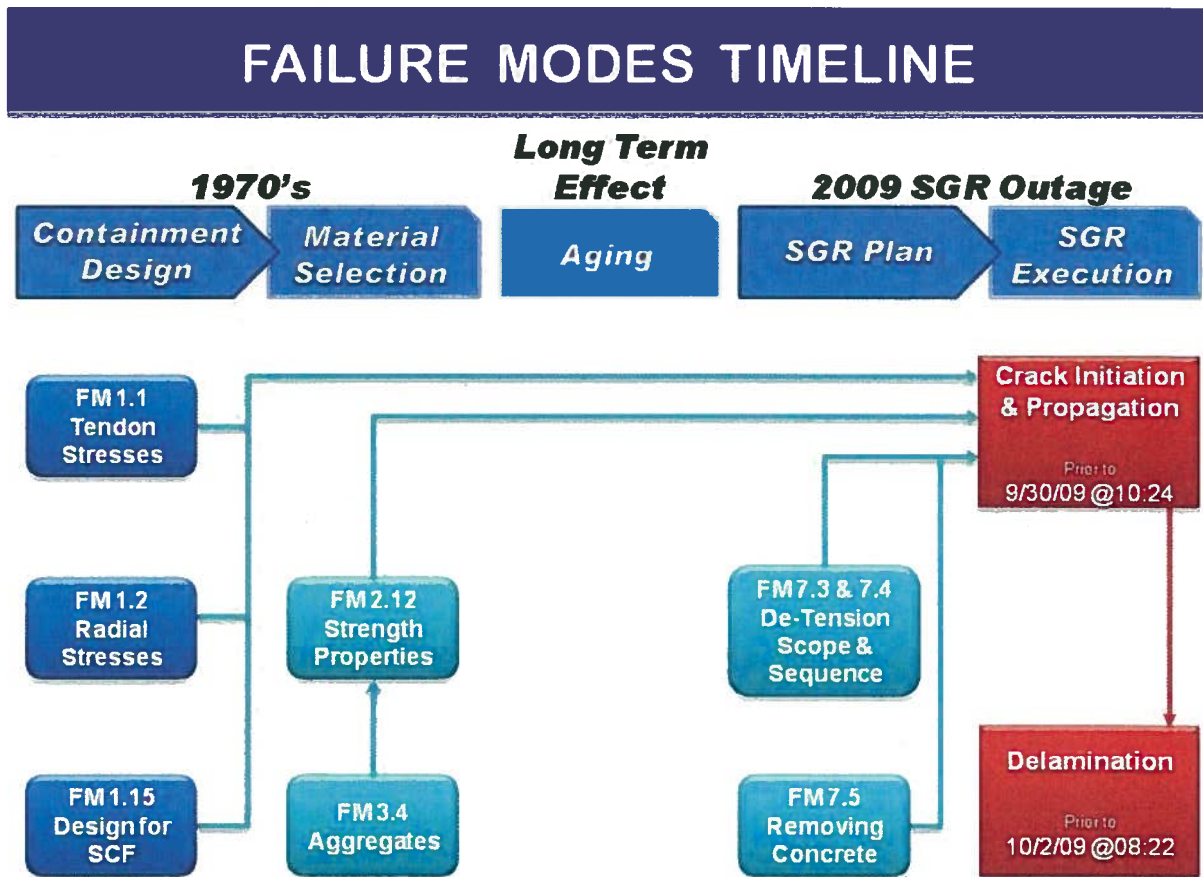


Figure 2.1 Failure Mode Timeline

The information in the next few sections will cover several topics related to the delamination event. The timeline in Figure 2.1 identifies how these topics converged to create the delamination. Section 7 provides a computer simulation of the delamination event. Section 8 integrates the individual elements and clarifies the overall process by which the root cause was determined.

The eight failure modes correlate with five time periods and topic categories.

- ◆ Original structure design from the 1970's
- ◆ Original material selection and construction in the 1970's
- ◆ Aging of materials from the 1970's to 2009
- ◆ Determination and execution of the de-tensioning scope and sequence in 2009
- ◆ Physical removal of concrete in 2009



3. GROUP 1: CONTAINMENT DESIGN

Confirmed Failure Modes:

- 1.1 Excessive vertical and hoop stress
- 1.2 Excessive radial tensile stresses/no radial reinforcement
- 1.15 Inadequate design analysis methods of radial tensile stresses (near sleeves, no radial reinforcement)

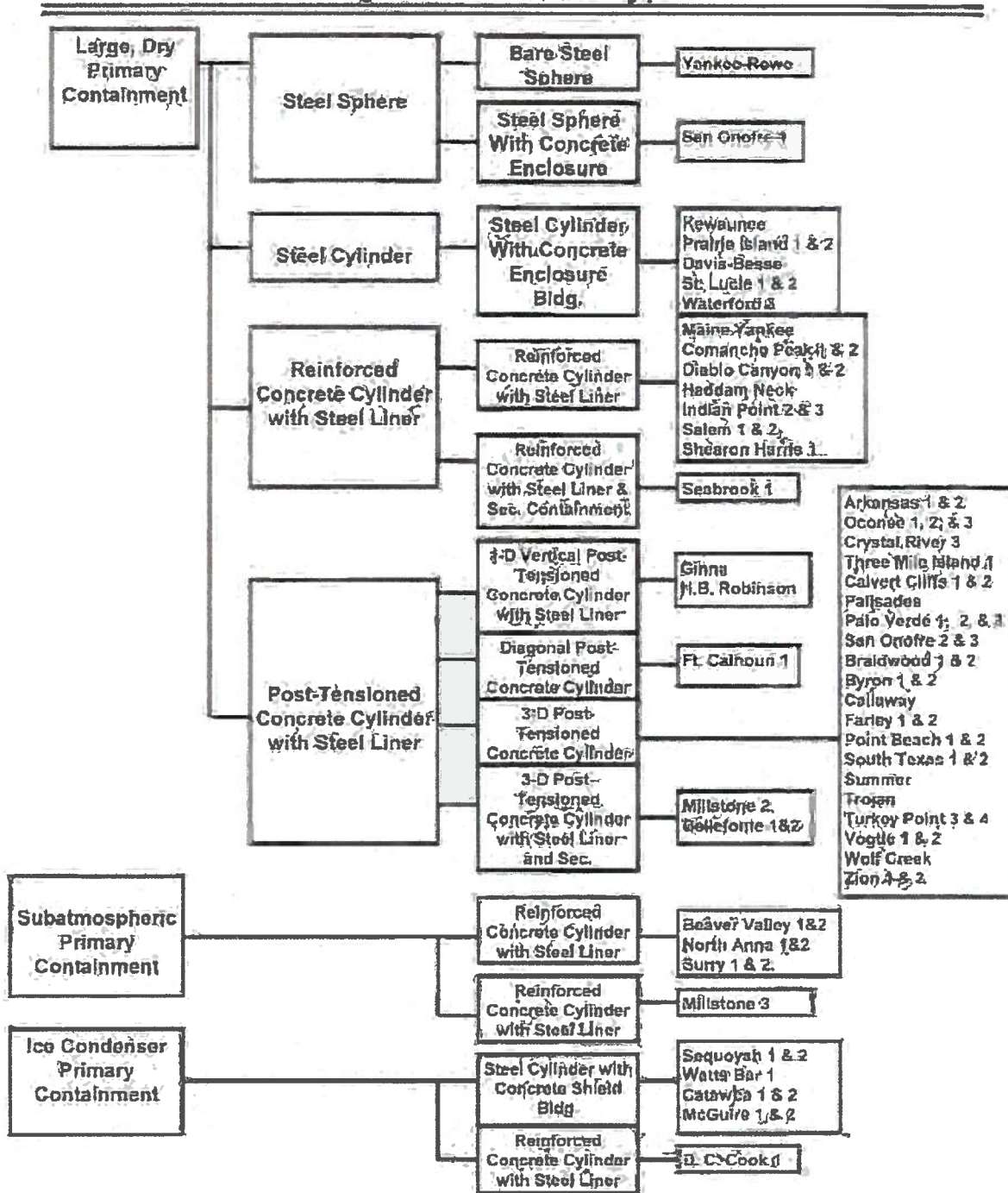
Summary:

FM 1.1 determines that CR3's containment design results in high vertical and hoop compression stresses and radial tensile stresses when compared to the designs of other plants. FM 1.15 determines that stress concentration factors (SCFs) were not explicitly considered in the original design of the containment building. FM 1.2 determines that radial stresses in the containment structure are high and that no radial reinforcement is currently in place. As with all the confirmed Failure Modes, the conclusions reached indicate that these issues did not individually cause the delamination, but rather contributed to the conditions that resulted in delamination.

Discussion:

Three Failure Modes in the design area related to vertical and hoop compression stresses, and radial tensile stresses contributed to the delamination of CR3. To evaluate the original design plan of CR3 and how it may have affected levels of stress, a comparison to seven other containment structures is made. CR3 is one of many containment buildings in service in the United States that uses post tensioned tendons to provide compression to the concrete structure. Figure 3.1 summarizes the various containment designs that have been built in the U.S.

PWR Containments in the United States by Construction Type



From US NRC PWR EAWL Real Riskmaking Package

Figure 3.1 The various containment designs in the U.S.

NON-PROPRIETARY VERSION

Within the post-tensioned category of containment buildings, there are several variations, one of which is the six buttress design used at Crystal River. A comparison group was selected from containment designs used in other plants comprised of seven units of the six buttress designs which have successfully undergone construction of an opening in the containment structure.

Within the comparison group are three tendon designs, the largest of which is the Crystal River design with 163 wires of 7 mm (0.276") diameter wire. One comparison plant has a design with 169 wires of ¼" diameter wire. The other 6 units have tendons with 90 wires of ¼" diameter wire. All units initially lock off their tendons to 70% guaranteed ultimate tensile strength. The importance of this design difference is that the larger the tendon cross section the higher the peak compressive stress on the concrete immediately in contact with the tendon sleeve. This directly translates into higher peak radial tensile stress at the vertical centerline of the hoop tendons.

Relative Individual Tendon Force	
Crystal River:	100%
Plant A*	85%
Plants B to G*	45%

* Nuclear plants A-G comprise a population of plants with a six buttress design most like CR3 which have successfully created containment construction openings.

The large diameter tendons have another impact as well. They are located at a depth of 10 inches from the outer containment wall with a set of tendons about every 39 inches. At that depth 27% of the cross-sectional area has the concrete displaced by tendon sleeves. The absence of concrete at this location increases the stress on the remaining concrete at exactly the location of the radial tensile stress at the top and bottom of each horizontal tendon sleeve. The nominal (average) radial stress in this location is 1.4 times what it would be without the displacement of the concrete by the tendon.

Figure 3.2 shows that there is no radial reinforcement provided beyond the horizontal tendons which results in the outermost 10 inches of concrete being radially un-reinforced while being subjected to tensile stresses.

NON-PROPRIETARY VERSION

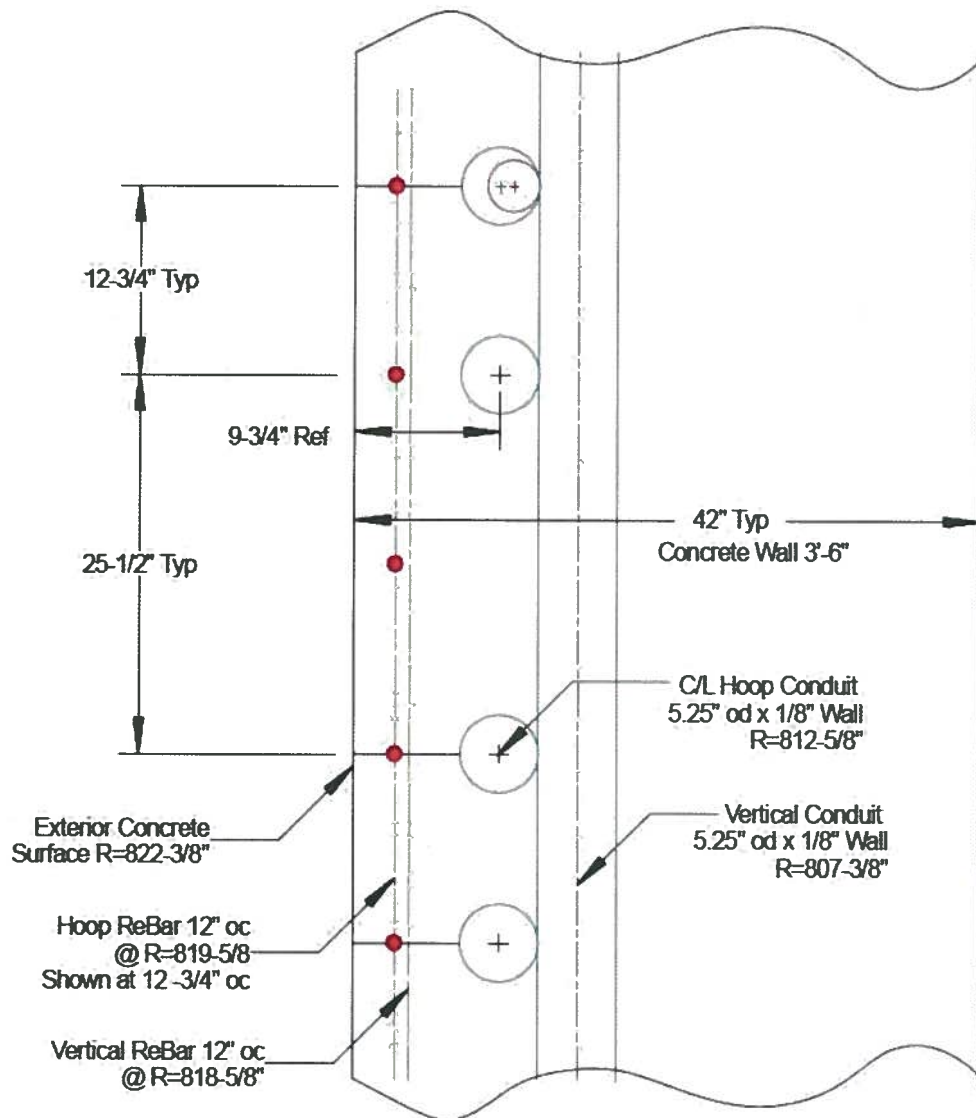


Figure 3.2 Layout of horizontal tendon sleeves in the CR3 containment wall (R is the containment inner radius in inches)

The following is a summary of the main design features of the containment wall.

The wall is 42 inches thick with a 3/8" steel liner on the inner surface. Approximately 10 inches into the concrete on the outside, the horizontal tendons (sleeve OD is 5.25 inches) each typically provides about 1400 kips of force (hoop tendon) to post-stress the concrete wall. Just inside the horizontal tendons are the vertical tendons.

There are a total of 94 horizontal tendons in the containment wall which covers one-third of the circumference for a total of 282 tendons. Each tendon has a near neighbor 13" away and a far neighbor on the other side 26" away. Each tendon has a length of 1/3 of the circumference of the containment from one buttress past one buttress to the next buttress. Buttress #1 is facing north and buttress #2 is at WNW 60 degrees counter-clockwise.

NON-PROPRIETARY VERSION

The remaining buttresses are numbered sequentially. Each of the six wall segments are located between two buttresses. Thus bay 34 lies between buttress 3 and buttress 4. Horizontal tendon 42H21 runs between buttress 4 and buttress 2 and is the 21st tendon going up from 42H1 at the bottom of the containment wall. Bay 34 also has 53H21 which is the other tendon in the set.

A horizontal tendon provides the radial compressive stress of about 340 psi averaged over the diameter of the tendon sleeve. The average over the entire cross-section of concrete being radially compressed by that horizontal tendon is about 100 psi. Normally the average radial tensile stress would be 23 psi but due to concrete displacement it is 31 psi at the centerline of the horizontal tendons.

The tensile stress peaks at a very high value right at the edge of the horizontal tendon hole at the intersection with a vertical tendon due to the vertical and horizontal tendons. It reaches 1630 psi at the hole and drops off rapidly by a factor of 2 about every inch away. More generally, tensile stress peaks at about 510 psi on the edge of a horizontal tendon away from the vertical tendons and drops off about a factor of 2 every inch away. Figures 3.3 to 3.6 show a general display of stress variations along various directions in the containment concrete assuming no cracking in the concrete. For exact values refer to the specific calculations of design parameters found in the applicable FMs and the figures in Section 7 of this report.

Using a cylindrical coordinate system, there are three dimensions used to locate a unique point in the containment wall. The radial direction extends outward from the center vertical axis of the circular building. The azimuthal angle is the horizontal angle, measured counter clockwise (looking down) from the north. Elevation defines the vertical distance from the ground reference point. A review of stresses throughout the wall due to horizontal tendons follows.

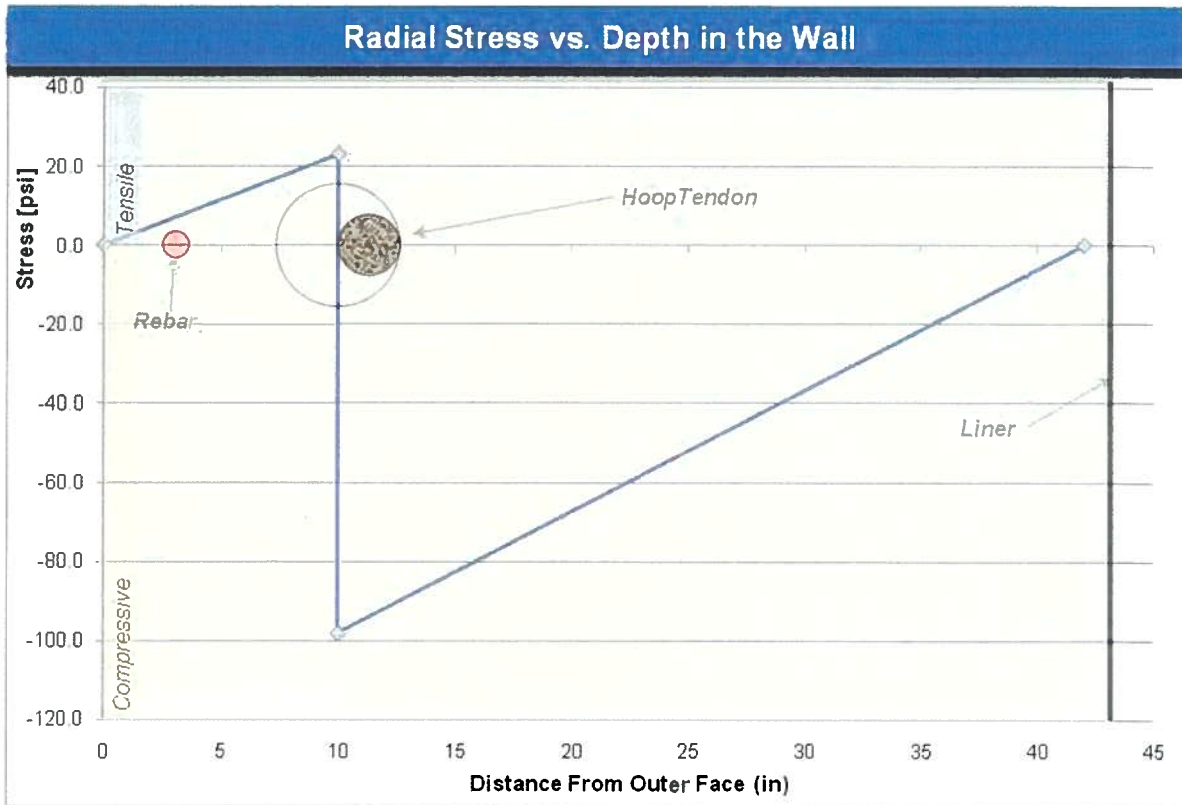


Figure 3.3 Tensile and compressive stresses in concrete wall cross-section due to horizontal tendons.

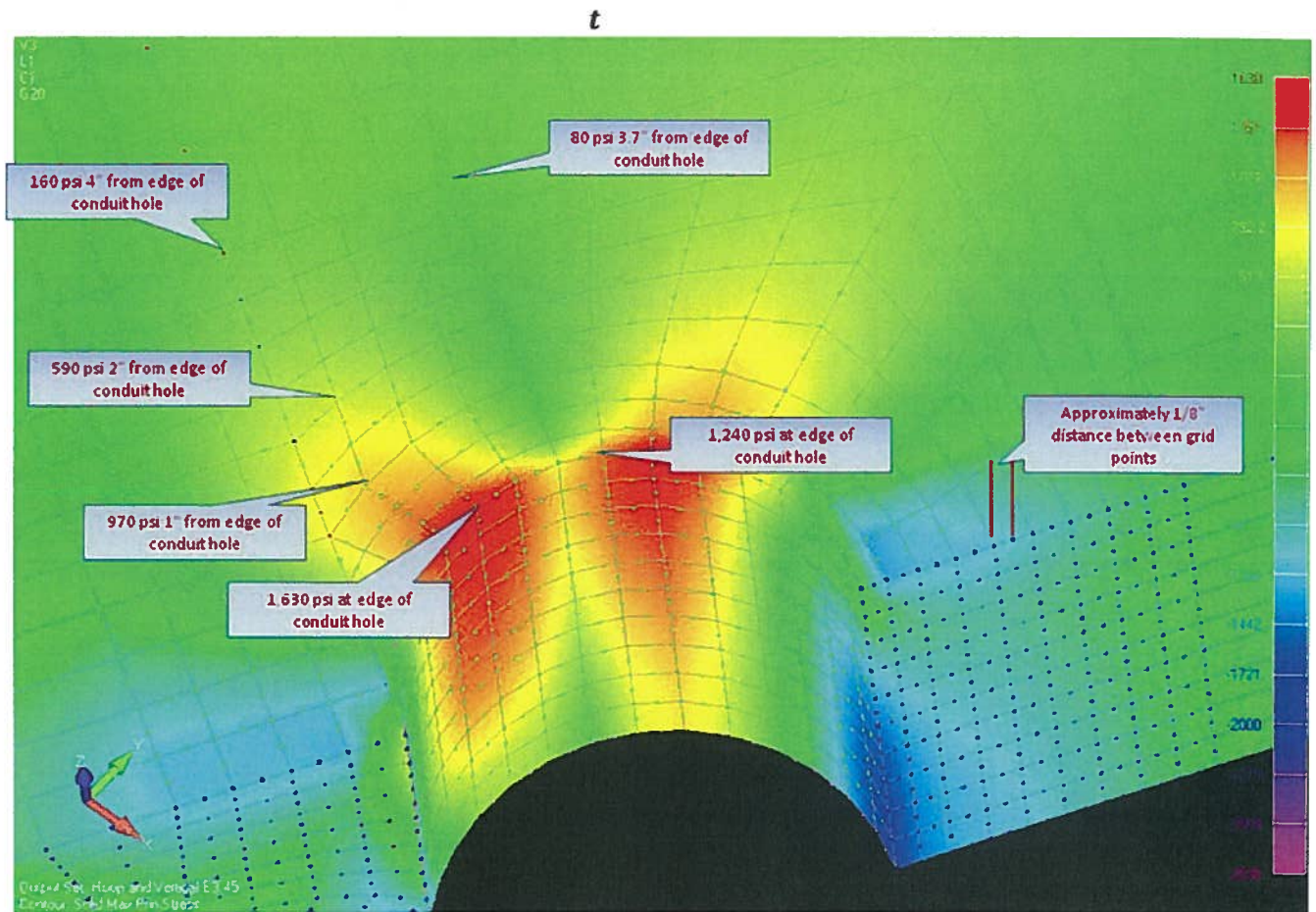
COMPUTER CODE INPUTS

The report will be providing some computer model plots which had the following inputs that were used based upon testing and modeling.. PII does not use NASTRAN to quantify concrete fracture so fracture parameters are not applicable. Abaqus applies creep correction only for long time period intervals such as the time step of 30 years of operation with the containment tensioned. E0 is the elasticity modulus and E1 is the creep adjusted elasticity modulus. F't is tensile capacity and G't is the fracture energy. 3.45 E6 psi is the average modulus measured on 22 CR3 containment cores. Fracture energy was measured to be 0.40 lbf/in (reference 11 in Section 11 of this report).

Figure	Model	E0 psi	E1 psi	F't psi	G't lbf/in	Creep
3.4	Abaqus Detail	3.45 E6	3.45 E6	360	0.08	2.2
3.5	Abaqus Detail	3.45 E6	3.46 E6	360	0.08	2.2
3.6	Nastran	4.29 E6	4.29 E6	NA	NA	0

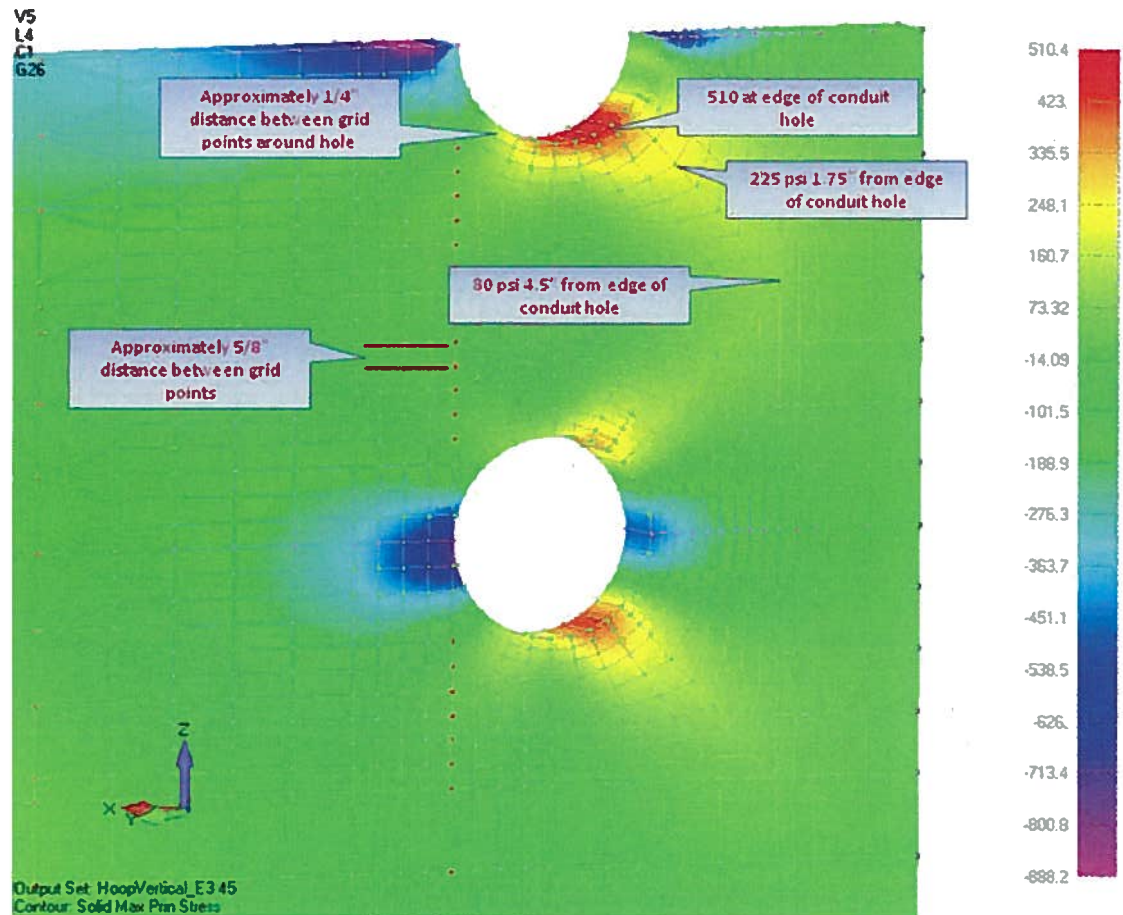
NON-PROPRIETARY VERSION

The area around a representative horizontal tendon is shown in Figure 3.4. This is a critical area due to the high stresses and displacement of concrete by the tendon sleeves. This is the location along which the delamination propagated from the top and bottom of the holes to the next hole vertically or propagated circumferentially (azimuthally) around a segment of the building. Notice that the peak tensile stress at the edge of the horizontal tendon hole near a vertical tendon (Figure 3.4) is well in excess of the tensile capacity of the CR3 concrete. It is likely that small cracks formed at these intersections but then stopped propagating when they reached a location where the stress was too low to continue.



Detailed FEM at Conduit Intersections – Lockoff Hoop & Vertical Loading, $E_c=3.45 \times 10^6$ psi

Figure 3.4 Stress contours for normally tensioned conditions at the intersection of a vertical and horizontal tendon.(3 Dimensional Effect Looking Through a Hoop Tendon Hole)



Expanded FEM *Between* Vertical Conduits – Lockoff Hoop & Vertical Loading, $E_c=3.45 \times 10^6$ psi

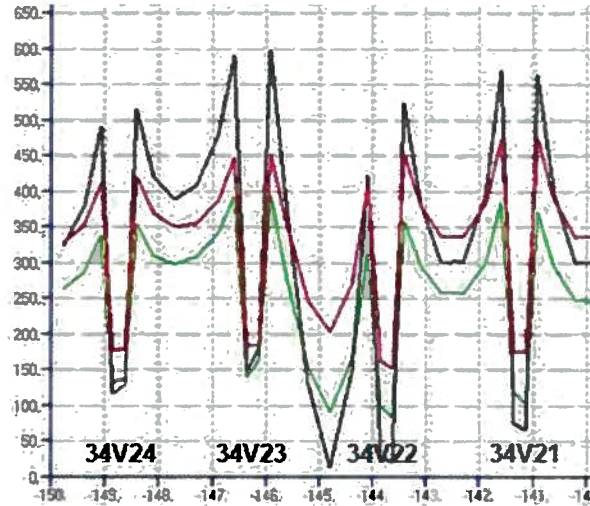
Slide 5 of 5

Figure 3.5 Stress contours for normally tensioned conditions in between intersections of a horizontal tendon with vertical tendons.(Section View)

Concrete is weaker in tension and the peak radial tension stress is located near the top and bottom of the sleeve holes. The circumferential surface through the vertical centerline of the hoop tendons has the least concrete surface area. Of the containment structures studied, all three of those that experienced delamination (Turkey Point dome, Crystal River dome, and Crystal River wall) failed along the equivalent high tensile stress locations.

Figure 3.6 shows stresses in the containment structure going around its circumference. Local stress peaks are caused by the vertical tendons spaced evenly around the containment at about 3 foot intervals. The three graphs show pre-SGR conditions, post SGR de-tensioning, and post SGR concrete removal. It is intended to simply show the changing stress seen traveling from one vertical tendon to the next.

Maximum Principal Stress Going Around Containment



Circumferential Distance, feet and tendon number

Figure 3.6 Plot of maximum principal stress as a function of distance around the containment circumference. (Black is pre-SGR, Green is Post SGR de-tensioning, Red is post SGR concrete removal.)

While the vertical tendons also displace concrete they are located inside the horizontal tendons in the area where the radial forces are compressive so the effect of displacement of concrete is not significant to the cause of cracking because concrete is strong in compression. Figure 3.6 is similar to Figures 3.4 and 3.5 showing the sharp stress changes near vertical tendons.

The specific design outlined above results in an area of reduced concrete area and high radial stress. The absence of concrete is a result of the tendon holes. The existence of high peak radial stress at the edge of the conduit hole is a material response to the compressive stresses of the tendons. This could be compensated for by using radial reinforcement but that was not required based upon the design requirements of the building as a containment. Figure 3.7 below shows a retrofitted radial reinforcement in the CR3 dome repair. This modification provided radial reinforcement on the dome as part of the required repair. It should be noted, however that many containments were designed and constructed without radial reinforcement, so this is only one of several considerations relevant to this root cause analysis.

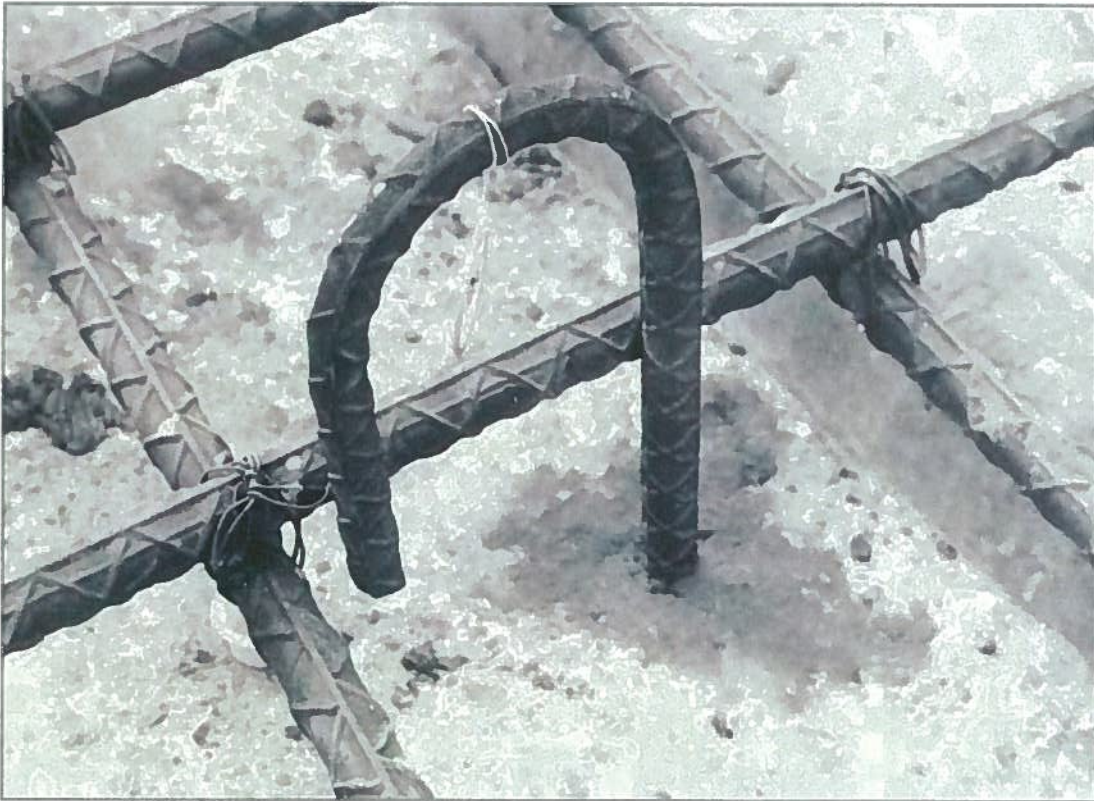


Figure 3.7 Photograph of a radial reinforcement installed as a corrective action to the CR3 Dome delamination

FM 1.1 determines that CR3's containment design results in a somewhat higher potential for delamination than other similar designs on the basis of Compressive-Tensile Stress Interaction. FM 1.2 finds that radial tensile stresses are high (refer to Figure 3.4) and there is no radial reinforcement. Large tendons lead to high peak stresses. FM 1.15 identified that stress concentration factors were not explicitly considered in the original design of the containment building. As with all the confirmed failure modes, they conclude that these issues did not individually cause the delamination but contributed to the conditions that resulted in delamination.

Considered alone, the stresses involved in the CR3 containment design are well within the capability of the concrete material used. However, when stresses occur for other reasons, such as local stresses resulting from de-tensioning of tendons and cutting the opening, these additional stresses at CR3 contribute to the overall stress condition.

4. GROUP 2: CONCRETE CONSTRUCTION

Confirmed Failure Modes:

2.12 Inadequate Strength Properties

Discussion:

The second step in the failure mode chronology was the selection of construction materials. CR3 used Type II cement and Florida Limestone aggregate. (FM 2.12) The resulting concrete met all design requirements and its properties were in the expected range for that type of concrete. Tensile strength tests on post delamination cores have shown, however, that the average tensile strength for concrete in bay 34 was up to 10% lower than that of cores from other parts of containment (compared to a standard deviation of 10% for the entire population) and similar variability in the dome. Direct tensile test results are 75% of the split tensile results when 88% to 95% would be expected. Measured compressive strength was 7707 +/- 634 psi.

Limestone in general is an acceptable aggregate that can produce high quality concrete. The limestone used for CR3 (Brooksville limestone) includes a significant portion of soft/friable particles that weakens the physical properties of the concrete (See FM 3.4). Even though the concrete compressive strength met project specifications, the variability and instances of low tensile strength led to the conclusion that this failure mode contributed to the delamination. This finding was largely based upon the performance of the aggregate used which is addressed in FM 3.4 Inadequate Aggregates.



5. GROUP 3: USE OF MATERIALS

Confirmed Failure Modes:

3.4 Inadequate Aggregates

Discussion:

Hardened concrete is composed of three main phases - aggregates, hardened cement paste (HCP) and the interface between them. The weakest part that normally controls strength is the interface where microcracks form and cracks originate. Since the aggregate is normally significantly stronger than the HCP it provides a stable medium that helps arrest and slows the progression of cracks.

Analysis revealed that the coarse aggregate used at CR3 was a locally available calcareous limestone (Brooksville Limestone) which included up to 50% soft/friable material that was not appreciably stronger than the HCP and allowed cracks to propagate directly through the aggregate.

In the three delamination events that have occurred in the U.S. nuclear industry, all involved Florida limestone aggregates.

Additionally, experience in other delamination events points to sensitivity for delamination when the tensile strength is low. For example, similar delamination during tensioning of the Kaiga containment dome in India involved concrete with tensile strength of 489 psi (3.37 MPa) ([Reference 2](#)) which is lower than the average tensile strength of 600 psi as measured at Crystal River (using the Brazilian splitting tensile strength test).

FM 3.4 is a discussion of the selected coarse aggregate. The aggregate used at CR3 was relatively soft, porous, and gap graded. While its properties were sufficient to satisfy the specifications and design requirements, it resulted in concrete tensile strength, modulus of elasticity, and ability to arrest cracks that was significantly lower than at most other nuclear containment structures.

This FM impacts the plant because it contributes to the tensile strength of the concrete discussed in [FM 2.12 Inadequate Strength](#). For that reason FM 3.4 is shown as feeding in [FM 2.12](#) on the FM Timeline.



6. GROUP 7: SGR ACTIVITIES

Confirmed Failure Modes:

- 7.3/7.4 Inadequate de-tensioning sequence and scope
- 7.5 Added stress due to removing concrete at the opening

Discussion:

FMs 7.3/7.4 addresses de-tensioning sequence and scope.

Normally, the containment is in a symmetric state of loads and deformations. When changes cause it to transition into non-symmetric state, it experiences stresses and strains that may exceed its capacity. One symmetric state existed at the time the containment was complete, but prior to prestressing any of the tendons. The symmetric load consisted primarily of the dead load of the structure. Another symmetric state existed when the structure was fully tensioned because of the symmetry built into the tendon pattern. In either situation the transition was smooth and free of bends in the concrete that can promote delamination. Excessive stresses and/or strains can develop when transitioning between two symmetric states because of the sharp local transition from a series of tensioned tendons and a series of de-tensioned tendons. However, the potential for a prestress force load imbalance on the containment shell as the tendons are globally stressed is precluded since the prestress force is applied in gradual and symmetric manner governed by procedure. For example, in the hoop direction the original stressing procedure sequence required stressing the tendons in complete rings of three tendons and also tensioning every fourth ring of tendons until $\frac{1}{4}$ of the total hoop prestress was applied to the shell. The process was repeated until another $\frac{1}{4}$ of the hoop prestress was applied et cetera..

Figure 7.11 shows the radial displacement that occurred during the SGR de-tensioning. Delamination occurs where radial stress is high. That occurs at sharp bends in the wall. The de-tensioned region ran horizontally from elevation 183' to 210' for a span of 27'. Horizontally the bulge extended across the bay for span of about 60' so there was a smoother transition in that direction. Note in Figure 7.11 that the radial displacement associated with de-tensioning is linear. This means that the stress that develops is monotonically increasing and other sequences of de-tensioning the same number of tendons would not change the end-point which is the highest stress condition.

The ability to control radial stress comes mainly from the manner (selecting the right number and location of additional tendons to be de-tensioned along with the sequence to be de-tensioned) in which the horizontal tendons are de-tensioned. What is important is the number of tendons involved, the symmetry of the tendons affected, and whether the sequence employed increases or decreases local peak stress. We know approximately when delamination occurred based upon observed cracking in the hydro demolition demonstration area and water observed coming out of the containment wall. In an area as large as bay 34 and with the large stress concentration factors on a detailed scale, it is probable that cracking began in isolated points of highest stress. As the stresses increased (due to the growing number of de-tensioned tendons), and shifted (due to the various tendons de-tensioned), small cracks grew and joined until they eventually covered the entire delaminated area. More detail is available in [Attachment 4](#).

NON-PROPRIETARY VERSION

The last four steps of the actual de-tensioning were to de-tension tendons 53H32 through 53H35 in order. However tendons 42H32, 42H33, and 42H34 were in between these last tendons and they had been previously de-tensioned so there was some alternation in the sequence used to minimize the transition from tensioned to de-tensioned tendon..

The scope and sequence used is so intertwined that the two FMs 7.3 and 7.4 were combined and it was concluded that they did contribute to the delamination. Although the building felt the impact of de-tensioning, it is clear from the finite element analysis that the localized de-tensioning in bay 34 led to curvature which contributed to the delamination. The March, 2010 analysis and subsequent de-tensioning for repair found that use of more symmetrical de-tensioning of the entire circumference was required to avoid delamination in other bays and the building was successfully de-tensioned.

(FM 7.5) addresses the removal of concrete. Photographs taken after concrete removal started, the day before the final two horizontal tendons were de-tensioned, show cracks existed at that time. The next day after more concrete removal the discovery of water flowing out of the containment wall more than 20 feet away from the hydro-lasing work area indicates that delamination occurred prior to large scale removal of concrete. Given the stresses caused by the demolition and those created in the remaining concrete when a large area is removed, it contributed to the overall de-lamination event.



7. FAILURE MODE TIMELINE

This section of the report discusses the timing of the contribution for each failure mode. Figure 7.1, below shows the timeline.

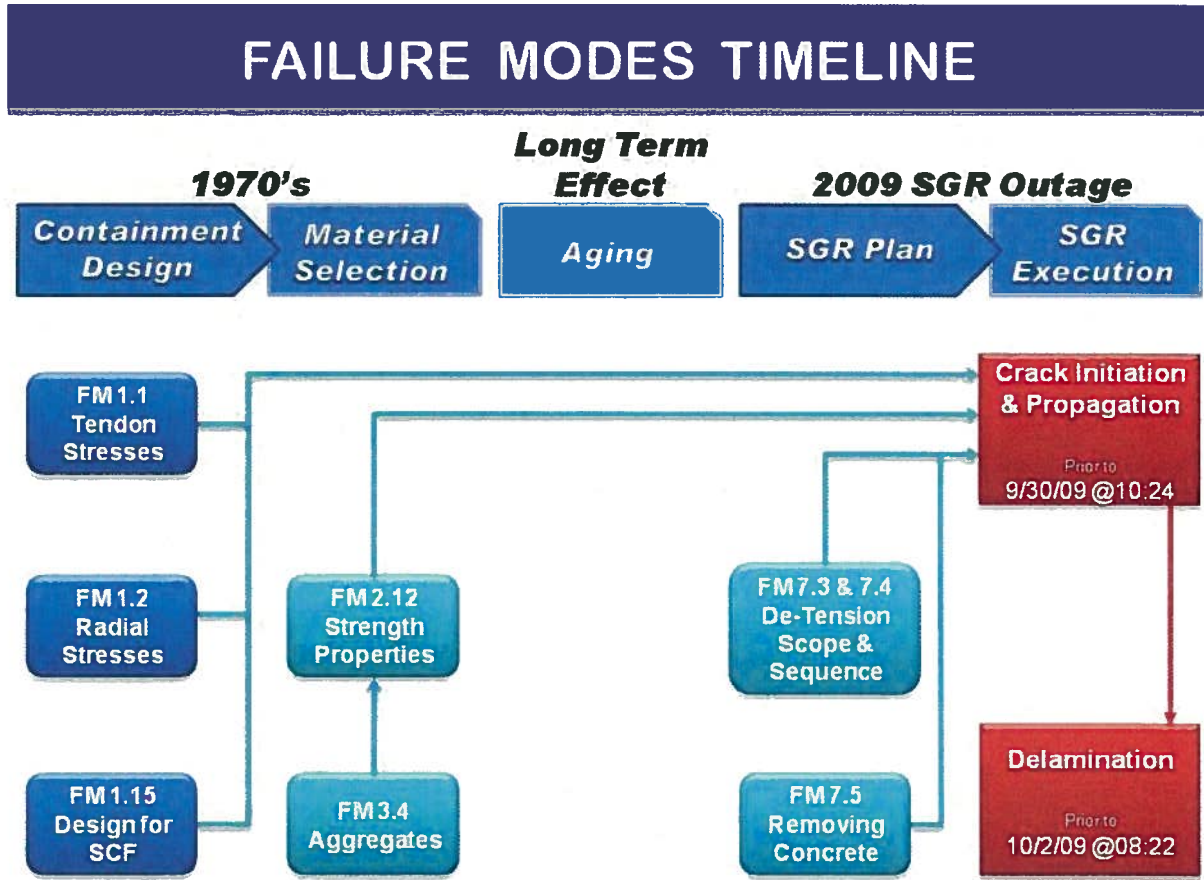


Figure 7.1 Failure Modes flow chart

The first step in the timeline was the original design of the containment building. That design specified the tendon sizes, locations, and no radial reinforcement for radial stress which ultimately played a part in the delamination four decades later.

The next step was the selection of materials for the concrete. The materials selected met the design requirements but resulted in concrete that had lower tensile strength and aggregate properties than concrete at other nuclear plants.

A part of the SGR project scope was to design a successful de-tensioning and containment opening project. The variables that were available were the scope of tendon de-tensioning, sequence of de-tensioning, and the nature of the containment opening made.

At this stage of the root cause assessment all the contributors have been identified and assessed. The next step is to simulate the tendon de-tensioning by Finite Element Analyses that reflect

loads and geometry related to the timeline and see under what conditions and when the concrete cracks.

Sequence of Steps:



The following sequence of steps provides an overall image of the de-tensioning process and its impact on bay 34. The displacements discussed below are from the Abaqus global model. The computer model simplified the de-tensioning process. It did not relax the tendons in order but, instead, relaxed all the tendons partially at the same time. Thus 25% through the de-tensioning means all tendons are stressed to 75% of their lock-off value.

1. The containment is initially constructed with straight vertical walls. Radial displacement is 0 inches since this is the measurement baseline (Figure 7.2).
2. Upon completion of tendon tensioning the building is mostly symmetrical and each bay has an inwardly curved wall with a maximum deflection of -0.5 inch (Figure 7.3).
3. Over the next three decades the concrete creeps and radial displacement grows to a maximum of -1" (Figure 7.4).
4. As SGR de-tensioning proceeds, bay 34 begins to move radially outward. Bays 23 and 45 also begin to move radially outward at half the rate of bay 34 because bay 34 has shared tendons with each of bays 23 and 45. The other bays begin to move inward in response to the buttresses having unbalanced side loads. The building develops an overall vertical curvature (Figure 7.5).

Figures 7.2 to 7.5 show the progression of containment shape over time. It was originally a cylinder but it became concave with the tensioning of the tendons. The SGR de-tensioning sequence resulted in a building-wide change in shape and bay 34 moved out close to its original tensioned position prior to creep. (Figure 7.11) Local stresses increased since the rest of the bay was still restrained by tensioned tendons. (Figures 7.16 to 7.23.) The situation ultimately led to localized cracking that propagated over most of bay 34. (Figures 7.26 and 7.28)

Detailed Computer Simulation:



The individual failure modes have been identified and placed in a timeline; results of the computer simulation follow.

There are three essential pieces to a credible computer simulation. They are:

- ◆ A discussion of the computer model being used. This is presented in [Attachment 1](#).
- ◆ A detailed discussion of the benchmarking performed to ensure the model accurately reproduces the conditions being simulated. This is discussed in [Attachment 2](#) so as not to distract from the discussion of the sequence of events presented in this section.
- ◆ A detailed presentation of the simulation results including a discussion of the important conclusions and expected results is discussed below.

In order to properly understand this event, it is necessary to develop a suitable computer model and simulate the response of the entire containment structure to changing conditions. For detailed information refer to [Attachment 1](#). To have confidence in a computer model's ability to simulate the events of root cause investigation, inputs must be realistic and predictions must be

validated. For this reason, PII developed progressively more rigorous analytical tools. A detailed discussion of the codes is available in [Attachment 1](#).

Next, a detailed comparison between the Abaqus radial displacement predictions will be compared to measured displacements using laser scanning. Greater detail is provided in [Attachments 2 and 4](#).

COMPUTER CODE INPUTS

The report will be providing some computer model plots which had the following inputs that were used based upon testing and modeling. PII does not use NASTRAN to quantify concrete fracture so fracture parameters are not applicable. Abaqus applies creep correction only for long time period intervals such as the timestep of 30 years of operation with the containment tensioned. E0 is the elasticity modulus and E1 is the creep adjusted elasticity modulus. F't is tensile capacity and G't is the fracture energy. 3.45 E6 psi is the average modulus measured on 22 CR3 containment cores. Fracture energy was measured to be 0.40 lbf/in. Abaqus Global does not calculate fracture so those parameters are Not Applicable for it.

Figure	Model	E0 psi	E1 psi	F't psi	G't lbf/in	Creep
7.2, 7.3, 7.5, 7.6, 7.7, 7.8, 7.10	Abaqus Global	3.45 E6	3.45 E6	NA	NA	2.2
7.12, 7.13, 7.15-7.24	Abaqus Global Bay sub model	3.45 E6	3.45 E6	108	0.08	2.2
7.4,7.9, 7.11	Abaqus Global	3.45 E6	1.1 E6	NA	NA	2.2
7.15,7.26,7.27,7.28,7.29	Abaqus Global Detailed sub model	3.45 E6	3.45E 6	360	0.08	2.2

Whole Containment Radial Displacement Simulation:



The following discussion of containment, due to its complexity, will be presented sequentially, starting with radial displacement calculations for the following milestones:

1. Un-tensioned (circa 1973)
2. Fully tensioned (circa 1976)
3. Fully tensioned in 2009 (after 30 years of creep)
4. Post SGR de-tensioning
5. Post SGR opening completion

NON-PROPRIETARY VERSION

The sequence of events starts with an un-tensioned containment building (circa 1973). This is shown in Figure 7.2.



Step: Step-01-Tensioning
Increment 0: Step Time = 0.000
Primary Var: U, U1 (Cyl)
Deformed Var: U Deformation Scale Factor: +2.000e+02

Figure 7.2 CR3 containment un-tensioned - facing bay 34 – baseline case.
Note the equipment hatch and buttresses 3 and 4. The parameter displayed (U) is radial displacement.

NON-PROPRIETARY VERSION

The next step is the containment building after being fully tensioned.

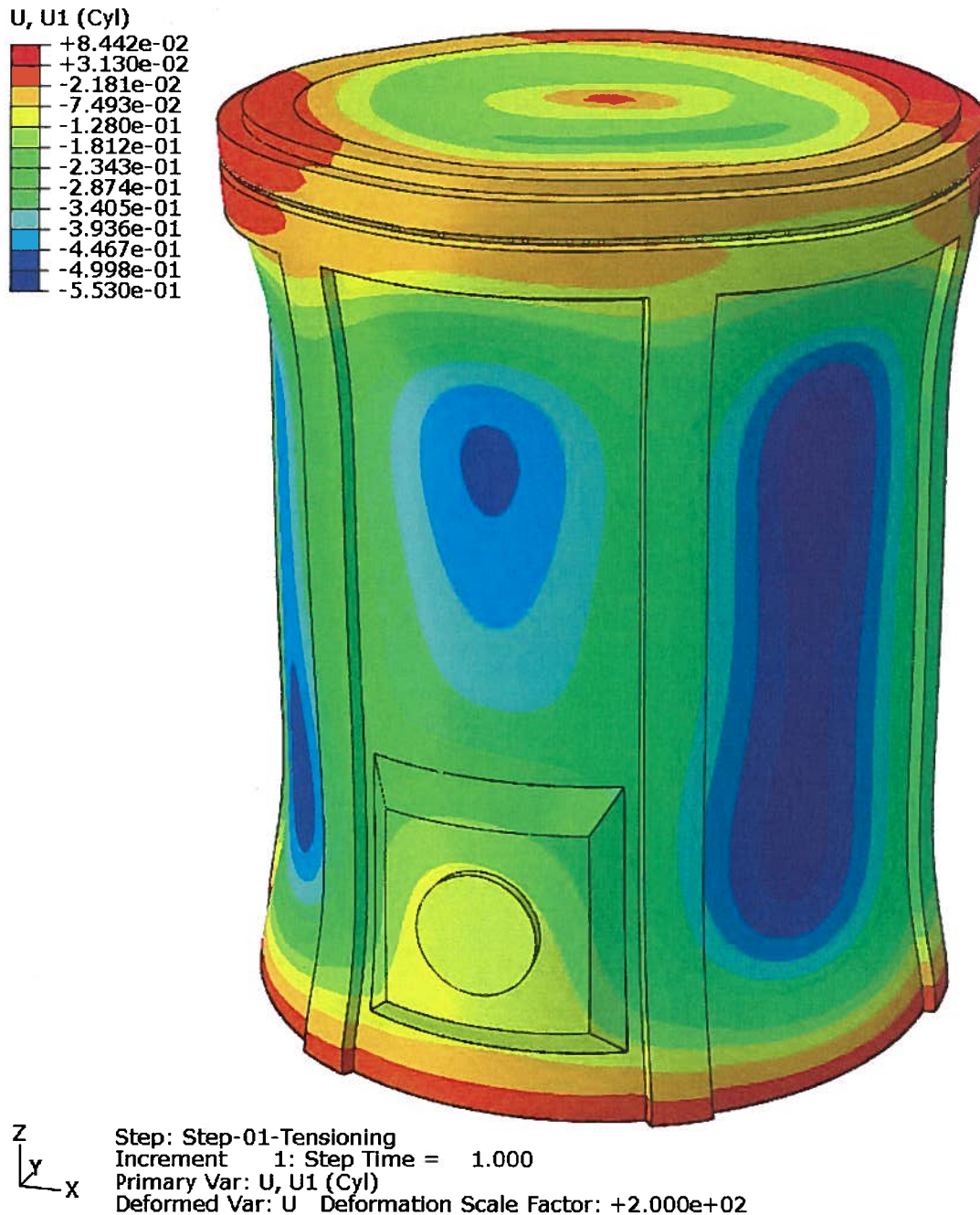


Figure 7.3 CR3 containment building fully tensioned.
The parameter being displayed (U) is radial displacement.

The overall effect of tensioning the tendons in the building was to cause the building to contract under the force of the tendons. Blue denotes the maximum contraction (of about -0.5") and red shows a slight expansion around the ring header and the foundation. Bay 34 is different from the

NON-PROPRIETARY VERSION

other bays due to the presence of the reinforced equipment hatch. As expected, the influence of the equipment hatch fades with distance. Also, as expected, the center of each bay deflects inward more than the edges which are anchored to the buttresses.

The next milestone is the effect of 30 years of creep in the concrete.

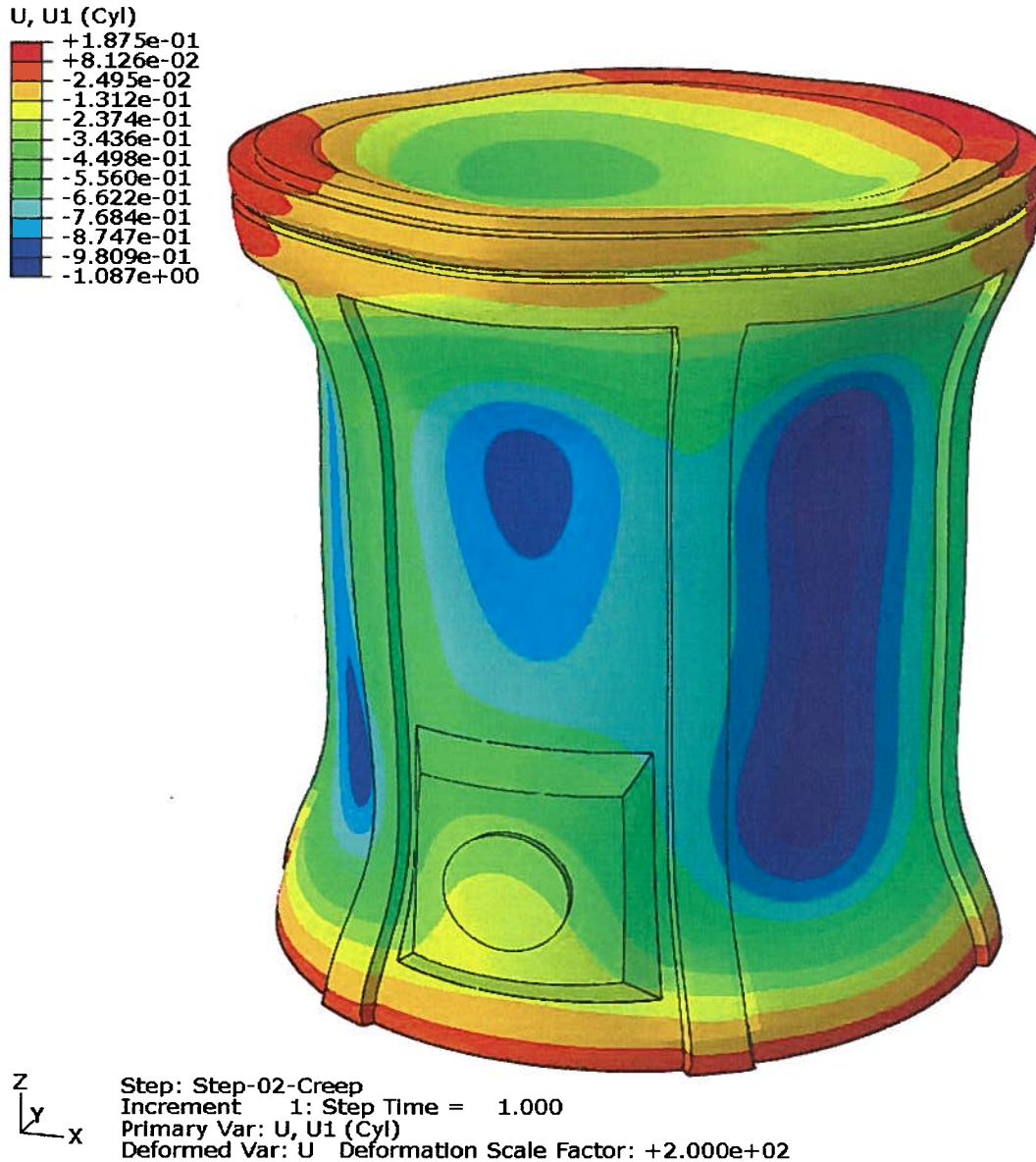


Figure 7.4 CR3 containment radial displacement after 30 years of creep.

Creep is the gradual displacement of concrete under long term stress so one would expect additional radial displacement over time. The effect of creep is visible in the depth of the dome, the narrowing of the waist of the building, and the displacement of the equipment hatch.

NON-PROPRIETARY VERSION

The next milestone is the completion of the SGR de-tensioning in 2009. This consisted of de-tensioning 17 horizontal and 10 vertical tendons. The de-tensioned zone extends from about elevation 183' to 210' with a maximum effect at elevation 197'.

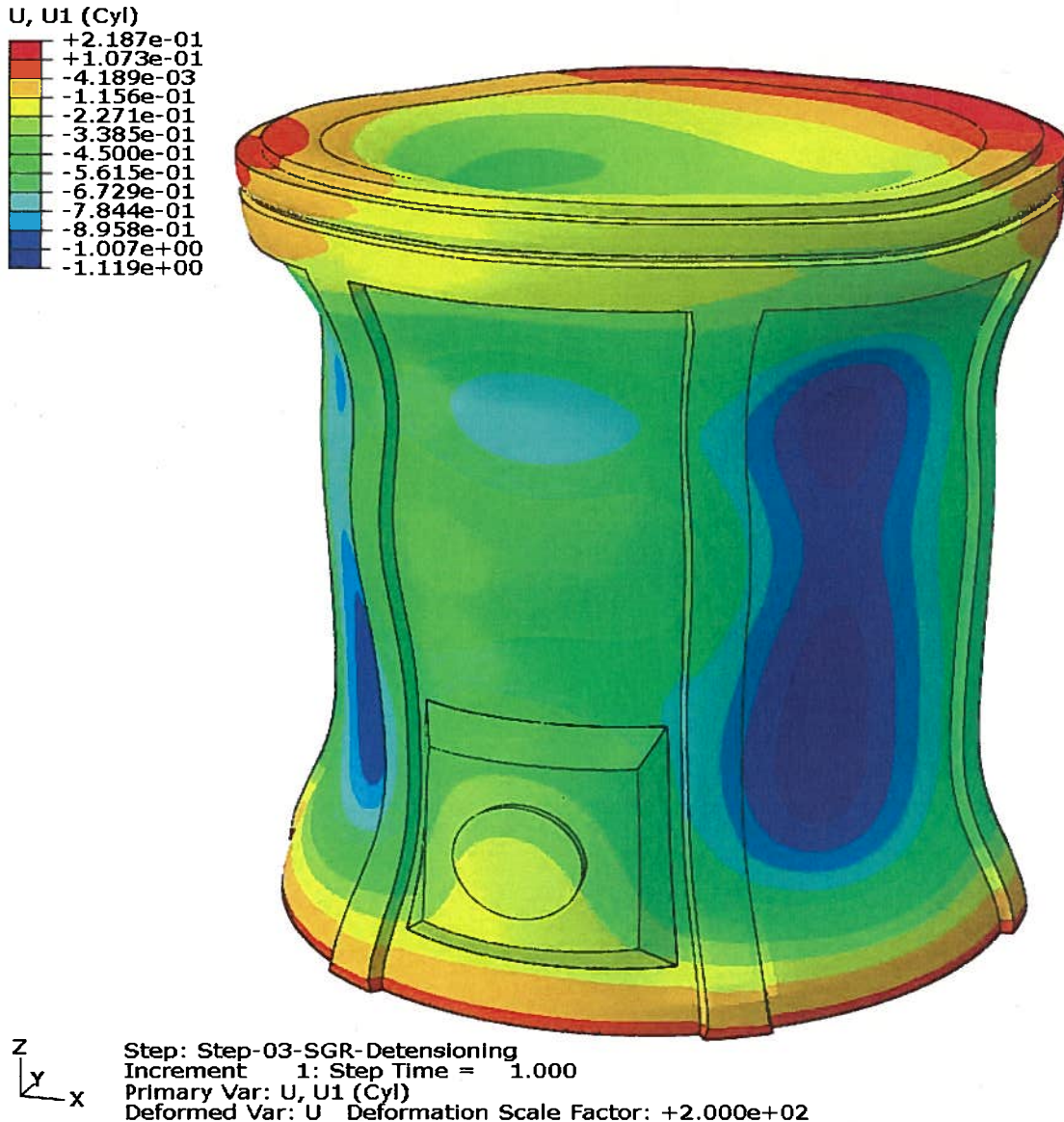


Figure 7.5 CR3 containment radial displacement post-SGR de-tensioning

The shape of buttress 3 in profile has changed from a gradual C curve into an S curve because of the development of a bulge in the center of bay 34. The blue spot indicating radial contraction is now missing from bay 34 and is somewhat reduced in bay 45 (which experienced a reduction of nine tendons (due to tendons extending across two bays)). Bay 23 is not visible but also sees a reduced effect due to eight of its tendons being de-tensioned.

Figure 7.6 is a special case. The containment wide Global Abaqus model is not designed to handle the consequences of concrete cracking. The additional complexity involved with handling crack propagation and load distribution in a cracked environment would be prohibitive for the full containment model. That analysis is performed in the sub-models. In Figure 7.6 the analysis was stopped at Figure 7.5 and the ties between the inner and outer layers were manually broken to determine what the containment-wide response would be. The result is that an hourglass shape has developed in the bulged area of bay 34, matching the actual delamination pattern, and is caused by the interaction of the building causing the center of bay 34 to bulge outward. The de-tensioned zone at the sides of the SGR opening reduces the propensity to crack. The result is an hour glass shape with the peak displacement in the fully tensioned area just above and below the bulge in the middle of the bay.

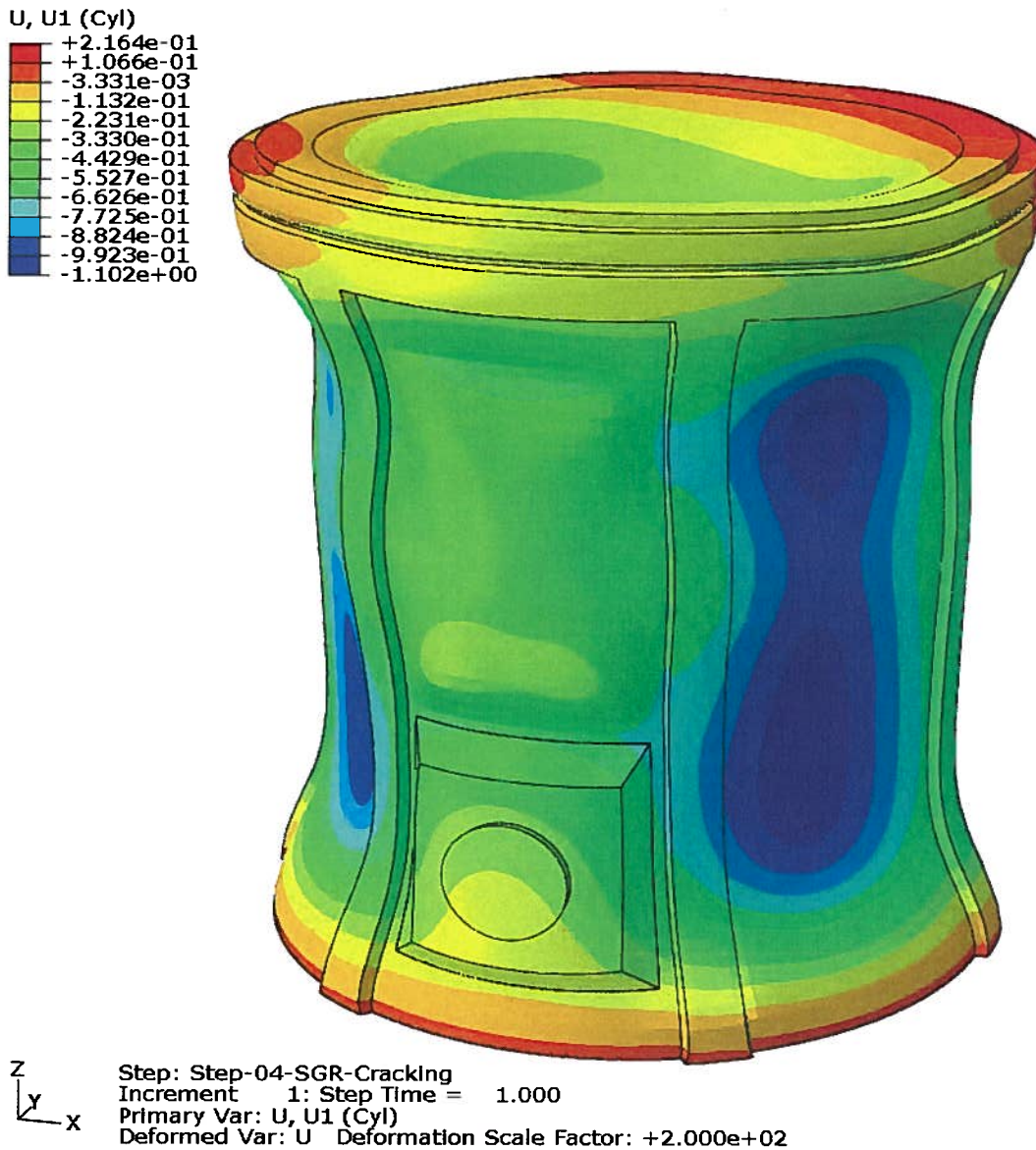


Figure 7.6 CR3 containment radial displacement post SGR de-tensioning

NON-PROPRIETARY VERSION

The final milestone occurs where the conditions in Figure 7.5 are then subjected to removing the concrete completing the SGR opening. To follow the actual progression of the delamination progression refer to Figures 7.16 through 7.23.

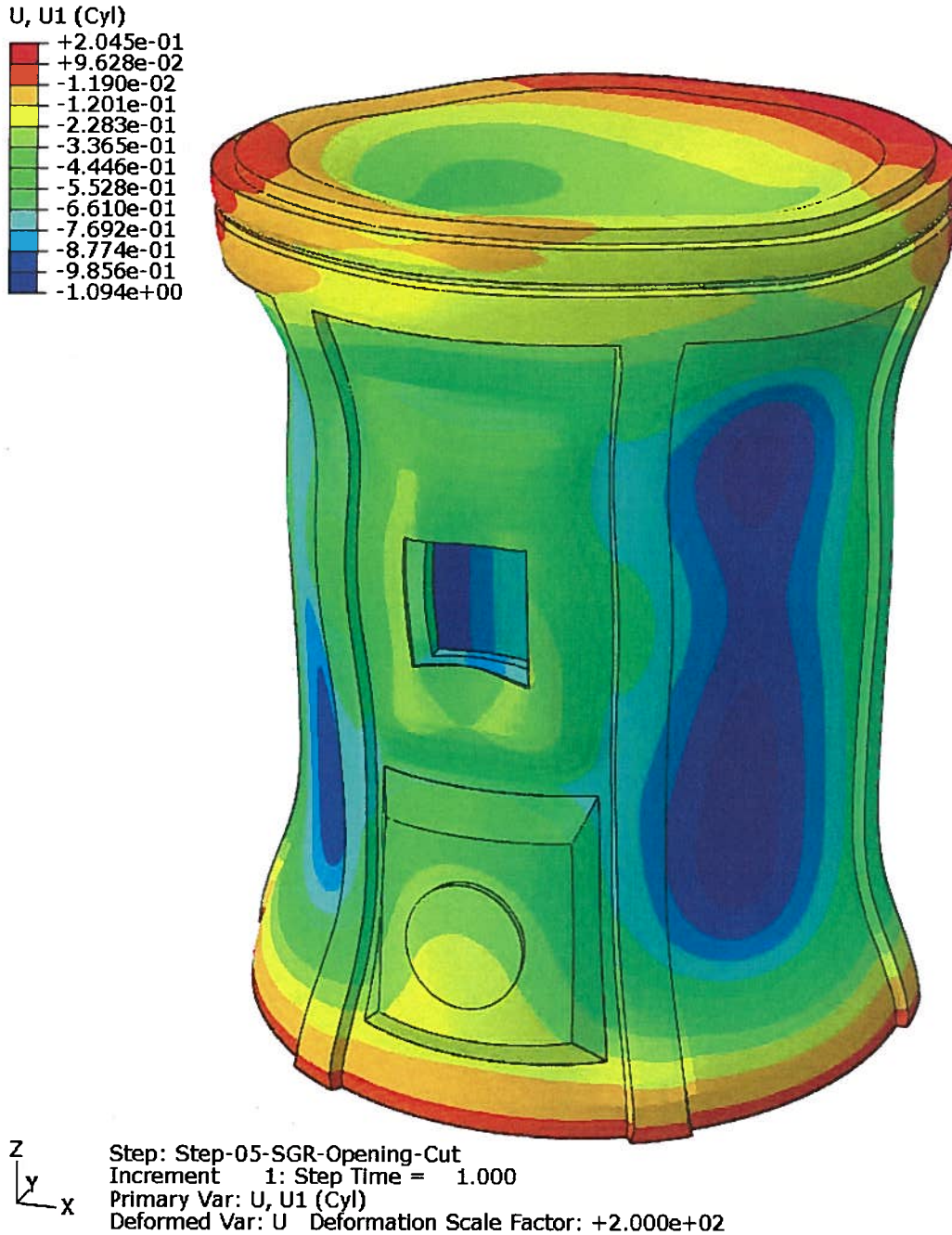


Figure 7.7 CR3 containment radial displacement after SGR opening completion.

Detailed Local Wall Radial Displacement Response:



Up until this point the entire containment has been displayed, which is useful to understanding the overall forces at work but it does not explain the local conditions that ultimately result in delamination. Figure 7.8 is a cut-away profile of the bay 34 wall showing radial displacement as it was immediately after tensioning in 1976.

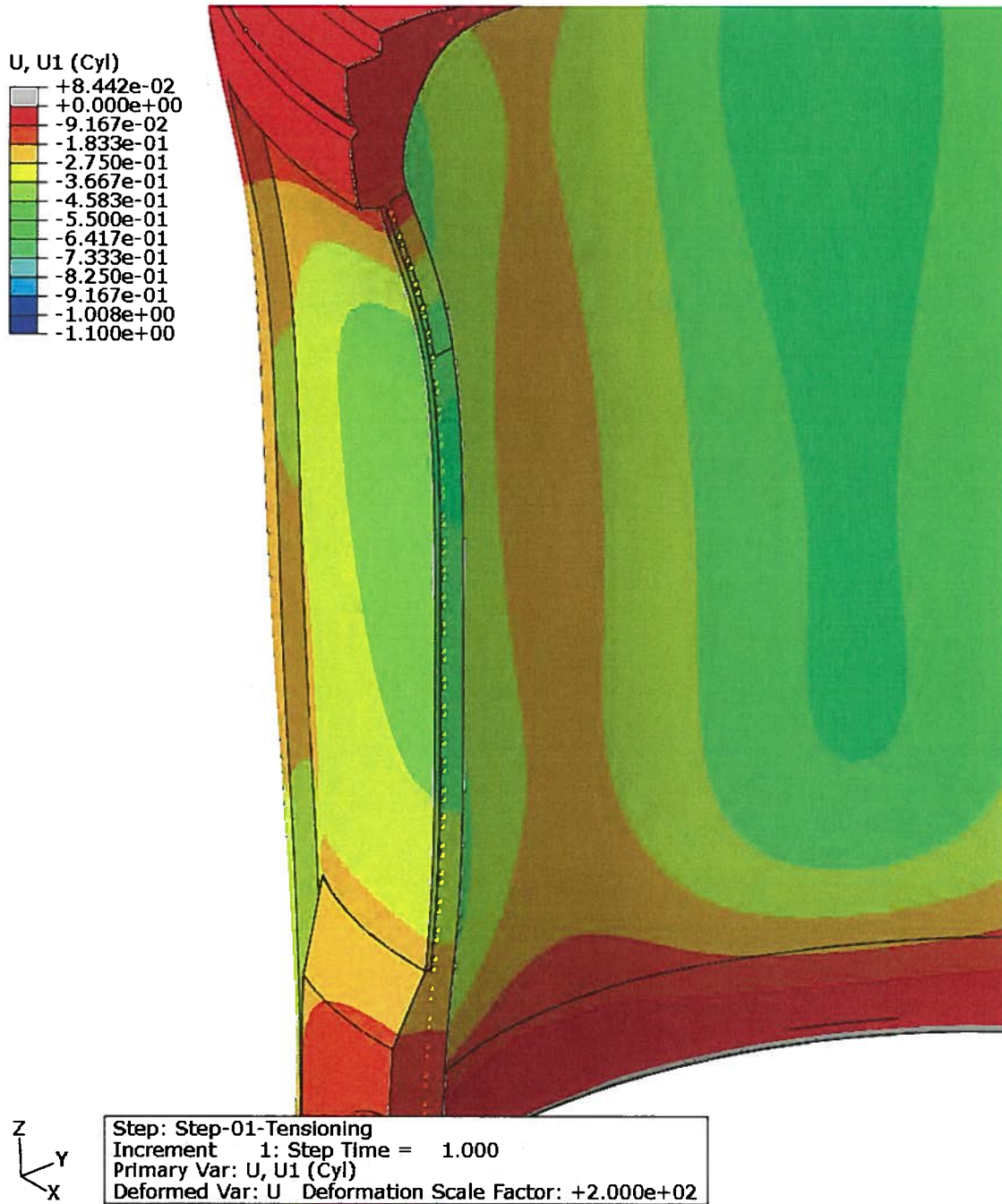


Figure 7.8 CR3 Bay 34 wall profile radial displacement post initial tensioning in 1975. The next milestone is in 2009 after 30 years of creep.

NON-PROPRIETARY VERSION

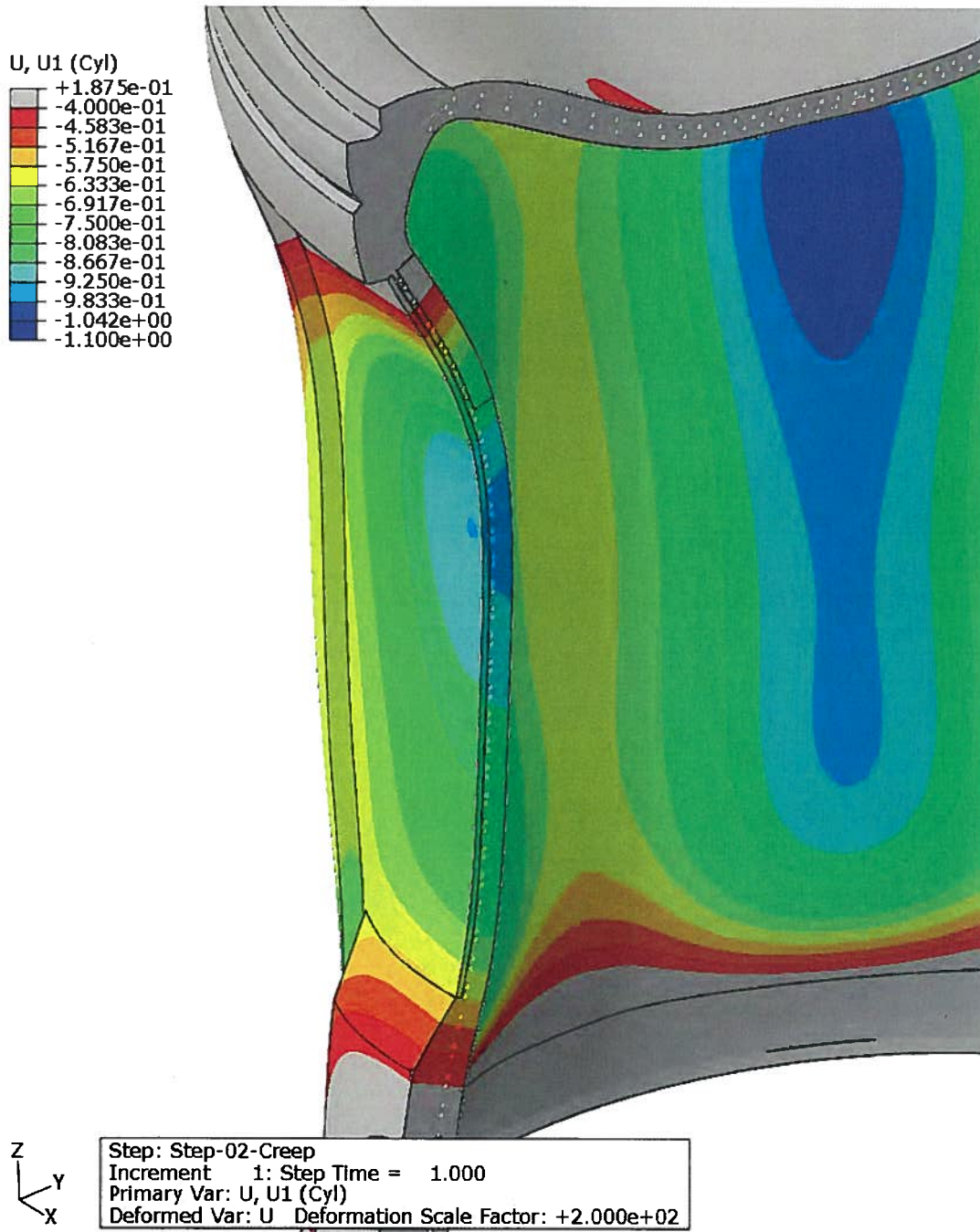


Figure 7.9 CR3 containment cut-away profile showing radial displacement after 30 years of creep.

The next milestone is post SGR de-tensioning.

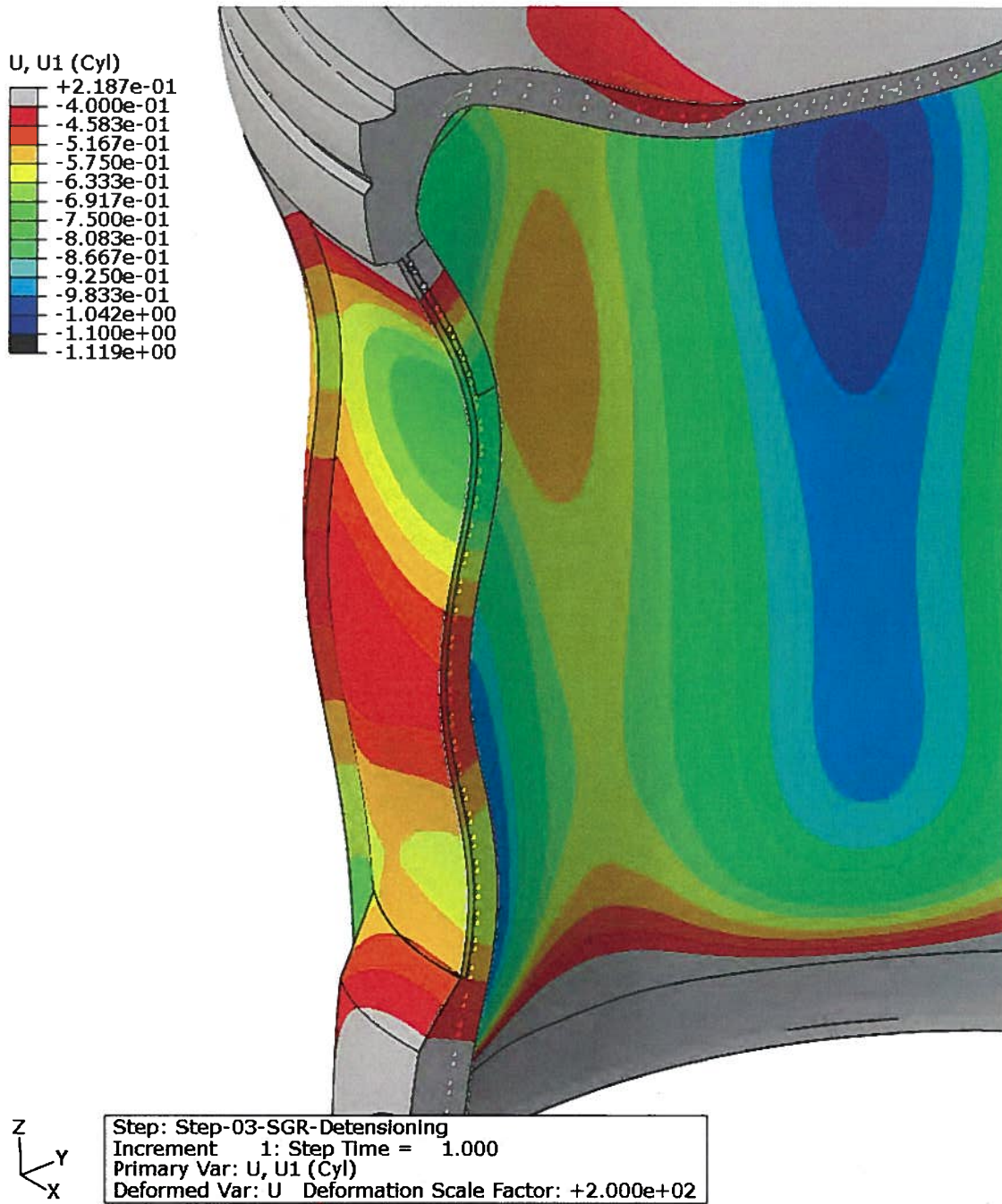


Figure 7.10 CR3 containment wall cut-away profile of radial displacement following the SGR

Here, an S curve has developed in the wall. Delamination stems more from the rate of change in the profile than from the magnitude of the change in profile. The inward displacement of the wall was greater prior to SGR de-tensioning than after de-tensioning, but its margin to delamination was greater because the contraction was smooth. In this plot, the maximum curvatures are at elevations 173' and 220'. The maximum delamination gap widths measured were centered around 175' and 216' (See Figure 7.14) which is good agreement.

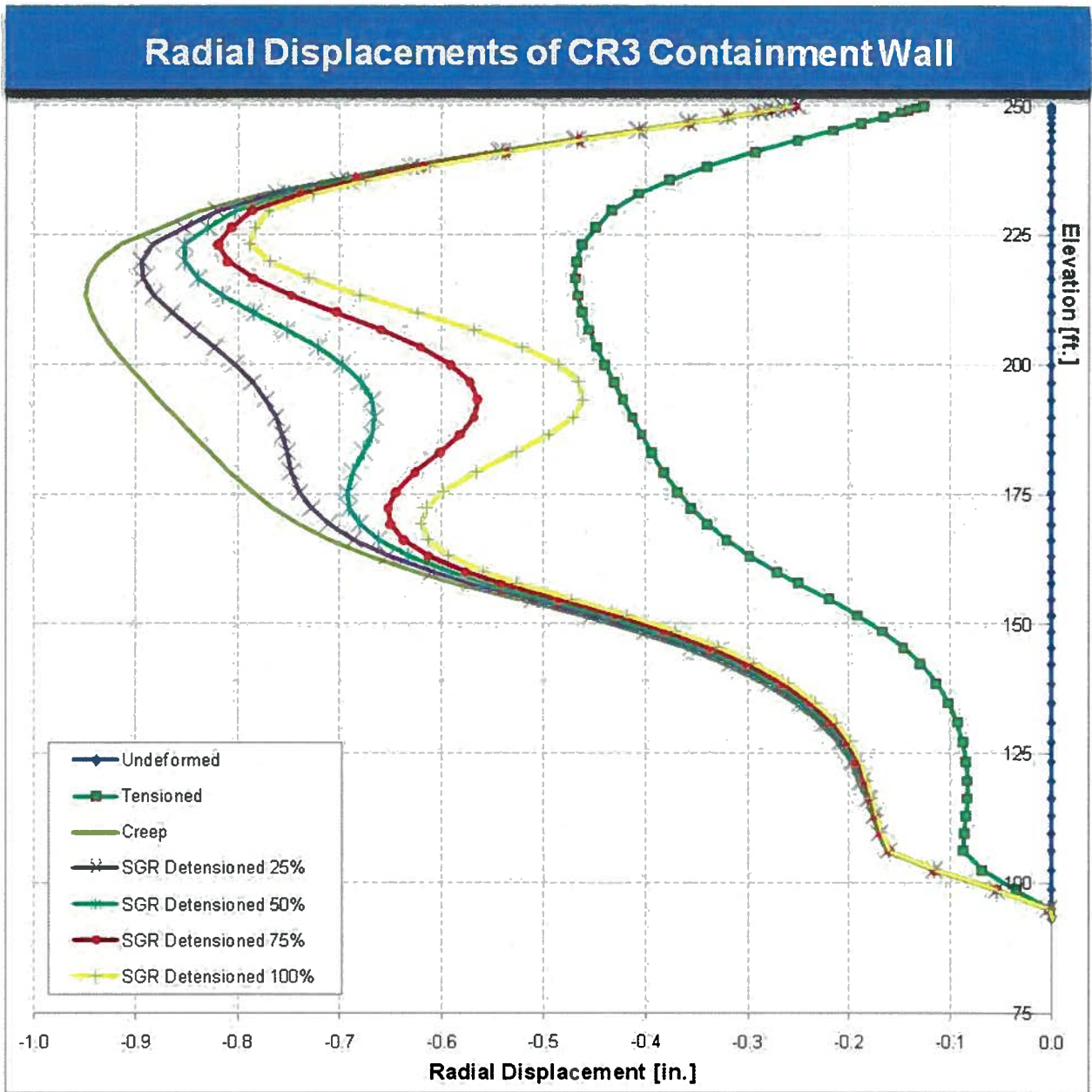


Figure 7.11 Bay 34 midline profile for progressive SGR de-tensioning

As expected, the un-tensioned case shows no radial displacement. The 1976 tensioned case shows uniform displacement of 0.5” inward. Creep increases that displacement to 1” inward by 2009. The SGR de-tensioning shows the impact of de-tensioning 10 vertical and 17 horizontal tendons in creating a double peaked profile with a much sharper curvature than was experienced previously. The intermediate lines are partial de-tensioning points going from fully tensioned to de-tensioned for SGR. The model did not remove each tendon sequentially. Instead, it de-tensioned all the selected tendons incrementally. While that is not the exact sequence used, the model gives a realistic view of the transition felt by the bay 34 wall. In the fully tensioned case (Creep), the curvature is approximately 0.05” over a 25’ span or 170 $\mu\text{in/in}$. De-tensioning 10

vertical tendons and then 17 horizontal tendons in a row created two sharp peaks with a curvature of 0.15" in 40' or 310 $\mu\text{in/in}$ and 0.3" in 50' or 500 $\mu\text{in/in}$, indicating that there should be more severe damage above the opening (centered at 225') and less severe damage below the opening (centered at 170'). However, the actual de-tensioning sequence de-tensioned the higher tendons last, which indicates that the lower peak was accentuated during most of the de-tensioning sequence, so the curves presented here may not exactly match the transient peaks seen until de-tensioning was complete. In Figure 7.14 the two centers of damage are at 216' and 175', and the damage appears similar above and below the opening. Overall there was good agreement between the predictions of the computer model and the delamination observed. Looking at bay 34 from the outside, at the end of de-tensioning the wall has two concave curves and one convex curve. It is worth noting that the peak concave curvature occurred in tensioned areas, so the concrete exposed to the peak curvature still had the tensile peak due to normal tendon force on the area around the horizontal tendons.

The center of the de-tensioned zone was at 192' and this is the point in the graph which showed the greatest outward displacement (bulging) by moving about 0.025" for each horizontal tendon de-tensioned.

Figure 7.12 shows the predicted effect of delamination. The wall separates into an inner section and an outer section. The separation is not uniform because the bulge area tends to close the gap in the center. The center area is de-tensioned so the force separating the two sections is reduced.

The Abaqus bay sub-model was used to calculate the response of bay 34 to the SGR de-tensioning sequence. The results are shown in Figures 7.12 and 7.13. The delamination event alone is shown in Figure 7.12. Figure 7.13 shows the bay response to removing the concrete after delamination. Notice the size of the crack that develops is not uniform and it is not greatest in the middle of the bay. It is greatest above and below the middle of the bay. This makes sense if the non-delaminated concrete on the outside of the neck of the hour-glass is restraining the crack opening. It also makes sense in terms of the area in which the tendons are de-tensioned. Note the similarity between the computer predictions in Figures 7.12 and 7.13 and the actual crack width data taken by core bore and Impulse Response monitoring. Also note that the crack opening does not significantly change due to removing the concrete. That explains the lack of change in the cracks visible at the edges of the opening when compared between 10/3/09 and 10/28/09. The depth of concrete removed on 10/3/09 was about 15" and on 10/28/09 it was 100%. It is recognized, however, that the model predicts about 0.5" for the crack and the peak cracking was about 2.5" so the relative dimensions should be considered rather than the absolute values.

NON-PROPRIETARY VERSION

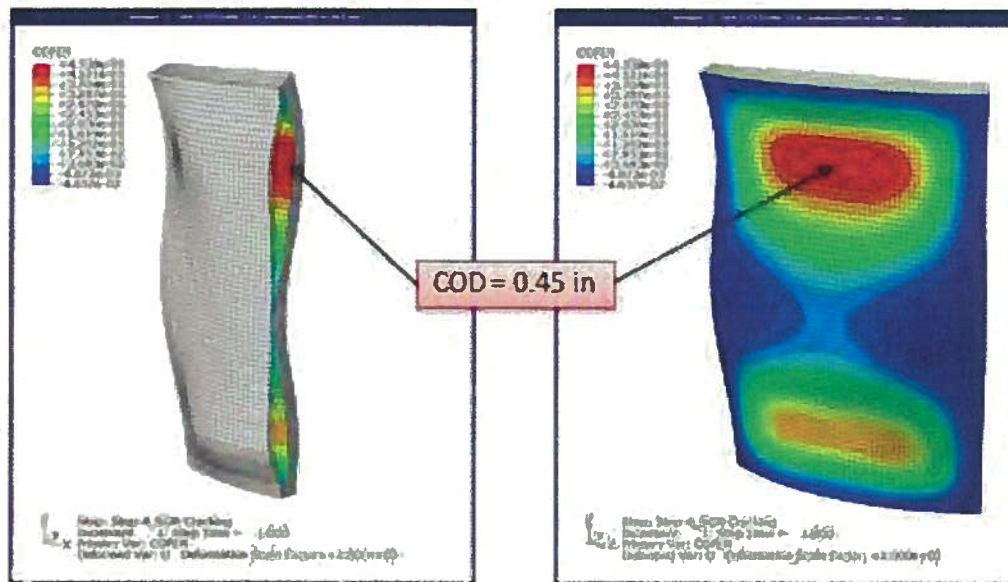


Figure 7.12 The Dimensional response to delamination – Step 4 SGR Cracking
Crack Opening Distance (COD) is the width of the crack that develops. Note the similarity of the pattern in this Figure to that in Figure 7.14.

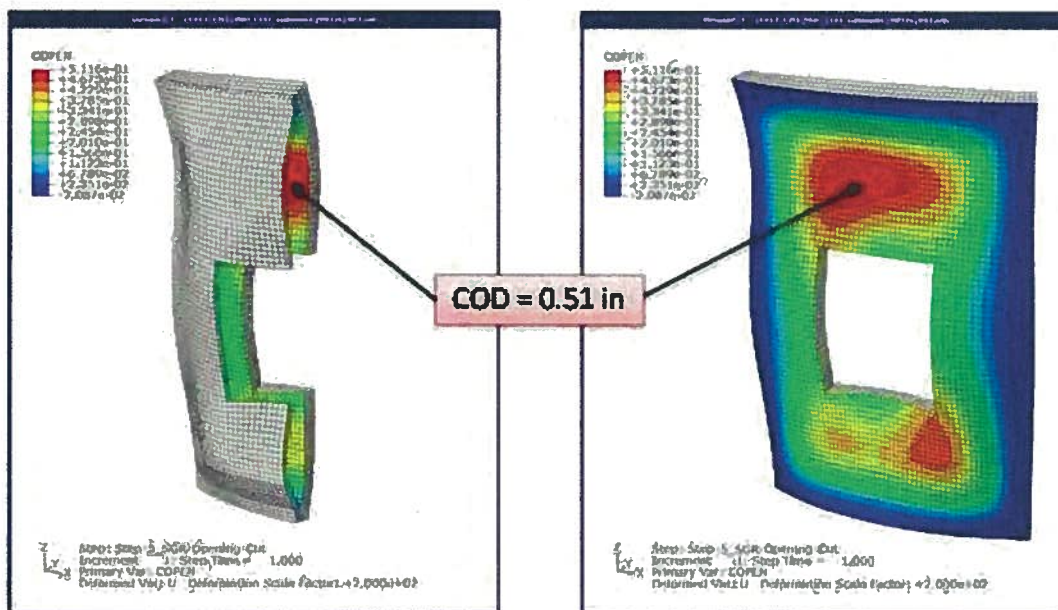


Figure 7.13 Crack Opening Distance (COD) after Concrete Removal – Step 5.
Note the width of the crack increased by about 10% due to concrete removal. Concrete removal does cause an increase but not a significant one.

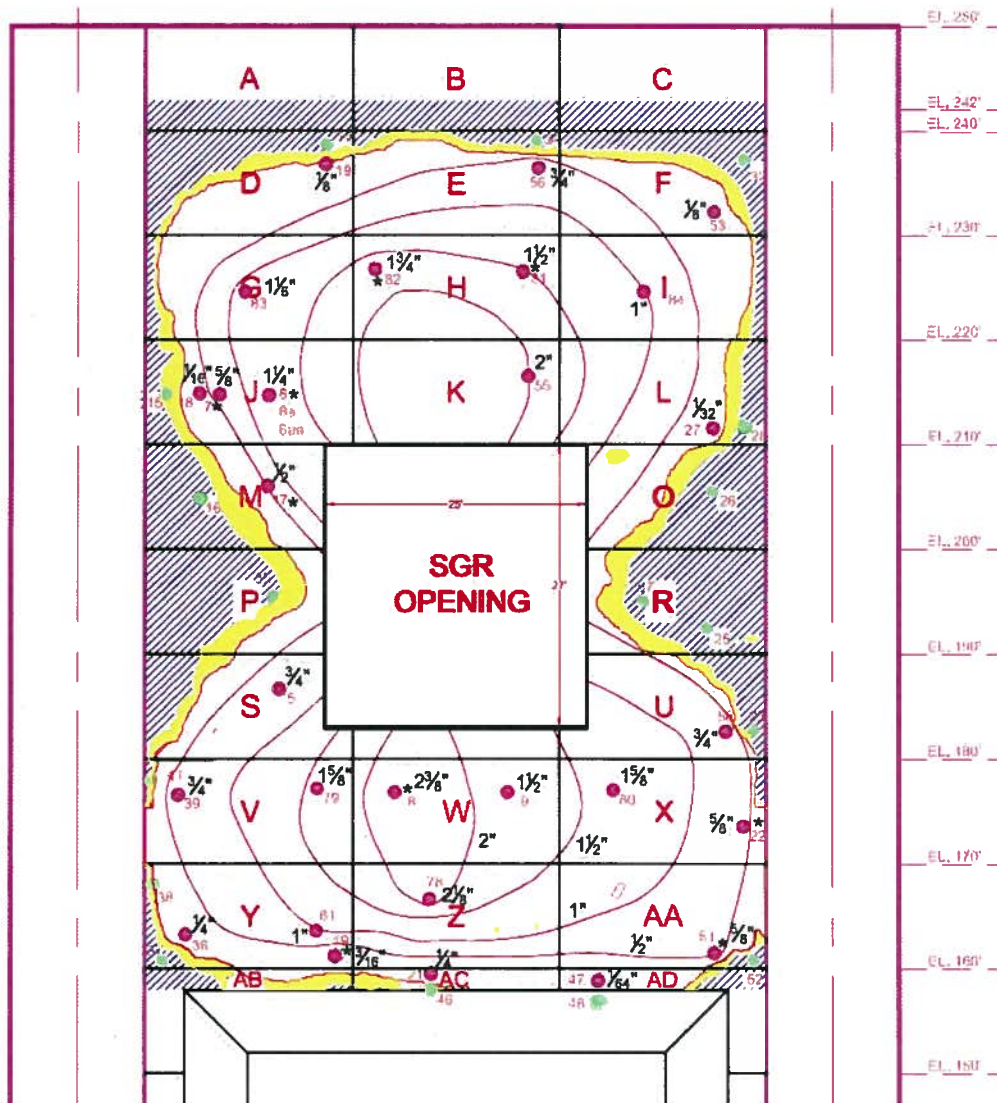


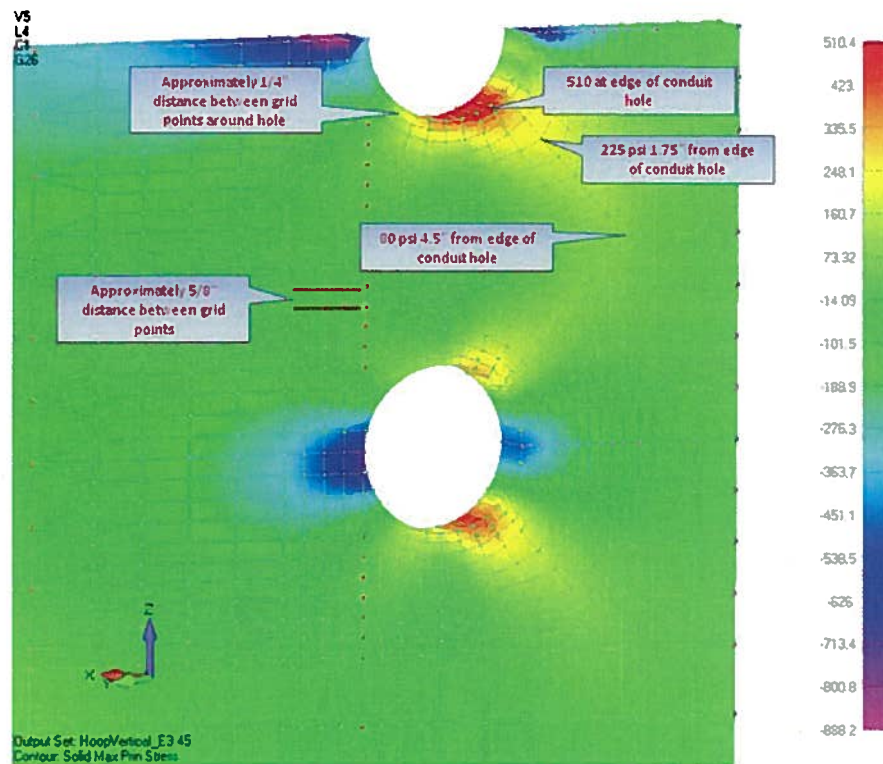
Figure 7.14 Plot of delamination damage in Bay 34. Shown are the measurements of the delamination gap both by impulse response test and by core bores.

Figure 7.14 displays the amount of separation due to delamination that was measured in bay 34. Compared with the radial displacement shown in Figure 7.13, the general agreement of the shape over the entire bay is an indication of the accuracy of the computer mode.

For completeness the effect of cutting out the concrete in the opening is also included in Figure 7.13, which increases the gap between with a mesh size of 1 square inch rather than the 1 square foot mesh of Abaqus Global.

At this point the analysis will switch from discussing large structures and will focus on small scale details. The scale will move from feet to inches. When the tendons were tensioned, the concrete underwent displacement which distributed the force exerted by the tendon into stress in

the concrete. Figure 7.15 shows the stress distribution around the horizontal tendons. Note the high compressive and tensile peaks on the edges of the horizontal tendons.



Expanded FEM *Between* Vertical Conduits – Lockoff Hoop & Vertical Loading, $E_c=3.45 \times 10^6$ psi

Slide 5 of 5

Figure 7.15 Stress contours for normally tensioned conditions in between intersections of a horizontal tendon with vertical tendons. (Section View)

The peak tensile stress in Figure 7.15 is about 500 psi in the area immediately next to the horizontal tendons near the top and bottom positions. In the absence of outside influences, the peak stress is just at the tensile capacity of the concrete and may indicate very small cracks at the top and bottom of each horizontal tendon sleeve hole. Figures 7.16 to 7.23 show the maximum principal stress added as a result of the bending of the containment wall.

The computer simulation is not a tendon-by-tendon scenario. Instead, it takes the total effect of de-tensioning all the selected tendons and divides it into twenty steps so each frame in the figures below corresponds to a 5% change in all of the tendons rather than 100% of one tendon. The overall effect is unchanged, but some special effects may be lost by this technique.

NON-PROPRIETARY VERSION

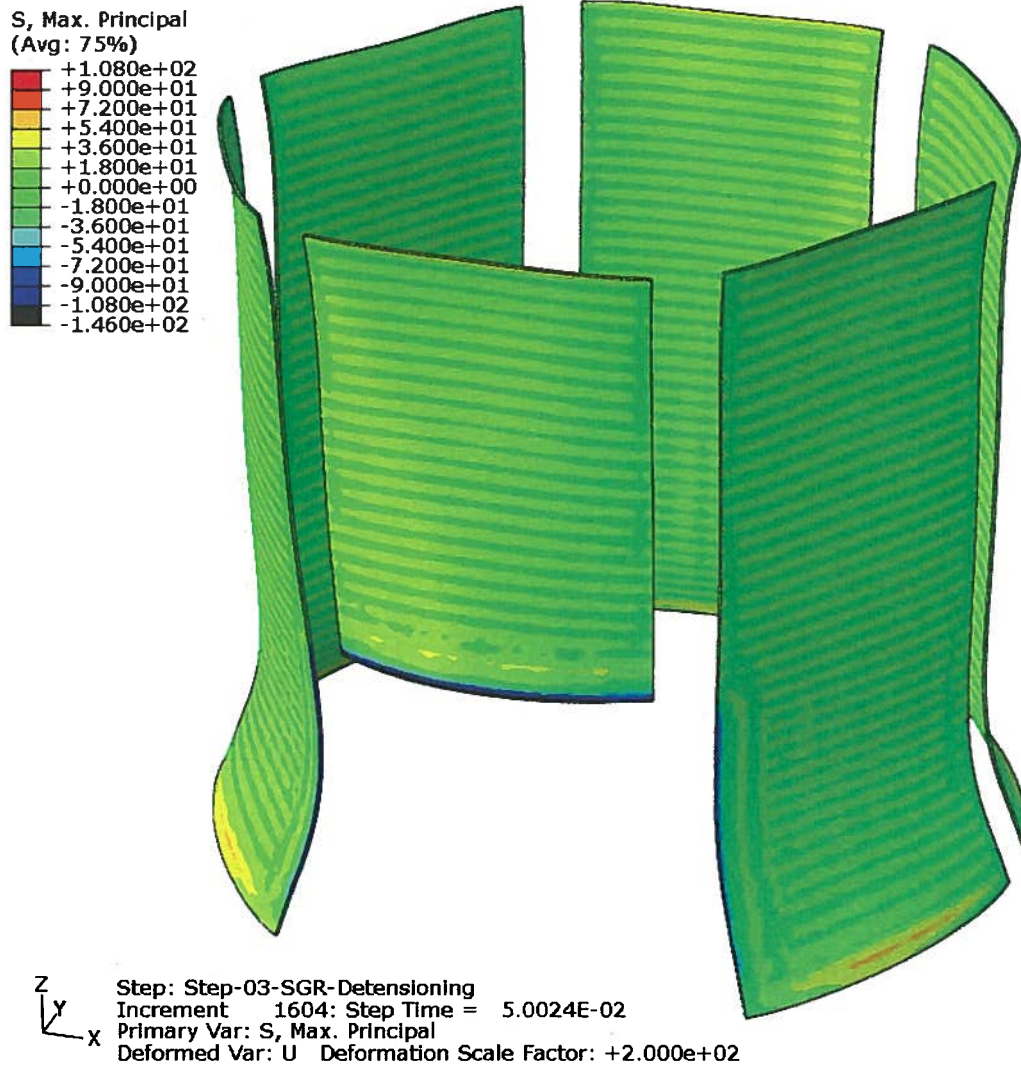


Figure 7.16 Step 1 of 20 time-steps in simulating the SGR de-tensioning.
Maximum principle stress (psi)

NON-PROPRIETARY VERSION

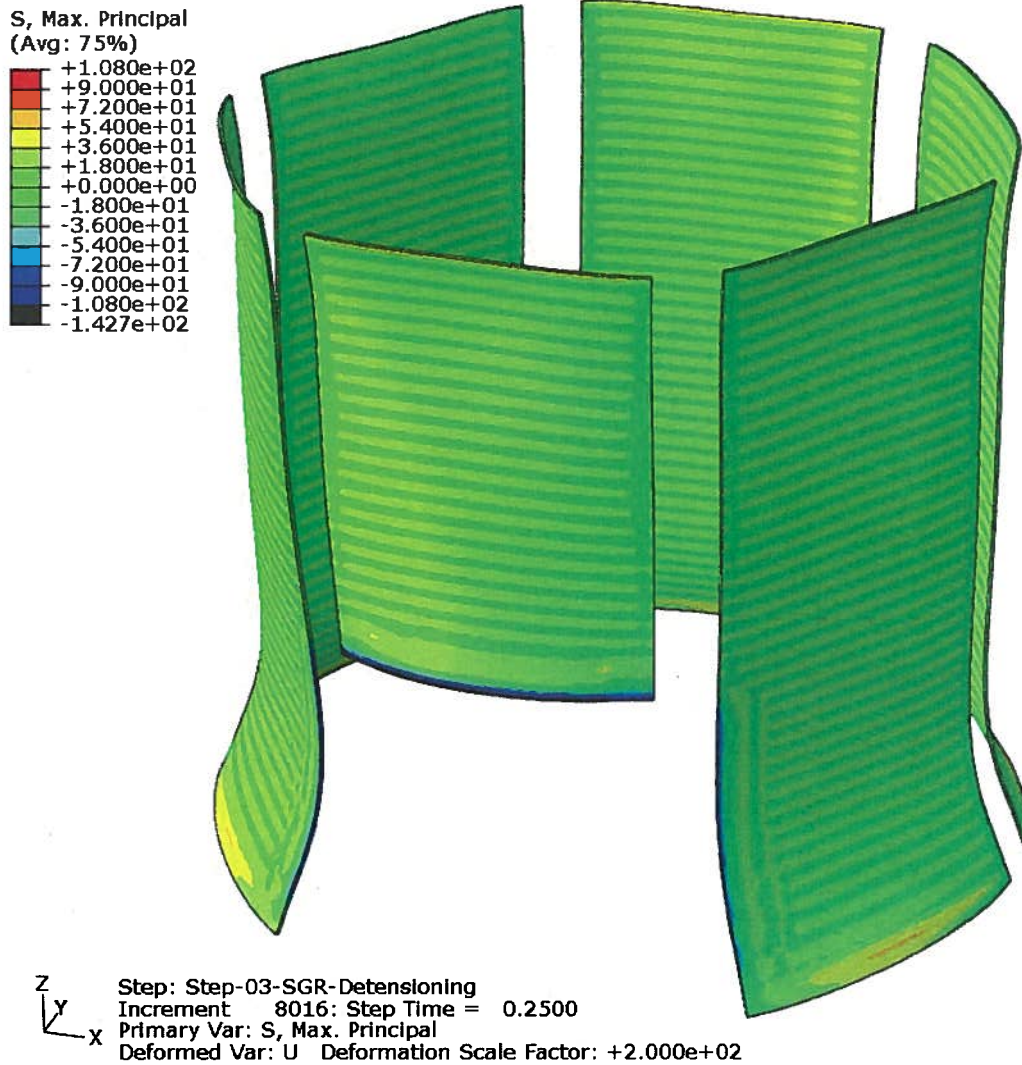


Figure 7.17 Step 5 of 20 in simulating the SGR de-tensoning.
Maximum principle stress (psi)

NON-PROPRIETARY VERSION

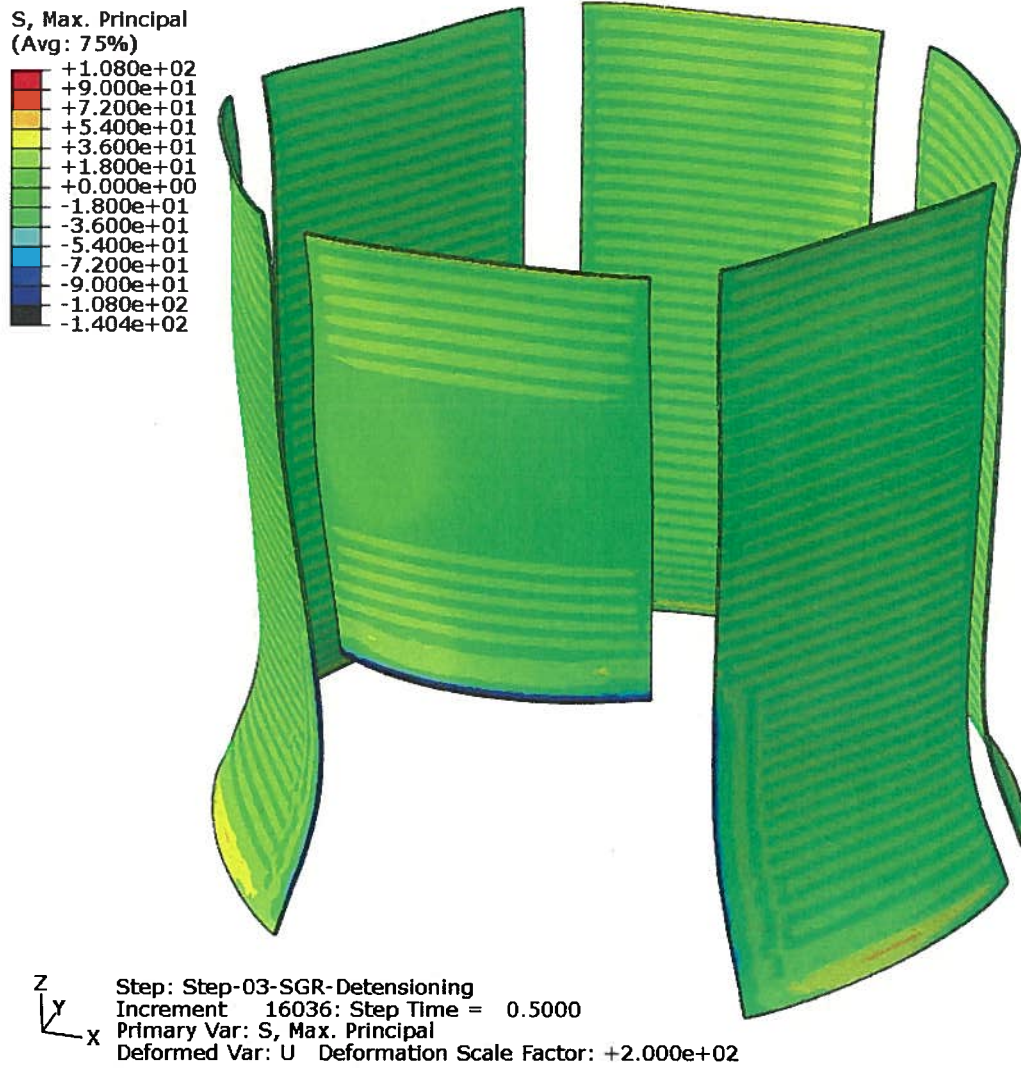


Figure 7.18 Step 10 of 20 in simulating the SGR de-tensioning.
Maximum principle stress (psi)

NON-PROPRIETARY VERSION

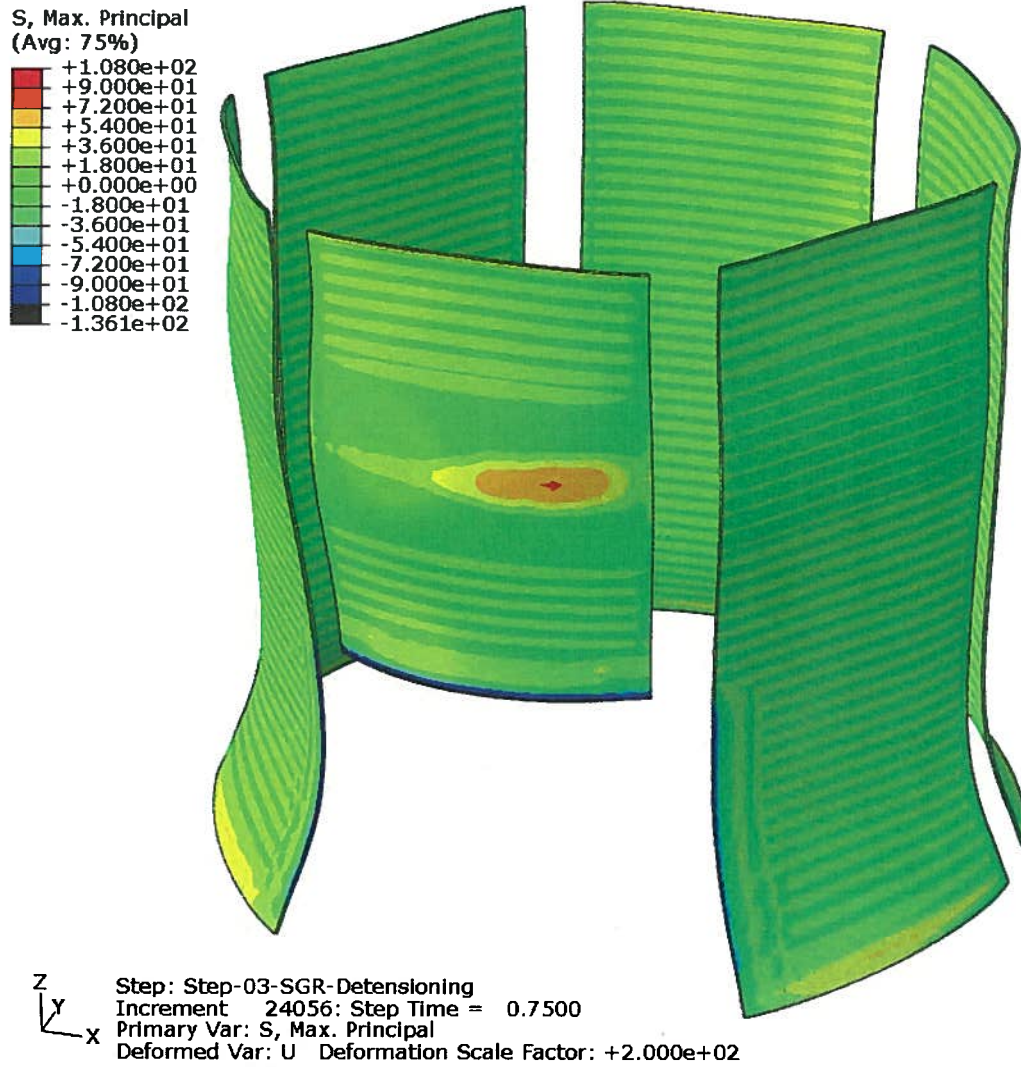


Figure 7.19 Step 15 of 20 in simulating the SGR de-tensioning.
Maximum principle stress (psi)

NON-PROPRIETARY VERSION

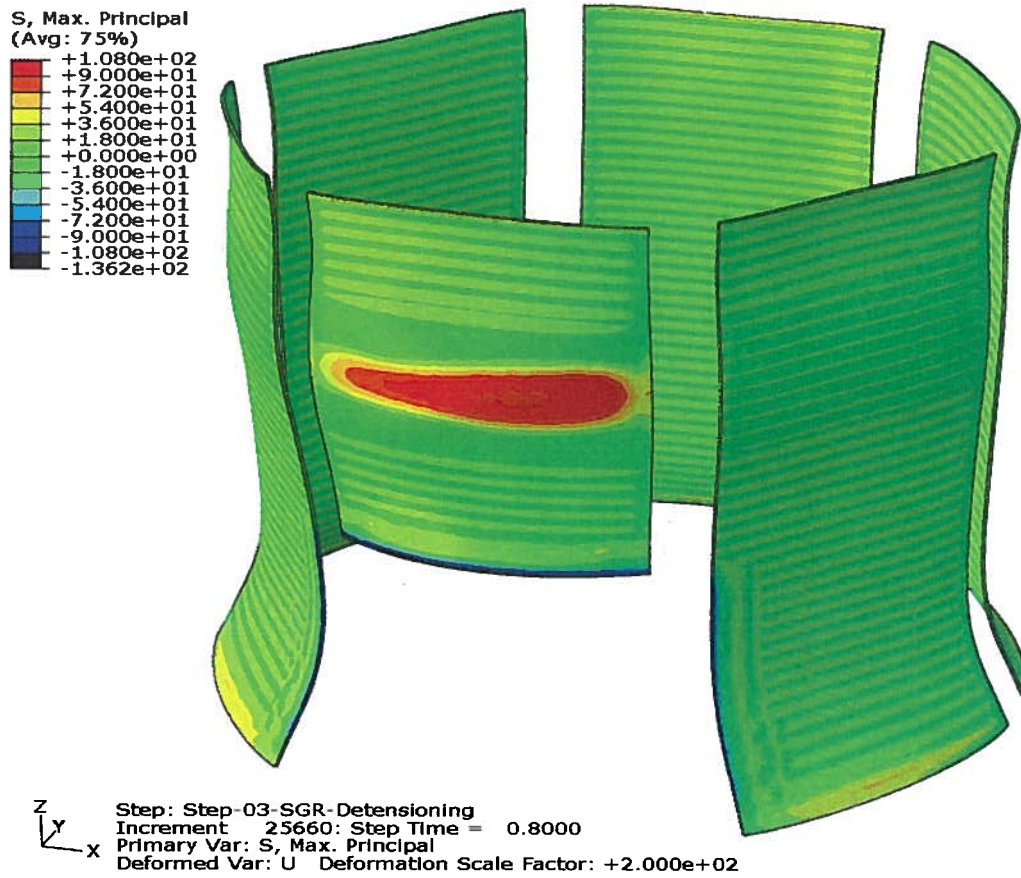


Figure 7.20 Step 16 of 20 in simulating the SGR de-tensioning.
Maximum principle stress (psi)

NON-PROPRIETARY VERSION

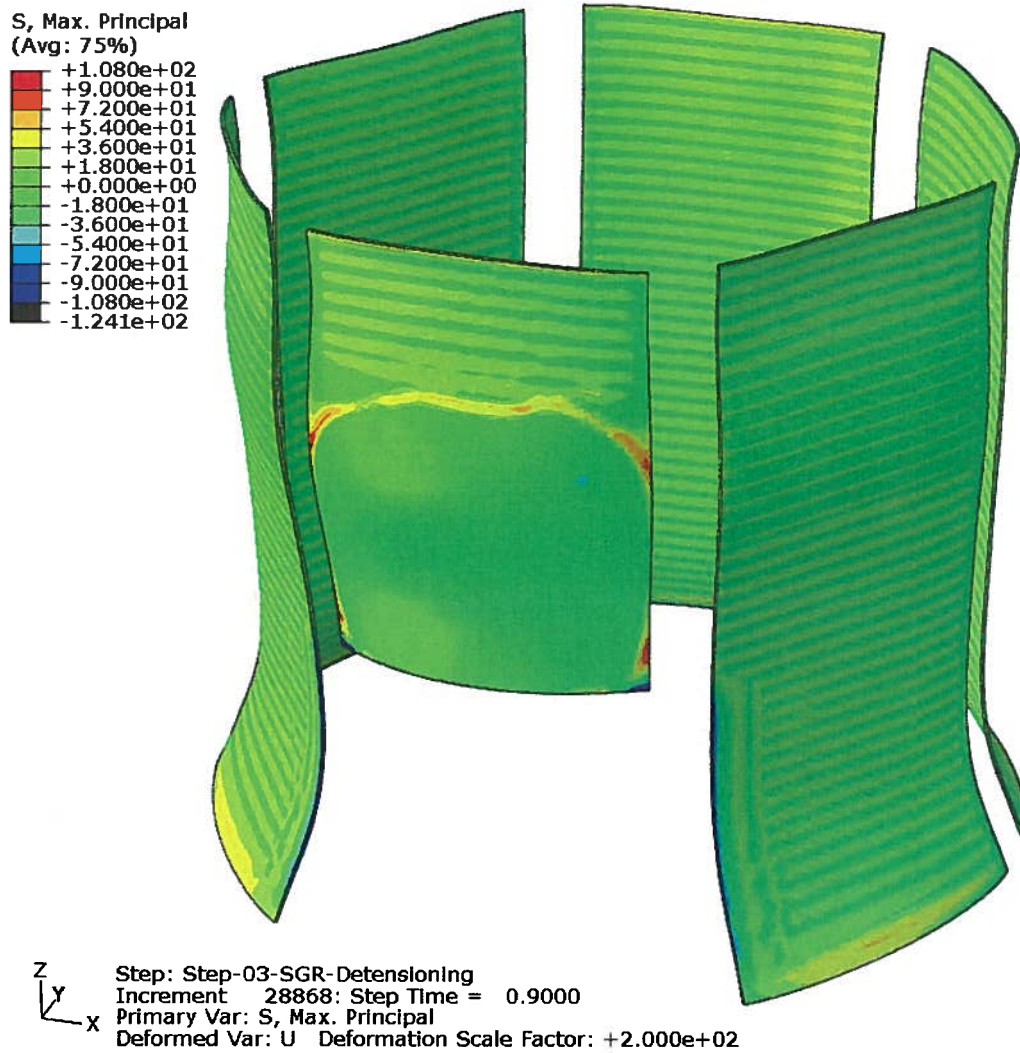


Figure 7.21 Step 18 of 20 in simulating the SGR de-tensioning.
Maximum principle stress (psi)

Note that at this step delamination has occurred and the stress has been relieved which can appear to be a relaxation of stress.

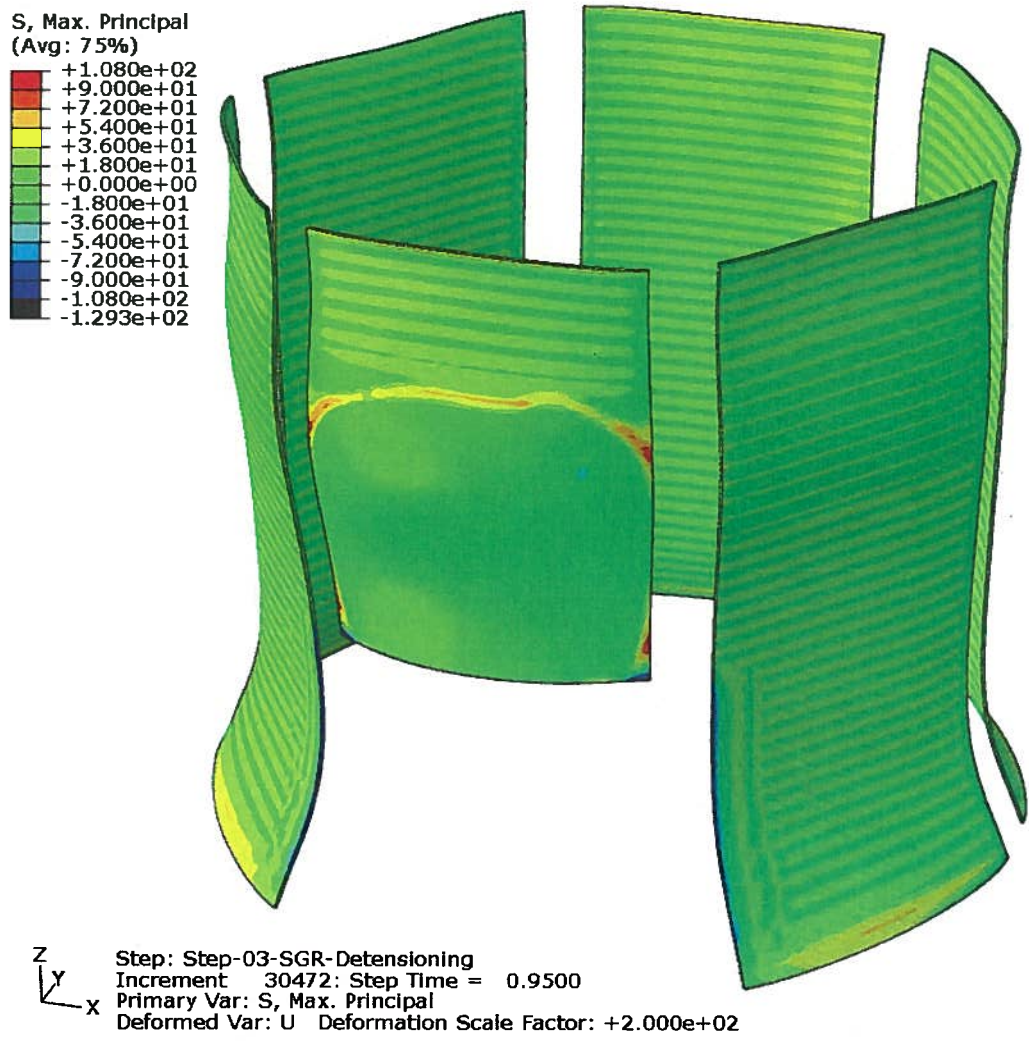


Figure 7.22 Step 19 of 20 in simulating the SGR de-tensioning.
Maximum principle stress (psi)

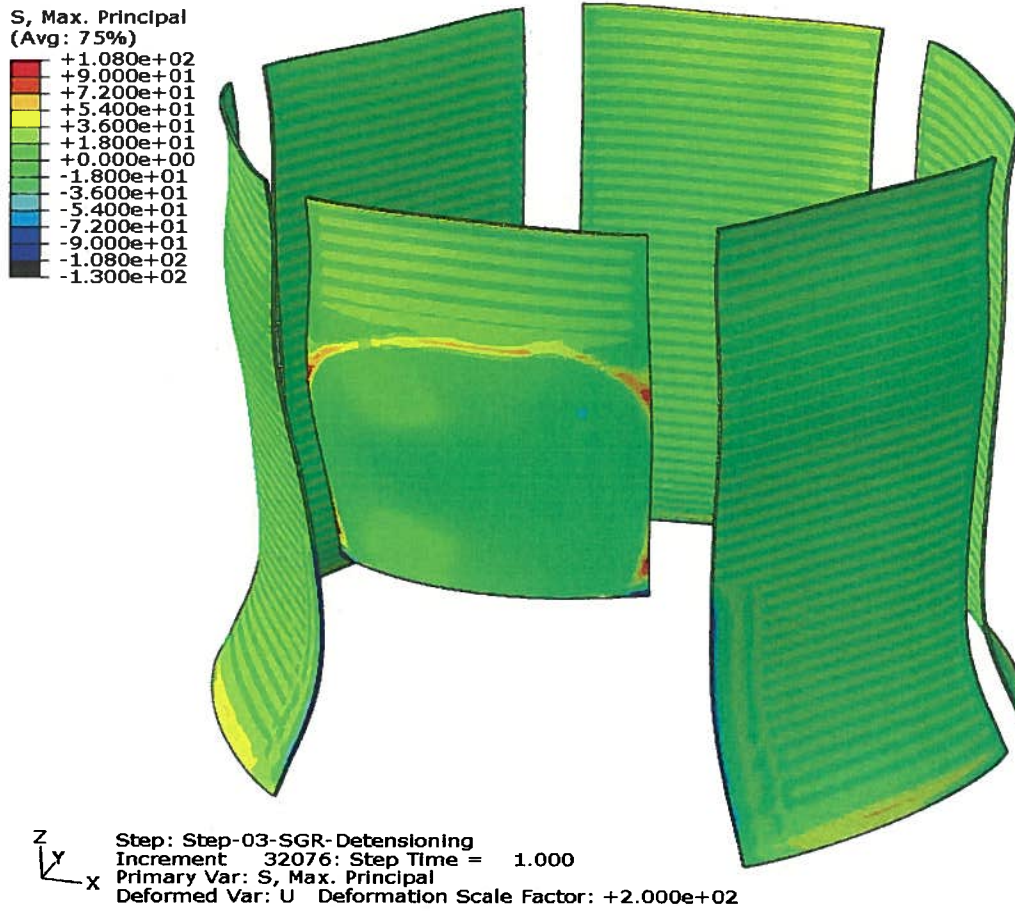


Figure 7.23 Step 20 of 20 in simulating the SGR de-tensioning. Simulation Complete.
Maximum principle stress (psi)

Figures 7.24 and 7.25 show the azimuthal shape and the vertical shape of the bulge. Figure 7.24 is a profile of bay 34 taken along its circumference at elevation 196'. Figure 7.11 was a profile taken at the middle of bay 34 going vertically so that between them both cross-sections are illustrated.

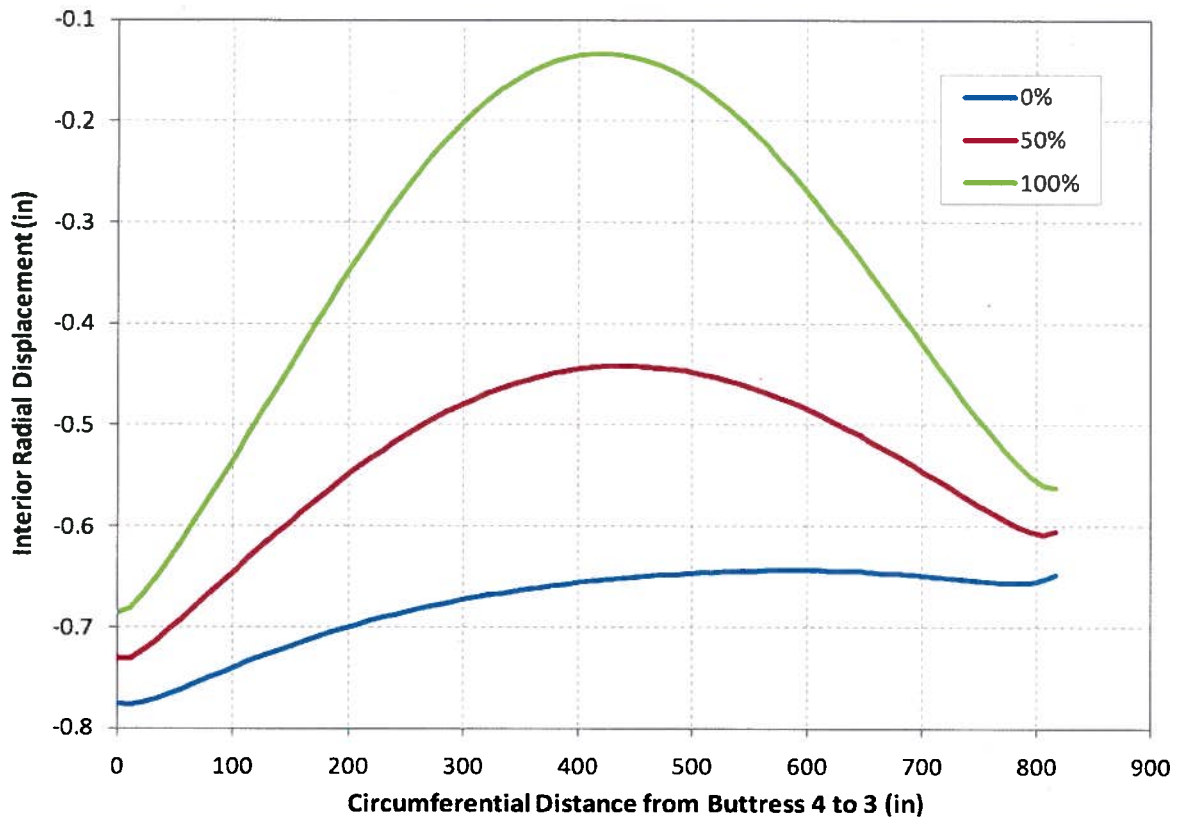


Figure 7.24 Azimuthal dependence of Bay 34 post SGR de-tensioning.

The asymmetric response in Figure 7.24 is due to an asymmetry in the dome tendon attachment arrangement that was correctly reflected in the model.

Figure 7.25 is a different version of the radial displacement as a function of elevation. It is a relative plot of displacement (0 is fully tensioned and 1 is fully un-tensioned) showing the displacement of one location to the next if there were no curvature prior to de-tensioning. It is idealized to show the relative displacement due only to de-tensioning tendons and the various plots are based upon the actual SGR de-tensioning sequence. Step 8 and step 12 both show an irregularity which is caused by skipping tendons so that a tendon remains tensioned after those around it have been de-tensioned.

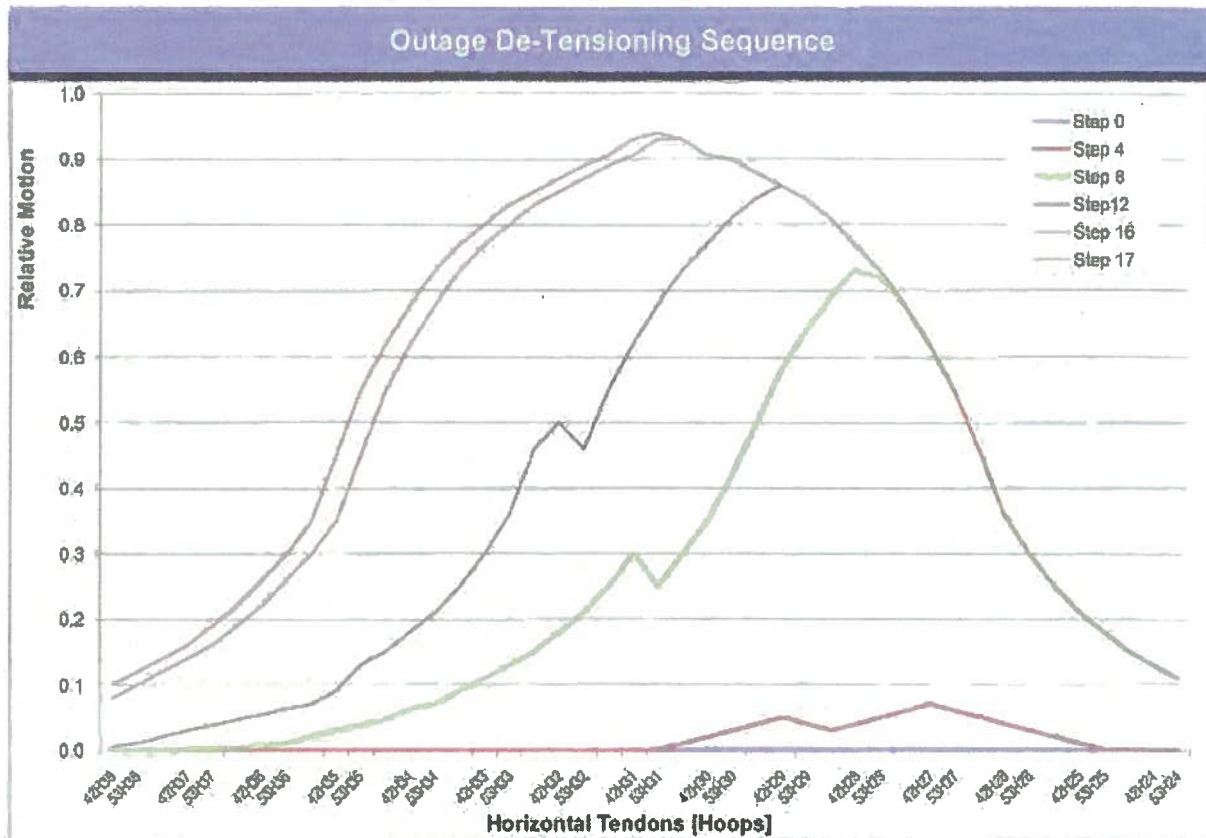


Figure 7.25 A Plot of the radial displacement in Bay 34 as SGR tendon de-tensioning progressed. The full displacement was 0.5”.

The information below helps correlate de-tensioning steps to calendar dates. The first step commenced the de-tensioning of tendons, which extended over several days. This is followed by the removal of the concrete in the SGR opening. Dates, times, and photographs of events as they unfolded are also included.

On 9/26/09	four vertical tendons were de-tensioned.	Total	4
On 9/27/09	six tendons were de-tensioned.	Total	10
On 9/28/09	six tendons were de-tensioned	Total	16
On 9/29/09	five tendons were de-tensioned	Total	21
On 9/30/09	two tendons were de-tensioned, the hydro-laser demonstration began, followed by two more horizontal tendons being de-tensioned	Total	25
On 10/1/09	the last two horizontal tendons were de-tensioned	Total	27

The conclusion of the computer simulation is that the de-tensioning scope and sequence used resulted in an oval shaped bulge in the bay 34 wall and created stresses in excess of the tensile strength of the concrete which delaminated as a result.

NON-PROPRIETARY VERSION

These results were generated from the Abaqus Global Model and the discussion about peak stress values as a function of model cell size in Attachment 1 applies here.

You will note that the maximum principle stress seems quite low. The global model assumed a tensile capacity of 108 psi to accommodate the coarse mesh being used. The next step is to reduce the mesh size and assume a material property closer to tested values. This is done below.

The tensile capacity assumed for the detailed mesh analysis below was 360 psi.

CRACKS OCCUR:

Cracking and then delamination began at some point in the de-tensioning and concrete removal process. Figures 7.26 to 7.29 show the results of the detailed Abaqus sub-model assuming tensile capacity of 360 psi. DAMAGET is a damage scale, a numerical measure of the ability of the concrete to pass load. The range is 0 to 1.0 where pristine material is 0 and fully fractured material is 1.0 and can pass no load.

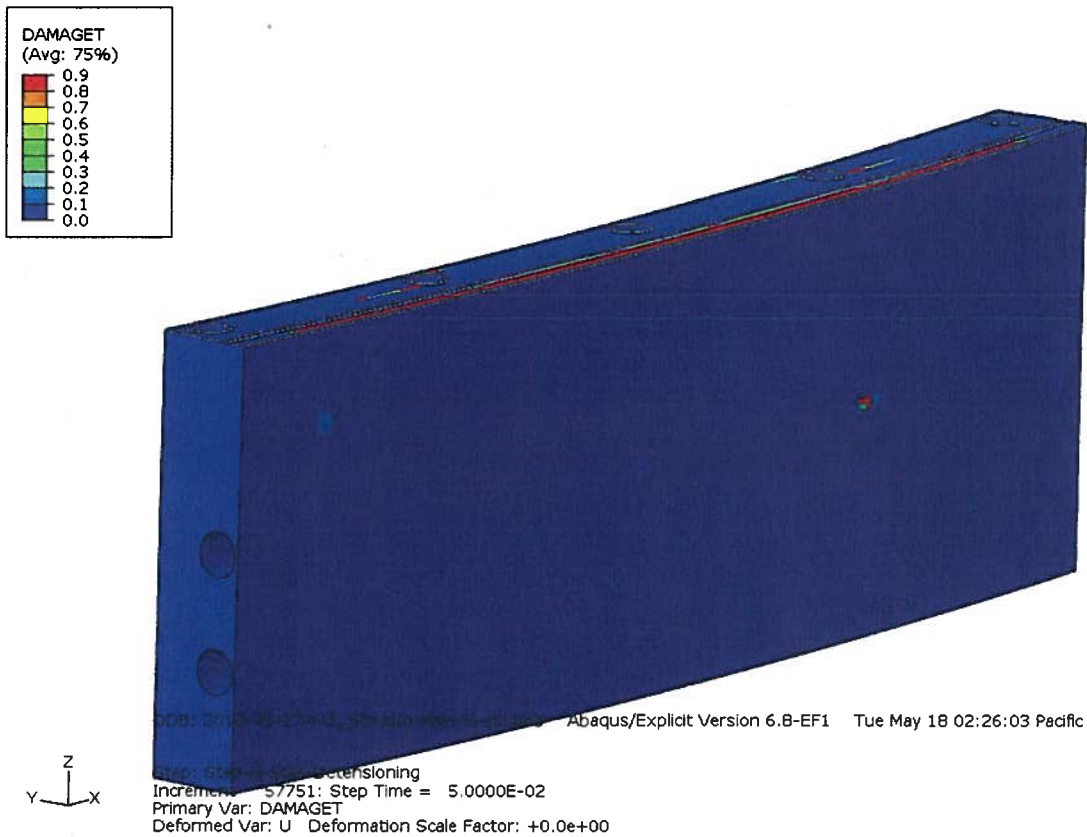


Figure 7.26 A Plot of a bay 34 wall segment approaching delamination.

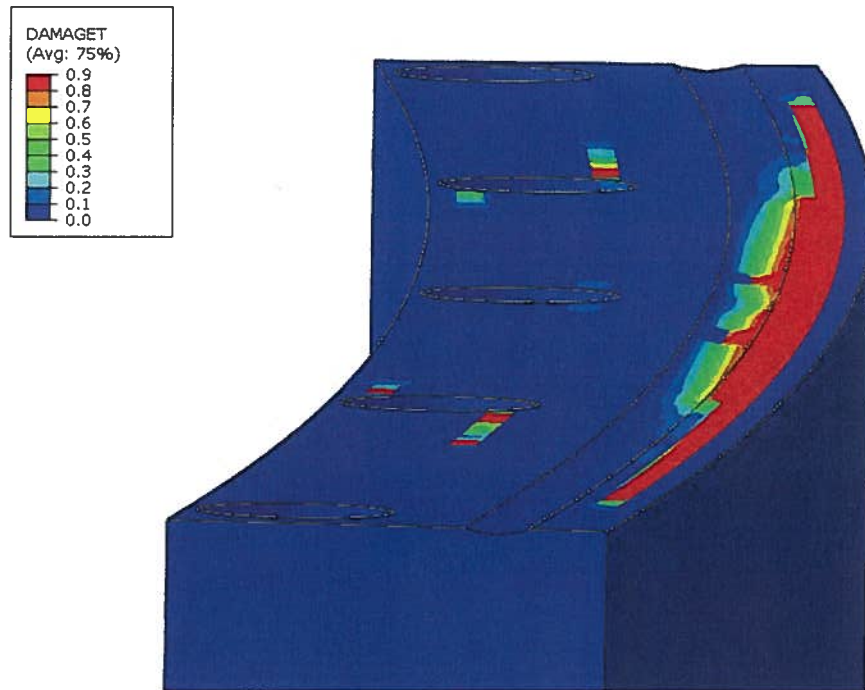


Figure 7.27 A Plot of a bay 34 wall segment delaminating

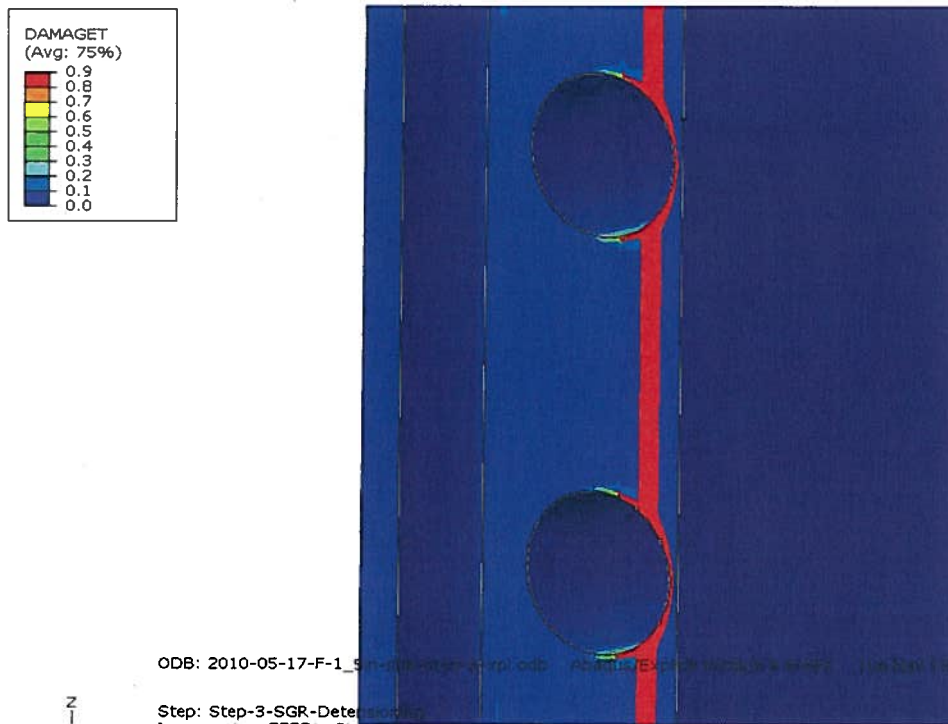


Figure 7.28 A Plot of a bay 34 wall segment delaminating $F't= 360$ psi

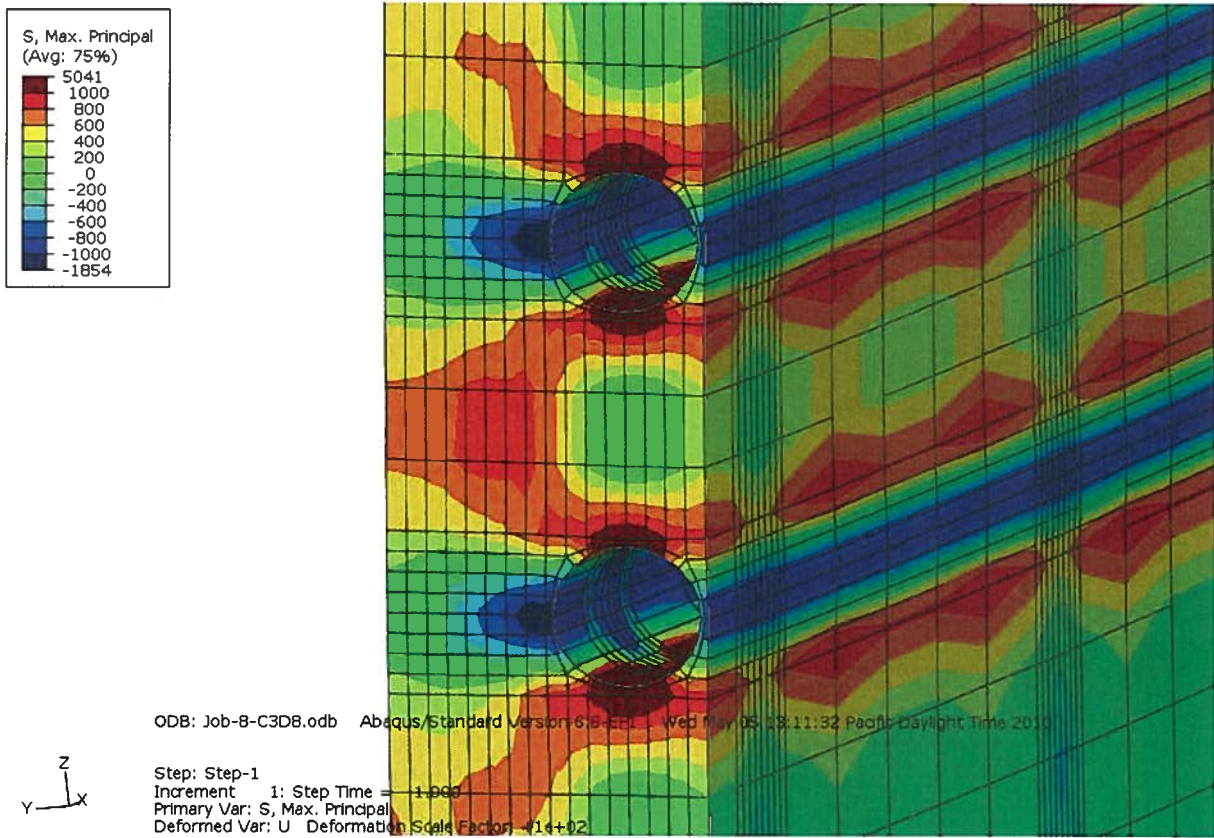


Figure 7.29 A Plot of maximum principal stresses in delamination. F't =360 psi

Sheet Delamination:

Cracking occurred in the area of the SGR opening. The cracks then propagated to form the unique hour glass shape in bay 34. Figure 7.25 shows a vertical slice through the bulge that formed in bay 34. The total deformation increases sharply as the total number of de-tensioned tendons increases. The absence of this transition in a de-tensioned environment is what prevented cracking in the neck of the hour glass.

Spontaneous propagation of a crack requires a tensile stress at the tip of the crack which exceeds the tensile capacity of the material. The cracks that spontaneously propagated were caused by stresses in the concrete caused by removal of the prestress force loading locally at that location. The cracking boundary was approached that either limited the deformation which drove the cracking (such as at a buttress) or limited the tensile stress involved (such as a region of de-tensioned tendons).

Figures 7.27 and 7.28 shows the Abaqus Detailed model prediction of delamination assuming tensile capacity of 360 psi. The peak stress locations on the top and bottom of the horizontal tendons extend out under the high radial tension conditions until they connect with the next tendon hole.



Scenario Validation:

Following is a summary of the failure scenario. Seventeen tendons from elevation 183' to 210' are de-tensioned. Ten vertical tendons, centered on azimuthal angle 150 degrees, are also de-tensioned. Generally the vertical tendons were de-tensioned first. This creates an imbalance in the pre-stress loads on the containment building and a bulge develops in bay 34 centered on elevation 196' and azimuthal angle 150 degrees. The bays on the opposite side of the building curve inward. The analysis also indicates that initial tensioning causes more inward displacement of the middle of a bay than around the edges. No displacement scans were performed during the SGR de-tensioning but the plant remained in the partially de-tensioned condition until March, 2010 when it was largely de-tensioned for delamination repair work. The scope of the repair de-tensioning was to de-tension essentially all horizontal tendons in all bays from H17 to H44 (elevation 152' to elevation 239'). This de-tensioning was accomplished in eleven steps from pass 1 to pass 11. Laser scanning was performed after each pass from pass 4 to pass 11. Thus, the laser scan only captured part of the de-tensioning but it does afford a comparison between the expectations of the scenario and the actual response of the plant. The laser data is presented as the radial displacement change using the un-tensioned condition after pass 11 as the baseline, so outward motion is negative and inward motion is positive. The point-by-point detailed comparison is discussed in Attachment 4.

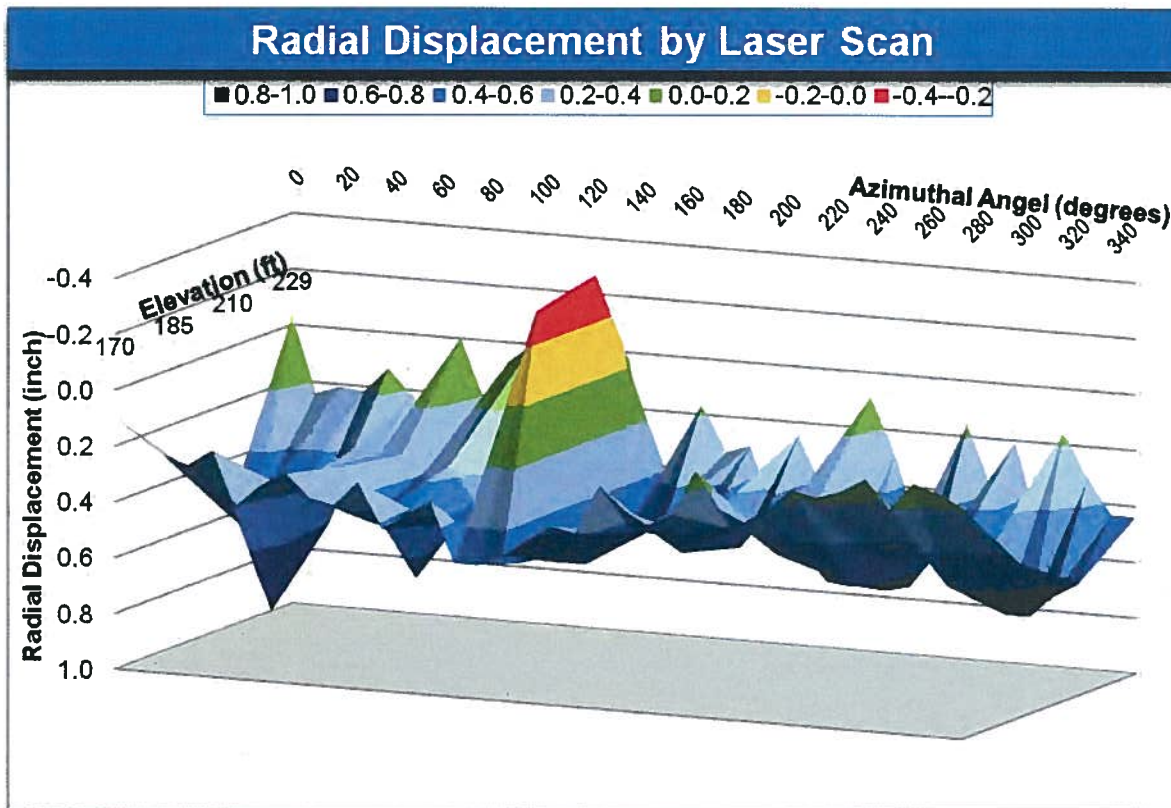


Figure 7.30 Three dimensional representation of radial displacement as a function of azimuthal angle and elevation.

NON-PROPRIETARY VERSION

In a sense, it is a snapshot of the conditions that existed at the end of the SGR opening project. The most prominent feature in figure 7.30 is the bulge at azimuthal angle 150 degrees. In addition each of the six bays is recognizable with its edges relatively fixed and its center sections bowed inward under tendon tension. Please note that these data indicate a change in displacement rather than an absolute displacement. Almost all points moved outward as the containment was de-tensioned in March, 2010. The notable exception was the area immediately around the SGR opening.

A large amount of additional benchmarking of computer models was performed using building data during de-tensioning. This is discussed in [Attachment 2](#).



8. ROOT CAUSE AND CONTRIBUTING CAUSES

Summary Conclusions:

The construction of a temporary containment opening has been accomplished successfully numerous times. PII has determined that the CR3 delamination did not exist prior to the SGR activities of de-tensioning and concrete removal. Rather, the delamination appears to have been caused by the combination and interplay of (1) certain design features of the CR3 containment structure; (2) the type of concrete used in the CR3 containment structure and (3) the acts of de-tensioning and opening the containment structure. Through a state-of-the-art computer model that PII developed, and using data and information specific to CR3 which PII was able to gather after the delamination had taken place, PII was able to determine that none of the individual contributing factors to the delamination, taken alone, would have caused delamination to occur. Rather, the complex interplay between all the contributing causes led to the delamination as discussed in detail in this report.

Despite the complex interplay of unrelated factors, it is possible to identify a root cause whose elimination will ensure the event will not be reproduced. That root cause was the scope and sequence of tendon de-tensioning associated with the containment SGR activities which generated additional stress beyond the capacity of the original design. The additional local loading exceeded the fracture capacity of the concrete and resulted in cracking along the line of least concrete area available for resistance. As the cracks propagated and joined, delamination occurred over a wide area. The O&P evaluation concluded that the inability of industry accepted tools to predict delamination was the programmatic root cause of the event. PII found that six methodology improvements were needed to accurately analyze the containment response.

Corrective action has been identified to address the issue at CR3.

Failure Mode Evaluation:

The purpose for performing a root cause evaluation is to fully identify the scope and conditions under which the failure took place so that corrective actions to prevent recurrence may be taken. The root cause is that single item which, if effectively corrected will ensure the event will not be repeated. Viewed in that light, PII has considered the individual FMs.

In general, the contributing conditions that have been identified are discussed in the context of delamination rather than fulfillment of the specifications established in the original design. The design and materials, as originally delineated, were sufficient to meet the requirements of a fully constructed containment structure.

FM 1.1 Excessive Vertical and Hoop Stresses - The stresses in question are inherent in the containment design and could not be changed significantly without rebuilding the structure. It is also not clear that modification of these stresses alone would preclude a repeat failure given the additional stresses imposed by some tendon tensioning/de-tensioning sequences.

FM 1.2 Excessive Radial Stresses/No Radial Reinforcements - This FM contributed to the event and radial reinforcement is recommended in the repair of the bay as it is an effective modification and can be implemented practically. However installing radial support is not

practical as a general solution because it would require rebuilding of the structure and may not, by itself, preclude recurrence.

FM 1.15 Inadequate Design Analysis Methods For Stress Concentration Factors- PII concludes that this FM was a contributor because high stress concentrations exist at the tendon sleeves. However, it is impractical at this point to change the design.

FM 2.12 Inadequate Strength Properties - This FM addresses the variability of measured strength from concrete cores. None of the strength tests of core samples indicated concrete below the required design strength. Because the Bay 34 concrete currently in place cannot be practically changed short of being removed, the strength properties, while an important consideration, cannot be a root cause.

FM 3.4 Inadequate Aggregate - The limestone aggregate used in the structure contributed to the delamination because of its properties. At this point, the FM may be taken into consideration when repairing bay 34 but otherwise it is impractical to replace the aggregate.

NOTE: The FMs existing at the time of this evaluation are historical and the containment met the requirements for normal and design basis conditions as a containment structure.

FM 7.3/7.4 Inadequate De-tensioning Sequence and Scope – the order of tendons that were de-tensioned and the selection of which and how many should be de-tensioned.

An expanded scope and sequence was developed in March, 2010 and it successfully de-tensioned the containment without delamination in the other bays.

FM 7.5 Added Stress Due to Removing Concrete - Photographic evidence proves the containment was cracked before any significant concrete removal occurred. However, concrete removal made stresses worse and so did contribute to the overall delamination. It can't be the root cause because tensioning and de-tensioning are pre-requisites for concrete removal but concrete removal alone will not preclude delamination if an inadequate sequence or scope of de-tensioning occurs.

In conclusion, and based on all the factors and information which will be discussed in the following sections, PII has determined that the immediate cause of the delamination event was the addition of stresses as a result of the containment SGR activities resulting in additional stress beyond original design and structure capacity. The added load exceeded the fracture capacity of the concrete and resulted in cracking along the high stress line connecting the horizontal tendons. As the cracks propagated and joined, delamination occurred over a wide area. Despite the complex interplay of unrelated factors, it is possible to identify a root cause whose elimination will ensure the event will not be repeated. That root cause is an inadequate scope and sequence of de-tensioning of containment tendons.

Frequently Asked Questions:



This section provides a convenient overall summary of the event in the form of the questions typically asked by people unfamiliar with the event.

1. What happened?

As a part of the SGR project, a series of horizontal and vertical tendons were de-tensioned in bay 34. For the particular tendon de-tensioning sequence selected for CR3 SGR opening, tensile stress is created at the interface between tensioned and de-tensioned tendons and increases with the number of de-tensioned tendons involved. As the number of de-tensioned horizontal tendons increased the load was amplified until it exceeded the fracture capacity of the concrete and cracking developed between the horizontal tendons. Continued de-tensioning and concrete removal exacerbated the cracking so severely that the cracks began to propagate spontaneously, growing together to form a delaminated sheet.

2. Why hasn't this happened elsewhere during SGR activities?

To some extent it has happened before in the form of dome delaminations assumed to be during initial tensioning of tendons. In order for delamination to occur at CR3 four factors must exist. All four are necessary and none of the contributing factors is sufficient to cause delamination. The factors are:

- ◆ Lack of radial reinforcement(No Radial)
- ◆ High stress peaks due to large tendons and wall design (Tendon Large)
- ◆ Certain material characteristics (Materials)
- ◆ Large tensile stress - typically associated with the interface between several tensioned tendons and several de-tensioned tendons (typically during SGR) (De-tensioning)

Of the peer plants considered only CR3 had all four factors.

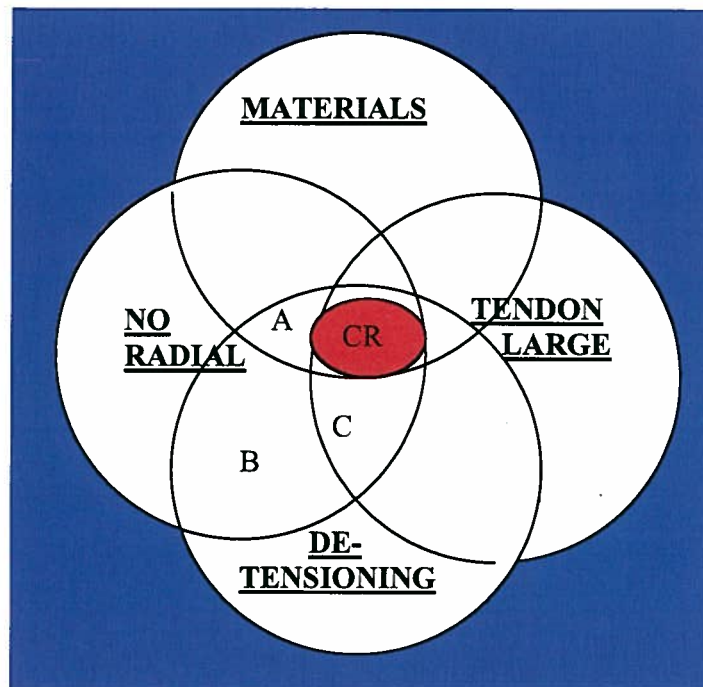


Figure 8.1 Venn diagram of plants with critical characteristics. A, B, and C are similar plants.

3. Why didn't this happen before at CR3?

The particular tensile stress generated is a very complicated function. During initial tensioning, the entire containment was involved rather than one concentrated band in one spot of the containment wall.

4. Why wasn't the damage limited to the small area of de-tensioned tendons?

The containment design is such that, given a large enough crack, the crack will grow spontaneously and will only stop when it approaches a boundary (such as a buttress) which limits the strain driving the delamination, or when it reaches an area of de-tensioned tendons. De-tensioned tendons allow the concrete to move so that their internal strain is reduced, and that strain is what drives the delamination.

5. Why did bay 34 delaminate in an hour glass fashion with the largest cracks centered above and below the opening?

All else being equal, the delamination would have occurred all around the bay (though inhibited at the edges). However, delamination did not occur in two symmetric isolated spots. Those spots form the neck of the hour glass and did not delaminate because the horizontal tendons in that area were de-tensioned. The tensile stress is highest in the center of the bay where the tendons most deform the concrete so the largest cracks would be in that area. The neck area has limited displacement due its location near the edge of the bay and to being in the de-tensioned tendon zone.

6. Is there anything unique about bay 34 that made it more sensitive to delamination?

Nothing of significance was found to set bay 34 apart from the other bays, though it is different in a couple of ways. The equipment hatch effectively shortens the bay but the delamination issue

NON-PROPRIETARY VERSION

occurred far enough away from the equipment hatch that it was not a contributor to the event. Bays 34 and 45 see daily thermal cycling but analysis showed the impact was not significant.

7. Was the absence of a de-tensioned margin around the opening a contributor to the event?

Delamination occurred due to a combination of de-tensioning and concrete removal. A primary factor was the number of de-tensioned tendons that were located in a row.

8. What have we learned?

The de-tensioning for the repair work in March, 2010 required extensive iteration to develop a sequence that would not cause excessive stresses or further delamination. The re-tensioning after repair will require an analysis similar to the one performed for the de-tensioning. Also CR3 should limit the simultaneous de-tensioning of tendons unless a detailed analysis is performed to ensure stresses are acceptable.



9. RECOMMENDATIONS TO PREVENT RECURRENCE

CORRECTIVE ACTIONS TO PREVENT RECURRENCE

A. Capturing the Operating Experience

There is always the possibility that some future event will require changes to containment that are not currently anticipated. Programmatic requirements typically ensure such situations are flagged for special consideration.

A.1 Establish programmatic controls to prevent de-tensioning more than one tendon/group without a detailed analysis validated using CR3 delamination experience.

B. Repair De-Tensioning Analysis

In March, 2010 it was necessary to de-tension bay 34 so that delaminated concrete could be removed and replaced. As such, this represented the conditions addressed in recommendation items A and C. The specific action for this topic (B.1) was performed prior to de-tensioning and it is included here to maintain consistency between this report and the Progress Energy assessment.

B.1 Perform a detailed analysis of the tendon de-tensioning plan in support of the containment repair effort. Modify the plan as necessary and ensure the stresses show positive margin as validated using CR3 delamination data. (Performed successfully in March, 2010.)

C. Re-Tensioning Containment in R 16

Delamination is typically associated with the process of changing tendon tension on a large scale so the upcoming re-tensioning of the containment is relevant

C.1 Perform a detailed analysis of the tendon re-tensioning plan in support of the containment repair effort. Modify the plan as necessary and ensure the stresses show positive margin as validated using CR3 delamination data.

BETTERMENT ACTIONS

C.2 Monitor displacement of the RB walls during re-tensioning to confirm the building response relative to computer prediction.

C.3 Monitor the RB wall with strain gauges and acoustic instruments during re-tensioning to ensure responses are within established limits per the repair design documents.

D. Life Extension

Accumulated stress cycles can impact material properties over time. The impact of plant evolutions on these properties appears to be small but should be monitored over the projected life of the plant.

D.1 Perform a detailed analysis of the stress consequences of typical activities such as heating up and cooling down of containment in outages or solar heating of an entire bay. Ensure there is no cumulative impact with time.

E. Aging Characteristics

E.1 Establish an inspection plan to periodically monitor containment concrete condition to ensure there are no unexpected changes. The inspection should use Non Destructive Examination (NDE) such as Impulse Response mapping of the area and selective core drilling in areas identified as suspect by NDE.

E.2 Establish a monitoring program that evaluates the response of the installed containment monitoring sensors to ensure the two types of concrete in bay 34 are behaving consistently as an indication of good coupling.

10. ORGANIZATIONAL AND PROGRAMMATIC ROOT CAUSE

1. The central issue associated with the delamination was the inability of industry accepted tools to predict delamination. The only reasonable way to have identified this inability would have been to benchmark the codes against industry experience. Outside of numerous successful SGR projects, the only available experience was the dome delamination information at Turkey Point 3 and at CR3. Six methodology improvements were needed to accurately analyze the situation. Benchmarking of industry codes using the Turkey Point 3 dome delamination would not have clearly identified the issue relative to the CR3 containment walls. The root cause of the Turkey Point 3 dome delamination was found to be a combination of insufficient concrete contact area and unbalanced post-tensioned loads. The root cause of the CR3 dome delamination was radial stresses that combined with biaxial compression to initiate laminar cracking in a concrete having lower than normal direct tensile capacity and limited crack arresting capability. The root cause of the CR3 dome delamination is more directly applicable to a containment wall analysis. The materials involved in the CR3 dome and wall were the same. The specific radial stresses and biaxial compression would be different however. The distinction was that the dome involved all of the dome tendons as opposed to the SGR opening which was believed to only involve a limited number of vertical and horizontal tendons in part of one bay. In addition, there was uncertainty about when and under what circumstances the dome delamination occurred. Tendon tensioning may have been underway but it is only speculation. In addition, de-tensioning was viewed as stress reduction and so not a challenge to the concrete the way containment wide tendon tensioning would be.

Comparison of Turkey Point 3 Dome, CR3 Dome, and Possible Applicability
to SGR Project

Turkey Point 3 Dome	Crystal River 3 Dome	Applicable to CR3 SGR Project?
Insufficient Concrete Contact		Not Applicable
Unbalanced Tendon Loads	Possibly Involved Tensioning	Limited De-tensioning
Dome	Dome	Different than Wall
Initial Tensioning	Sometime Early In Life	After 33 years of Operation
	Concrete Material Properties	Applicable
	Bi-axial Stresses	Different Geometry

2. Given the industry success at performing temporary openings in containments using standard analysis tools there was no indication (other than 30 year old dome delamination data of questionable applicability) that the tools were non-conservative. Usually a scoping calculation that demonstrates a large margin of safety is adequate.

NON-PROPRIETARY VERSION

3. Post event research and modeling by PII determined that very rigorous application of typical industry tools would not have been able to accurately predict margin to delamination and therefore would have been insufficient to prevent this failure.

4. PII noted that six major breakthroughs in the development of a state-of-the-art modeling methodology were needed to obtain accurate results. Those six improvements are (1) use of fracture energy parameters, versus tensile strength, as failure thresholds, (2) modeling of visco-elastic effects of concrete creep, in conjunction with the fracture energy based fracture thresholds, to account for stress reversal effects (i.e., from compression to tensile), (3) use of a 360 degree, realistic whole containment modeling to reveal realistic containment displacements, (4) incorporate the creep fracture phenomenon around the sleeves to account for a lower tensile strength near the conduits (thus initiating small cracks which could be delamination initiation sites), (5) use of fine meshes (about 1.0 cubic inch mesh) to reveal local stress concentration for crack initiation, and (6) the use of a variable elasticity and fracture toughness based upon local strain. Without these breakthroughs in modeling, delamination cannot be accurately predicted with measured, realistic input parameters to the methodology.

5. Using such a validated model avoids the non-conservative results otherwise obtained. Since this corrective action is already implemented as a result of the technical root cause evaluation, no additional corrective actions are required.

11. REFERENCES



1. Moreadith, F.L. et al, "Delaminated Prestressed Concrete Dome: Investigation and Repair", Journal of Structural Engineering, vol 109, no. 5, May 1983, pp. 1235-1249.
 2. MPR Associates, "Crystal River Unit 3 Nuclear Power Plant Local Tensile Stresses in Containment Dome Resulting From Post-Tensioning Load", MPR-531, October, 1976
 3. Final Revisions to the Crystal River Unit No. 3 Reactor Building Dome Delamination Report, Docket No. 50-302, June 1, 1976
 4. Turkey Point Unit 3 Containment Dome, Delamination of the Dome Concrete During Post-Tensioning, Docket 5-250, U.S. Nuclear Regulatory Commission. (1972)
 5. Ashar, H and Naus, D, "Overview of the Use of Prestressed Concrete in U.S. Nuclear Power Plants", Office of Nuclear Regulatory Research, U.S. Nuclear Regulatory Commission, May 1994.
 6. Basu, P.C. et al, "Containment Dome Delamination", Transactions, SMiRT 16, Washington, DC, August 2001, Paper #1557
 7. Acharya, S. and Memon, D, "Prediction of radial stresses due to prestressing in PSC shells", Nuclear Engineering and Design, 225 (2003) pp 109-125
 8. Basu, Prabir and Gupthup, Vijay, "Safety Evaluation of Delaminated Containment Dome Re-Engineering" Transactions SMiRT , 16, Washington, DC, August, 2001
 9. PII Document, "Margin-To-Delamination Analysis of Proposed CR3 Detensioning Sequence Option 10 F, March 7, 2010
 10. Gilbert Associates Report 1930, "Crystal River Unit Three Nuclear Generating Plant Reactor Containment Building Structural Integrity Test", 12/7/1976.
 11. Saouma, V. et al, "Creep Fracture Tests of CR-3 Concrete", internal PII document in support of the CR-3 Root Cause Assessment. See Appendix 10 of this report.
-



ATTACHMENT 1: COMPUTER MODELING

Modeling Assumptions

The assumed values for physical parameters is an important consideration when evaluating the credibility of any computer model. To facilitate that evaluation, the results presented in this report are generally the output of the Abaqus global model or its sub-models. They consistently use the parameter values listed below. When this is not the case the parameters used for a specific figure will be identified with the figure.

To ensure full understanding of the delamination process at Crystal River, PII followed parallel paths in development of computer solutions. The conditions involved in the delamination event can be modeled using a wide variety of crack propagation techniques that will lead to significantly different conclusions. Because benchmarking is an important validation technique, the codes used in this computer analyses were benchmarked against the known plant response to the Structural Integrity Test performed in 1976. In addition, the computer model predictions were compared with containment interior laser scanning performed in March, 2010 during the de-tensioning that was done prior to repair bay 34. Benchmark comparisons are provided in [Attachment 2](#).

Pure analytic solutions for many material properties are limited to simple geometries and homogeneous materials. For more complicated problems the technique of choice is the computer based solution of simultaneous equations known as Finite Element Analysis (FEA).

FEA has been successfully used to simulate a wide variety of engineering situations for both spatial variation and time dependence. There are, however, some limitations. The first difficulty is that the computer code will not converge to a unique solution unless the time steps and cell dimensions are small enough to closely approximate a continuous solution. The second limitation is that the number of computer steps needed to obtain a solution grows geometrically with the number of time steps and computational cells used. Thus, there is a trade-off between the accuracy of the solution and the time needed to obtain the solution.

When the structure being analyzed is large and closely coupled, commonly used techniques must be augmented by combining highly detailed regions in the areas of interest with a larger scale model which sets boundary conditions for the detailed cells.

Analysis of the Crystal River containment found that the delamination ultimately depends on very complex local conditions that are impacted by the response of the building as a whole. As a result, PII created a series of computer codes to simulate the entire building and execute detailed calculations for the particular area of interest. The role that each code part played in the larger framework of the computer model is detailed below.

Immediately after the delamination event PII found that industry standard computer codes provided solutions which showed significant margin to delamination' when applied to CR3.

As an interim measure until more accurate modeling techniques could be developed, PII relied upon NASTRAN and its linear-elastic model to calculate local conditions and then Abaqus to evaluate the local conditions and determine if damage resulted. However, due to limitations in the model, it was necessary to assume a modulus of elasticity of

NON-PROPRIETARY VERSION

1.1E6 psi throughout the structure. While this assumption allowed the model to predict the onset of delamination it had significant uncertainty.

PII now uses an Abaqus Global model using a visco-elastic fracture model and a detailed sub-model for decreased mesh sizing to provide accurate stress predictions. There are four input values which can be adjusted to make the computer model output match the benchmark data. They are listed below

Parameter	Typical Value	Abaqus Global/Detailed	Impact
Tensile Capacity	500 psi	█*	Onset of Cracking
Fracture Energy	0.40 lbf/in	█*	Onset of Cracking
Elasticity Modulus	3.45 E6 psi	█	Radial Displacement
Creep Coefficient	2.2	█	Radial Displacement

*Note: Adjustments in Tensile Capacity and Energy reflect the analysis mesh size used.

The treatment of creep is an important consideration. Abaqus Global applies a creep coefficient for long term changes (such as 30 years of tensioned operation) but does not apply it for short term changes such as de-tensioning. The creep coefficient is used to modify the modulus of elasticity by the equation:

$$E' = E/(1+c)$$

where E is the measured coefficient of 3.45 E6 psi and if the standard creep coefficient of █ is used $E' = \text{█}$.

The effect you see is a shift in radial displacement over a long time period but no corresponding return immediately after de-tensioning. Refer to Figure 7.11. The Tensioned line is generated immediately after initial tensioning using $E = 3.45 \text{ E6 psi}$. The next line is Creep and this shows the gradual shift in radial displacement over time due to █ as a creep corrected elasticity. The remaining lines use $E = 3.45 \text{ E6 psi}$ because they occur over a few days. The result is that the de-tensioned state does not immediately return to the un-tensioned state that existed in 1973.

One measure of the precision of the modeling is the degree to which it is necessary to adjust the measured physical values in order to obtain good agreement with benchmarking. Unless indicated otherwise, the PII models use the typical values listed above.

PII was able to reduce the level of uncertainty by developing a linear elastic super-model, but this model still suffered from the limitations of linear elastic modeling, such as difficulty dealing with creep in concrete. The creep effect makes concrete respond more like a viscous fluid than an elastic solid in very particular conditions and unless the model is capable of applying the different properties selectively as appropriate to the situation, one set of properties must be applied throughout the model, which leads to non-physical material properties being used.

In response to these limitations, PII recently developed a Global Visco-elastic Abaqus model that selectively applies the appropriate creep response for the local conditions. The result is

NON-PROPRIETARY VERSION

appropriate calculation of delamination with realistic material parameters and radial displacements that agree well with benchmark data. The model uses the Lee-Fenves concrete damaged plasticity properties. The concrete Poisson's ratio used [REDACTED]. The model includes individual tendons and specifically models the steel properties of the liner, conduits, and rebar assuming steel elasticity of 29 E6 psi and a steel Poisson's ratio of 0.27.

The Abaqus global model is run using the sparse solver in Abaqus/Standard and the various sub-models are run in both Abaqus/Standard and Abaqus/Explicit. The global model provides displacement data to the edges of the panel sub-models and other sub-models, which further provide higher resolution of localized behavior. The driven sub-models include stress models and concrete damaged plasticity models, all within Abaqus.

Every curved tendon in the containment is modeled explicitly using embedded beam elements in the global model. The tendons are assigned the cross-sectional stiffness of the sleeves and loads are applied as described below. The beam sections are sized such that only the curved length that applies load to the concrete is modeled. Tendon forces are calculated and applied as line loads to the embedded beam elements. These values are ramped appropriately to account for designed loads, creep, and surveillance loads.

The dome is partitioned into four layers, representing the layers above, below, and in between the dome conduits. All 123 of the dome sleeves are modeled explicitly and at their respective as-designed radii. The dome conduits are not placed at an average radius or joined together directly. Instead, the solid continuum host elements' layer surfaces are aligned with the dome sleeve centerlines in order to improve accuracy and efficiency. The dome conduit "tails" are also modeled explicitly and aligned with the dome solid continuum element mesh. The dome sleeve tails are applied appropriate loading with respect to whether they belong to a subset of the dome tendon tails that are curved and apply either upward or downward force on the concrete.

[REDACTED]


[REDACTED]

The dome tendon lock-off loads are applied to an angled surface on the outer edge of the ring girder such that the total force balance is properly equilibrated. The angle of the lock-off surface is calibrated to ensure the sum of all the forces is zero.

Partitions are included in the structure to allow for the selective removal of concrete in the SGR opening, in the SGR delamination crack region, in the excavation regions of bay 34, and at the openings of the equipment and personnel hatches.

Rebar is included in both the global and sub-models. This is implemented using the *REBAR capability within Abaqus, which entails converting all of the host elements to solid continuum shell elements with stack directions (sweep directions) oriented radially. Sleeve and tendon host

elements remain as solid continuum elements and rebar host elements are implemented using continuum shell formulation.



Because the tendons are all modeled explicitly in both the global model and the sub-models, the tendon loads are added or removed individually as dictated in each de-tensioning or re-tensioning pass specification.

The elastic modulus of all the embedded steel is adjusted appropriately to account for the overlap in volume between the concrete and the steel. The liner is included explicitly in both the global model and all of the sub-models.

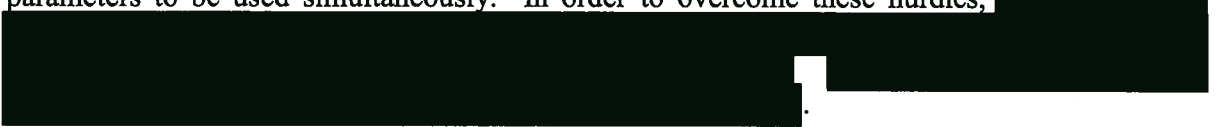
The global model has approximately [REDACTED]. The element size through the dome and cylinder cross-sections range from [REDACTED] in thickness. The various sub-models have on the order of [REDACTED] of freedom each. There are a total of [REDACTED] discrete geometric cells and [REDACTED] surface patches in the global model.

The global model dome has [REDACTED] elements through its cross-section, all of which are fully integrated solid continuum elements. The bay walls have [REDACTED] elements through each cross-section, consisting of both solids and continuum shells. Solid cells are meshed with hexagonal fully integrated –C3D8” elements and continuum shell sections are meshed with reduced-integration –SC8R” elements with 5 integration points.

A mesh study was performed on each region of the structure, including the dome, the ring girder, and the bay walls, which determine that the mesh response is converged.

Long term visco-elastic creep is calculated by the Abaqus solver [REDACTED]. Creep is calculated from the actual stress state after design-load tensioning, which accounts for local variations in the stress, rather than by applying an approximation such as a global average shrinkage strain.

The global displacements, stress state, creep law, and the concrete damaged plasticity parameters are all implemented into the sub-models. This results in two technical barriers: Abaqus does not normally allow both mapping of the stress state and sub-modeling to be used simultaneously; and, Abaqus does not normally allow the creep law and the concrete damaged plasticity parameters to be used simultaneously. In order to overcome these hurdles, [REDACTED]



The Abaqus Global model has four sections in the containment wall: a steel liner plate, an inner concrete cylinder, a hoop tendon sleeve layer, and an outer concrete cylinder. Curved sections of tendon sleeves are matched to the mesh. The global model uses about [REDACTED]. The sub-model uses [REDACTED]. If you refer to Figure 3.4 you will see the issue of detail. The average value of tensile stress is about 23

psi. It increases to 31 psi due to concrete displacement. [REDACTED]

[REDACTED] Until recently the resolution was to adjust the tensile capacity of the concrete to compensate for this. That is why a capacity of [REDACTED] psi was assumed in global calculations. It does not affect radial displacement but it does facilitate the delamination evaluation. With the creation of the detailed sub-model the peak stresses become more visible and a tensile capacity of [REDACTED] becomes appropriate. Note that even at a [REDACTED] inch mesh size there is still significant averaging of peak stresses occurring. [REDACTED]

[REDACTED] Recent analysis shows marginal improvement going from a [REDACTED] [REDACTED] such that the underestimation of peak stress by about [REDACTED]. Applying that factor to the assumed tensile capacity of [REDACTED] for an infinitely small mesh. That corresponds to the measured tensile capacity of CR3 concrete. The average direct tensile capacity measured in 9 samples was 448 +/- 73 psi. The average split tensile capacity measured in 10 samples was 594 +/- 59 psi and it is generally accepted that tensile capacity is 90% of the tested split tensile capacity. That gives 535 psi. Fracture energy is similarly impacted.

There are a number of ways to address the mesh issue. For radial displacements or general stress calculations, [REDACTED] mesh is sufficient to obtain realistic values. For scenarios which depend heavily on peak stress values one approach is to use a stress concentration factor. Recent comparisons indicate that for global Abaqus that factor would be about [REDACTED]. For the detailed sub-model it would be about [REDACTED]. Another way to achieve exactly the same result is to adjust the tensile capacity of the concrete. For events such as the onset of delamination, the details of the process are very sensitive to the peak stresses involved and fine mesh analysis is the best approach. Once initiated, delamination is less sensitive to peak parameters so the overall extent and width of cracking can be well described by a detailed sub-model or even the normal sub-model.

Liner

The liner is modeled using 3/8 in thick conventional shell elements with elements located on the inner surface of the concrete (R 780.375). Shell offset is used to account for correct placement of center section of the liner.



Figure A1.1 Containment steel liner model

Inner Cylinder

The inner cylinder is located from the liner at R 780.375 to R 810 (IR of hoop conduits). Two layers of continuum shell elements each with 5 integration point though the thickness are included for bending accuracy.



Figure A1.2 Containment inner cylinder (30" thick) model



Performance Improvement International

ROOT CAUSE ASSESSMENT CRYSTAL RIVER UNIT 3 CONTAINMENT CONCRETE DELAMINATION



August 10, 2010

NON-PROPRIETARY VERSION

This report is a Root Cause Assessment (RCA) of the Crystal River Unit 3 containment concrete delamination identified on October 2, 2009. The assessment was performed by Performance Improvement International (PII) at the request of Progress Energy.

Chong Chiu, PhD, Team Leader
Marci Cooper, Assistant Team Leader
Patrick Berbon, PhD, Assistant Team Leader
Ray Waldo, PhD, Assistant Team Leader
Avi Mor, Dr. Eng.
Joe Amon, PE
Henric Larsson
Tyson Gustus
David Brevig
Gary Hughes, PhD
Mostafa S. Mostafa, PhD
David Dearth, PE
Jan Cervenka, PhD
Doug Marx
Luke Snell, PhD

Note: The information in this report should not be used as “design basis input” for any design basis analyses unless the specific information has been validated to have been obtained under an approved 10CFR50 Appendix B program.



INTRODUCTION

Issue:

Progress Energy Florida's (PEF) Crystal River Unit 3 (CR3) nuclear power plant discovered a delamination in one section of the reactor containment structure wall during the process of cutting a temporary opening in the containment to be used to replace the steam generators. PEF subsequently engaged Performance Improvement International (PII) to perform a comprehensive root cause assessment to identify the cause or causes of the delamination. This report provides the results of PII's root cause assessment both for the technical cause of the concrete delamination and for the Organizational and Programmatic (O&P) aspects of the project.

Report Structure:

This report is intended to be a single point reference document that includes the detailed information needed to understand the circumstances and conclusions associated with the containment wall delamination at CR3. The report has a pyramidal structure. The Executive Summary provides detailed summary and overall conclusions. [Section 1](#) provides a brief description of CR3 and the delamination event. The first step in the analysis process is to identify potential Failure Modes (FMs) to determine the overall scope of the issues to be investigated. A total of 75 potential FMs in nine general groups were identified to encompass the scope of possible contributors to the delamination event. This report provides a discussion of the eight confirmed failure modes grouped by topic area. [Sections 2](#) through [6](#) discuss the failure mode process and the individual Failure Modes that contributed to the delamination. The nature of the FMs is that they cover all aspects of the event so that a review of each FM correlates from issue to issue. The contributing FMs are organized into a failure mode timeline in [Section 7](#). This method of presentation assembles the contributors into a chronological analysis of the interactions and individual factors that created the conditions for the delamination to occur. Next, the computer simulations are presented which provides a visual display of the actual circumstances that led to the delamination. [Section 8](#) discusses the root cause of the event. [Section 9](#) provides recommendations to prevent recurrence of the issue. [Section 10](#) provides the O&P evaluation. [Attachment 1](#) provides a detailed discussion of the computer models used. [Attachment 2](#) describes the benchmarking done to validate the computer modeling results. The individual failure mode assessments are provided in [Attachment 6](#).

Note: All TOC elements are clickable links. Additional links to referenced locations can be found throughout the document.



EXECUTIVE SUMMARY

Through a complex process which involved deductive investigation of data and information that was available to PII after the delamination event at CR3, PII was able to create a state-of-the-art computer model. This model allowed PII to start with information now known about how the CR3 containment structure behaves and work backwards in time to determine what factors contributed to the delamination event. Using this process, PII has identified seven discrete factors that, working in conjunction, caused the delamination. These factors are: (1) tendon stresses; (2) radial stresses; (3) design for stress concentration factors; (4) concrete strength properties; (5) aggregates; (6) de-tensioning sequence and scope; and (7) removing concrete.

Considered alone, none of these individual contributing factors would have led to a delamination. For example, the type of concrete and aggregates used at CR3, while a contributing collective cause, would not alone have caused a delamination without the combined interplay of the other contributing factors acting in concert while the containment structure was being de-tensioned and while the Steam Generator Replacement (SGR) opening was created. Thus, it is important to understand both the specifics of each contributing factor as well as how all of those factors worked together.

Of particular importance in this analysis is that typical industry containment structure analysis tools have consistently shown large margins for stress tolerance when creating containment openings in other similar projects by using average tensile stress values. Other projects have typically included de-tensioning tendons around the containment opening so that the containment structure was in a state to accept replacement concrete after the major equipment movements in and out of containment were complete. PII's computer model, however, has shown that the CR3 containment structure had a lower margin of tolerance to cracking than other plants which have used common industry calculations. PII further determined that the de-tensioning of more tendons immediately around the containment opening in CR3 may have exacerbated the delamination event, a result that would not have been apparent from experiences with other Steam Generator Replacement (SGR) projects. Both of these examples demonstrate the complexity and the unique nature of PII's investigation into delamination.

PII has determined that the delamination did not exist prior to the work to create the containment opening by the SGR. Rather, the delamination appears to have been caused by the combination and interplay of (1) certain design features of the CR3 containment structure; (2) the type of concrete used in the CR3 containment structure; and (3) the acts of de-tensioning and cutting the containment structure. Through a state-of-the-art computer model that PII developed CR3 specific information, available to PII after the delamination had taken place, PII was able to determine that none of the individual contributing factors to the delamination, on its own, would have caused a delamination. Rather, the complex interplay between all the contributing causes led to the delamination as discussed in detail in this report.

In conclusion, PII has determined that the immediate cause of the delamination event was the redistribution of stresses as a result of the containment opening activities resulting in additional stress beyond original containment design. The condition exceeded the fracture capacity of the concrete and resulted in cracking along the high stress plane connecting the horizontal tendons. As the cracks propagated and joined, delamination occurred over a wide area. Evaluation of the contributing failure modes identified only one practical root cause subject to control and that was inadequate scope/sequence of tendon de-tensioning used in the SGR outage. The O&P

NON-PROPRIETARY VERSION

evaluation concluded that the inability of industry accepted tools to predict delamination was the programmatic root cause of the event. PII found that six methodology improvements were needed to accurately analyze the containment response.



TABLE OF CONTENTS

Note: All TOC elements are clickable links. Additional links to referenced locations can be found throughout the document.

INTRODUCTION	3
EXECUTIVE SUMMARY	4
1. PLANT DESCRIPTION AND HISTORY	8
GENERAL DESIGN:	8
PREVIOUS INDUSTRY OPERATING EXPERIENCE:	8
STEAM GENERATOR REPLACEMENT OUTAGE EVENT CHRONOLOGY:	8
2. FAILURE MODE PROCESS	144
INTRODUCTION:	14
3. GROUP 1: CONTAINMENT DESIGN	166
CONFIRMED FAILURE MODES:	166
SUMMARY:	166
DISCUSSION:	16
4. GROUP 2: CONCRETE CONSTRUCTION	26
CONFIRMED FAILURE MODES:	26
DISCUSSION:	26
5. GROUP 3: USE OF MATERIALS	277
CONFIRMED FAILURE MODES:	27
DISCUSSION:	27
6. GROUP 7: SGR ACTIVITIES	288
CONFIRMED FAILURE MODES:	28
DISCUSSION:	28
7. FAILURE MODE TIMELINE	30
SEQUENCE OF STEPS:	31
DETAILED COMPUTER SIMULATION:	31
WHOLE CONTAINMENT RADIAL DISPLACEMENT SIMULATION:	32
DETAILED LOCAL WALL RADIAL DISPLACEMENT RESPONSE:	39
SHEET DELAMINATION:	59
SCENARIO VALIDATION:	60
8. ROOT CAUSE AND CONTRIBUTING CAUSES	62
SUMMARY CONCLUSIONS:	62
FAILURE MODE EVALUATION:	62
FREQUENTLY ASKED QUESTIONS:	64
9. RECOMMENDATIONS TO PREVENT RECURRENCE	67
CORRECTIVE ACTIONS TO PREVENT RECURRENCE	67
A. RE-TENSIONING CONTAINMENT IN R 16	67
B. CAPTURING THE OPERATING EXPERIENCE	67
BETTERMENT ACTIONS	67

NON-PROPRIETARY VERSION

C. LIFE EXTENSION	67
D. DIFFERENTIAL AGING CHARACTERISTICS	68
10. ORGANIZATIONAL AND PROGRAMMATIC ROOT CAUSE	70
11. REFERENCES	73
ATTACHMENT 1: COMPUTER MODELING	74
ATTACHMENT 2: FLEXING OF CONTAINMENT WALLS	84
PURPOSE:	84
EXPECTED BUILDING RESPONSE:	84
CONCLUSION:	96
COMPARISON OF LASER SCANNING AND COMPUTER MODEL SIMULATION	92
ATTACHMENT 3: CONTAINMENT WALL INTERNAL RESPONSE	978
ATTACHMENT 4: SGR OPENING SEQUENCE	989
EVENT CHRONOLOGY:	989
ATTACHMENT 5: REVIEWER TABLE AND RESUMES	105
FAILURE MODE AUTHOR AND REVIEWER LIST:	1055
RESUMES OF PII PARTICIPANTS:	1077
ATTACHMENT 6: CONFIRMED AND REFUTED FAILURE MODE ASSESSMENTS	1478
1. CONTAINMENT DESIGN AND ANALYSIS	1478
2. CONCRETE CONSTRUCTION	147
3. USE OF CONCRETE MATERIALS	147
4. CONCRETE SHRINKAGE, CREEP, AND SETTLEMENT	148
5. CHEMICALLY OR ENVIRONMENTALLY INDUCED DISTRESS	148
6. CONCRETE-TENDON-LINER INTERACTIONS (DURING OPERATION)	1489
7. CONTAINMENT CUTTING	148
8. OPERATIONAL EVENTS	148
9. EXTERNAL EVENTS	1499



1. PLANT DESCRIPTION AND HISTORY

This discussion is limited to a brief summary of the plant and its history to ensure the reader understands the general flow of events. Detailed discussions of specific plant data are delayed until they are addressed in the analysis of each applicable topic.

General Design:

Prior to the current outage, Crystal River 3 was a 2609 thermal megawatt Babcock and Wilcox pressurized water reactor located in Crystal River, Florida. Gilbert Associates was the architect engineer for the plant. The plant went online for the first time on 3/13/1977.

Construction of the CR3 containment wall was completed in 1973. The dome concrete was placed from February to July, 1974. Post tensioning was completed in early 1975. The nominal inner radius is 65'-0" and thickness of 42". Horizontal tendons are arranged in pairs that are located at 39" intervals. Each tendon is housed in a 5.25" diameter conduit. The inner containment surface has an integral 3/8" steel liner. The containment building is generally a right circular cylinder but it contains six buttresses with six bays that form the containment walls between the buttresses.

Previous Industry Operating Experience:

In April, 1976, workmen identified a delamination of the concrete on the dome of CR3. The delaminated concrete was removed and additional radial reinforcing was grouted into the remaining 24" thickness of concrete. New concrete was placed, reinforced with meridional and hoop steel, and a nominal thickness of 12" new concrete was placed. The event investigation concluded, "...that radial stresses combined with biaxial compression to initiate laminar cracking in a concrete having lower than normal direct tensile capacity and limited crack arresting capability".

Prior to the CR3 dome delamination, on 6/17/70 Turkey Point Unit 3 also identified delamination of their containment dome during post tensioning after 2/3 of the tendons had been tensioned. This occurred three months after the last concrete was placed.

Additionally containment dome delamination occurred during construction of the Kaiga Atomic Power Project Unit 1 in 1994. The event occurred during the post-tensioning process after 1/3 of the tendons had been tensioned. It was accompanied by a collapse of the inner surface of the dome (Reference 6).

Steam Generator Replacement Outage Event Chronology:

On 9/26/09 the Crystal River steam generator replacement outage began. This included the creation of an access opening in the containment wall. The construction opening was a 27' by 25' rectangle running from elevation 183' to 210'. The centerline of the opening was coincident with the centerline of panel 34. Tendon cutting began on 9/26/09. The first two tendons (V12 and V13) were hydraulically de-tensioned. The remaining 25 tendons were de-tensioned by flame cutting under full tension (FM 7.6 evaluates this practice). A demonstration of hydro-lasing was conducted on 9/30/09. The final tendon was de-tensioned on 10/1/2009. Detailed information is available in Attachment 4. Figure 1.1 below shows the area of interest.



Figure 1.1 Photograph of the steam generator opening worksite.
Note the newly constructed rectangular opening above the existing circular equipment hatch.

The pictures of cracks between horizontal tendons taken on 9/30/09, the day before the final two tendons were de-tensioned, and before any significant concrete removal, provide a rough estimate for the onset of cracking in the Failure Mode Timeline.

On 10/2/09 plant personnel identified a delamination of the concrete about 10 inches into the 42 inch thick concrete containment wall in the plane of the horizontal tendon conduits. Shortly thereafter, process water was noted seeping out of the concrete about 20 feet away from the hydro-lasing work area (Figure 1.2). The appearance of water is the most compelling evidence that the delamination occurred during the last stages of the de-tensioning rather than as a result of concrete removal. For water to travel a significant distance inside the wall there must have been an extensive network of delamination which provided an estimate for its onset in the Failure Mode Timeline. Action Request (AR) 358724 was opened to address this event.



Figure 1.2 Photograph of water leakage from the containment wall (10/3/2009).

Figure 1.3 shows the extent of delamination visible on the edge surfaces of the SGR construction opening. Figure 1.4 is a sketch identifying the most important features of the containment wall construction.



Figure 1.3 Photograph of delamination crack running from horizontal tendon to horizontal tendon, parallel to the wall surface, approximately 10 inches deep. (Photo taken after partial concrete demolition)

NON-PROPRIETARY VERSION

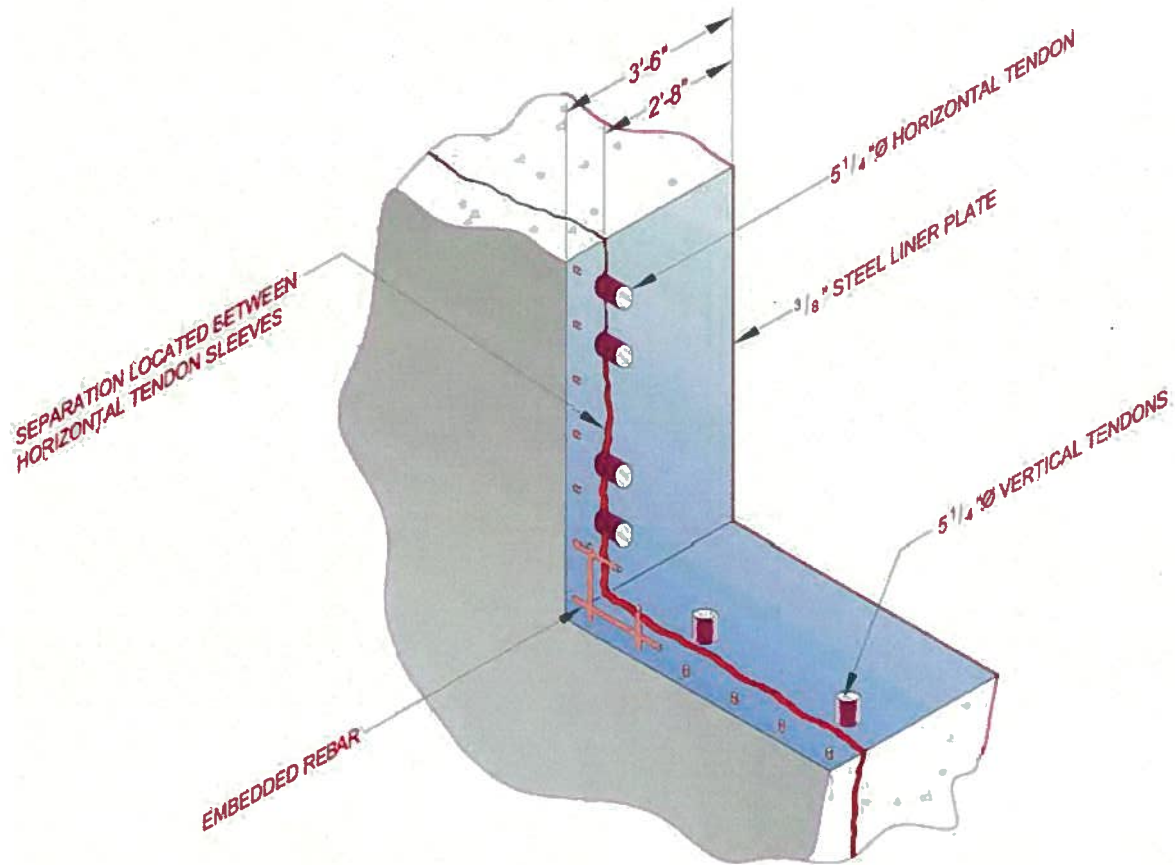


Figure 1.4 Sketch of the delamination cracking in the bay 34 wall.

With identification of the delamination, a detailed extent of condition assessment plan was developed. Impulse Response inspections and core drills have been performed at many locations around the containment with a good correlation between the two techniques. Delamination was only found in bay RBCN-0015 (containing the equipment hatch and steam generator replacement opening), also known as bay 34 because it lies between buttresses 3 and 4. Figure 1.5 shows a map of all six containment bays.

During the investigation and repair process other items were identified. Action Request (AR) 00359670 documents a surface separation in the containment concrete approximately 22 feet away from the SGR opening. AR 00368389 documents an isolated crack beneath the equipment hatch support area; however, this area was not impacted by the delamination event or its causes. AR 388332 identifies a crack in a core bore sample of the dome concrete at the interface of the original concrete and the concrete used to repair the dome delamination in 1976. The interface area was not impacted by the delamination event or its causes. Both of these isolated cracks are far removed from the area of high stress resulting from tendon de-tensioning, and they are physically separated from the delaminated concrete. The conditions were determined to be unrelated and will be dispositioned separately by the station.

NON-PROPRIETARY VERSION



Figure 1.5 Sketch of the containment structure unfolded.

Figure 1.5 shows the details of each containment bay and the 10' by 20' panels in each bay. Having discussed the history and plant conditions associated with Crystal River, Unit 3, the analysis then focused on the potential failure modes for the event.



2. FAILURE MODE PROCESS

Introduction:

At the start of the root cause evaluation, PII identified possible contributing factors and then systematically assessed the individual importance of each factor to the event. These possible contributors are called Failure Modes (FMs) and are organized into logical groupings. Each failure mode is investigated and the resulting conclusions are reviewed within PII, by the utility, and also by third party reviewers. A primary component in the analysis of each Failure Mode is the identification of information needed to either confirm or refute the Failure Mode as a contributor to the event. This information is then obtained and analyzed.

Nine groups containing 75 individual Failure Modes were identified as possible contributors for this event. The analysis sheets for each of the Failure Modes may be found in [Attachment 6](#). Of the 75 Failure Modes, 67 were refuted and did not contribute to this event, eight were confirmed as contributors. The eight Failure Modes that were not explicitly refuted are individually discussed in the next few sections of the report with one section for each group containing a confirmed Failure Mode. Attachment 6 of this report contains each of the 75 FMs evaluated. The entire Failure Mode file, including exhibits, is found in the appendices of this report.

Once the analysis of Failure Modes was complete, a Failure Modes Timeline was generated to identify when the issue arose and how it contributed to the event. This timeline is shown in [Figure 2.1](#).

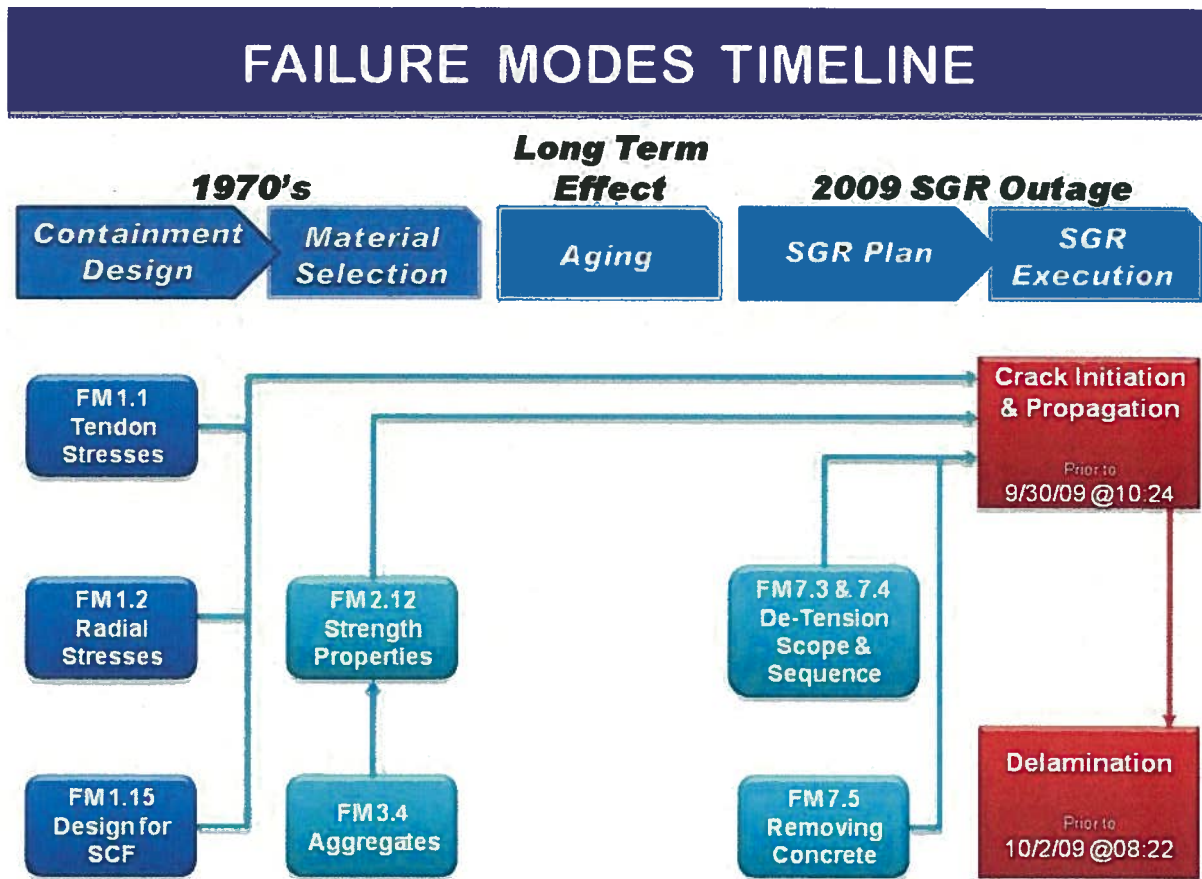


Figure 2.1 Failure Mode Timeline

The information in the next few sections will cover several topics related to the delamination event. The timeline in Figure 2.1 identifies how these topics converged to create the delamination. Section 7 provides a computer simulation of the delamination event. Section 8 integrates the individual elements and clarifies the overall process by which the root cause was determined.

The eight failure modes correlate with five time periods and topic categories.

- ◆ Original structure design from the 1970's
- ◆ Original material selection and construction in the 1970's
- ◆ Aging of materials from the 1970's to 2009
- ◆ Determination and execution of the de-tensioning scope and sequence in 2009
- ◆ Physical removal of concrete in 2009



3. GROUP 1: CONTAINMENT DESIGN

Confirmed Failure Modes:

- 1.1 Excessive vertical and hoop stress
- 1.2 Excessive radial tensile stresses/no radial reinforcement
- 1.15 Inadequate design analysis methods of radial tensile stresses (near sleeves, no radial reinforcement)

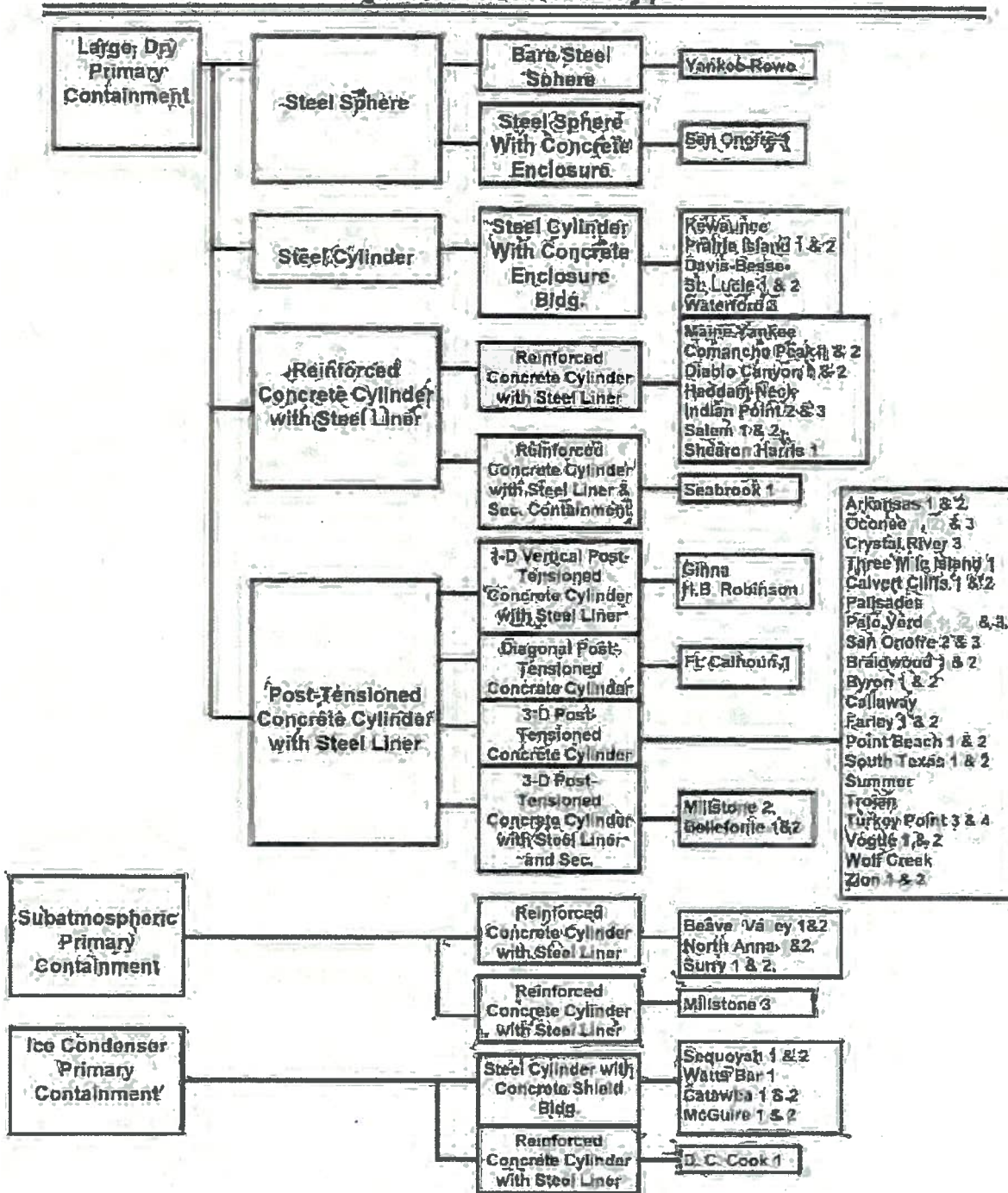
Summary:

FM 1.1 determines that CR3's containment design results in high vertical and hoop compression stresses and radial tensile stresses when compared to the designs of other plants. FM 1.15 determines that stress concentration factors (SCFs) were not explicitly considered in the original design of the containment building. FM 1.2 determines that radial stresses in the containment structure are high and that no radial reinforcement is currently in place. As with all the confirmed Failure Modes, the conclusions reached indicate that these issues did not individually cause the delamination, but rather contributed to the conditions that resulted in delamination.

Discussion:

Three Failure Modes in the design area related to vertical and hoop compression stresses, and radial tensile stresses contributed to the delamination of CR3. To evaluate the original design plan of CR3 and how it may have affected levels of stress, a comparison to seven other containment structures is made. CR3 is one of many containment buildings in service in the United States that uses post tensioned tendons to provide compression to the concrete structure. Figure 3.1 summarizes the various containment designs that have been built in the U.S.

PWR Containments in the United States by Construction Type



From USNRC: www.nrc.gov/reading_rm/reports/2002/02-010

Figure 3.1 The various containment designs in the U.S.

NON-PROPRIETARY VERSION

Within the post-tensioned category of containment buildings, there are several variations, one of which is the six buttress design used at Crystal River. A comparison group was selected from containment designs used in other plants comprised of seven units of the six buttress designs which have successfully undergone construction of an opening in the containment structure.

Within the comparison group are three tendon designs, the largest of which is the Crystal River design with 163 wires of 7 mm (0.276") diameter wire. One comparison plant has a design with 169 wires of ¼" diameter wire. The other 6 units have tendons with 90 wires of ¼" diameter wire. All units initially lock off their tendons to 70% guaranteed ultimate tensile strength. The importance of this design difference is that the larger the tendon cross section the higher the peak compressive stress on the concrete immediately in contact with the tendon sleeve. This directly translates into higher peak radial tensile stress at the vertical centerline of the hoop tendons.

Relative Individual Tendon Force	
Crystal River:	100%
Plant A*	85%
Plants B to G*	45%

* Nuclear plants A-G comprise a population of plants with a six buttress design most like CR3 which have successfully created containment construction openings.

The large diameter tendons have another impact as well. They are located at a depth of 10 inches from the outer containment wall with a set of tendons about every 39 inches. At that depth 27% of the cross-sectional area has the concrete displaced by tendon sleeves. The absence of concrete at this location increases the stress on the remaining concrete at exactly the location of the radial tensile stress at the top and bottom of each horizontal tendon sleeve. The nominal (average) radial stress in this location is 1.4 times what it would be without the displacement of the concrete by the tendon.

Figure 3.2 shows that there is no radial reinforcement provided beyond the horizontal tendons which results in the outermost 10 inches of concrete being radially un-reinforced while being subjected to tensile stresses.

NON-PROPRIETARY VERSION

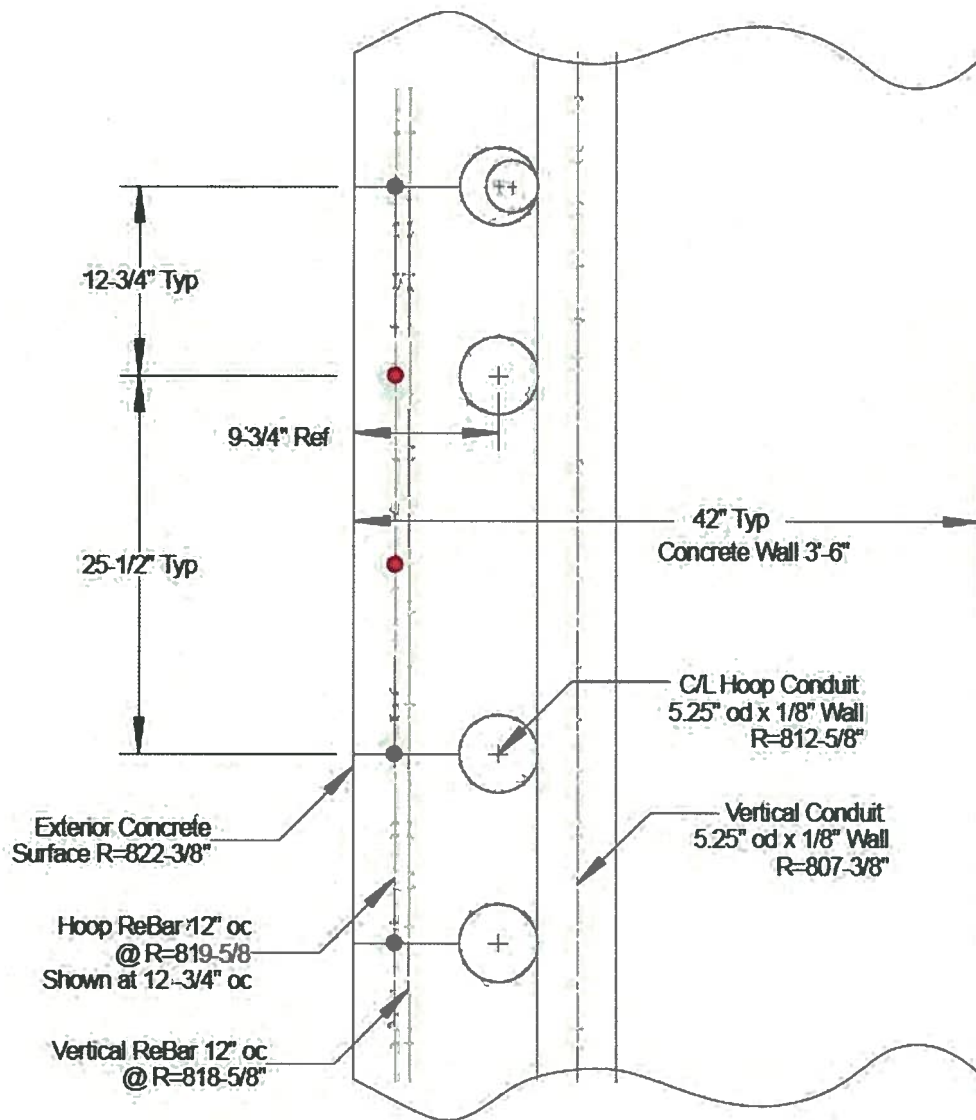


Figure 3.2 Layout of horizontal tendon sleeves in the CR3 containment wall (R is the containment inner radius in inches)

The following is a summary of the main design features of the containment wall.

The wall is 42 inches thick with a 3/8" steel liner on the inner surface. Approximately 10 inches into the concrete on the outside, the horizontal tendons (sleeve OD is 5.25 inches) each typically provides about 1400 kips of force (hoop tendon) to post-stress the concrete wall. Just inside the horizontal tendons are the vertical tendons.

There are a total of 94 horizontal tendons in the containment wall which covers one-third of the circumference for a total of 282 tendons. Each tendon has a near neighbor 13" away and a far neighbor on the other side 26" away. Each tendon has a length of 1/3 of the circumference of the containment from one buttress past one buttress to the next buttress. Buttress #1 is facing north and buttress #2 is at WNW 60 degrees counter-clockwise.

NON-PROPRIETARY VERSION

The remaining buttresses are numbered sequentially. Each of the six wall segments are located between two buttresses. Thus bay 34 lies between buttress 3 and buttress 4. Horizontal tendon 42H21 runs between buttress 4 and buttress 2 and is the 21st tendon going up from 42H1 at the bottom of the containment wall. Bay 34 also has 53H21 which is the other tendon in the set.

A horizontal tendon provides the radial compressive stress of about 340 psi averaged over the diameter of the tendon sleeve. The average over the entire cross-section of concrete being radially compressed by that horizontal tendon is about 100 psi. Normally the average radial tensile stress would be 23 psi but due to concrete displacement it is 31 psi at the centerline of the horizontal tendons.

The tensile stress peaks at a very high value right at the edge of the horizontal tendon hole at the intersection with a vertical tendon due to the vertical and horizontal tendons. It reaches 1630 psi at the hole and drops off rapidly by a factor of 2 about every inch away. More generally, tensile stress peaks at about 510 psi on the edge of a horizontal tendon away from the vertical tendons and drops off about a factor of 2 every inch away. Figures 3.3 to 3.6 show a general display of stress variations along various directions in the containment concrete assuming no cracking in the concrete. For exact values refer to the specific calculations of design parameters found in the applicable FMs and the figures in Section 7 of this report.

Using a cylindrical coordinate system, there are three dimensions used to locate a unique point in the containment wall. The radial direction extends outward from the center vertical axis of the circular building. The azimuthal angle is the horizontal angle, measured counter clockwise (looking down) from the north. Elevation defines the vertical distance from the ground reference point. A review of stresses throughout the wall due to horizontal tendons follows.

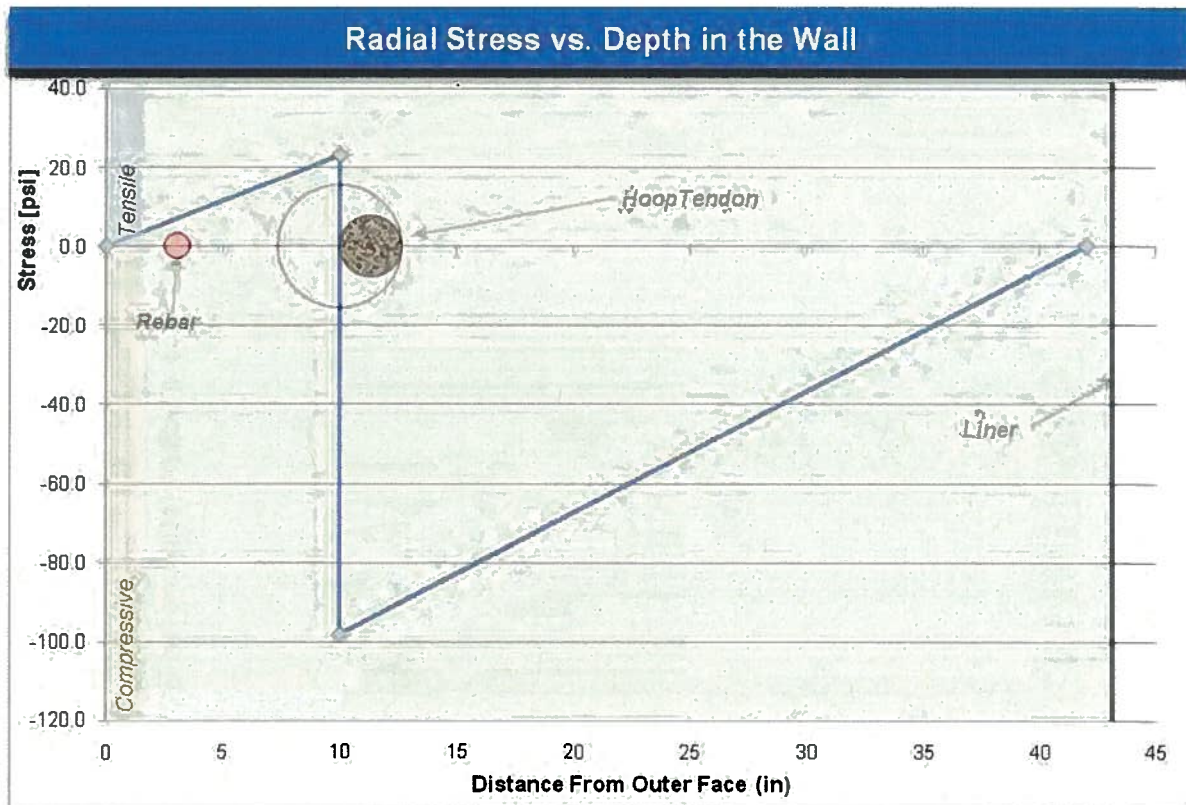


Figure 3.3 Tensile and compressive stresses in concrete wall cross-section due to horizontal tendons.

COMPUTER CODE INPUTS

The report will be providing some computer model plots which had the following inputs that were used based upon testing and modeling. PII does not use NASTRAN to quantify concrete fracture so fracture parameters are not applicable. Abaqus applies creep correction only for long time period intervals such as the time step of 30 years of operation with the containment tensioned. E0 is the elasticity modulus and E1 is the creep adjusted elasticity modulus. F't is tensile capacity and G't is the fracture energy. 3.45 E6 psi is the average modulus measured on 22 CR3 containment cores. Fracture energy was measured to be 0.40 lbf/in (reference 11 in Section 11 of this report).

Figure	Model	E0 psi	E1 psi	F't psi	G't lbf/in	Creep
3.4	Abaqus Detail	3.45 E6	3.45 E6	360	0.08	2.2
3.5	Abaqus Detail	3.45 E6	3.46 E6	360	0.08	2.2
3.6	Nastran	4.29 E6	4.29 E6	NA	NA	0

NON-PROPRIETARY VERSION

The area around a representative horizontal tendon is shown in Figure 3.4. This is a critical area due to the high stresses and displacement of concrete by the tendon sleeves. This is the location along which the delamination propagated from the top and bottom of the holes to the next hole vertically or propagated circumferentially (azimuthally) around a segment of the building. Notice that the peak tensile stress at the edge of the horizontal tendon hole near a vertical tendon (Figure 3.4) is well in excess of the tensile capacity of the CR3 concrete. It is likely that small cracks formed at these intersections but then stopped propagating when they reached a location where the stress was too low to continue.

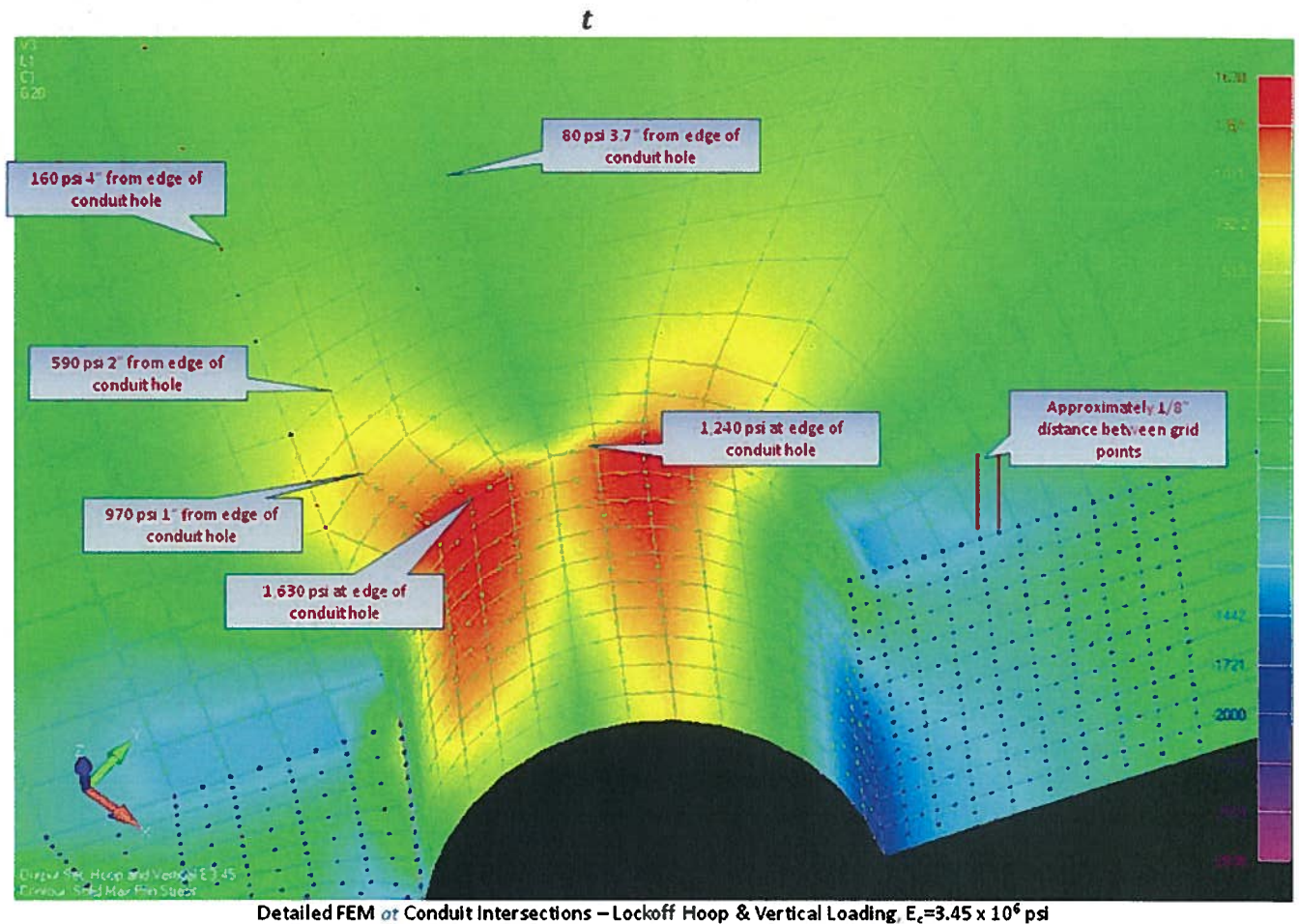
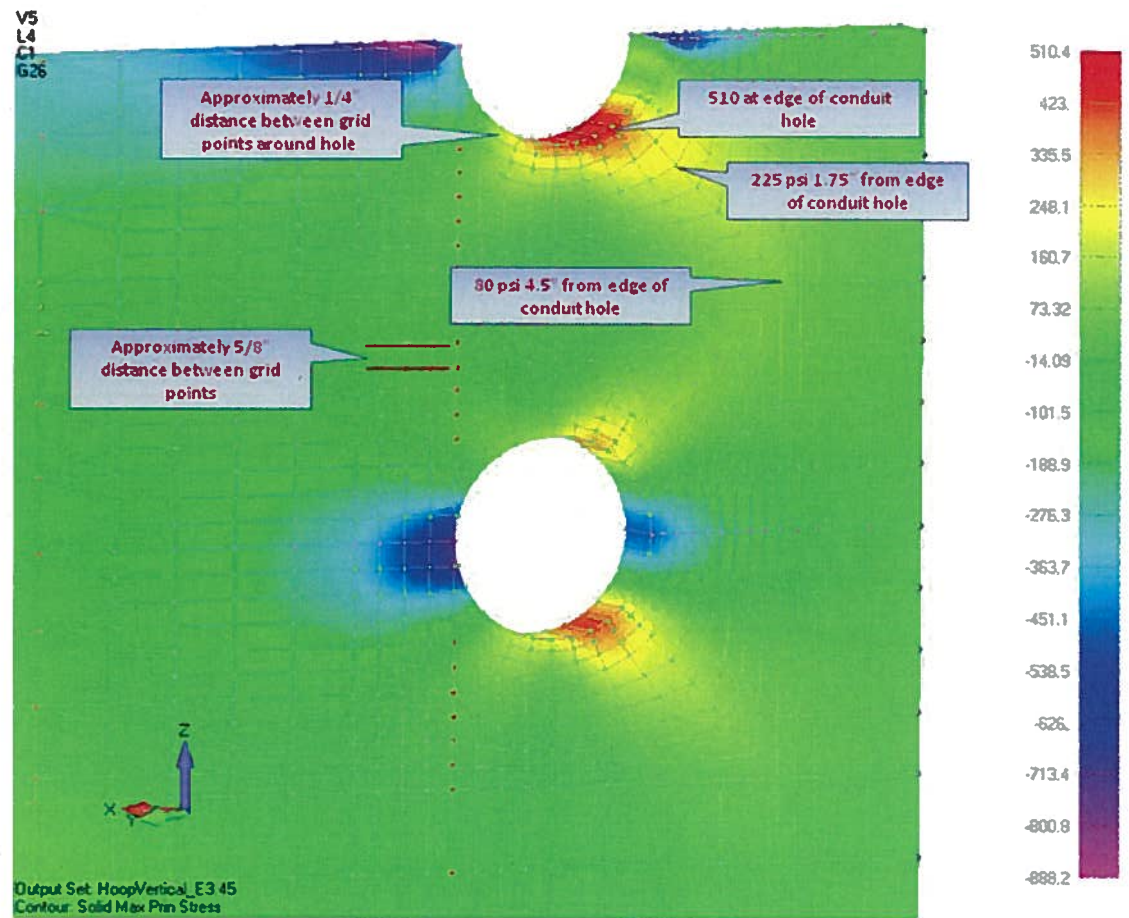


Figure 3.4 Stress contours for normally tensioned conditions at the intersection of a vertical and horizontal tendon.(3 Dimensional Effect Looking Through a Hoop Tendon Hole)

NON-PROPRIETARY VERSION



Expanded FEM *Between* Vertical Conduits – Lockoff Hoop & Vertical Loading, $E_c=3.45 \times 10^6$ psi

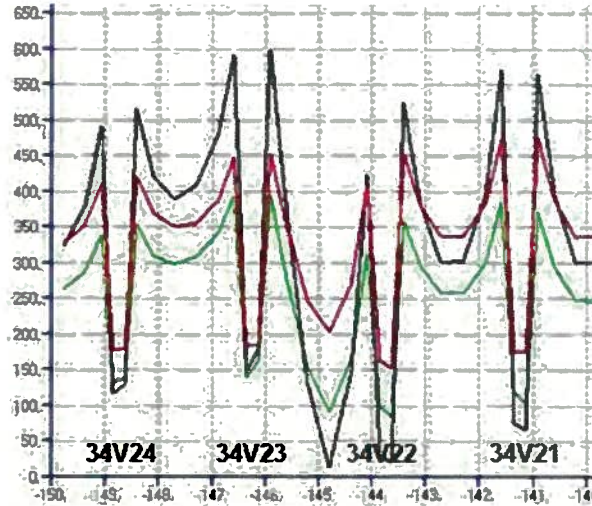
Slide 5 of 5

Figure 3.5 Stress contours for normally tensioned conditions in between intersections of a horizontal tendon with vertical tendons.(Section View)

Concrete is weaker in tension and the peak radial tension stress is located near the top and bottom of the sleeve holes. The circumferential surface through the vertical centerline of the hoop tendons has the least concrete surface area. Of the containment structures studied, all three of those that experienced delamination (Turkey Point dome, Crystal River dome, and Crystal River wall) failed along the equivalent high tensile stress locations.

Figure 3.6 shows stresses in the containment structure going around its circumference. Local stress peaks are caused by the vertical tendons spaced evenly around the containment at about 3 foot intervals. The three graphs show pre-SGR conditions, post SGR de-tensioning, and post SGR concrete removal. It is intended to simply show the changing stress seen traveling from one vertical tendon to the next.

Maximum Principal Stress Going Around Containmentment



Circumferential Distance, feet and tendon number

Figure 3.6 Plot of maximum principal stress as a function of distance around the containment circumference. (Black is pre-SGR, Green is Post SGR de-tensioning, Red is post SGR concrete removal.)

While the vertical tendons also displace concrete they are located inside the horizontal tendons in the area where the radial forces are compressive so the effect of displacement of concrete is not significant to the cause of cracking because concrete is strong in compression. Figure 3.6 is similar to Figures 3.4 and 3.5 showing the sharp stress changes near vertical tendons.

The specific design outlined above results in an area of reduced concrete area and high radial stress. The absence of concrete is a result of the tendon holes. The existence of high peak radial stress at the edge of the conduit hole is a material response to the compressive stresses of the tendons. This could be compensated for by using radial reinforcement but that was not required based upon the design requirements of the building as a containment. Figure 3.7 below shows a retrofitted radial reinforcement in the CR3 dome repair. This modification provided radial reinforcement on the dome as part of the required repair. It should be noted, however that many containments were designed and constructed without radial reinforcement, so this is only one of several considerations relevant to this root cause analysis.

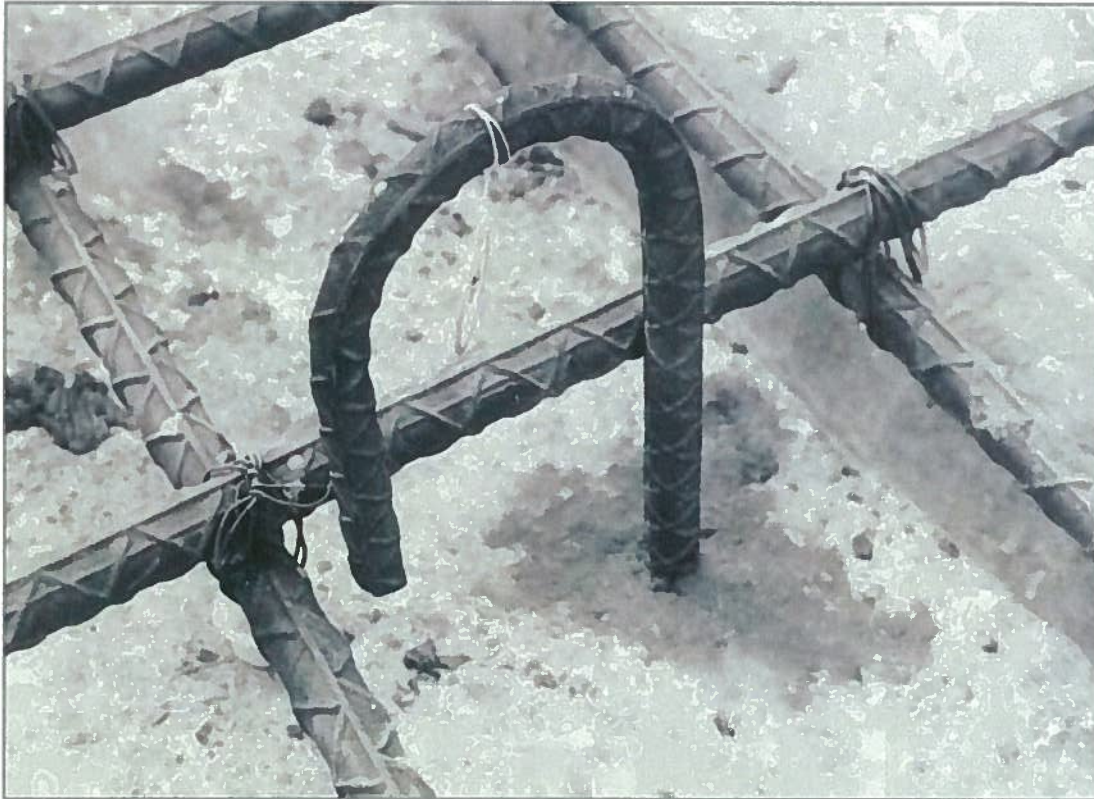


Figure 3.7 Photograph of a radial reinforcement installed as a corrective action to the CR3 Dome delamination

FM 1.1 determines that CR3's containment design results in a somewhat higher potential for delamination than other similar designs on the basis of Compressive-Tensile Stress Interaction. FM 1.2 finds that radial tensile stresses are high (refer to Figure 3.4) and there is no radial reinforcement. Large tendons lead to high peak stresses. FM 1.15 identified that stress concentration factors were not explicitly considered in the original design of the containment building. As with all the confirmed failure modes, they conclude that these issues did not individually cause the delamination but contributed to the conditions that resulted in delamination.

Considered alone, the stresses involved in the CR3 containment design are well within the capability of the concrete material used. However, when stresses occur for other reasons, such as local stresses resulting from de-tensioning of tendons and cutting the opening, these additional stresses at CR3 contribute to the overall stress condition.

4. GROUP 2: CONCRETE CONSTRUCTION

Confirmed Failure Modes:

2.12 Inadequate Strength Properties

Discussion:

The second step in the failure mode chronology was the selection of construction materials. CR3 used Type II cement and Florida Limestone aggregate. (FM 2.12) The resulting concrete met all design requirements and its properties were in the expected range for that type of concrete. Tensile strength tests on post delamination cores have shown, however, that the average tensile strength for concrete in bay 34 was up to 10% lower than that of cores from other parts of containment (compared to a standard deviation of 10% for the entire population) and similar variability in the dome. Direct tensile test results are 75% of the split tensile results when 88% to 95% would be expected. Measured compressive strength was 7707 +/- 634 psi.

Limestone in general is an acceptable aggregate that can produce high quality concrete. The limestone used for CR3 (Brooksville limestone) includes a significant portion of soft/friable particles that weakens the physical properties of the concrete (See FM 3.4). Even though the concrete compressive strength met project specifications, the variability and instances of low tensile strength led to the conclusion that this failure mode contributed to the delamination. This finding was largely based upon the performance of the aggregate used which is addressed in FM 3.4 Inadequate Aggregates.



5. GROUP 3: USE OF MATERIALS

Confirmed Failure Modes:

3.4 Inadequate Aggregates

Discussion:

Hardened concrete is composed of three main phases - aggregates, hardened cement paste (HCP) and the interface between them. The weakest part that normally controls strength is the interface where microcracks form and cracks originate. Since the aggregate is normally significantly stronger than the HCP it provides a stable medium that helps arrest and slows the progression of cracks.

Analysis revealed that the coarse aggregate used at CR3 was a locally available calcareous limestone (Brooksville Limestone) which included up to 50% soft/friable material that was not appreciably stronger than the HCP and allowed cracks to propagate directly through the aggregate.

In the three delamination events that have occurred in the U.S. nuclear industry, all involved Florida limestone aggregates.

Additionally, experience in other delamination events points to sensitivity for delamination when the tensile strength is low. For example, similar delamination during tensioning of the Kaiga containment dome in India involved concrete with tensile strength of 489 psi (3.37 MPa) (Reference 2) which is lower than the average tensile strength of 600 psi as measured at Crystal River (using the Brazilian splitting tensile strength test).

FM 3.4 is a discussion of the selected coarse aggregate. The aggregate used at CR3 was relatively soft, porous, and gap graded. While its properties were sufficient to satisfy the specifications and design requirements, it resulted in concrete tensile strength, modulus of elasticity, and ability to arrest cracks that was significantly lower than at most other nuclear containment structures.

This FM impacts the plant because it contributes to the tensile strength of the concrete discussed in FM 2.12 Inadequate Strength. For that reason FM 3.4 is shown as feeding in FM 2.12 on the FM Timeline.



6. GROUP 7: SGR ACTIVITIES

Confirmed Failure Modes:

- 7.3/7.4 Inadequate de-tensioning sequence and scope
- 7.5 Added stress due to removing concrete at the opening

Discussion:

FMs 7.3/7.4 addresses de-tensioning sequence and scope.

Normally, the containment is in a symmetric state of loads and deformations. When changes cause it to transition into non-symmetric state, it experiences stresses and strains that may exceed its capacity. One symmetric state existed at the time the containment was complete, but prior to prestressing any of the tendons. The symmetric load consisted primarily of the dead load of the structure. Another symmetric state existed when the structure was fully tensioned because of the symmetry built into the tendon pattern. In either situation the transition was smooth and free of bends in the concrete that can promote delamination. Excessive stresses and/or strains can develop when transitioning between two symmetric states because of the sharp local transition from a series of tensioned tendons and a series of de-tensioned tendons. However, the potential for a prestress force load imbalance on the containment shell as the tendons are globally stressed is precluded since the prestress force is applied in gradual and symmetric manner governed by procedure. For example, in the hoop direction the original stressing procedure sequence required stressing the tendons in complete rings of three tendons and also tensioning every fourth ring of tendons until $\frac{1}{4}$ of the total hoop prestress was applied to the shell. The process was repeated until another $\frac{1}{4}$ of the hoop prestress was applied et cetera..

Figure 7.11 shows the radial displacement that occurred during the SGR de-tensioning. Delamination occurs where radial stress is high. That occurs at sharp bends in the wall. The de-tensioned region ran horizontally from elevation 183' to 210' for a span of 27'. Horizontally the bulge extended across the bay for span of about 60' so there was a smoother transition in that direction. Note in Figure 7.11 that the radial displacement associated with de-tensioning is linear. This means that the stress that develops is monotonically increasing and other sequences of de-tensioning the same number of tendons would not change the end-point which is the highest stress condition.

The ability to control radial stress comes mainly from the manner (selecting the right number and location of additional tendons to be de-tensioned along with the sequence to be de-tensioned) in which the horizontal tendons are de-tensioned. What is important is the number of tendons involved, the symmetry of the tendons affected, and whether the sequence employed increases or decreases local peak stress. We know approximately when delamination occurred based upon observed cracking in the hydro demolition demonstration area and water observed coming out of the containment wall. In an area as large as bay 34 and with the large stress concentration factors on a detailed scale, it is probable that cracking began in isolated points of highest stress. As the stresses increased (due to the growing number of de-tensioned tendons), and shifted (due to the various tendons de-tensioned), small cracks grew and joined until they eventually covered the entire delaminated area. More detail is available in [Attachment 4](#).

NON-PROPRIETARY VERSION

The last four steps of the actual de-tensioning were to de-tension tendons 53H32 through 53H35 in order. However tendons 42H32, 42H33, and 42H34 were in between these last tendons and they had been previously de-tensioned so there was some alternation in the sequence used to minimize the transition from tensioned to de-tensioned tendon..

The scope and sequence used is so intertwined that the two FMs 7.3 and 7.4 were combined and it was concluded that they did contribute to the delamination. Although the building felt the impact of de-tensioning, it is clear from the finite element analysis that the localized de-tensioning in bay 34 led to curvature which contributed to the delamination. The March, 2010 analysis and subsequent de-tensioning for repair found that use of more symmetrical de-tensioning of the entire circumference was required to avoid delamination in other bays and the building was successfully de-tensioned.

(FM 7.5) addresses the removal of concrete. Photographs taken after concrete removal started, the day before the final two horizontal tendons were de-tensioned, show cracks existed at that time. The next day after more concrete removal the discovery of water flowing out of the containment wall more than 20 feet away from the hydro-lasing work area indicates that delamination occurred prior to large scale removal of concrete. Given the stresses caused by the demolition and those created in the remaining concrete when a large area is removed, it contributed to the overall de-lamination event.



7. FAILURE MODE TIMELINE

This section of the report discusses the timing of the contribution for each failure mode. Figure 7.1, below shows the timeline.

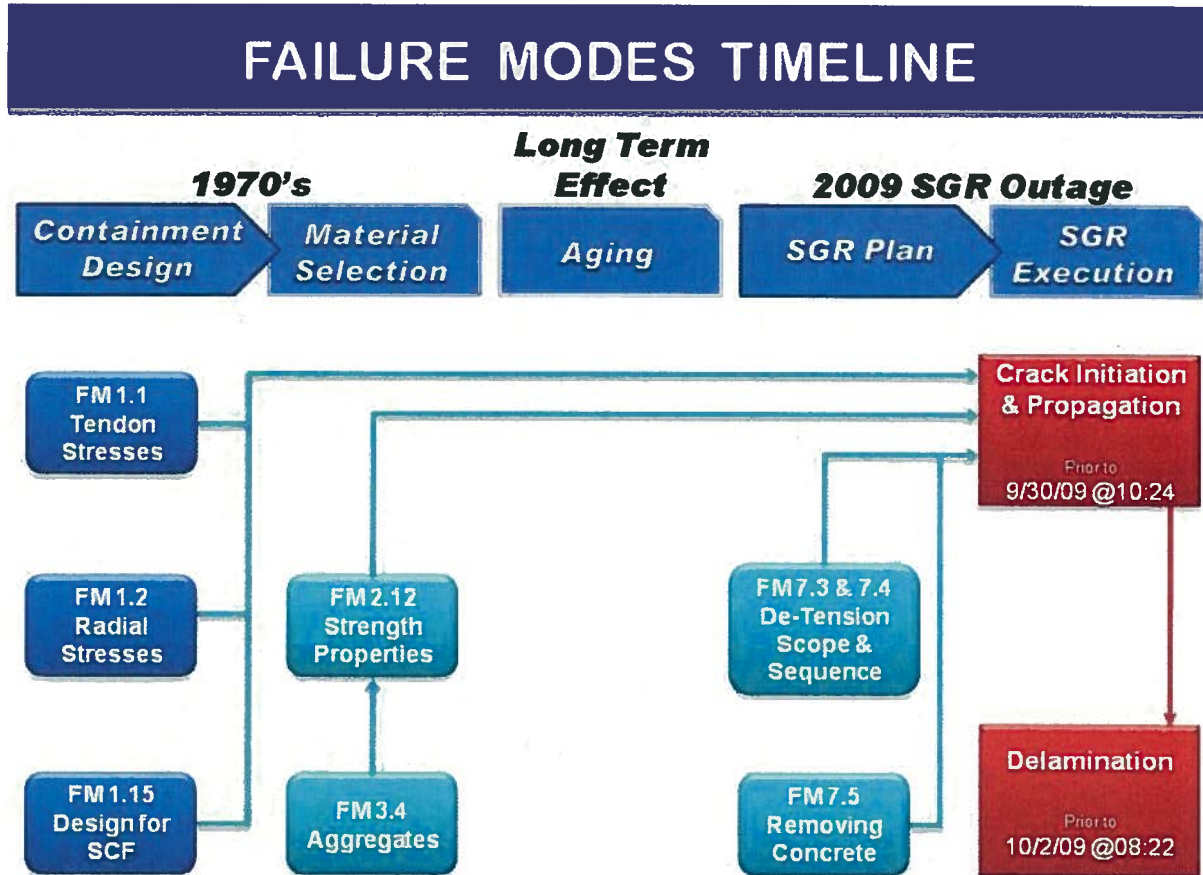


Figure 7.1 Failure Modes flow chart

The first step in the timeline was the original design of the containment building. That design specified the tendon sizes, locations, and no radial reinforcement for radial stress which ultimately played a part in the delamination four decades later.

The next step was the selection of materials for the concrete. The materials selected met the design requirements but resulted in concrete that had lower tensile strength and aggregate properties than concrete at other nuclear plants.

A part of the SGR project scope was to design a successful de-tensioning and containment opening project. The variables that were available were the scope of tendon de-tensioning, sequence of de-tensioning, and the nature of the containment opening made.

At this stage of the root cause assessment all the contributors have been identified and assessed. The next step is to simulate the tendon de-tensioning by Finite Element Analyses that reflect

loads and geometry related to the timeline and see under what conditions and when the concrete cracks.

Sequence of Steps:

The following sequence of steps provides an overall image of the de-tensioning process and its impact on bay 34. The displacements discussed below are from the Abaqus global model. The computer model simplified the de-tensioning process. It did not relax the tendons in order but, instead, relaxed all the tendons partially at the same time. Thus 25% through the de-tensioning means all tendons are stressed to 75% of their lock-off value.

1. The containment is initially constructed with straight vertical walls. Radial displacement is 0 inches since this is the measurement baseline (Figure 7.2).
2. Upon completion of tendon tensioning the building is mostly symmetrical and each bay has an inwardly curved wall with a maximum deflection of -0.5 inch (Figure 7.3).
3. Over the next three decades the concrete creeps and radial displacement grows to a maximum of -1" (Figure 7.4).
4. As SGR de-tensioning proceeds, bay 34 begins to move radially outward. Bays 23 and 45 also begin to move radially outward at half the rate of bay 34 because bay 34 has shared tendons with each of bays 23 and 45. The other bays begin to move inward in response to the buttresses having unbalanced side loads. The building develops an overall vertical curvature (Figure 7.5).

Figures 7.2 to 7.5 show the progression of containment shape over time. It was originally a cylinder but it became concave with the tensioning of the tendons. The SGR de-tensioning sequence resulted in a building-wide change in shape and bay 34 moved out close to its original tensioned position prior to creep. (Figure 7.11) Local stresses increased since the rest of the bay was still restrained by tensioned tendons. (Figures 7.16 to 7.23.) The situation ultimately led to localized cracking that propagated over most of bay 34. (Figures 7.26 and 7.28)

Detailed Computer Simulation:

The individual failure modes have been identified and placed in a timeline; results of the computer simulation follow.

There are three essential pieces to a credible computer simulation. They are:

- ◆ A discussion of the computer model being used. This is presented in [Attachment 1](#).
- ◆ A detailed discussion of the benchmarking performed to ensure the model accurately reproduces the conditions being simulated. This is discussed in [Attachment 2](#) so as not to distract from the discussion of the sequence of events presented in this section.
- ◆ A detailed presentation of the simulation results including a discussion of the important conclusions and expected results is discussed below.

In order to properly understand this event, it is necessary to develop a suitable computer model and simulate the response of the entire containment structure to changing conditions. For detailed information refer to [Attachment 1](#). To have confidence in a computer model's ability to simulate the events of root cause investigation, inputs must be realistic and predictions must be

validated. For this reason, PII developed progressively more rigorous analytical tools. A detailed discussion of the codes is available in [Attachment 1](#).

Next, a detailed comparison between the Abaqus radial displacement predictions will be compared to measured displacements using laser scanning. Greater detail is provided in [Attachments 2 and 4](#).

COMPUTER CODE INPUTS

The report will be providing some computer model plots which had the following inputs that were used based upon testing and modeling. PII does not use NASTRAN to quantify concrete fracture so fracture parameters are not applicable. Abaqus applies creep correction only for long time period intervals such as the timestep of 30 years of operation with the containment tensioned. E0 is the elasticity modulus and E1 is the creep adjusted elasticity modulus. F't is tensile capacity and G't is the fracture energy. 3.45 E6 psi is the average modulus measured on 22 CR3 containment cores. Fracture energy was measured to be 0.40 lbf/in. Abaqus Global does not calculate fracture so those parameters are Not Applicable for it.

Figure	Model	E0 psi	E1 psi	F't psi	G't lbf/in	Creep
7.2, 7.3, 7.5, 7.6, 7.7, 7.8, 7.10	Abaqus Global	3.45 E6	3.45 E6	NA	NA	2.2
7.12, 7.13, 7.15-7.24	Abaqus Global Bay sub model	3.45 E6	3.45 E6	108	0.08	2.2
7.4,7.9, 7.11	Abaqus Global	3.45 E6	1.1 E6	NA	NA	2.2
7.15,7.26,7.27,7.28,7.29	Abaqus Global Detailed sub model	3.45 E6	3.45E 6	360	0.08	2.2

Whole Containment Radial Displacement Simulation:

The following discussion of containment, due to its complexity, will be presented sequentially, starting with radial displacement calculations for the following milestones:

1. Un-tensioned (circa 1973)
2. Fully tensioned (circa 1976)
3. Fully tensioned in 2009 (after 30 years of creep)
4. Post SGR de-tensioning
5. Post SGR opening completion



NON-PROPRIETARY VERSION

The sequence of events starts with an un-tensioned containment building (circa 1973). This is shown in Figure 7.2.



Step: Step-01-Tensioning
Increment 0: Step Time = 0.000
Primary Var: U, U1 (Cyl)
Deformed Var: U Deformation Scale Factor: +2.000e+02

Figure 7.2 CR3 containment un-tensioned - facing bay 34 – baseline case.
Note the equipment hatch and buttresses 3 and 4. The parameter displayed (U) is radial displacement.

NON-PROPRIETARY VERSION

The next step is the containment building after being fully tensioned.

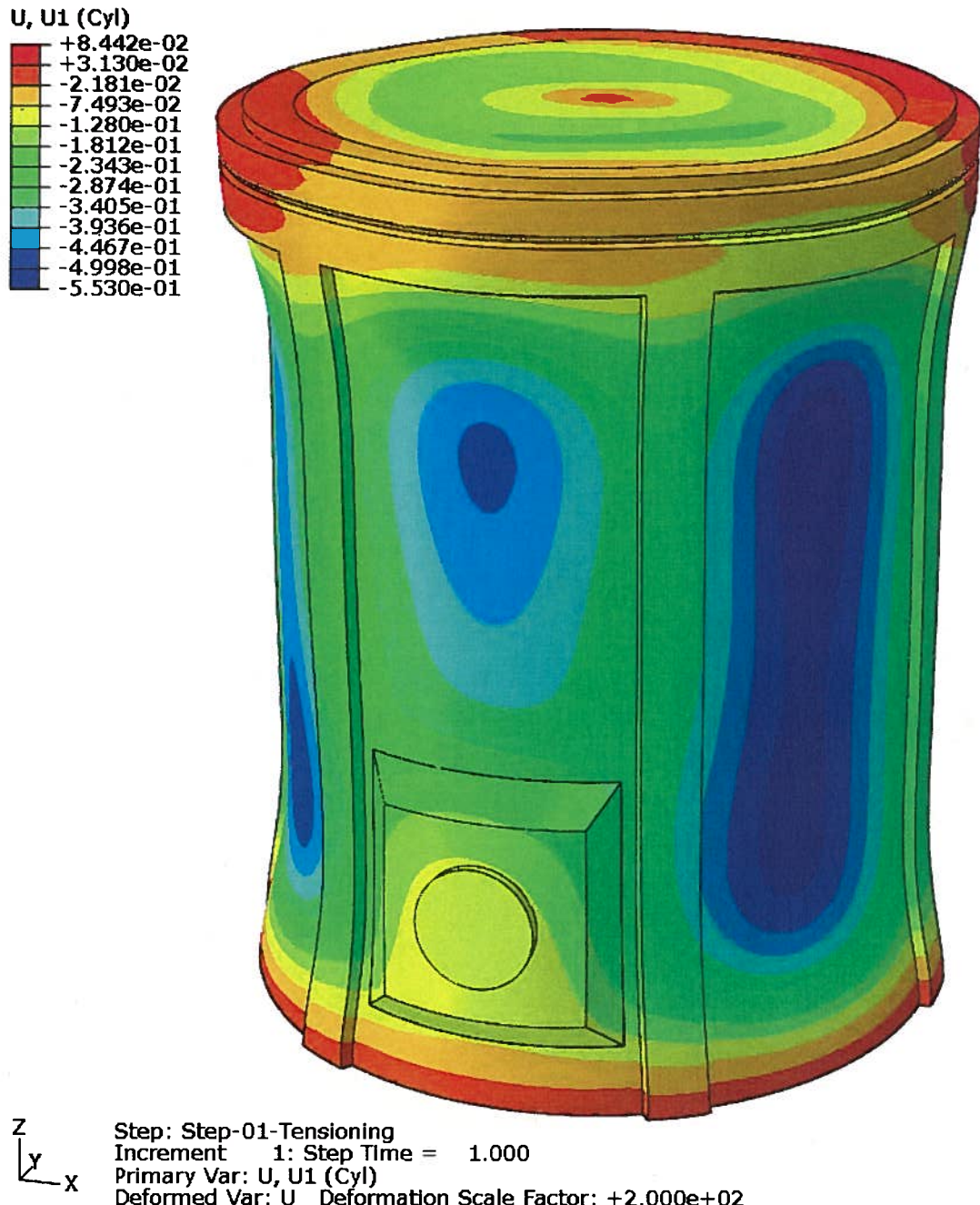


Figure 7.3 CR3 containment building fully tensioned.
The parameter being displayed (U) is radial displacement.

The overall effect of tensioning the tendons in the building was to cause the building to contract under the force of the tendons. Blue denotes the maximum contraction (of about -0.5") and red shows a slight expansion around the ring header and the foundation. Bay 34 is different from the

NON-PROPRIETARY VERSION

other bays due to the presence of the reinforced equipment hatch. As expected, the influence of the equipment hatch fades with distance. Also, as expected, the center of each bay deflects inward more than the edges which are anchored to the buttresses.

The next milestone is the effect of 30 years of creep in the concrete.

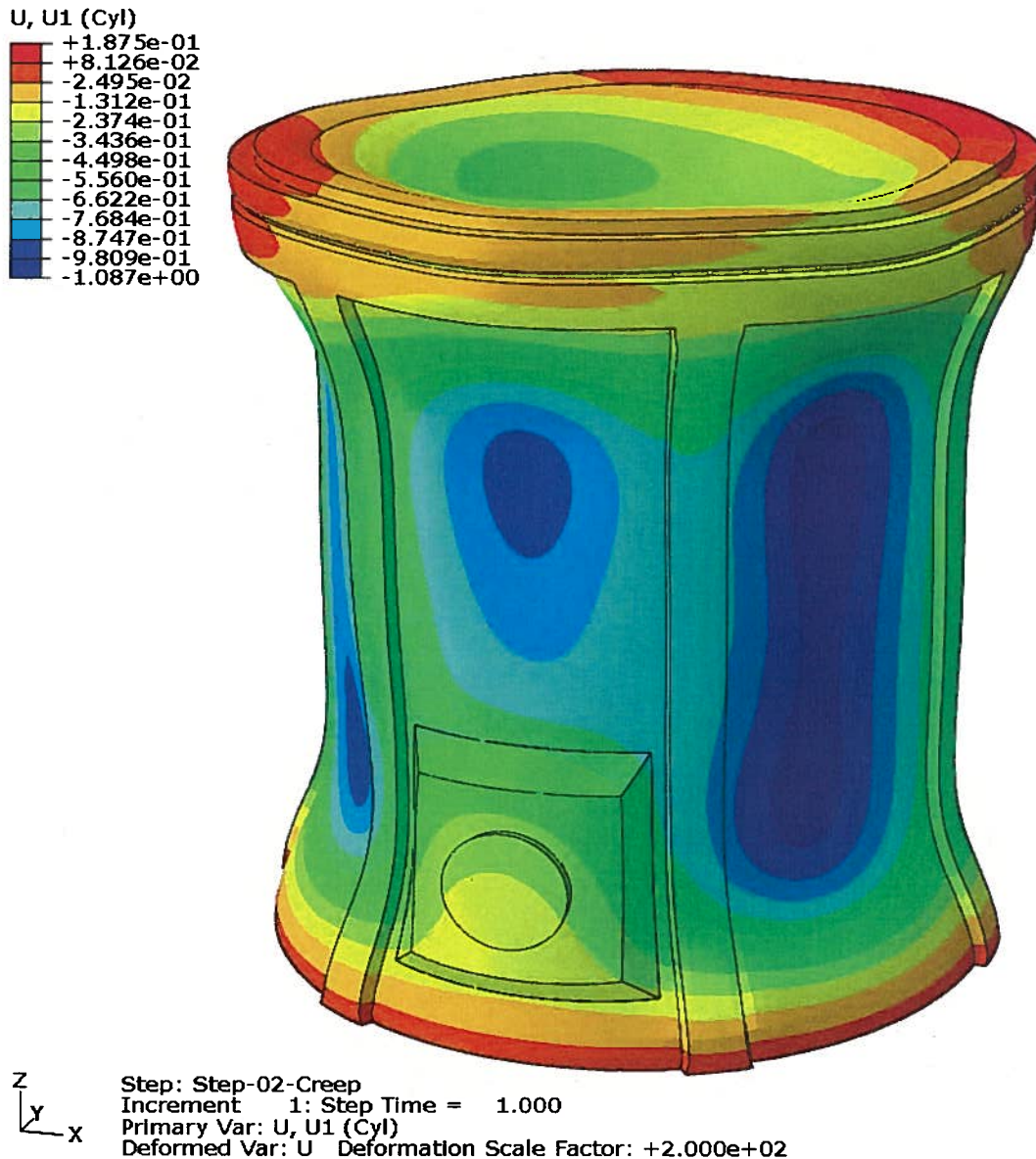


Figure 7.4 CR3 containment radial displacement after 30 years of creep.

Creep is the gradual displacement of concrete under long term stress so one would expect additional radial displacement over time. The effect of creep is visible in the depth of the dome, the narrowing of the waist of the building, and the displacement of the equipment hatch.

NON-PROPRIETARY VERSION

The next milestone is the completion of the SGR de-tensioning in 2009. This consisted of de-tensioning 17 horizontal and 10 vertical tendons. The de-tensioned zone extends from about elevation 183' to 210' with a maximum effect at elevation 197'.

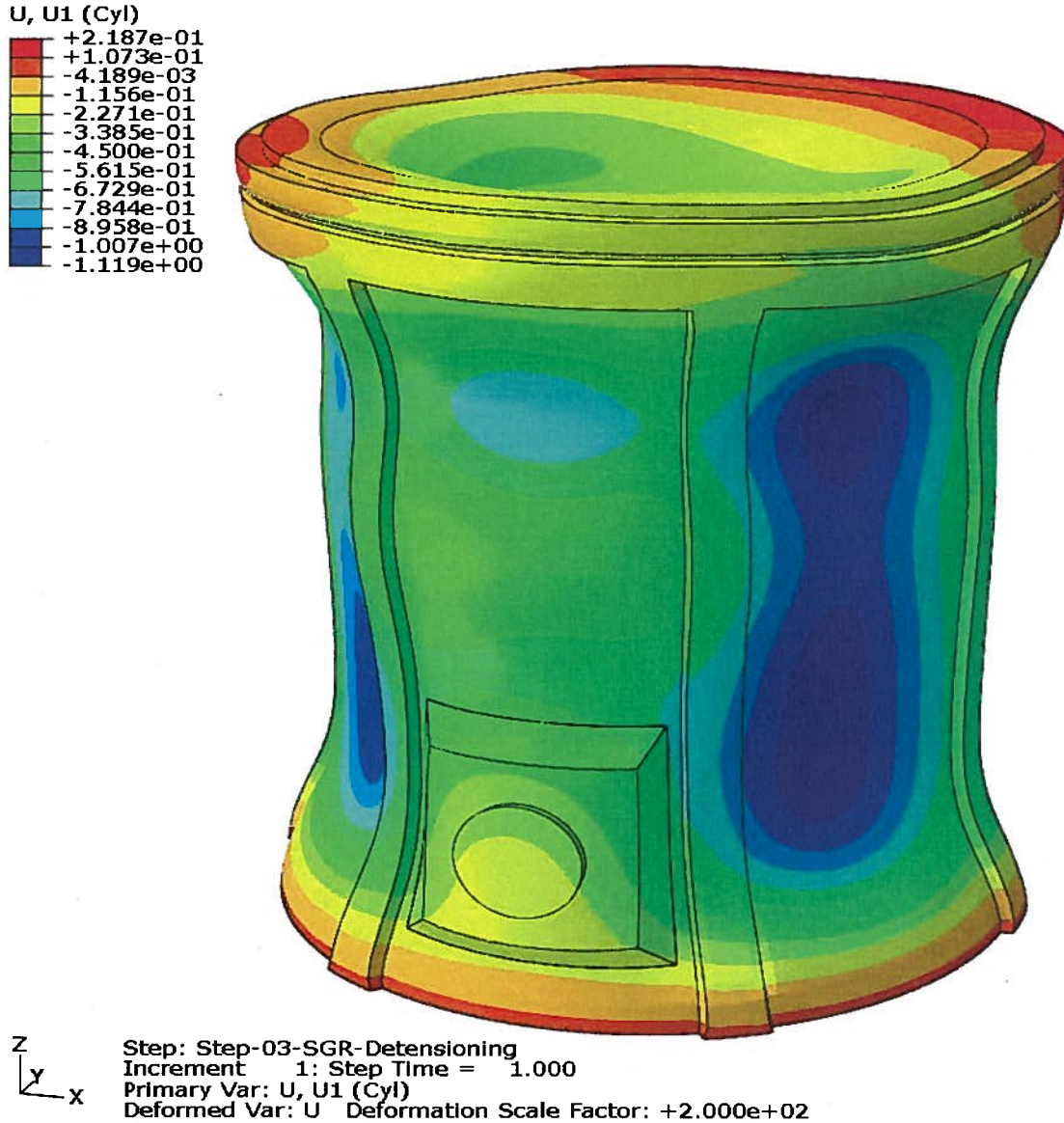


Figure 7.5 CR3 containment radial displacement post-SGR de-tensioning

The shape of buttress 3 in profile has changed from a gradual C curve into an S curve because of the development of a bulge in the center of bay 34. The blue spot indicating radial contraction is now missing from bay 34 and is somewhat reduced in bay 45 (which experienced a reduction of nine tendons (due to tendons extending across two bays)). Bay 23 is not visible but also sees a reduced effect due to eight of its tendons being de-tensioned.

Figure 7.6 is a special case. The containment wide Global Abaqus model is not designed to handle the consequences of concrete cracking. The additional complexity involved with handling crack propagation and load distribution in a cracked environment would be prohibitive for the full containment model. That analysis is performed in the sub-models. In Figure 7.6 the analysis was stopped at Figure 7.5 and the ties between the inner and outer layers were manually broken to determine what the containment-wide response would be. The result is that an hourglass shape has developed in the bulged area of bay 34, matching the actual delamination pattern, and is caused by the interaction of the building causing the center of bay 34 to bulge outward. The de-tensioned zone at the sides of the SGR opening reduces the propensity to crack. The result is an hour glass shape with the peak displacement in the fully tensioned area just above and below the bulge in the middle of the bay.

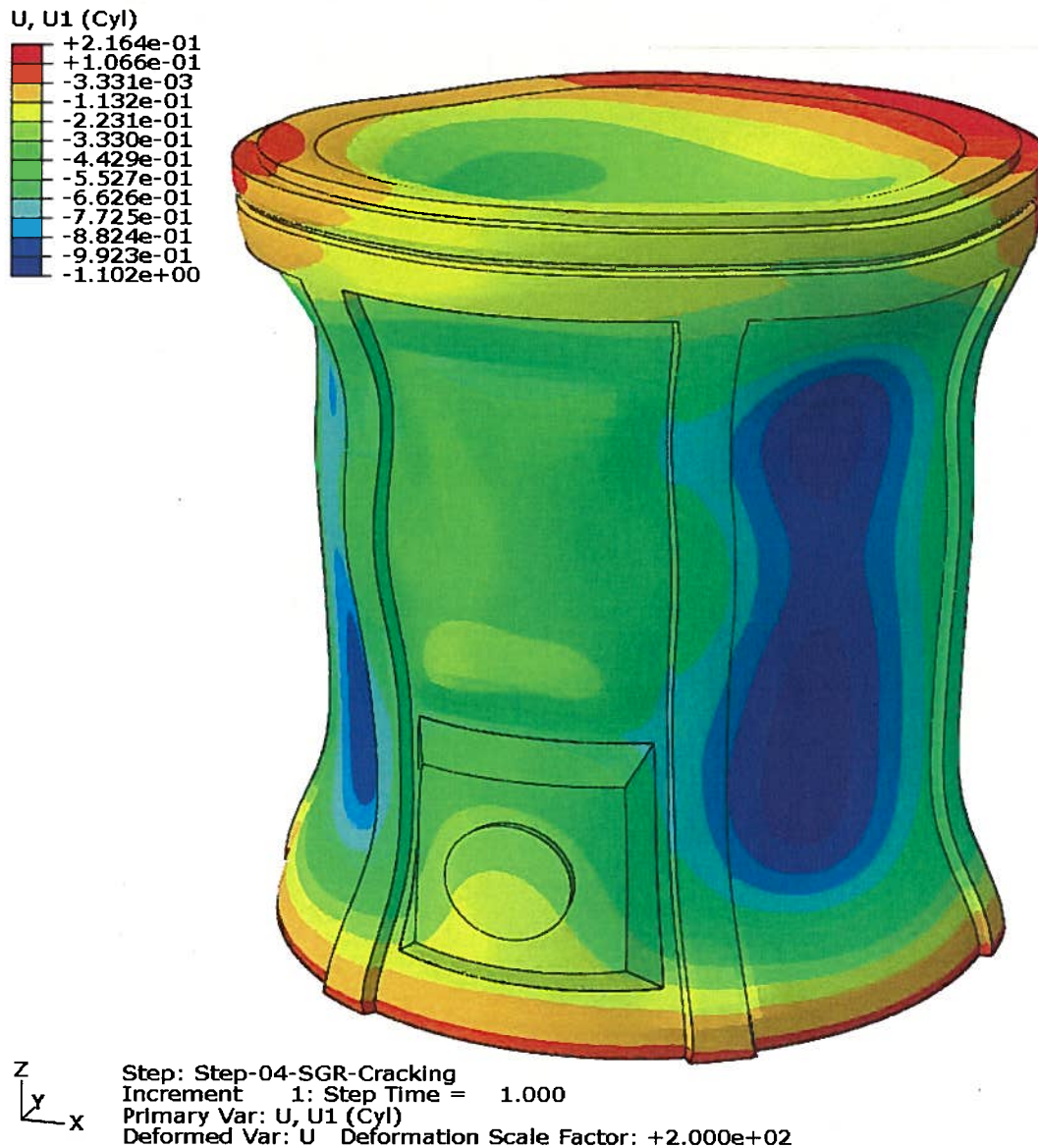


Figure 7.6 CR3 containment radial displacement post SGR de-tensioning

NON-PROPRIETARY VERSION

The final milestone occurs where the conditions in Figure 7.5 are then subjected to removing the concrete completing the SGR opening. To follow the actual progression of the delamination progression refer to Figures 7.16 through 7.23.

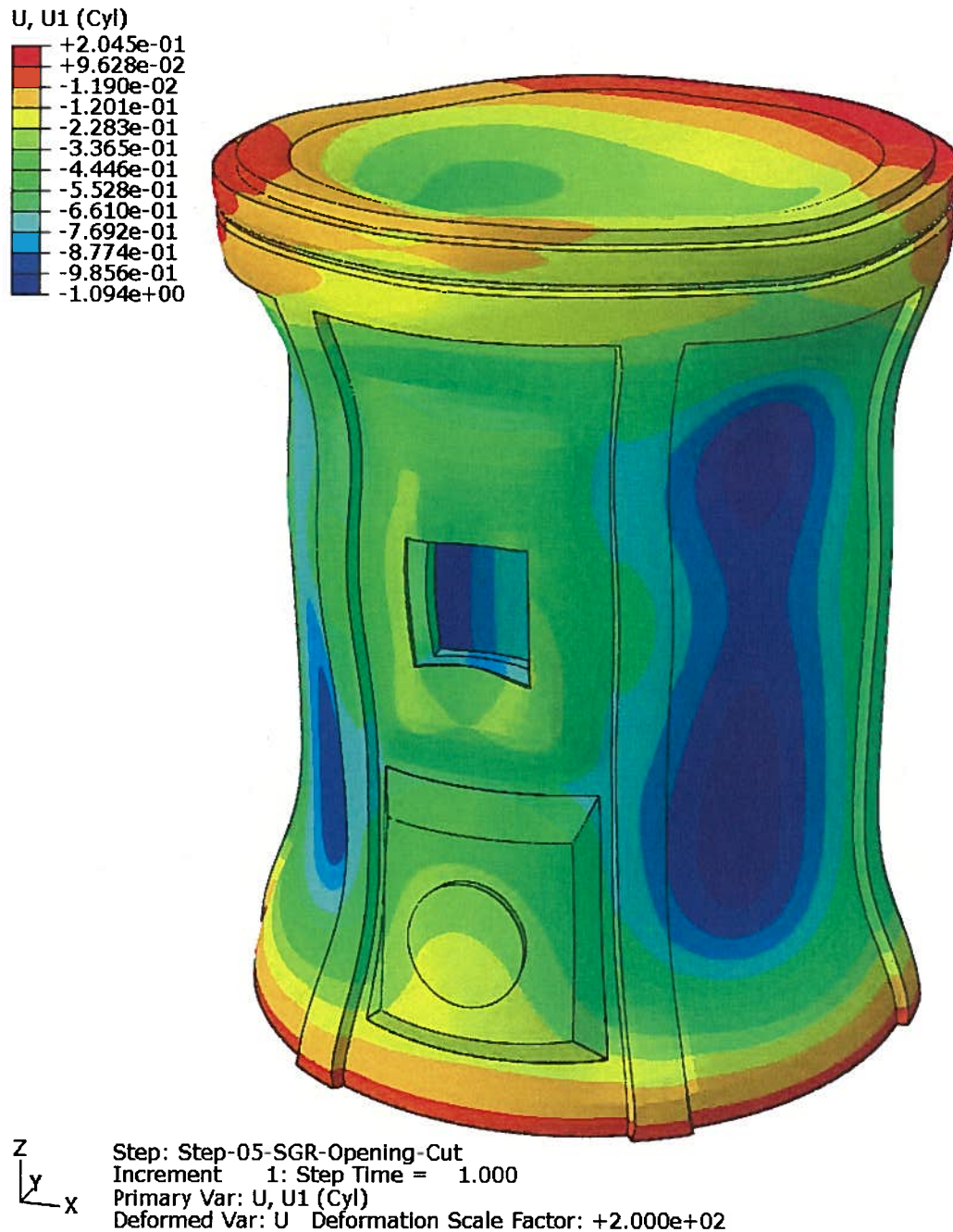


Figure 7.7 CR3 containment radial displacement after SGR opening completion.

Detailed Local Wall Radial Displacement Response:



Up until this point the entire containment has been displayed, which is useful to understanding the overall forces at work but it does not explain the local conditions that ultimately result in delamination. Figure 7.8 is a cut-away profile of the bay 34 wall showing radial displacement as it was immediately after tensioning in 1976.

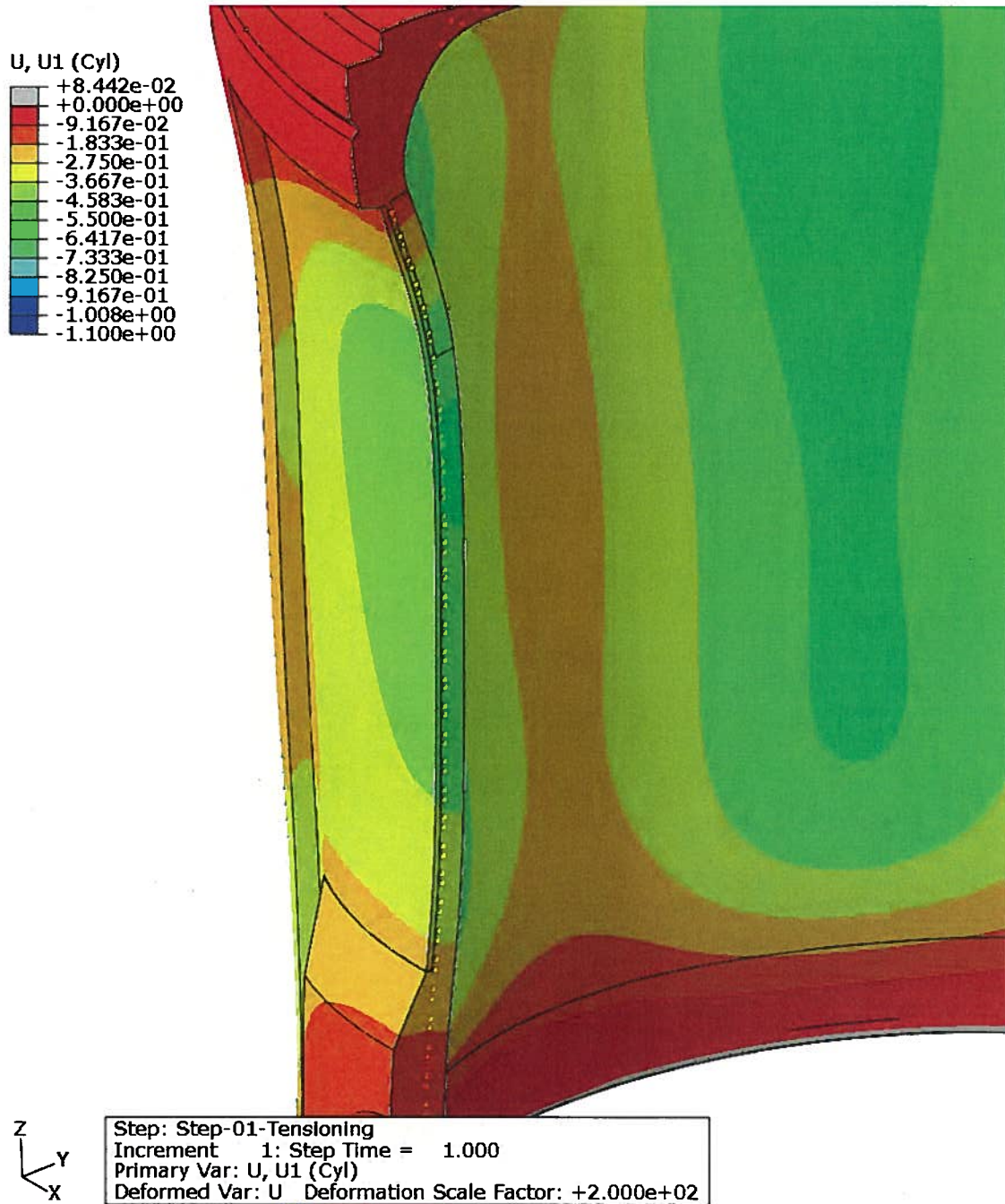


Figure 7.8 CR3 Bay 34 wall profile radial displacement post initial tensioning in 1975. The next milestone is in 2009 after 30 years of creep.

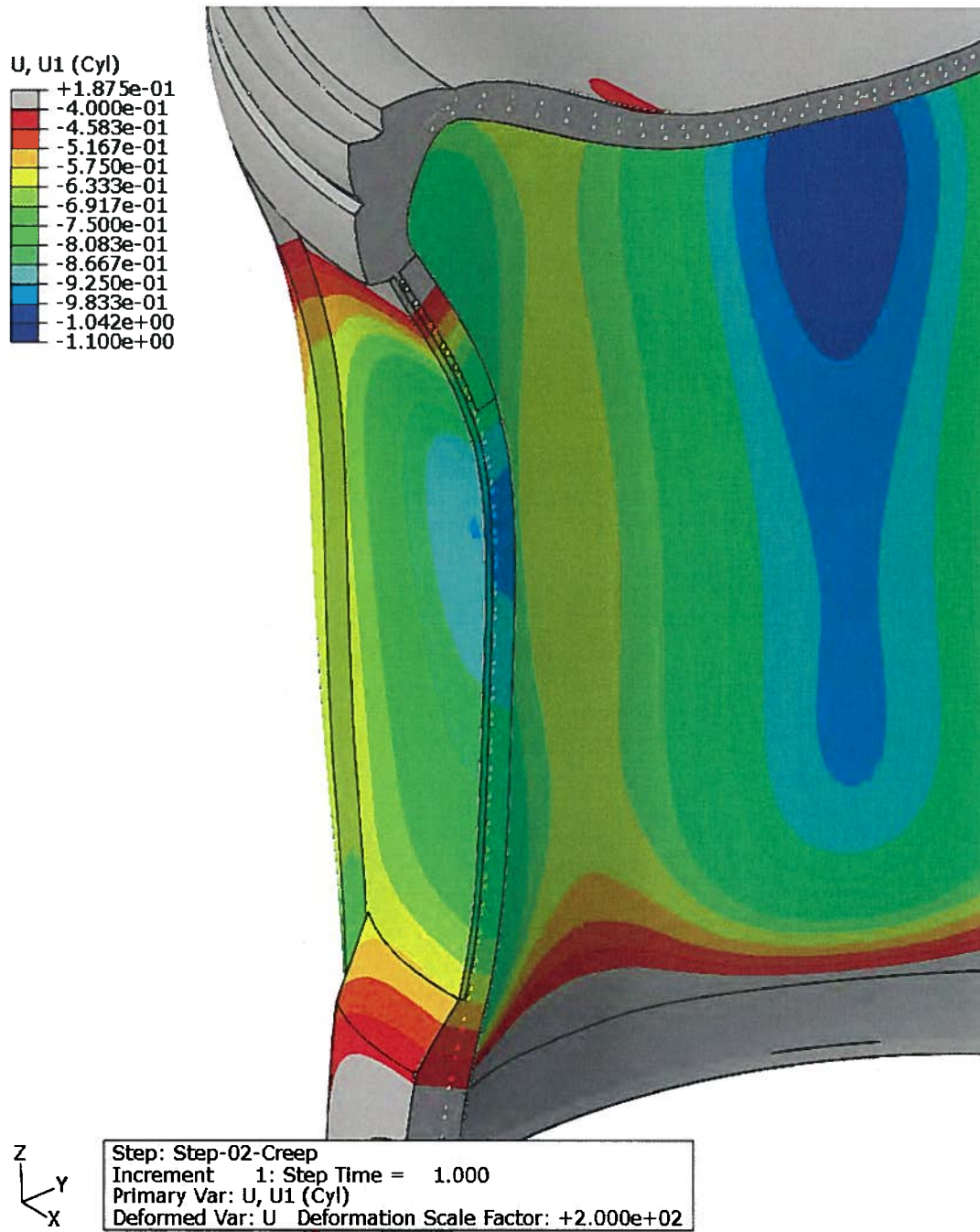


Figure 7.9 CR3 containment cut-away profile showing radial displacement after 30 years of creep.

The next milestone is post SGR de-tensioning.

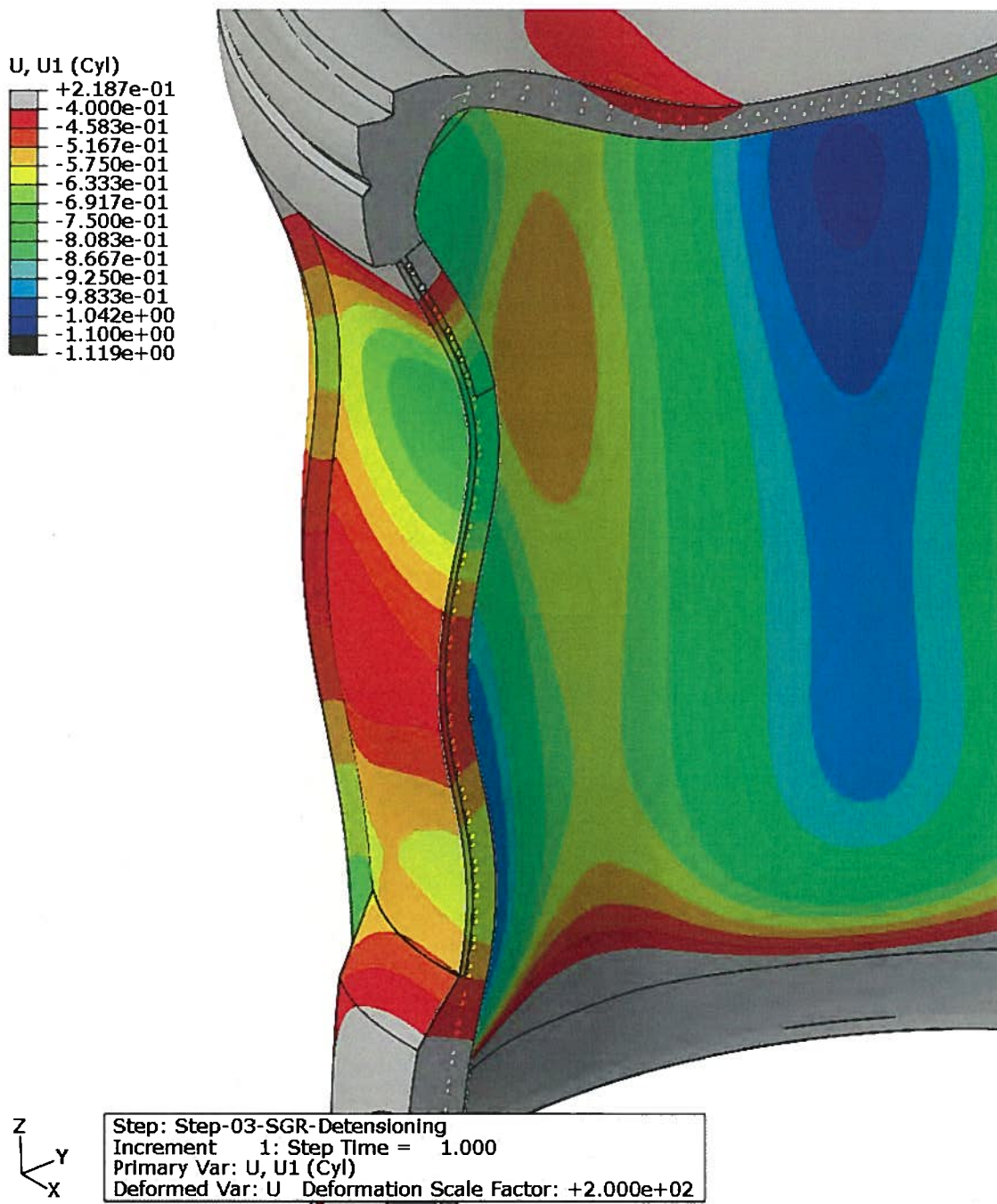


Figure 7.10 CR3 containment wall cut-away profile of radial displacement following the SGR

Here, an S curve has developed in the wall. Delamination stems more from the rate of change in the profile than from the magnitude of the change in profile. The inward displacement of the wall was greater prior to SGR de-tensioning than after de-tensioning, but its margin to delamination was greater because the contraction was smooth. In this plot, the maximum curvatures are at elevations 173' and 220'. The maximum delamination gap widths measured were centered around 175' and 216' (See Figure 7.14) which is good agreement.

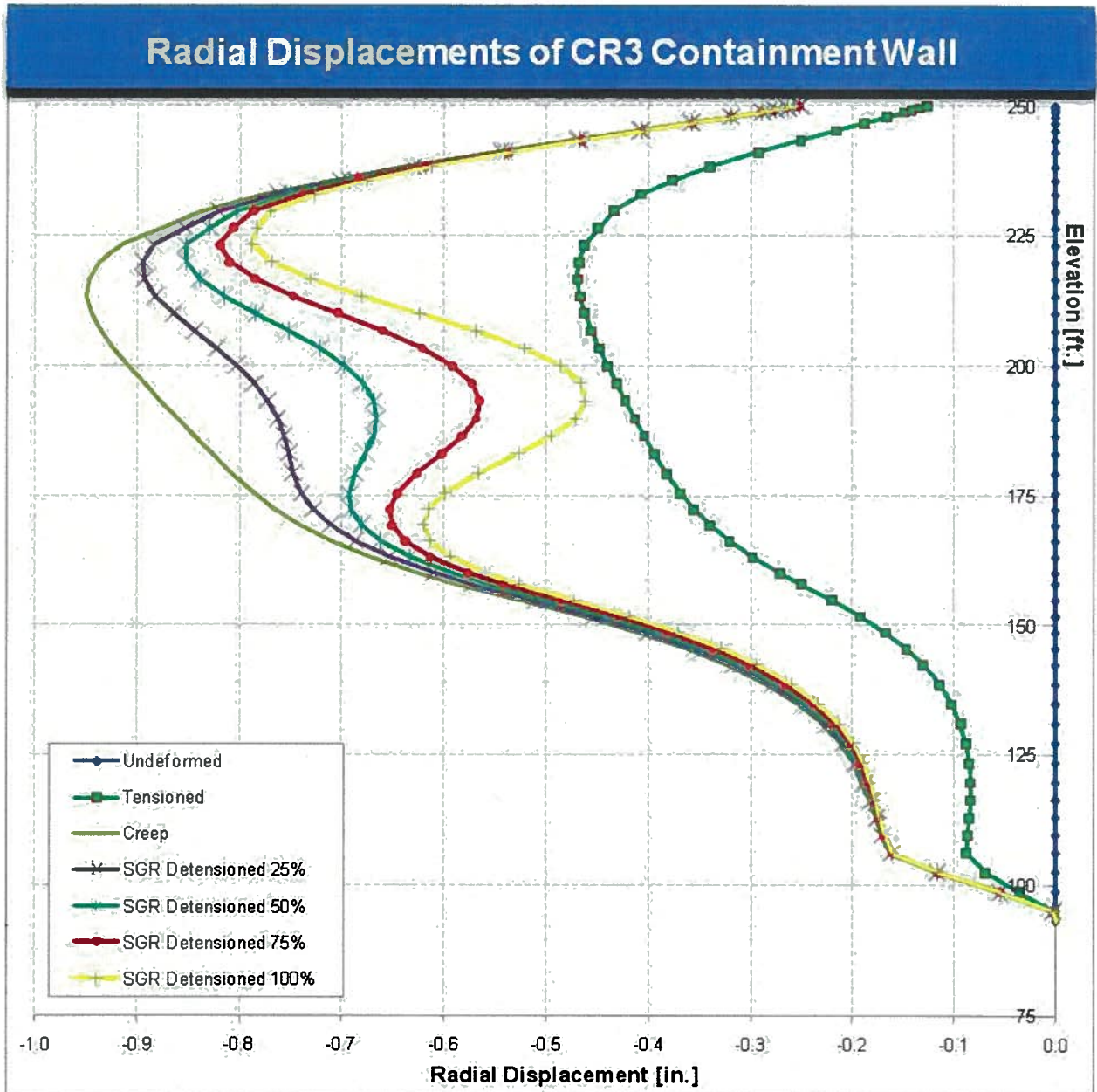


Figure 7.11 Bay 34 midline profile for progressive SGR de-tensioning

As expected, the un-tensioned case shows no radial displacement. The 1976 tensioned case shows uniform displacement of 0.5" inward. Creep increases that displacement to 1" inward by 2009. The SGR de-tensioning shows the impact of de-tensioning 10 vertical and 17 horizontal tendons in creating a double peaked profile with a much sharper curvature than was experienced previously. The intermediate lines are partial de-tensioning points going from fully tensioned to de-tensioned for SGR. The model did not remove each tendon sequentially. Instead, it de-tensioned all the selected tendons incrementally. While that is not the exact sequence used, the model gives a realistic view of the transition felt by the bay 34 wall. In the fully tensioned case (Creep), the curvature is approximately 0.05" over a 25' span or 170 μ in/in. De-tensioning 10

vertical tendons and then 17 horizontal tendons in a row created two sharp peaks with a curvature of 0.15" in 40' or 310 $\mu\text{in/in}$ and 0.3" in 50' or 500 $\mu\text{in/in}$, indicating that there should be more severe damage above the opening (centered at 225') and less severe damage below the opening (centered at 170'). However, the actual de-tensioning sequence de-tensioned the higher tendons last, which indicates that the lower peak was accentuated during most of the de-tensioning sequence, so the curves presented here may not exactly match the transient peaks seen until de-tensioning was complete. In Figure 7.14 the two centers of damage are at 216' and 175', and the damage appears similar above and below the opening. Overall there was good agreement between the predictions of the computer model and the delamination observed. Looking at bay 34 from the outside, at the end of de-tensioning the wall has two concave curves and one convex curve. It is worth noting that the peak concave curvature occurred in tensioned areas, so the concrete exposed to the peak curvature still had the tensile peak due to normal tendon force on the area around the horizontal tendons.

The center of the de-tensioned zone was at 192' and this is the point in the graph which showed the greatest outward displacement (bulging) by moving about 0.025" for each horizontal tendon de-tensioned.

Figure 7.12 shows the predicted effect of delamination. The wall separates into an inner section and an outer section. The separation is not uniform because the bulge area tends to close the gap in the center. The center area is de-tensioned so the force separating the two sections is reduced.

The Abaqus bay sub-model was used to calculate the response of bay 34 to the SGR de-tensioning sequence. The results are shown in Figures 7.12 and 7.13. The delamination event alone is shown in Figure 7.12. Figure 7.13 shows the bay response to removing the concrete after delamination. Notice the size of the crack that develops is not uniform and it is not greatest in the middle of the bay. It is greatest above and below the middle of the bay. This makes sense if the non-delaminated concrete on the outside of the neck of the hour-glass is restraining the crack opening. It also makes sense in terms of the area in which the tendons are de-tensioned. Note the similarity between the computer predictions in Figures 7.12 and 7.13 and the actual crack width data taken by core bore and Impulse Response monitoring. Also note that the crack opening does not significantly change due to removing the concrete. That explains the lack of change in the cracks visible at the edges of the opening when compared between 10/3/09 and 10/28/09. The depth of concrete removed on 10/3/09 was about 15" and on 10/28/09 it was 100%. It is recognized, however, that the model predicts about 0.5" for the crack and the peak cracking was about 2.5" so the relative dimensions should be considered rather than the absolute values.

NON-PROPRIETARY VERSION

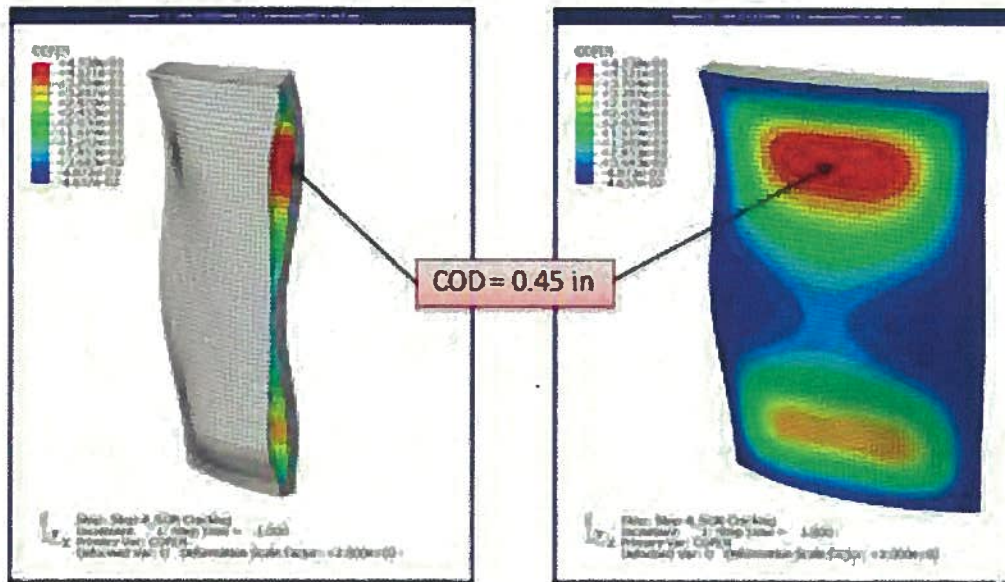


Figure 7.12 The Dimensional response to delamination – Step 4 SGR Cracking
Crack Opening Distance (COD) is the width of the crack that develops. Note the similarity of the pattern in this Figure to that in Figure 7.14.

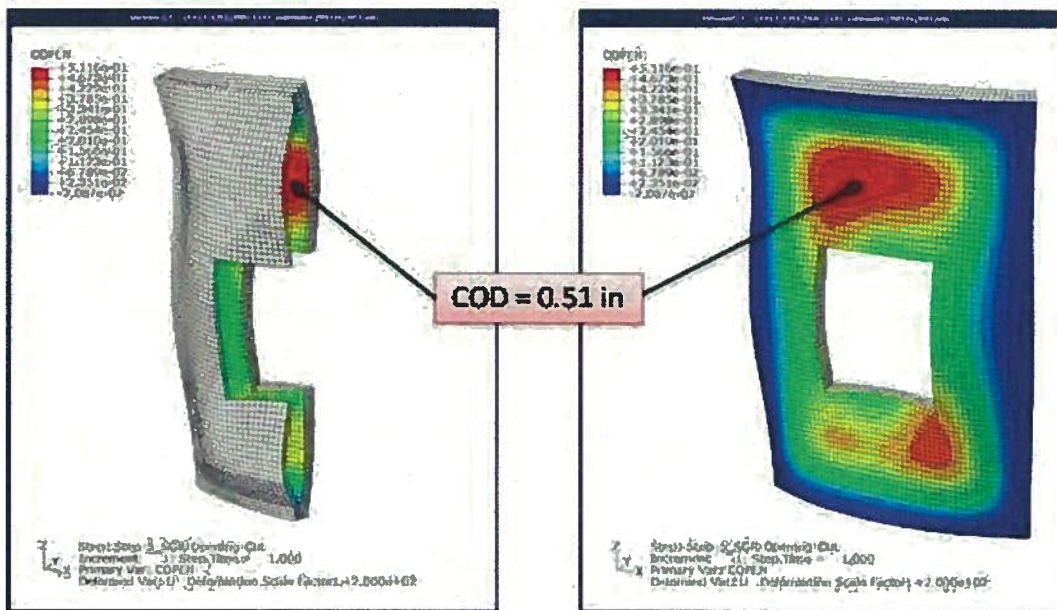


Figure 7.13 Crack Opening Distance (COD) after Concrete Removal – Step 5.
Note the width of the crack increased by about 10% due to concrete removal. Concrete removal does cause an increase but not a significant one.

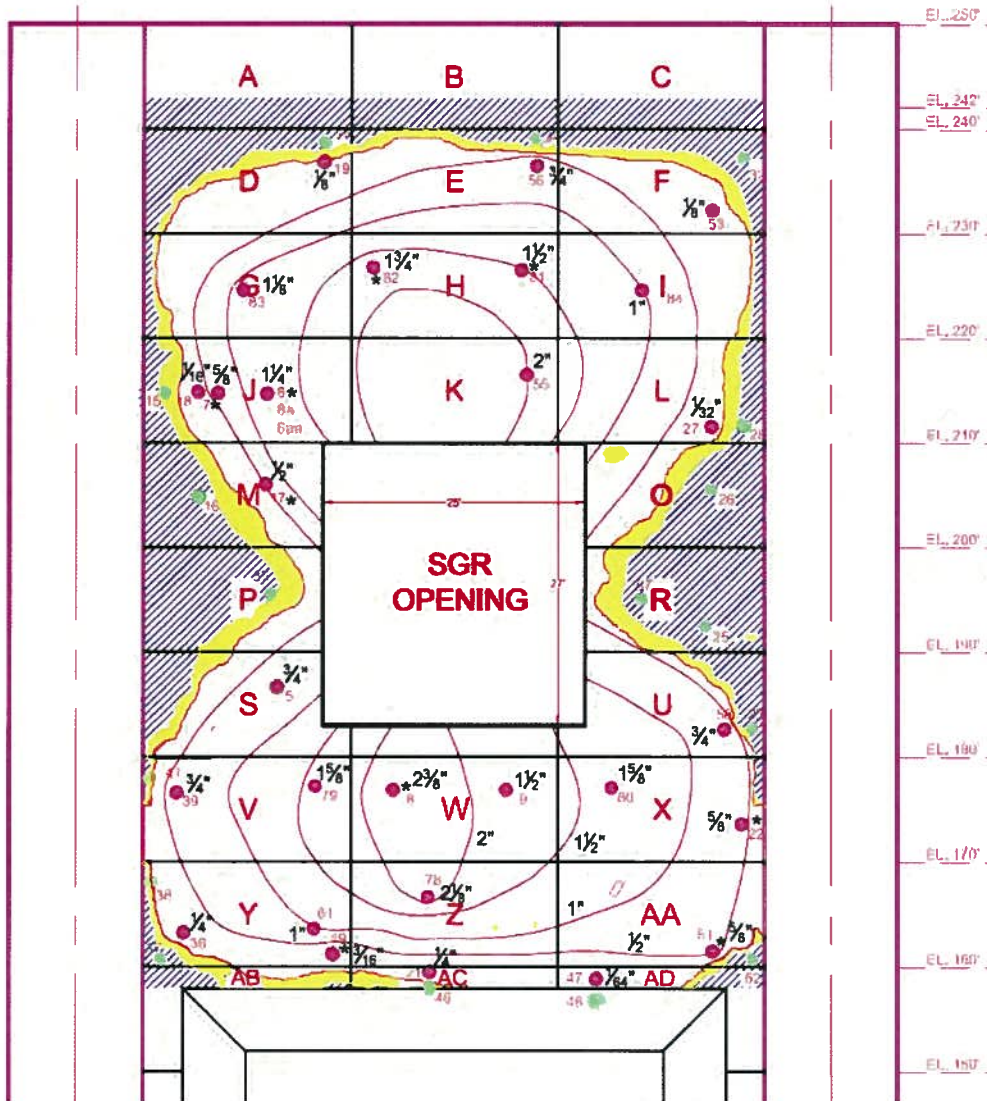


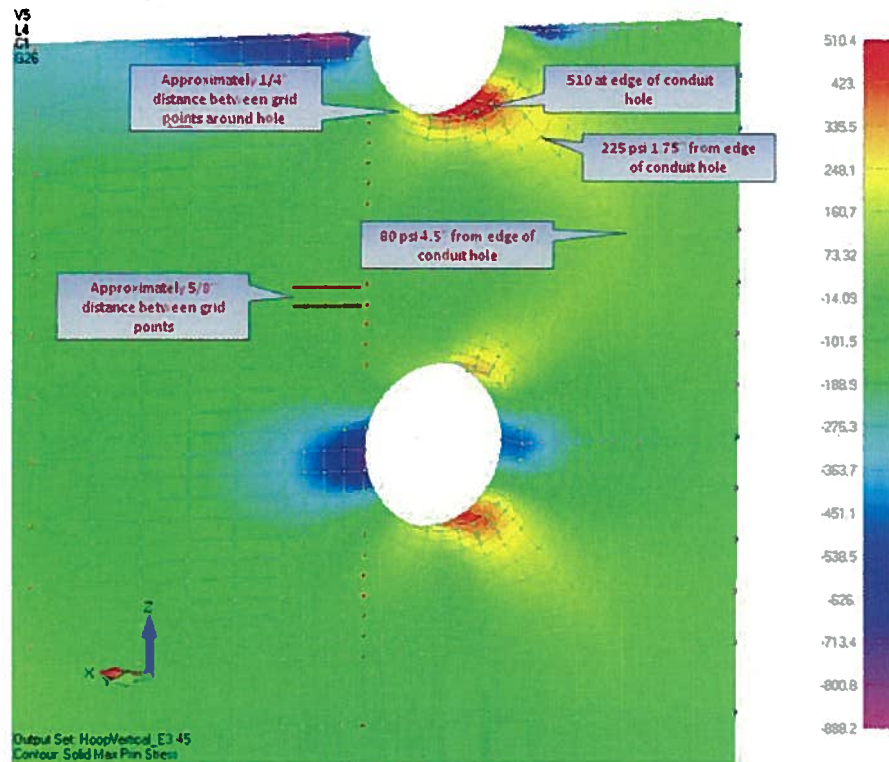
Figure 7.14 Plot of delamination damage in Bay 34. Shown are the measurements of the delamination gap both by impulse response test and by core bores.

Figure 7.14 displays the amount of separation due to delamination that was measured in bay 34. Compared with the radial displacement shown in Figure 7.13, the general agreement of the shape over the entire bay is an indication of the accuracy of the computer mode.

For completeness the effect of cutting out the concrete in the opening is also included in Figure 7.13, which increases the gap between with a mesh size of 1 square inch rather than the 1 square foot mesh of Abaqus Global.

At this point the analysis will switch from discussing large structures and will focus on small scale details. The scale will move from feet to inches. When the tendons were tensioned, the concrete underwent displacement which distributed the force exerted by the tendon into stress in

the concrete. Figure 7.15 shows the stress distribution around the horizontal tendons. Note the high compressive and tensile peaks on the edges of the horizontal tendons.



Expanded FEM *Between* Vertical Conduits – Lockoff Hoop & Vertical Loading, $E_c = 3.45 \times 10^6$ psi

Slide 5 of 5

Figure 7.15 *Stress contours for normally tensioned conditions in between intersections of a horizontal tendon with vertical tendons. (Section View)*

The peak tensile stress in Figure 7.15 is about 500 psi in the area immediately next to the horizontal tendons near the top and bottom positions. In the absence of outside influences, the peak stress is just at the tensile capacity of the concrete and may indicate very small cracks at the top and bottom of each horizontal tendon sleeve hole. Figures 7.16 to 7.23 show the maximum principal stress added as a result of the bending of the containment wall.

The computer simulation is not a tendon-by-tendon scenario. Instead, it takes the total effect of de-tensioning all the selected tendons and divides it into twenty steps so each frame in the figures below corresponds to a 5% change in all of the tendons rather than 100% of one tendon. The overall effect is unchanged, but some special effects may be lost by this technique.

NON-PROPRIETARY VERSION

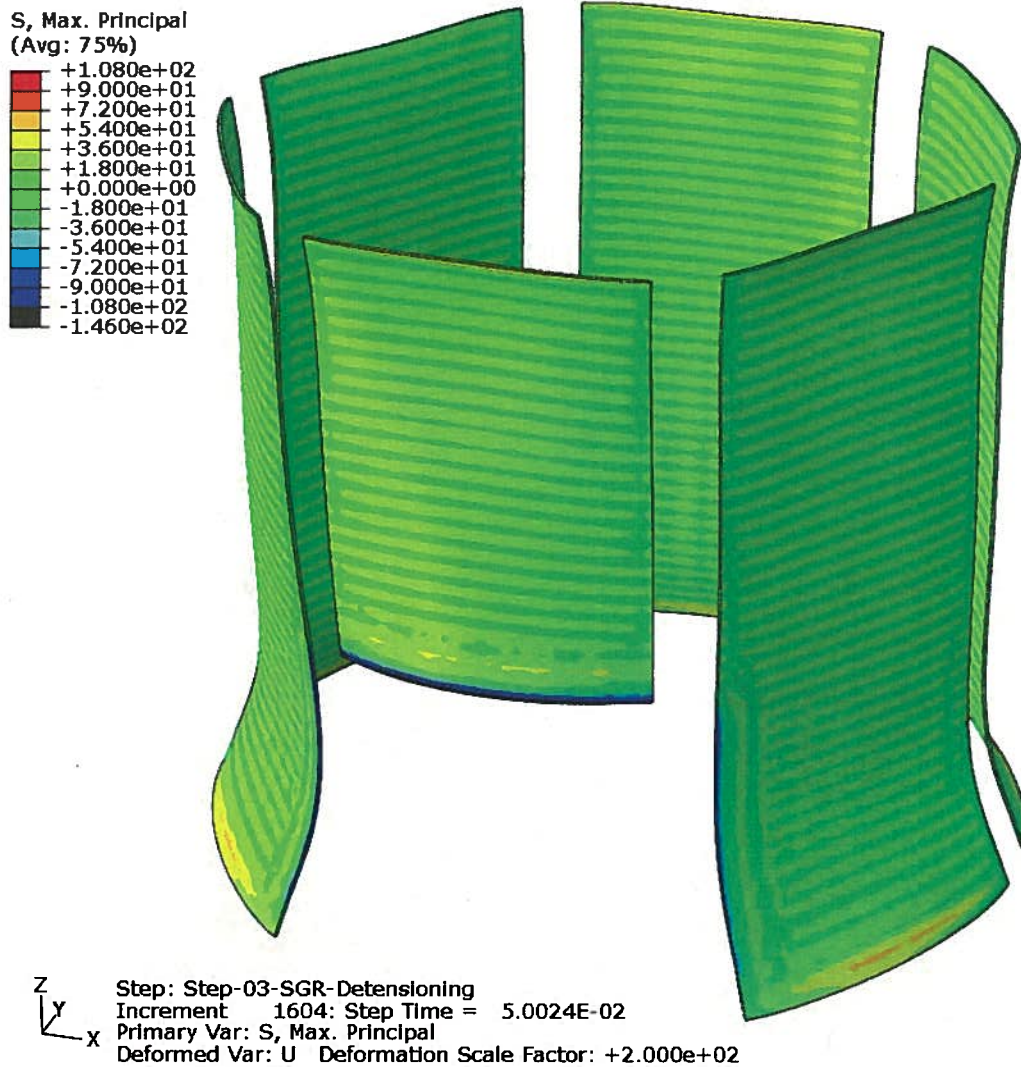


Figure 7.16 Step 1 of 20 time-steps in simulating the SGR de-tensioning.
Maximum principle stress (psi)

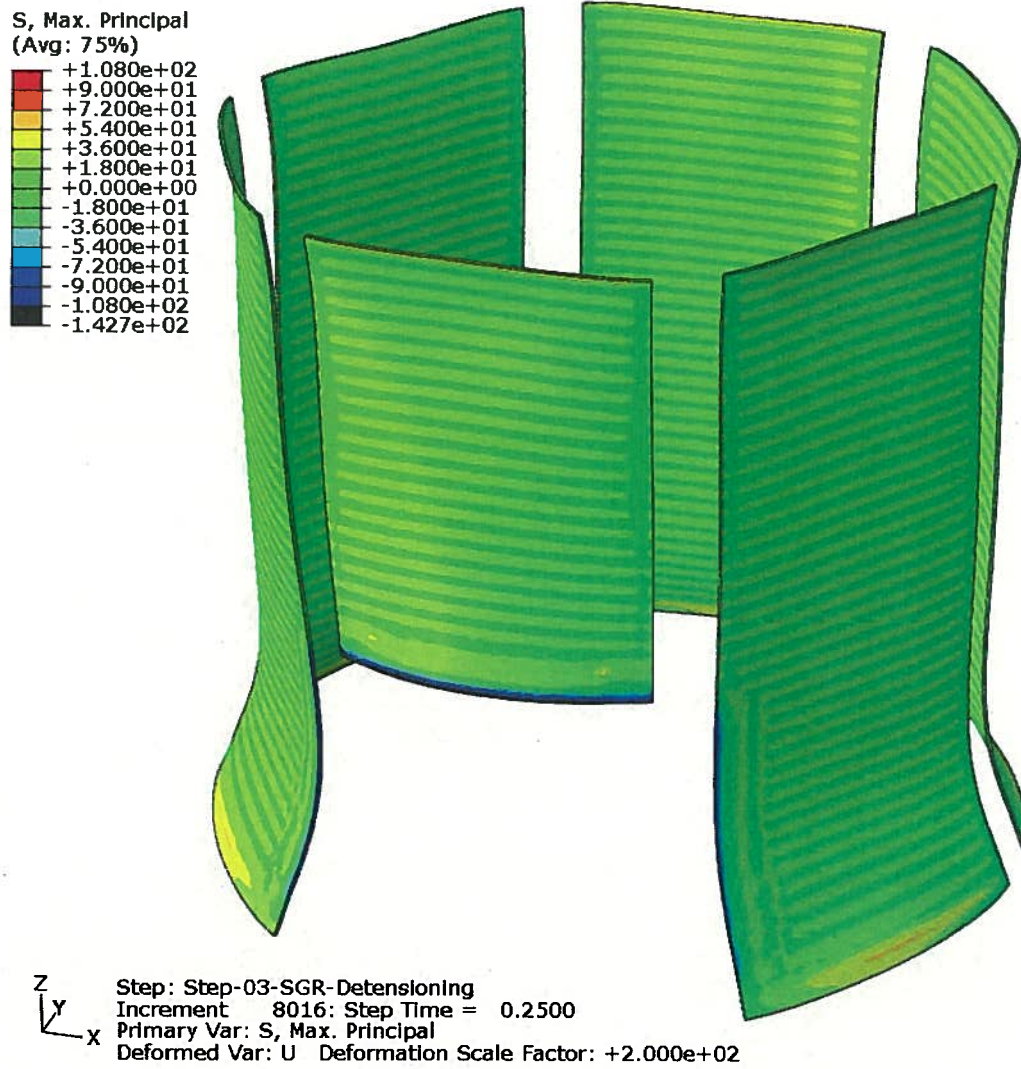


Figure 7.17 Step 5 of 20 in simulating the SGR de-tensioning.
Maximum principle stress (psi)

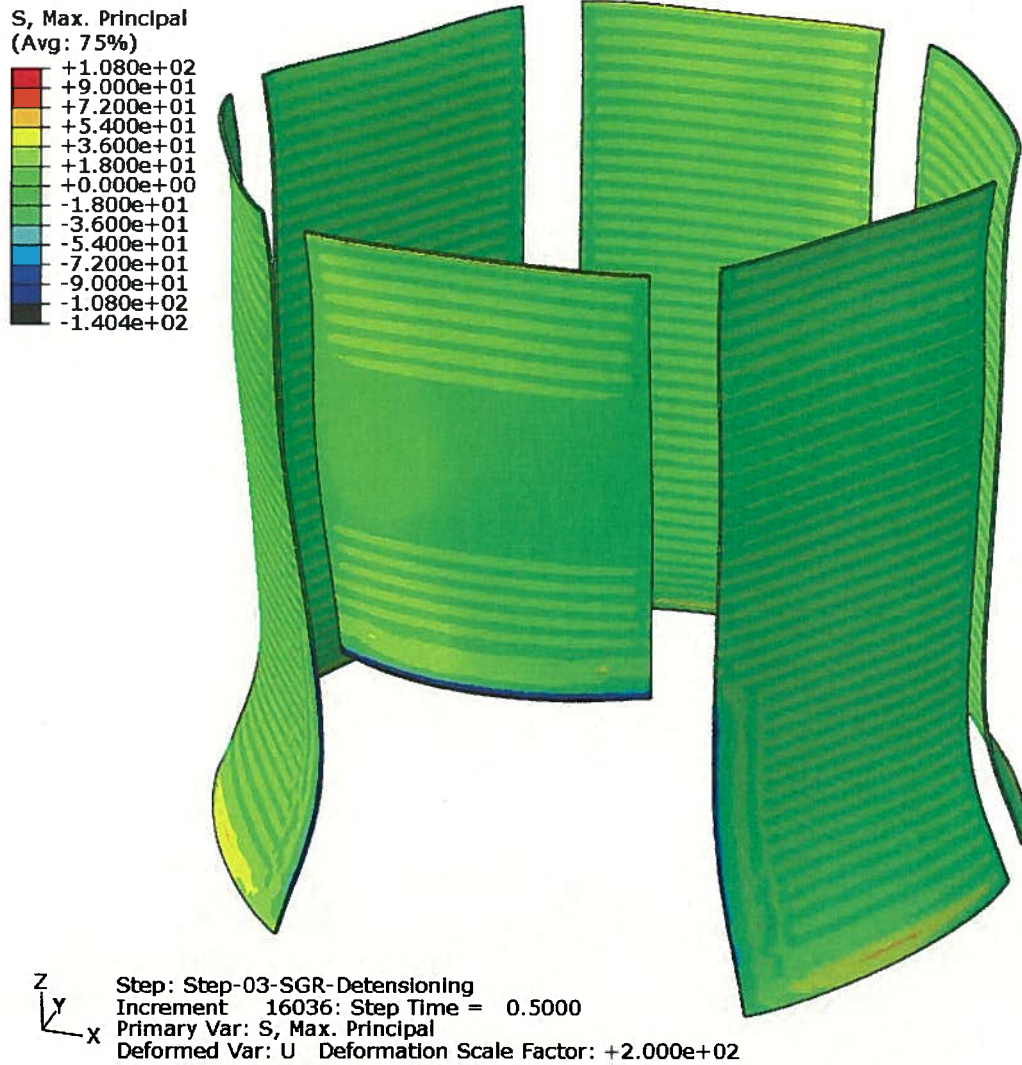


Figure 7.18 Step 10 of 20 in simulating the SGR de-tensioning.
Maximum principle stress (psi)

NON-PROPRIETARY VERSION

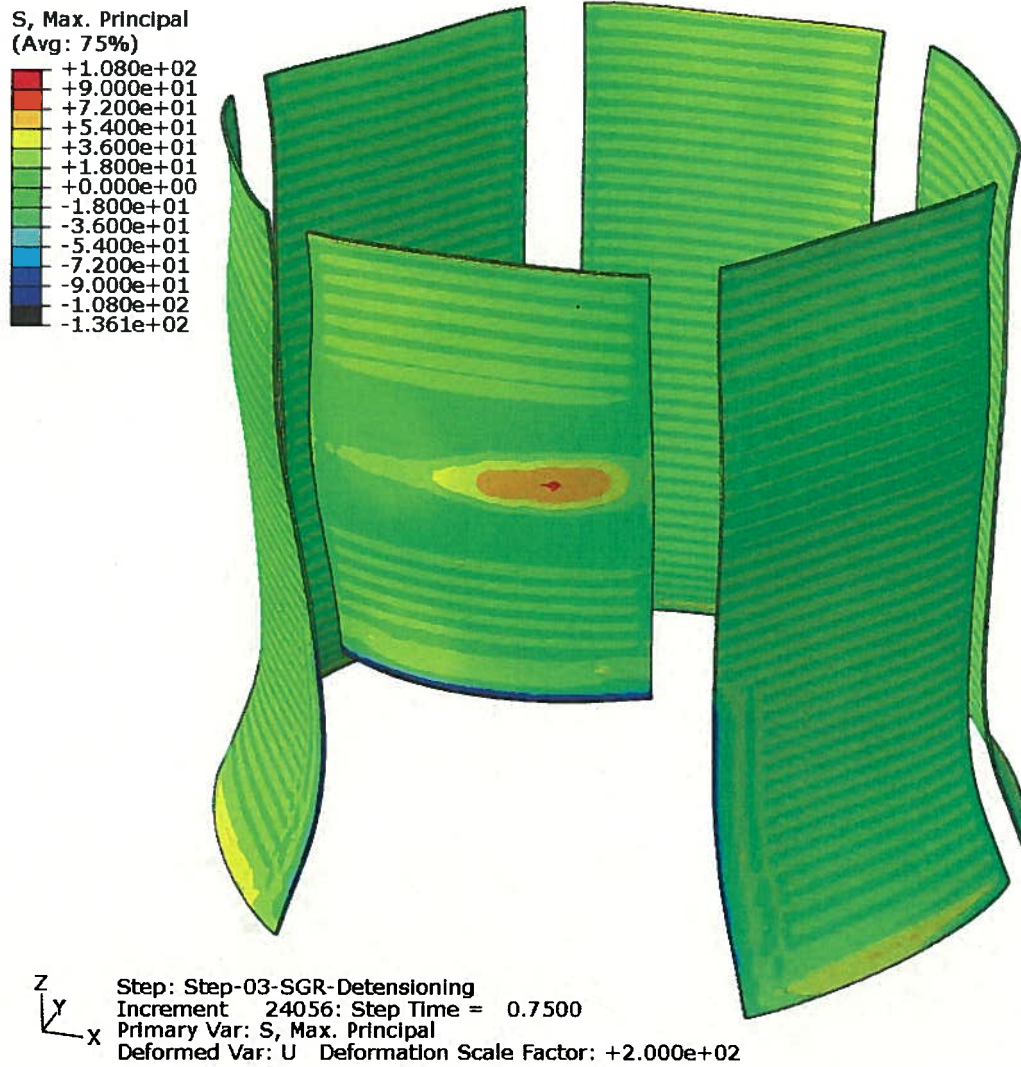


Figure 7.19 Step 15 of 20 in simulating the SGR de-tensioning.
Maximum principle stress (psi)

NON-PROPRIETARY VERSION

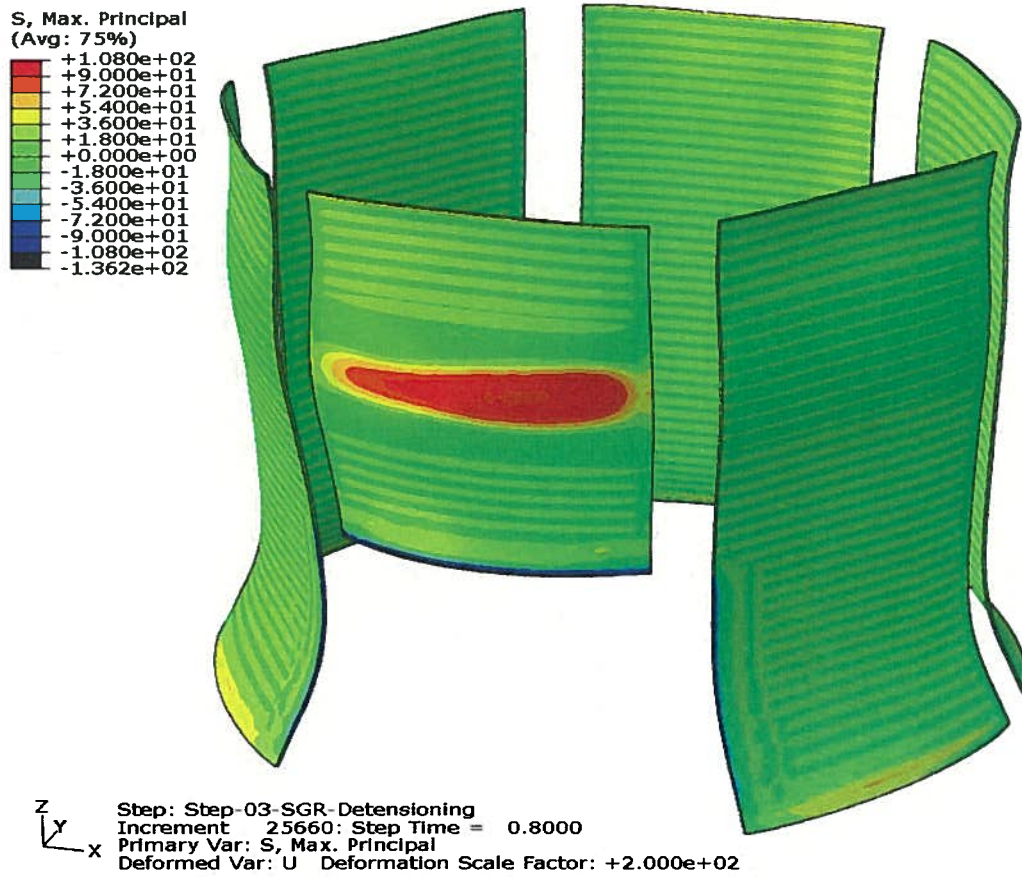


Figure 7.20 Step 16 of 20 in simulating the SGR de-tensioning.
Maximum principle stress (psi)

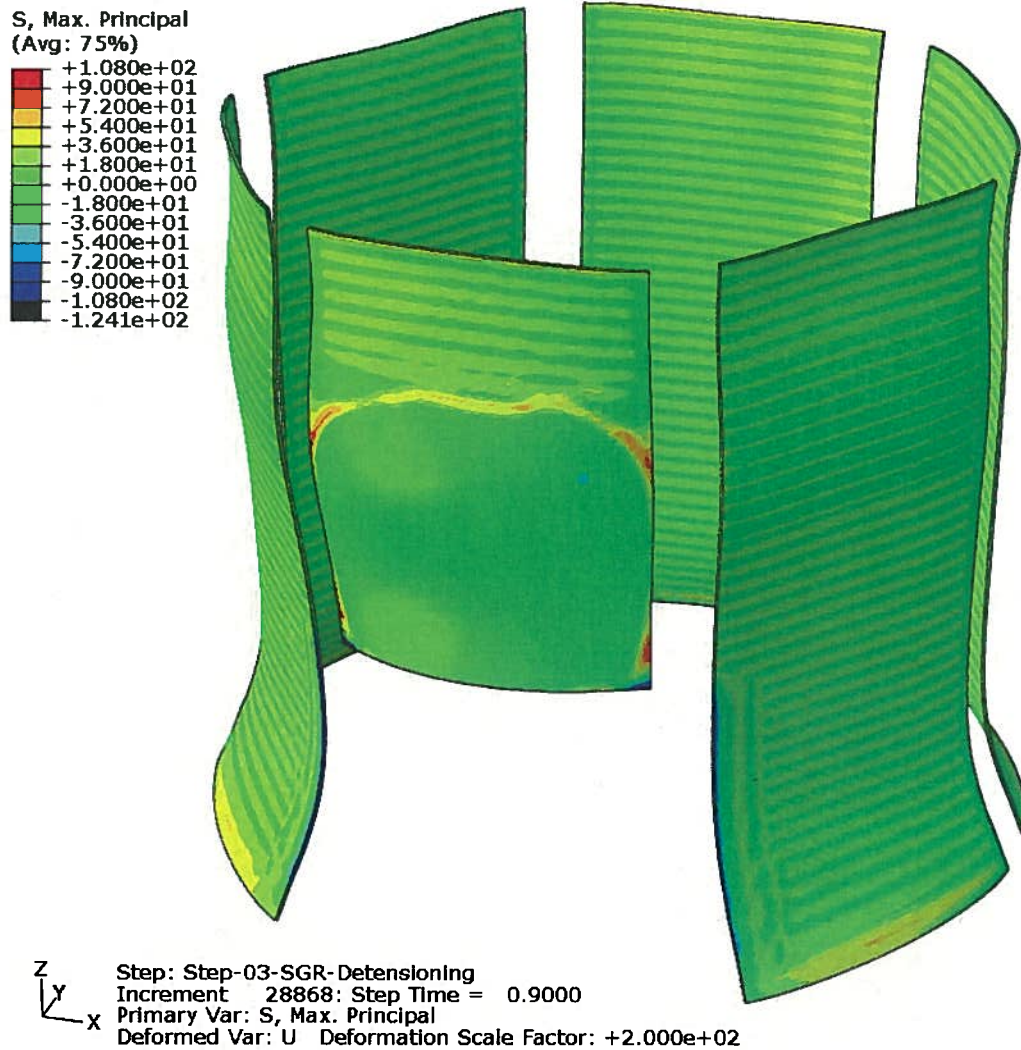


Figure 7.21 Step 18 of 20 in simulating the SGR de-tensioning.
Maximum principle stress (psi)

Note that at this step delamination has occurred and the stress has been relieved which can appear to be a relaxation of stress.

NON-PROPRIETARY VERSION

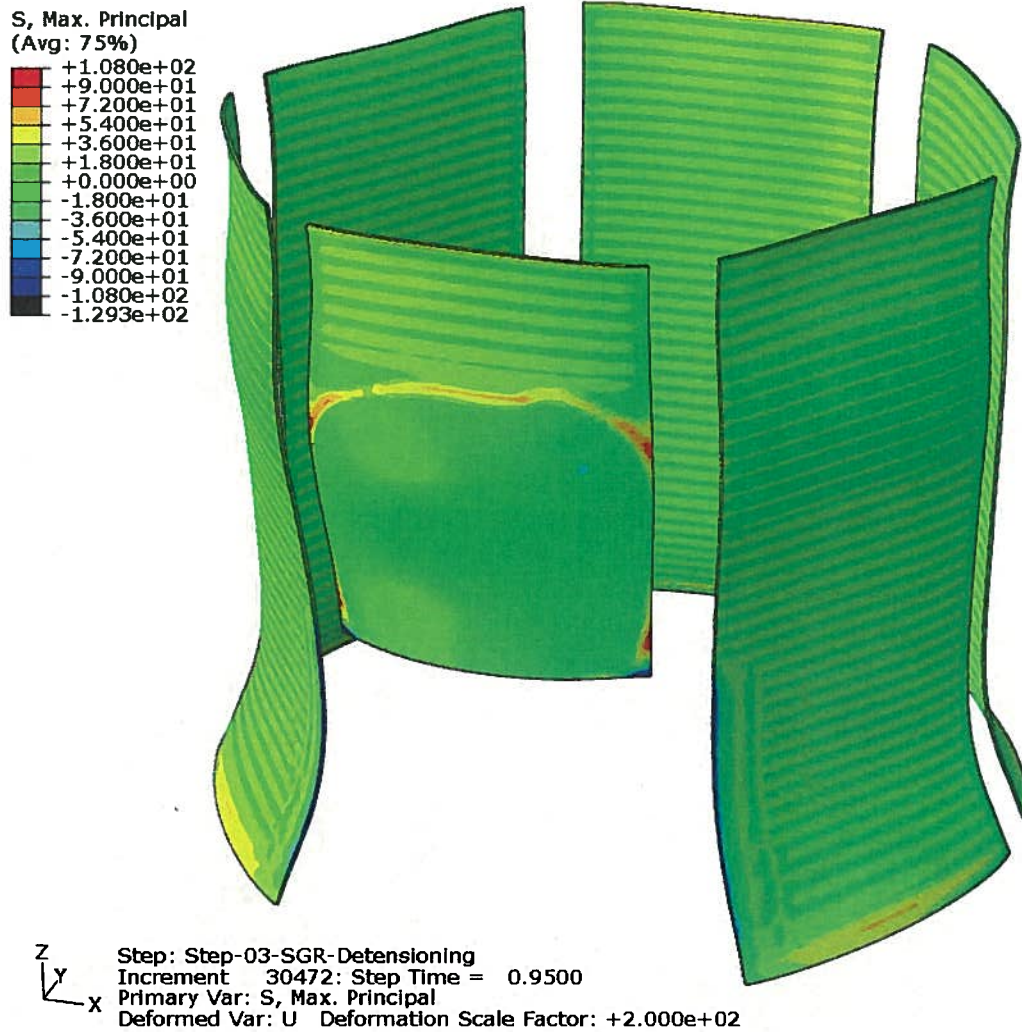


Figure 7.22 Step 19 of 20 in simulating the SGR de-tensioning.
Maximum principle stress (psi)

NON-PROPRIETARY VERSION

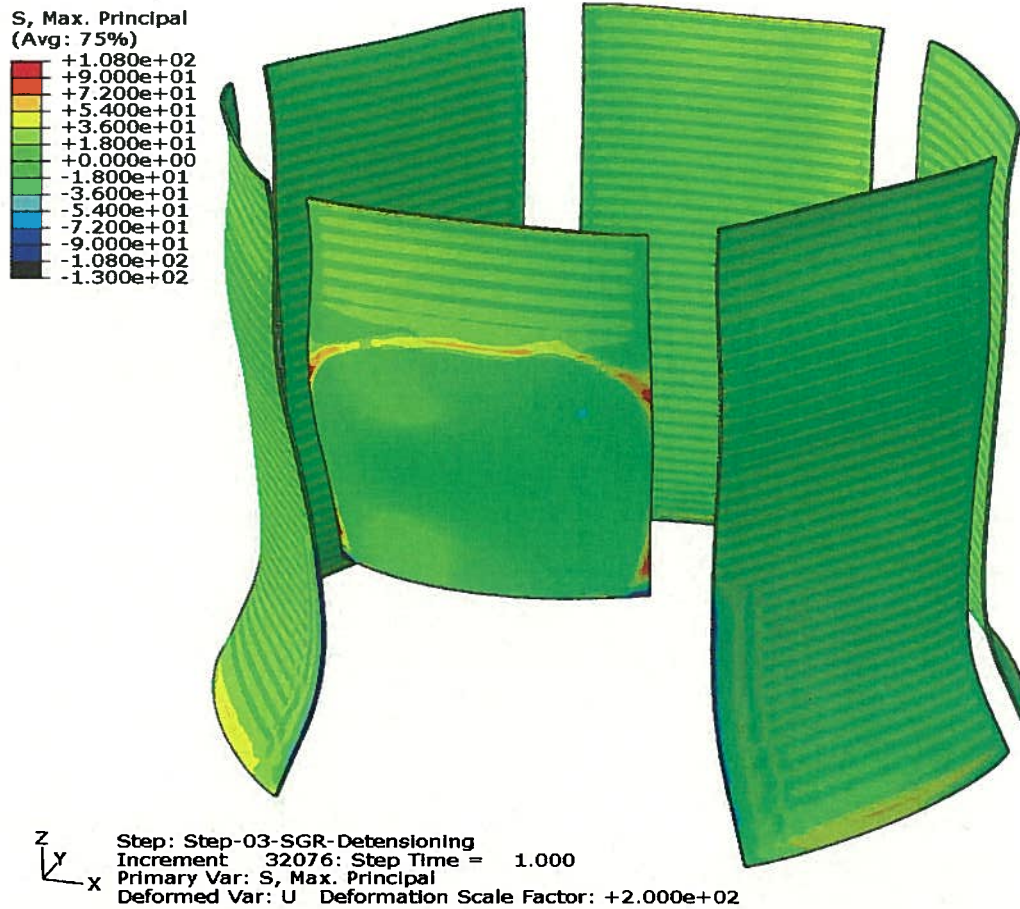


Figure 7.23 Step 20 of 20 in simulating the SGR de-tensioning. Simulation Complete.
Maximum principle stress (psi)

Figures 7.24 and 7.25 show the azimuthal shape and the vertical shape of the bulge. Figure 7.24 is a profile of bay 34 taken along its circumference at elevation 196'. Figure 7.11 was a profile taken at the middle of bay 34 going vertically so that between them both cross-sections are illustrated.

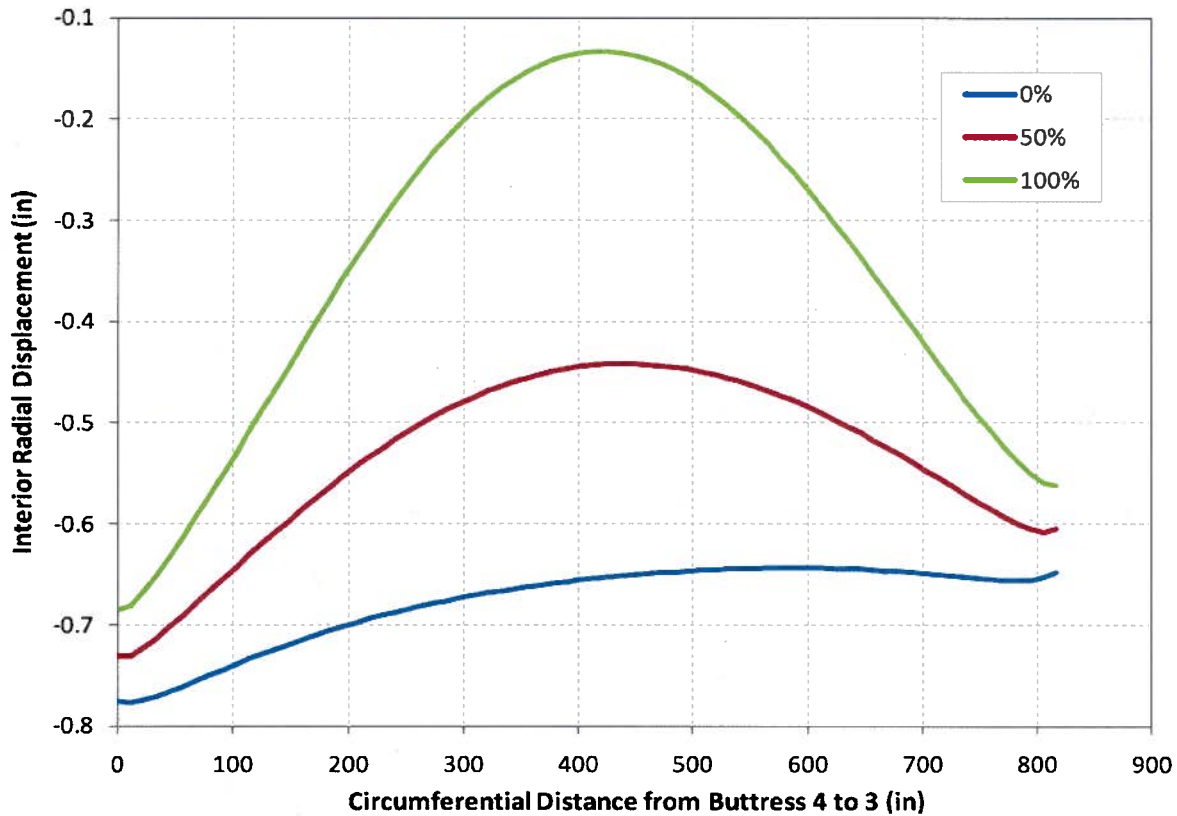


Figure 7.24 Azimuthal dependence of Bay 34 post SGR de-tensioning.

The asymmetric response in Figure 7.24 is due to an asymmetry in the dome tendon attachment arrangement that was correctly reflected in the model.

Figure 7.25 is a different version of the radial displacement as a function of elevation. It is a relative plot of displacement (0 is fully tensioned and 1 is fully un-tensioned) showing the displacement of one location to the next if there were no curvature prior to de-tensioning. It is idealized to show the relative displacement due only to de-tensioning tendons and the various plots are based upon the actual SGR de-tensioning sequence. Step 8 and step 12 both show an irregularity which is caused by skipping tendons so that a tendon remains tensioned after those around it have been de-tensioned.

NON-PROPRIETARY VERSION

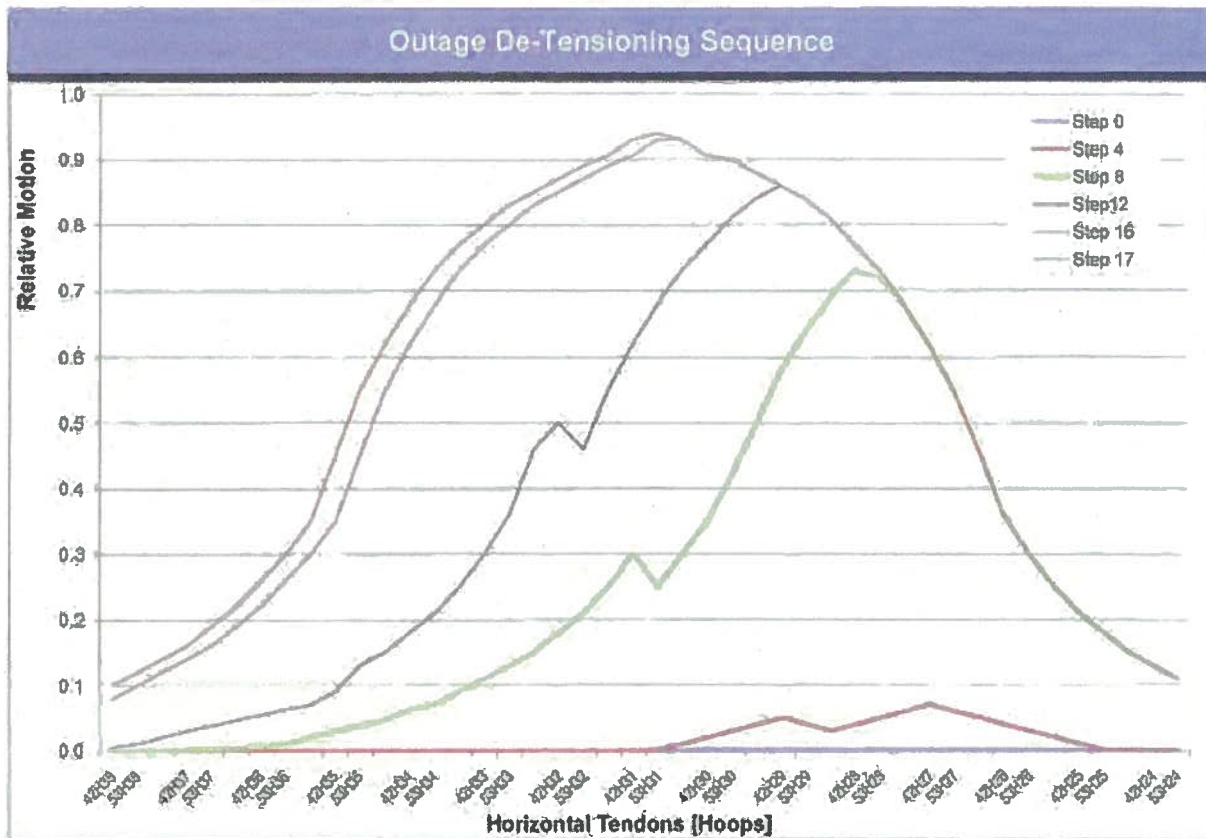


Figure 7.25 A Plot of the radial displacement in Bay 34 as SGR tendon de-tensioning progressed. The full displacement was 0.5”.

The information below helps correlate de-tensioning steps to calendar dates. The first step commenced the de-tensioning of tendons, which extended over several days. This is followed by the removal of the concrete in the SGR opening. Dates, times, and photographs of events as they unfolded are also included.

On 9/26/09	four vertical tendons were de-tensioned.	Total	4
On 9/27/09	six tendons were de-tensioned.	Total	10
On 9/28/09	six tendons were de-tensioned	Total	16
On 9/29/09	five tendons were de-tensioned	Total	21
On 9/30/09	two tendons were de-tensioned, the hydro-laser demonstration began, followed by two more horizontal tendons being de-tensioned	Total	25
On 10/1/09	the last two horizontal tendons were de-tensioned	Total	27

The conclusion of the computer simulation is that the de-tensioning scope and sequence used resulted in an oval shaped bulge in the bay 34 wall and created stresses in excess of the tensile strength of the concrete which delaminated as a result.

These results were generated from the Abaqus Global Model and the discussion about peak stress values as a function of model cell size in Attachment 1 applies here.

You will note that the maximum principle stress seems quite low. The global model assumed a tensile capacity of 108 psi to accommodate the coarse mesh being used. The next step is to reduce the mesh size and assume a material property closer to tested values. This is done below.

The tensile capacity assumed for the detailed mesh analysis below was 360 psi.

CRACKS OCCUR:

Cracking and then delamination began at some point in the de-tensioning and concrete removal process. Figures 7.26 to 7.29 show the results of the detailed Abaqus sub-model assuming tensile capacity of 360 psi. DAMAGET is a damage scale, a numerical measure of the ability of the concrete to pass load. The range is 0 to 1.0 where pristine material is 0 and fully fractured material is 1.0 and can pass no load.

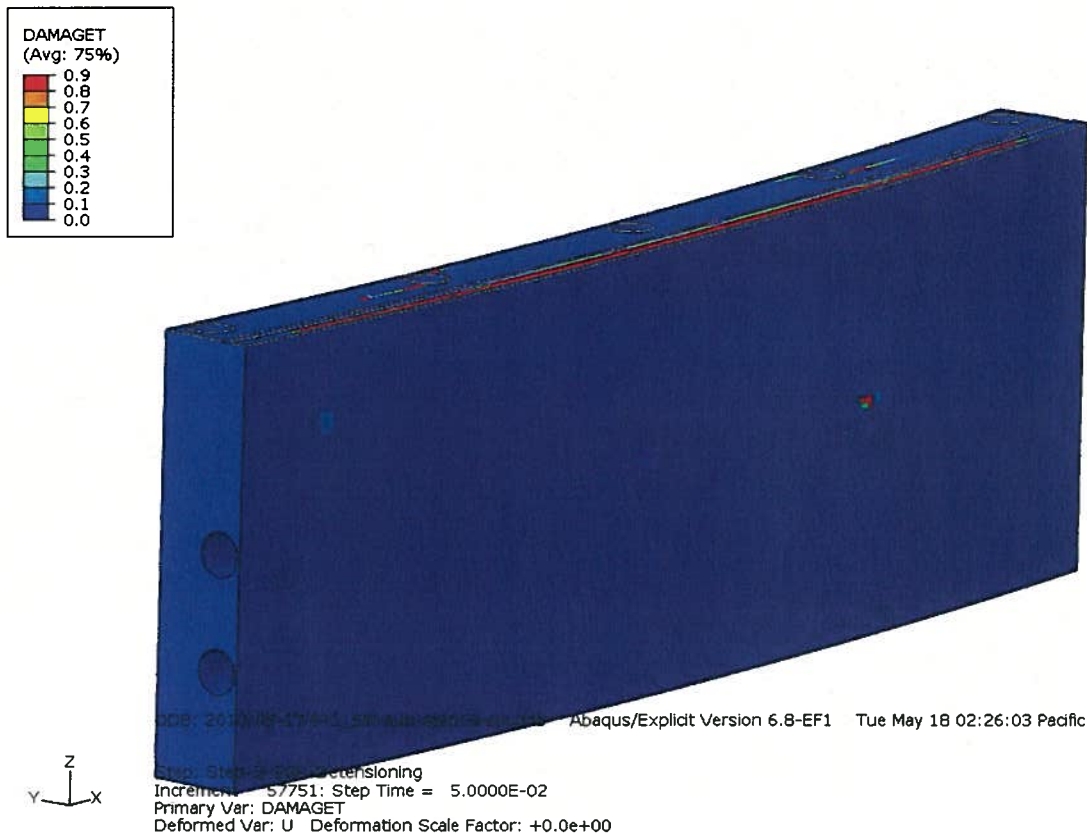


Figure 7.26 A Plot of a bay 34 wall segment approaching delamination.

NON-PROPRIETARY VERSION

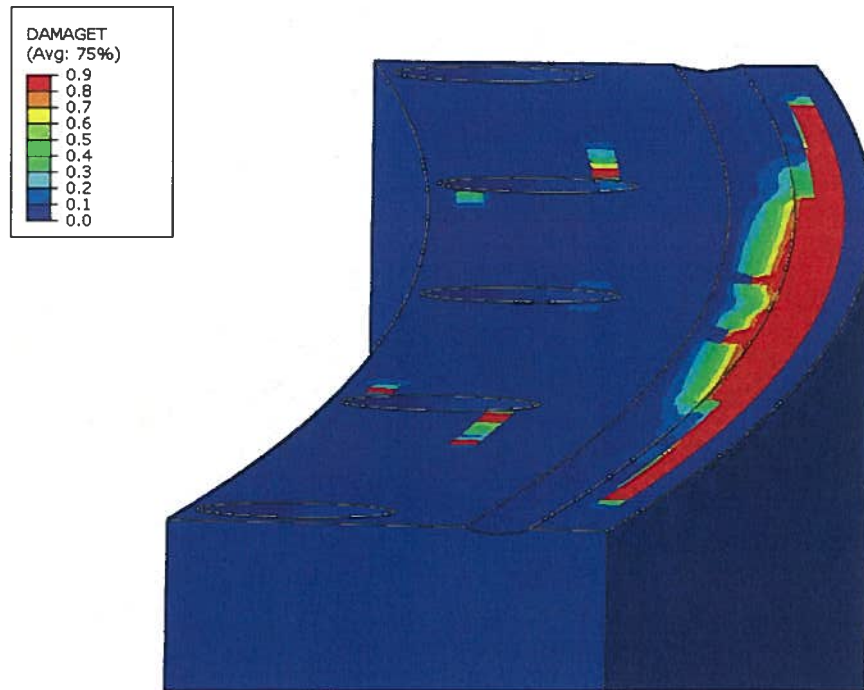


Figure 7.27 A Plot of a bay 34 wall segment delaminating

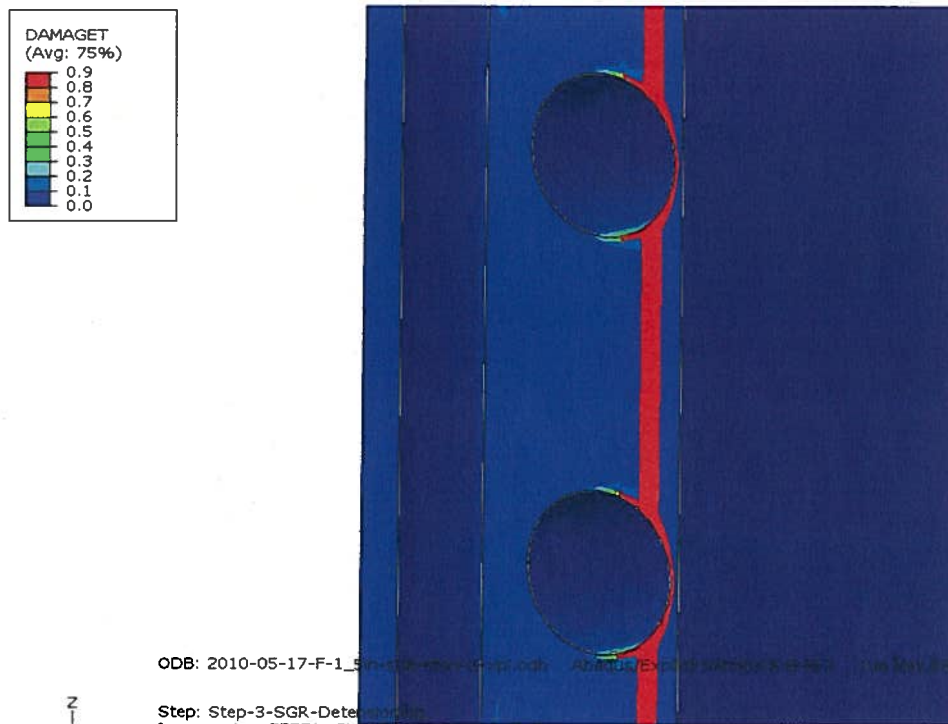


Figure 7.28 A Plot of a bay 34 wall segment delaminating $F't= 360$ psi

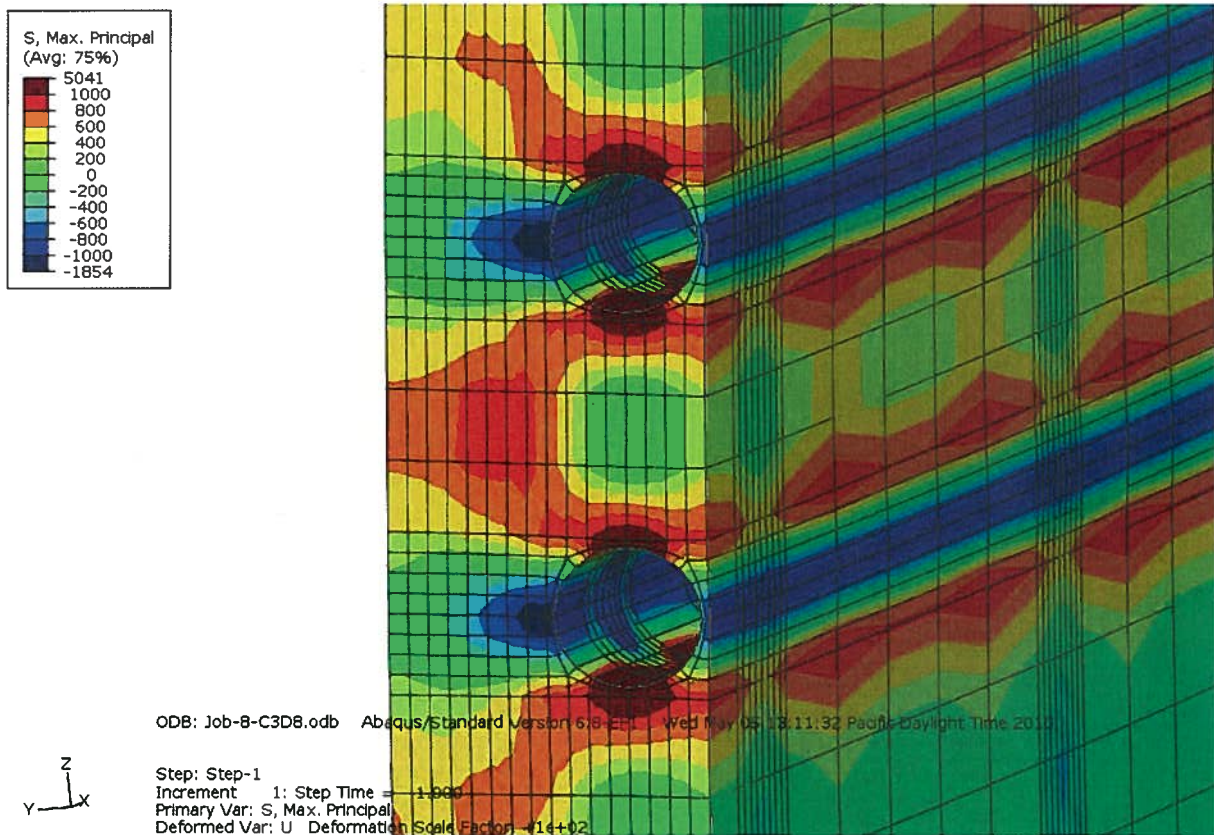


Figure 7.29 A Plot of maximum principal stresses in delamination. $F't = 360$ psi

Sheet Delamination:

Cracking occurred in the area of the SGR opening. The cracks then propagated to form the unique hour glass shape in bay 34. Figure 7.25 shows a vertical slice through the bulge that formed in bay 34. The total deformation increases sharply as the total number of de-tensioned tendons increases. The absence of this transition in a de-tensioned environment is what prevented cracking in the neck of the hour glass.

Spontaneous propagation of a crack requires a tensile stress at the tip of the crack which exceeds the tensile capacity of the material. The cracks that spontaneously propagated were caused by stresses in the concrete caused by removal of the prestress force loading locally at that location. The cracking boundary was approached that either limited the deformation which drove the cracking (such as at a buttress) or limited the tensile stress involved (such as a region of de-tensioned tendons).

Figures 7.27 and 7.28 shows the Abaqus Detailed model prediction of delamination assuming tensile capacity of 360 psi. The peak stress locations on the top and bottom of the horizontal tendons extend out under the high radial tension conditions until they connect with the next tendon hole.



Scenario Validation:

Following is a summary of the failure scenario. Seventeen tendons from elevation 183' to 210' are de-tensioned. Ten vertical tendons, centered on azimuthal angle 150 degrees, are also de-tensioned. Generally the vertical tendons were de-tensioned first. This creates an imbalance in the pre-stress loads on the containment building and a bulge develops in bay 34 centered on elevation 196' and azimuthal angle 150 degrees. The bays on the opposite side of the building curve inward. The analysis also indicates that initial tensioning causes more inward displacement of the middle of a bay than around the edges. No displacement scans were performed during the SGR de-tensioning but the plant remained in the partially de-tensioned condition until March, 2010 when it was largely de-tensioned for delamination repair work. The scope of the repair de-tensioning was to de-tension essentially all horizontal tendons in all bays from H17 to H44 (elevation 152' to elevation 239'). This de-tensioning was accomplished in eleven steps from pass 1 to pass 11. Laser scanning was performed after each pass from pass 4 to pass 11. Thus, the laser scan only captured part of the de-tensioning but it does afford a comparison between the expectations of the scenario and the actual response of the plant. The laser data is presented as the radial displacement change using the un-tensioned condition after pass 11 as the baseline, so outward motion is negative and inward motion is positive. The point-by-point detailed comparison is discussed in Attachment 4.

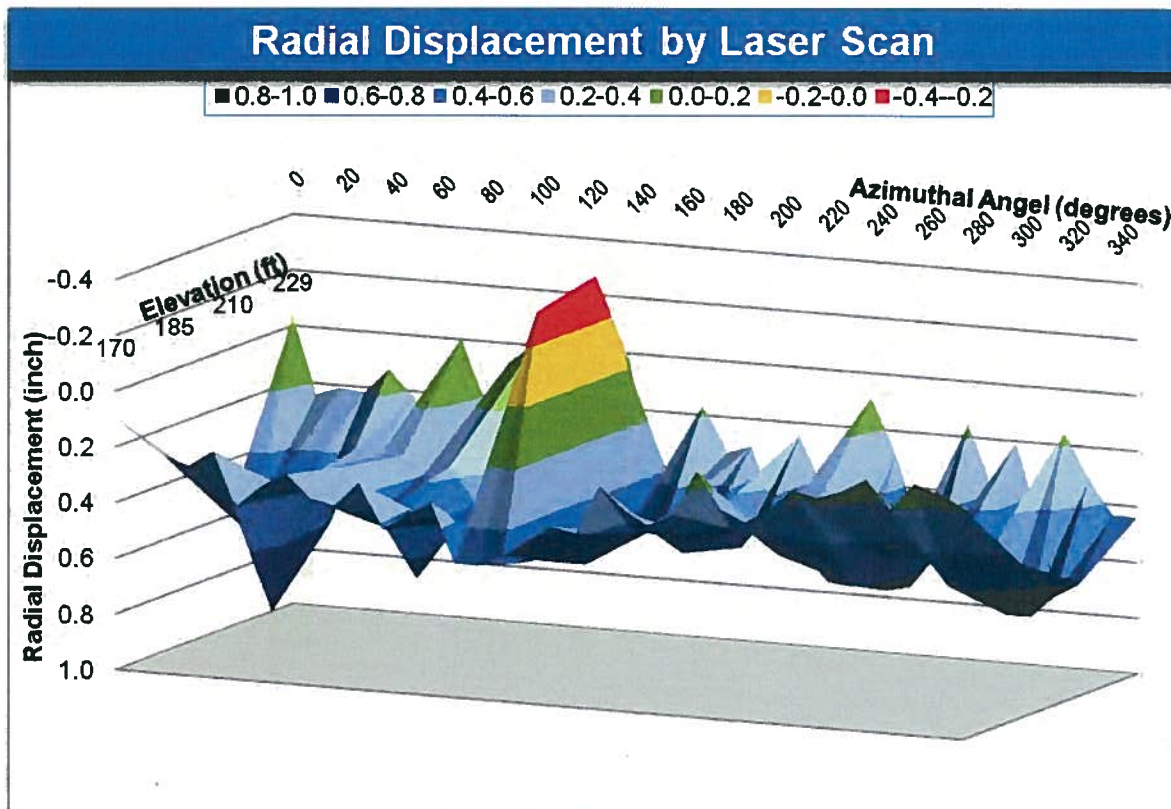


Figure 7.30 Three dimensional representation of radial displacement as a function of azimuthal angle and elevation.

NON-PROPRIETARY VERSION

In a sense, it is a snapshot of the conditions that existed at the end of the SGR opening project. The most prominent feature in figure 7.30 is the bulge at azimuthal angle 150 degrees. In addition each of the six bays is recognizable with its edges relatively fixed and its center sections bowed inward under tendon tension. Please note that these data indicate a change in displacement rather than an absolute displacement. Almost all points moved outward as the containment was de-tensioned in March, 2010. The notable exception was the area immediately around the SGR opening.

A large amount of additional benchmarking of computer models was performed using building data during de-tensioning. This is discussed in [Attachment 2](#).



8. ROOT CAUSE AND CONTRIBUTING CAUSES

Summary Conclusions:

The construction of a temporary containment opening has been accomplished successfully numerous times. PII has determined that the CR3 delamination did not exist prior to the SGR activities of de-tensioning and concrete removal. Rather, the delamination appears to have been caused by the combination and interplay of (1) certain design features of the CR3 containment structure; (2) the type of concrete used in the CR3 containment structure and (3) the acts of de-tensioning and opening the containment structure. Through a state-of-the-art computer model that PII developed, and using data and information specific to CR3 which PII was able to gather after the delamination had taken place, PII was able to determine that none of the individual contributing factors to the delamination, taken alone, would have caused delamination to occur. Rather, the complex interplay between all the contributing causes led to the delamination as discussed in detail in this report.

Despite the complex interplay of unrelated factors, it is possible to identify a root cause whose elimination will ensure the event will not be reproduced. That root cause was the scope and sequence of tendon de-tensioning associated with the containment SGR activities which generated additional stress beyond the capacity of the original design. The additional local loading exceeded the fracture capacity of the concrete and resulted in cracking along the line of least concrete area available for resistance. As the cracks propagated and joined, delamination occurred over a wide area. The O&P evaluation concluded that the inability of industry accepted tools to predict delamination was the programmatic root cause of the event. PII found that six methodology improvements were needed to accurately analyze the containment response.

Corrective action has been identified to address the issue at CR3.

Failure Mode Evaluation:

The purpose for performing a root cause evaluation is to fully identify the scope and conditions under which the failure took place so that corrective actions to prevent recurrence may be taken. The root cause is that single item which, if effectively corrected will ensure the event will not be repeated. Viewed in that light, PII has considered the individual FMs.

In general, the contributing conditions that have been identified are discussed in the context of delamination rather than fulfillment of the specifications established in the original design. The design and materials, as originally delineated, were sufficient to meet the requirements of a fully constructed containment structure.

FM 1.1 Excessive Vertical and Hoop Stresses - The stresses in question are inherent in the containment design and could not be changed significantly without rebuilding the structure. It is also not clear that modification of these stresses alone would preclude a repeat failure given the additional stresses imposed by some tendon tensioning/de-tensioning sequences.

FM 1.2 Excessive Radial Stresses/No Radial Reinforcements - This FM contributed to the event and radial reinforcement is recommended in the repair of the bay as it is an effective modification and can be implemented practically. However installing radial support is not

practical as a general solution because it would require rebuilding of the structure and may not, by itself, preclude recurrence.

FM 1.15 Inadequate Design Analysis Methods For Stress Concentration Factors- PII concludes that this FM was a contributor because high stress concentrations exist at the tendon sleeves. However, it is impractical at this point to change the design.

FM 2.12 Inadequate Strength Properties - This FM addresses the variability of measured strength from concrete cores. None of the strength tests of core samples indicated concrete below the required design strength. Because the Bay 34 concrete currently in place cannot be practically changed short of being removed, the strength properties, while an important consideration, cannot be a root cause.

FM 3.4 Inadequate Aggregate - The limestone aggregate used in the structure contributed to the delamination because of its properties. At this point, the FM may be taken into consideration when repairing bay 34 but otherwise it is impractical to replace the aggregate.

NOTE: The FMs existing at the time of this evaluation are historical and the containment met the requirements for normal and design basis conditions as a containment structure.

FM 7.3/7.4 Inadequate De-tensioning Sequence and Scope – the order of tendons that were de-tensioned and the selection of which and how many should be de-tensioned.

An expanded scope and sequence was developed in March, 2010 and it successfully de-tensioned the containment without delamination in the other bays.

FM 7.5 Added Stress Due to Removing Concrete - Photographic evidence proves the containment was cracked before any significant concrete removal occurred. However, concrete removal made stresses worse and so did contribute to the overall delamination. It can't be the root cause because tensioning and de-tensioning are pre-requisites for concrete removal but concrete removal alone will not preclude delamination if an inadequate sequence or scope of de-tensioning occurs.

In conclusion, and based on all the factors and information which will be discussed in the following sections, PII has determined that the immediate cause of the delamination event was the addition of stresses as a result of the containment SGR activities resulting in additional stress beyond original design and structure capacity. The added load exceeded the fracture capacity of the concrete and resulted in cracking along the high stress line connecting the horizontal tendons. As the cracks propagated and joined, delamination occurred over a wide area. Despite the complex interplay of unrelated factors, it is possible to identify a root cause whose elimination will ensure the event will not be repeated. That root cause is an inadequate scope and sequence of de-tensioning of containment tendons.



Frequently Asked Questions:

This section provides a convenient overall summary of the event in the form of the questions typically asked by people unfamiliar with the event.

1. What happened?

As a part of the SGR project, a series of horizontal and vertical tendons were de-tensioned in bay 34. For the particular tendon de-tensioning sequence selected for CR3 SGR opening, tensile stress is created at the interface between tensioned and de-tensioned tendons and increases with the number of de-tensioned tendons involved. As the number of de-tensioned horizontal tendons increased the load was amplified until it exceeded the fracture capacity of the concrete and cracking developed between the horizontal tendons. Continued de-tensioning and concrete removal exacerbated the cracking so severely that the cracks began to propagate spontaneously, growing together to form a delaminated sheet.

2. Why hasn't this happened elsewhere during SGR activities?

To some extent it has happened before in the form of dome delaminations assumed to be during initial tensioning of tendons. In order for delamination to occur at CR3 four factors must exist. All four are necessary and none of the contributing factors is sufficient to cause delamination. The factors are:

- ◆ Lack of radial reinforcement(No Radial)
- ◆ High stress peaks due to large tendons and wall design (Tendon Large)
- ◆ Certain material characteristics (Materials)
- ◆ Large tensile stress - typically associated with the interface between several tensioned tendons and several de-tensioned tendons (typically during SGR) (De-tensioning)

Of the peer plants considered only CR3 had all four factors.

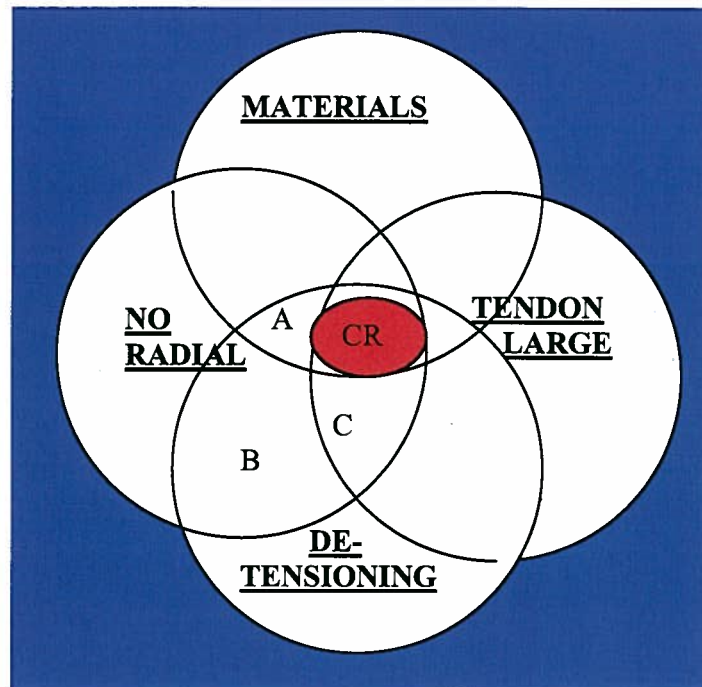


Figure 8.1 Venn diagram of plants with critical characteristics. A, B, and C are similar plants.

3. Why didn't this happen before at CR3?

The particular tensile stress generated is a very complicated function. During initial tensioning, the entire containment was involved rather than one concentrated band in one spot of the containment wall.

4. Why wasn't the damage limited to the small area of de-tensioned tendons?

The containment design is such that, given a large enough crack, the crack will grow spontaneously and will only stop when it approaches a boundary (such as a buttress) which limits the strain driving the delamination, or when it reaches an area of de-tensioned tendons. De-tensioned tendons allow the concrete to move so that their internal strain is reduced, and that strain is what drives the delamination.

5. Why did bay 34 delaminate in an hour glass fashion with the largest cracks centered above and below the opening?

All else being equal, the delamination would have occurred all around the bay (though inhibited at the edges). However, delamination did not occur in two symmetric isolated spots. Those spots form the neck of the hour glass and did not delaminate because the horizontal tendons in that area were de-tensioned. The tensile stress is highest in the center of the bay where the tendons most deform the concrete so the largest cracks would be in that area. The neck area has limited displacement due its location near the edge of the bay and to being in the de-tensioned tendon zone.

6. Is there anything unique about bay 34 that made it more sensitive to delamination?

Nothing of significance was found to set bay 34 apart from the other bays, though it is different in a couple of ways. The equipment hatch effectively shortens the bay but the delamination issue

NON-PROPRIETARY VERSION

occurred far enough away from the equipment hatch that it was not a contributor to the event. Bays 34 and 45 see daily thermal cycling but analysis showed the impact was not significant.

7. Was the absence of a de-tensioned margin around the opening a contributor to the event?

Delamination occurred due to a combination of de-tensioning and concrete removal. A primary factor was the number of de-tensioned tendons that were located in a row.

8. What have we learned?

The de-tensioning for the repair work in March, 2010 required extensive iteration to develop a sequence that would not cause excessive stresses or further delamination. The re-tensioning after repair will require an analysis similar to the one performed for the de-tensioning. Also CR3 should limit the simultaneous de-tensioning of tendons unless a detailed analysis is performed to ensure stresses are acceptable.



9. RECOMMENDATIONS TO PREVENT RECURRENCE

CORRECTIVE ACTIONS TO PREVENT RECURRENCE

A. Capturing the Operating Experience

There is always the possibility that some future event will require changes to containment that are not currently anticipated. Programmatic requirements typically ensure such situations are flagged for special consideration.

A.1 Establish programmatic controls to prevent de-tensioning more than one tendon/group without a detailed analysis validated using CR3 delamination experience.

B. Repair De-Tensioning Analysis

In March, 2010 it was necessary to de-tension bay 34 so that delaminated concrete could be removed and replaced. As such, this represented the conditions addressed in recommendation items A and C. The specific action for this topic (B.1) was performed prior to de-tensioning and it is included here to maintain consistency between this report and the Progress Energy assessment.

B.1 Perform a detailed analysis of the tendon de-tensioning plan in support of the containment repair effort. Modify the plan as necessary and ensure the stresses show positive margin as validated using CR3 delamination data. (Performed successfully in March, 2010.)

C. Re-Tensioning Containment in R 16

Delamination is typically associated with the process of changing tendon tension on a large scale so the upcoming re-tensioning of the containment is relevant

C.1 Perform a detailed analysis of the tendon re-tensioning plan in support of the containment repair effort. Modify the plan as necessary and ensure the stresses show positive margin as validated using CR3 delamination data.

BETTERMENT ACTIONS

C.2 Monitor displacement of the RB walls during re-tensioning to confirm the building response relative to computer prediction.

C.3 Monitor the RB wall with strain gauges and acoustic instruments during re-tensioning to ensure responses are within established limits per the repair design documents.

D. Life Extension

Accumulated stress cycles can impact material properties over time. The impact of plant evolutions on these properties appears to be small but should be monitored over the projected life of the plant.

D.1 Perform a detailed analysis of the stress consequences of typical activities such as heating up and cooling down of containment in outages or solar heating of an entire bay. Ensure there is no cumulative impact with time.

E. Aging Characteristics

E.1 Establish an inspection plan to periodically monitor containment concrete condition to ensure there are no unexpected changes. The inspection should use Non Destructive Examination (NDE) such as Impulse Response mapping of the area and selective core drilling in areas identified as suspect by NDE.

E.2 Establish a monitoring program that evaluates the response of the installed containment monitoring sensors to ensure the two types of concrete in bay 34 are behaving consistently as an indication of good coupling.

10. ORGANIZATIONAL AND PROGRAMMATIC ROOT CAUSE

1. The central issue associated with the delamination was the inability of industry accepted tools to predict delamination. The only reasonable way to have identified this inability would have been to benchmark the codes against industry experience. Outside of numerous successful SGR projects, the only available experience was the dome delamination information at Turkey Point 3 and at CR3. Six methodology improvements were needed to accurately analyze the situation. Benchmarking of industry codes using the Turkey Point 3 dome delamination would not have clearly identified the issue relative to the CR3 containment walls. The root cause of the Turkey Point 3 dome delamination was found to be a combination of insufficient concrete contact area and unbalanced post-tensioned loads. The root cause of the CR3 dome delamination was radial stresses that combined with biaxial compression to initiate laminar cracking in a concrete having lower than normal direct tensile capacity and limited crack arresting capability. The root cause of the CR3 dome delamination is more directly applicable to a containment wall analysis. The materials involved in the CR3 dome and wall were the same. The specific radial stresses and biaxial compression would be different however. The distinction was that the dome involved all of the dome tendons as opposed to the SGR opening which was believed to only involve a limited number of vertical and horizontal tendons in part of one bay. In addition, there was uncertainty about when and under what circumstances the dome delamination occurred. Tendon tensioning may have been underway but it is only speculation. In addition, de-tensioning was viewed as stress reduction and so not a challenge to the concrete the way containment wide tendon tensioning would be.

Comparison of Turkey Point 3 Dome, CR3 Dome, and Possible Applicability
to SGR Project

Turkey Point 3 Dome	Crystal River 3 Dome	Applicable to CR3 SGR Project?
Insufficient Concrete Contact		Not Applicable
Unbalanced Tendon Loads	Possibly Involved Tensioning	Limited De-tensioning
Dome	Dome	Different than Wall
Initial Tensioning	Sometime Early In Life	After 33 years of Operation
	Concrete Material Properties	Applicable
	Bi-axial Stresses	Different Geometry

2. Given the industry success at performing temporary openings in containments using standard analysis tools there was no indication (other than 30 year old dome delamination data of questionable applicability) that the tools were non-conservative. Usually a scoping calculation that demonstrates a large margin of safety is adequate.

NON-PROPRIETARY VERSION

3. Post event research and modeling by PII determined that very rigorous application of typical industry tools would not have been able to accurately predict margin to delamination and therefore would have been insufficient to prevent this failure.

4. PII noted that six major breakthroughs in the development of a state-of-the-art modeling methodology were needed to obtain accurate results. Those six improvements are (1) use of fracture energy parameters, versus tensile strength, as failure thresholds, (2) modeling of visco-elastic effects of concrete creep, in conjunction with the fracture energy based fracture thresholds, to account for stress reversal effects (i.e., from compression to tensile), (3) use of a 360 degree, realistic whole containment modeling to reveal realistic containment displacements, (4) incorporate the creep fracture phenomenon around the sleeves to account for a lower tensile strength near the conduits (thus initiating small cracks which could be delamination initiation sites), (5) use of fine meshes (about 1.0 cubic inch mesh) to reveal local stress concentration for crack initiation, and (6) the use of a variable elasticity and fracture toughness based upon local strain. Without these breakthroughs in modeling, delamination cannot be accurately predicted with measured, realistic input parameters to the methodology.

5. Using such a validated model avoids the non-conservative results otherwise obtained. Since this corrective action is already implemented as a result of the technical root cause evaluation, no additional corrective actions are required.

11. REFERENCES



1. Moreadith, F.L. et al, "Delaminated Prestressed Concrete Dome: Investigation and Repair", Journal of Structural Engineering, vol 109, no. 5, May 1983, pp. 1235-1249.
 2. MPR Associates, "Crystal River Unit 3 Nuclear Power Plant Local Tensile Stresses in Containment Dome Resulting From Post-Tensioning Load", MPR-531, October, 1976
 3. Final Revisions to the Crystal River Unit No. 3 Reactor Building Dome Delamination Report, Docket No. 50-302, June 1, 1976
 4. Turkey Point Unit 3 Containment Dome, Delamination of the Dome Concrete During Post-Tensioning, Docket 5-250, U.S. Nuclear Regulatory Commission. (1972)
 5. Ashar, H and Naus, D, "Overview of the Use of Prestressed Concrete in U.S. Nuclear Power Plants", Office of Nuclear Regulatory Research, U.S. Nuclear Regulatory Commission, May 1994.
 6. Basu, P.C. et al, "Containment Dome Delamination", Transactions, SMiRT 16, Washington, DC, August 2001, Paper #1557
 7. Acharya, S. and Memon, D, "Prediction of radial stresses due to prestressing in PSC shells", Nuclear Engineering and Design, 225 (2003) pp 109-125
 8. Basu, Prabir and Gupthup, Vijay, "Safety Evaluation of Delaminated Containment Dome Re-Engineering" Transactions SMiRT , 16, Washington, DC, August, 2001
 9. PII Document, "Margin-To-Delamination Analysis of Proposed CR3 Detensioning Sequence Option 10 F, March 7, 2010
 10. Gilbert Associates Report 1930, "Crystal River Unit Three Nuclear Generating Plant Reactor Containment Building Structural Integrity Test", 12/7/1976.
 11. Saouma, V. et al, "Creep Fracture Tests of CR-3 Concrete", internal PII document in support of the CR-3 Root Cause Assessment. See Appendix 10 of this report.
-



ATTACHMENT 1: COMPUTER MODELING

Modeling Assumptions

The assumed values for physical parameters is an important consideration when evaluating the credibility of any computer model. To facilitate that evaluation, the results presented in this report are generally the output of the Abaqus global model or its sub-models. They consistently use the parameter values listed below. When this is not the case the parameters used for a specific figure will be identified with the figure.

To ensure full understanding of the delamination process at Crystal River, PII followed parallel paths in development of computer solutions. The conditions involved in the delamination event can be modeled using a wide variety of crack propagation techniques that will lead to significantly different conclusions. Because benchmarking is an important validation technique, the codes used in this computer analyses were benchmarked against the known plant response to the Structural Integrity Test performed in 1976. In addition, the computer model predictions were compared with containment interior laser scanning performed in March, 2010 during the de-tensioning that was done prior to repair bay 34. Benchmark comparisons are provided in [Attachment 2](#).

Pure analytic solutions for many material properties are limited to simple geometries and homogeneous materials. For more complicated problems the technique of choice is the computer based solution of simultaneous equations known as Finite Element Analysis (FEA).

FEA has been successfully used to simulate a wide variety of engineering situations for both spatial variation and time dependence. There are, however, some limitations. The first difficulty is that the computer code will not converge to a unique solution unless the time steps and cell dimensions are small enough to closely approximate a continuous solution. The second limitation is that the number of computer steps needed to obtain a solution grows geometrically with the number of time steps and computational cells used. Thus, there is a trade-off between the accuracy of the solution and the time needed to obtain the solution.

When the structure being analyzed is large and closely coupled, commonly used techniques must be augmented by combining highly detailed regions in the areas of interest with a larger scale model which sets boundary conditions for the detailed cells.

Analysis of the Crystal River containment found that the delamination ultimately depends on very complex local conditions that are impacted by the response of the building as a whole. As a result, PII created a series of computer codes to simulate the entire building and execute detailed calculations for the particular area of interest. The role that each code part played in the larger framework of the computer model is detailed below.

Immediately after the delamination event PII found that industry standard computer codes provided solutions which showed significant margin to delamination' when applied to CR3.

As an interim measure until more accurate modeling techniques could be developed, PII relied upon NASTRAN and its linear-elastic model to calculate local conditions and then Abaqus to evaluate the local conditions and determine if damage resulted. However, due to limitations in the model, it was necessary to assume a modulus of elasticity of

NON-PROPRIETARY VERSION

1.1E6 psi throughout the structure. While this assumption allowed the model to predict the onset of delamination it had significant uncertainty.

PII now uses an Abaqus Global model using a visco-elastic fracture model and a detailed sub-model for decreased mesh sizing to provide accurate stress predictions. There are four input values which can be adjusted to make the computer model output match the benchmark data. They are listed below

Parameter	Typical Value	Abaqus Global/Detailed	Impact
Tensile Capacity	500 psi	██████████*	Onset of Cracking
Fracture Energy	0.40 lbf/in	██████████*	Onset of Cracking
Elasticity Modulus	3.45 E6 psi	██████████	Radial Displacement
Creep Coefficient	2.2	██████████	Radial Displacement

*Note: Adjustments in Tensile Capacity and Energy reflect the analysis mesh size used.

The treatment of creep is an important consideration. Abaqus Global applies a creep coefficient for long term changes (such as 30 years of tensioned operation) but does not apply it for short term changes such as de-tensioning. The creep coefficient is used to modify the modulus of elasticity by the equation:

$$E' = E/(1+c)$$

where E is the measured coefficient of 3.45 E6 psi and if the standard creep coefficient of ██████████ is used $E' =$ ██████████.

The effect you see is a shift in radial displacement over a long time period but no corresponding return immediately after de-tensioning. Refer to Figure 7.11. The Tensioned line is generated immediately after initial tensioning using $E = 3.45 E6$ psi. The next line is Creep and this shows the gradual shift in radial displacement over time due to ██████████ as a creep corrected elasticity. The remaining lines use $E = 3.45 E6$ psi because they occur over a few days. The result is that the de-tensioned state does not immediately return to the un-tensioned state that existed in 1973.

One measure of the precision of the modeling is the degree to which it is necessary to adjust the measured physical values in order to obtain good agreement with benchmarking. Unless indicated otherwise, the PII models use the typical values listed above.

PII was able to reduce the level of uncertainty by developing a linear elastic super-model, but this model still suffered from the limitations of linear elastic modeling, such as difficulty dealing with creep in concrete. The creep effect makes concrete respond more like a viscous fluid than an elastic solid in very particular conditions and unless the model is capable of applying the different properties selectively as appropriate to the situation, one set of properties must be applied throughout the model, which leads to non-physical material properties being used.

In response to these limitations, PII recently developed a Global Visco-elastic Abaqus model that selectively applies the appropriate creep response for the local conditions. The result is

NON-PROPRIETARY VERSION

appropriate calculation of delamination with realistic material parameters and radial displacements that agree well with benchmark data. The model uses the Lee-Fenves concrete damaged plasticity properties. The concrete Poisson's ratio used [REDACTED]. The model includes individual tendons and specifically models the steel properties of the liner, conduits, and rebar assuming steel elasticity of 29 E6 psi and a steel Poisson's ratio of 0.27.

The Abaqus global model is run using the sparse solver in Abaqus/Standard and the various sub-models are run in both Abaqus/Standard and Abaqus/Explicit. The global model provides displacement data to the edges of the panel sub-models and other sub-models, which further provide higher resolution of localized behavior. The driven sub-models include stress models and concrete damaged plasticity models, all within Abaqus.

Every curved tendon in the containment is modeled explicitly using embedded beam elements in the global model. The tendons are assigned the cross-sectional stiffness of the sleeves and loads are applied as described below. The beam sections are sized such that only the curved length that applies load to the concrete is modeled. Tendon forces are calculated and applied as line loads to the embedded beam elements. These values are ramped appropriately to account for designed loads, creep, and surveillance loads.

The dome is partitioned into four layers, representing the layers above, below, and in between the dome conduits. All 123 of the dome sleeves are modeled explicitly and at their respective as-designed radii. The dome conduits are not placed at an average radius or joined together directly. Instead, the solid continuum host elements' layer surfaces are aligned with the dome sleeve centerlines in order to improve accuracy and efficiency. The dome conduit "tails" are also modeled explicitly and aligned with the dome solid continuum element mesh. The dome sleeve tails are applied appropriate loading with respect to whether they belong to a subset of the dome tendon tails that are curved and apply either upward or downward force on the concrete.




The dome tendon lock-off loads are applied to an angled surface on the outer edge of the ring girder such that the total force balance is properly equilibrated. The angle of the lock-off surface is calibrated to ensure the sum of all the forces is zero.

Partitions are included in the structure to allow for the selective removal of concrete in the SGR opening, in the SGR delamination crack region, in the excavation regions of bay 34, and at the openings of the equipment and personnel hatches.

Rebar is included in both the global and sub-models. This is implemented using the *REBAR capability within Abaqus, which entails converting all of the host elements to solid continuum shell elements with stack directions (sweep directions) oriented radially. Sleeve and tendon host

elements remain as solid continuum elements and rebar host elements are implemented using continuum shell formulation.



Because the tendons are all modeled explicitly in both the global model and the sub-models, the tendon loads are added or removed individually as dictated in each de-tensioning or re-tensioning pass specification.

The elastic modulus of all the embedded steel is adjusted appropriately to account for the overlap in volume between the concrete and the steel. The liner is included explicitly in both the global model and all of the sub-models.


The global model has approximately [REDACTED]. The element size through the dome and cylinder cross-sections range from [REDACTED] in thickness. The various sub-models have on the order of [REDACTED] of freedom each. There are a total of [REDACTED] discrete geometric cells and [REDACTED] surface patches in the global model.

The global model dome has [REDACTED] elements through its cross-section, all of which are fully integrated solid continuum elements. The bay walls have [REDACTED] elements through each cross-section, consisting of both solids and continuum shells. Solid cells are meshed with hexagonal fully integrated -C3D8" elements and continuum shell sections are meshed with reduced-integration -SC8R" elements with 5 integration points.

A mesh study was performed on each region of the structure, including the dome, the ring girder, and the bay walls, which determine that the mesh response is converged.

Long term visco-elastic creep is calculated by the Abaqus solver [REDACTED]. Creep is calculated from the actual stress state after design-load tensioning, which accounts for local variations in the stress, rather than by applying an approximation such as a global average shrinkage strain.

The global displacements, stress state, creep law, and the concrete damaged plasticity parameters are all implemented into the sub-models. This results in two technical barriers: Abaqus does not normally allow both mapping of the stress state and sub-modeling to be used simultaneously; and, Abaqus does not normally allow the creep law and the concrete damaged plasticity parameters to be used simultaneously. In order to overcome these hurdles, [REDACTED]



The Abaqus Global model has four sections in the containment wall: a steel liner plate, an inner concrete cylinder, a hoop tendon sleeve layer, and an outer concrete cylinder. Curved sections of tendon sleeves are matched to the mesh. The global model uses about [REDACTED]. The sub-model uses [REDACTED]. If you refer to Figure 3.4 you will see the issue of detail. The average value of tensile stress is about 23

NON-PROPRIETARY VERSION

psi. It increases to 31 psi due to concrete displacement. [REDACTED]

[REDACTED] Until recently the resolution was to adjust the tensile capacity of the concrete to compensate for this. That is why a capacity of [REDACTED] psi was assumed in global calculations. It does not affect radial displacement but it does facilitate the delamination evaluation. With the creation of the detailed sub-model the peak stresses become more visible and a tensile capacity of [REDACTED] becomes appropriate. Note that even at a [REDACTED] inch mesh size there is still significant averaging of peak stresses occurring. [REDACTED]

[REDACTED] Recent analysis shows marginal improvement going from a [REDACTED] such that the underestimation of peak stress by about [REDACTED]. Applying that factor to the assumed tensile capacity of [REDACTED] for an infinitely small mesh. That corresponds to the measured tensile capacity of CR3 concrete. The average direct tensile capacity measured in 9 samples was 448 +/- 73 psi. The average split tensile capacity measured in 10 samples was 594 +/- 59 psi and it is generally accepted that tensile capacity is 90% of the tested split tensile capacity. That gives 535 psi. Fracture energy is similarly impacted.

There are a number of ways to address the mesh issue. For radial displacements or general stress calculations, [REDACTED] mesh is sufficient to obtain realistic values. For scenarios which depend heavily on peak stress values one approach is to use a stress concentration factor. Recent comparisons indicate that for global Abaqus that factor would be about [REDACTED]. For the detailed sub-model it would be about [REDACTED]. Another way to achieve exactly the same result is to adjust the tensile capacity of the concrete. For events such as the onset of delamination, the details of the process are very sensitive to the peak stresses involved and fine mesh analysis is the best approach. Once initiated, delamination is less sensitive to peak parameters so the overall extent and width of cracking can be well described by a detailed sub-model or even the normal sub-model.



Liner

The liner is modeled using 3/8 in thick conventional shell elements with elements located on the inner surface of the concrete (R 780.375). Shell offset is used to account for correct placement of center section of the liner.



Figure A1.1 Containment steel liner model

Inner Cylinder

The inner cylinder is located from the liner at R 780.375 to R 810 (IR of hoop conduits). Two layers of continuum shell elements each with 5 integration point though the thickness are included for bending accuracy.



Figure A1.2 Containment inner cylinder (30" thick) model

Hoop Conduits

All hoop conduits are explicitly modeled as beams with pipe section. There is matching mesh between the hoop conduits and the concrete mesh. Only curved sections modeled on which a radial line load is applied.



Figure A1.3 Containment horizontal tendon sleeves

Hoop Layer

The hoop conduit layer is positioned between R 810 to R 815.25 inches. Solid Elements are used here. The grey areas have special Concrete Damaged Plasticity material property which is based on the Lee-Fenves model. These regions are allowed to crack and potentially delaminate. The green regions are not allowed to crack since those regions are reinforced with steel



Figure A1.4 Hoop layer for monitoring delamination

Outer Cylinder

The outer cylinder is positioned at R 815.25 to R 822.375. One layer of continuum shell elements with 5 integration points is used for accurate bending representation



The outer rebar cage consisting of two layers of rebars (one vertical layer at R 818.625, and one horizontal layer at R 819.625 in) are embedded in the shell elements to account for the steel reinforcement.

Figure A1.5 Outer concrete cylinder (7" thick)

Damage Material Regions

This figure shows the regions of the hoop layer which has the Concrete Damaged Plasticity material properties. These regions are allowed to crack and may result in a delamination of the outer cylinder from the inner cylinder.



Figure A1.6 Damage material region within the horizontal tendon layer (capable of cracking and delaminating.)

Driven Regions

The regions depicted here are driven by the displacements from the global model. The displacements are synchronized with the loadings in the delamination model. Hence, the global effects due to, tensioning, creep, and SGR detensioning (including the unloading of 10 vertical tendons) are accounted for.



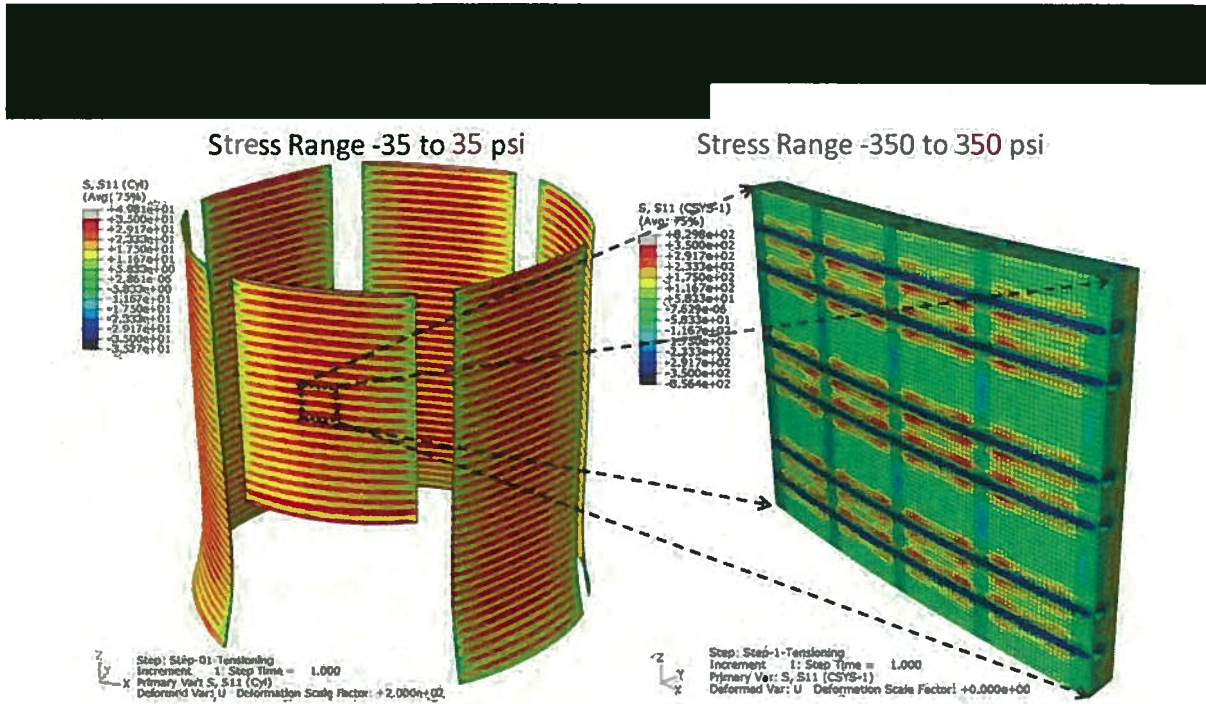
Figure A1.7 The global model provides displacement values which load the driven regions creating boundary conditions for the sub-model.



Figure A1.8 Detailed model including 6 horizontal and 3 vertical tendons

One of the toughest problems in modeling is optimizing the model mesh size. The smaller the size the more accurate are the depictions of local variations but the computer takes correspondingly longer to reach a solution. If peak values are important (such as peak stress for the onset of cracking), the mesh size needs to match the dimensions of the peak. For example,

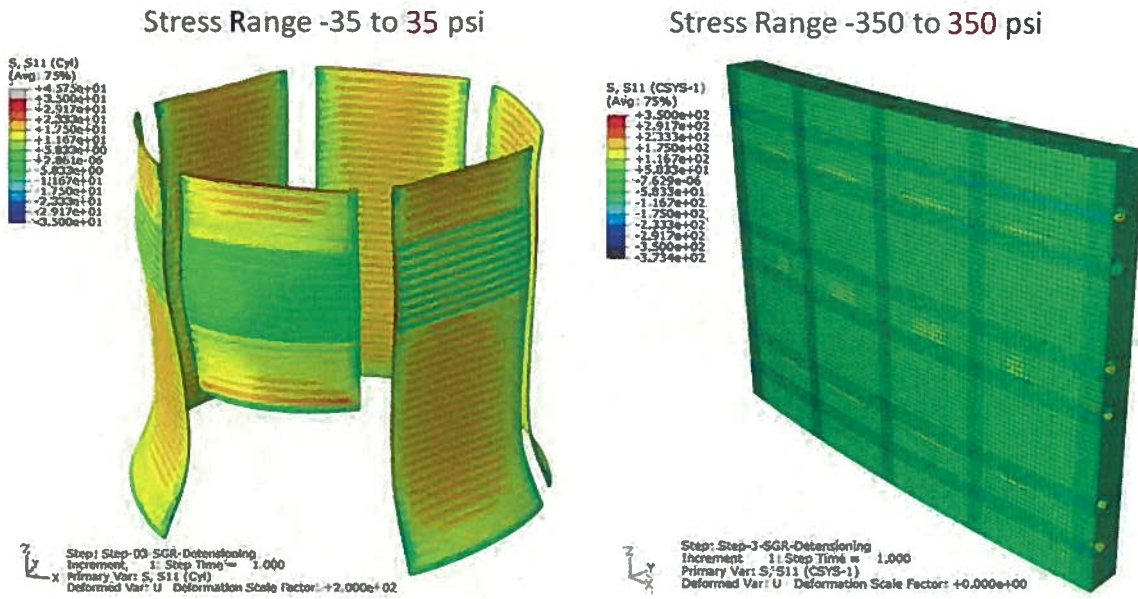
NON-PROPRIETARY VERSION



Approximately a factor of 10 difference in peak radial stress on outside of the hoop layer

Figure A1.9 Comparison of indicated peak stress between the Abaqus sub-model and the detailed model - Step 1: Tensioned.

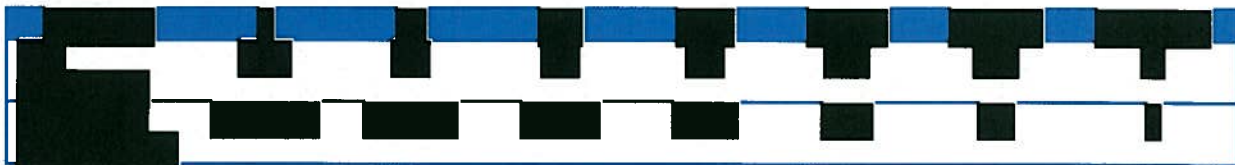
NON-PROPRIETARY VERSION



The radial tensile stress concentrations is reduced during the SGR de-tensioning

Figure A1.10 Comparison of indicated peak stress between the Abaqus sub-model and the detailed model - Step 3: SGR de-tensioning

To demonstrate the issue of mesh size, consider this example. Imagine a tank of water (density of 1) that is a cube 100 inches on each side. Imagine as well that hanging in the center of this tank is a 1" cube of metal with a density of 2. If you used a Finite Element model to identify the peak density in the tank the answer you would get is dependent upon the size of the mesh used.



In order to accurately calculate a peak value, the model must eventually use a cell size of no more than the dimension of the peak being studied. For the CR3 containment, the peak tensile stress is at the very edge of the horizontal tendon sleeve hole.

The conclusion is that a global model will naturally under-estimate the size of a peak stress unless it ultimately has a cell size equal to the size of the peak being studied. That does not make the global model unreliable. It simply means that additional study on a detailed level is needed to obtain the actual answer. Thus, one would not be surprised, in looking at containment wide or bay wide stress mappings, to see peak values that are lower than the actual peak values.

NON-PROPRIETARY VERSION

Clearly, an analysis which does not utilize a suitably small mesh size will conclude that peak stresses are acceptably low in a situation in which they are not.

Inevitably, the credibility of the computer model is based upon its ability to accurately reproduce predictions comparable to the benchmark data available without stretching the input assumptions by using non-physical material properties, as discussed above. [Attachment 2](#) provides the detailed analysis of benchmark studies of the Abaqus Global model versus the actual plant response.



ATTACHMENT 2: FLEXING OF CONTAINMENT WALLS

--BENCHMARKING THE COMPUTER MODEL AGAINST PLANT DATA--

Purpose:

This attachment focuses upon the comparison of computer generated plant simulations with actual plant data to confirm the accuracy of the computer models.

Expected Building Response:

The containment building was constructed as a cylinder, but when the tendons were tensioned, they modified the shape of the bays. The figure below shows this using an exaggerated degree of change to illustrate the point. The amount of radial displacement is actually about 0.5" immediately after tensioning and about 1" after 30 years of creep are added in.

Figure A2.1 shows a simplified drawing of the building response to tensioning its tendons. It also shows the bulge that developed as a result of the SGR partial de-tensioning.

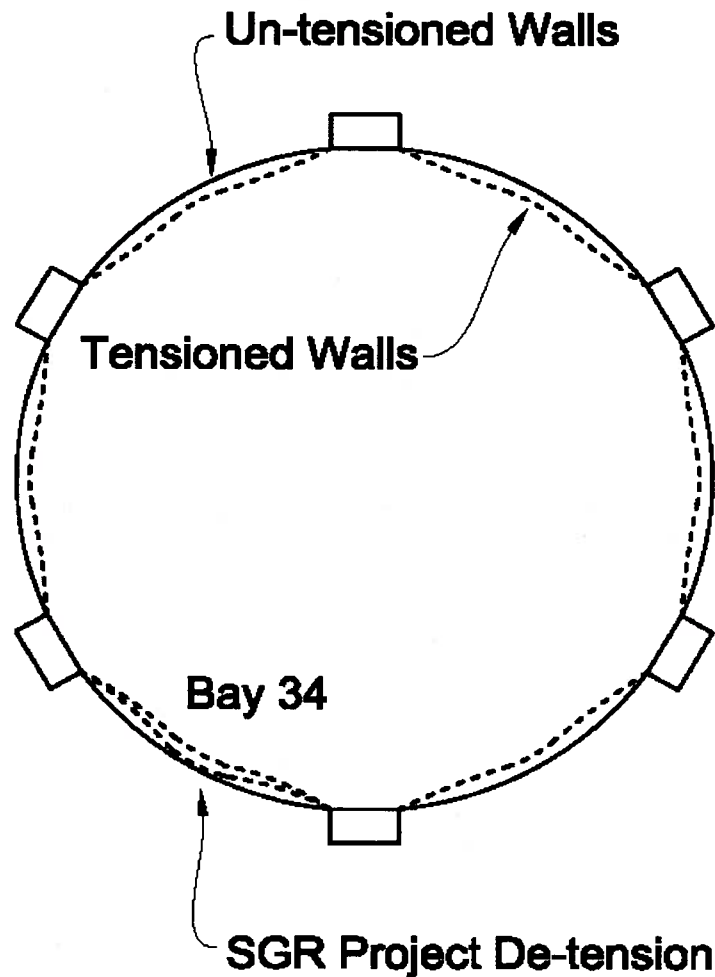


Figure A2.1 The effect of tensioning on containment walls

NON-PROPRIETARY VERSION

- 1) Initially the walls form a cylinder. They are attached to six buttresses which are essentially fixed.
- 2) When a tendon is tensioned, it pulls the center of the bay inward and decreases the curvature of the original arc.
- 3) When fully tensioned, the building looks slightly like a hexagon as the tendons decrease the curvature of the original bays.
- 4) If tendons are then de-tensioned, the affected walls move outward again. One would expect the outward motion to end when the wall reached its un-stressed location. If the containment is completely de-tensioned, that is what happens (except for the effects of creep).
- 5) However, if the de-tensioning is asymmetric, then the building can impose additional stress on the bay and the de-tensioned wall may create a double curve

COMPUTER CODE INPUTS

The report will be providing some computer model plots which had the following input assumptions. Abaqus applies creep correction only for long time period intervals such as the time step of 30 years of operation with the containment tensioned. E0 is the elasticity modulus and E1 is the creep adjusted elasticity modulus. F't is tensile capacity and G't is the fracture energy. 3.45 E6 psi is the average modulus measured on 22 CR3 containment cores. Fracture energy was measured to be 0.40 lbf/in. However Abaqus Global does not calculate cracking so those parameters are Not Applicable.

Figure	Model	E0 psi	E1 psi	F't psi	G't lbf/in	Creep
All computer comparisons	Abaqus Global	3.45 E6	3.45 E6	NA	NA	2.2

STRUCTURAL INTEGRITY TEST (SIT) BENCHMARKING

In 1976 CR3 performed a Structural Integrity Test (Reference 10) which involved pressurizing containment. The building was instrumented and dimensional changes were recorded which offer an opportunity to benchmark computer model predictions. Figure A2.2 shows a comparison between the PII computer model to the building's actual response in the SIT.

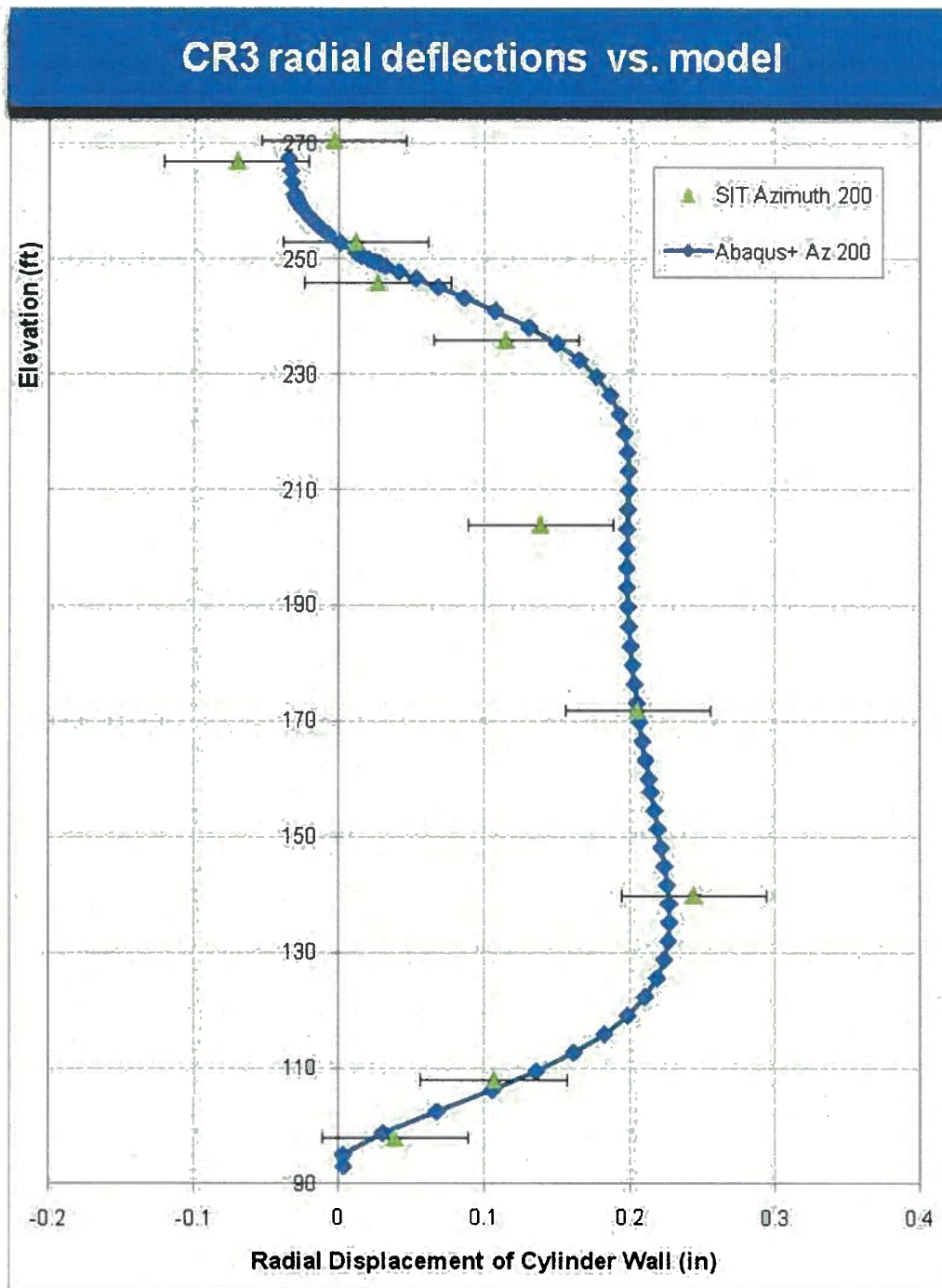


Figure A2.2 Comparison of measured radial deflections during the 1976 CR3 SIT taken at azimuth 200 degrees (Az 200) with PII computer model predictions

Overall the agreement between the computer models and the plant data is good. There is a slight discrepancy in radial displacement around elevation 220'. One would expect to see good agreement on a benchmark like this because it is a uniform application of pressure to all parts of containment.

LASER SCANNING DATA BENCHMARKING

A more stringent test is modeling an evolution which creates asymmetries in the building. Such a situation occurred in May, 2010 when the containment was de-tensioned to repair the delamination in bay 34. Laser scanning was performed after each group of tendons (referred to as a Pass) was de-tensioned from after Pass 4 until after Pass 11. Pass 4 was taken as the baseline for all the readings so the Pass 11 data represents the change in radial displacement from Pass 4 through Pass 11. The laser scans were taken roughly every 10 degrees around containment at four different elevations (170°, 185°, 210°, and 229°). The corresponding computer model predictions were obtained and plotted below.

FEA-Predicted Radial Displacements *RELATIVE TO END OF PASS 4* vs. Azimuth, Elevation 229'

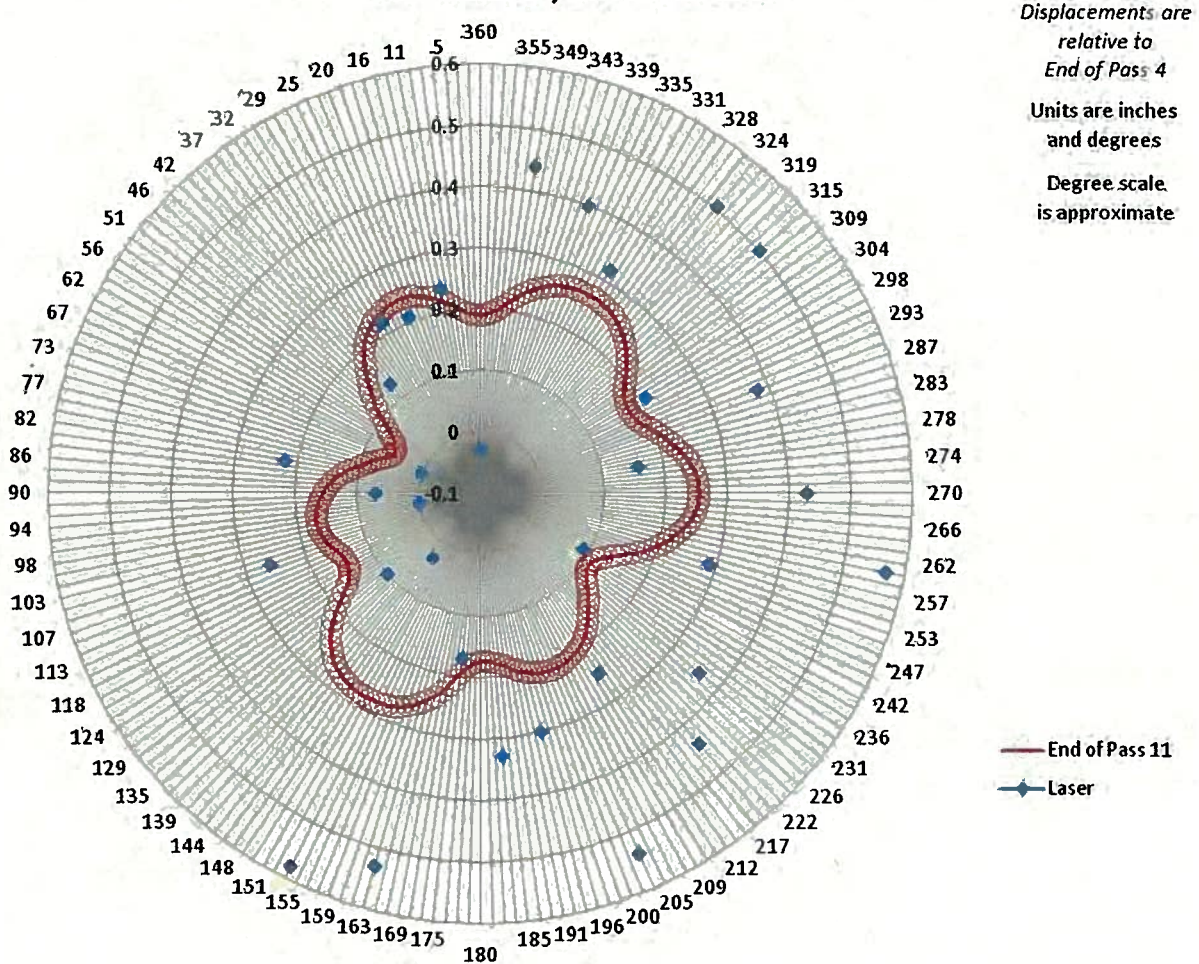


Figure A2.3 Comparison of PII computer model predictions for radial displacement from pass 4 through pass 11 at elevation 229' to the laser scanning data.

**FEA-Predicted Radial Displacements *RELATIVE TO END OF PASS 4*
vs. Azimuth, Elevation 210'**

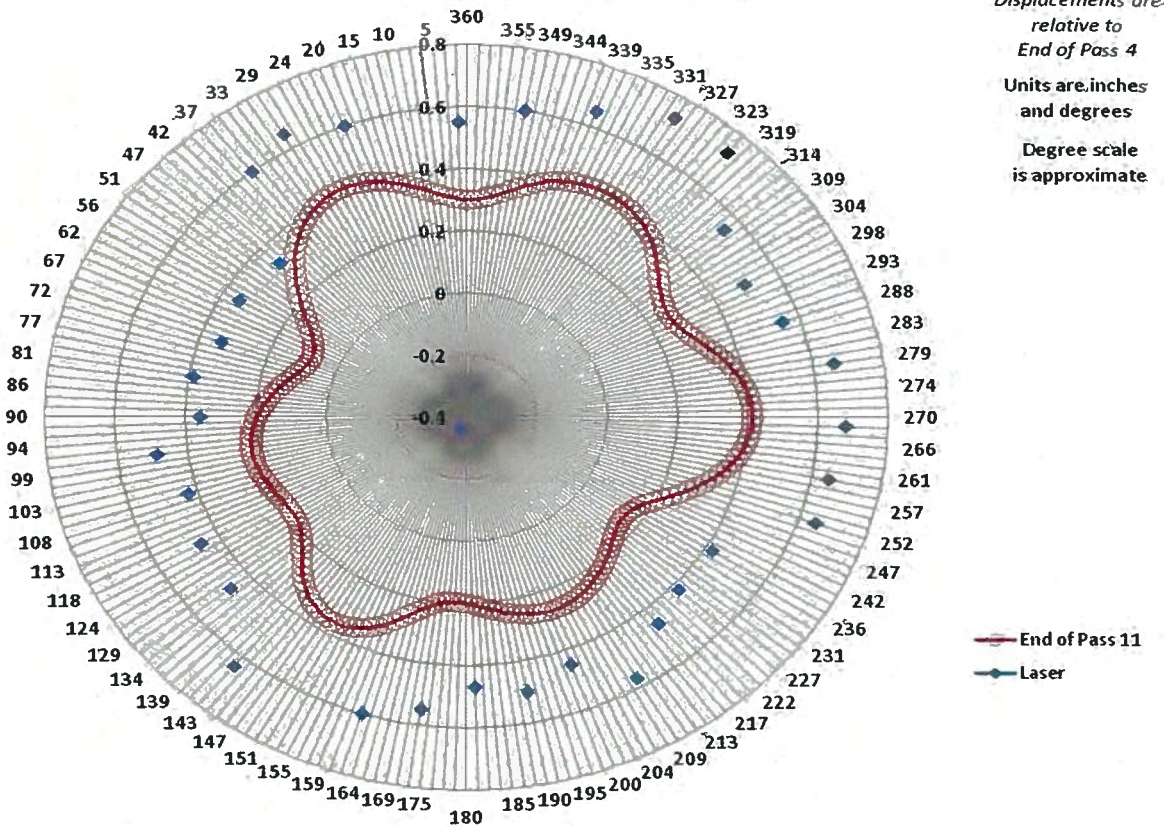


Figure A2.4 Benchmark comparison of PII computer predictions versus laser scanning data for elevation 210'.

**FEA-Predicted Radial Displacements *RELATIVE TO END OF PASS 4*
vs. Azimuth, Elevation 185'**

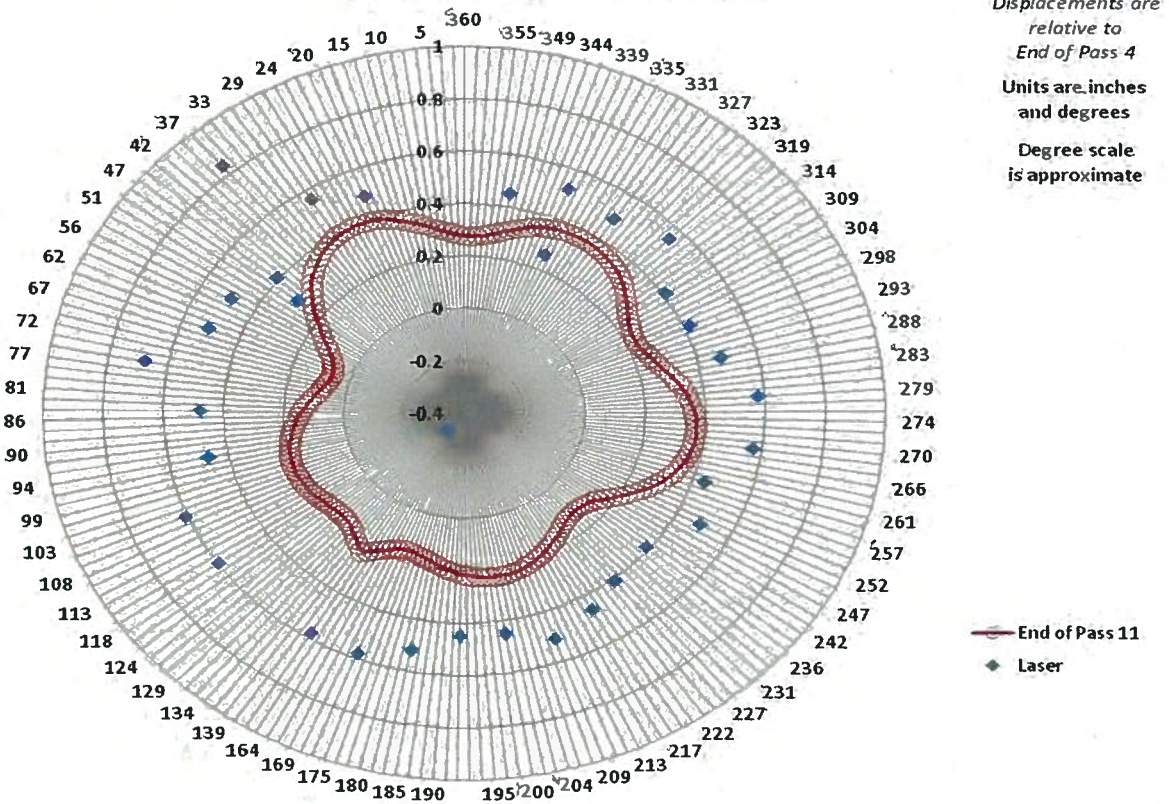


Figure A2.5 Benchmark comparison of PII computer model predictions with laser scanning for elevation 185'.

**FEA-Predicted Radial Displacements *RELATIVE TO END OF PASS 4*
vs. Azimuth, Elevation 170'**

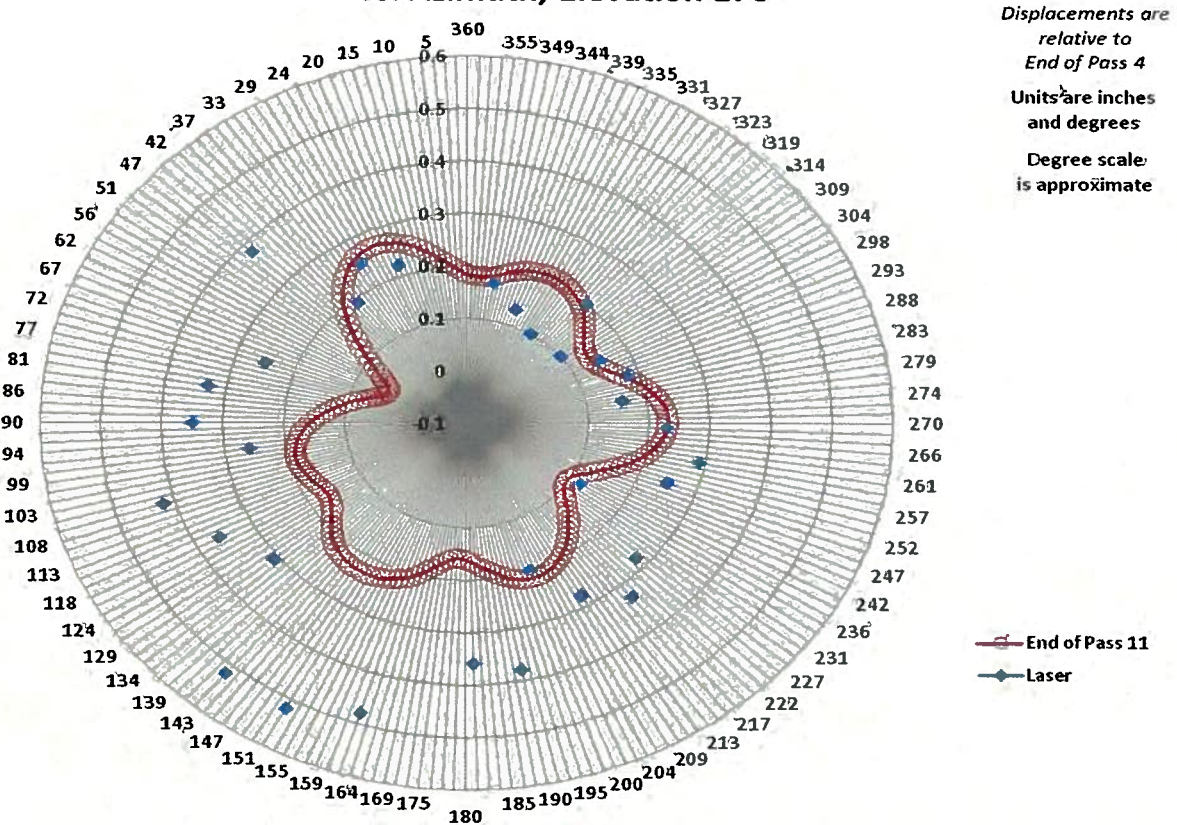


Figure A2.6 Benchmark comparison of PII computer models with laser scanning data for elevation 170'.

Primarily, the computer predictions show features that are expected. The six buttresses (at 0 degrees, 60 degrees, et cetera) show some movement but less than the bay midlines. However, the level and distribution of correlation between the model and the laser data is more difficult to explain. On elevation 229' there is considerable scatter in the laser data. Generally the laser data agree with the model predictions from 0 to 180 degrees (with the exception of immediately around the SGR opening at 150 degrees). Interestingly, in 1976 the agreement was better at 270 degrees than at 90 degrees. In 2010 the laser data from 180 degrees to 360 degrees is scattered and generally larger than the computer model predictions.

At elevation 210' the laser data show less scatter. Whereas the computer prediction averages about 0.3" radial displacement, the laser saw about 0.5". As with elevation 229' the computer predictions were lower than the plant data in 2010 but higher than the data in 1976. The shapes of the buttresses and bays are clearly visible in the laser data.

Elevation 185' is very similar to the features identified for elevation 210'.

Elevation 170' is similar to elevation 229'. The laser data agree well with the model from 260 degrees to 45 degrees and then the laser data is scattered and larger than the computer model predictions for the rest of the circle. Figure A2.7 shows the containment surface surveyed by the laser scanning equipment.

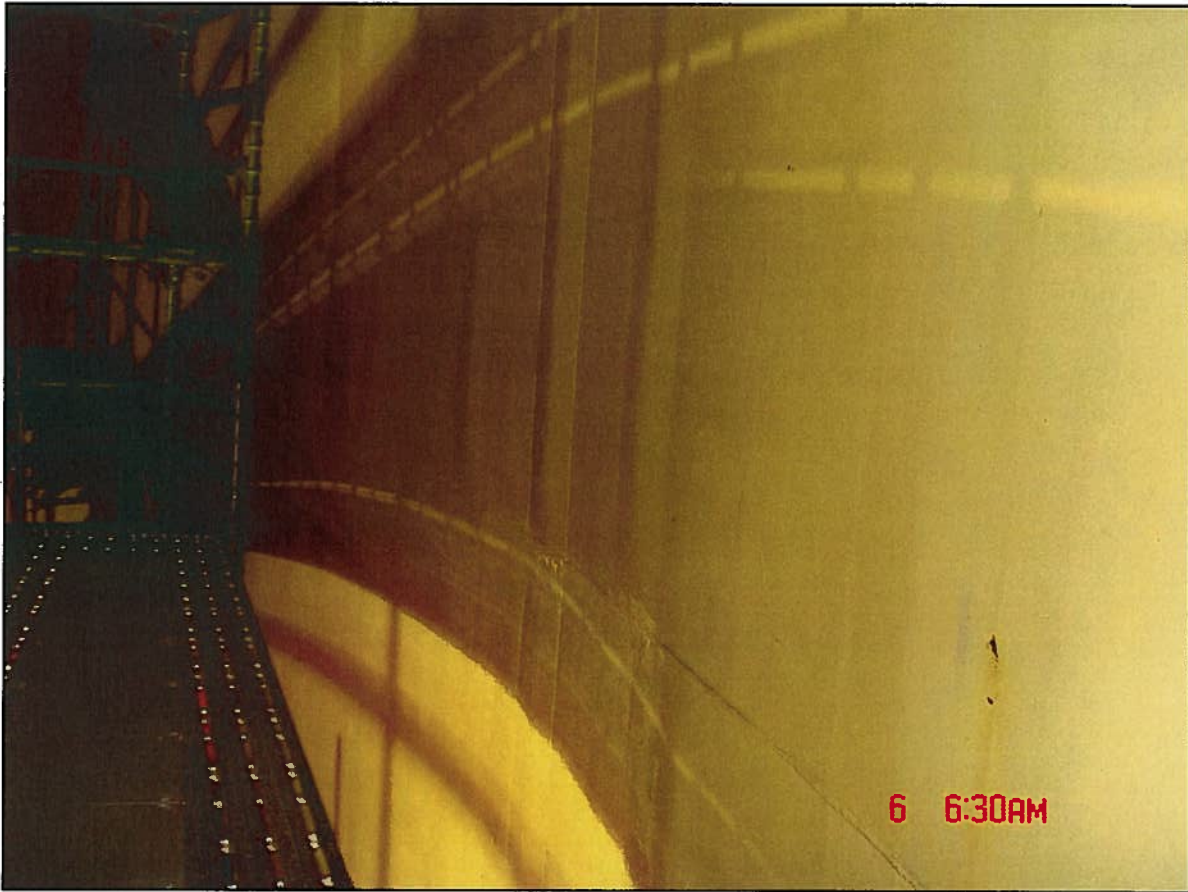


Figure A2.7 Photograph of the containment inner liner.

Figure A2.8 shows the results of the laser scan illustrated in three dimensions, displaying a very detailed image of the changes in radial deflection from the middle of the March, 2010 de-tensioning sequence to the end of that sequence.

The data demonstrating the bulge area in the center of bay 34, as shown in Figure A2.6, exhibit how, while every other part of the containment moved outwards during the de-tensioning in March, 2010, the area around azimuth 150 degrees from elevation 180' to 210' moved inwards. This is the reaction that would be expected had a bulge existed at the start and been deflated by the de-tensioning evolution. The laser would estimate the height of the bulge at 0.4" (based upon the partial evolution monitored) and the computer model would estimate it at 0.4" based on the information in Figure 7.12.

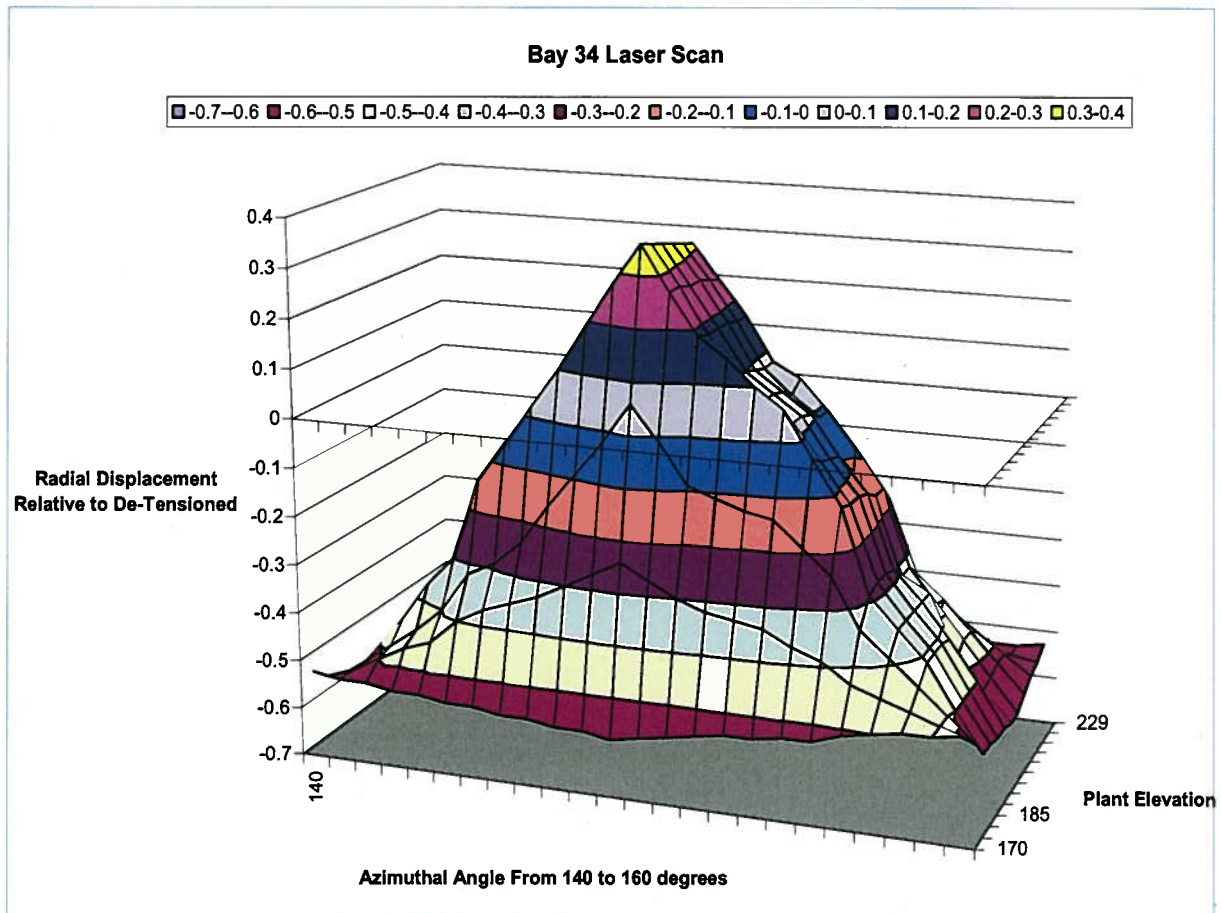


Figure A2.8 Three dimensional laser scan results for Bay 34.

Figure A2.8 is another method to display the laser scan data in the center of bay 34. The above comparison indicates that laser scanning confirms the salient points in the delamination scenario relative to radial displacement of bay 34.

Overall, the comparison is a valuable one, validating both the laser scanning methodology and the relative displacement model of containment. The general shape and variation in the containment interior wall is visible on elevation 210'. The individual buttresses and bay curvatures are quite visible. While the agreement is better for the SIT data the deflection expected from a uniform pressurization of containment is easier to model than the partial de-tensioning of containment. The 210' elevation data indicate a consistency in the laser data consistent with its quoted uncertainty of 0.1" and perhaps better in a relative sense. The agreement is not as good on the 180' elevation. There appears to be more random variation in the individual data points but much of the shape is discernable. The same is true at the 170' elevation but with more variation in the laser data. Elevation 229' is not particularly useful due to scatter in the laser data. The value in the laser benchmarking is the validation of the general predicted shape in a very large change in containment conditions. As discussed in Attachment 1, the modulus of elasticity selected for modeling has a significant influence on predicted absolute displacements and it is not surprising that an adjustment is needed for comparison to actual displacements.

NON-PROPRIETARY VERSION

Computer modeling is presented in more detail in Attachment 1.

A tabulated version of the laser comparison to the computer model is provided below:

Elevation	117 deg	133 deg	140 deg	150 deg	160 deg	166 deg	180 deg
229' laser	-	0.10"	0.03"	0.58"	0.53"	0.17"	0.33"
229'model	0.14"	0.19"	0.25"	0.28"	0.27"	0.23"	0.17"
210'laser	0.46"	0.47"	0.64"	-0.36"	0.60"	0.55"	0.47"
210'model	0.19"	0.22"	0.28"	0.36"	0.31"	0.24"	0.20"
185' laser	0.47"	0.61"	0.60"	-0.31"	0.58"	0.58"	0.52"
185'model	0.18"	0.18"	0.23"	---	0.23"	0.19"	0.17"
170' laser	0.36"	0.31"	0.52"	0.52"	0.48"	-	0.36"
170'model	0.17"	0.20"	0.22"	0.23"	0.21"	0.19"	0.16"

Elevation	300 deg	310 deg	320 deg	330 deg	340 deg	350 deg	360 deg
229' laser	0.21"	0.52"	0.16"	0.32	0.44"	0.44"	-0.03"
229'model	0.18"	0.20"	0.24"	0.27"	0.25"	0.21"	0.19"
210' laser	0.50"	0.55"	0.73"	0.73"	0.65"	0.60"	0.55"
210'model	0.26"	0.29"	0.37"	0.42"	0.39"	0.32"	0.30"
185'laser	0.42"	0.41"	0.55"	0.49"	0.52"	0.45"	---
185'model	0.23"	0.25"	0.32"	0.37	0.35"	0.29	0.28"
170'laser	0.15"	0.10"	0.20"	0.10"	0.13"	0.17"	---
170'model	0.14"	0.14"	0.18"	0.21"	0.21"	0.18"	0.18

Table A.2.1 Comparison of laser scanning and computer model prediction of radial displacement in bays 34 & 61 between SGR de-tensioning to full de-tensioning.

PLANT STRAIN GAUGE DATA COMPARISON

A second indication of accuracy in the computer models is the comparison of displacement gauge data taken during the March, 2010 de-tensioning activity. Responses were collected from displacement gauge channel 31 in bore hole 81 and channel 32 in bore hole 51, both of which are located in bay 34. Hole 51 is located about 7 feet from the buttress and 5 feet from the equipment hatch support. Hole 81 is located about 23 feet from the buttress and 23 feet from the ring girder. The displacement experienced by hole 81 (center) is consistently three times what hole 51 (edge) experiences. For further discussion of instrument response inside the concrete refer to Attachment 3.

Another indication of modeling accuracy comes from installed radial strain gauges. Four radial strain gauges are located in bore hole 104 in the middle of bay 45 at elevation 171'. Two other radial strain gauges are located in bore hole 30. The figure below shows the locations of the detectors.

Core Bore #104 Location and Strain Gauge Channels

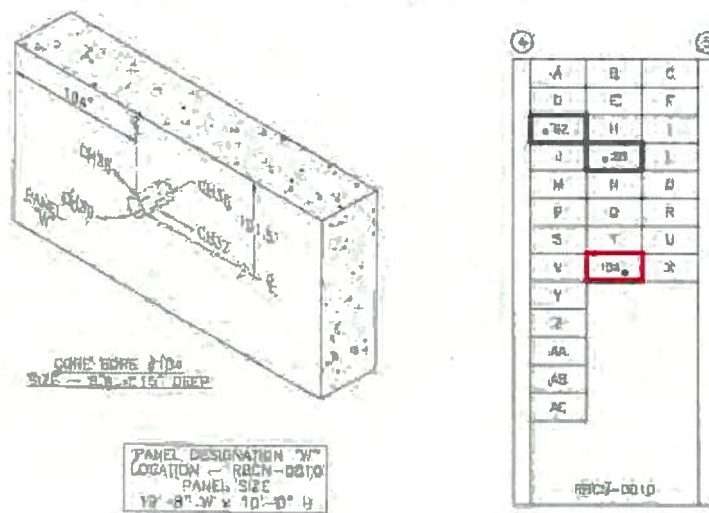


Figure A2.9 Detectors #36 to #39 in bore hole 104 and the location of bore hole 30.

Strain gauge responses to the individual tendon de-tensioning in March, 2010 were investigated and it was found that their amplitude is a simple exponential function of the distance between the tendon and the sensor. The amplitude drops by a factor of 2 every 6 feet further away you go from the sensor. This relationship allowed estimation of the total strain felt due to fully tensioned tendons. The results are summarized below.

NON-PROPRIETARY VERSION

Table A2.2 Estimated Total Strain Removed Due to Tendon De-tensioning ($\mu\text{in/in}$)

Channel #	Location	Depth (inches)	Total Strain ($\mu\text{in/in}$)	
			Method 1	Method 2
34	#30 hole	14	95	163
35	#30 hole	10	164	149
36	#104 hole	13.2	181	107
37	#104 hole	10.5	175	128
38	#104 hole	10.4	170	140
39	#104 hole	6.8	53	19

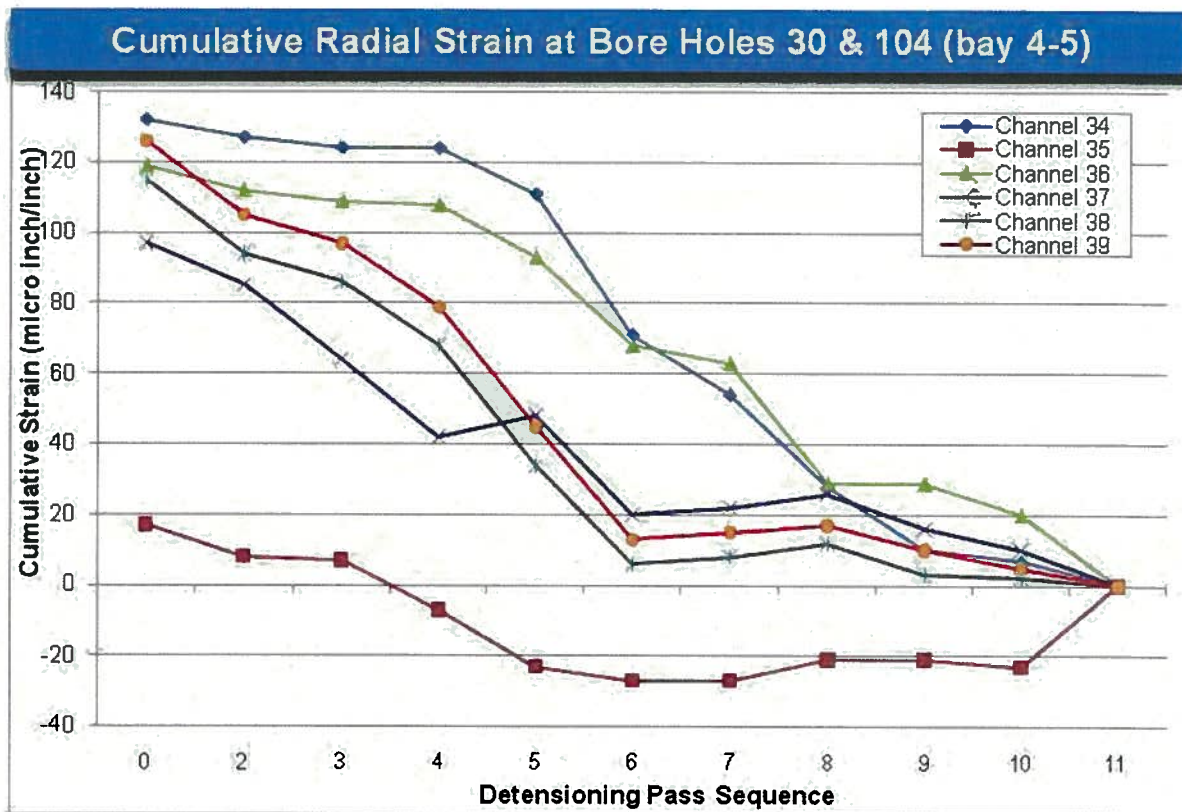
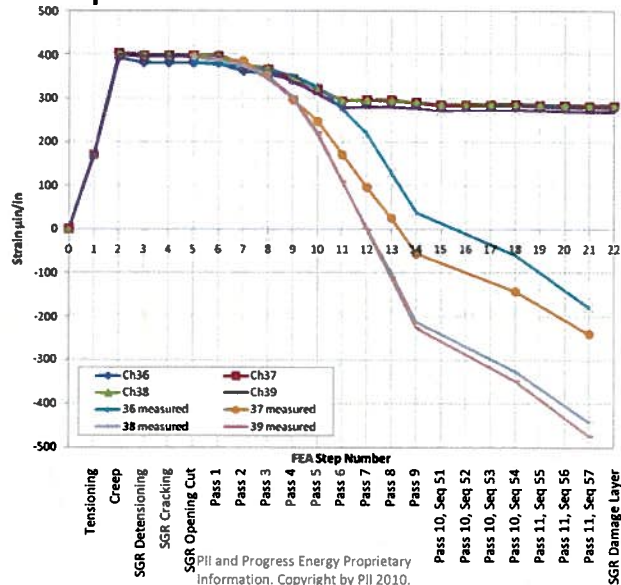


Figure A2.10 Cumulative radial strain readings as the containment was de-tensioned in March, 2010

Note that the readings are normalized to zero in the de-tensioned state. The two deepest sensors (#34 at 14" and #36 at 13") behave similarly. Sensor #35, at 10" deep, was located in a section of the bay that underwent a lesser total strain change than deeper in the concrete or at the other sensor, which indicates that the containment at elevation 215' in Bay 45 straightened out during the de-tensioning. This is confirmed in the computer model. The computer model also indicates that the most extreme displacement occurs at pass 6 and that the cumulative data shows a distinct change at that pass in sensors 37, 38, and 39.



Comparison to Measurements



3/30/2010

PII and Progress Energy Proprietary Information. Copyright by PII 2010.

8

Figure A2.11 Comparison of computer predictions with observed detector response

Channel #36 shows good agreement through pass 6 and then deviates. Channels #37, #38 and #39 deviated after pass 3. These benchmarking opportunities allow for refining of the computer models, a process which is discussed in more detail in Attachment 1.

The purpose of this discussion was to address actual bay movements and the benchmarking of modeling codes.

If, indeed, there is cycling of the bays and the center of the bay experiences most of the stress, it might be possible to see this in the average material properties of the concrete as a long term phenomenon.

Conclusion:

The computer model reasonably predicts the general shape and magnitude of radial displacements for a variety of plant changes. If anything, the computer model under-predicts the size of these displacements. Certainly, the conclusion that the SGR de-tensioning scope and sequence created a bulge in the wall and that the stress created by the curvature of the bay wall precipitated the cracking and delamination of bay 34 is credible. The fact that the March, 2010 de-tensioning evolution was successful even though it involved 8 times the number of tendons also indicates the scope and sequence of tendon de-tensioning is an important contributor to the delamination event.



ATTACHMENT 3: CONTAINMENT WALL INTERNAL RESPONSE

The containment wall is also subjected to other tensile stresses (such as thermal heating due to solar radiation) and bending stresses which can be different on the outside surface of the wall than further into the concrete.

An example of the routine radial strains encountered by the concrete containment is the variation on strain actually observed in the Crystal River containment sensors at various depths into the concrete. The graph below displays actual typical data.

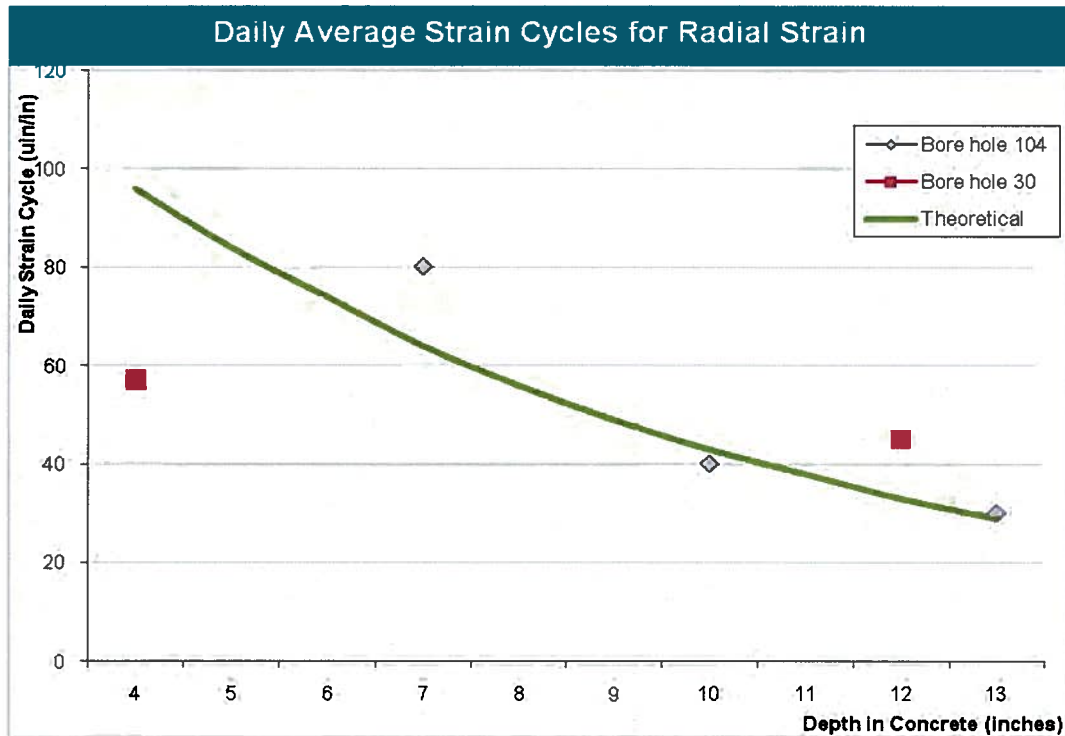


Figure A3.1 Plot of average daily radial strain cycles as a function of depth in concrete

These cycles are driven by the temperature variation due to solar heating and have been directly correlated to the equivalent temperature readings as a function of depth in the concrete. This shows the concrete sees a strain of about 40 µin/in at the critical depth of 10 inches.



ATTACHMENT 4: SGR OPENING SEQUENCE

Event Chronology:

On 9/26/09 the Crystal River steam generator replacement (SGR) outage began. It included the creation of an access opening in the containment wall. The construction opening was a 27' by 25' rectangle running from elevation 183' to 210' centered on the centerline of bay 34. From 9/27/09 to 10/1/09 plasma cutting of 17 horizontal and 8 vertical tensioned tendons occurred. Two additional vertical tendons were de-tensioned with jacks for possible reuse.

On September 30, 2009 a limited concrete removal began. The photograph in Figure A4.1 (after the fact) that there were indications of cracks as soon as the area around the horizontal tendons became exposed. This was the day before the last two horizontal tendons were de-tensioned.



Figure A4.1 The first indication of cracking between horizontal tendons taken on 9/30.



Figure A4.2 Photograph of overall status of demolition taken on 9/30/09.at 17:38



Figure A4.3 Another crack photograph taken on 10/01/09

Figure A4.2 shows the limited scope of concrete removal on 9/30/09. Only about 0.5% of the total amount to be removed had been removed when cracks were uncovered.

NON-PROPRIETARY VERSION

Figure A4.4 below shows the concrete removal status as of October 1, 2009. Note the large blocks of broken concrete in the middle of the opening. This is indicative of delamination since hydro-lasing does not normally generate large debris.



Figure A4.4 Photograph of demolition on the evening of 10/1/09. Note the large blocks of broken concrete in the middle of the opening.



Figure A4.5 Another early photograph (10/1/09) of concrete debris, showing the distribution of horizontal tendons. The horizontal tendons come in pairs centered 13 inches apart. The distance between pairs is 26 inches. The horizontal tendons are outside the vertical tendons and define the transition from radial tension stress to radial compression stress in the concrete.



Figure A4.6 Delamination crack running vertically between horizontal tendons about 10" deep.
Taken on 10/3/2009

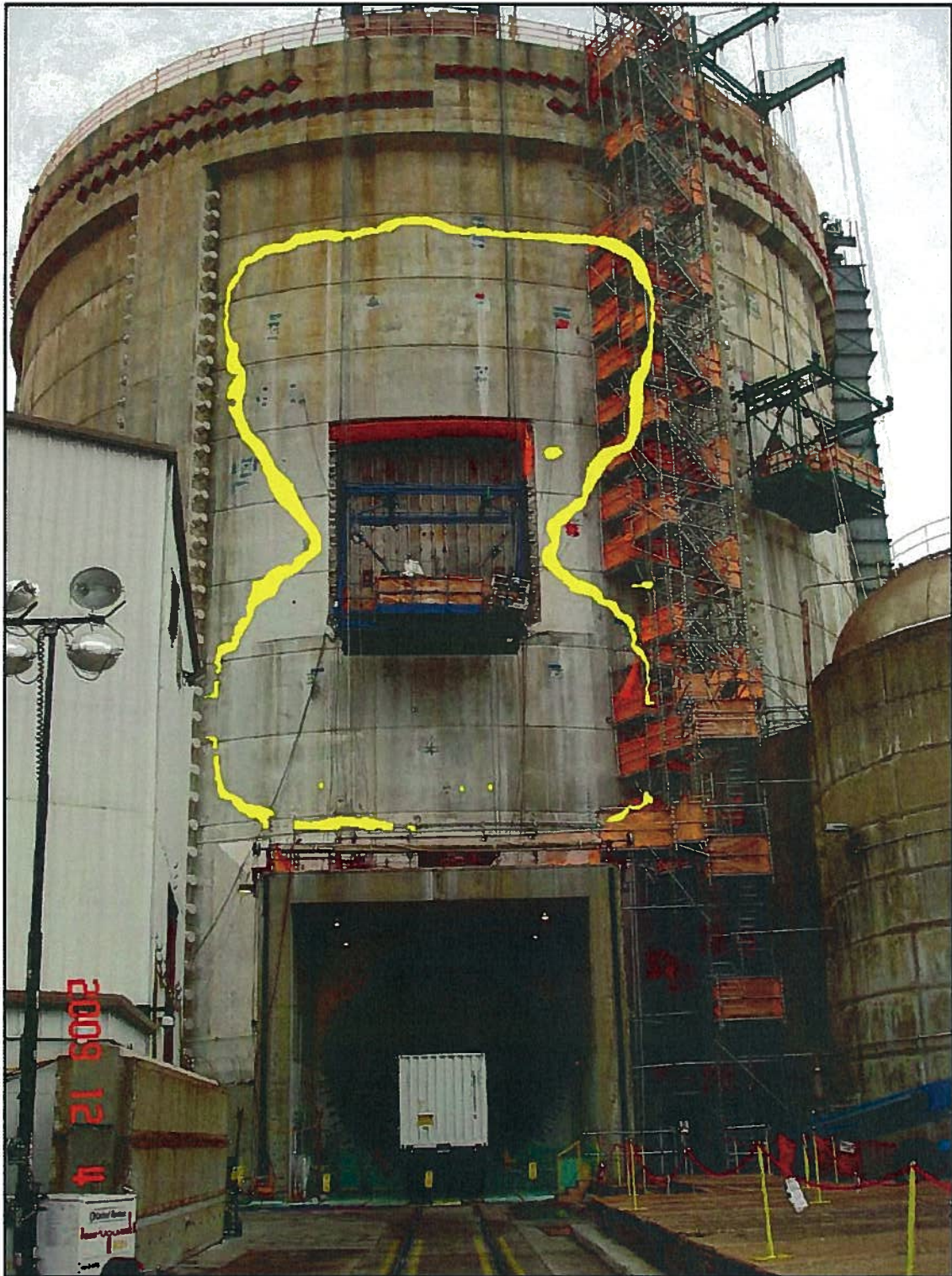


Figure A4.7 Delamination zone outline overlaid on the containment wall above and below the SGR opening

NON-PROPRIETARY VERSION

Figure A4.8 shows the delaminated area as determined through non-destructive testing (NDT), and confirmed through core drilling and fiberscope follow-up:

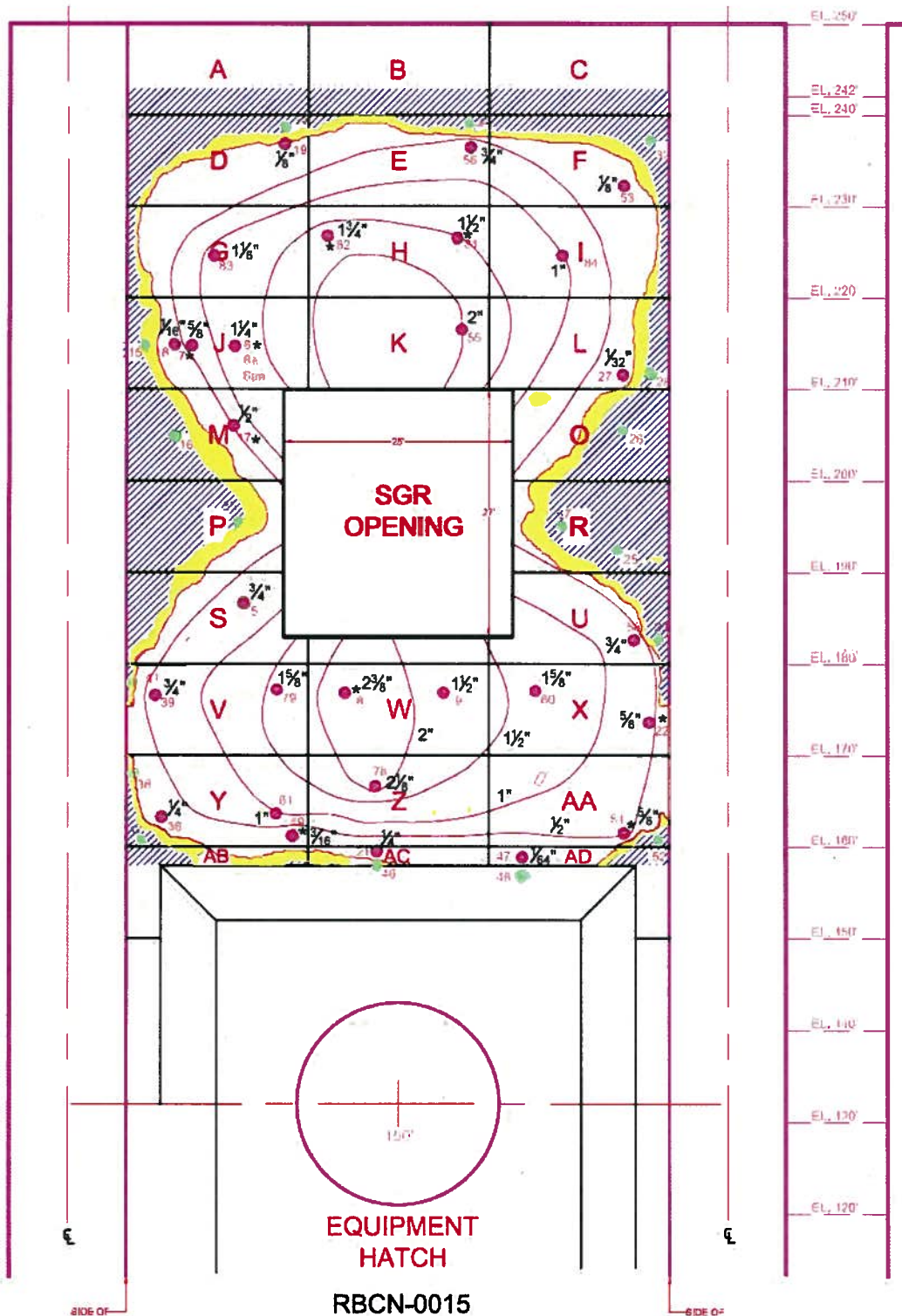


Figure A4.8 Displacement map showing the distribution of delamination depth



ATTACHMENT 5: REVIEWER TABLE AND RESUMES

Failure Mode Author and Reviewer List:

Table A5.1 PII Failure Mode Author and Reviewer Table

FM #	Subject	Author	Reviewer	Reviewer	Reviewer
1.1	Tendon Stresses	Berbon	Cooper	Brevig	
1.2	Radial Stress	Berbon	Cooper	Brevig	
1.3	Horizontal Tensioning	Berbon	Hughes	Brevig	
1.4	Vertical Tensioning	Berbon	Hughes	Brevig	
1.5	Foundation	Amon	Snell	Mor	Berbon
1.6	Ground Movement	Amon	Snell	Mor	Berbon
1.7	Vibrations	Berbon	Cooper		
1.8	Tendon out of plane	Berbon	Hughes	Waldo	Brevig
1.9	Tendon Spacing	Berbon	Mor	Cooper	
1.10	In 2.7	Mor	Berbon	Cooper	Brevig
1.11	Micro-cracks	Mor	Berbon	Cooper	Brevig
1.12	Tendon sleeve size	Berbon	Cooper	Mor	
1.13	Net loading area	Berbon	Cooper	Brevig	
1.14	Equipment Hatch	Waldo	Mor	Cooper	
1.15	SCF Design	Berbon	Waldo		
2.1	Curing	Mor	Cooper		
2.2	Pouring	Mor	Amon	Cooper	
2.3	Slump (includes 3.6)	Mor	Cooper		
2.4	Early Age	Mor	Berbon	Cooper	Snell
2.5	Temperature	Mor	Snell	Cooper	Waldo
2.6	Mix Design	Mor	Amon	Snell	
2.7	Vibration	Mor	Snell	Cooper	
2.8	Tendon	Mor	Waldo		
2.9	Forms	Mor	Snell	Amon	
2.10	Early Tension	Mor	Waldo		
2.11	Cold Joint	Mor	Snell		
2.12	Strength Properties	Mor	Amon	Snell	Berbon
3.1	Air	Mor	Waldo		
3.2	Grouting	Mor	Cooper		
3.3	Cement	Mor	Snell	Cooper	
3.4	Aggregates	Mor	Amon	Snell	
3.5	Admixtures	Mor	Cooper		
3.6	In 2.3	Mor	Waldo		
3.7	Testing	Mor	Amon	Brevig	Cooper
4.1	Plastic shrinkage	Mor	Snell	Amon	
4.2	Shrinkage	Mor	Snell		
4.3	In 4.2	√	√	√	

NON-PROPRIETARY VERSION

4.4	In 4.2	√	√	√	
4.5	Creep	Berbon	Waldo		
4.6	In 4.5	√			
4.7	Segregation	Mor	Cooper	Snell	
4.8	Cyclic Loading	Mor	Waldo		
5.1	Foreign Material	Mor	Brevig	Berbon	Cooper
5.2	Salt Water	Mor	Snell	Saouma	Cooper
5.3	Maintenance	Mor	Waldo		
5.4	Form Release	Mor	Brevig	Berbon	
5.5	Corrosion	Mor	Brevig	Berbon	
5.6	Grease	Brevig	Waldo		
5.7	Physical attack	Mor	Brevig	Snell	Snell
5.8	Chemical attack	Mor	Brevig	Berbon	Cooper
6.1	Uneven Force along tendon	Berbon	Waldo		
6.2	Tendon wires	Berbon	Waldo		
6.3	Grease thermal effects	Berbon	Waldo		
6.4	Rigid/flex sleeves	Berbon	Waldo		
6.5	Re-tensioning	Berbon	Waldo		
6.6	Initial tensioning	Berbon	Waldo		
7.1	Accumulated damage	Mor	Brevig	Waldo	
7.2	Hydro shock/vibration	Berbon	Mor	Hughes	
7.3	De-tensioning sequence	Berbon	Mor	Cooper	
7.4	De-tensioning scope	Berbon	Cooper	Brevig	
7.5	Removing Concrete	Waldo	Brevig	Cooper	
7.6	Cutting Vibrations	Berbon	Brevig		
7.7	Pre-existing Delamination	Berbon	Cooper		
7.8	Water jet pressure	Berbon	Mor	Brevig	
7.9	Hydro Nozzle rate	Berbon	Mor		
7.10	Cracks from hydro	Berbon	Waldo		
7.11	Pulling tendon stress	Berbon	Waldo		
8.1	Spray pressure	Brevig	Cooper	Berbon	
8.2	Spray temp	Brevig	Cooper	Berbon	
8.3	ILRT	Brevig	Cooper	Berbon	
8.4	IWL	Brevig	Cooper	Mor	Berbon
8.5	Purge	Brevig	Cooper	Berbon	
9.1	Hurricane tornado	Brevig	Cooper	Berbon	
9.2	Seismic	Brevig	Cooper	Mor	Berbon
9.3	Ground Movement	Amon	Waldo		



RESUMES of PII PARTICIPANTS:

- ❖ Chong Chiu, PhD, Team Leader
- ❖ Ray Waldo, PhD, Assistant Team Leader
- ❖ Marci Cooper, Assistant Team Leader
- ❖ Patrick Berbon, PhD, Assistant Team Leader
- ❖ Avi Mor, Dr. Eng.
- ❖ David Brevig
- ❖ Henric Larsson
- ❖ Tyson Gustus
- ❖ Joe Amon, PE
- ❖ David Dearth, PE
- ❖ Luke Snell, PhD
- ❖ Gary Hughes, PhD
- ❖ Mostafa S. Mostafa, PhD
- ❖ Jan Cervenka, PhD



Chong Chiu, Ph.D.

Technical Background

Dr. Chong Chiu graduated from M.I.T. nuclear engineering department with a Ph.D. (1977) and a M.S. degree (1976). He had a grade point average of 5.0, highest achievable at M.I.T. His Ph.D. thesis was performed at the Mechanical Engineering Department under Professor Warren Rohsenow and Neil Todreas. He has taught at MIT Summer Safety courses on prevention of programmatic and organizational failures, human performance problems, equipment failures, and safety leadership during 2000-2006. He has personally performed more than 500 root cause investigations since 1977 many of which are related to safety leadership.

Publications

Dr. Chiu has published more than 50 technical papers in the areas of management and human error reduction, integrated approaches to prevention, detection and correction, equipment performance improvement, and safety culture improvements. His professional interest throughout his career is to improve safety through design improvement and root cause analysis. He has authored two books, "Root Cause Guidebook" and "Failure Diagnostic Guidebook", both of which are in circulation with over 12,500 copies used at most U.S., European, and Asian power plants.

Achievements

Dr. Chiu worked for ABB-CE from 1977 to 1985. During that period of time, he was a manager for safety system design. Among other achievements, he successfully completed the design of the first generation of digital protection and monitoring systems at ABB-CE (COLSS/CPC). These types of systems have been widely used by all later designs and the advanced reactors.

In 1985, he joined SCE (Southern California Edison) as the Assistant Technical Manager. He then became the Safety Engineering Manager at Southern California Edison in 1988. He led a task force to help San Onofre Nuclear Station (3 units) reduce the scram rate from 15 per year in 1988 to 0 in 1989.

Dr. Chiu founded FPI International (currently Performance Improvement International) in 1987 with the sole mission to improve safety and performance by preventing failures through root cause analysis, management consultation and training. The formation of this company was endorsed by SCE senior management due to its strong research orientation in failure prevention through root cause analysis. His research, case studies, and seminars at Performance Improvement International and FPI International have covered three types of failures:

- ◆ Human Errors
- ◆ Equipment Failures
- ◆ Organizational/Programmatic and Executive Leadership Failures

Over the past 20 years, he has achieved the following:



- He has lead over a hundred research projects, providing consultation support and conducting training seminars funded by the power industry to help reduce safety problems related to human errors and equipment failures. These projects include:
 - Accountability Systems
 - Human Error Reduction Methods for Field Workers, Supervisors, Engineers, and Managers
 - Complacency
 - Organization and Safety Culture
 - Organizational Effectiveness
 - Reduction of Human Errors Involving Injuries
 - Leadership Safety Behavior (at Daya Bay Nuclear Power Plant in 2006)
 - Manager Error Reduction
 - Manager's Role in Highly Performing Organizations
- From 1987 to 2008, he helped establish component root cause analysis programs at more than 86 power plants (86% of all U.S. plants, 11 European plants, 3 Taiwan plants and 4 China plants) as well as in many other industries.
- From 1987 to 2008, he has delivered seminars on how to solve human error (including work injury) problems and helped many industries and organizations to achieve the highest safety performance possible. His seminars in human error reduction have been used by many organizations including China Daya Bay Nuclear Management Company, American Electric Power, Duke Power Corporation, TVA, Wisconsin Electric, Entergy, Evergreen International Group, etc. as a means to improve safety performance.
- From 2003 to 2009, he has served on the Senior Nuclear Safety Oversight Board of China Daya Bay Nuclear Management Company.
- He developed a comprehensive method (quantitative method) to assess work process failure rate. The method has been used at both nuclear and non-nuclear industries for work process safety assessments.
- He has given seminars at the NRC and DOE (US Government) on human error reduction and O&P root cause analysis (NRC Region IV and Region II). More than 500 NRC staff members have attended Dr. Chiu's seminars.
- Since 1987, he has been called upon by many companies to solve urgent equipment failures. After his findings of the root causes and implementing corrective actions, there has been *no recurrence*. The total number of cases solved by Dr. Chiu and his PII team between 1987 to 2008 is over 5,000. Some of the well-known cases are listed as follows:
 - Taiwan nation-wide blackout event in July (1999)



- San Francisco electrical blackout in December (1998)
- USA west coast blackout (1996)
- American Electric Power's repeat breaker failures (1996)
- TVA Transformer and breaker failures (1996, 1998)
- TVA-EPRI Statcom Failures (1997)
- Los Angeles distribution 25 outages (1995-1998)
- Entergy plant trip with spurious water high level (1994)
- Big Rock Point water hammer (1990)
- PG&E's Diablo Canyon letdown line cracking (1990)
 - Nebraska Public Power's Cooper RHR valve fracture (1991)
 - Nine Mile Point 2 loss of power event due to UPS failures
 - APS battery failures (1994)
 - Baltimore Gas & Electric's Calvert Cliffs repeat turbine trips (1994)
 - Detroit Edison's Fermi turbine failures (1993)
 - Trojan safety valve failures (1991)
- NASA Space Shuttle hydrogen leak
 - Davis Besse auxiliary feedwater control valve failures (1994)
- Westinghouse Generator Failures (1987)
- GE Generator Failures of Hydrogen Leak and Stator Winding Failures (1989)
- Three Mile Island accident (1979)
- Los Angeles blackout investigation (2000)
- TAMU Bon Fire Collapse investigation (2000)
- Iatan Pipe Rupture event (two fatalities) at KCP&L (2007)
- DC Cook Turbine Blade failure event investigation (2008)
- California fire (Cox Fire) investigation (2009)
- Mississippi Power and Light Scaffold collapse (one fatality) investigation (2008)
- Daya Bay Diesel Generator failure investigation (2007)
- Daya Bay RCP pump bearing failure investigation (2007)



Past Awards

- 1979 ABB-CE Outstanding Achievement Award for developing the first generation of digital protection and monitoring system for PWRs
- 1986 SCE Management Achievement Award for reducing scram rate and radioactive waste significantly at San Onofre Nuclear Station
- 1989 ANS Reactor Operations Meritorious Performance
- 1990 ABB-CE Special Award for helping achieve ABB-CE's national record of continuous operation among all its PWRs
- MIT Outstanding Teaching Assistant Award (1977)
- American Nuclear Society Fellow (1995) for Human Performance Improvement

More detailed information about Dr. Chiu's resume will be provided upon request



Raymond W. Waldo, PhD.

Career Summary

A nuclear engineer for over 30 years with experience in academic research, test reactors, and power reactors. This experience includes engineering, operations, and executive management. These roles included frequent interaction with both the Nuclear Regulatory Commission (NRC) and the Institute of Nuclear Power Operations (INPO). Oversight experience includes Academic Review Board for the Nuclear Engineering Department of U.C. Berkeley and membership on the Palo Verde Offsite Review Board.

Professional Experience

Performance Improvement International 2007- Present
 Human Performance and Equipment Failure Consultant responsible for onsite investigations and programmatic evaluations for large scale industrial applications including both nuclear and non-nuclear experience.

Southern California Edison, San Onofre Nuclear Generating Station..... 1980 – 2007
 Vice President, Nuclear Generation..... 2005 – 2007
 Executive responsibility for 1,000 employees in Operations, Maintenance, Health Physics, Chemistry, Training, and Emergency Preparedness at a two Unit PWR.
 Station Manager 2002 – 2005
 Managing 800 employees in Operations, Maintenance, Health Physics, and Chemistry. Responsible for the safe and compliant operations of San Onofre.
 Operations Manager..... 1990 – 2002
 Managing 300 employees in Operations. Responsible for the licensed and non-licensed Operators.
 Engineering Supervisor..... 1983 – 1990
 Supervising 40 Reactor Engineers, Computer Engineers, and Technicians. Responsible for physics testing and digital reactor protection.
 Reactor Engineer..... 1980 – 1983
 Responsible for Reactor Engineering group of eight people.
 Lawrence Livermore National Laboratory 1977 – 1980
 Reactor Supervisor for 3 MWth Livermore Pool Type Reactor.
 Georgia Institute of Technology 1976
 NRC licensed Operator at the 5 MWth heavy water Georgia Tech Research Reactor.
 ERDA fellowship at Georgia Tech.

Education

Ph.D. in Nuclear Engineering, Georgia Tech, Atlanta GA..... 1980
 M. S. in Nuclear Engineering, Georgia Tech, Atlanta GA 1976
 B. S. in Physics, Caltech, Pasadena, CA..... 1972

Qualifications

INPO Senior Nuclear Plant Manager Course Mentor..... 2006



Ontario Hydro Nuclear Development Seminar Mentor.....	2003
INPO Ops Manager Mentor.....	1997
INPO Senior Nuclear Plant Managers Course,.....	1996
College Instructor for Introduction to Nuclear Energy at Cal Poly, Pomona.....	1986-1987
Shift Technical Advisor, San Onofre Unit 1.....	1985
Senior Reactor Operator (SRO), San Onofre Units 2/3,.....	1983
Reactor Supervisor Qualification, Livermore Pool Type Reactor,.....	1977
Reactor Operator (RO), Georgia Tech Research Reactor,.....	1976
ERDA Fellowship, Georgia Tech,	1975
High School Science and Math teacher in the Peace Corps,	1973-1975
Academic Research	
Heat Treat Optimization at San Onofre	1993
Rhodium Self Powered Incore Detector Signal Depletion versus Accumulated Charge	1988
N-16 Steam Generator Tube Leakage Monitoring, San Onofre Units 2/3	1987
RCS Leakage Monitoring Using Radioactive Isotopic Analysis.....	1986
Long Lived Neutron Sources, San Onofre Unit 1.....	1985
Delayed Neutron Yield from Transuranic Elements (Ph.D. thesis).....	1980
Professional Affiliations	
Member, American Nuclear Society	
Palo Verde Offsite Review Board	
University of California, Berkeley, Nuclear Engineering Department Academic Review Board	
EPRI Fuel Integrity Sub-committee (1985-1986)	



Patrick Berbon, PhD

PROFESSIONAL EXPERIENCE

PERFORMANCE IMPROVEMENT INTERNATIONAL, Oceanside, California

Senior Expert 2007 – present

PII provides consulting in O&P and equipment root analysis.

- Sector expertise in Materials Science, particularly composite materials;
- Expertise in Mechanical design and structural materials;
- Background in Metallurgy, with knowledge of most engineering materials;
- Background in Failure analysis and Root cause investigations;

DUE DILIGENCE GROUP, San Francisco, California

Co-founder and Managing Partner 2003 – 2007

Due Diligence Group provides technology assessment, technology transfer, and business development services to investors, start-ups, and entrepreneurs.

- Technical expertise in Clean technologies and Renewable energy.

CALIFORNIA NANOTECHNOLOGIES, LA and San Francisco, California

Co-founder, President and Board Member 2005 – 2007

California Nanotechnologies (CNO) is engaged in the development, processing, characterization, marketing, and sale of high-performance nano-crystalline metallic and composite materials that impart superior structural properties to final components, as well as value-added components, in diverse applications including energy, transportation, aerospace and sports and recreation. CNO is publicly-traded on the Toronto Venture exchange.

- CNO was built around DDG Cryogenics (DDC), a spin out from Rockwell Scientific;
- Built the business into a recognized leader in this field with contracts from General Electric, Boeing, Ceracon, Alberta Research Council, UC Davis, Rockwell, and others;
- Co-founder, president, and lead technologist for CNO.

ROCKWELL SCIENTIFIC COMPANY, Thousand Oaks, California

Research Scientist, Materials Science 1998 - 2005

Started as the central R&D lab for Rockwell International in the 1960s, Rockwell Scientific Company (RSC) became an independent high-tech enterprise in 2002, conducting R&D services and deriving commercial revenue from a diverse product portfolio and its outlicensing arm.

- Led advanced research in processing and consolidation of aluminum and titanium based nano-composite materials;
- Extensive experience in materials characterization, including Scanning Electron Microscopy and Transmission Electron Microscopy;
- Extensive experience in testing of materials, including tensile strength, shear strength, ductility, and toughness for aerospace components, fuel cells, and high temperature applications;



- Led research on advanced superalloy material for oxidation resistance, including environmental degradation of properties;
- Customers included Boeing, General Electric, FuelCell Energy, US Air Force, NASA, and DARPA;
- Lead multidisciplinary teams spanning organizations and participated in technology roadmap initiatives of various agencies;
- Managed projects from budgetary and human resource perspectives.

EDUCATION

Ph.D. 1998

Material Science and Engineering, University of Southern California, Los Angeles, California

- Doctorate thesis emphasis on creep (high-temperature deformation of materials) and superplasticity (large elongation at high temperature);

Master of Science, 1994

Ecole Centrale de Lyon, Lyon, France and Tsinghua University, Beijing, China

- Master thesis emphasis on ceramic materials and sintering processes;

Bachelor of Science, 1993

Ecole Centrale de Lyon, Lyon, France

AFFILIATIONS AND PUBLICATIONS

Member Materials Research Society

Member American Society for Materials

San Fernando Valley Engineers Council, Chairman (2007), Vice-Chairman (2005-2006)

American Society of Materials (ASM), Orange County Chairman (2006-2007), San

Fernando Valley Chairman (2002)

USC Engineering Graduate Student Association, President (1997) and Vice President (1996)

Co-Editor, "Superplasticity: Current Status and Future Potential," Material Research Society

Co-Editor: "Materials Science & Engineering volume 410-411 (Nov 2005), Structural

Materials: Properties, Microstructure and Processing", TMS

Authored 30+ scientific publications in peer-reviewed international journals

LANGUAGES

Fluent English

Fluent French

Conversational Mandarin Chinese



Avi Mor, Dr. Eng.

Doctor Mor is an expert in the areas of concrete technology, construction methods, and construction materials with over 28 years' experience in the industry. His expertise includes construction, problem solving, testing and evaluation, quality assurance, nondestructive evaluation, and research. He is an expert consultant, lecturer and author with numerous articles and presentations to his credit. His background as a scientist, lecturer and builder provides a solid basis of technical and practical knowledge for evaluation of complex **construction failure** cases

Education

Doctor of Engineering, Concrete Technology, University of California Berkeley, 1987

M.Eng. in Construction Management, University of California Berkeley, 1984

M.Sc. in Construction Materials, Technion, Israel Institute of Technology, 1982

B.Sc. in Civil Eng., Technion, Israel Institute of Technology, 1980

Experience

Consultant, Dr. Mor & Associates, Inc., Los Angeles, CA, 1991 present

Forensic engineering and construction consulting on concrete technology.

Quality Control, Parsons/Dillingham JV, Pasadena, CA, 1992

Quality assurance of concrete construction on the Metro Red Line, LA.

Dr. Engineering, Twining Laboratories, Long Beach, CA, 1989-1991

Engineering supervision of testing and inspection activities. Performed special testing services, including nondestructive testing and load testing. Provided consulting services and expert advice to clients on construction materials and methods.

Associate Specialist, University of CA, Berkeley, 1987-1988

Responsible for test program evaluating the marine uses and **durability** of structural LWA concrete for the US Navy.

Consultant, Ben C. Gerwick, Inc., San Francisco, CA, 1984-1989

Provided consulting services on construction materials for construction companies and public agencies, with emphasis on marine and **sulfate** attack durability.

Research Assistant, University of CA, Berkeley, 1982-1987

Investigated fatigue of high strength concrete, **sulfate** and acid resistance of concrete, prestressed lightweight concrete, and freeze thaw resistance.

Supervising Engineer and General Contractor, 1980-1982

Development and construction of single family residential units.

Professional Memberships



PII - Providing a competitive advantage through research and applications

American Society for Testing and Materials (ASTM)

ASTM Technical committee C09 - Concrete

American Concrete Institute (ACI)

ACI Technical committee 201 - Durability of Concrete

ACI Technical committee 213 - Lightweight Aggregate and Concrete

ACI Technical committee 214 - Evaluation of Results of Tests Used to Determine the Strength of Concrete

ACI Technical committee 215 - Fatigue of Concrete

ACI Technical committee 228 - Nondestructive Testing of Concrete

ACI Technical committee 304 - Measuring, mixing, transporting, and placing concrete

ACI Technical committee 311 - Inspection of Concrete

International Conference of Building Officials (ICBO)

International Code Council

Registration

CE, Israel, 1982 (#00030627)

Certified Special Inspector - Reinforced Concrete (ICBO #1028361-88)

Other

Guest editor and contributing author for the international magazine Concrete Construction.

Authored numerous articles and technical presentations.

Lectured on concrete construction at the University of California, Berkeley and at the Technion.

Provide advice and information through a Web Site dedicated to concrete technology – <http://drmor.com/>



L. David Brevig

SUMMARY Mr. Brevig has over 48 years of nuclear plant experience; most in project management related to nuclear propulsion or nuclear power generation, including 10 years that were directly related to planning and conducting the decommissioning of a commercial nuclear facility, San Onofre Nuclear Generating Station Unit 1 (SONGS 1). Recently, I provided consulting services relative to decommissioning project management, decommissioning project planning, and evaluating and establishing an industrial safety culture for large nuclear decommissioning facilities for ENRESA in Spain and EdF/CIDEN in France.

RELEVANT EXPERIENCE

PERFORMANCE IMPROVEMENT INTERNATIONAL (PII)

3/2009- Present

Performance and Equipment Failure Consultant

Fall 2009 to Present – Progress Energy – Member of PII Team conducting an RCA for Crystal River 3 delamination event

Summer 2009 – TVA – Formulated a Prevention Detection and Correction strategy to address lessons learned from the Browns Ferry Nuclear Unit 1 return to service and provide their application to the completion of the Watts Bar Nuclear Unit 2.

SOUTHERN CALIFORNIA EDISON

06/99 – 2/2007

External Affairs Manager

Responsible for ensuring the decommissioning project is, and remains, unrestrained by Nuclear Regulatory Commission (NRC), California Public Utility Commission (CPUC), California State Lands Commission, California Coastal Commission, EPA, and other federal, state, and local regulations and requirements. These activities required the ability to effectively communicate project issues to various groups and individuals, who often had opposing views, for the end result of attaining satisfactory agreements to the parties. Responsible for the preparation of applications and testimony for regulatory authority approval related to decommissioning matters.

9/96 – 06/1999

Decommissioning Project Manager

Responsible for overall strategy and long-term business planning of the initial decommissioning activities for SONGS 1. Established the initial framework for the safe and efficient decommission of SONGS 1, in accordance with applicable regulations and project cost & schedule.

7/92—6/1999

Manager, Nuclear Rate Regulation

Responsible for providing a central management function for all Nuclear CPUC/CEC activities, which include preparation and development of compelling and strategically effective Nuclear Operation testimony for the General Rate Case, Energy Cost Adjustment Clause rate case, and other CPUC rate case matters.

2/89—7/1992

Supervisor, Onsite Nuclear Licensing

Responsible for establishing and managing contact with Nuclear Regulatory Commission (NRC) personnel (Resident and Regional Inspectors) with respect to inspections, investigations, and licensing activities performed at the Site. Managed the development and submittal of all nuclear related correspondence to the NRC.



- 7/88—2/1989 **Senior Engineer II**
Responsible for coordinating 28 Technical Specification revisions that recognized the refueling interval change from 18 months to 24 months for the SONGS 2 & 3 Units.
- 5/87—7/1988 **ILLINOIS POWER COMPANY**
Project Manager, Chemistry and Radiation Monitor Improvement Program--
Responsible for evaluating all installed in-line chemistry instrumentation (132) and all radiation monitors (157) for service applicability.
Project Manager, Radiation Protection Procedure Task Group—
Managing a team for the rewriting of 41 Radiation Monitor channel calibration and functional test procedures. **Supervisor**, Chemistry Radiation Protection and Radioactive Waste Management Programs--Responsible for providing recommendations for improving Chemistry, Radiation Protection programs based upon industry developments and new technologies.
Appointed Member of the Nuclear Review and Audit Group (NRAG)--NRAG serves as an independent committee responsible for performing senior management directed reviews and exercising an overview of activities affecting nuclear safety. NRAG reports directly to the Vice President-Nuclear.
- 6/86—5/1987 **Project Manager/Consultant, ASTA, Inc.**
Responsible for revising effluent technical specifications, developing the Zero Liquid Radwaste Discharge Program, revising the Chemistry QA program, and the Data Trending Program.
- 7/85—6/1986 **SOUTHERN CALIFORNIA EDISON**
Senior Engineer I
Responsible for the development and management of the Hazardous Waste Program and the Condition Monitoring Program, a supplemental program to the Environmental Qualification Program. Managed the application of the California Underground Tank Regulations for all site underground tanks.
- 7/82—7/1985 **Supervisor of Nuclear Plant Chemistry**
Responsible for the development, implementation, and management of the Site Chemistry and Effluent Monitoring Programs for the three operating nuclear plants. Managed the team effort to develop the Chemistry Quality Assurance Program. Initiated the activity and participated in the development of the Primary Chemistry Guidelines document for the commercial PWR nuclear industry.
- 1961-1982 **UNITED STATES NAVY (22 years)**
Assigned to various positions of responsibility on five nuclear submarines involving the supervision, operation, maintenance, refueling, and overhaul of a nuclear propulsion plant. Qualified for Command of a nuclear submarine and Engineer in the Navy Nuclear Propulsion Program, qualified on S5G, S4W, and three different versions of the S5W nuclear propulsion plants.

EDUCATION/QUALIFICATIONS

1969 – BSME, University of Oklahoma

1976 – MSNE, Rensselaer Polytechnic Institute

NON-PROPRIETARY VERSION



PII - Providing a competitive advantage through research and applications

1986 – MBA, National University

2006 - Southern California Edison - Qualified Rigger and Rigging Supervisor



Joseph A. Amon, PE

Vice President/Managing Principal Ardaman & Associates, Inc., Tampa, Florida

Education:

Masters of Engineering, University of Louisville, 1972

B.S. Engineering, University of Louisville, 1971

Professional Registration:

Registered Professional Engineer: Kentucky, Ohio, and Florida (# 43576)

Previously Registered: Indiana, Nevada, Tennessee, West Virginia

Florida Division of Standards, Bureau of Fair Ride Inspections, Inspector No. 0305-164

Career Summary:

After graduation Mr. Amon joined Law Engineering in 1972. He served as a Staff Geotechnical/Materials Engineer in the Tampa, Florida office. In 1972 he entered the United States Air Force where he served as a Base Civil Engineering Officer providing Structural, Geotechnical, and Materials engineering support to the Base Design Group. After a short assignment in 1975 in Las Vegas, Nevada with Strobeck and Associates as a Project Geotechnical and Construction Engineer, he practiced as a Senior Geotechnical and Materials Engineer through 1976 with Milton M. Greenbaum & Associates in Louisville, Kentucky. In late 1976, Mr. Amon returned to Law Engineering as a Senior Project Geotechnical and Materials Engineer and opened Law's Louisville office. There he served as Department Manager, Office Manager, and Chief Engineer. In 1982, he became Branch Manager of the Nashville Branch which included the Louisville, Lexington and Indianapolis offices. Mr. Amon remained in Nashville until 1989 when he became the Branch Manager of the Tampa, Florida Branch which included Daytona, Orlando, Ft. Myers, and the Naples offices. In 1994, Law Engineering designated Florida as a separate region and named Mr. Amon the Regional Manager. He was responsible for the operation and business development of ten offices within the State of Florida with aggregate annual fees in excess of \$30,000,000. A further reorganization in 1996 brought him back to the West Coast of Florida where he was responsible for Senior business and technical leadership of a 130 person Engineering and Scientific Services office. In 1998, Mr. Amon joined Ardaman & Associates, Inc. as a Vice President and Managing Principal of their Tampa office. He is responsible for the business and technical leadership of the 42 person Tampa staff and provides Senior Materials Engineer Consulting to Ardaman's 525 member staff throughout Florida.



Construction Material Testing

Mr. Amon has managed and provided senior technical review on over 2000 investigations that provided performance evaluation of engineered materials in the constructed environment. The materials included soils, rock, concrete, asphalt, steel, building stone, brick, concrete masonry unit, wood, plastics, roofing materials, sealant and construction metals. Many of these studies required using state of the art diagnostic tools in a wide variety of tasks. These tools included physical testing, electronic evaluation and microscopic techniques.

Mr. Amon has also published and lectured extensively on use and performance of construction materials. He has had experience in forensic evaluations and testifying in cases involving damage caused by construction materials and techniques of construction.

Mr. Amon has published successful techniques for non-destructive evaluation of concrete repairs that have become standard procedures. He has performed hundreds of evaluations using Ultrasonics and Surface Penetrating Radar.

Geotechnical Investigations:

Mr. Amon has performed, managed, and consulted on over two thousand geotechnical investigations related to residential and commercial developments, dams, low and high pressure pipelines, towers, power plants, industrial facilities, mines, airports, roadways, bridges and waste treatment and disposal facilities. His experience included the following foundation types: spread footings, slabs-on-ground, drilled piers, auger cast piles, driven piles, vibro replacement, and grouting. His experience includes failure investigations of subsidence, erosion, blasting, dewatering, slope instability, retaining wall failure, sheeting collapse, foundation movement and pavement distress.

Structural Analysis:

Mr. Amon has extensive experience in structural analysis, design and repair. Projects have included buildings, bridges, retaining structures, waste treatment and disposal facilities, towers, tanks and silos. For these projects he evaluated needs, analyzed conditions and future use and designed structures or modifications to structures to meet the required needs. He was able to find cost effective solutions to structural requirements while maintaining safety and low life cycle costs.

Other Relevant Experience:

Specialty Coating Systems consulting
Roof Systems consulting
Concrete Pipe Manufacturing, design and construction
Fiber reinforced concrete consulting
Mold Evaluation and Consulting
Forensic Engineering and Expert Witness consulting

Professional Publications:

Amon, Joseph A., Feasibility Study An Addition to the University Center Building University of Louisville, 1972 (Master Thesis)



- Amon, Joseph A. and Snell, Luke M. "The Use of Pulse Velocity Techniques to Monitor and Evaluate Epoxy Grout Repair to Concrete." American Concrete Institute, November, 1978 "Concrete International, Design and Construction" American Concrete Institute, December, 1979 Volume 1, No. 12
- Amon, Joseph A. "Flowable Fill - A Maintenance Solution" Tennessee Concrete, Spring, 1989 Volume 3, No. 1
- Amon, Joseph A. "Controlled Low-Strength Material - Concrete's Low-Cost Cousin" The Construction Specifier, December, 1990
- Amon, Joseph A. and McGillivray, Ross T. "Design of a Low Strength Cementations Grout for Control of Ground Subsidence over Shallow Tunnels" American Concrete Institute, 2002
- Amon, Debby and Amon, Joseph A. "An Oil Tycoon and Railroad Baron Build Florida Dreams Out of Portland Cement Concrete In 1885" American Concrete Institute, 2004

Special Technical Activities:

- Instructor, 1979 through 1981, Structures and Geotechnical Sciences, Louisville Technical Institute, Louisville, Kentucky.
- Guest Lecturer, 1979 and 1980, Concrete Testing Techniques, Southern Illinois University at Edwardsville.
- Committee Member, 1979 to Present, American Concrete Institute, Committee 437, Strength Evaluation of Existing Concrete Buildings.
- Member of 5-person Subcommittee of 437 to author "Load Tests of Concrete Structures: Methods, Magnitude, Protocols and Acceptance Criteria", published March 2007.
- Committee Member, 1987 to Present, American Concrete Institute, Committee E-702, Education, Structural Design. Chairman 2005 to Present.
- Committee Member, 1988 to 1992, 1999 to Present, American Concrete Institute 229, Controlled Low Strength Materials.
- Committee Member, 1988 to 1990, 1999 to Present, American Concrete Institute C-610, Field Technician Certification.
- Committee Member, 2003 to Present, American Concrete Institute 120, History of Concrete.
- Seminar Lecturer, February 1989, Tennessee Ready Mix Association, "Flowable Fill."
- Seminar Lecturer, 1990 to 1996, Concrete Technician Level II, Suncoast Chapter, American Concrete Institute.
- Seminar Lecturer, 1996, Florida Ready Mix Concrete Association.
- Seminar Lecturer, December, 2005, American Sports Builders Association, "Moisture in Concrete Floor Slabs."
- Citizens Advisory Committee, Transportation; Hillsborough County Metropolitan Planning Organization; Member 2001 to Present, Chairman 2003 to Present
- Florida Historical Commission, appointed by Senate President, Member June 2005 to January 2008.

Professional Associations:

- American Society of Civil Engineers, Member, 1970 to Present.
- National Society of Professional Engineers, Member, 1972 to Present.
- Florida Engineering Society, Member, 1990 to Present.
- American Concrete Institute, National Member, 1977 to Present.
- American Concrete Institute, Middle Tennessee Chapter, Founding Member, 1984 to 1989.
- American Concrete Institute of Florida, Suncoast Chapter, Member, 1989 to Present, Board of Directors, 1993 to 1996 and 1998 to 2005. Special Advisor to Board 2005 to Present.
- American Water Works Association, Member, 1996 to Present
- Associated General Contractors of America, Greater Florida Chapter, Associate Member, 1998 to Present, Board of Directors, 1999 to 2005, Advisory Board 2005 to Present.
- Society of American Military Engineers, MacDill AFB Post, 1989 to Present



PII - Providing a competitive advantage through research and applications

Chi Epsilon National Civil Engineering Honor Society, 1994 to Present

Special Recognition:

In November 2005, Mr. Amon was honored by the American Concrete Institute for being one of the founders of the Technician Certification Program.

In April 2007, Mr. Amon was elected a Fellow of The American Concrete Institute.



Henric Larsson

Experience

Consultant/Senior Expert (January 2009 – Present)

Performance Improvement International, Oceanside, CA

- Mechanical Equipment Failure, Stress, and Vibration Analysis
- Finite Element Analysis (Abaqus) and Traditional Engineering Calculations

FEA Analyst/Engineer (Summer 2002 – Present)

Hewlett-Packard, Rancho Bernardo, CA – Large Consumer Products Environment

- (MCAE) Mechanical Computer-Aided Engineering Expert & Engineering Support
- Products Analyzed: Inkjet Printers, Scanners, Printing Presses, Media Conversion, etc.
- Finite Element Analysis (FEA) using ABAQUS, ANSYS, HyperMesh & OptiStruct
- Developed custom test procedures and new constitutive material model
- Electronics cooling simulations and heat sink optimization using FlowTherm
- Rigid Body Dynamics analysis using ADAMS and RecurDyn
- Engineering calculations using: Matlab, Mathematica, & Fortran
- CAD Software: CoCreate, SolidWorks, & ProEngineer

Finite Element Analyst (September 2001 – June 2002)

Solus Micro Technologies, Inc., Westlake Village, CA – Small Start-Up Environment

- Design, analysis and packaging of precision opto-electronic fabry-perot interferometer
- Micro-ElectroMechanical Systems (MEMS) design (SolidWorks, AutoCAD, L-View)
- Curvature and stress measurements and finite element analysis of structures with dielectric films for optical mirrors and anti-reflective (HR and AR) coatings

MEMS Test Engineer (March 2001 – September 2001)

OMM, Inc., San Diego, CA – Large Pre IPO Environment

- Test and reliability of 3D MEMS mirror using DSP (Digital Signal Processor), PSD (Photo Sensitive Device) & Polytec interferometer and Visual Basic
- Design, modeling and characterization of MEMS fiber optic micro-mirror switch
- Instrumentation using MATLAB and dSPACE for real-time DSP characterization



Member of the Technical Staff (June 1997 – March 2001)

Rockwell Scientific, Thousand Oaks, CA – Large Corporate Research Environment

- FE analysis using ANSYS, ABAQUS, LS-DYNA, and Coventor
- Products and devices analyzed: Rocket engine composite material parts; MEMS sensors, switches, filters and actuators; automotive braking, suspension and tire systems; plastic parts, flip-chip packages, piezoelectric linear motors, etc.
- Human Computer Interaction
- Software engineering using MS Visual C++, MS Visual Basic and FORTRAN
- Applied Noise, Vibration and Harshness (NVH) testing, modeling and analysis

Graduate Research Assistant, Full-Time (August 1995 – June 1997)

Center for Advanced Friction Studies, SIU, Carbondale, IL

- Modeling, simulation and analysis of systems with friction-induced vibration

Education

Master of Science in Mechanical Engineering (August 1995 – June 1997)

Southern Illinois University at Carbondale (SIU)

- Grade Point Average: 4.0 (on a 4.0 scale)
- Related Classes: Kinematic Synthesis, Mechanical Engineering Controls, Mechanical System Vibrations, Nonlinear Vibrations, Finite Element Analysis

Bachelor of Science in Mechanical Engineering (August 1992 – June 1995)

University of Borås, Sweden

- Related Classes: Quality Control, Industrial Economics, Production Systems, Industrial Organizations & Logistics, Design of Experiments, Statistical Process Control, Project Control, Systems Control, FEA

Computer Proficiency

FEA: ABAQUS/Standard, ABAQUS/Explicit, ANSYS, MARC, MENTAT, LS-DYNA, FEMAP, HyperMesh, HyperView, OptiStruct, COSMOS, Harpoon, pro/ENGINEER (pro/Mechanica), Coventor

CFD: Fluent, Gambit, CFX, ANSYS, FlowTherm

MBD: ADAMS, RecurDyn

CAD: CoCreate (A.K.A. SolidDesigner, OneSpaceDesigner), AutoCAD, SolidWorks, Pro/ENGINEER, ANSI 14.5 skills

Programming: MS Visual C++, MS Visual Basic, FORTRAN, Python



Modeling: Matlab, Simulink, dSPACE, Mathematica, Mathcad

Statistical: JMP, VisVSA

Publications and Patents

- Larsson, H., and Doan, L - Hewlett-Packard Co. –“Paper Feeding Performance of an All-in-One Printer,” 2006 West Regional ABAQUS Users’ Meeting
- Herbert, C., Annis, J., Yao, J., Morris, W., Larsson, H., Harris, R., Kretshmann, R., –“MicroElectroMechanical System with Improved Beam Suspension,” Patent. No. 10950886 filed on 2004-09-27 by Rockwell Automation Technologies, Inc.
- Larsson, H. and Pan, J., –“Noise, Vibration and Harshness of Wet Disc Brake Systems – A New Modeling Approach,” 1999 SAE Brake Colloquium
- Larsson, H. and Farhang, K., –“Vibration and Analysis of Multi-Disk Friction Systems,” 1998 ASME Design Engineering Technical Conferences (DETC)
- Larsson, H. and Farhang, K., –“Investigation of Stick-Slip Phenomenon Using a Two-Disk Friction System Vibration Model,” 1997 ASME DETC



Marci Cooper

Summary

Over 25 years power industry experience in broad range of progressive technical, managerial, leadership and executive positions. Solid technical, regulatory, business, and production experience base in both nuclear and fossil generation. Broad utility P&L service organization business management and leadership experience. Strong strategic, organizational, leadership and communication experience and skills. High level of intellect, initiative, discipline, flexibility and drive.

Experience

Present: Performance Improvement International Oceanside, CA

Director

- Identify performance problems and effective corrective actions, mentor and coach implementation
- Provide driving force for culture transformation in large organizations
- Implement new organizational core values by providing training, feedback and reinforcement
- Develop and provide training for improving critical supervisor skills such as problem solving, field surveillance, communication, planning/scheduling, coordination, worker briefing. Provide effective tools to reinforce the use of these skills
- Conduct assessments and root cause investigations determining organizational problems and provide improvement solutions
- Participate in the analysis of various processes, both human and industrial, to improve performance, emphasizing safety, utilization, environment, output, and quality.

2004 - 2008 Tennessee Valley Authority (TVA) Chattanooga, TN

Sr. Vice President, Fossil Engineering & Technical Services, Fossil Power Group

- Management and direction of FPG engineering and design to support over 14,000 MW of generating capacity and \$500M in annual capital project expenditures
- Management and direction for TVA-wide central laboratories and TVA-wide integrated maintenance and repair facilities and associated field operations - self supporting profit centers involving \$75-100M in annual revenues
- Leadership in reducing cost and improving quality of critical support services involving projects, outages, O&M, and major programs
- Strategic development and deployment of programmatic initiatives to improve availability and reduce delivered cost of power
- Leadership development assignment related to power supply and generation planning, portfolio risk management, competitive analysis, optimizing system dispatch and future generation mix.

2002-2004 Tennessee Valley Authority Stevenson, AL

Site General Manager, Widows Creek Fossil Plant

- Management of 8-unit, 1600 MW station; \$50M annual O&M budget.
- Installation and initial operation of SCR's on two large units

NON-PROPRIETARY VERSION



PII - Providing a competitive advantage through research and applications

- Instrumental in driving significant budgetary and performance improvements, transforming culture and strategy, and laying foundation for sustaining long term performance

2000-2002 Tennessee Valley Authority

Chattanooga, TN

General Manager, Methods & Process

- Facilitation and coordination of fossil system process standardization
- Sponsorship of Human Performance initiative and Maintenance Optimization project systemwide

1999-2000 Tennessee Valley Authority

Chattanooga, TN

General Manager, Fossil Operations - Western Plants

- Management and direction of over 8000 MW of fossil generation
- Drove major initiatives for operational improvements

1998-1999 Tennessee Valley Authority

Chattanooga, TN

General Manager, Maintenance & Testing Services

- Management of over \$100M cost recovery businesses including Power Service Shops, Heavy Equipment Division and Central Laboratories

1997-1998 Tennessee Valley Authority

Chattanooga, TN

Manager Component Engineering, TVA Nuclear

- Management of corporate major component expertise, plant support and programmatic direction for multiple nuclear sites. Included Maintenance Rule and turbine generator, pump, motor, breaker, and valve programs.

1996-1997 Tennessee Valley Authority

Chattanooga, TN

Manager of Operations Projects, TVA Nuclear

- Responsible for project management and direction for multi-discipline projects affecting multiple nuclear sites.

1994-1996 Tennessee Valley Authority

Soddy Daisy, TN

Technical Support Manager, Sequoyah Nuclear Plant

- Management and direction of plant systems, program and reactor engineers in conduct of associated testing, refueling, engineering evaluation and operations/maintenance support activities.

1993-1994 Tennessee Valley Authority

Soddy Daisy, TN

Maintenance Manager, Sequoyah Nuclear Plant

- Management and direction of permanent and contract resources for conduct of plant maintenance activities, programs, and outage recovery.

1993 Tennessee Valley Authority

Soddy Daisy, TN

Restart Manager, Sequoyah Nuclear Plant

- Development, direction and management of restart plan, including regulatory approval and extensive unit recovery efforts resulting from erosion/corrosion outage.

1986-1993 Tennessee Valley Authority

Soddy Daisy, TN

Site Licensing Manager, Sequoyah Nuclear Plant



PII - Providing a competitive advantage through research and applications

- Management and direction of site licensing organization, and all regulatory interface functions. Extensive experience in NRC regulatory interface and assurance of regulatory compliance programs. Period includes supporting manager positions leading to this position in 1990.

1982-1986 Tennessee Valley Authority

Soddy Daisy, TN

Various Engineer Positions, Sequoyah Nuclear Plant

- Licensing, testing and mechanical engineering positions. On shift, Operations Shift Technical Advisor (STA).

1981-1982 Tennessee Valley Authority

Chattanooga, TN

Mechanical Engineer, Division of Energy Demonstration & Technology

- Advanced utility gas turbine research and power cost of electricity studies.

1978-1981 Pratt & Whitney Aircraft

West Palm Beach, FL

Analytical Design Engineer, Government Products Division

- Advanced engine combustion design.

Education or Certifications

1978 BS, Mechanical Engineering, University of Tennessee, Knoxville, TN

1984 Shift Technical Advisor (STA) certification, Sequoyah Nuclear Plant, Soddy Daisy, TN

1999 MBA, Finance - University of Tennessee, Chattanooga, TN



Luke Snell, P.E. FACI

EDUCATION:

- B.S.C.E., 1969; M.S.C.E. 1970, University of Oklahoma:
- Advanced Graduate Studies in Construction Materials, WVU, 1972 – 1974
- Registered Professional Engineer – Arizona, Illinois and Missouri

PROFESSIONAL EXPERIENCE:

- 2009 – Present, Consultant , Performance Improvement International
- 2008- Present, Eminent Scholar, Del E. Webb School of Construction, Arizona State University (ASU)
- 2006 – 2008, Director of the Concrete Industry Management, Del E. Webb School of Construction, Arizona State University (ASU)
- 2000 – 2006, Professor of Construction and Director of Concrete Construction Resource Unit (SIUE)
- 1979 – 2000, Professor and Chair of Construction, Southern Illinois University Edwardsville (SIUE)

PUBLICATIONS AND PRESENTATIONS: (5)

- “How ACI Certification Program Got its Start,” Concrete International, October 2005
- “Using Infrared Thermometers in Concrete Construction,” Concrete Plant International, February 2007
- “History of the Hoover Dam,” presented at the World of Concrete, Las Vegas, Nevada, 2006- 2009
- “Acceptance of Concrete Test Results”, Concrete Knowledge Center, ACI Website, 2007
- “A Model for Establishing ACI Chapters in Developing Countries” , Concrete International, April, 2010

Other Publications (5)

- “Prevention of Plastic Shrinkage Cracks in Fresh Concrete”, Proceedings, International Conference on Advances in Cement Based Materials and Applications in Civil Infrastructures, Lahore, 2007
- “Radioactivity in Fly Ash”, Proceeding, 5th Annual Mongolian Concrete Conference, Ulaanbaatar, 2006
- “Certification Programs for Quality and Durable Concrete Association of Consulting Engineers, Bangalore, 2008
- “ Mixing Certification with Higher Education”, Concrete International, November, 2008



- Low Strength Concrete Problems, National Ready Mixed Concrete, New York City and St. Louis , April and May ,2010

Synergistic Activities

Extensive consulting work on construction and concrete projects

Written over 225 articles on concrete, construction and construction education

Invited lecturer to over 500 groups on concrete and construction-related topics

Activities with American Concrete Institute (ACI)

- Chair – International Committee
- Member – Construction Liaison Committee
- Past Chair – Chapter Activities Committee
- Past Chair – Education Activities Committee
- Past Chair – E702 Design Concrete Structures
- Past Chair – 517 Accelerated Curing of Concrete
- Past Member – Board of Direction
- Past Member – Financial Activities Committee

AWARDS RECEIVED:

- Fellow – ACI, 1994, and American Society of Civil Engineers, 1994
- Joe W. Kelly Award (for innovative teaching of concrete) – ACI, 1995
- Educators Make A Difference Award, Kappa Delta Pi (an International Honors Society in Education), 1997
- Professional Engineer in Education, Missouri Society of Professional Engineers, 1997
- Chapter Activities Award, ACI, 1997
- Great Teacher of the Year Award, SIUE's Alumni Association, 1997
- "Concrete Person of the Year", Missouri Chapter of ACI, 1999
- Education Committee Member of the Year, ACI, 2002
- Honorary Professor, Mongolian University of Science and Technology, 2005



R. Tyson Gustus

SKILLS & EXPERTISE

- Finite Element Analysis, including nonlinear analysis, thermal, structural, statics and dynamics
- Solving design problems in mechanical, thermal, electrical, and multi-physics domains
- Extensive experience with solar concentrators, electronic packaging, aerospace structures, composites and concrete
- Extensive experience with implantable medical devices, shape memory & hyper-elastic metals, and exotic materials
- Superior problem solving skills, logical and analytical ability
- Writing patents and proposals
- Project management
- Complex numerical modeling and systems analysis using spreadsheets, statistics, complex logic, and analysis tools
- Comprehensive knowledge of FEA best practices and a meticulous understanding of common mistakes
- Fluent in Solidworks, Abaqus/CAE, Abaqus/Standard, Abaqus/Explicit, Microsoft Project and Excel

EXPERIENCE

PERFORMANCE IMPROVEMENT INTERNATIONAL

Oceanside, California

FULL-TIME FEA CONSULTANT

March 2010 – Present

Analysis of the Progress Energy Crystal River 3 Nuclear Generating Station Containment Structure

- Creation of a state-of-the-art FEA tool suite for performing analysis on pre-stressed concrete using Abaqus

21st CENTURY ENGINEERING

San Diego, California

PRINCIPAL/OWNER/SOLE PROPRIETOR

May 2005 – Present

Design and analysis services to the medical device, electronic packaging, and green technology industries

- Creating tangible value by exposing specific details of the underlying physics and design trade-offs within a product, facilitated by modeling and analysis tools, applied judiciously and accurately, across platforms and industries.
- Meticulously exploring the details to improve the analysis and design of structures and devices ranging from turbine engine components and satellite structures to electronic packaging, solar concentrators, and medical devices.
- Helping clients better understand physical test data, uncovering bad assumptions and faulty data with good modeling.
- Authoring analysis reports for submission to federal panels, facilitating dozens of regulatory approvals.

ENERGY INNOVATIONS

Pasadena, California

FULL-TIME FEA CONSULTANT

Dec 2008 – June 2009

Provided design and analysis services to this concentrating photovoltaic (CPV) start-up

- Created from scratch this company's first accurate, fully 3D analysis model, incorporating CFD data and multiple load scenarios, in order to identify necessary design improvements and potential cost savings.



- Design improvements were identified and analyzed, resulting in highly superior long term reliability.
- Potential cost savings identified, amounting to over \$600,000 in savings for every 10 MW installation.

**MINNOW MEDICAL
PRINCIPAL ENGINEER**

San Diego, California
July 2006 – Sept 2008

Head of Finite Element Analysis (FEA) effort

Led development and implementation of analysis program leading to vast improvement in clinical outcomes

- Contributed essential innovation that enabled the feasibility of core technology and launch of human clinical trials.
- Developed and presented a fully 3D analysis model of the heat transfer and Joule heating of human arterial tissue; calibrated the model to bench top experimental data with extremely high accuracy, resulting in a highly detailed understanding of the treatment delivery, leading to reduction in patient pain and improvement in clinical outcomes.

Project Management

Selected to lead project management efforts within engineering department

- Developed long term project schedules, FMEA and FTA risk analyses for regulatory submission package 510k.
- Championed short term project schedules as the most effective way to manage day-to-day operations within a department of 7 engineers in this highly challenging start-up environment.
- Mentored engineering staff on time management and prioritization techniques.

Legal/Patent Committee and Inventor

Provided technical expertise and patent writing innovation to legal team

- Wrote the main claims in multiple patents central to the defense of core technology.
- Employed novel techniques to define the scope of inventions, leading to better protection [Back to List](#) technology.
 - Reviewed and edited all final drafts of patent claims, receiving accolades from the CEO and patent counsel.



David R. Dearth, P.E.

Background:

David Dearth is an engineering consultant specializing in areas of traditional design, metallurgy, failure analysis, mechanical analysis, environmental testing and other disciplines as required achieving technical excellence. He directs, manages and assists in developing new products; expand emerging technologies and improving current designs.

Experience:

Thirty-four (34) years mechanical engineering experience performing detailed analysis, durability and damage tolerance, fatigue, material allowable and dynamics using metallic and advanced composite structures in design and analysis. Thirty-two (32) year's experience using mainframe and PC based computer-aided design (CAD) and finite element analysis (FEA) programs.

Fifteen (15) years experience as a part time professor at California State University at Long Beach, instructing both graduate and undergraduate courses in mechanical engineering courses in structural analysis, vibrations and dynamics.

Experience

1990-Present: Consultant, Performance Improvement International, LLC (1990-Present)

Mr. Dearth has participated in more than 34 equipment failure investigations, including welding failures, radial stacker collapse, pump shaft failures, cooling tower structure failures, and fatigue cracking of piping and heat exchangers.

Applied Analysis & Technology, Inc., Huntington Beach, CA.

- Engineering consulting company involved in CAD design and FEM analyses projects covering a vast array of industries. Client lists include leading companies in aerospace, computer peripherals, medical devices, dental implantology, nuclear & fossil fuel power plants... etc. In addition to high tech industries, client lists include general manufacturing, injection molded & die cast component design, custom software and test equipment development... etc. Beta tester for MSC/Nastran software
- Hoover Dam Visitors Center redesign of rotating amphitheatre support system.
- 767 Tanker Air Refueling system design & analysis.
- Boeing 787 redesign of the center fuselage/wing structural interface.
- Northrup/Grumman X-47B NLG & MLG durability and damage tolerance.

1985-1987: Contract consultant engineer, McDonnell Douglas Corporation, Long Beach, CA.

- Monitored T-45A structural element fatigue program for material allowable and Fatigue & Damage Tolerance analysis. Created computer program for automated fatigue analysis of T-45 landing gear.



- Structural analysis of C-17 Wing Group Bulkheads. Refined FEA model of C-17 upper wing surface using MDAC CGSA program.
- Conversion of McDonnell Douglas FEA models of MD-11 & MD-12 aircraft from CGSA/CASD format into Patran and Nastran.

1981-1984: Manager, Cartridge Engineering, Archive Corporation, Costa Mesa, CA.

- Head to tape mechanical interface analysis & design. Structural analysis, Heat Transfer & Thermal Structural response.
- Environmental testing, shock, vibration and thermal.
- Component specifications and test plans.
- Customer interface, CRO, MRB and DCB responsibility.

1980-1981: Senior Staff Engineer, Printronix, Irvine, CA.

- Dynamic analysis of dot matrix printer systems.
- Finite element analysis in heat transfer and structural problems using ANSYS and STARDYNE.
- Conventional stress analysis, material fatigue and component design. Cam profiles idealization using custom FORTRAN program.

1979-1980: Senior Research and Development Engineer, BASE Video Corp., Fountain Valley, CA.

- Analysis of tape transport system dynamics, shock & vibration isolation, environmental testing, video tape cartridge mechanics, acoustic analysis and responsible engineer for tape cassettes.

1976-1986, 1998-Present: Part-time faculty member in the Mechanical Engineering Department of California State University, Long Beach.

- Instructing under-graduate and graduate level engineering classes in static's, strength of materials, mechanics of deformable bodies, dynamics, vibrations and computer programming analysis using FORTRAN and CSSL-4. Courses taught are the following:
 - ◆ ME 273: Solid Mechanics - Static's & Strength of Materials
 - ◆ ME 305: Numerical Methods in Mechanical Engineering - Applied Numerical Methods for Digital Computation.
 - ◆ ME 373: Mechanics of Deformable Bodies - Engineering Mechanics of Materials.
 - ◆ ME 403: Introduction to Computer Simulation of Mechanical Systems.
 - ◆ ME 576: Engineering Vibrations - Elements of Vibration Analysis. [Graduate Course]

1976-1979: Engineer, Ford Aerospace and Communications Corporation, Aeronutronic Division, Newport Beach, CA [DOD Secret Security Clearance]

- Mechanical analysis, design and environmental testing of primary missile airframe components.
- Computer programming in propulsion, thermodynamics, airframe inertias, vibration & dynamic response analysis and finite element analysis of airframe components using STARDYNE.



1973-1976: Engineer/Scientist, McDonnell Douglas Corporation, Long Beach, CA.

- Detailed layout, design, some analysis and liaison' work on the YC-15 Advanced Short Take-off and Landing Transport prototype, a.k.a. C-17 Transport.
- Primary Adhesive Bonded Structures (P.A.B.S.T.) research and development program at McDonnell Douglas X-Shop.
 - a.) Detailed design and finite element idealization of bonded structural concepts using MDAC in house FEA program software CGSA & CASD.
 - b.) Preparation and presentation of design concepts to Air Force and inter-company personnel.

Education

Masters of Science in Engineering Mechanics (MSE);
California State University, Long Beach, CA - 1979.

Bachelor of Science in Aeronautical and Astronautical Engineering (BSAAE);
The Ohio State University, Columbus, Ohio - 1973.

1974-1979: MSE: *Masters of Science in Engineering* - Primary interest: Finite element analysis, Vibrations and Elasticity; Thesis subject: "The Method of Ritz Applied to Hamilton's Law of Varying Action".

1973-1979: Completion of company sponsored courses in materials, dynamics, advanced FORTRAN programming techniques, Direct Access Computing (DAC); MCAUTO McDonnell Douglas.

1967-1973: BSAAE: *Bachelor of Science in Aeronautical and Astronautical Engineering* - Primary interest, Structural analysis by Hamilton's Principal, Aeroelasticity, dynamics, computer programming analysis using 2 and 3 dimensional computer graphics. Earned entire college living expenses and tuition by managing fast food restaurants and working in a bakery.

Inventions & Product Development

- Developed custom test equipment for test evaluation and receiving inspection of 3M series DC300 – DC600 tape cartridges used for mass data storage. Automated test evaluations runs in real-time environment with multi-test capability controlled by a computerized interface.
- Developed automated test stations for measuring performance characteristics and for receiving inspection of Brushless DC motors by back EMF method in real-time.

Professional Affiliations

- Professional Engineer: California Department of Consumers Affairs, License Registration No. 20894.
- Member: American Society of Mechanical Engineers, ASME No. 0022419907.



- Member: American Institute of Aeronautics and Astronautics, AIAA No.
- Member: United Professors of California. [1976 to 1987]
- Member: American National Standards Institute, ANSI Committee XB55. [1980-1985]
- Charter Member: American Engineers Association. [1973-1987]

Miscellaneous Affiliations

Race Committee Chairman for *Kalifornia Outrigger Association* [1984-1988]. Duties included organization, officiating, directing as well as participating in regional, state, national and international competition of open ocean outrigger canoe racing. Regions of interest were State of California, Hawaii and Tahiti. Other responsibilities included working with various Olympic committees in efforts to make outrigger canoe racing an Olympic event.

Publications

- 1.) "*Vibrational Characteristics of Elastic Beam Systems with Multiple Discontinuities: Direct Approach*"; Masters Thesis, California State University at Long Beach, August 1979.
- 2.) "*Finding Deflections of Complex Beams*", Machine Design magazine, October 1979.
- 3.) "*Specifying Random Vibration Severity*", Machine Design magazine, July 1985.
- 4.) "*Magnetic Permeability Study - Finite Element Analogous Field Study*", Algor FEA Technical Publication, February 1989.
- 5.) "*What-if Analysis Moves to the Desktop*", Design News magazine, Cover Story, January 1995.
- 6.) "*Eagle Optimization Program - Impeller Fan Casting*", Algor Design World Spotlight, April 1995.
- 7.) "*Aerospace Engineering Made Easy*", Computer Graphics magazine, Aerospace section, April 1996.
- 8.) "*FEA Determines Duct Assembly Strength*", Design News magazine, July 1996.
- 9.) "*Finite Element Modeling Tools Aid Aerospace*", Aerospace America magazine, Systems & Software column, May 1995.
- 10.) "*FEA Today - Trends in Finite Element Analysis*", Design News magazine, December 1996.
- 11.) "*Shape Optimizer Trims Excess Weight From Aircraft Parts*", Machine Design magazine, News Off the Wire column, 10 March 1998.
- 12.) "*Manual Meshing Could Solve Some Modeling Problems*", Machine Design magazine, Finite Element Update column, 6 August 1998.
- 13.) "*A Few Guidelines for Meshing Circular Regions*", Machine Design magazine, Finite Element Update column, 14 January 1999.
- 14.) "*Stress Concentrations Pose Sticky Meshing Problems*", Machine Design magazine, Finite Element Update column, 8 July 1999.
- 15.) "*Recognizing Correct Solutions to Resonant Vibration Problems*", Machine Design magazine, Finite Element Update column, 10 February 2000.
- 16.) "*Understanding Your Thermal Code*", Machine Design magazine, Finite Element Update column, 3 August 2000.
- 17.) "*When To Go Nonlinear With FEA*", Machine Design magazine, Finite Element Update



- column, 7 June 2001.
- 18.) **–Analysis for the Design Crowd**”, Computer-Aided Engineering magazine, Product Review Feature Article, September 2001.
 - 19.) **–FEA gets designers started with analysis**”, Machine Design magazine, User Review column, 11 October 2001.
 - 20.) **–Predicting Dynamic Response**”, Machine Design magazine, Finite Element Update column, 8 November 2001.
 - 21.) **–Determining Harmonic Response**”, Machine Design magazine, Finite Element Update column, 13 December 2001.
 - 22.) **–Code Breakers – The Bug Hunters**”, Design News magazine, Cover story on software beta testers, 7 April 2003.
 - 23.) **–Why Did It Fail – FEA Helps Find Out**”, Machine Design magazine, Redesign of rotating turntable for Visitor’s Center at Hoover Dam, 19 June 2003.
 - 24.) **–FEA Lets Designers Take First Cut Analyses**”, Product review of CosmosWorks 2003 finite element software package, Machine Design magazine, 9 July 2003.
 - 25.) **–Heat Transfer 101**”, Machine Design magazine, Finite Element Update column, 7 August 2003.
 - 26.) **–Simulating Bolts in Finite Element Assemblies**”, Machine Design magazine, Finite Element Update column, 9 December 2004.
 - 27.) **–Find The Load, Then Size The Bolts**”, Machine Design magazine, Finite Element Update column, 3 February 2005.
 - 28.) **–Sizing Bolts for Flexible Brackets**”, Machine Design magazine, Finite Element Update column, 3 March 2005.
 - 29.) **–Heat Transfer 201: Cooling Without Fans**”, Machine Design magazine, Finite Element Update column, 7 July 2005.
 - 30.) **–Steady-State Heat Transfer Problem: Cooling Fin**”, HDBK of Heat-Transfer Calculations – Chapter 5, McGraw-Hill Books, November 2005.
 - 31.) **–Transient Heat Transfer Problem: Tape Pack Cooling**”, HDBK of Heat-Transfer Calculations – Chapter 12, McGraw-Hill Books, November 2005.
 - 32.) **–Sneaking Up On a Solutions**”, Machine Design magazine, Finite Element Update column, 14 December 2005.
 - 33.) **–FEA Program Unites Design with Analysis**”, Machine Design magazine, Software Review column CosmosWorks 2006, 23 February 2006.
 - 34.) **–FEA Inside CAD Simplifies Complex Analysis**”, Machine Design magazine, Software Review column CosmosWorks 2007, 22 November 2006.
 - 35.) **–Residual-Compressive Stresses Can Pump Fatigue Strength**”, Machine Design magazine, Finite Element Update column, 7 June 2007.
 - 36.) **“Handbook of Finite Element Methods”**; 275 pages, in progress.
 - 37.) **“How to Succeed In College”**; 150 pages, in progress.
- ”Statics - A Work Book for Review and Study”**, in progress.



GARY A. HUGHES, PhD

Summary of Qualifications

Gary Hughes is a distinguished professional electrical and nuclear engineer who has established an outstanding record in his field. His interest in nuclear safety has led him to become an expert in the fields of human performance and root cause investigation, with the responsibility of providing independent verification that activities are performed correctly and human error reduced as much as possible.

He has established the reputation of being an ethical and thorough investigator who is able to look at both detail and the big picture. He is knowledgeable and experienced in examining plant operating characteristics, NRC issuances, industry advisories, reportable events and other sources of plant design and operating experience information. He is able to communicate the information collected in understandable form. He has traveled across the United States, requested by NRC, WANO and INPO to lend his effective interview techniques and problem-solving skills. He is a sought after speaker and trainer within the industry, and his teaching and mentoring skills have taken him to Great Britain, Rome, Bratislava and Brazil. A natural facilitator, Gary has been elected by his peers to numerous leadership positions within industry groups.

Proven Areas of Expertise

- Effective investigation and interview techniques
- In depth issue and trend analysis
- Human performance issues
- Operating experience
- Operational productivity
- Problem solving and conflict resolution
- Leadership and team-building skills
- Global safety perspective
- Organizational development
- Reactor trip reduction and equipment reliability

Professional Work Experience

Present	Performance Improvement International
Senior Expert - Consultant	
2001 – 2007	Ameren-Union Electric, Callaway Plant
	Supervising Engineer QA



1995 – 2001 Responsible for Independent Technical Reviews
Ameren-Union Electric, Callaway Plant
Supervising Engineer, ISEG

1981 – 1995 Union Electric, Callaway Plant
Supervising Engineer, Nuclear Safety

1979 – 1981 University of Missouri-Columbia
Ph.D. Candidate, Nuclear Engineering
Research Assistant position at MURR and Teaching
Assistant position while completing Ph.D.

1979 - 1994 U.S. Naval Reserve (Retired as Commander)

1968 – 1979 U.S. Navy (Active service)
Nuclear engineer, submarine service
Active Duty Commissioned Officer 1974 - 1979
Active Duty Enlisted 1968-1974

Education

University of Missouri – Columbia 1979 - 1981
Ph.D. Nuclear Engineering
Research in loss of coolant accident.

University of Missouri – Columbia 1971 - 1974
M.S. Nuclear Engineering
Developed the thermo-hydraulic/kinetics work submitted to NRC for the MURR 10MW
upgrade.

B.S. Electrical Engineering

Additional Professional Education

- Probabilistic Risk Assessment / IPE
- Human Reliability Assessment (HRA)
- Management Oversight and Risk Tree investigation (MORT)
- Human Performance Evaluation System (HPES)
- TAP Root Cause
- PWR Senior Reactor Operator Systems Theory
- Shift Technical Advisor PWR
- Quality Assurance Lead Auditor
- PWR Mitigating Core Damage
- Crisis Communication Skills
- Quality Improvement Process (Team Leadership and Facilitator Courses)
- Problem Solving and Decision Making



- Management Techniques
- Organizational Development
- Writing and Business Management
- Management Planning

Regulatory and Assessment Experience

- University of Missouri Research Reactor 10 MW upgrade (1973-74)
- NUREG – 0737 TMI Response and Callaway Implementation of ISEG, OE and STA (1981)
- SAMG Implementation (1991 – 1999)
 - EPRI Severe Accident Chairman during TBR issuance
 - WOG Committee on SAMG
 - Callaway Implementation
- QA member during Tech Spec Improvement process
- University of Missouri Research Reactor Employee Concerns (1995)
- RUG IV member / Day to Day NRC support (1996-97)
- IPE development support and HRA support
- Contributor to recent INPO document on Equipment Reliability Single Power Failure Reduction
- Contributor to EPRI NP – 6748 1990 Control Room Operator Alertness and Performance in Nuclear Power Plants
- Nuclear industry reviewer to NUREG / CR 6046 Alertness performance and off duty sleep on 8 hour and 12-hour night shift
- Previous responsibility for INPO and NRC information notice OE reviews and Event Reduction
- NSRB Support and sub-committee
 - Secretary 1984 –2001
 - Subcommittee 1984 – present
- QA ORC member 2000 – present
- Developed and taught a Root Cause / Corrective Action course for IAEA in Bratislava, Slovakia
- 16 plant assessments at plants in U.S., Canada and England. Several were meeting NRC committed actions
- STA previously qualified and performed first verification and validation on Westinghouse Emergency Procedures in 1982
- Supervised STAs and ensured INPO accredited training program
 - 1981 – 1992 Supervised all STAs
 - 1992 – 2000 Supervised day STAs



Recognitions

Two EPRI Innovator awards

Three major INPO Nuclear Professional articles on Operating Experience
2000 University of Missouri Alumni / Faculty Award

Professional Affiliations

University of Missouri Nuclear Engineering Adjunct Professor



Mostafa S. Mostafa, PhD

Experience

1985-1990 - Expert Witness at LM Laboratories (laboratory manager 1984-1986) with several OSHA litigation cases (one case involving fatalities at Unocal, one case involving Mohave pipe rupture related fatalities)

1990 – Current, PII Chief Metallurgist and Senior Expert

At PII, Dr. Mostafa has worked on more than 100 root cause cases throughout the nuclear and fossil power industries. His root cause investigation experience includes the following major cases:

- Fort Calhoun flow assisted corrosion pipe rupture case
- Millstone flow assisted corrosion pipe rupture case
- Pressurizer tube, Inconel-600 cracking
- San Onofre water hammer event
- Portugal weld cracking case
- Zion tube fracture failures
- San Onofre erosion-corrosion case
- South Texas Project nozzle cracking case
- Palo Verde battery and steam generator tube rupture failure case

1990 – Current, Consulting Engineer at Southern California Edison

As a consulting engineer at SCE, Dr Mostafa has helped San Onofre Nuclear Generating Station to solve its technical issues.

Education

1974 - B.S., Metallurgy at Cairo University, Egypt,

1974-1978 - Teaching and Research at Cairo University, Egypt

1978 - Engineering Masters Degree in Metallurgy at Cairo University, Egypt

1985 - PhD, Material Science, University of California at Irvine



Jan Červenka, Dipl.-Ing., PhD

Personal data:

Birth date: May, 22, 1966, Birth place: Praha, Czech Republic

Education:

1994, Ph.D., University of Colorado, Boulder, USA
1990, Dep. Civil Eng., Czech Tech. Univ., Prague;

Professional positions:

2008-today, principal, Cervenka Consulting Ltd, Czech Republic, Prague
1996-2008, technical director, Cervenka Consulting, Czech Republic, Prague
1995-1996, assistant professor, Dep. of Structural Mechanics, Fac. of Civil Eng., CTU
1995, research associate, CEAE Dep. University of Colorado Boulder, U.S.A.
1990-1994, research assistant, CEAE Dep. University of Colorado, Boulder, USA;

Professional profile:

I have a strong practical as well as research oriented experience in numerical analysis of reinforced concrete structures, non-linear finite element method, fracture mechanics and plasticity. My professional goal is to improve these methods and bring them closer to practicing engineers and to extend the applicability of these modern methods in engineering practice.

Recent Consulting Projects

- Containment non-linear analysis, Okiluoto 3 NPP, AREVA, Finland,
- Tunnel Dobrovskeho in Brno, optimization of tunnel RC lining, Metrostav, Praha
- Tunnel Brezno, failure analysis, SUDOP, Praha
- Berounka Bridge, Novak & Partner, Praha, analysis of construction process of segmental prestressed concrete bridge.
- Liner anchor optimization, Ishikawajima Harima Heavy Industries, Nuclear power div., Japan,
- Pre-stressed concrete vessels under seismic loads, Oriental Construction, Japan,
- Development of pre-stressing anchors, M.Borer, Switzerland,

Recent Research projects

- EU 6th Framework project "Sustainable Railway Bridges",
- EU 6th Framework project "Smart and Safe Buildings".
- EU GROWTH project GRD1-2001-40739 "UPTUN - Upgrading of existing tunnels", 2002-2005 (joint applicant)
- GA CR 103/07/1660 "Damage analysis of concrete structures due to high temperature"
- GA ČR 103/99/0755, "Numerical model of concrete under local confining pressure", 1999-2001
- EU project IST-1999-11508, "ISTforCE - Intelligent Service Tools for Concurrent Engineering", 2000-2002 (joint applicant)
- GA ČR 103/00/1563, "Long-term effects in nonlinear computational models of reinforced concrete structures", 2000-2002



Selected Publications: overall 54 publications in journal or conf. proceedings

- CERVENKA, J., PAPANIKOLAOU, V.K., Three Dimensional Combined Fracture-Plastic Material Model for Concrete, International Journal of Plasticity, Vol 24(12), pp. 2192-2220, 2008
- CERVENKA, J., CERVENKA, V., PUKL, R., JANDA, Z.: Assessment of remaining structural capacity by computer simulation. Int. fib Symposium 2008, May 19-22, De Meerwart Congress Centre, Amsterdam; Tailor Made Concrete Structures – Walraven & Stoelhorst (eds) © 2008 Taylor & Francis Group, London, ISBN 978-0-415-47535-8; pp.665-671.
- CERVENKA, J., CERVENKA, V., JANDA, Z., PUKL, R.: Safety assessment of railway bridges by non-linear and probabilistic methods. Bridge Maintenance, Safety, Management, Health Monitoring and Informatics – Koh & Frangopol (eds) © 2008 Taylor & Francis Group, London, ISBN 978-0-415-46844-2. pp.3708-3715.
- JENDELE L., CERVENKA J., On the Solution of Multi-Point Constraints - Application to FE Analysis of Reinforced Concrete Structures, Computers and Structures, doi:10.1016/j.compstruc.2008.04.018, 2008
- CERVENKA, J., SUROVEC, J., KABELE, P., ZIMMERMAN, T., STRAUSS, A., BERGMEISTER, K., 2007, Numerical simulation of fracture and damage in RC structures due to fire., Fracture Mechanics of Concrete and Concrete Structures, ISBN 978-0-415-44616-7, pp. 727-736, 2007
- CERVENKA, V., ČERVENKA, J., JANDA, Z, Posouzení bezpečnosti železobetonových konstrukcí v nelineárních výpočtech, Beton Technologie Konstrukce Sanace, (1) 2007, 68-72
- JENDELE, L., CERVENKA, J., Modelling Bar Reinforcement with Finite Bond, Computers and Structures, 84, 1780-1791, 2006
- CERVENKA, J., BAZANT, Z.P., AND WIERER, M., Equivalent localization element for crack band approach to mesh-sensitivity in microplane model, Int. J. Numer. Meth. Engng 2005, Vol. 62, pp. 700-726, 2005
- CANER, F. C., BAŽANT, Z. P., ČERVENKA, J.: Vertex Effect in Strain-softening Concrete at Rotating Principal Axes. Journal of Engineering Mechanics, Vol. 128, No.1, 24-33, Januar 2002
- ČERVENKA, J., ČERVENKA, V., and ELIGEHAUSEN, R. (1998) "Fracture-plastic material model for concrete. Application to analysis of powder actuated anchors", Proceedings of the 3rd International Conference on Fracture Mechanics of Concrete Structures - FraMCoS 3, Gifu, Japan, eds. H. Mihashi and K. Rokugo, Aedificatio Publishers, Freiburg, Germany, Vol. 2, pp. 1107-1116.
- ČERVENKA, J., KISHEN, J. M. C., SAOUMA, V. E.: Mixed Mode Fracture of Cementitious Bimaterial Interfaces; Part II. Numerical. Engineering Fracture Mechanics, Vol. 60, No.1, 95-107, May 1998
- KISHEN, J. M. C., ČERVENKA, J., SAOUMA, V. E., Mixed Mode Fracture of Cementitious Bimaterial Interfaces; Part I: Experimental Results, Part I: Experimental Results", Engineering Fracture Mechanics, Vol.60, No.1, pp.83-94
- CERVENKA, J., SAOUMA, V.E., Numerical evaluation of 3-D SIF for arbitrary finite element meshes, Engineering Fracture Mechanics, Vol. 57, Number 5, July 1997, pp. 541-563 (23), 1997



ATTACHMENT 6: CONFIRMED AND REFUTED FAILURE MODE ASSESSMENTS

(Y) indicates a confirmed failure mode; (R) indicates a refuted failure mode

NOTE: The entire FM file including exhibits can be found in the Appendix files of this report.

1. CONTAINMENT DESIGN AND ANALYSIS

- 1.1 Excessive vertical and hoop stress (Y)
- 1.2 Excessive radial tensile stresses/no radial reinforcement (Y)
- 1.3 Excessive tensioning of horizontal tendons (R)
- 1.4 Excessive tensioning of vertical tendons (R)
- 1.5 Foundation settling (R)
- 1.6 Inadequate design against ground movement (R)
- 1.7 Containment long term, low-level vibrations (R)
- 1.8 Added stress from tendons not in the same plane (R)
- 1.9 Added stress from variations in tendon spacing (R)
- 1.10 Added stress from voids around tendon sleeves (R)
- 1.11 Effect of micro cracks (R)
- 1.12 Added stress from inadequate size of tendon sleeves (R)
- 1.13 Inadequate net loading area due to presence of horizontal sleeves (R)
- 1.14 Added stress from equipment hatch located underneath in same bay (R)
- 1.15 Inadequate design analysis methods of radial tensile stresses (Y)

2. CONCRETE CONSTRUCTION

- 2.1 Inadequate concrete curing (R)
- 2.2 Inadequate concrete pouring (R)
- 2.3 Inadequate slump (Includes FM 3.6) (R)
- 2.4 Inadequate control of early age cracking (R)
- 2.5 Inadequate temperature control (R)
- 2.6 Inadequate mix design (R)
- 2.7 Inadequate vibration during pour (R)
- 2.8 Inadequate support of tendons during pouring (R)
- 2.9 Void or cracks due to inadequate forms (leaky, insecure, early stripping) (R)
- 2.10 Concrete deformation from tensioning too early (R)
- 2.11 Inadequate construction cold joint (R)
- 2.12 Strength Properties (Y)

3. USE OF CONCRETE MATERIALS

- 3.1 Inadequate air content (R)
- 3.2 Inadequate grouting materials (R)
- 3.3 Inadequate cement materials (R)
- 3.4 Inadequate aggregates/weak aggregate (Y)
- 3.5 Inadequate admixtures (R)
- 3.6 Inadequate slump (Included in FM 2.3) (R)
- 3.7 Inadequate break test used to verify compliance (R)



4. CONCRETE SHRINKAGE, CREEP, AND SETTLEMENT

- 4.1 Excessive plastic shrinkage (R)
- 4.2 Excessive shrinkage (Includes FM 4.3 and 4.4) (R)
- 4.3 Excessive autogenous shrinkage (R)
- 4.4 Excessive carbonation shrinkage (R)
- 4.5 Excessive basic creep (R)
- 4.6 Excessive drying creep (R)
- 4.7 Stresses due to Differential Material Properties (R)
- 4.8 Non-vibration induced fatigue cracking (R)



5. CHEMICALLY OR ENVIRONMENTALLY INDUCED DISTRESS

- 5.1 Foreign material intrusion/contaminants during construction (R)
- 5.2 Salt water intrusion (R)
- 5.3 Chemicals introduced during routine maintenance (R)
- 5.4 Concrete form release (R)
- 5.5 Corrosion of rebars, sleeves, and tendons (R)
- 5.6 Inadequacy of grease lubrication capability (R)
- 5.7 Physical attack (R)
- 5.8 Chemical attack (R)

6. CONCRETE-TENDON-LINER INTERACTIONS (DURING OPERATION)

- 6.1 Uneven tension distribution along the tendon due to excessive local duct friction (R)
- 6.2 Inadequate tendon wires (R)
- 6.3 Added stress from thermal effects of greasing (R)
- 6.4 Added stress from differences between rigid and flexible sleeves (R)
- 6.5 Inadequate tendon re-tensioning in surveillance activities (R)
- 6.6 Inadequate initial tensioning of tendons(R)

7. CONTAINMENT CUTTING

- 7.1 Accumulated Low Level Damage (R)
- 7.2 Shock or concrete separation due to resonant vibrations during hydro-blasting (R)
- 7.3 Inadequate pattern of de-tensioning of tendons (Y)
- 7.4 Inadequate de-tensioning scope(Y)
- 7.5 Added stress due to removing tendons and concrete at opening (Y)
- 7.6 Vibrations due to cutting tendons under tension (R)
- 7.7 Cracking due to pre- existing defects in this area (R)
- 7.8 Excessive water jet pressure (R)
- 7.9 Inadequate hydro-blasting rate (R)
- 7.10 Formation of fine micro-cracks from hydro-lasing (R)
- 7.11 Added stress from pulling tendons out of sleeves and grease after cutting (R)

8. OPERATIONAL EVENTS

- 8.1 Prior spray event leading to low pressure inside containment (R)
- 8.2 Thermal stresses due to containment spray (R)
- 8.3 Effect of faster pressurization/depressurization rates during last ILRT (R)
- 8.4 Inadequate concrete structure monitoring/maintenance (IWL) (R)
- 8.5 Containment depressurization due to inadequate purging operation (R)



9. EXTERNAL EVENTS

- 9.1 Hurricanes or Tornados (R)
- 9.2 Seismic events (R)
- 9.3 Ground movements (sink holes or geo-sliding) (R)



1.1 Excessive Vertical and Hoop stresses / Compressive-Tensile Interaction

Description:

Post-tensioned concrete structures use tension cables or tendons to introduce large compressive stresses in the concrete material. In the case of a nuclear plant, the reactor and the steam generators are contained in a large strong containment structure designed to contain possible radioactive material release under various postulated design loading combinations. The two typical approaches are to use reinforced-concrete or to use post-tensioned concrete (FM 1.1 Exhibit 6 is a list of US Pressurized Water Reactors (PWR) and their containment type). A description of pre-stressed concrete nuclear containment structures can be seen in FM 1.1 Exhibit 1. A list of nuclear reactor containments that use the post-tensioned approach can be seen in FM 1.1 Exhibit 2.

This FM focuses on the as-designed overall level of pre-stress for the CR-3 containment and whether it could have led to or contributed to the observed delamination. Note that issues specifically associated with the high radial tensile stresses are analyzed in FM 1.2 and the issues specifically associated with stress concentration factors are analyzed in FM 1.15. Note that PII modelling results are available with the PII root cause analysis report and are not attached as exhibits. The potential for Compressive-Tensile stress interaction will also be assessed.

Data to be collected and Analyzed:

1. Detailed 3D Finite Element Analysis (FEA) of the entire CR3 post-tensioned concrete containment structure subjected to internal compressive loading;
2. Verify and evaluate loads and stresses generated by hoop tendons (FM 1.1 Exhibit 3 is a calculation of the forces and stresses generated by the hoop tendons);
3. Comparison CR3 pre-stress numbers with pre-stress numbers from other nuclear reactor containments (FM 1.1 Exhibit 4 is a Bechtel Topical Report on the topic of "Pre-stressed Concrete Nuclear Reactor Containment Structures" and FM 1.1 Exhibit 5 is a PII calculation containing available pre-stress levels for CR3 and TMI
4. Observation of the fracture surface at the intersection with a tendon sleeve (FM 1.1 Exhibit 9 is the result of phenolphthalein testing of the fracture surface to determine crack age).
5. Comparison of CR3 and Ocone for compressive-tensile interaction. (FM 1.1 Exhibit 10)

Verified Supporting Evidence:

1. Phenolphthalein experiments confirm the presence of pre-existing cracks around tendon sleeves (FM 1.1 Exhibit 9). This is based upon finding areas of low pH on concrete samples.
2. Plotting of Compressive-Tensile interaction indicates a slightly higher interaction for CR3 as compared to peers such as Ocone. (FM 1.1 Exhibit 10)

Verified Refuting Evidence:

1. The hoop pre-stress level is around 2,000 psi (using a simplified analysis, assuming maximum tendon force ignoring stress in the liner plate and Poisson's effects) (FM 1.1 Exhibit 3). The concrete used at CR3 has a specified 28 days compressive strength of 5,000 psi and a tested 32 years (today) compressive strength of 7,500 psi with a standard deviation of 820 psi. The pre-stress level is therefore only around 40% of the specified f_c and 27% of the measured f_c . This remains too low to damage the material in compression;
2. CR3 successfully operated for 30 years without shell delamination that might result from excessive as-designed tensile stress (see FM 1.2 for further discussion on this topic);
3. Post event condition assessment did not identify delamination outside bay 34.



1.1 Excessive Vertical and Hoop stresses / Compressive-Tensile Interaction

Discussion:

The design of containments has evolved with successive generations of nuclear plants in the US. For example, the CR3 containment design was largely completed by end of 1969. The first containment design criteria in the U.S. was published in 1972 as ACI 349-72, "Criteria for Reinforced Concrete Nuclear Power Containment Structures" Reported by ACI Committee 349. The BC-TOP-5-A (FM 1.1 Exhibit 4) was published in February 1975, and the containments listed in Table 2.1 include ones designed much prior to this, as was CR3. Containment design evolved over time as design criteria such as ACI 349-72 became available.

Of particular importance, ACI 349-72 (Section 2.5.6.2) has provisions for establishing the level of prestress. In ACI 349-72, the recommendation in Section 2.5.6.2 was to provide sufficient prestress to eliminate membrane tension away from discontinuities for two load combinations. The first was for the LOCA condition (unfactored) involving $1.0 P_a + 1.0 T_a$. The second load combination was for the condition of $1.2 P_a$ without T_a , which is nearly the SIT load condition. Since the DBA LOCA condition includes a 1.5 load factor on P_a , containments designed for this latter criterion had significantly less prestress and far more reinforcement than CR3, TMI 1, Oconee 1, 2, 3 and others.

We can note that the original Gilbert Associates calculations specified a hoop pre-stress level of 829 kips/ft (FM 1.1 Exhibit 7). This is in rough agreement with our calculated end-of-life value of 815 kips/ft (FM 1.1 Exhibit 3).

Note that the tendon force per unit length in FM 1.1 Exhibit 4 and FM 1.1 Exhibit 5 are for minimum design tendon force.

Forces and stresses generated by the vertical tendons are only half those generated by the hoop tendons (FM 1.1 Exhibit 8).

Although hoop stress is higher at CR3 than for other plants, this does not translate into higher probability for delamination. The analytical technique illustrated by the Compression-Tension Interaction Diagram in FM 1.1 Exhibit 10 does show a greater potential for delamination at CR3.

Conclusion:

High level of as-designed hoop pre-stress did not alone cause delamination. However, the higher level of pre-stress likely reduced the margin to delamination by augmenting inherent weakness in the potential delamination hoop tendon sleeve plane.



1.2 Excessive Radial Stresses / No Radial Reinforcements (Contributing factor)

Description:

Post-tensioned systems using curved tendons are known to exert radial compression on the inner region of the containment structure and radial tension on the outer region (FM 1.2 Exhibit 1 is a 2003 paper in Nuclear Engineering and Design). The common theoretical approach to calculating forces and stresses is a shell analysis giving an average tensile stress value (FM 1.2 Exhibit 2 is a typical industry shell calculation performed by MPR Associates).

It is noted that it is not common to use radial restraints, such as radial reinforcing steel and/or radial stirrups. Both the Gilbert Associates plants and the Bechtel plants often use no radial reinforcement in the cylinder section of the containment wall. Only a few plants have radial reinforcements in the containment cylinder, namely Farley, Vogtle, Summer, South Texas, Calvert Cliffs, Wolf Creek, and San Onofre (FM 1.2 Exhibit 3 is a list of post-tensioned containment of the type used at CR3).

It is very common to have radial reinforcements in containment domes because:

1. Tendons are located closer to the inner radius;
2. There are often three sets of intersecting tendons;
3. The dome is thinner than the cylinder.

During plant operation, the radial tensile stresses present in this area of the containment wall originate from:

1. Compressive force due to the hoop tendons induces radial tension in the outer region of the containment structure, as described in FM 1.2 Exhibit 1;
2. Stress concentration factors lead to localized tensile stresses (see FM 1.15 for a detailed analysis of the stress concentration factors);
3. Thermally-induced tensile stresses due to temperature differentials and solar effect on the concrete wall (see FM 4.8 for an in-depth analysis of daily, seasonal, and outage temperature effects).

CR3 added radial reinforcement as a corrective measure after the dome delamination in 1976.

Note that this FM is only considering the radial stresses present in the tensioned structure during normal operation. All additional stresses induced by the SGR opening are considered in the family of FM 7.

Note that issues specifically associated with the high pre-stress level are analyzed in FM 1.1 and the issues specifically associated with stress concentration factors are analyzed in FM 1.15. Note that PII modelling results are available with the modes.

Data to be collected and Analyzed:

1. Extent of condition of delamination around the containment (FM 1.2 Exhibit 4 is a CTL report on Impulse Response testing of the entire CR3 containment and FM 1.2 Exhibit 5 is a Progress Energy calculation showing a sketch of the delamination that documented the delamination condition and extent; Finite Element Modelling (FEM) of a local area around hoop tendons showing the stress levels in the concrete around the tendon sleeves due to tensioned vertical and hoop tendons (FM 1.2 Exhibit 6);
2. Observation of the use of radial reinforcements in containment cylinders at other post-tensioned concrete nuclear plants (FM 1.2 Exhibit 3);
3. Original Gilbert design calculations for CR3 (FM 1.2 Exhibit 7).

Verified Supporting Evidence:

1. Observations show that there is a large-scale delamination mostly in the plane containing the hoop tendons which is the point of maximum as-designed tensile radial stress i.e., at the interface between the inner cylinder subject to post-tensioned radial compressive stress and the outer shell cylinder operating under radial tension (FM 1.2 Exhibit 5 pages 16 of 20 and 18 of 20);



1.2 Excessive Radial Stresses / No Radial Reinforcements (Contributing factor)

2. Design pre-stress levels for the CR-3 containment are among the highest of the population of similar plants, thereby resulting in higher radial stresses (see FM 1.1 for more analysis).

Verified Refuting Evidence:

1. Non-destructive testing using Impulse Response technique shows that the containment is not delaminated in the five panels that were not subjected to the SGR opening (FM 1.2 Exhibit 4). This implies that the radial tensile stresses present in the plane of the hoop tendons during normal operating conditions were not sufficient to generate the delamination;
2. It is common to have no radial reinforcements in the cylinder section of a post-tensioned concrete nuclear containment (FM 1.2 Exhibit 3). A number of similar plants with fairly high design pre-stress, such as TMI-1, Oconee, and Turkey Point, do not have radial reinforcements and have not experienced a delamination type failure like CR3, either before or after creating an opening in their containment.

Discussion:

Note that vertical compression from the vertical tendons leads to an increase in radial and hoop tendon tension by Poisson's effect. As a simple approximation, the vertical compressive stress is approximately 1,000 psi and the Poisson's ratio is approximately 0.2 so that the tensile stresses generated could be of the order of 200 psi. Comparison of radial tensile stresses near vertical tendons and away from vertical tendons show the vertical tendons do contribute to radial tensile stress (FM 1.2 Exhibit 6).

Conclusion:

As designed radial tensile stresses without radial reinforcements were not, alone, sufficient to cause delamination. However, the high level of design pre-stress without radial reinforcements reduced the margin to delamination. Therefore, radial tensile stresses did contribute to delamination of the containment in the plane of the hoop tendons.



1.3 Excessive Tensioning Hoop Tendons

Description:

The design calls for tensioning the Hoop tendons to 1,635 kips with a design minimum of 1252 kips. When considering the number of hoop tendons and the height of the containment building, we can calculate the number of hoop tendons per unit height and the hoop tendon force per unit height. The design minimum number 770 kips/ft can be compared to typical industry standard for this type of containment.

Additionally, occasional excessive tensioning, as allowed by normal operation, can damage the concrete by generating localized micro-cracks and/or enhanced creep.

Data to be collected and Analyzed:

1. Calculate loads and stresses generated by hoop tendons (FM 1.3 Exhibit 1 is a PII calculation of the stresses generated in the concrete by the post-tensioning tendons);
2. Compare with equivalent numbers from other nuclear reactor containments (FM 1.3 Exhibit 2 is a 1975 Bechtel study on post-tensioned nuclear containments with similar design as CR3 and FM 1.3 Exhibit 5 is a PII calculation performed for CR3 data.);
3. NCR incidents in the past that may have involved over-tensioning of horizontal tendons;
4. Procedure review for writing NCR for overstressing tendons;
5. Interview with experienced and knowledgeable engineers (FM 1.3 Exhibit 3 is an interview with the CR3 Lead Engineer for IWE/IWL inspections);
6. Review WO 681043-01 and PSC procedures to confirm that the maximum tension is 80% of Guaranteed Ultimate Tensile Strength (GUTS) (FM 1.3 Exhibit 4).

Verified Supporting Evidence:

1. The hoop pre-stress at CR3 is generally higher than the pre-stress level at most equivalent nuclear power plant containment buildings (FM 1.3 Exhibit 2, in particular table 2.1 page 20 of 21). Compare 770 kips/ft Design Minimum at CR3 from FM 1.3 Exhibit 1 (section C) with a maximum of 730 kips/ft design minimum from FM 1.3 Exhibit 2 table 2.1 (page 32 of 64) at Bechtel-built plants and 798 for one other plant (FM 1.3 Exhibit 5).

Verified Refuting Evidence:

1. The higher pre-stress level results in a hoop pre-stress around 2,000 psi from a simplified analysis (ignoring stress in the liner plate and Poisson's effects) (FM 1.3 Exhibit 1). The concrete used at CR3 has a specified 28 days compressive strength of 5,000 psi and a tested 32 years (today) compressive strength of 7,500 psi with a standard deviation of 820 psi. The pre-stress level is therefore only around 40% of the specified f_c and 27% of the measured f_c . This remains too low to damage the material in compression;
2. Tendon tensioning records and interview results show no evidence of over-tensioning (FM 1.3 Exhibit 3). Additionally, no NCRs were reported;
3. Additionally, the worst case scenario of having tendon force at 80% of GUTS increases the existing radial stress by only 14%.

Discussion:

We can note that the original Gilbert Associates calculations specified a hoop pre-stress level of 829 kips/ft (FM 1.3 Exhibit 8). This is in strong agreement with our calculated end-of-life value of 831 kips/ft (FM 1.3 Exhibit 1 section B.1.2).



1.3 Excessive Tensioning Hoop Tendons

The higher pre-stress level leads to higher creep for a given concrete material and a given specific creep given in terms of $\mu\text{in/in per psi}$ (FM 1.3 Exhibit 6 is the Schupack and Associates creep study performed initially for Oyster Creek unit 2, then used by TMI, and then used at CR3). In particular in the study done by Schupack and Associates, "Report on recommended concrete creep and shrinkage values for computing prestressing losses", the conclusion is given in terms of a specific creep of $0.4 \mu\text{in/in per psi}$ (FM 1.3 Exhibit 6, page 6 of 33).

The NCRs for over-stressing tendons are contained in the PSC procedure on tendon surveillances (FM 1.3 Exhibit 7). The procedure calls for writing an NCR if the tendon lift-off force exceeds 80% GUTS. It does not call for writing an NCR if the measured lift-off force is higher than the "predicted" tendon force from tendon force loss predictions (see FM 6.5 and FM 6.6 for details).

Conclusion:

No excessive tensioning of horizontal tendons has been identified. It is concluded that excessive tensioning of the horizontal tendons did not contribute to the 2009 delamination of the containment concrete.



1.4 Excessive Tensioning of Vertical Tendons

Description:

The design calls for tensioning the Vertical tendons to 1,635 kips with an upper limit at 1,878 kips during tensioning (80% of Guaranteed Ultimate Tensile Strength (GUTS)) and 1,721 kips afterwards (FM 1.4 Exhibit 3 is the CR3 tendon surveillance program). When considering the number of vertical tendons and the diameter of the containment building, we can calculate the number of vertical tendons per unit circumference and the vertical tendon force per unit circumference (FM 1.4 Exhibit 1 is a PII calculation of the pre-stress generated when tensioning the vertical tendons).

Additionally, occasional excessive tensioning, as allowed by normal operation, can damage the concrete by generating localized micro-cracks and/or enhanced creep.

Note: All design values above were obtained from DBD 1.1 and CR3 Calc. S80-0020.

Data to be collected and Analyzed:

1. Calculate loads and stresses generated by vertical tendons (FM 1.4 Exhibit 1);
2. NCR incidents in the past that may have involved over-tensioning of vertical tendons;
3. Procedure review for when to write an NCR for overstressing tendons (FM 1.4 Exhibit 3 and FM 1.4 Exhibit 5 is the 1997 pre-surveillance package from Precision Surveillance Corporation (PSC) for the CR3 tendons);
4. Interview with experienced and knowledgeable tendon engineers (FM 1.4 Exhibit 2 is an interview with Richard Portmann, the CR3 Responsible Engineer for IWL/IWE surveillance);
5. PSC procedures which state that the maximum tension is 80% of the yield (FM 1.4 Exhibit 5).

Verified Supporting Evidence:

None

Verified Refuting Evidence:

1. The pre-stress generated by vertical tendons is low compared to the compressive strength of the material (FM 1.4 Exhibit 1). It is also low compared to the hoop pre-stress generated by the hoop tendons (1,106 psi versus 2,000 psi). The concrete used at CR3 has a specified 28 days compressive strength of 5,000 psi and a tested 32 years (today) compressive strength of 7,500 psi with a standard deviation of 820 psi. The vertical pre-stress level is therefore only around 22% of the specified f_c and 15% of the measured f_c . This remains too low to damage the concrete material in compression;
2. Personnel interview documents that no evidence of over-tensioning was recorded. Search by Progress found no NCRs written on the subject (FM 1.4 Exhibit 2);
3. Additionally, the worst case scenario of having tendon force at 80% of GUTS increases the existing vertical pre-stress by less than 14%. This is not sufficient to initiate damage in the material.

Discussion:

We can note that the original Gilbert Associates calculations specified a vertical pre-stress level of 457 kips/ft (FM 1.4 Exhibit 4). This is in strong agreement with our calculated end-of-life value of 451 kips/ft (FM 1.4 Exhibit 1).

The requirements for writing NCRs for over-stressing tendons are contained in the PSC procedure on tendon surveillances (FM 1.4 Exhibit 3). The procedure calls for writing an NCR if the tendon lift-off force exceeds 80% GUTS. It does not call for writing an NCR if the measured lift-off force is higher than the "predicted" tendon force from tendon force loss predictions (see FM 6.5 and FM 6.6 for details).

The surveillance procedure is performed the same way for horizontal and vertical tendons, except that lift-



1.4 Excessive Tensioning of Vertical Tendons

off measurements are only performed at the lower end (tendon gallery) for the vertical tendons since the upper end (at the ring girder) is not accessible. Since the vertical tendons are straight, unlike the curved hoop tendons, the tendon force angular friction is not a factor and the force is much more homogeneous along a vertical tendon. The exceptions would be the vertical tendons going around the equipment and personnel hatches (see FM 1.14).

Conclusion:

It is concluded that excessive tensioning of the Vertical tendons did not contribute to the 2009 delamination of the containment concrete.



1.5 Foundation

Description:

Foundation settling can cause added, asymmetrical stress in certain area in the containment.

Data to be collected and Analyzed:

1. Review previous condition reports involving foundation cracks. No condition reports written since no foundation cracks were observed.
2. Review memo to file from Glenn Pugh, 22 October, 2009. (FM 1.5 Exhibit 1)
3. Buttress and Dome survey data. (FM 1.5 Exhibit 2)
4. Review FSAR Section for containment foundation. (FM 1.5 Exhibit 3, FSAR Chapter 2, Section 2.5.7)

Verified Supporting Evidence:

None

Verified Refuting Evidence:

1. None of the personnel contacted by Mr. Pugh was able to remember an incident where equipment required adjustment because of settlement issues. (FM 1.5 Exhibit 1)
2. Buttress surveys do not have historical baseline data for comparison, but looking at the tilt or plumbness may indicate foundation settling. On buttresses that could be measured on both sides, a large difference in measured tilt from one buttress to another is judged to be a result of construction tolerance rather than foundation settlement. Buttress #2 was measured as having a lateral offset of 2.37 inches on one side and 0.522 inch on the other. Foundation settlement would result in tilt at both locations. Buttress #4 was measured with very small tilt of 0.45 inch. No foundation settlement indicated. (FM 1.5 Exhibit 2)
3. The Dome Survey is based on benchmarks on the structure. The Dome survey points are used to monitor relative movement of the Dome. If large differential movements were recorded they could be indicative of structural movement or possible settlement of the foundation. Dome survey data compares elevation change data from 1982 and 2009. The measured change from 1982 to 2009 ranged from a +0.060 to - 0.240 inch. This movement is considered to be insignificant and not indicative of differential foundation settlement. (FM 1.5 Exhibit 2)
4. There is no record of containment cracking at or around the foundation consistent with the FSAR conclusions relative to the potential for foundation settlement. (FM 1.5 Exhibit 3)

Conclusion:

There is no indication of containment settlement sufficient to cause added, asymmetrical stress in the containment.

1.6 Inadequate design against ground movement (R)



1.6 Inadequate Design against Ground Movement

Description:

Ground movement, improper geo-strength selection, elastic deformation of the foundation base rock, dissolution of the ground limestone, etc. can distort the containment structure resulting in localized, added stress in certain areas of containment. The stress could result in crack initiation.

Data to be collected and Analyzed:

1. Gilbert Geo-technical Study, Sections 1.2.11.5, 1.2.11.6, 1.2.11.7 (1971) (FM 1.6 Exhibit 1)
2. FSAR Chapter 2 Sections 2.5.8. (FM 1.6 Exhibit 2)

Verified Supporting Evidence:

None

Verified Refuting Evidence:

1. The 1971 Gilbert Study found Inglis and Avon rock limestone units below the area on which the containment was to be built. The Inglis was highly solutioned, the Avon rock less so. Where sound rock was encountered, the rock had a bearing capacity much greater than required to support the containment design. (FM 1.6 Exhibit 1, Section 1.2.11.5)
2. Settlement calculations predicted that settlement of 7/8 in occurring concurrently with loading during construction. To assure the continuity and integrity of the limestone, cement grouting under the containment was recommended. An additional study concluded cement alone was insufficient and chemical grouting was added. The Gilbert Study also confirms a successful grouting program under the containment was conducted. (FM 1.6 Exhibit 1, Sections 1.2.11.6 and 1.2.11.7)

The FSAR and sited reports confirm the containment, including the grouting program, are compliant with the Geo-technical Study. (FM 1.6 Exhibit 2 Section 2.5.8)

Conclusion:

Reviewed data confirms that the containment design is adequate against ground movement.

1.7 Containment long term, low-level vibrations (R)



1.7 Containment Long Term Low Level Vibrations

Description:

During operation, the containment is subjected to long-term low-level vibrations due to the large rotating equipment located within or in the vicinity of it, and due to the wind. Rotating equipment generates “humming” vibrations that are typically low level but are present constantly over the years. In addition, the outside wind blowing on the containment also generates low level continuous vibrations. This failure mode investigates the long-term low-level vibrations induced by large rotating equipment and vortex shedding from the cross winds and whether they could have imparted a meaningful contribution or driver to long term fatigue induced micro-cracking leading to the observed delamination.

Data to be collected and Analyzed:

1. Natural frequencies of the containment (FM 1.7 Exhibit 1 is a PII Abaqus calculation of the resonant frequencies of the CR3 containment building);
2. Details of the largest rotating machinery, the Reactor Cooling Pump (RCP) (FM 1.7 Exhibit 2 is the section of the Design Basis Document related to the RCP);
3. Wind velocity as described in the Design Basis Document (FM 1.7 Exhibit 3 is an excerpts of the DBD11 document including the typically Design Basis wind velocities) for vortex shedding calculation.

Verified Supporting Evidence:

None

Verified Refuting Evidence:

1. The RCP pump operates at 1,185 rpm = 19.7 Hz (FM 1.7 Exhibit 2). This is a higher frequency than the first 11 modes frequencies of the containment building (FM 1.7 Exhibit 1);
2. The turbine operates at 1,800 rpm = 30 Hz, far away from the building frequencies (FM 1.7 Exhibit 1);
3. The vortex frequency is calculated in FM 1.7 Exhibit 4, using the data from the DBD (FM 1.7 Exhibit 3). The frequency is 0.2 Hz. This is far away from the first fundamental at 4.3 Hz (FM 1.7 Exhibit 1). Additionally, the wind speed of 110 mph is a Design Basis worst case wind velocity load, not a long term life of the plant "average" wind loading so the actual frequency would actually be even lower for most days and this is a very conservative bounding calculation.

Conclusion:

Long term low level vibrations were not significant and therefore did not provide any meaningful contribution to the delamination.

1.8 Added stress from tendons not in the same plane (R)



1.8 Tendon Sleeves Not in Same Plane

Description:

Design calculations assume that the hoop and vertical tendons are located in the same radial plane. In practice, due to limitations in construction, that may not be the case. This potential misalignment leads to changed stress conditions from those assumed in the design that could result in damage to the concrete and/or contribute to delamination initiation.

Another factor to consider is the possibility that the sleeves moved during concrete setting due to hoop forces applied on them from the buttresses. The delaminated panel, number 34, together with panel 16, was poured after the adjacent panels had already hardened. The installed sleeves ability to expand freely, either in the radial direction outward from the center of containment or within the plane of the sleeves, upon concrete pouring, particularly as the temperature rises due to cement hydration, depends on the method used to attach the sleeve sections together and the sleeve ends inside the buttresses. Fixed ends can lead to bending of the sleeves and high stresses in the concrete.

The radial position of the hoop sleeves with respect to the theoretical plane of the hoop sleeves is analyzed in this FM.

Data to be collected and Analyzed:

1. Gather evidence of out-of-plane tendons (FM 1.8 Exhibit 1 shows a photograph of hoop tendon sleeves);
2. Stress analysis of local stress with out-of-plane sleeve arrangements (FM 1.8 Exhibit 2 is a diagram of out-of-plane tendons effect on the supporting area and FM 1.8 Exhibit 5 is a more quantitative analysis of the subject);
3. Calculate elongation of sleeve due to temperature and outward movement generated when both ends are fixed (FM 1.8 Exhibit 3 is a hand calculation of potential sleeve movements);
4. Sleeve installation documents and drawings (FM 1.8 Exhibit 4 is a discussion and drawings on the topic of sleeve connections).

Verified Supporting Evidence:

1. Photographs show that some hoop tendons are out-of-plane (FM 1.8 Exhibit 1).

Verified Refuting Evidence:

1. With out-of-plane hoop tendon sleeves, the radial stress that tends to pull the outer layer apart is in fact decreasing with a larger radial loading area and this reduces the driving force to delaminate (FM 1.8 Exhibit 2 and FM 1.8 Exhibit 5);
2. Deviation in planar positioning by one inch to the inside increases the peak tensile stress by a factor of 1.1 only. This is not a major contributor to the overall failure scenario due to the small magnitude and isolated occurrence (FM 1.8 Exhibit 5);
3. Deviation in planar positioning to the outside reduces peak tensile stresses (FM 1.8 Exhibit 5);
4. Construction documents show that the ends of the sleeves in the cylindrical walls at the buttresses were not welded and most likely not constrained from movement in the direction of the plane of the sleeves. Therefore, the potential exists for movement in the sleeve plane if they expanded in that plane during concrete pouring and subsequent temperature rises. (FM 1.8 Exhibit 4).

Discussion:

The appearance of the sleeve/concrete interface on FM 1.8 Exhibit 1 can be explained in at least two ways:



1.8 Tendon Sleeves Not in Same Plane

1. Misalignment during installation of the sleeves before pouring of the concrete. Note that this was pointed out in the case of the vertical tendon sleeves in FM 2.8;
2. Movement of the sleeves during concrete pouring due to thermal expansion of a thick steel sleeve having both ends fixed which would create very high stresses in the concrete early in the age of the containment.

Observation of construction documents shows no evidence that the tendon sleeves in the cylindrical sections of containment were fixed in the plane of the sleeves to keep them perfectly rigid during the concrete curing process. They most likely moved and slid slightly, just enough to accommodate the thermal expansion of the sleeve.

Consideration of the changing peak tensile stresses as the hoop tendon sleeves radial position changes within the containment wall show that the increase is limited to 10% when the sleeve comes 1" closer to the inside while all other factors decrease peak tensile stress (FM 1.8 Exhibit 5). The effect of having a tendon 2" inset is to increase peak stress by 20%.

Conclusion:

Tendon sleeves not in the same plane did not lead to the delamination.

1.9 Added stress from variations in tendon spacing (R)



1.9 Tendon Spacing / Tendons Bending around Penetrations

Description:

The design spacing for horizontal tendon (hoops) alternated between 13 inches and 26 inches. The tendons running between two same buttresses are uniformly spaced 39 inches. In order to accommodate the end of the next tendon, in the panel where they cross, the tendons from buttresses n to $n+2$ are not centered around tendons from buttresses $n+1$ to $n+3$ (FM 1.9 Exhibit 1 is the basic tendon arrangement from the Gilbert Calculations book 2 of 5).

Inadequate tendon spacing can potentially result in undesirable, uneven stress distribution or concentrations that could contribute to crack initiation or delamination propagation.

Additionally, at penetrations, there are significant variations in tendon spacing where the tendons curve around the penetrations. This is observed for example around the equipment hatch for the vertical tendons (FM 1.9 Exhibit 2 is a drawing of the vertical tendons bending around the equipment hatch) and for the hoop tendons (FM 1.9 Exhibit 3 is a drawing of the hoop tendons bending around the equipment hatch and of the hoop tendons running two at the same elevation).

Note that the tendons installed at wrong positions and/or moving during concrete pouring are addressed in FM 2.8 and local stress concentration around the hoop sleeves is addressed in FM 1.15.

Data to be collected and Analyzed:

1. As designed distances between hoop tendons (FM 1.9 Exhibit 1) and between vertical tendons (FM 1.9 Exhibit 2);
2. Effect of vertical and hoop tendons bending around penetrations (FM 1.9 Exhibit 3);
3. The original Gilbert calculations for stresses at various liner and containment penetrations (FM 1.9 Exhibit 4 is a partial sample of the calculations performed);
4. List and containment design for other nuclear plants that have performed Steam Generator Openings (SGR) (FM 1.9 Exhibit 5 is a list of post-tensioned nuclear containments similar to CR3).

Verified Supporting Evidence:

1. Design drawings show significant tendon bending around penetrations, leading to very complex stress states in those areas (FM 1.9 Exhibit 2 and FM 1.9 Exhibit 3).

Verified Refuting Evidence:

1. Stress distribution in the hoop direction, where the stresses are highest and compressive, is not strongly influenced by tendon spacing because the force on the tendons is distributed into the concrete through the thicker buttresses;
2. Stress distribution in the vertical direction, where stresses are high and compressive, is not strongly influenced by tendon spacing because the force on the tendons is distributed into the concrete through the thicker ring girder;
3. The tendon arrangement is very similar to all containments having six buttresses and the spacing is similar as well. Several of these plants have had a successful Steam Generator Replacement opening performed in the concrete containment (FM 1.9 Exhibit 5);
4. Extensive analysis was performed to ensure the stresses around penetrations are not excessive (FM 1.9 Exhibit 4).

Discussion:



1.9 Tendon Spacing / Tendons Bending around Penetrations

As can be seen in FM 1.9 Exhibit 4, the tendon spacing at penetrations, both vertical and hoop, was analyzed very carefully. The bending radii of each tendons were calculated, the spacing between adjacent bent tendons were optimized, the distance between the penetration and the first tendon was optimized, the added radial forces due to tendon bending were calculated, and the tendon friction losses were calculated.

In particular, the radial forces are very significant as the post-tensioning will tend to crush the opening. Each penetration must therefore be built strong enough to handle these additional forces.

In the case of the hoop tendons going around the equipment hatch two in the same plane, there is now twice the radial hoop force applied in this area. The additional compressive force on the inside of the hoop tendons is not important as the radial compressive stresses are very small compared to the compressive strength of the concrete (say a few hundred psi versus 5,000 psi). The local radial tensile stresses also are not important as the radial compressive stress generated on the inside of the outer tendon is larger than the radial tensile stress generated on the outside of the inner tendon. Additionally, the spacing between hoop tendons at the same elevation is at least 12 inches (FM 1.9 Exhibit 4, page 84 of 188) and therefore the stress distribution in the hoop direction is not very different from that due to the regular vertical spacing of 13 inches between close adjacent tendons.

From results of the PII modeling, the delamination is largely determined by the amount of bulges (global displacement) that a panel has after detensioning. A spacing variation of 1" to 2" for some tendons will not change the shapes of the bulges, and therefore will have little effect on the delamination.

Finally, possible additional loads in the equipment hatch area are mitigated by a much thicker concrete section and high amounts of reinforcements (FM 1.9 Exhibit 4, page 2 of 2).

Conclusion:

Variations in tendon spacing and did not contribute to the delamination.



1.10 Included in Failure Mode 2.7 Vibration

Description:
Data to be collected and Analyzed:
Verified Supporting Evidence:
Verified Refuting Evidence:
Discussion:
Conclusion:



1.11 Design for Excessive Microcracking

Description:

Very fine cracks (commonly called microcracks) exist at the interface between coarse aggregate and cement paste even prior to application of load on the concrete. These cracks remain stable up to stresses of about 30% or more of ultimate strength and then begin to increase in length, width and number as the stress increases. New micro-cracks form in concrete as stress reaches 40-60% of ultimate strength. When stresses reach 70-90% of ultimate strength the cracks start bridging across the mortar, creating a continuous crack pattern. As the stress approaches ultimate strength the cracks grow until failure occurs.

The existence of microcracks explains how two materials (aggregates and cement paste) with nearly linear stress-strain behavior produce concrete that switches from linear stress-strain behavior at low stresses to non-linear behavior leading to ultimate failure.

Microcracks existence and development also help explain the mechanism of fatigue where concrete cycled at stresses lower than ultimate strength undergoes progressive degradation, leading to eventual failure without exceeding ultimate stress.

This document is intended only to answer the question if the design at CR3 accounted for the microcracking of the concrete. Since normally microcracks are not analyzed as part of the design process, this document will only attempt to verify that normal design process would not have resulted in excessive microcracking.

Data to be collected and Analyzed:

1. Literature regarding bond properties of aggregates and concrete used at CR3 (FM 1.11 Exhibit 1).
2. Background on microcracking in concrete (FM 1.11 Exhibit 2 is from ACI 224R report on Control of Cracking)
3. Petrographic analysis of CR3 concrete (FM 1.11 Exhibits 3, 4, 5 are Petrographic reports with references to bond and/or microcracking).

Verified Supporting Evidence: None

Verified Refuting Evidence:

1. The aggregate used at CR3 (Limestone) is known for producing better bond with the cement paste (FM 1.11 Exhibit 1).
2. Petrographic analysis confirmed good bond properties (FM 1.11 Exhibits 3, 4, 5).
3. Petrographic reports identified relatively low level of microcracking (FM 1.11 Exhibits 3, 5).

Discussion:

1. Limestone aggregate will, in addition to the mechanical bond, form chemical bonds that help strengthen the paste/aggregate interface and reduce voids/microcracks around the aggregate.
2. It is concluded based on Petrographic reports that original volume and extent of microcracking was lower than expected for average concrete. Therefore, concrete designed in compliance with standards and codes is expected to account for the likely microcracking and will exceed expected properties thanks to its improved microcracking state.

Conclusion:

Design consideration for microcracking was not deficient and was not a cause of the delamination.

- 1.12 Added stress from inadequate size of tendon sleeves (R)
 1.13 Inadequate net loading area due to presence of horizontal sleeves (R)



1.13 Size of tendon sleeves / Inadequate Net Loading Area (Includes FM 1.12)

Description:

The tendons used in the post-tension design are located within sleeves that are installed when the concrete forms are installed and are subsequently used as conduits (sleeves). The diameter of the sleeves used in the cylinder at Crystal River Unit 3 (CR3) is 5.25 inches.

This failure mode addresses the size of the sleeves in terms of:

1. Sleeve size in relation to the area needed to contain the tendons;
2. Sleeves act as a hole in the concrete and locally reduce the effective area (area where concrete is actually present over total area (sometimes called gross area)).

All the hoop tendons are in the same radial plane from the center of the containment. This leads to a radial plane with reduced effective concrete area. The only elevation where this does not hold is around the equipment hatch where some hoop tendons are located at the same elevation.

All the vertical tendons also are in the same radial plane from the center of the containment. This generates a plane with reduced effective concrete area, creating a weak plane in the concrete. The location of this weak plane is addressed in FM 1.13 Exhibit 10. Refer to CR3 drawing SC 421-006

Details regarding the types of sleeves used in the cylinder, rigid versus flexible, and the consequences of that are addressed in FM 6.4. Issues regarding vibration of the tendon sleeves are addressed in FM 7.2. Local stress concentration around the hoop sleeves is addressed in FM 1.15.

Data to be collected and Analyzed:

1. Calculate ratio of tendon wires area to tendon sleeve area (FM 1.13 Exhibit 4 is a PII calculation of the area fraction of steel wires into the CR3 sleeves);
2. Calculate area percentage taken by the sleeves in the plane of the hoop tendons (FM 1.13 Exhibit 5 is a PII calculation of the effective concrete area when considering the free space taken by the tendon sleeves);
3. Calculate area percentage taken by the sleeves in the plane of the vertical tendons (FM 1.13 Exhibit 5 is a PII calculation of the effective concrete area when considering the free space taken by the tendon sleeves).

Note: Exhibits 1, 2, and 3 are no longer included with this document

Verified Supporting Evidence:

1. In the plane of the hoop tendons, the sleeve area fraction is 27 %. In the plane of the vertical tendons, the sleeve area fraction is 20%. This is a large area reduction. The PII calculation is in general agreement with the MPR calculation highlighted on page 13 of 15 of FM 1.13 Exhibit 9. When combining the reduced area of the hoop and vertical tendons, the sleeve area fraction is then 42% (FM 1.13 Exhibit 5). This is a large area reduction;
2. The observed delamination generally runs in the plane of the hoop tendon sleeves (FM 1.13 Exhibit 6 is a Progress Energy calculation on SGR opening wall effective width showing the general path of the delamination.

Verified Refuting Evidence:

1. The text of the CR3 FSAR states that "Aside from other functions, this relatively heavy conduit acts as additional reinforcement. Thus, the loss-of-gross section resulting from the presence of tendon conduit, does not yield unacceptable stress levels" (FM 1.13 Exhibit 7 is an excerpt of the CR3 FSAR Section 5.2.5.2.1).



1.13 Size of tendon sleeves / Inadequate Net Loading Area (Includes FM 1.12)

Discussion:

The containment building wall has a weak plane where the net concrete loading area is dramatically reduced (at least 27%) due to the presence of the hoop tendon sleeves.

Additionally, as shown in FM 1.13 Exhibit 10:

1. There is a radial tensile stress in that plane;
2. Stress concentration effects occur in the concrete at the close periphery of the pre-stressing tendon sleeves (, see also FM 1.15).

This design is standard to all containment buildings and it is inherent to all post-tensioned construction. Post-tensioned concrete can be and has been successfully designed with this inherent condition, as evidenced by many operating years in absence of delamination. Some containment buildings use smaller tendons into smaller tendon sleeves and use more of them, such as Oconee. In such cases, the vertical tendons often are separated into two planes (FM 1.13 Exhibit 8 is a drawing of the vertical tendons at Oconee unit 1).

Following on FM 1.13 Exhibit 4, note that there are three 6 buttresses designs:

1. Crystal River: sleeve OD 5.25", tendon spacing 19.5", and percentage tendons 27%;
2. TMI: sleeve OD 4.57", tendon spacing 16.66", and percentage tendons 27%;
3. Oconee et al: sleeve OD 3.5", tendon spacing 10.11", and percentage tendons 35%;

The "percentage tendon" here is the linear fraction of the height of containment at the critical depth (10") which is lost to tendons. The Oconee design is the same as several other plants including Turkey Point.

Note that our calculation excludes the overlapping area when combining the reduced area of the hoop and vertical tendons, and we get the sleeve area fraction of 42% (FM 1.13 Exhibit 5). The MPR calculation does not exclude the overlap and therefore gets a somewhat higher value of 48% (FM 1.13 Exhibit 9 page 13 of 15).

The conduit has a 0.085 inch wall thickness, as measured on tendon sleeves recovered from the SGR opening. This corresponds to 6.4% of the available volume $(5.25^2 - (5.25 - 2 * 0.085)^2) / (5.25^2)$. The thickness is required to maintain integrity during installation (must support a 200 lbs man in case construction workers use the sleeves as a ladder), to handle the grease pressure upon tendon greasing (up to 85 psi hydraulic pressure), and then to provide a reliable path for the tendons. Given the small volume fraction involved, there is no benefit in considering reduction of the sleeve thickness. Sleeve thickness is within typical design specifications for application and has minor impact on overall area reduction.

Conclusion:

The CR3 design configuration did not cause the delamination.

1.14 Added stress from equipment hatch located underneath in same bay (R)



1.14 Presence of Equipment Hatch

Description:

The SGR opening was created above the equipment hatch and is where the delamination occurred. The location of the equipment hatch represents a major structural difference between this bay and the other five bays. This failure mode goes through the various possible issues that could be created by the presence of the equipment hatch on this bay.

There are a series of issues potentially associated with the location of the equipment hatch:

- 1.14a. Added stress due to the weight of the concrete forming the hatch. In particular it is possible to create a large bending moment in the wall above the equipment hatch (FM 1.14 Exhibit 2);
- 1.14b. The containment wall in the area of the equipment hatch is twice the normal thickness and so resistant to bending. That effectively shortens the bending length of the remainder of the wall. This could increase the bending stresses in the wall for a given forced displacement (FM 1.14 Exhibit 2);
- 1.14c. Hoop tendons are bent to go around the equipment hatch. This redistributes the forces in the concrete, potentially creating high localized stresses relative to those in the surrounding areas. In particular, the density of hoop tendons just above and below the hatch is such that they run two in the same horizontal plane (FM 1.14 Exhibit 3 page 2 of 4);
- 1.14d. Vertical tendons going around the equipment hatch also redistribute the forces and stresses in the area. In particular, the vertical tendons are now creating hoop forces (FM 1.14 Exhibit 3 page 3 of 4);
- 1.14e. The added weight from the thickened containment wall also changes the resonant frequency. This bay does not behave like the others in terms of vibration. (FM 1.14 Exhibit 2)
- 1.14f. Problems associated with the special construction of the equipment hatch as an insert in the wall. (FM1.14 Exhibit 2)

Data to be collected and reviewed:

1. Drawings of the equipment hatch, additional reinforcements used in this area. (FM 1.14 Exhibit 4);
2. Evaluation of the weight of the equipment hatch concrete (FM 1.14 Exhibit 1);
3. Evaluation of the bending moment created on the wall above the hatch (FM 1.14 Exhibit 1);
4. Comparison of the lengths of the different bays (FM 1.14 Exhibit 1).

Verified Supporting Evidence:

None

Verified Refuting Evidence:

1. The equipment hatch was carefully incorporated in the design. The design required the equipment hatch to be heavily reinforced (FM 1.14 Exhibit 4);
2. It effectively shortens the height of the bay but is not significant to conditions in the area of the containment SGR opening.

Conclusion:

This failure mode is refuted.

1.15 Inadequate design analysis methods of radial tensile stresses (Return to list)



1.15 Inadequate Design Analysis Methods for Local Stress Concentrations (Contributing factor)

Description:

Post-tensioned systems are known to induce tensile stresses on the backside of the pre-stressing tendons (FM 1.15 Exhibit 1 is a 2003 paper in Nuclear Engineering and Design). The common theoretical approach to calculating forces and stresses is a shell analysis giving an average tensile stress value (FM 1.15 Exhibit 2 is a typical industry shell calculation performed by MPR Associates). Standard industry analysis of this type has led to the mindset that large margins exist and a delamination as observed at CR3 would not have been predicted using industry standard calculation tools.

The original analysis (circa 1973) utilized hand calculations to estimate requirements for steel reinforcement bars. These calculations relied upon estimations of forces and moments at various critical locations in the concrete containment structure. Any computer model associated with this work idealized the containment walls as "thin shells" or plates. As such, high local stress concentrations in the concrete around the discontinuity created by the tendon conduit were not included.

The compressive stress produces secondary tension effects in regions of discontinuity such as holes in the concrete created by tendon conduits occurs in the general area of each tendon sleeves that contain the post-tensioning tendons. In essence, they behave like built-in "holes" in the structure. These higher tensile stresses resulting from high stress can create small, non-active cracks.

NOTE: Exhibits 3 and 4 are not used.

Data to be collected and Analyzed:

1. Review the original design calculation for methodology used to calculate loads, moments, and stresses in the concrete containment cylinder wall (FM 1.15 Exhibit 5 is an excerpt of the original Gilbert calculations used for CR3);
2. Review standard industry calculation for CR3 as performed as of 2009 (FM 1.15 Exhibit 2);
3. Observation of the fracture surface at the intersection with a tendon sleeve (FM 1.15 Exhibit 8 is the result of phenolphthalein testing of the fracture surface of sample from bay 3-4 of the containment);
4. Develop Finite Element Model of the concrete containment and observe local stress concentrations (FM 1.15 Exhibit 6 is a Finite Element Model calculating stresses around tendon sleeves and at the intersection of hoop and vertical sleeves).

Verified Supporting Evidence:

1. Stress concentration does take place in all post-tensioned concrete containment cylinders due to the geometry and the presence of "holes" at the location of the tendon sleeves. This is confirmed using FEM analysis showing high maximum principal stresses (FM 1.15 Exhibit 6);
2. Cracks were observed at the intersection of fracture surface and sleeves using the phenolphthalein experiments (FM 1.15 Exhibit 8); The test results indicate that the crack was pre-existing
3. Review of section 1.01.4 "cylindrical wall" of Gilbert calculations book 2 of 5 (FM 1.15 Exhibit 5) shows that the sizing estimates for reinforcing bar were performed using gross section areas, as is typical per industry standard shell calculation methodology and did not address local stress concentrations;
4. Typical industry shell calculation does not consider stress intensification at tendon conduits as seen in note 1 on page 4 of 15 of FM 1.15 Exhibit 2.

Verified Refuting Evidence:

1. The stress concentration observed here around "holes" in the structure is common to all post-tensioned concrete nuclear containment. Delamination in that wide population of containment shells



1.15 Inadequate Design Analysis Methods for Local Stress Concentrations (Contributing factor)

- has not been observed;
2. Additionally, this type of effect has been well known since the 19th century (FM 1.15 Exhibit 7 shows a reference to work performed by Kirsch and published in 1898). This is not a specific feature of the CR3 containment;
 3. Elevated stress concentrations rapidly fall-off a close distance from the hole. Small structural cracks potentially created by these localized higher stresses would be self-limiting and non-active.

Discussion:

The pre-existence of small cracks emanating from the tendon sleeves in the plane of the hoop tendon sleeves has been used in the PII modeling and it has been used in the PII uncertainty analysis in the Margin-to-Delamination calculation. It is likely that such non-active cracks would be present in other plants not analyzed here because the stresses calculated using linear elastic mechanics (Nastran or Ansys basic calculations) are very large and would exceed the tensile strength of all concrete materials. It is important to realize that these are structural cracks (not micro-cracks) and they will not allow transfer of stresses across the crack opening. It is also important to realize that these cracks are non-active, meaning that the localized high stresses are eliminated by the cracking. With that said, tendon sleeve hole locations and hoop planes generically possess higher potential for crack propagation if exposed to additional sufficient drivers, due to this “weakening” of an already reduced effective concrete thickness between the ducts.

Conclusion:

Standard industry analysis of this type has consistently shown that large margins exist in post-tensioned systems and a delamination, as observed at CR3 would not have been predicted using industry standard calculation tools. Thus, industry standard calculations and models used to predict stress margins led to larger margins than actually existed being predicted.

2.1 Inadequate concrete curing (R)



2.1 Inadequate Concrete Curing

Description:

Curing is the maintaining of an adequate moisture content and temperature in concrete at early age so that it can develop its design properties. Excessive early drying will result in drying shrinkage before the concrete gains sufficient strength to resist cracking stresses. It may also deprive the concrete of moisture needed for the chemical reactions through which it achieves the desired strength and durability. In cold climate it is also necessary to maintain the concrete at a temperature that allows adequate strength development through chemical reactions.

Curing is achieved through the physical protection of the concrete from the environment, and by maintaining its surface moist for a recommended period (seven or more days).

Protection can be provided by leaving the forms for the desired period or by protecting the concrete with impervious membranes (plastic sheets or applied curing compounds). Moisture may be applied to the surface with water spray, soaked fabric, etc.

Data to be collected and Analyzed:

1. Records of curing procedures. (FM 2.1 Exhibit 1 provides samples of curing logs)
2. Review specification for curing related requirements (FM 2.1 Exhibit 2)
3. Inspect concrete for curing related defects like Plastic and Drying shrinkage.

Verified Supporting Evidence:

None

Verified Refuting Evidence:

1. Original inspection records, including the "concrete curing log", documented curing conditions. Wet curing was performed by sprinkling water using a perforated hose for a period of 7 to 10 days (Minimum specified was 7 days). (FM 2.1 Exhibit 1).
2. No indication of Plastic or drying shrinkage was found in visual inspections.

Conclusion:

Concrete curing was adequate and did not contribute to the delamination.



2.2 Inadequate Placement

Description:

Concrete placement is the process of transporting the fresh concrete into the forms in a way that will result in uniform distribution and properties throughout the element with minimal separation of coarse aggregate (per specs). The two most common methods are pumping and transport by buckets. Pumping has the advantage of providing easy reach into spaces with limited accessibility whereas buckets allow placement of less workable concrete. The disadvantage of pumping is the need for more workable concrete, usually with higher cement and water contents, and the need to "lubricate" the pipes with grout (about 1 cu/yd per 1000 ft of pipe). Moreover, pumping equipment requires considerable additional cleaning and maintenance for efficient operation. Buckets, although simpler to operate, have limited reach and may not allow the same flexibility in concrete spreading as can be achieved with pumps.

This document will address the "transport" and "deposit" parts only. Other placement issues, such as grout, joint treatment and vibration are discussed in other Failure Modes.

Data to be collected and Analyzed:

1. Records of concrete pours. (FM 2.2 Exhibit 1 is a representative example of pour card showing placement equipment)
2. Review specification for placement related requirements (FM 2.2 Exhibit 2)
3. Inspect concrete for placement related defects like segregation and non-uniform concrete (FM 2.2 Exhibit 4 – photos and FM 2.2 Exhibit 5 - NCR).

Verified Supporting Evidence:

1. Excessive amount of grout was used to start each pour, resulting in grout pockets and non-uniform concrete at the joints. (FM 2.2 Exhibit 3 - summary of pours; FM 2.2 Exhibit 4 and FM 2.2 Exhibit 5).

Verified Refuting Evidence:

1. Original pour cards indicate that a combination of pumps and buckets were used. (FM 2.2 Exhibit 1).
2. Project specifications and original pour cards indicate that grout was specified and used to start each pour. (FM 2.2 Exhibits 1, 2).
3. QC record show that pump/bucket related issues were inspected and verified prior to any pour (FM 2.2 Exhibit 6)

Conclusion:

Concrete placement complied with project specifications but resulted in non-uniformity of the concrete without reducing its strength (FM 3.2 shows that grout was as strong as the concrete). This issue did not contribute to the delamination.

2.3 Inadequate slump (Includes FM 3.6) (R)



2.3 Inadequate Slump (Includes FM 3.6)

Description:

Slump is a standard measured property used to define workability and the ease of flow of concrete into various forms of confined areas (such as in the rebar cage, between conduits and rebars, etc.). Slump is normally specified as a maximum, not to exceed, value that is used in field testing to verify compliance with approved mix design and detect variations in the uniformity of a mix. Lower slump makes placing and consolidation more difficult, which in turn can result in the formation of voids. Higher slump makes concrete more workable, but may be an indication of excess water and a higher w/c ratio than desired. Excess water can lead to segregation, impact the concrete strength properties, lead to increased shrinkage, and increase creep in the long term. It is important to remember that slump alone does not define workability. It is possible to make low slump concrete that is workable when the right materials and tools are used.

Data to be collected and Analyzed:

1. Review concrete pour cards for slump data. FM 2.3 Exhibit 1 is a table summary of pour tickets for RBCN 0012 and RBCN 0015. RBCN 0015 is between buttresses 3 and 4 where the delamination happened, and RBCN 0012 is located on the opposite side between buttresses 1 and 6. These panels were placed during the same time frame using the same materials and techniques. FM 2.3 Exhibits 2 is a graph of the same data.
2. Examine if excessive voids exist through core sample and boroscopic examinations.
3. Review original project documents for required and allowed slump (FM2.3 Exhibit 4)
4. Provide drawing of bays RBCN-0012 and 0015 for reference of pour locations. (FM 2.3 Exhibit 3)

Verified Supporting Evidence:

1. A number of concrete loads with slump under 2" were reportedly placed into the concrete forms between the buttresses (for example, FM 2.3 Exhibit 7 includes pour cards for pour 695 – in the delamination area). However, although stiffer than what is normally considered workable, they were not out of specification. (FM 2.3 Exhibit 1 is a summary of all concrete placed in bays RBCN-0012 and 0015. FM 2.3 Exhibit 3 is a drawing of these bays)
2. A NCR was issued when concrete with slump of 1.5" was mixed with grout and placed in bay RBCN-0015 (FM 2.3 Exhibit 5). Surface defects were found in two pours (Pour 528 below the equipment hatch and pour 737 at elevation 220' as shown in FM 2.3 Exhibit 6) of the same bay.

Verified Refuting Evidence:

1. Original specifications and mix design called for 3" maximum slump. A letter (FM2.3 exhibit 4) refers to previous approval to accept 4" slump at the discharge pipe and 4.5" at the truck. Pour data (FM 2.3 Exhibit 1) shows compliance with these values.
2. Inspection/pour records indicate that trucks were rejected when slump was inadequate (for example: pour 729 - rejected 5 of 21 loads). (FM 2.3 Exhibit 1)
3. Cores and boroscope investigation did not detect any significant voids or aggregate pockets. Visual observation during and after demolition did not detect voids across the full thickness.

Discussion:

The supporting evidence reveals some problems in achieving and maintaining workable concrete. A number of trucks with out-of-spec concrete were delivered, some of which were subsequently rejected,



2.3 Inadequate Slump (Includes FM 3.6)

causing disruption of the process (especially when partial trucks were rejected). Also noted was a number of trucks that exceeded the allowed mixing time and were rejected after a partial unload. However, as shown in the refuting evidence, all concrete actually placed in bay RBCN-0015 met project specifications and was placed and consolidated successfully using the specified vibrators. Minor surface defects were reported and corrected.

Conclusion:

It is concluded that slump was not a contributing factor to the delamination.

2.4 Inadequate control of early age cracking (R)



2.4 Inadequate Control of Early Age Cracking

Description:

Early age cracking can occur when concrete is exposed to stresses exceeding its tensile capacity before it matured and gained strength. These cracks are usually the result of early, excessive drying shrinkage. They may also occur when forms and supports are removed too early and excessive loads are imposed on the structure before the concrete reached its design strength. These cracks can extend the full depth of the element and lead to early failure from strength loss and/or durability related distress.

Data to be collected and Analyzed:

1. Review reports from original construction regarding curing and form removal procedures. (FM 2.4 Exhibit 1)
2. Review strength development of original concrete. (FM 2.4 Exhibit 2)
3. Review project specifications for related requirements (FM 2.4 Exhibit 3)

Verified Supporting Evidence:

None

Verified Refuting Evidence:

1. Records of construction methodology, and especially curing and form stripping records, indicate that the concrete was not exposed to the environment or allowed to dry for at least seven (7) days after pouring as recommended by concrete industry standards and required in the specifications. (a representative sample is included in FM 2.4 Exhibit 1)
2. Form stripping records show that the concrete was supported for at least seven (7) days, at which time it reached 70-80% of measured 28 day strength. Four graphs related to strength gain with time are presented in FM 2.4 Exhibit 2.
3. Original specifications provided curing guidelines (selected pages in FM 2.4 Exhibit 3)

Conclusion:

Early age cracking was not a problem and was not a contributor to the delamination.



2.5 Inadequate Temperature Control During Pour

Description:

Concrete hardens through chemical reactions that generate heat. Maintaining low temperatures in the fresh concrete will minimize stress levels in the hardened concrete due to volume change caused by subsequent temperature drop.

Excessive higher temperature can cause rapid set, reduced workability, and loss of control over placing and finishing operations.

Excessive lower temperatures can delay set, damage concrete through early-age freezing, and lead to damage from pre-mature form removal.

Data to be collected and Analyzed:

1. Review temperature records from delivery/pour tickets
2. Review strength results at early age (7 days) from pour records
3. Analyze strength development between seven (7) and twenty-eight (28) days
4. Review all concrete related NCRs for temperature related problems (FM 2.5 Exhibit 5).

Verified Supporting Evidence:

1. NCR 95 reports on a single incidence where concrete was placed at a temperature exceeding 70 degrees. The Engineer accepted the non-compliant concrete based on its location in the structure and small variation (FM 2.5 Exhibit 5)

Verified Refuting Evidence:

1. Project specifications limited containment concrete temperature to 70 deg F (FM 2.5 Exhibit 6). Pour records show that all concrete was placed between 50 to 70 deg F. (FM 2.5 Exhibit 1 are plots for all concrete placed between buttresses 3-4 and 6-1)
2. Review of pour tickets show that ice was used to control concrete temperature as needed. (example in FM 2.5 Exhibit 2)
3. Seven day strength is adequate. No significant variation over time and temperature range. (All available strength data in FM 2.5 Exhibit 3)
4. Ratio of 7/28 days strength is in normal range with acceptable variation. (FM 2.5 Exhibit 4 includes all available tests for buttresses 1-6 and 3-4)

Conclusion:

Temperature control was not a contributing factor to the delamination since all concrete was placed and finished at an acceptable temperature range.

2.6 Inadequate mix design (R)



2.6 Inadequate Mix Design

Description:

Concrete mix design is a process of determining the right combination of cement, aggregates, water, and admixtures for making concrete that will have specified properties. Part of the process includes a trial mix and physical testing intended to prove compliance and to fine-tune the proportions. Once a mix-design is approved it should not be modified without evaluation of property changes and without approval from the responsible engineer.

Inadequate mix-design can result in deficiencies in the fresh concrete's properties, such as workability, and in deficient hardened concrete physical properties, i.e., air content, strength and modulus of elasticity. These deficiencies could contribute to distress from physical attack, and to stress induced cracking.

This Failure Mode addresses the Mix-Design process only. Material choices and concrete properties are discussed in FM 2.12 and FM 3.1 to 3.7

Data to be collected and Analyzed:

1. Original project specifications (FM 2.6 Exhibit 7)
2. Original mix designs by Law Engineering (FM 2.6 Exhibit 1)
3. Record of changes to the original mix-design (FM 2.6 Exhibit 4 is Gilbert report on mix design written after Dome delamination; FM 2.6 Exhibit 8 is a summary of proportions for all mixes used)
4. Daily pour reports (Representative sample of pour records are included in FM 2.6 Exhibit 2)
5. Original concrete test reports. (FM 2.6 Exhibit 3 is a summary of 28 days strength for containment building concrete)
6. Strength testing and modulus of elasticity testing of core samples by S&ME. (Selected sample of cores, FM 2.6 Exhibit 5)

Note: Exhibit 6 is no longer used in this FM.

Verified Supporting Evidence:

1. Original mix design by Law Engineering (FM 2.6 Exhibit 1) was modified slightly (reduced 16 lbs sand and added 4.8 lbs water) into mix DM-5 which underwent a complete evaluation testing by PTL in 1970. Mix DM-5 was later modified into mix DM-5-M (add 47 lbs cement and remove 40 lbs sand) with no record of testing or approval. In 1972 it was modified again into mix 727550-2 (add another 23 lbs cement, remove 20 lbs sand, add 10 lbs water and increase admixture content) which was tested by PTL for fresh concrete properties and compressive strength at 7 and 28 days. A final modification into mix 727550-2-M (add another 47 lbs cement) has no record of testing or approval (FM 2.6 Exhibit 8).

Verified Refuting Evidence:

1. Original mix design by Law Engineering in 1969 was done in accordance with CR3 specification SP-5569 (FM 2.6 Exhibit 7), and verified with ASTM tests for fresh concrete and strength tests at ages 7, 14, 21, and 28 days.
2. The mix design used initially in the containment structure (designated DM-5) was thoroughly tested by PTL and the results reported in January 1970 (FM 2.6 Exhibit 4)
3. The mix design used later in the containment structure (designated 727550-2) was tested by PTL and the results reported in June 1972 (FM 2.6 Exhibit 4)
4. Compressive strength tests from original construction testing and from cores taken from subject concrete verify compressive strength complied with the 5000 psi specification. (FM 2.6 Exhibits 3 and 5)



2.6 Inadequate Mix Design

Discussion:

1. The mix design process was done properly, following industry standards and project specifications.
2. Both of the approved mix designs were modified during the construction process without documentation of the reasons, methodology, and any tests that may have been performed. There is also no record of approval for the modifications.
3. Both modifications involved an increase in the cement content with a corresponding decrease in the water to cement (W/C) ratio. The measured strength prior to the changes was in full compliance with the specifications and the changes did not appear to increase the compressive strength significantly.
4. The most likely reasons for the changes may be aggregate gap-grading, workability and problems with pumping low slump concrete.
5. At the time of CR3 construction, adding cement without modifying other ingredients was an acceptable industry practice.
6. The only creep tests were reported on the first mix design in 1970.
7. The final (727550-2-M) mix design had 18% more cement than the first (DM-5) mix design (752 compared to 635 lbs per cubic yard) with a similar increase in the Hardened Cement Paste (HCP) in the concrete.
8. HCP is the concrete phase where shrinkage and creep occur. Therefore, such increase could change the creep and shrinkage properties of the containment concrete. However, basic creep, drying creep and shrinkage were ruled out as contributors (FM 4.5, 4.6 and 4.2).
9. According to ACI-318-71 no more than 1% of tests can be more than 500 psi below f'_c (4500 psi for f'_c of 5000 psi) and no more than 1% of tests can have an average of three consecutive tests below f'_c . Analysis of twenty eight (28) days strength tests (FM 2.6 Exhibit 3) shows compliance with both requirements for concrete with f'_c of 5000 psi.

Conclusion:

The original mix design was adequate and did not contribute to the delamination.

2.7 Inadequate vibration during pour (R)



2.7 Inadequate Vibration during Concrete Pour

(Includes FM 1.10)

Description:

Concrete, especially low slump concrete, requires mechanical vibration in order to achieve optimal consolidation levels. Vibration helps remove excess entrapped air and water, resulting in denser concrete. However, excessive vibration could result in segregation of concrete constituents, while too little vibration could result in voids and aggregate pockets even when the concrete slump is within specifications. The containment structure is pre-stressed with minimal reinforcement above ground and away from openings. The tendons and rebars are spaced in a way that allows unimpeded access for the workmen to place and consolidate the concrete.

Voids around tendon conduits (originally FM 1.10) and other inserts are also minimized by effective consolidation.

Data to be collected and Analyzed:

1. Review specification for consolidation/vibration requirements. (FM 2.7 Exhibit 3 & 5)
2. Review vibration inspection reports. (A representative sample is provided in FM 2.7 Exhibit 1).
3. Review pour records for NCRs about segregation/voids (FM 2.7 Exhibit 4)
4. Review Petrographic reports for existence of voids and aggregate pockets. (FM 2.7 Exhibit 2)
5. Review Petrographic reports for bleeding and for segregation of concrete constituents. (FM 2.7 Exhibit 2)

Verified Supporting Evidence:

None

Verified Refuting Evidence:

1. Specifications provided instructions for proper vibration methodology (selected sections in FM 2.7 Exhibit 3)
2. QA procedures established framework for ensuring proper vibration (selected sections in FM 2.7 Exhibit 5)
3. According to reports on concrete placement adequate mechanical vibration was provided in compliance with specifications. (Selected pour tickets included in FM 2.7 Exhibit 1).
4. Although NCRs addressed voids and aggregate pockets that required corrections and were repaired, they are more a manifestation of slump issues than vibration (results of exhaustive search in FM 2.7 Exhibit 4)
5. Visual and Petrographic observations show relatively dense matrix with air voids typical of well consolidated air entrained concrete. No evidence of bleeding or segregation was found (FM 2.7 Exhibits 2a & 2b).

Conclusion:

Data analyzed indicates that adequate vibration was applied and that concrete vibration was not a contributing factor in the delamination.

2.8 Inadequate support of tendons during pouring (R)



2.8 Inadequate Support of Tendon Sleeves (conduits) during Pouring

Description:

If the tendon sleeves (conduits) are not supported well, they may move during concrete pouring. Such movements have the potential to result in either or both, (1) localized friction between the tendon and its conduit and (2) non-uniform stress in the concrete over the length of the tendon.

Due to limited documentation from original construction it was necessary to evaluate this issue based on photographic records taken during construction and during demolition.

Data to be collected and Analyzed:

1. Examine supports of hoop sleeves during construction.
2. Examine supports of vertical sleeves during construction.
3. Examine sleeve location and condition during SGR hole cut.
4. Review NCR reports from original construction (FM 2.8 Exhibit 2)

Verified Supporting Evidence:

1. Non-conformance and Correction Report (NCR 0043) discusses an incidence where 9 vertical tendon conduits were out of allowable tolerance (FM 2.8 Exhibit 2). Corrective measures were taken and the conduits were brought back into tolerance.
This evidence demonstrates that a QC system was in place to evaluate conduit alignment and corrections were done as needed.

Verified Refuting Evidence:

1. Photos from original construction demonstrate the support system. (FM 2.8 Exhibit 1, 1973 photos)
2. Photos taken during demolition show that the sleeves were evenly distributed in the zone and not deformed. (FM 2.8 Exhibit 1, 2009 photos)

Conclusion:

Based on the available evidence it is concluded that sleeve (conduit) support during pouring was proper and was not a contributing cause of the delamination.

2.9 Void or cracks due to inadequate forms (leaky, insecure, early stripping) (R)



2.9 Inadequate Concrete Forms

Description:

Forms constructed improperly with gaps between sections or with inadequate strength will likely result in concrete seepage between sections and/or in form deformation. Seepage could result in voids, aggregate pockets, and non-uniform surface finish. Form deformation could result in excessive fins and/or an uneven outer surface.

Data to be collected and Analyzed:

1. Conduct a visual inspection of the outside containment surface for evidence of grinding.
2. Review construction documents for containment surface repair (FM 2.9 Exhibit 1).

Verified Supporting Evidence:

1. Visual observations of the structure post demolition revealed evidence of limited localized grinding – most likely associated with leaks from form joints. No record was found in NCRs or other documents.

Verified Refuting Evidence:

1. IWL visual inspection (summary of a 2007 report is attached in FM 2.9 Exhibit 2) detected multiple instances of wood embedded in the concrete which they attributed to plywood delamination. They also reported one instance of deflection which they attributed to “form slippage during original construction.” In every case their conclusion was that it did not cause degradation of the concrete.
2. A total of thirteen (13) concrete related NCRs were located for the containment structure. One (1) reported surface damage discovered upon form removal and corrected (FM 2.9 Exhibit 1). It was not clear if the defect was related to vibration or form deficiency. Other minor surface blemishes were reported on “concrete surface defect forms” and repaired. None was identified as caused by form deficiency.

Discussion:

Occasional minor honeycombing was reported upon form removal and the concrete was repaired. Visual inspections by PII of the concrete surface found good quality concrete surface. IWL inspections detected a few minor form related defects which did not cause degradation of the concrete.

Conclusion:

Concrete forms did not contribute to the delamination.

2.10 Concrete deformation from tensioning too early (R)



2.10 Concrete Deformation from Tensioning too Early

Description:

Applying full design preload to the installed post-tension tendons before the concrete achieves sufficient maturity can result in excessive creep and deformation.

Data to be collected and Analyzed:

1. Review strength development over time. (FM 2.10 Exhibit 1)
2. Compare dates of tensioning and pouring. (Selected pour tickets and a table of tendon tensioning reports are provided as FM 2.10 Exhibit 2)

Verified Supporting Evidence:

None

Verified Refuting Evidence:

1. Average of strength tests up to ninety (90) days exceeded design strength by close to 30%. (FM 2.10 Exhibit 1)
2. Additional gain of 10-20% is estimated after 90 days and prior to the application of post-tension
3. Cores tested in 2009 averaged over 7000 psi (over 40% above design strength)
4. Construction schedule allowed sufficient time between pouring and tensioning. (FM 2.10 Exhibit 2 shows a year and ten months separation for vertical tendons and 1 year and six months for hoop tendons)

Conclusion:

The evidence shows that the concrete achieved sufficient maturity before tensioning and there is no evidence that excessive creep or deformation occurred. This failure mode did not contribute to the delamination.

2.11 Inadequate construction cold joint (R)



2.11 Inadequate Horizontal Cold Joints

Description:

Special procedures are specified when fresh concrete is to be placed over hardened concrete in a "cold joint". The old concrete surface has to be thoroughly cleaned, roughened and brought to a saturated-surface-dry condition. These steps are required in order to ensure good bond between the hardened concrete and the newly placed concrete. Common practice at the time of original construction at CR3 was to apply a thin layer of grout (fluid concrete without the coarse aggregate fraction) directly on the cleaned concrete and place the fresh concrete on top of the grout bed. Excessive stresses, debonding and/or cracking are possible if a cold joint has physical properties that are not compatible with the rest of the concrete.

Data to be collected and Analyzed:

1. Review original project specifications for cold joint procedures. (FM 2.11 Exhibit 2 and 3)
2. Perform review of Non-Conformance Reports (NCRs) for joint related problems. (FM 2.11 Exhibit 1)
3. Perform analysis of pour records. (FM 2.11 Exhibit 4)
4. Review photographic records from demolition for joint related issues. (FM 2.11 Exhibit 5)
5. Review core strength tests for concrete and mortar (FM 2.11 Exhibit 6)

Verified Supporting Evidence:

None

Verified Refuting Evidence:

1. Original project specifications provided guidance for joint construction. (FM 2.11 exhibits 2 & 3 and discussion on next page)
2. One NCR was found for joint issues. (FM 2.11 exhibit 1 and discussion on next page)
3. Pour record analysis confirmed that joints were in compliance with specifications. (FM 2.11 exhibit 4 and discussion next)
4. Photographic records show the existence of well defined joints. There did not appear to be a problem with debonding or cracking at the joint. (FM 2.11 exhibit 5)
5. Core tests confirmed that the mortar at the joints had strength properties similar to the bulk of the concrete (FM 2.11 Exhibit 6)

Discussion:

1. Original project specifications provided guidance for joint construction. FM 2.11 Exhibit 2 is SP-5618 whose section 4:01.2 requires that "The horizontal joints shall be dampened (but not saturated), then covered with coat of neat cement mortar of similar proportions to the mortar in the concrete. The mortar shall be at least ½ inch thick...". However, section 5:01.6 of SP-5618 requires that "...a ½ inch layer of neat grout shall be applied before concrete is deposited".
After a review of pour tickets we were able to determine that a grout composed of sand and cement with w/c ratio of 0.4 was used. The amount of grout used exceeded the ½" specification but met the "at least ½ inch" called for. It appears that six (6) cubic yards of grout were placed on each joint, bringing the height of the grout layer to nearly 7.5 inches. Concrete was pumped on top of this layer, resulting in partial mixing, grout pockets, and non-uniform concrete. It also appears, based on NCR 99 (FM 2.11 exhibit 1) that concrete with low slump (1.5") was mixed with the grout in order to facilitate pumping, and that this was considered standard construction practice.



2.11 Inadequate Horizontal Cold Joints

2. When reviewing photos taken during the demolition process it is possible to discern a darker band of material along the joint line. That band has varying amount of aggregate and is darker due to the higher cement content at the location. It was not possible to determine from the photos if there were any cracks that originated from the band. Measurements indicate that the band varies from 5" to 15" high between the outside face and the liner. This observation confirms the theory that pumping concrete onto the grout layer caused displacement and "splashing" of the mortar – resulting in non-uniform transition layer between pours.
3. Cores obtained from grout areas were tested for strength under compressive loading. The three (3) samples averaged 8700 psi, which is about 20% higher than the average concrete core strength. It is therefore doubtful that the presence of thick grout layer could weaken the joint. (note: the grout cores were taken from locations outside the delaminated panel – however, they are considered representative of the grout used in the containment structure)
4. Debonding and/or cracking at the horizontal cold joint are unlikely to have a direct effect on delamination in the vertical plane.

Conclusion:

Based on the available evidence it is concluded that horizontal cold joints were not a contributing cause of the delamination.



2.12 Inadequate Strength Properties

Description:

The main concrete strength properties used in design are compressive strength (f'_c) and Tensile strength (f_t). Of those, the most commonly used is f'_c which is easy to measure and can be related to all other properties through empirical expressions. Direct tensile strength is difficult to measure accurately and is normally replaced with Splitting Tensile Strength (f_{tsp}) that is measured with the "Brazilian" test.

Concrete strength properties are influenced by multiple parameters, the most important of which include the water to cement (W/C) ratio, aggregate properties, and total voids. These parameters are analyzed separately in other Failure Modes.

When evaluating strength properties for failure analysis it is advantageous to analyze the strength at three distinct time frames (if data is available): the strength at twenty eight (28) days compared to the specifications and design parameters; strength development during the early period (up to 90 days) to evaluate potential variations in material properties and curing conditions; and strength changes over the life of the structure to evaluate potential degradation caused by chemical or physical interactions.

Data to be collected and Analyzed:

1. Original project specifications (FM 2.12 Exhibit 1)
2. Analysis of original design (FM 2.12 Exhibit 2 is analysis prepared by Progress Energy in 2000)
3. Code requirements at the time of the containment structure construction (FM 2.12 Exhibit 4 is from ACI 318-63)
4. Cylinder strength test results from the original construction (FM 2.12 Exhibits 7, 8 and 9 are database analyses of all samples from the Reactor Building at 7, 28 and 90 days respectively; FM 2.12 Exhibit 3 is a graphic representation of the average cylinder strength at early ages for concrete in two bays (out of six) of the containment structure; FM 2.12 Exhibit 6 is the original cylinder test records for bay RBCN-0015 (where delamination occurred).
5. Core tests in 2009-2010 and their correlation to original cylinder tests at the containment structure (FM 2.12 Exhibit 5 is a graphical representation of core tests and original cylinder strength results taken from the core test location; FM 2.12 Exhibit 10 is a table summary of all the available information for these locations)
6. Analysis of locations where the four different mix-designs were used in the containment structure (FM 2.12 Exhibit 12 is a graphical presentation of the mix- design and cylinder strength test overlaid on a plan of bays RBCN-0015 and RBCN-0012; these two bays were placed during the same period of time and using the same materials; bay RBCN-0015 is the delaminated bay).
7. Gilbert report on Dome Delamination from 1976 (FM 2.12 Exhibit 13 is the section reporting on concrete properties)

Verified Supporting Evidence:

1. The data presented in the Dome Delamination Report (FM 2.12 Exhibit 13) reveals variable and sometimes low tensile strength of concrete.
2. Measured Direct Tensile strength at the delaminated bay was lower than elsewhere in the structure (FM 2.12 Exhibit 10).

Verified Refuting Evidence:

1. Original cylinder compressive strength tests were in compliance with the requirements of ACI 318-63 (FM 2.12 Exhibit 4) for concrete with specified strength, f'_c , of 5000 psi. At twenty eight (28) days the average concrete cylinder strength exceeded 5700 psi.



2.12 Inadequate Strength Properties

2. Strength development during the first ninety (90) days followed the expected trend for concrete of the type used at CR3 (Type II cement without pozzolanic admixtures). By the time the structure was pre-stressed the concrete had gained more than 15% over the 28 days average compressive strength.
3. In the 30 years that followed the concrete gained, on average, 28% more compressive strength as compared to the tested strength at 28 days strength (see discussion 7 below).

Discussion:

1. Project specifications (FM 2.12 Exhibit 1) require twenty eight (28) days minimum compressive strength of 5000 psi. There are no specifications for tensile strength – splitting, direct or flexural.
2. Design documents use the relationship $3(f_c)^{1/2}$ for allowed tensile stress (212 psi for concrete with $f_c=5000$)
3. Analysis of cylinder tests (FM 2.12 Exhibit 8) shows compliance with ACI 318 requirements for 5000 psi concrete when evaluated according to ACI 214 methods. Design analysis/Calculation (FM 2.12 Exhibit 8) performed in the year 2000 provides a detailed analysis of the strength gain and compliance for the as-built condition.
4. Analysis of cylinder strength development during the first 90 days (FM 2.12 Exhibit 3 is a graphical representation of the strength development in bay RBCN-0015 and RBCN-0012 respectively) reveals the following:
 - 4.1. Early age strength development, as measured by the ratio of strength at seven (7) days to strength at twenty eight (28) days, was in a range of 71% to 88%.
 - 4.2. There was significant difference in strength (mostly for 7 and 28 days tests) between pours. This may be explained by the four (4) different mix-designs used in the structure (FM 2.12 Exhibit 12 is an elevation view of the wall overlaid with pour numbers and data for concrete mix-designs and strength at 28 days). By age 90 days the strength differences between pours were smaller, as seen in the statistical analysis (average and standard deviation) in FM 2.12 Exhibit 10.
5. Empirical relationships between concrete compressive strength (f_c) and splitting tensile strength (f_{tsp}) have been established through long term experience. Such relationships are provided in ACI 318, CEB-FIB (Comité Euro-International du Béton-International Federation for Structural Concrete) and numerous published papers. Of those, the one that best fits the experimental data from tests on the concrete cores from CR3 is the CEB-FIB formula ($f_{tsp}=0.3f_c^{2/3}$ MPa). When applied to the average compressive strength of all cores (50.9 MPa or 7385 psi), it accurately predicts the measured splitting tensile strength average of 4.14 MPa (600 psi). The ACI 318 expression used in design ($f_{tsp}=0.56f_c^{0.5}$ MPa) predicts f_{tsp} of 4.0 MPa (580 psi) which is lower (more conservative) than the average CR3 concrete.
 Direct Tensile strength can be calculated using empirical formula 3.2 from ACI 224.2R (or 2-4 from ACI 209R) where $f_t=0.0069[W_c(f_c)]^{1/2}$ MPa. CR3 concrete cores with average f_c of 50.9 MPa (7385 psi) and W_c of 2515 Kg/m³ (157 lb/ft³) resulted in calculated f_t of 2.53 MPa (358 psi). Tests of direct tensile strength averaged 453 psi and the lowest test result was 350 psi. It can be concluded that the measured direct tensile strength met or exceeded the values expected for the CR3 concrete.
 Based on the above, it can be concluded that the tensile strength properties of the original concrete were in the expected range for the design and code requirements.
6. Empirical relationships in design manuals provide guidance for calculating direct tensile strength from splitting tensile strength. Neville, in his text book "Properties of Concrete" states that f_{tsp} is 5-12% higher than f_t , whereas BS EN 12390-6, BS EN 1992-1-1 permits using 90% of tested f_{tsp} for calculated f_t . At CR3 the ratio is close to 75%. This is likely caused by a large percentage of porous soft particles in the aggregate since the direct tensile test is more sensitive to anomalies in the total sample volume.
7. Analysis of strength development over the life of the structure (FM 2.12 Exhibit 10 is a table summary



2.12 Inadequate Strength Properties

of concrete properties at locations where both original cylinder data and current core test data are available; FM 2.12 Exhibit 11 is a graphical representation of the relationship between common strength properties from the table in Exhibit 10) reveals the following:

- 7.1. The 2009-2010 core compressive strength ranged from 1% to 35% above the ninety (90) days average cylinder strength. This spread reflects the possibility that the cores and the cylinder location were not from the same ready-mixed truck (within the same pour). It can also be explained by fast early age strength gain, core damage (ACI 318 allows 15% adjustment to core strength when compared to cylinders for acceptance criteria), or exposure over the life of the structure. This type of variation is not uncommon in investigations of older structures and the exact cause is often left unexplained.
- 7.2. On average, concrete compressive strength development is in line with that expected from high strength concrete made with Type II cement and Florida Limestone aggregate. Seven (7) days compressive strength was 76% of the twenty eight (28) days compressive strength. Beyond 28 days the concrete gained another 14% by age 90 days, and another 14% by the year 2010. Total compressive strength gain after age 28 days was on average 27%.
- 7.3. When comparing core strength to cylinder strength for design analysis it is possible to estimate equivalent in-place strength of the concrete at the location from which the cores were taken. According to ACI 214.4R section 8.1 it is permissible to multiply the core measured strength by 1.06 to account for damage due to drilling (our cores were 4" diameter and tested "as-received" – so no other corrections were allowed). This calculation was not performed since the purpose of the long term analysis was to determine trends and not to establish design values.
- 7.4. Direct tensile strength tests performed in 2010 show concrete tensile strength in the delaminated bay is about 10% lower (on average) than tensile strength measured in an adjacent bay and opposing bay. These values may have been further reduced in the tendon plane (where delamination occurred) due to higher local stresses caused by reduced concrete cross-section and thermal cycling (as discussed in FM 4.8). These test result are in agreement with results reported in 1976 for the Dome Delamination report (FM 2.12 Exhibit 13)

Conclusion:

Based on the analysis above, it can be concluded that even though average strength properties met design criteria established for CR3, the tensile strength of the concrete was not adequate for radial stresses produced during the activities of tendon detensioning and of cutting the opening for the SGR Project. Therefore, the variable and, in some cases, low tensile strength was a contributor to the delamination

3.1 Inadequate air content (R)



3.1 Inadequate Air Content

Description:

The amount, size, and distribution of air voids inside concrete have significant influence on its physical properties and durability. For strength considerations, air voids have the same effect as other voids by creating initiation points for cracking. For durability, small, well distributed voids help protect the concrete against damage from freezing and thawing cycles. The "beneficial" voids are formed by specialized, air-entraining admixture that is added to the fresh concrete during batching. The other type of air voids are those entrapped through the process of mixing and placing the fresh concrete. The entrapped air is composed of larger, non-uniform voids that are randomly distributed in the concrete. Concrete specifications provide requirements for total air content and for the type and quantity of air-entraining admixture to be used.

Data to be collected and Analyzed:

1. Petrographic analysis (FM 3.1 Exhibits 1, 2, 5 & 7)
2. Review pour tickets for measured air during construction (FM 2.8 Exhibit 3).
3. FM 2.8 Exhibit 4 is a graph of the air reported on all available pour tickets for panels RB12 & RB15. RB15 is the delaminated panel and RB12 is the opposite panel constructed at the same time frame.
4. Review project specifications (FM 2.8 Exhibit 6).

Verified Supporting Evidence:

None

Verified Refuting Evidence:

1. Analysis of measured air in fresh concrete during construction confirmed that air content was within specifications of 3-6%. (FM 3.1 Exhibit 4 and 6)
2. The amount of entrained air is within specified range according to Petrographic analysis. (FM 3.1 Exhibits 1, 2, 5 & 7; Exhibits 1 & 7 refer to samples from the dome during the 1976 delamination. The dome concrete used the same mix-design and materials as the concrete in the wall)
3. Pour ticket review shows the air entrained admixture (DAREX) was used in all concrete pours in accordance with the mix design specifications. (FM 3.1 Exhibit 3 is a sample of typical tickets)

Conclusion:

Based on the available evidence it is concluded that air content was not a contributing cause of the delamination.

3.2 Inadequate grouting materials (R)



3.2 Inadequate Grouting Materials

Description:

Mortar and grout (which appear to be used interchangeably in the documentation) were used in mortar beds between pours and in repairs of defects (voids & aggregate pockets) in the concrete. From review of project data it appears that the material used was mortar (concrete without the coarse aggregate) or grout (mortar of fluid consistency) and not "neat grout" (as it was called in one specification). We will use the term grout to describe this material in our analysis. A grout bed was specified when fresh concrete was to be placed over hardened concrete in a "cold joint". The grout was required in order to ensure a good bond between the hardened concrete and the newly placed concrete. Its other function was to prepare the pump and its pipes for the relatively dry concrete by smoothing the surface with a layer of wet mortar.

The purpose of this document is to determine the adequacy of the materials and proportions used in the production of the grout. Grout application and construction considerations are included in another Failure Mode.

Data to be collected and Analyzed:

1. Review core strength tests for concrete and grout (FM 3.2 Exhibit 1)
2. Review original project specifications for cold joint procedures. (FM 3.2 Exhibit 2)
3. Review grout mix design. (FM 3.2 Exhibit 3)
4. Perform analysis of pour records. (FM 3.2 Exhibit 4)

Verified Supporting Evidence:

None

Verified Refuting Evidence:

1. Core tests confirmed that the grout at the joints had strength properties similar to the bulk of the concrete (FM 2.11 Exhibit 1)
2. Original project specifications provided guidance for joint construction. (FM 3.2 exhibits 2 and discussion a.)
3. Grout (typically identified on pour cards by mix designation SCM) was batched with similar materials and Water to Cement (W/C) ratio (0.4) as the concrete. (FM 3.2 exhibits 3 and 4)

Discussion:

1. Based on pour tickets we were able to determine that grout composed of sand and cement with w/c ratio of 0.4 was used. Proportions of sand to cement in the grout (2 to 1) were similar to those of the original concrete mix design (DM-5).
2. Cores obtained from mortar areas (sampled outside the delaminated panel) were tested for strength under compressive loading. The three (3) samples averaged 8700 psi, which is about 20% higher than the average concrete core strength. This trend was expected since the concrete included coarse aggregate with lower strength properties.

Conclusion:

Based on the available evidence it is concluded that proper grouting materials were used and the grouting materials were not a contributing cause of the delamination.

3.3 Inadequate cement materials (R)



3.3 Inadequate Cement Materials

Description:

Cement properties can have considerable impact on the physical properties and durability of the concrete when the cement fails to meet specifications and industry standards. The standards (ACI and ASTM) referenced by the original specifications create the basis for testing and acceptance program of cement. Some of the main potential problems with cement include: 1. Slow reacting cement can slow strength gain; 2. Fast reacting cement can cause rapid loss of workability and early set; 3. High C3A cement can support failure when exposed to Sulphates (as well as accelerate reactions); and 4. High Alkali cement may cause problems when reactive aggregates are used. Problems may also be caused by imbalance between the cement's main compounds, particle size that is too large (slow, incomplete reactions) or too fine, or the inclusion of contaminants that affect the cement's performance. ASTM C150 covers the production and use of cement and is normally used to determine compliance and suitability of the cement for the intended application.

Data to be collected and Analyzed:

1. Original cement test records including mill certificates. (FM 3.3 Exhibit 1)
2. Records of strength tests on original concrete (FM 3.3 Exhibits 2)
3. Petrographic analysis of original concrete and current samples (FM 3.3. Exhibit 6, 5, 4 and 3)

Verified Supporting Evidence:

None

Verified Refuting Evidence:

1. "Tests of Cement" reports dated 4/2/1974 and 4/22/1974 by PTL conclude that the cement meets all specifications and ASTM standards within acceptable standard deviation. (FM 3.3 Exhibit 1)
2. The PTL test found that the cement was slightly finer and faster settling than specified. However, it was concluded that the variation was acceptable. (FM 3.3 Exhibit 1 pg 2 of 3)
3. "Mill Certificate" dated 4/2/1974 from "General Portland Inc." meets all applicable ASTM standards. (FM 3.3 Exhibit 1 pg 3 of 3)
4. Original test records show satisfactory variation and strength level. When cement quality is not satisfactory it is often possible to see unusual strength trends over the life of a project. (FM 3.3 Exhibit 2- strength graphs)
5. Original Petrography reports by Erlin and Hime (FM 3.3 Exhibit 3 and 6), current CTL Petrography Report dated 11/2/2009 (FM 3.3 Exhibit 4), and MacTec report dated 11/11/2009 (FM 3.3 Exhibit 5) reported no irregularities with the cement.

Conclusion:

All documents reviewed show that the cement materials meet all requirements and are not a contributing factor in the delamination.



3.4 Inadequate Aggregate

Description:

Aggregates occupy 60-75% of concrete volume and therefore have large influence on the mix design, physical, chemical, and thermal properties.

The aggregate's gradation, strength, porosity, mineral composition, hardness, and chemical stability are evaluated through a set of ASTM standards which determine its suitability for use in concrete. Aggregate with deficiency in any of these properties may still make good concrete when combined with proper ingredients in a proper mix design. Therefore, failure in any of these tests does not automatically disqualify the aggregate for use in concrete. It is common practice to accept aggregates based on their proven ability to produce concrete with the specified strength through long term local experience.

This document will review the original requirements, tests, properties of the aggregates, how these aggregates affected the properties of the concrete in the containment structure, and if the aggregates contributed to the delamination.

Data to be collected and Analyzed:

1. Original project specifications (FM 3.4 Exhibit 1)
2. Reports on testing and evaluation of the aggregates during construction (FM 3.4 Exhibit 2 is Law Engineering report)
3. Aggregate Quality Control (QC) program at the batch plant (FM 3.4 Exhibit 11 is a summary followed by original detailed test records of aggregates)
4. Available information on the Florida aggregates (FM 3.4 Exhibits 12a, 12b, 12c, 12d, and 12e).
5. Physical properties of the concrete
6. Chemical properties of the concrete
7. Petrographic analysis reports (FM 3.4 Exhibit 3, 4, 5, 6, 7, 7a)
8. Strength properties of concrete and grout (FM 3.4 Exhibit 10)
9. Historical records (FM 3.4 Exhibit 13 is a summary of 1976 observations by Fred Moreadith of Gilbert Associates)

Verified Supporting Evidence:

1. The coarse aggregate included up to 50% softer, porous and fossiliferous particles that reduce the concrete's strength and modulus of elasticity (FM 3.4 Exhibit 4 and 13).
2. Aggregate was gap-graded, causing modifications to the mix design and increase of 18% in cement used to improve workability (FM 3.4 Exhibit 11 is a summary and details of grading reports during construction; details of mix-design modifications are discussed in another Failure Mode).
3. Concrete strength records show the effect of coarse aggregate presence. Tests of grout cores (Concrete without the coarse aggregate used to start each pour) were significantly stronger (pours 487 and 452 with grout mix SCM averaged 8700 psi) than concrete from the adjacent pours (pours 712, 685, 683, and 695 with mix DM-5-m averaged 7700 psi). Water to cement ratio (W/C) for the concrete mix averaged 0.41 and for the grout 0.40. (FM 3.4 Exhibit 10)

Verified Refuting Evidence:

1. Project specifications required aggregate compliance with ACI 301 and ASTM C 33 and concrete strength of 5000 psi at 28 days. (FM 3.4 Exhibit 1)
2. Original testing program (Law Engineering FM 3.4 Exhibit 2) confirmed that the aggregate complied with ASTM C 33 requirements and project specifications, and that the concrete met project specifications.



3.4 Inadequate Aggregate

3. Aggregates were tested for Alkali Reactivity and passed the ASTM C-277 mortar bar test. Subsequent Petrographic analysis confirmed that the aggregate was innocuous (FM 3.4 Exhibit 3, 4, 7, 7a).

Discussion:

1. Aggregate test data from time of original construction is very limited. It was therefore necessary to use industry reference (FM 3.4 Exhibit 12a, 12b, 12c, 12d) and current tests in the evaluation process.
2. Multiple Petrographic reports over the life of the structure provided the following:
 - a. Petrography identified the coarse aggregates as crushed limestone of various types, mainly microcrystalline and fossiliferous, many of which exhibit high porosity and permeability.
 - b. FM 3.4 Exhibit 4 indicated that about half of the CA particles were dense and firm while the rest were porous with chalky texture and contained shell fragments and fossils.
 - c. There was no evidence that the aggregate had been either chemically or physically unsound (FM 3.4 Exhibit 3, 4). PCA report (FM 3.4 Exhibit 5) identified one CA particle similar to those causing ASR reactions in Florida aggregates; however, no actual reaction was reported. CTL report (FM 3.4 Exhibit 6) agrees that there was no evidence of deleterious chemical reactions. Mactec report (FM 3.4 Exhibit 7 & 7a) identified CA pieces that retained moisture longer than other portions of a sample and exhibited localized evidence of alkali silica reaction (ASR) which is not a concern.
 - d. The aggregate contained less than 0.1% clay lumps (FM 3.4 Exhibit 4) while ASTM C 33 allows up to 5.0%; these soft and friable particles are expected to degrade during mixing and do not pose a problem.
 - e. Aggregate grading was lacking in the finer sizes of the coarse aggregate and coarser sizes of the fine aggregate (FM 3.4 Exhibit 3).
 - f. According to CTL report (FM 3.4 Exhibit 6) the aggregate/paste bond was tight and there was a "lack of major cracks and microcracks."
3. Exhaustive search of reports and publications over the years provided information regarding the properties of the Brookville coarse aggregate (FM 3.4 Exhibit 12a, 12b, 12c, and 12d are summaries). The highlights of the relevant properties include:
 - a. Shrinkage of concrete made with limestone is lower than most other types of aggregate (FM 3.4 Exhibit 12a). However, the Brookville aggregate used at CR3 exhibited the highest average shrinkage rates when compared to other Florida limestone.
 - b. Thermal coefficient of expansion for limestone is the lowest of all common aggregate types (FM 3.4 Exhibit 12b). Thermal diffusivity is among the highest of all aggregate types, indicating the enhanced ability to transfer heat through the material. There are no specific studies for the Brookville aggregate.
 - c. Aggregate reactivity potential exists in the Brookville limestone which may include lenses of reactive silica (FM 3.4 Exhibit 12c). However, the reactive silica is encountered in minimal quantities, and tests confirm that the aggregate is innocuous.
 - d. Modulus of Elasticity (E_c) of concrete made with Florida limestone is normally low and may be only 90% of the value calculated from the ACI 318 formula for normal concrete. Tests performed in 2009-2010 at CR3 on cores from the containment structure (FM 3.4 Exhibit 10) reveal much lower values than would be expected from high strength concrete (average measured E_c was 3.4E6 psi compared to calculated values of over 5E6 psi when using either compressive strength or weight in ACI 318 formulas). This may be caused by the coarse aggregate properties.
4. The coarse aggregate did not meet all the requirements of ASTM C-33 as specified:
 - a. According to FM 3.4 Exhibit 8 (appendix A attachment 2) the aggregate failed the ASTM C 88 test for soundness of aggregate (13.47% loss instead the 12% loss allowed) but was accepted based on service record.
 - b. Initially, the coarse aggregate did not meet the ASTM C-117 test for 200 sieve wash loss (2.3%



3.4 Inadequate Aggregate

compared to 1% maximum allowed according to FM 3.4 Exhibit 9). The ASTM C-117 test was repeated on a washed sample which passed the test (loss of 0.8%). According to FM 3.4 Exhibit 8 (appendix A attachment 2) the specified limit was raised to 1.5% to account for the fact that the material is crushed aggregate.

5. Deviations from ASTM C 33 grading requirements were made for Fine Aggregate based on satisfactory experience in local applications and the fact that both the US Corp of Engineers and the Florida State Road Department have modified the specifications to allow the use of these native aggregates. ASTM C 33 (AASHTO M 6) requirement for Fineness Modulus (FM) range of 2.3-3.1 was changed at CR3 to 2.2-2.7 to match the finer local sands.
6. The aggregate was ultimately accepted based on its local record of use and serviceability as well as acceptable properties of the concrete made with it (as allowed by ASTM C-33).
7. Analysis of aggregate grading (FM 3.4 Exhibit 11) establish the following:
 - a. Both CA and FA are lacking in particles in the #8 to #16 size range. As a result, the combined aggregate is "gap graded" and required additional cement to achieve the workability needed (cement quantities went from 635 lbs/cu.yd. in the initial mix-design to 682, 705 and 752 lbs/cu.yd as the project progressed). The strength and workability requirements of the concrete were met, but the additional Hardened Cement Paste (HCP) may have contributed to other potential problems such as creep and shrinkage.
 - b. Fineness Modulus (FM) was used as acceptance criteria for fine aggregates and shipments with FM below 2.2 were rejected. The coarse aggregate did not have FM as acceptance criteria and shipments with FM exceeding the recommended 6.5-6.9 range were regularly incorporated into the concrete (see Summary of Quality Control (QC) reports in FM 3.4 Exhibit 11).
8. Analysis of concrete strength records lead to the conclusion that aggregate strength limited concrete strength development. Grout cores (Concrete without the coarse aggregate that used to start each pour) tested significantly stronger than concrete from the same pour (FM 3.4 Exhibit 10 page 1-2 shows selected concrete test results while page 3 shows the test results for grout cores). These observations indicate that the presence of aggregate limits the tested strength of the concrete. This conclusion is further validated based on the observation of core fracture – where all cracks propagate through the aggregate and not around the interface zone. Although the concrete at CR3 is in full compliance with design criteria (5000 psi at 28 days) the aggregate limited the concrete's ability to reach the full strength potential of its low W/C and cement paste properties.
9. The relationship between compressive strength (f_c) and modulus of elasticity (E_c) has many different expressions in the literature and codes. Using these empirical relationships, the CR3 concrete would be expected to have E_c in the range of 4.75 to 5.25x10⁶ psi. However, the measured E_c was substantially lower, averaging 3.4x10⁶ psi. This can be explained by a lower than normal modulus of elasticity for the aggregate.
In general, aggregate properties will affect concrete E_c much more than its compressive strength. Accordingly, concrete made with weaker aggregate can meet strength specification while failing to achieve the E_c calculated from design formulas.
10. The aggregate impact on creep/shrinkage properties is governed by two mechanisms – it will either restrain creep by providing a volume of inert hard material, or increase creep by providing weakened interface zone on its surface. For the same aggregate volume, fine aggregate will have more surface area than coarse aggregate. Therefore, it will require more cement paste with larger effect on the creep properties. At CR3, the aggregates' grading resulted in increase of the finer fractions with the corresponding increase of creep and shrinkage potential. The presence of softer coarse aggregate reduced its ability to restrain that creep and shrinkage.
11. Normally, the coarse aggregate serves as a crack-arrestor in the concrete thanks to its higher



3.4 Inadequate Aggregate

strength and density. The presence of porous and fossiliferous particles introduces weakened locations where cracks may originate, or where existing cracks may propagate. The CR3 concrete had up to 50% of these weaker particles, which would have significant influence on its ability to stop propagation of cracks.

This would have a detrimental effect on the tensile strength and fracture energy of the concrete, especially when subjected to high tensile or shear stresses.

12. Analysis performed by PII in 2010 determined that reduced tensile strength properties of the concrete contributed to the delamination.

Conclusion:

Based on the available evidence it is concluded that the aggregate used for concrete at CR3 was relatively soft, porous, and gap graded. It produced concrete that met acceptable guidelines and requirements, but whose tensile strength, modulus of elasticity and ability to arrest cracks were substantially lower than expected from high-strength concrete. These reductions contributed to the delamination at the containment building through tensile stress failure and excessive shrinkage and creep.

3.5 Inadequate admixtures (R)



3.5 Inadequate Admixtures

Description:

Admixtures are materials, other than cement, water, aggregates, and reinforcement, used as ingredient of concrete and added to the batch immediately before or during mixing. Original records indicate that the two admixtures used were a water reducing retarding admixture (Daratard by W.R. Grace conforms to ASTM C-494) and air entraining admixture (Darex by W.R. Grace conforms to ASTM C-260). Air entrainment is normally added to concrete exposed to potentially destructive exposure such as freezing thawing cycles. It may also provide a limited benefit in workability improvement. Water reducer/retarder improves workability of low slump concrete while allowing more time for placing in high temperature conditions. Admixture use must be carefully controlled since excessive amounts of air can result in strength deficiencies, whereas excessive amounts of retarders can lead to delays in setting and early strength gain.

Data to be collected and Analyzed:

1. Original project specifications. (FM 3.5 Exhibit 1)
2. Concrete mix designs (FM 3.5 Exhibit 2)
3. Records of pour tickets (FM 3.5 Exhibits 3 is a representative example of all pour cards reviewed) and analysis of air measured (FM 3.5 Exhibit 4 analyzes data from all pour cards in RBCN-0012 and RBCN-0015)
4. Petrographic analysis (FM 3.5. Exhibit 5, 6 and 7)

Verified Supporting Evidence: None

Verified Refuting Evidence:

1. Project specifications (SP-5569) provide guidelines for admixture use (FM 3.5 Exhibit 1). Final specifications dated June 23, 1971 require 3-6% air entrainment, allow the use of Daratard, and forbid the use of admixtures containing Calcium Chloride.
2. Review of concrete mix designs (FM 3.5 Exhibit 2) and pour tickets (examples in FM 3.5 Exhibit 3) indicate that specifications were followed. Fly ash and admixtures containing calcium chloride were not used in concrete.
3. Analysis of total air content tests performed during construction show compliance with specified range of 3-6% air (FM 3.5 Exhibit 4).
4. Petrographic analysis was performed during the dome repair and in 2009. Analysis of Petrographic reports follows:
Original Petrography report by Erlin and Hime dated 5/10/1976 (FM 3.5 Exhibit 5) concluded that total air content was 5.5% and the "parameters of the air-void system are judged to be effective for protecting critically saturated concrete exposed to cyclic freezing."
5. CTL Petrography Report dated 11/2/2009 (FM 3.5 Exhibit 6) estimated that the concrete had 2-4% air content and that it could be considered "marginally air entrained..."
6. MacTec report dated 11/11/2009 (FM 3.5 Exhibit 7) indicated that "the concrete appeared to be air entrained and had a total air content estimated to around 2 to 3%."

Conclusion:

All documents reviewed show that the admixtures meet all requirements and are not a contributing factor in the delamination.

[Back to List](#)

3.6 Inadequate slump (Included in FM 2.3) (R)

3.7 Inadequate break test used to verify compliance (R)



3.7 Inadequate Concrete Testing

Description:

Construction projects require a quality assurance (QA) program that, among other things, involves the selection of test methods, establishing test criteria, testing the fresh concrete, testing the hardened concrete, statistical analysis of test results, and follow-up procedures.

Fresh concrete is tested for its workability (Slump test), temperature, and air content.

Hardened concrete is tested for its strength under compressive loading. The purposes of strength tests of concrete are to determine compliance with a strength specification and to measure the variability of concrete (ACI 214 provides a discussion of methods and analysis for strength tests of concrete).

It is necessary to establish the quality of the test program in order to be able to evaluate its results and conclusions.

Data to be collected and Analyzed:

1. Review project QA program (FM 3.7 Exhibits 1, 2, 10)
2. Review test procedures and results (FM 3.7 Exhibits 3, 4, 7)
3. Review analysis and reporting procedures (FM 3.7 Exhibit 9).
4. Analyze follow-up procedures (NCRs). (FM 3.7 Exhibit 5)
5. Analyze test program for compliance with industry standards. (FM 3.7 Exhibit 6, 9).

Note: Original exhibit 8 is no longer part of FM 3.7.

Verified Supporting Evidence:

None

Verified Refuting Evidence:

1. The established QA program was found to be comprehensive and covered all critical testing areas.
2. All pour records for RBCN-0015 were reviewed and found to comply with the parameters of the QA program.
3. Although some strength test results appear to be erroneous, the overall program meets industry standards for Good Control.
4. When errors are found in individual strength tests it is possible to make proper evaluation of the concrete strength by analyzing earlier (7 days) or later (90 days) tests from the same cylinder set. It is believed that no under-strength concrete was allowed in the structure as a result of inadequate testing.

Discussion:

1. Fresh concrete is subjected to a set of "acceptance" tests that determine whether it should be used or discarded. The test criteria and procedures were established in PTL's documents shown in FM 3.7 Exhibit 3 and specifications FM 3.7 Exhibits 1 & 2.
 - a. The Slump test is a practical test for workability that is also useful in determining if the concrete was modified or if it was mixed for extended period of time. Project specifications allowed Slump of 4.5" at the pump and 4" at the discharge (FM 3.7 Exhibit 10). Analysis of all pour records for RBCN-0015 and 0012 indicate that a strict inspection/testing process was followed and that multiple trucks were rejected when the allowed slump was exceeded. (Representative examples of reported tests and rejection handling in FM 3.7 Exhibit 4). A more complete discussion can be found in FM 2.3.
 - b. Air content was measured using the pressure meter on selected trucks. The specifications called for air in the range of 3-6%. All tests fell in that range and no concrete was rejected because of air.



3.7 Inadequate Concrete Testing

(Representative examples of reported tests in FM 3.7 Exhibit 4)

- c. Ambient and concrete temperatures were recorded on selected loads. Trucks were rejected (or accepted after Engineer's approval) when concrete temperature exceeded 70 degrees. (Specifications at FM 3.7 Exhibit 2; examples of reported tests in FM 3.7 Exhibit 4 and rejection handling in FM 3.7 Exhibit 5). A more complete discussion can be found in FM 2.5.
2. Hardened concrete was tested for compliance with design strength over time by crushing site-made cylinders after 7, 28, and 90 days.
 - a. Records of Statistical analysis of compressive tests from original construction time, as recommended by ACI 214, were not found.
 - b. Spot checks (by PII) of random test results revealed problems with laboratory strength tests. An example in FM 3.7 Exhibit 6 reports test results from two adjacent samples taken on 2/16/73 from pour 712RB. Cylinder 2181 shows normal strength gain between 7 and 28 days (28%) and very small gain between 28 and 90 days (7%). Cylinder 2182 shows small strength gain between 7 and 28 days (7%) and very large gain between 28 and 90 days (37%). At 28 days cylinder 2181 was 28% stronger than cylinder 2182, whereas at 90 days the trend reversed and 2181 was 10% weaker than 2182. The most likely explanation is testing error at 28 days.
According to the pour tickets these two loads were practically identical and in full compliance with the mix design (FM 3.7 Exhibit 7).
There is no record of concern or corrective measures arising from these tests.
- c. Current analysis by PII of all cylinders from 5000 psi concrete placed in the Reactor Building (RB) is included in FM 3.7 Exhibit 9. Besides providing a complete picture of the 28 days strength tests, it established that the test program met ACI 214's requirements for "Good" Standard of Concrete Control (ACI 214-77, Table 3.5 assigns Good control when Standard Deviation (StD) is in the range of 500-600 psi). 200 tests for mix 727550-2 had a StD of 541 and 239 tests for mix DM-5 had a StD of 508. The combined 439 samples had a StD of 527.
The "Good" Standard of Control for general field construction testing may be explained by the multiple mix-designs used and by testing problems as demonstrated above

Conclusion:

The testing program and follow up procedures for concrete material that was placed in the containment wall was adequate and testing was not a contributor to the delamination.

4.1 Excessive plastic shrinkage (R)



4.1 Excessive Plastic Shrinkage

Description:

Plastic shrinkage cracks occur when fresh concrete is allowed to dry before setting is complete. These cracks are usually parallel, shallow, and do not extend through joints. In general, plastic cracking is not considered a cause for strength deficiency or durability problems.

Plastic cracks can be a problem when they serve as initiation for later cracking due to stresses through the life of the structure.

Data to be collected and Analyzed:

1. Review reports from original construction regarding plastic shrinkage. (representative records in FM 4.1 Exhibit 1)
2. Inspect SGR hole cut zone for visible surface cracks.

Verified Supporting Evidence:

None

Verified Refuting Evidence:

1. Search for reports or NCRs addressing plastic shrinkage of the containment structure did not locate any.
2. Records of construction methodology, and especially curing and form stripping records, indicate that the concrete was not exposed or allowed to dry for at least seven (7) days after pouring as recommended by concrete industry standards. (representative sample from exhaustive search in FM 4.1 Exhibit 1; specifications sample in FM 4.1 Exhibit 2)
3. Visual inspections of the SGR hole cut zone by PII did not identify cracks with the typical appearance of plastic shrinkage cracks.
4. Plastic shrinkage cracks (when present) are perpendicular to the surface and would not be a factor in the observed delamination.

Conclusion:

Plastic shrinkage was not excessive and was not a contributor to the delamination.

4.2 Excessive shrinkage (Includes FM 4.3 and 4.4) (R)

**4.2 Excessive Shrinkage** (Includes FMs 4.3 and 4.4)**Description:**

Concrete will shrink when it dries. In fresh concrete, the volume of water mixed with the cement and aggregates can be significant. As concrete dries, the excess water is removed - causing shrinkage in the HCP and leaving behind voids of various sizes. Cracks may result if the concrete is restrained. The extent of shrinkage depends on a combination of factors including the volume of water in the fresh concrete, the aggregate/cement paste ratio, the water to cement ratio and the concrete's strength and rigidity at the time of moisture loss. Coarse aggregate properties, especially its modulus of elasticity and content, are also important factors in concrete shrinkage. Therefore, to minimize drying shrinkage, concrete should be batched with the smallest volume of water needed for workability and the largest aggregate fraction practical. It should also be kept moist (wet cured) until it gains enough strength and rigidity to withstand the stresses of drying shrinkage. When these preventive steps are deficient, the concrete may crack and/or develop micro-cracks where cracks initiate due to stresses later in its life. Concrete shrinkage may also be the result of autogenous process where water is consumed in the hydration process without external loss (formerly FM 4.3). Another shrinkage cause is carbonation shrinkage which is a byproduct of the carbonation process (formerly FM 4.4). These secondary processes result in limited shrinkage whose effect cannot be separated from drying shrinkage.

Data to be collected and Analyzed:

1. Review original pour records for water to cement ratio and water content.
2. Observe microstructure of concrete for indications of early volume changes due to drying shrinkage (microscopic analysis through Petrography).
3. Test for carbonation levels and depth by Petrographic analysis
4. Review curing specifications and records.

Verified Supporting Evidence:

None

Verified Refuting Evidence:

1. Water to Cement ratio and total water content were relatively low. (analysis of pour cards in FM 4.2 Exhibit 6)
2. No shrinkage cracks were reported in regular inspection reports over the years and none were observed in cores obtained from the structure. (see discussion next)
3. Observed carbonation levels were low. (Petrographic reports FM 4.2 Exhibits 1, 2 & 5 and following discussion)
4. Curing was found to be satisfactory. (selective curing logs in FM 4.2 Exhibit 3 and specifications in FM 4.2 Exhibit 4)

Discussion:

Petrographic analysis reports did not provide direct evaluation of shrinkage history. However, both CTL and Mactech reports (FM 4.2 Exhibits 2 & 5) indicate minimal depth of carbonation (4-5mm from outer surface in CTL report; ¼ to ½ inch in Mactech report) and therefore no issue of carbonation shrinkage. CTL report also noted that only a small number of randomly oriented micro cracks were observed. Erlin & Hime report did not address either of these issues and did not provide insight (FM 4.2 Exhibit 1 was included here for completeness only). Curing log reports show that the concrete was not allowed to dry for at least seven (7) days, at which time



4.2 Excessive Shrinkage (Includes FMs 4.3 and 4.4)

it exceeded 4000 psi compressive strength. It is therefore expected that early drying shrinkage was not an issue.

Original pour records (summarized in FM 4.2 Exhibit 6) show a relatively low water to cement ratio (W/C in the range of 0.38 to 0.40) and low total water content (note: w/c range reflects the fact that multiple mix designs were used).

Petrographic analysis indicates relatively low W/C ratio and relatively dense cement paste. These observations leads us to conclude that the concrete had relatively low potential for drying shrinkage.

Exhaustive review of IWL surveillance reports of the containment structure did not identify any surface cracks of the type expected from excessive shrinkage (typically parallel, evenly spaced cracks)

Conclusion:

Shrinkage during the early age, due to drying, autogenous shrinkage, or carbonation was not excessive and was not a contributor to the delamination.

4.5 Excessive basic creep (R)

4.6 Excessive drying creep (R)



4.5 Creep (basic and drying) (Includes FM 4.6)

Description:

Basic (or true) creep is the time-dependent increase in strain under sustained load of a concrete specimen in which moisture losses or gains are prevented (sealed specimen). Drying creep is the additional creep occurring in a specimen exposed to the environment and allowed to dry. In the case under consideration it is not practical or necessary to separate the two and the following will address the total creep experienced by the structure.

Many of the terms used in this FM are found in FM 4.5 Exhibit 8, a study performed on the replacement concrete to be used at CR3 to fill the SGR opening.

Creep is influenced by multiple variables including:

1. Concrete properties: aggregate/paste volume, modulus of elasticity of the paste and aggregate;
2. Environmental: temperature and humidity;
3. Structural: restraint, size effect, stresses, and time.

Since creep happens in the hardened cement paste (HCP) through moisture and void redistribution, the total quantity as well as quality of the HCP is a major consideration. The larger the HCP volume and the lower its modulus of elasticity (E_c) the larger the total creep. The aggregates can reduce creep by reducing the total HCP content and by providing restraint due to their stability and rigidity. In high strength concrete, or when soft aggregate is used, the aggregate may be unable to provide restraint and could undergo creep as well.

Creep is primarily the result of reduction of void volume in the HCP. Therefore, it has the potential for increasing the strength and reducing the apparent micro-cracking in the concrete. This makes a positive contribution to the concrete properties. However, in pre-stressed structures, concrete creep results in at least three issues (FM 4.5 Exhibit 18):

1. Time-dependent losses in the pre-stressing force that could result in pre-stress levels below design requirements;
2. Large deformations of the containment structure;
3. Residual stresses induced as the loading conditions change.

A typical creep curve can be seen in the study performed by CR3 on the replacement concrete to use at the end of the SGR opening operation (FM 4.5 Exhibit 17).

Removal of the load results in instantaneous elastic recovery, followed by creep recovery (FM 4.5 Exhibit 8 Figure 7 on page 18 of 31). This can cause localized increase in micro-cracks with corresponding reduction in strength properties. This creep spring-back can contribute to micro-cracking during detensioning.

This FM combines basic creep (FM 4.5) and drying creep (FM 4.6).

Data to be collected and Analyzed:

1. Calculation of the order of magnitude of elastic and creep strains to be expected in a post-tensioned concrete containment such as CR3 (FM 4.5 Exhibit 1 lists the basic calculations used to get an order of magnitude of the numbers involved);
2. Calculate relationship between creep strain, creep coefficient, and tendon force losses (FM 4.5 Exhibit 2 is a detailed derivation of the specific creep parameter, and FM 4.5 Exhibit 3 is an estimate of the creep coefficient at CR3);
3. Review tendon force loss mechanisms (FM 4.5 Exhibit 4) and tendon force loss calculations (FM 4.5 Exhibit 5);
4. Review input parameters to force loss curves (FM 4.5 Exhibit 6 is a part of the CR3 Design Basis Documents);
5. Review original basis for the specific creep values used at CR3 (FM 4.5 Exhibit 7 is the original



4.5 Creep (basic and drying) (Includes FM 4.6)

Schupack study used to determine the specific creep value at CR3);

6. Review tendon surveillance lift-off data and compare the Shop and Field lift-off data collected during containment IWL inspections (FM 4.5 Exhibit 9 displays the tendons that were tested during surveillance activities over the years, FM 4.5 Exhibit 10 displays the shop and field measurement data for the various surveys and FM 4.5 Exhibit 11 is a summary of all these data);
7. Investigate possible correlation between hoop tendon force lift-off non-symmetry and location of the lift-off (FM 4.5 Exhibit 12);
8. Draw tendon force curves for hoop tendons tested multiple times in bay 34 (FM 4.5 Exhibit 13);
9. Measurements to determine if the containment was subjected to gross deformation due to creep (FM 4.5 Exhibit 19 is a laser scanning study of the inside circumference of containment, performed on the liner plate, and FM 4.5 Exhibit 20 is a survey study of the dome and of the buttresses);
- 10 Creep tests performed at the University of Colorado on concrete material cores taken from CR3 containment (FM 4.5 Exhibit 14 reports on the experimental tests performed, and FM 4.5 Exhibit 15 is an analysis of the results).

Verified Supporting Evidence:

1. Examination of the tendon surveillance records indicate series of adjacent hoop tendons that did not meet the requirement of being above 95% predicted value (FM 4.5 Exhibit 9 and FM 4.5 Exhibit 10);
2. There are examples of tendon force loss curves that show a force loss with time that is faster than predicted values. For example, in FM 4.5 Exhibit 13, re-tensioning was performed on tendons between buttresses 4 and 2 and between buttresses 6 and 4;
3. The correlation of the lift-off measurements with the mix design and pour time is good (FM 4.5 Exhibit 12). Specifically, panels 34 and 61 were poured with a mix richer in cement (mix DM-5M, richer by about 8%) and were poured later than panel 12, 23, 45, and 56. FM 4.5 Exhibit 12 shows the correlation between lift-off measurement point location and presence of mix DM-5M. The force measured near panels 34 and 61 is higher than that measured at other panels. This indicates a differential creep between the various panels.

Verified Refuting Evidence:

1. Creep is primarily the result of reduction of void volume in the HCP. Therefore, it has the potential for increasing the strength and reducing the apparent micro-cracking in the concrete. This is a positive contribution to the material;
2. No gross deformation of the entire containment structure was detected with laser scanning of the inside of containment and survey of the dome and buttresses (FM 4.5 Exhibit 19 and FM 4.5 Exhibit 20);
3. Very high creep strains, for example associated with a creep coefficient of 5.0, would be obvious in terms of tendon force losses (FM 4.5 Exhibit 1). This was not observed in practice (FM 4.5 Exhibit 10)

Discussion:

In a large concrete structure like the CR3 containment, where the surface to volume ratio of the concrete is small, drying creep tends to be negligible (FM 4.5 Exhibit 7).

Additionally, shrinkage is also governed by the surface to volume ratio, and is expected to be very small for a large structure with little access to the surface to lose or gain moisture (FM 4.5 Exhibit 7).

This study of creep is to determine the magnitude of the effect of creep in the delamination event.

The CR3 containment tendon surveillance history for measured tendon liftoff forces shows numerous tendons with liftoff forces that were below the predicted "base" values. There are four phenomenon combined in the tendon force losses as measured by lift-off forces in the tendons over time (FM 4.5 Exhibit 4 and FM 4.5 Exhibit 5):



4.5 Creep (basic and drying) (Includes FM 4.6)

1. Elastic shortening;
2. Concrete shrinkage;
3. Concrete creep;
4. Wire relaxation.

Elastic shortening and concrete shrinkage occur early in the life of the containment, while concrete creep and wire relaxation are time-dependant and continue to progress over the years. As the concrete creeps, the strain in the concrete drops, and thereby the tendon force drops.

FM 4.5 Exhibit 1 shows that a creep strain of 500 micro-strains corresponds approximately to the elastic strain upon loading of the concrete (creep coefficient equals 1). It also shows that 500 creep micro-strains corresponds to a tendon force loss of 140 kips on the hoop tendons. Looking at the order of magnitude of force losses at CR3 (FM 4.5 Exhibit 10), it appears that the creep coefficient is not larger than 2.0 (for a loss lower than 280 kips). Based on FM 4.5 Exhibit 2 work on specific creep in the case of CR3, we concluded that the creep coefficient is approximately 1.63 (FM 4.5 Exhibit 3).

Note that the most convenient approach to working with creep in a tri-axial stress state as present in a nuclear concrete containment is to determine the specific creep of the material, or creep strain per unit load applied, typically given in micro-strains per psi. This is the approach taken in FM 4.5 Exhibit 2, in FM 4.5 Exhibit 7, and in FM 4.5 Exhibit 16 page 3 of 7.

The analysis of the creep tests performed on CR3 concrete conclude that the ultimate creep coefficient is 2.39 and that for all periods of time less than infinity, the creep coefficient will be lower than 2.39 (FM 4.5 Exhibit 15). This is in general agreement with our calculation.

A large number of adjacent tendons with high asymmetry might be indicative of:

1. Differences in concrete condition along the tendon arc, such as a section of pre-existing cracked/delaminated concrete;
2. Differences in concrete condition along the tendon arc, such as a section with varying creep;
3. A bias in lift off measurement equipment utilization at one end of the tendon during surveillance.

The correlation of the lift-off measurements with the neighbor panel is excellent (FM 4.5 Exhibit 12). Specifically, panels 34 and 61 were poured with a mix richer in cement (mix DM-5M, richer by about 8%) and were poured later than panel 12, 23, 45, and 56. FM 4.5 Exhibit 12 shows the correlation between lift-off measurement point location and presence of mix DM-5M. The force measured near panels 34 and 61 is higher than that measured at other panels. This is the first successful correlation discovered regarding the non-symmetrical lift-off measurements at CR3.

Note that in modeling the structure, the time-dependant creep is often treated using a creep coefficient and an effective modulus of elasticity that is reduced to account for the addition of creep strain to the elastic strain (FM 4.5 Exhibit 16 page 2 of 7 and page 6 of 7). This has been applied extensively in the PII models.

Panels 34 and 61 have a concrete mix richer in HCP. This can lead to higher creep strains and higher shrinkage strains. Panels 34 and 61 also were poured later and therefore were younger at the time of concrete tensioning. This can also lead to higher creep strains and higher shrinkage strains.

Conclusion:

Creep is higher at CR3 than predicted in the tendon force loss calculations. A likely number for the creep coefficient today is 1.63. Creep did not generate the delamination.



4.7 Excessive stresses from differential material properties

Description:

When concrete mixes of different physical properties are combined they may perform differently under stress. These differences can cause stress concentrations at the interface, leading to bond failure and cracking. In concrete construction it is possible to have concretes of different strength placed adjacent to each other while expected to perform as a uniform material with the same properties.

The purpose of this document is to determine if such conditions existed at the delamination area and contributed to the delamination.

Data to be collected and Analyzed:

1. Review original records for concrete mixes used in the construction of the structure (FM 4.7 Exhibit 3).
2. Review pour records for information on materials used in adjacent lifts (FM 4.7 Exhibit 4 is a graphical summary).
3. Test core samples from different concrete/grout mixes. (FM 4.7 Exhibit 1 is a summary of core tests, presented with original strength data for the corresponding pours)

Verified Supporting Evidence:

1. Three different concrete mixes were used in bay RBCN-0015. A total of four concrete mixes were used in the containment structure for the 5000 psi level.

Verified Refuting Evidence:

1. Different concrete mixes were used in the containment structure. It appears that this was allowed as long as the strength exceeded the design strength and the strength variation was acceptable. FM 4.7 Exhibit 2 is a statistical analysis of the four main mixes used anywhere in the containment structure. It shows that for mixes DM-5, DM-5-M, 727550-2, and 727550-2-M the average strength was 5690 psi, 6000 psi, 5900 psi, and 5700 psi (with Standard deviation of 495 psi, 500 psi, 620 psi, and 390 psi) respectively.

Discussion:

1. The concrete mixes used in the containment wall had similar physical properties and are not expected to have significantly different strength properties. The same materials (aggregates, cement and admixtures) were used for all concrete variations. (FM 4.7 Exhibit 3)
2. Statistical analysis was performed only on compressive strength results since a statistically significant number of tests was available for compressive strength only. However, Modulus of Elasticity and Tensile strength are directly related to compressive strength and are expected to show the same trends. This was confirmed by a small set of core tests.
3. Even when placed on top of each other, different fresh concrete mixes in the same pour (mostly concrete placed over grout) were blended at the interface by adequate vibration (see FM 2.7). This procedure prevents the creation of defined interface and eliminates differential properties at the location.
4. All interfaces between different concrete mixes in the wall were horizontal and full depth. It is not expected that such interface could have a significant effect on delamination in the vertical plane.

Conclusion:

There were no excessive stresses from differential material properties in the containment wall and this Failure Mode did not cause the delamination.



4.8 Cyclic Loading

Description:

Concrete structures exposed to cyclic changes in stresses, humidity, or temperature can be damaged by fatigue even when the cyclic stresses are not large enough to cause failure in one application. Fatigue damage starts at the pre-existing microcracks at the aggregate interface, inserts interface and voids. A large number of these cycles can lead to propagation and extension of the micro-cracks into larger, structurally significant cracks. These cracks can expose the concrete to environmental attacks and allow increased deflections. The structure will fail as a result of excessive cracking, excessive deflections, or brittle fracture.

Normally, concrete structures are designed to codes which limit design stress levels to a point that fatigue is not an issue. However, localized fatigue damage may develop at locations exposed to excessive cyclic loading such as at machine connections.

The purpose of this document is to determine if the containment structure was exposed to excessive cyclic loading and if it contributed to the delamination.

Data to be collected and Analyzed:

1. Design for fatigue (FM 4.8 Exhibit 1 is a section of ACI 215R)
2. Containment structure exposure to cyclic loads.
3. Indications of fatigue related degradation.
4. Analysis of thermal stresses in mass concrete (FM 4.8 Exhibit 3 is a presentation of thermal stress analysis by P. K. Mehta of UC Berkeley)
5. Physical properties of the concrete (FM 4.8 Exhibit 4 is a summary of measured physical properties for the concrete used in the delaminated panel at the CR3 containment; FM 4.8 Exhibit 5 is a report of concrete tests dated June 1971)
6. Thermal analysis of containment structure interior (FM 4.8 Exhibit 6 and 7)
7. Dome delamination report on thermal stresses (FM 4.8 Exhibit 2)

Verified Supporting Evidence: None

Verified Refuting Evidence:

1. The containment structure has not been subjected to significant high cycle fatigue loadings (such as vibration or impact) during its operations history.
2. The only significant cyclic stresses are from thermal cycles that are not large enough to cause significant damage (see discussion)
3. There are no indications of failure (see discussion)

Discussion:

1. Thermal stresses inside the concrete are a function of its restraint, elastic modulus, coefficient of thermal expansion, creep coefficient and temperature change, expressed as:

$$\sigma_t = K_r \frac{E}{1 + \phi} \alpha \Delta t$$

(from page 4 of FM 4.8 Exhibit 3)

In the case of CR3, the elastic modulus (E) was measured at 3.63E6 psi (FM 4.8 Exhibit 4) and the coefficient of thermal expansion (α) was 6.5E-6 in/in/deg F (FM 4.8 Exhibit 5). The degree of restraint (K_r) can vary between 1.0 (fully restrained) and 0.0 (unrestrained). A conservative estimate of K_r for interior of the wall at mid-span at CR3 is taken as 0.75. Because of the short thermal cycle time (daily)



4.8 Cyclic Loading

it is determined that creep was not significant and the creep coefficient (ϕ) for the calculation was taken as zero.

The resulting expression for thermal stress at CR3 is therefore: $\sigma_t = 17 \cdot \Delta t$ (each degree change results in 17 psi stress)

Because of the conservative estimates this expression will result in tensile stresses that are at the high end of possible stresses.

2. Design considerations from ACI 215R (FM 4.8 Exhibit 1- Fig. 1) correlate probability of failure to number of cycles and the ratio of stress to ultimate strength. For example, 10,000 cycles at 70% of ultimate strength have a 5% probability of failure. At 80% of ultimate strength the probability of failure is as high as 80%. At 60% of ultimate strength we will need a million cycles to reach a probability of failure of 5%.
3. Measured tensile strength of the concrete at CR3 averages about 600 psi (split tensile tests). It will require over 10000 cycles with stresses exceeding 420 psi (70% of 600 psi) to reach a probability of failure of 5%.
4. Reported daily temperatures over time for the area were analyzed. The effect of solar exposure was also analyzed and added to the ambient temperatures in order to arrive at outside wall temperatures at the location of maximum exposure (south facing panel).
5. During normal operations the interior of the containment building is maintained near 130°F (FM 4.8 Exhibit 6). These temperatures are higher than the calculated external wall temperatures and will not cause tensile stresses in the concrete. Therefore days of normal operation do not contribute to the thermal cycles.
6. During outages the interior temperature is significantly lower and the thermal differences will be sufficient to cause higher tensile stresses in the concrete. Only these days count towards the total number of cycles that introduce significant tensile stresses in the concrete.
7. Based on temperature records over the years and the number of expected outages it is estimated that the structure will experience between 1400 to 1900 significant daily cycles (with solar exposure) during outages in its expected lifetime of 60 years. Temperature range (inside the concrete) during these days is estimated to average about 10°F (conservative estimate of Δt from FM 4.8 Exhibit 7). This range is equivalent to 170 psi ($17 \cdot \Delta t$) maximum tensile stress experienced by the concrete.
8. The temperature inside the concrete was estimated using measurements taken in 2010 during the current delamination investigation (FM 4.8 Exhibit 7).
9. Based on the above it is determined that there is substantially less than 5% probability of damage to the concrete as a result of thermal cycles over its lifetime.
10. Damage to concrete from thermal cycles would be the result of tensile stresses that cause microcracks to grow and multiply. Theoretically, such damage might be detected through Petrography and through comparative strength tests between damaged and undamaged areas. However, due to the normal scatter of strength tests it is not possible to determine such damage to any significant certainty. Tensile strength tests throughout the structure did not provide any usable indication of distress level since the expected test variation exceeds the differences observed in the tests. Petrographic studies on concrete from the outer ten inches of the wall showed no significant pattern of increase in microcracking. This issue of microcracking is covered in depth in another Failure Mode (FM 1.11).
11. Analysis performed during the Dome Delamination event on 1976 reached the same conclusions using a different approach. FM 4.8 Exhibit 2 is that analysis and is provided here as a reference.

Conclusion:

There were no excessive stresses from cyclic loading in the containment wall and this Failure Mode did not cause or contribute to the delamination.



5.1 Contamination during construction

Description:

During construction operations it is possible for contaminants to get mixed with the fresh concrete. Some of these materials have the potential to weaken the concrete and/or affect its durability. Source of contamination can be dirty aggregate that may include organic material or other reactive elements. Another source is construction related material such as grease/oil, nails/ties, tools and safety items, clothing, cigarettes, food, and other debris.

Foreign material can impact the concrete by either replacing sound concrete with weak/incompatible filler, or by adding reactive elements that react inside the concrete. Contamination can be detected by inspections during construction, visual inspections for signs of distress such as spalls and cracks, and analysis of concrete removed from the structure (during demolition and coring).

Precautions involve strict control of aggregate sources, good construction and safety practices, and effective Quality Control (QC) program that monitors potential for contaminations.

The purpose of this document is to establish if any contaminants were found in the concrete, and if these contaminants contributed to the delamination.

Data to be collected and Analyzed:

1. Review project specifications for requirements
2. Review project QC procedures
3. Review aggregate evaluation from original construction (FM 5.1 Exhibit 5 is a report by Law Engineering)
4. Review Non Compliance Reports (NCR)
5. Review Petrographic reports for signs of contamination.
6. Review inspection records (IWL), observations during demolition, and core inspections for indication of contamination.

Verified Supporting Evidence:

1. Exhaustive review of NCR reports revealed an incidence where sand pocket was found after form removal. (FM 5.1 Exhibit 3) QC procedures failed to detect the contaminant before concrete placement (FM 5.1 Exhibit 4). It was, however, detected upon form removal and corrective measures were taken to repair the problem. A second incidence mentioned in FM 5.1 Exhibit 3 was in pour #644 which is not in the delaminated panel.

Verified Refuting Evidence:

1. Project specifications included cleaning requirements for forms and existing concrete prior to concrete pour. (FM 5.1 Exhibit 1)
2. Project QC specifications provided requirements for preventing contaminations and for proper inspections and reporting (FM 5.1 Exhibit 2)
3. The isolated incidents mentioned above demonstrate that even when a problem was missed by pre-pour inspections it was detected and corrected in post-pour inspections. Overall, the QC program proved effective in preventing contamination.
4. Tests on original aggregate by Law Engineering are reported in FM 5.1 Exhibit 5. There was no mention of any organic impurities or other contaminants.
5. Multiple Petrographic reports on concrete cores taken in 1975 and 2009 did not encounter contaminants (FM 5.1 Exhibit 6 is a representative report by Mactec). There was also no indication of weakened aggregate/paste interface as might be expected from dirty aggregates.



5.1 Contamination during construction

6. Exhaustive review of inspection reports (IWL) found no indication of spalling or cracking that could be attributed to contaminants.
7. Detailed review of cores taken during 2009 found no indication of contaminants. Thorough analysis of photos taken during and after the demolition did not detect any signs of contamination in the concrete.

Discussion:

The evidence presented above describes a system that provided guidelines and inspection tools needed to prevent contamination of the concrete. The isolated report (FM 5.1 Exhibit 3 & 4) of contaminant in the concrete also describes the methodology for removing and repairing the contaminated concrete.

Although QA/QC is not the subject of this FM, a limited discussion was included for completeness in order to establish the methodology for detecting and removing contaminants.

Conclusion:

There is no evidence of undetected contamination during construction and it was not a contributing factor to the delamination.



5.2 Salt Water related distress

Description:

Concrete exposed to salt water can, over time, lose its ability to protect the embedded iron from corrosion. Concrete exposed to wetting/drying by salt water can suffer deterioration related to chemical reactions and cycles of shrinkage/expansion.

This document will attempt to determine whether the concrete was exposed to sea water, without addressing the corrosion issue that is analyzed in another Failure Mode.

Data to be collected and Analyzed:

1. Determine areas where salt water is utilized.
2. Evaluate concrete samples for effects of salt water exposure. (Petrographic reports in FM 5.2 Exhibit 1, 2 and 3)
3. Test concrete for Chloride exposure.

Verified Supporting Evidence:

None

Verified Refuting Evidence:

1. Salt water used for cooling is separate from the containment structure. There is no direct exposure of the containment concrete to raw sea water.
2. The containment structure is not exposed to chloride ions from spray (located over 1.25 miles from the Gulf of Mexico)
3. Concrete cores obtained from the structure showed no evidence of salt water exposure. (FM 5.2 Exhibit 1, 2 and 3 – Petrographic reports by CTL, Mactech, and Erlin & Hime)
4. Chloride profile of a concrete cores shows insignificant chloride content (FM 5.2 Exhibit 4)

Discussion:

Petrographic analysis did not note any signs of salt water related distress. CTL (FM 5.2 Exhibit 3) concluded that “no evidence is exhibited of any deleterious chemical reactions involving the cement paste and/or aggregates.” The other two Petrographic reports are included as exhibits for completeness and do not contain direct reference to distress typical of sea water exposure.

Chloride profile confirmed that there was no significant exposure to salt water.

Conclusion:

Salt water did not impact the structure and did not cause distress related to the delamination.

5.3 Chemicals introduced during routine maintenance (R)



5.3 Chemicals introduced during routine maintenance

Description:

Routine maintenance of industrial structures can involve the application of deleterious materials, including solvents, cleaning agents, or aggressive water.

ACI committee 515 compiled a list of potential deleterious materials, most of which are either harmless to good quality concrete, require high concentrations, will only attack porous concrete, and/or must be dissolved in water in order to penetrate the concrete.

The issue of chemical attack is addressed in another Failure Mode (FM).

This document is intended to identify any materials used in maintenance of the concrete shell and determine if these materials could have damaged the concrete.

Data to be collected and Analyzed:

1. Interview Crystal River 3 personnel regarding practices that might affect the concrete (FM 5.3 Exhibit 1, 3 and 4).
2. Review and analyze information regarding possible deleterious materials (FM 5.3 Exhibit 2 is the comprehensive list of potential harmful chemicals compiled by ACI 515).
3. Review Petrographic reports for signs of contamination.

Verified Supporting Evidence:

None

Verified Refuting Evidence:

1. Interviews with personnel of Crystal River 3 (CR3) reveal that no chemicals were applied to the concrete during regular maintenance.
2. Grease solvent was used occasionally to clean grease stains outside the delamination area. There is no expectation or indication of damage to the concrete from the Petroleum Hydrocarbon Distillate.
3. FM 5.3 Exhibit 1 mentions a onetime application of linseed to the dome after delamination repairs in 1976. Linseed is not considered harmful to concrete, was used as a sealant for the newly repaired dome, and had no impact on the containment wall where the delamination happened.
4. Multiple Petrographic reports on concrete cores taken in 1975 and 2009 did not encounter contaminants (FM 5.3 Exhibit 5 is a representative report by Mactec).

Conclusion:

Routine maintenance did not involve significant exposure of the concrete to deleterious chemicals and was not a contributing factor to the delamination.



5.4 Concrete Form Release Agent

Description:

Release agents are applied to the form contact surfaces to prevent bond and facilitate stripping. They may be applied to the form before each use, at which time care must be exercised to prevent coating adjacent construction joint surfaces or reinforcing steel. A good release agent should provide a clean and easy release without damage to either the concrete face or the form, while contributing to the production of blemish free surface. It should have no adverse effect upon either the form or the concrete surface. When applied improperly, form oil may prevent bond between the concrete and reinforcing bars or weaken joints by preventing bond of old to new concrete.

Data to be collected and Analyzed:

1. Review concrete placement specifications.
2. Review Quality Control (QC) specifications.
3. Review QC reports.

Verified Supporting Evidence:

None

Verified Refuting Evidence:

1. Project specifications (FM 5.4 Exhibit 1 – Specification SP-5618) require that forms are thoroughly cleaned after each use, and surfaces in contact with concrete be coated with form oil which has been approved by the OWNER.
2. Project QC specifications (FM 5.4 Exhibit 2) included requirements for verifying form oiling and cleanliness of all surfaces prior to concrete placement.
3. QC reports (representative example in FM 5.4 Exhibit 3) show that inspectors followed the established QC specifications and monitored proper form coating. They also verified that the rebar was clean.
4. Exhaustive review of Non-Conformance Reports (NCRs) found no evidence of improper application of form oil during the construction of the containment building.

Conclusion:

Form release agents were applied properly and were not a contributing factor to the delamination.

5.5 Corrosion of rebars, sleeves, and tendons (R)



5.5 Corrosion of Rebars, Tendons, and Inserts

Description:

Corrosion of embedded metal is one of the main causes of failure of concrete structures (ACI 201.2R, ACI 222R). The critical elements needed for corrosion to occur are water, oxygen, and chloride ions, which in turn makes permeability the main concrete property that influences corrosion resistance. The high alkalinity (pH>12.5) of the concrete protects the thin iron-oxide film on the surface of the steel, thus making the steel passive to corrosion. The alkalinity can be reduced by carbonation or exposure to acidic solutions, allowing corrosion when oxygen and moisture are available. In the presence of chloride ions, the pH threshold for corrosion initiation is considerably higher than when chlorides are not present.

The initial stage of corrosion often produces cracking, spalling, and staining in the surrounding concrete. These can be detected by visual observations.

This document will attempt to identify basic properties of the concrete, type of exposure, and service conditions that affect its corrosion resistance.

Data to be collected and Analyzed:

1. Permeability of the concrete.
2. Design parameters that affect corrosion resistance.
3. Availability of chloride ions
4. Petrographic analysis for extent of carbonation
5. Visual observations of the tendons, rebars and sleeves over the life of the structure (IWL report in FM 5.5 Exhibit 7; highlighted summary of findings from the report in FM 5.5 Exhibit 8).
6. Chlorides profile in concrete cores (FM 5.5 Exhibit 9)

Verified Supporting Evidence:

None

Verified Refuting Evidence:

1. The concrete meets industry recommendations for low permeability required for durability (FM 5.5 Exhibit 1 – correlation between W/C and permeability; FM 5.5 Exhibit 2 – mix design; FM 5.5 Exhibit 3 – representative Petrographic reports; FM 5.5 Exhibit 4 – graph of water/cement ratio from pour cards).
2. Providing adequate cover of low-permeability concrete was part of the original design. Original plans called for concrete cover of 2 ¼" over the reinforcing bars (FM 5.5 Exhibit 5 is a copy of a representative plan with enlarged details).
3. Measurements taken during the demolition in 2009 show cover size in line with the plan requirements (FM 5.5 Exhibit 6 includes three representative photos taken in 2009 at the containment wall) and with ACI 117 (Standard Specifications for Tolerances for Concrete Construction and Materials) that allows cover variation of ±½" in elements thicker than 12".
4. The containment structure does not have direct exposure to chloride ions from spray (it is located over 1.25 miles from the Gulf of Mexico) or artificial sources (such as deicing salts). Salt water canals are located less than 100 yards from the structure and may add to the chloride exposure.
5. Petrographic analysis revealed a dense, low-permeability concrete with low depth of carbonation after over 30 years in service (FM 5.5 Exhibit 3b and 3c – reported measured carbonation depth of 0.2" to 0.5"). This level of carbonation is an indication that the concrete in the structure is not losing its ability to protect the metal inserts from corrosion.
6. Visual inspections over the life of the structure (2007 IWL in FM 5.5 Exhibits 7 and 8) detected multiple



5.5 Corrosion of Rebars, Tendons, and Inserts

instances of rust staining, spalling and cracking of the concrete. Most refer to staining from rusting nails and tie-wires embedded in the concrete. A few refer to corrosion of exposed reinforcing bars (not protected by cover) which did not cause degradation of the rebar or concrete and did not require remedial work. These bars were not part of the structure's reinforcing system

7. Tendon sheaths are located more than seven (7) inches from the outer surface of the wall. There was no indication of corrosion on sheaths or tendons removed during the 2009 demolition.
8. Chloride levels profile of the concrete proved that there was no significant intrusion of chlorides into the concrete (FM 5.5 Exhibit 9). Measured levels of 0.008 and 0.014 [% wt] are well below the ACI 201 recommendation of 0.06. Deeper measurements at the rebar level dropped to 0.002 which reflects the natural chlorides included in the original concrete.

Discussion:

Industry standards use water to cement (W/C) ratio as an indication of concrete's permeability. It has been established that concrete with W/C of 0.4 or lower has voids system that is mostly made of disconnected discreet small voids – making it practically impermeable (FM 5.5 Exhibit 1). FM 5.5 Exhibit 4 is a graph based on data from all pour cards of concrete used in panel RB-15 of the containment structure. It shows that all the concrete was placed with W/C ratio of less than 0.41, with an average of 0.40. FM 5.5 Exhibit 2 is a summary of mix designs used in the construction. These designs were prepared with W/C of either 0.41 or 0.38.

Based on the above it is concluded that the concrete has very low permeability.

Another source of moisture and chloride ingress can be surface cracks. IWL inspections did not identify open cracks through the surface concrete that exposed rebar or tendon. All rebars in the containment wall are protected by a low permeability cover of concrete, meeting design criteria and industry standards.

Conclusion:

The concrete in the containment structure did not experience corrosion of rebars or tendons. Therefore corrosion was not a contributor to the delamination.



5.6 Inadequate Grease Protection Capability

Description:

Grease is placed into the tendon sleeves primarily to protect the tendons. Routine tendon surveillance provides opportunities to evaluate grease losses, examine the grease for deterioration, and provide opportunities for grease contamination; all of which may result in tendon capability loss.

Data to be collected and Analyzed:

1. Interview tendon engineer regarding practices on grease maintenance (FM 5.6 Exhibit 1).
2. Review tendon surveillance specifications for grease analysis, grease replacement criteria, and leakage detection. (FM 5.6 Exhibits 2 and 3)
3. Review latest IWL surveillance for any issues related to tendon grease. (FM 5.6 Exhibits 4 and 5)

Verified Supporting Evidence:

None

Verified Refuting Evidence:

1. Latest Tendon grease inspection results demonstrate that no grease degradation occurred, grease chemical analysis results were all in specifications, and the grease provided the appropriate protection to the tendons. (FM 5.6 Exhibits 4, 5, and 9) See also FM 5.5 relative to no tendon corrosion.
2. Grease losses noted during last IWL (2007) were within specified limits. (FM 5.6 Exhibit 6)

Discussion:

1. Following surveillances over the last few years, Progress Energy has added higher density grease to the vertical tendon sleeves to make up for apparent grease losses. It has been concluded that grease settling in vertical tendons causes a need for more makeup grease in vertical tendons than would be required to replace the grease removed from the surveillance activity. (FM 5.6 Exhibit 1) If grease losses were occurring, then the grease would potentially not be available for tendon protection, and therefore, provide the opportunity for tendon reduced capacity.
2. PSC Procedure SQ 12.1 provisions PSC to Notify CR3 Engineering by an NCR if the absolute difference between the amount of grease removed from the tendon and the amount of grease replaced exceeds 10% of the net duct volume. (FM 5.6 Exhibit 3)
3. Interviews and containment pictures reveal no grease collecting in the area around the SGR Project opening that could have indicated grease losses from the sleeves removed in that area, thereby, confirming surveillances that grease losses were not occurring. (FM 5.6 Exhibit 1)
4. Grease was recently observed leaching from containment concrete surface cracks located under the equipment hatch. However, an investigation showed that the crack was not in the plane of the delamination. Although the source of the grease was not identified (FM 5.6 Exhibit 7, sample pictures), Progress Energy does not intend to treat the leaching during this outage. In addition, multiple reports of grease stains on the buttresses (at the ends of the tendon sleeves) have been detected, were analyzed, and determined to not require any corrective action. (FM 5.6 Exhibits 1 and 8).

Conclusion:

Adequate grease protection has been provided to the tendons and was not a contributor to the delamination.

5.7 Physical attack (R)



5.7 Physical Attack

Description:

Concrete is vulnerable to multiple mechanisms of physical attack that may lead to deterioration over time and potential failure. Physical processes include non-structural cracking, salt crystallization, freezing and thawing, abrasion and erosion, thermal exposure, irradiation, fatigue and vibration, and settlement. Shrinkage cracking, thermal exposure, fatigue and settlement are discussed elsewhere in separate Failure Modes.

Salt crystallization is a process where dissolved salts move through the concrete by capillary action and crystallize on or under the surface as the water evaporates. The growing crystals can exert pressure on the "skin" of the concrete, resulting in spalling of the surface. This process can continue as long as there is a ready supply of moisture from the soil or atmosphere and the concrete experiences cycles of wetting and drying.

Freezing and thawing is a process where water freezes inside the concrete, exerting pressure from the inside as it turns into ice of larger volume. Repeated cycles of freezing and thawing can cause spalling of the surface in concrete that is not adequately air-entrained.

Abrasion and erosion are processes where surface material is removed from the concrete by either dry rubbing/grinding or impact of fluid carried particles.

Irradiation by either neutrons or gamma rays can cause changes to concrete's physical properties and/or volume change of aggregates (a summary of concrete irradiation is provided FM 5.7 Exhibit 5)

This document will attempt to identify potential processes and determine if any occurred in a way that impacted the observed failure.

Data to be collected and Analyzed:

1. Permeability of the concrete (Industry Standards; mix design; Petrographic reports; pour card analysis)
2. Air entrainment from pour records.
3. Freezing temperature information for CR3
4. IWL inspections record of damage related to physical attacks
5. Radiation exposure records

Verified Supporting Evidence: None

Verified Refuting Evidence:

1. The concrete has very low Water to Cement (W/C) ratio and permeability (FM 5.7 Exhibit 2 is a graph summary of pour records).
2. Petrographic reports did not detect salt crystallization inside the concrete (FM 5.7 Exhibit 3).
3. IWL reports did not identify significant surface salt crystallization (efflorescence) or concrete spalling that is associated with salt crystallization (FM 5.7 Exhibit 4 is a summary of the latest IWL report).
4. IWL Inspections did not detect any indication of damage due to other physical attack processes (FM 5.7 Exhibit 4).
5. The structure was not exposed to abrasion or erosion causing processes from mechanical abrasion or flowing water.
6. Irradiation levels are low (FM 5.7 Exhibits 6 is a summary prepared in 2010 by Dr. Ray Waldo of PII) and will not have a detrimental effect on the containment structure's concrete.
7. Review of winter temperature records at CR3 revealed that during the 2002-2009 period there were a total of thirteen (13) freezing incidences (FM 5.7 Exhibit 7 is a graphical record of temperatures measured at CR3 by Progress Energy). When extrapolated to the 1970-2009 period this level is



5.7 Physical Attack

insignificant for air-entrained concrete and no freezing/thawing damage is expected.

Discussion:

1. Industry standards use water to cement (W/C) ratio as an indication of concrete's permeability. It has been established that concrete with W/C of 0.4 or lower has voids system that is mostly made of disconnected discreet small voids – making it practically impermeable (FM 5.7 Exhibit 1). FM 5.7 Exhibit 2 is a graph based on data from all pour cards of concrete used in panel RB-15 of the containment structure. It shows that all the concrete was placed with $\frac{3}{4}$ " aggregate and W/C ratio of less than 0.41 (average W/C of 0.40). Based on the above it is concluded that the concrete has very low permeability.
2. Some of the physical attack modes mentioned above require moisture transmission through the concrete. Impermeable concrete will be resistant to damage by salt crystallization and will have reduced exposure to freezing.
3. W/C ratio is also a good indicator of concrete strength. The low W/C ratio resulted in strong concrete, able to resist higher stresses caused by physical attack.
4. The adequate air entraining found in the containment structure provides the concrete with resistance to damage from freezing/thawing cycles. The number of freezing cycles the structure experiences is very low and would not create a problem.
5. Irradiation levels at the containment wall are very low and would not have significant effect on the concrete's physical properties.

Conclusion:

The containment structure's concrete did not undergo physical attack. Therefore, physical attack was not a contributor to the delamination.



5.8 Chemical Attack

Description:

Concrete is vulnerable to multiple mechanisms of chemical attack that may lead to deterioration over time and potential failure. In porous materials, water can be the source of chemical processes of degradation by transporting aggressive ions. Therefore, controlling permeability is the main method for limiting chemical related damage. The two other factors affecting durability are the availability of aggressive ions, and the presence of concrete constituents that are vulnerable to these ions. Chemical attack may be prevented by reducing permeability, using non-reactive concrete components, and preventing aggressive ions from penetrating the concrete.

Chemical attack may be the result of Sulfate attack, acid and base attack, aggressive water attack, phosphate ion attack, Alkali Aggregate Reactions (AAR), Carbonation, efflorescence/leaching, and biological attack. A detailed discussion of these mechanisms is beyond the scope of this document and may be found in external sources (such as ACI 201).

The effects of chemical attack vary, but generally include loss of concrete cover accompanied by staining, erosion, reduction of concrete constituents, cracking, and spalling.

A visual survey is considered (ACI 349) an effective way of quantifying the effects of damage and identifying possible sources and composition of the aggressive chemicals.

This document will attempt to identify potential reactions and determine if any occurred in a way that impacted the observed failure.

Data to be collected and Analyzed:

1. Permeability of the concrete (Industry Standards; mix design; Petrographic reports; pour card analysis)
2. Availability of reactive concrete components (Petrographic reports)
3. Availability of aggressive ions (FM 5.8 Exhibit 12 is the 2008 annual emissions report)
4. Visual inspections (exhaustive search of IWL inspections was conducted)
5. Reports of damage related to chemical attacks (exhaustive search of IWL inspections was conducted)

Verified Supporting Evidence:

None

Verified Refuting Evidence:

1. The concrete meets industry standards for low permeability required for durability (FM 5.8 Exhibit 1 – ACI 201.2R-08 table 6.3; FM 5.8 Exhibit 2 – mix design; FM 5.8 Exhibit 3 – representative Petrographic reports; FM 5.8 Exhibit 4 – graph of water/cement ratio from pour cards).
2. Petrographic reports (FM 5.8 Exhibit 3b is CTL report) identified carbonation to a depth of 4-5 mm. This is a minimal amount for 30 years old concrete and does not reduce the concrete's ability to protect the embedded steel.
3. Petrographic reports (FM 5.8 Exhibit 3 and 5) found no evidence of destructive Alkali Aggregate Reaction (AAR). Although reactive components (chert) were found in some aggregates, the quantities were small and did not present an AAR problem.
4. Accelerated aggregate reactivity test (ASTM C1260 Potential Alkali Reactivity of Aggregates - FM 5.8 Exhibit 9) confirmed that the concrete exhibits innocuous behavior with expansion of 0.1% or lower (FM 5.8 Exhibit 8).
5. There is no indication that the structure was exposed to significant levels of water borne aggressive chemicals.
6. Inspections over the life of the structure did not detect any indication of damage due to chemical attack



5.8 Chemical Attack

(FM 5.8 Exhibit 10 and 11).

Discussion:

1. Industry standards, as demonstrated in FM 5.8 Exhibit 1 from ACI 201.2R-08, use water to cement (W/C) ratio as an indication of concrete's permeability. It has been established that concrete with W/C of 0.4 or lower has voids system that is mostly made of disconnected discreet small voids – making it practically impermeable (FM 5.8 Exhibit 6).
 FM 5.8 Exhibit 4 is a graph based on data from all pour cards of concrete used in panel RB-15 (between buttresses 4 and 3) of the containment structure. It shows that all the concrete was placed with W/C ratio of less than 0.41, with an average of 0.40.
 FM 5.8 Exhibit 2 is a summary of mix designs used in the construction. These designs were prepared with W/C of either 0.41 or 0.38.
 FM 5.8 Exhibit 3 includes pages from representative Petrographic reports that made an attempt at estimating the W/C ratio. Estimating W/C is notoriously inaccurate, as demonstrated by the estimates that range from 0.4 to 0.6 and as explained in the body of the CTL report (FM 5.8 Exhibit 3c).
 Based on the above it is concluded that the concrete has very low permeability.
2. Alkali Aggregate Reaction (AAR) requires the presence of reactive aggregates in sufficient quantities to cause destructive expansion, as well as sufficient moisture. According to Petrographic reports (FM 5.8 Exhibits 3 and 5), reactive aggregates (chert) were not present in quantities that support destructive expansion. This was confirmed by the low frequency of rims, indicative of a non-destructive level of AAR activity. After over 30 years in service the concrete did not exhibit typical AAR damage. Accelerated tests performed in 2009 confirm this conclusion (FM 5.8 Exhibit 8 and FM 5.8 Exhibit 9).
3. Sulfate attack is a process of forming expansive products in the hardened concrete by converting cement components into Ettringite and/or Gypsum. This process requires permeable concrete, moisture, and availability of sulfate ions.
 As demonstrated above, the concrete at CR3 has very low permeability and there are no readily available sources of sulfate ions, either from the soil or the environment.
 Petrographic analysis found no evidence of sulfate attack (FM 5.8 Exhibit 7).
4. Leaching and efflorescence are a process and indication of moisture transfer through the concrete, resulting in the removal of dissolved salts. These salts crystallize into white powder on the exposed surface when the water evaporates. No significant incidences of such process were reported in IWL inspection reports over the life of the structure, nor were any observed during visual inspections of the containment structure by PII in 2009.
5. Exposure to acids has the potential to cause significant damage to concrete. There is no indication that the containment structure was directly exposed to acids during its lifetime.
6. A report for air pollutant emitting facility (FM 5.8 Exhibit 12) provides emissions data from all four operating fossil units and the cooling towers at Crystal River during 2008. It identifies acceptable levels of potential acid rain causing emissions. However, there are no indications of acid exposure and damage to the concrete. A table summary of all potentially harmful chemicals from ACI 515.1R report is included in FM 5.8 Exhibit 13 for reference.
7. Virtually all the constituents of hydrated Portland cement are susceptible to carbonation. The results can be either beneficial or harmful, depending on the time, rate, and extent that they occur and the environmental exposure. Carbonation can improve the strength, hardness, and dimensional stability of concrete products, or it can result in deterioration and a decrease in the pH of the cement paste leading to corrosion of reinforcement near the surface.



5.8 Chemical Attack

Conclusion:

The containment structure's concrete did not undergo chemical attack. Therefore, chemical attack was not a contributor to the delamination.

6.1 Uneven tension distribution along the tendon due to excessive local duct friction (R)



6.1 Uneven Force Distribution along Tendons

Description:

This Failure Mode analyzes three separate but related issues:

- 6.1a. Effect of the non-uniform force along one tendon due to friction of the wires forming the tendon;
- 6.1b. Effect of the non-uniform force around penetrations due to bending around the penetrations;
- 6.1c. Cause of the asymmetries in tendon lift-off force measurements that have been previously reported at CR3, and consequences with respect to the 2009 delamination;

6.1a - The tendon force varies along the length of the tendon, with a maximum force at the jacking locations and a decreasing force towards the center of the tendon. These variations can lead to non-uniform pre-stress levels in the concrete material.

The load $F(x)$ at position x along the tendon is approximated by $F(x) = F(0) \exp(-\mu \alpha - K s)$, where $F(0)$ = Load at the jacking point, μ = Angular friction coefficient, α = Total angle change (rad), typically $\mu = 0.16$, K = Wobble friction coefficient, typically $K = 0.0003$, and s = Length of tendon "straight" portion (ft). FM 6.1 Exhibit 1 is the CR3 Design Basis Document 11 Rev.6 and contains numerical values.

6.1b - Around penetrations, tendon curvatures are larger and friction losses are larger than for typical horizontal tendons with less curvature. (FM 6.1 Exhibit 10 is an excerpt from the original Gilbert calculation on tendon force friction losses around the equipment hatch penetration).

The higher localized stresses can cause local micro-fracturing or local enhanced creep rates.

6.1c - A large number of adjacent tendons with high asymmetry might be indicative of:

1. Differences in concrete condition along the tendon arc, such as a section of pre-existing cracked/delaminated concrete;
 2. Differences in concrete condition along the tendon arc, such as a section with varying creep;
 3. A bias in lift off measurement equipment utilization at one end of the tendon during surveillance.
- These various hypotheses are addressed, together with their possible impact on the current delamination.

Note: Exhibit 2 is not used.

Data to be collected and Analyzed:

1. Draw expected tendon force along the 120' long tendons (FM 6.1 Exhibit 5 is a curve of the force along a hoop tendon drawn using the equation and numerical values in the above description);
2. Review tendon friction calculation around penetration and investigate the effects of non-uniform forces (FM 6.1 Exhibit 10);
3. Compare the shop and field lift-off data collected during containment IWL inspections (FM 6.1 Exhibit 3 displays the shop and field measurement data for the various surveillances and FM 6.1 Exhibit 4 is a summary of all these data);
4. Review data for another similar plant (FM 6.1 Exhibit 13 is a summary of the tendon lift-off force surveillance measurements);
5. Review grease losses in tendon sleeves (FM 6.1 Exhibit 6 displays the field measurement for grease losses for the various surveys and FM 6.1 Exhibit 7 is a summary of all these data);
6. Compare shims being used at the shop and field ends (FM 6.1 Exhibit 9 displays the shim thicknesses used at the shop and field ends as observed during surveillance 8 (last surveillance to date));
7. Investigate possible trend in the shop and field lift-off differences as a function of the concrete mix and pouring time (FM 6.1 Exhibit 11).

Verified Supporting Evidence:



6.1 Uneven Force Distribution along Tendons

1. The friction contributes to an un-even load distribution (FM 6.1 Exhibit 5). In particular around penetrations, the variation in the tendon force is large. For example, the difference between T1 = 172 ksi and T4 = 135 ksi (page 1 of 3 in FM 6.1 Exhibit 10) is equivalent to 25% variation;
2. Differences of 2-3% between the shop and field lift-off data are expected (see for example the summary for Farley Nuclear Plant in FM 6.1 Exhibit 13). CR3 surveillance data show much larger differences, up to 8% in survey 2 tendon 53H44, up to 12% in survey 4 tendon 13H40, up to 18% in survey 5 tendon 46H30, up to 20% in survey 6 tendon 42H33, up to 11% in survey 7 tendon 62H02, and up to 12% in survey 8 tendon 13H37 (FM 6.1 Exhibit 3 and FM 6.1 Exhibit 4);
3. Observations made by PSC personnel show the forces required to move the tendons out of the sleeves are much larger than the weight of the tendons (FM 6.1 Exhibit 8).

Verified Refuting Evidence:

1. The maximum force on a tendon running from buttress (n) to buttress (n+2) corresponds to the minimum force on a tendon running from buttress (n+1) to buttress (n+3). On average, the forces balance each other and the pre-stresses are relatively constant in various areas of the concrete;
2. The additional stresses generated by tendons curving around penetrations are addressed in the design (FM 6.1 Exhibit 10).

Discussion:

6.1a - A tendon running from buttress (n) to buttress (n+2) will have a maximum force at buttresses (n) and (n+2) (jacking points) and a minimum force at buttress (n+1) (its center) while a tendon running from buttress (n+1) to buttress (n+3) will have a maximum force at buttresses (n+1) and (n+3) (jacking points) and a minimum force at buttress (n+2) (its center) due to friction of the wires against the side of the tendon conduit. Overall, the tendons will compensate and the average pre-stress is essentially the same everywhere.

6.1b - Friction forces are particularly important around penetrations where the curvature of the tendons can be much larger. These local pre-stress gradients are in practice handled by the specific design of steel reinforcement in these regions of the concrete structure.

6.1c - Operator error or imprecision is discounted to explain the lift-off differences at shop and field ends as the equipment is much more precise than the errors recorded (FM 6.1 Exhibit 12).

The shim heights for the hoop tendons are similar between the shop and field ends as observed during IWL surveillance #8 (FM 6.1 Exhibit 9 outlines the values). This indicates that the different lift-off values recorded at the shop and field ends (FM 6.1 Exhibit 3 and FM 6.1 Exhibit 4) are not due to installation issues.

Additionally, grease losses are limited (FM 6.1 Exhibit 6 and FM 6.1 Exhibit 7) and cannot explain some of the tendon force differences.

Tendon removal force was determined to be reasonable (addressing Verified Supporting Evidence #3).

The correlation of the lift-off measurements with the mix design and pour time is good (FM 6.1 Exhibit 11).

Specifically, panels 34 and 61 were poured with a mix richer in cement (mix DM-5M, richer by about 8%) and were poured later than panel 12, 23, 45, and 56. FM 6.1 Exhibit 11 shows the correlation between lift-off measurement point location and presence of mix DM-5M. The force measured near panels 34 and 61 is higher than that measured at other panels.

Conclusion:

The uneven force along the tendons did not contribute to the delamination.



6.2 Inadequate Tendon Wires

Description:

The tendons in a concrete post-tensioned system are made of steel wires. The wires must have a very high tensile strength and must sustain high stress levels for long time periods with minimal stress relaxation. Cold-drawn steel wires are typically used. The wire quality, strength, uniformity, and corrosion are tested during regular surveillances, as described in the ASME Code Section XI, Subsection IWL (FM 6.2 Exhibit 1).

Relaxation of the tendon wires leads to reduced pre-stress levels in the concrete. Local strain variations and strain-hardening (work-hardening) along the tendon can lead to non-uniform pre-stress levels. Tendon wires are ASTM A421-65 high-strength steel with a guaranteed ultimate tensile strength (GUTS) of 240ksi (FM 6.2 Exhibit 2).

Data to be collected and Analyzed:

1. Check ASTM A421 requirements (FM 6.2 Exhibit 7);
2. Draw wire elongation variation along the tendon due to friction (FM 6.2 Exhibit 3);
3. Review surveillance data on tendon wires (FM 6.2 Exhibit 4);
4. Analyze wire surveillance data (FM 6.2 Exhibit 5);
5. Test wires recovered from removed tendons (FM 6.2 Exhibit 6 and FM 6.2 Exhibit 7).

Verified Supporting Evidence:

1. The strain in the wire is not uniform because the tendon force is not uniform (due to friction) (FM 6.2 Exhibit 3).

Verified Refuting Evidence:

1. Wire material ASTM A421 high-strength steel is the standard material specified in the industry. It is low relaxation and it is not subject to strain hardening / work hardening (FM 6.2 Exhibit 2);
2. Surveillance data on tendon wires show expected strength and ductility (FM 6.2 Exhibit 4, 5 and 6).

Discussion:

1. The strain of 5,000 $\mu\text{in/in}$ on a 120 ft wire leads to a displacement of 7.2in. This is consistent with observations made by PSC personnel;
2. There are no cyclic stresses imparted to the tendon wires so that the effects of strain hardening / work hardening are further limited;
3. The ASTM A421 chemical requirements on Sulfur (0.050% max) and Phosphorus (0.040 % max) are met by this material (FM 6.2 Exhibit 6). The wire material is left to the discretion of the manufacturer and a wire chemistry of 1080 carbon steel as found in FM 6.2 Exhibit 6 is acceptable;
4. Additionally, the tested wires meet the mechanical requirement of ASTM A421 (FM 6.2 Exhibit 6 and FM 6.2 Exhibit 7);
5. Upon installation, the tendon wires are stretched to 80% GUTS and then locked-off at 70% GUTS. Therefore the maximum possible over-stressing in a local area of a wire is only 20 to 30%. Above that, the GUTS of the wire would be reach and the wire would break. There are very few instances of broken wires and all are explained by other factors than over-stressing.

Conclusion:

There are no indications the tendon wire material used in CR3 tendons contributed to the delamination.



6.3 Thermal Effects of Greasing

Description:

The high-strength steel wires that make up the pre-stressing tendons are very sensitive to stress corrosion cracking while under tension. Corrosion protection was initially done by grouting the inside of the tendon sleeves after tendon original stressing. However, NRC RegGuide 1.107 (FM 6.3 Exhibit 1 is NRC RegGuide 1.107 Rev.1 from February 1977) and NRC RegGuide 1.90 (FM 6.3 Exhibit 2 is NRC RegGuide 1.90 Rev.1 from August 1977) moved the industry towards non-grouted tendons in order to fulfil in-service periodic inspections (FM 6.3 Exhibit 3 is a 1982 published paper by H. Ashar and D.J. Naus on the topic).

1. The procedure to grease the tendon during original installation is described in FM 6.3 Exhibit 4 (part of the documentation generated after the dome delamination event in 1976) and observed in the examples of FM 6.3 Exhibit 5 (typical pre-stressing field documentation including details of the greasing operation): Install the tendons inside the sleeves (the sleeves themselves were installed as part of the concrete form-work and they are embedded in the concrete);
2. Tension the tendons to lock-off force (the details of the tensioning procedure are investigated in other failure modes);
3. Grease the tendons (basically done by filling the sleeves with grease, all around the tendons themselves).

The grease is injected in the tendon sleeves at a pressure up to 85 psi and a temperature up to 160 °F (FM 6.3 Exhibit 4). The pressure and temperature cause thermal expansion of the duct and of the concrete surrounding the duct. Differences in expansion and/or rate of expansion can induce thermal stresses and possibly cause cracking.

The failure mode being investigated is the possibility to crack/delaminate the concrete due to differential expansion. Note the difference comes from thermal conductivity, NOT thermal expansion coefficient per se. Ultimately concrete and steel expand by the same amount. However, steel expands much faster and therefore we have transient stresses.

(Note that additional analysis of potential tensile strength degradation due to thermal effects is included in FM 4.8.)

Data to be collected and Analyzed:

1. Details of the original greasing procedure (FM 6.3 Exhibit 4 and FM 6.3 Exhibit 5);
2. Materials properties comparison (FM 6.3 Exhibit 6 shows pages 88-89 of P.K. Mehta reference book on concrete "Concrete: Structure, Properties, and Materials" and the summary of Coefficient of Thermal Expansion (CTE) values, and FM 6.3 Exhibit 8 is a summary of Thermal Conductivity values);
3. Calculate the heat transferred from the grease to the sleeve during tendon greasing (FM 6.3 Exhibit 9 is a thermal transfer analysis done by PII);
4. Calculate pressure capability of the tendon sleeves (FM 6.3 Exhibit 10 is a sleeve pipe pressure calculation done by Progress energy);
5. Calculate additional stress created by the grease injection at high temperature and pressure using first principles (FM 6.3 Exhibit 12 is a PII calculation of the stresses generated by the hot grease);
6. Investigate grease additions during surveillance activities (FM 6.3 Exhibit 15 shows re-greasing of tendons during surveillance activities, including typical grease losses recorded at CR3).

Note: Exhibit numbers 7 and 11 are not used in this FM.

Verified Supporting Evidence:

1. The Thermal Conductivity Coefficient of the steel and concrete are very different so that the sleeve expands much faster than the concrete and this creates a force from the hot sleeve to the still-cold



6.3 Thermal Effects of Greasing

- surrounding concrete (concrete 1.73 W/m.K and steel 43 W/m.K from FM 6.3 Exhibit 8);
2. This stress has the potential to create localized micro-cracks in the concrete around the hot tendon sleeves.

Verified Refuting Evidence:

1. Once the temperature has equilibrated at the sleeve/concrete interface, there is no thermal stress because the coefficient of thermal expansion of the sleeve steel material and of the concrete are very similar (FM 6.3 Exhibit 6);
2. The pressure capability of the tendon sleeves is high enough to support the 85 psi grease injection pressure (FM 6.3 Exhibit 10);
3. Stress analysis demonstrates that the additional stresses added due to thermal effects of greasing (less than 85 psi) in the concrete do not exceed the concrete tensile strength (measured at 450 psi direct tensile) (FM 6.3 Exhibit 12).

Discussion:

The files exemplified in FM 6.3 Exhibit 5 are from the original installation of the post-tensioning tendons. They are the "Crystal River 3 Reactor Building Pre-Stressing System Tendon History" files. The identification number is the number of the tendon in question.

The first example in FM 6.3 Exhibit 5 is tendon 12V2:

1. Tendon 12V2 is the second (2) Vertical tendon (V) between buttresses 1 and 2 (12), hence 12V2;
2. The tendon was received on-site on 1/16/1974;
3. And installed in the conduit (sleeve) on 7/3/1974;
4. No wires were removed or replaced;
5. The field anchor-head was button-headed on 8/27/1974;
6. And subsequently stressed on 10/14/1974;
7. All the elongation is on the same side as the vertical tendons are accessible only on the dome side for tensioning;
8. The total elongation is 12.5". This is the elongation from 1,500 psi (FM 6.3 Exhibit 5) or "an initial force that will remove all slack" (FM 6.3 Exhibit 13 chapter 1.0 Purpose), which was taken as 360 kips in practice (FM 6.3 Exhibit 13 chapter 3.0 Design Inputs). The theoretical elongation of 14.94 inches (FM 6.3 Exhibit 14) is longer than the actual elongation because of the wobble friction in the wires (FM 6.3 Exhibit 13);
9. The grease is then filled on 10/23/1974;
10. At a pressure of 112 psi and an Outlet temperature of 126 °F.

An important point to remember is that the issue of differential thermal expansion in this case is NOT associated with different Coefficient of Thermal Expansions (CTE) between the two materials but with different Thermal Conductivity Coefficients between the steel sleeve and the concrete. The sleeve expands much faster initially and this creates a load on the slowly heating and expanding surrounding concrete (see FM 6.3 Exhibit 4 from the dome analysis).

Additionally, the tendons are greased again during surveillance activities after they have been tested. It can be seen that there is very little grease loss in the surveillance operations (FM 6.3 Exhibit 15). From observation of the tendon surveillance data, the number of greasing cycles is under 4 for all tendons, and it is 1 for most tendons in the structure.

Conclusion:

The stresses due to high-temperature greasing did not lead to the delamination.



6.4 Stresses due to Rigid and Flexible Sleeves

Description:

In post-tensioned systems, sleeves are installed at the same time as reinforcing bars to be used later as conduits for the post-tensioning tendons. Note that they can alternately be called “sleeves”, “conduits”, or “sheaths”. We are using the former in this analysis.

Different types of tendon sleeves are used in Nuclear Power Plant containment structures. Rigid sleeves are used in straight sections while flexible sleeves must be used to go around containment penetrations.

6.4a: Vibration of rigid sleeves

The hydro-blasting high-pressure water jets can induce stresses on the sleeves and concrete. Additionally, hydro-blasting can induce vibration of the exposed rigid sleeves leading to cracking in the adjacent concrete. In particular, thick-wall rigid sleeves are more prone to vibration than thin-walled flexible sleeves that would typically simply crush under the impact of the water pressure.

6.4b: No tensile transfer at the smooth concrete / rigid sleeve interface

Rigid sleeves have a smooth surface that can lead to very low concrete/sleeve bonding and virtually no tensile carrying capability across the bond.

Data to be collected and Analyzed:

1. Review the types of tendon sleeves that are allowed in the Design Basis Document (FM 6.4 Exhibit 1 is an excerpts of the CR3 Design Basis Document rev 6, pages 4 and 5, containing the description of the tendon sleeves used in the CR3 containment) and the original CR3 Requirements Outline (Bidders Specification) (FM 6.4 Exhibit 2 is the Requirement Outline (RO) of Florida Power Corporation regarding the tendon sleeves, pages 20 to 24);
2. Examine the sleeves used at CR3 (FM 6.4 Exhibit 3 is a drawing of the CR3 panel 3-4 with an outline of the rigid and flexible vertical tendon sleeves, FM 6.4 Exhibit 4 is a photograph taken during the SGR opening showing evidence of rigid hoop sleeves, and FM 6.4 Exhibit 5 is a photograph taken on the CR3 containment in core #61 showing evidence of flexile hoop sleeves);
3. Calculate vibration due to possible excitation of rigid sleeves by hydro-blasting water jets (FM 6.4 Exhibit 6 is a PII Finite Element Modelling (FEM) analysis of the water jets impinging on the exposed hoop tendons);
4. Examine the effect of no tensile transfer capability across the concrete/sleeve interface.

Verified Supporting Evidence:

1. The very smooth surface and lack of mechanical bonding at the sleeve / concrete interface leads to virtually no tensile transfer at the concrete / sleeve interface.

Verified Refuting Evidence:

1. Using different types of sleeves is allowed by the Design Basis Document (FM 6.4 Exhibit 1 and FM 6.4 Exhibit 2);
2. Using smooth rigid sleeves is standard in other plants that have not experienced delaminations (FM 6.4 Exhibit 8 is a photograph of the TMI rigid hoop and vertical sleeves during their SGR opening);
3. Vibration analysis shows that the hydro-blasting water jets on the exposed sleeves do not generate stresses in the concrete that are large enough to create the delamination (FM 6.4 Exhibit 6).

Discussion:

Examination of the vertical tendon sleeves demonstrates a mixed use of flexible and rigid sleeves in the



6.4 Stresses due to Rigid and Flexible Sleeves

CR3 containment structure (FM 6.4 Exhibit 3 and FM 6.4 Exhibit 5). Photographs of the containment show rigid tendon sleeves for hoop and vertical tendons in the area of the SGR opening (FM 6.4 Exhibit 4).

Concrete pieces recovered after the demolition job show a very smooth interface between the concrete and the sleeve surface (FM 6.4 Exhibit 7);

The impulse generated by the high-pressure water on the concrete structure is not sufficient to generate the delamination through vibration (see the analysis done in FM 7.2). Because there is a layer of material where the radial tensile stresses are positive (albeit small on average) (see FM 1.2), once the crack is generated, it is "live" and can propagate until reaching a region of zero or compressive radial stress. This is the case near the buttresses and below the ring girder where the steel reinforcement can carry the tensile stresses.

The mixed use of flexible and rigid smooth tendon sleeves is standard in the industry and in the case at most plants in the USA.

Because virtually no tensile load can be carried across the sleeve / concrete interface, the sleeves act like defects in the structure. In the various models, this is taken into account by having no cohesion or tensile stress carrying capacity between the sleeves and the concrete. The sleeves become potential initiators of cracks, especially as a very large force is applied on one (but not the other) side of the sleeve.

This potential for crack nucleation is confirmed in the global PII FEM model. It is captured at each tendon sleeve location by a discontinuity where no tensile stress can be transferred. The analogy is that of tearing paper along pre-drilled aligned holes.

Conclusion:

6.4a: Hydro-blasting induced resonant vibration in the rigid sleeves did not cause the delamination.

6.4b: Poor bonding at the concrete / sleeve interface leads to considering the sleeves as 5.25" cracked regions in the structure for computer analysis. This is however an as-designed feature that was considered when the plant was first designed and constructed. As such, it did not contribute to the delamination by weakening the plane of the hoop tendons. FM 1.2 covers the impact of "as-designed features" such as this.



6.5 Inadequate Tendon Re-tensioning in Surveillance Activities

Description:

The 10CFR50.55a requires periodic inspections of the containment concrete and post-tensioning system following ASME Code Section XI, Subsection IWL (FM 6.5 Exhibit 1). The NRC provided acceptable methodology in NRC Reg Guides 1.35 (FM 6.5 Exhibit 2) and 1.35.1 (FM 6.5 Exhibit 3).

The predicted tendon force loss curves which establish acceptance criteria "base" values, are calculated for each tendon taking into account the causes of pre-stress losses as described in exhibits (FM 6.5 Exhibit 4 and FM 6.5 Exhibit 5 are excerpts of calculation S-95-0082 describing the four types of tendon force losses, FM 6.5 Exhibit 6 is a 1982 publication in Nuclear Engineering and Design) and design basis data taken from the plant's Design Basis Documents (FM 6.5 Exhibit 12 is an excerpts of the CR3 Design Basis Document showing the end-of-life minimum tendon forces for dome, vertical, and hoop tendons).

The CR3 containment tendon surveillance history for measured tendon liftoff forces shows numerous tendons with liftoff forces that were below the predicted "base" values. The predicted "base" values were developed conservatively and accounted for the pre-stress losses described in RG 1.35.1 technical position (see FM 6.5 Exhibit 7 is the second lift-off surveillance results for CR3 and FM 6.5 Exhibit 8 shows all the tendons that have been tested during the eight past surveillances).

Liftoff forces are measured on a sample of surveillance tendons in order to firstly demonstrate that the overall average level of pre-stress for each of the 3 groups of tendons (hoop, vertical, and dome) will remain greater than the minimum average required by design for the group until the next regularly scheduled surveillance. And secondly, the liftoff forces confirm that there is no unexpected degradation or unpredicted losses of force occurring over time for the tendons that could raise a question as to whether the minimum average force for a group of tendons will continue to meet the required minimum pre-stress average until the next surveillance in 5 years.

Surveillance tendons having lift-off forces below 95% of base value have been re-stressed to the established predicted base value for the tendon + 6% and -0% (FM 6.5 Exhibit 2).

This failure mode investigates whether the re-tensioning of these tendons to a higher but acceptable level of pre-stress force during tendon surveillance activities contributed to the delamination.

Data to be collected and Analyzed:

1. Review ASME Code Section XI, Subsection IWL (FM 6.5 Exhibit 1);
2. Review NRC RegGuide 1.35 (FM 6.5 Exhibit 2) and RegGuide 1.35.1 (FM 6.5 Exhibit 3);
3. Review tendon force loss mechanisms (FM 6.5 Exhibit 4) and tendon force loss calculations (FM 6.5 Exhibit 5);
4. Review input parameters to force loss curves (FM 6.5 Exhibit 12);
5. Review tendon surveillance lift-off data (FM 6.5 Exhibit 7 and FM 6.5 Exhibit 8);
6. Review regression analysis done by PSC and Progress Energy to explain tendons "failing" (FM 6.5 Exhibit 9);
7. Draw tendon force curves for hoop tendons tested multiple times in bay 34 (FM 6.5 Exhibit 10);
8. Review history (NCR's) for instances of tendon over-tensioning events;
9. Calculate stresses in the concrete from potential hoop tendon over-tensioning (FM 6.5 Exhibit 11)

Verified Supporting Evidence:

1. Examination of the tendon surveillance records indicate series of adjacent hoop tendons that did not meet the requirement of being above 95% predicted value (FM 6.5 Exhibit 7 and FM 6.5 Exhibit 8);
2. There are examples of tendon force loss curves that show a force loss with time that is faster than predicted values. For example, in FM 6.5 Exhibit 10, re-tensioning was performed on tendons between buttresses 4 and 2 and between buttresses 4 and 6.



6.5 Inadequate Tendon Re-tensioning in Surveillance Activities

Verified Refuting Evidence:

1. No NCRs were found that would indicate tendons were re-tensioned above the predicted force value plus 6%;
2. The four causes of pre-stress loss accounted to determine the predicted lift-off force in the tendons over time are elastic shortening, concrete shrinkage, concrete creep, and wire relaxation (FM 6.5 Exhibit 4). FM 6.5 Exhibit 9 provides a regression analysis performed by PSC and Progress Energy on measured tendon forces. It also provides the predicted curves (FM 6.5 Exhibit 9). It indicates that the force loss predicted curves used with the CR3 DBD numbers may have underestimated the expected force loss, particularly for the horizontal tendons, resulting in overly conservative acceptance criteria, additional testing expansion, and re-tensioning activities to a higher than necessary base predicted value (-0%,+6%). Re-tensioning was conservative in ensuring that sufficient compressive pre-stress was maintained above the minimum required level, and well below the 1,635 kips original tensioning value;
3. Re-tensioning above the predicted value but below the original tensioning of 1,635 kips cannot result in higher stresses in the containment wall than the stresses at the time the tendons were initially tensioned when the time dependent pre-stress force losses had not occurred (FM 6.5 Exhibit 11).

Discussion:

The "base" value in this discussion corresponds to the predicted liftoff force at the time of the tendon surveillance, not the original lock-off force when the tendon was first tensioned. The effect of re-tensioning tendons that fall below 95% base back to base value is conservative and relatively minor as far as pre-stress levels in the containment even if several adjacent tendons are re-tensioned to base (FM 6.5 Exhibit 11). In comparison, the effect on the pre-stress level locally is greater than the above condition when one tendon is fully detensioned from each group during each surveillance because that detensioned tendon represents about 1300 kips or more depending on the tendon. Detensioning one tendon fully is previously determined to be acceptable even when the plant is on line.

The issue of measured surveillance tendon liftoff forces being less than predicted liftoff forces calculated using theoretical pre-stress losses has been observed for at least the last three surveillances. The regression analyses curves for each tendon group generated by PSC (FM 6.5 Exhibit 9) using the liftoff data for numerous tendon liftoff forces taken over years of surveillances show a good fit with later data points, and confirm empirically that the force loss prediction curves for each tendon used for acceptance criteria on individual tendon liftoff force are too conservative. The conservative predicted liftoff force values have resulted in having to take more liftoff force measurements for adjacent tendons than would have been required if the predictions had justified additional predicted pre-stress losses. The increased population of surveillance liftoff force tendons, while resulting in more work during the surveillances, also resulted in re-tensioning more tendons back to the base level force predicted for the time of the surveillance. The relatively small additional pre-stress force added upon re-tensioning conservatively added by a small amount to the margin of pre-stress force available to counteract the internal pressure design load in event of the postulated accident. The small additional pre-stress was also insufficient to generate damage in the concrete (FM 6.5 Exhibit 11).

Regression analyses of the tendon liftoff force data for each group for many surveillances done by CR3 and PSC confirms that the calculated pre-stress losses taking into account the individual theoretical causes of tendon pre-stress losses reflected in the curves of base predicted values for each surveillance tendon are too conservative, resulting in having to perform liftoff force surveillance on more tendons than should be necessary. The result however of having to perform liftoff measurements on more tendons is conservative, resulting in more data that confirms the tendon pre-stress force requirements are met and when tendons are re-stressed to base level, some small amount of added pre-stress design margin is conservatively applied to the containment. In all cases the tendon surveillance results have confirmed that



6.5 Inadequate Tendon Re-tensioning in Surveillance Activities

the minimum required average pre-stress levels are met for each group and that there is no unexpected or unusual degradation occurring on the tendons on an individual basis as confirmed by the surveillance sample.

Conclusion:

Tendon re-tensioning during surveillance activities did not contribute to the delamination.



6.6 Inadequate Original Tensioning of Tendons

Description:

Excessive original tensioning above the pre-stress levels accounted for in the design can damage the concrete by generating localized micro-cracks and/or by increasing the creep deformation due to the higher stresses.

Also, unbalanced or incorrectly sequenced post-tensioning can lead to high local stresses, micro-cracks and/or delamination.

Initial tensioning of tendons, among other factors, can lead to excessive stresses in the containment structure. This is of particular importance as the CR3 containment dome did delaminate upon tendon original tensioning in 1976 (FM 6.6 Exhibit 4 is a letter from Florida Power Corporation to NRC describing the CR3 dome delamination event of 1976) as well as another Florida containment dome that delaminated at Turkey Point upon original tendon tensioning (FM 6.6 Exhibit 5 is an excerpt of a letter from Florida Power Corporation to NRC describing the Turkey Point dome delamination event of 1970).

When tensioning, the tendons are initially stressed to 80% Guaranteed Ultimate Tensile Stress (GUTS), shims are installed between the support plate and the back of the anchor head, and the loads is reduced and the tendons are locked-off at 70% GUTS.

Note that a strong distinction is made between this FM 6.6 and FM 1.1 dealing with the "Inadequate Pre-stress Design". The current FM 6.6 addresses the possibility that tendons were tensioned other than as designed /required and analyzes the potential results.

Data to be collected and Analyzed:

1. Review possible delamination Operating Experience upon tendon original tensioning (FM 6.6 Exhibit 4 and FM 6.6 Exhibit 5);
2. Review initial tendon force requirements (FM 6.6 Exhibit 1 is an excerpts of the Design Basis Document of 1985);
3. Review initial tendon tensioning data (FM 6.6 Exhibit 2 contains examples of the tensioning data sheet used during original tensioning of the CR3 tendons);
4. Review Non-Conformance Reports (NCR) related to original tendon over-tensioning;
5. Review first surveillance lift-off measurements (FM 6.6 Exhibit 3 shows the results of the first lift-off surveillance at CR3);
6. Review original tensioning sequence (FM 6.6 Exhibit 7 is the original CR3 tendon tensioning sequence, including the dome, vertical, and hoop tendons).

Verified Supporting Evidence:

1. First surveillance lift-off measurements did detect 3 over-tensioned vertical tendons (FM 6.6 Exhibit 3)

Verified Refuting Evidence:

1. The PII calculation in FM 6.6 Exhibit 10 shows that 10% over-tensioning in vertical tendons results in a concrete pre-stress that will not lead to any additional damage.
2. Original tensioning sheets did not report any over-tensioned hoop tendons. They did report some over-tensioned vertical tendons, however, item a above shows this did not damage the concrete;
3. No NCR were found related to original tendon over-tensioning;
4. First surveillance lift-off measurements did not detect any over-tensioned hoop tendons (FM 6.6 Exhibit 3);
5. The CTL condition assessment analysis showed there is no delamination in five of the six CR3 containment panels (FM 6.6 Exhibit 6, see Summary page 4 of 96). This supports the conclusion that



6.6 Inadequate Original Tensioning of Tendons

inadequate original tensioning of tendons did not cause the delamination crack between buttresses 3 and 4 in the vertical cylindrical shell.

Discussion:

The initial tendon tensioning was sufficient to cause delamination early in the life of the containments in the case of the CR3 dome and the Turkey Point dome (FM 6.6 Exhibit 4 and FM 6.6 Exhibit 5). In both cases, issues of radial tensile stresses, tension-compression interactions, and relatively low concrete tensile strength were indicated as root causes for the events.

Samples of the original tendon tensioning sheets are shown in FM 6.6 Exhibit 2. The tensioning sheets contain the hydraulic pressure on the jacks while the tendon force is the number typically referred to. The relationship between the two numbers is linear and well-known. Each jack is calibrated and the linear relationship is slightly different for each one (FM 6.6 Exhibit 8 is an example of the calibration sheet for the hydraulic jacks). For the original tensioning jacks used by VSL, the approximate relationship is that 6,800 psi of hydraulic pressure at the jack is equivalent to a tendon force of 1,635 kips.

Tendon 12V20 shows a lift-off force of 1785 kips at the first tendon surveillance even though the original stressing record does not indicate any special problem with this tendon (FM 6.6 Exhibit 9 is a compilation of issues that were found on vertical tendons). Tendon 12V20 does not go around any penetration. The greater than expected force was recorded again at the second surveillance (1740 kips) and then as-found tested in the third surveillance and found to be 1675 Kips, below the maximum tension of 1721 Kips allowed. Tendons 45V3 and 56V1 lift-off measurements were also above the 1,635 kips. The PII calculation in FM 6.6 Exhibit 10 shows that 10% over-tensioning in vertical tendons results in a concrete pre-stress that will not lead to any additional damage.

In addition to the level of pre-stress force in the tendons when they are tensioned, the sequence of tensioning is important, both in terms of elastic shortening losses for the various tendons, and in terms of asymmetrical loading of the concrete shell structure. Review of the CR3 required original tendon stressing sequence found that the sequence was appropriate, applying the tendon pre-stress forces in an engineered sequence that ensured gradual, even, and symmetrical distribution of pre-stress forces. For example in the early sequences, tensioning is done sequentially on tendons 31, 15, and 51 so as not to tension one side of the structure faster than the other two. It is also observed that neighboring tendons are not tensioned as a group but dispersed with tendons further away.

Review of the records of the CR3 dome delamination cracking during original plant construction found that the cracking within the thickness of the dome concrete shell was not observed during tendon pre-stressing or subsequently when the containment underwent the internal pressurization of the structural integrity test. The crack was discovered by workmen installing anchors in the area of the dome above the ring girder. It was not known just when the delamination crack in the dome had occurred. Similarly, no evidence of delamination cracking in the containment cylinder wall was observed by the required visual inspections of the concrete surface. The delamination between buttresses 3 and 4 was observed only after removal of concrete during installation of the large temporary opening for the steam generator replacement. Because neither the dome delamination crack nor the recent crack in the cylinder wall between buttresses 3 and 4 were detected by general visual observation on the concrete surface, it was essential that an investigation be performed to assess the condition of the entire vertical concrete shell, not just the area where the crack was observed between buttresses 3 and 4. The CTL investigation and condition assessment using several techniques such as core bores and Impulse Response technology determined that there was no delamination cracking in the other 5 of the 6 vertical cylindrical shell panels between the vertical buttresses (FM 6.6 Exhibit 6 is the CTL report on the topic, see Summary page 4 of 96).

Conclusion:



6.6 Inadequate Original Tensioning of Tendons

We found no evidence of inadequate original tensioning of tendons that could have been a contributor to the delamination.

7.1 Damaged properties/stresses Tensile Stresses from SGR Operations (Y)



7.1 Accumulated Low Level Damage

Description:

Concrete structures in service are exposed to multiple low level stresses on a regular basis. Normally these stresses can be safely ignored in distress analysis since they are too low to cause damage to the concrete.

Theoretically, such low level stresses may include:

1. Thermal stresses, daily, seasonally, and during outages (FM 4.8 has additional details on the subject)
2. Shrinkage and expansion due to drying/wetting cycles (FM 4.2 has additional details)
3. Construction related – specifically hydro-demolition loads and vibrations as well as impact from sudden release of prestress cables. (FM 7.2, 7.6 and 7.8 have additional details)

Each of these mechanisms has been refuted as a contributor to the delamination.

However, each mechanism has the potential to degrade the material by introducing defects, such as localized cracks and/or micro-cracks. As a result causing degradation of mechanical properties such as tensile strength and fracture energy. This type of degradation may be a contributing factor to the delamination.

Data to be collected and Analyzed:

1. Measurement of CR3 concrete mechanical properties (FM 7.1 Exhibit 1)
2. Petrographic analysis of CR3 concrete (FM 7.1 Exhibit 2)

Verified Supporting Evidence:

None

Verified Refuting Evidence:

1. Physical properties did not show significant variation from those expected of normal concrete (FM 7.1 Exhibit 1).
2. Petrographic analysis did not detect significant internal damage (FM 7.1 Exhibits 2).

Discussion:

Some of the low level stress mechanisms will actually cancel each other. For example, concrete that would expand when wet will shrink when the water cools it. In addition, concrete has the ability to “heal” itself by hydrating cement exposed in cracks, effectively repairing the small tight cracks. This phenomenon is especially effective in cases of low-level damage that does not expand rapidly towards failure.

The only practical way to determine if low level degradation occurred over time is to compare current physical properties to original properties, taking into account normal time-related changes.

Due to the large variation inherent in these tests and estimates it will require a very large change in properties in order to conclude that a statistically significant degradation occurred.

Analysis of concrete properties over time did not find evidence of significant variation from expected properties (FM 7.1 Exhibit 1).

Conclusion:

Accumulated low-level damage was not significant and did not cause the delamination.

7.2 Shock or concrete separation due to resonant vibrations during hydro-blasting (R)



7.2 Vibration Induced by Hydro-Blasting

Description:

During the Steam Generator Replacement (SGR) job at CR3, a large opening was created in the post-tensioned concrete containment. The method selected to remove the concrete was hydro-blasting. In hydro-blasting, high-pressure water jets impact the concrete to be removed (FM 7.2 Exhibit 1 is a September 2004 International Concrete Repair Institute (ICRI) Technical Guideline "Guide for the Preparation of Concrete Surfaces for Repair Using Hydro-demolition Methods"). The pressure is obtained by means of plunger positive displacement pumps. The water nozzles rotate at 500 rpm.

The water jet pressure that is used is nominally 20,000 psi (FM 7.9 Exhibit 2 is the Hydro-demolition work plan from Mac & Mac Hydro-Demolition Services to Progress Energy). The pressure used in the field was closer to 17,000 psi (FM 7.9 Exhibit 3 is an interview with Dave MacNeil, President of Mac & Mac).

There are several sources of vibrations in this process that need to be investigated. Damage to concrete may occur if the jet pulsation frequency, or the nozzle rotation frequency, or the pumps vibration frequency equal one of the resonant frequencies of any part of the containment, panels, or sleeves.

Data to be collected and Analyzed:

1. Determine natural frequencies associated with the Mac & Mac and American Hydro hydro-blasting technology (FM 7.2 Exhibit 3, FM 7.2 Exhibit 4 is an interview with Bob Nettinger, President of American Hydro, the leader in hydro-blasting projects of nuclear containments, FM 7.2 Exhibit 5 is a PII vibration analysis of the CR3 post-tensioned concrete containment building, FM 7.2 Exhibit 6 is a US patent showing the details of the American Hydro hydro-blasting system as applied to vertical surfaces, and FM 7.2 Exhibit 7 is an American Hydro calculation on hydro-blasting induced vibrations);
2. Measure the natural frequency of the containment building (FM 7.2 Exhibit 8 show the results of vibration frequency measurements performed on the CR3 containment building and panels);
3. Review natural frequency as calculated and reported in the CR3 Final Safety Analysis Report (FSAR) (FM 7.2 Exhibit 9 is an excerpt of the CR3 FSAR, Chapter 5, pages 62 to 64);
4. Finite Element Modeling (FEM) calculation of the natural frequency of the building (FM 7.2 Exhibit 5);
5. FEM calculation of the impulse force (forcing function) generated by the hydro-blasting water jets and machinery (FM 7.2 Exhibit 5 and FM 7.2 Exhibit 7);
6. FEM analysis of the vibration induced into the tendon sleeves by the impulse force (forcing function) of the high-pressure water jets (FM 7.2 Exhibit 16 is a PII FEM analysis of the vibration of the tendon sleeves exposed to hydro-blasting water jets);
7. Interviews with Progress Energy personnel present during hydro-blasting (FM 7.2 Exhibit 11);
8. Observations that may be related to vibrations induced by the hydro-blasting process (FM 7.2 Exhibit 12 is an NCR generated near the end of the concrete hydro-blasting process relating to paint spalling on the inside of containment, FM 7.2 Exhibit 13 shows photographs of the paint spalling);
9. Observation of phenomena that may be related to impact from the water jets (FM 7.2 Exhibit 15 shows photographs of vertical cracks observed on the left side of the SGR opening).

Note: Exhibit 10 is not used in this FM.

Verified Supporting Evidence:

1. Hydro-blasting pulsation due to the rotation of the injection nozzles is about 8.3Hz (equals 500 rpm). Hydro-blasting pulsation due to the positive displacement pumps is about 8.3Hz (FM 7.2 Exhibit 5). This is close to the resonant frequencies of the wall panels between buttresses of 6.4, 7.5, and 8.4 Hz



7.2 Vibration Induced by Hydro-Blasting

- (FM 7.2 Exhibit 5 page 1 of 11);
2. Frequency measurements on the building show resonant frequencies of 7.3 and 14.96 Hz (FM 7.2 Exhibit 8). They are in the same range as the hydro-blasting frequencies (FM 7.2 Exhibit 5);
 3. One witness observed vibrations on containment liner near the end of the hydro-blasting work (FM 7.2 Exhibit 11);
 4. Vibration of the liner resulted in paint spalling on the inside of containment (FM 7.2 Exhibit 12 and FM 7.2 Exhibit 13).

Verified Refuting Evidence:

1. The impulse force resulting from a 17,000 psi water jet is not sufficient to excite a structure of the size of the CR3 containment (FM 7.2 Exhibit 5 page 1 of 11). Displacements are under 350 μ strains and tensile stresses lower than 1 psi. Alternative mechanical and impact methods can damage the residual concrete that is to be repaired (see for example FM 7.2 Exhibit 1, pages 3 and 4 of 16);
2. The PII calculation (FM 7.2 Exhibit 5) also agrees with a calculation done by American Hydro (FM 7.2 Exhibit 7). They also conclude that the impulse force from the water jet is minimal;
3. The first time the hydro-blasting equipment was turned on, a demonstration operation was performed. This consisted of a small 8ft wide by 6ft high area, located at the lower right corner of the SGR opening, to be hydro-blasted about 10 inches deep. There are indications that the crack was present very early while this demonstration was being performed (FM 7.8 Exhibit 11 is a summary of observation of cracks very early in the hydro-blasting process). The cracks are observed on the side of the hydro-blasted area in Exhibit 11. This would indicate that the delamination may have been present before the hydro-blasting operation started;
4. The hydro-blasting power packs are located 400 ft (far) from the reactor opening location (FM 7.2 Exhibit 2) therefore vibrations from the pumps themselves cannot impact the containment wall.

Discussion:

The finite element analysis of the vibration response of the structure due to the hydro cutting pulsating load is analyzed. This analysis consists of two main steps. First the frequency analysis is performed after a static baseline analysis which includes the tensioning of the tendons and the application of gravity load. This step results in the first 50 free vibration natural frequencies and mode shapes. The second step is performing a transient dynamic modal analysis based on the 50 modes extracted in step 1. A linear super-positioning of the vibration modes with the associated participation factors and 2% critical damping is performed. Several forcing loads are applied to study the response. The forcing functions are assumed to be sine functions with varying amplitude and frequencies. The response is plotted as a function of time. When the response amplitude has reached a non-increasing state, the maximum stress is examined and reported.

The influence of the modulus of elasticity and Poisson's ratio on the stress is small. The analogy of bending in a slender member is used to demonstrate the modulus of elasticity insignificance. For example, the surface stress in a slender beam can be calculated with the Euler-Bernoulli equation $\text{Sigma} = (M * c) / I$, where Sigma is the stress, M is the moment, c is the distance from the neutral axis to the surface, and I is the second moment of area about the neutral axis. As seen in the equation the modulus of elasticity is not included. This demonstrates that stress is not significantly influencing the results.

The lowest natural frequency reported in the FSAR is 4.4 Hz (FM 7.2 Exhibit 9). This agrees very well with the PII-calculated resonant frequency for swaying of the whole building of 4.43 Hz (FM 7.2 Exhibit 5 page 1 of 11).

The presence of rather rigid hoop sleeves was not fully expected when the project started. It raises the question of the water jet impulse putting the partially exposed sleeves in resonant vibration. An FEM



7.2 Vibration Induced by Hydro-Blasting

analysis of the vibration induced into the tendon sleeves by the impulse force (forcing function) of the high-pressure water jets has been performed (FM 7.2 Exhibit 16). We conclude that the movement of the sleeves is small and the additional stress in the concrete is low.

Interviews with engineers at Mac & Mac and at American Hydro demonstrated that the two systems are similar. American Hydro has performed eight SGR openings into post-tensioned reactor building containments (seven were performed before the start of this investigation and one more was performed since then, at TMI). All were successful, demonstrating that it is possible to hydro-blast the SGR opening in a post-tensioned concrete containment in a non-damaging manner.

Additionally, all the literature we found on comparing the various means to perform concrete removal agree that hydro-blasting is the least damaging to the underlying structure.

The water pressure is listed at 20,000 psi in the Mac & Mac work instruction document. However, it was determined from interviews that the actual pressure was closer to 17,000 psi when operating at CR3.

Near the end of the hydro-blasting when the water jet was impacting close to the liner plate, there are several indications of vibration induced in the liner. It was reported by Progress personnel on the inside of containment (FM 7.2 Exhibit 11) and it was confirmed from analysis of cracked features in the concrete outside of containment close to the liner plate (FM 7.2 Exhibit 15). This indicates there was enough force in the water jets to induce radial displacement of the liner plate.

The ability of the water to vibrate the liner at that stage can be explained because the water at that stage in the hydro-blasting is impacting on a thin (3/8 in thick) long and wide (25 ft x 27 ft) plate of steel, loosely bonded on the four sides (mostly through mechanical locking due to the liner stiffeners).

There are three key discoveries leading to our refuting of this failure mode:

1. Although the vibration frequency induced by the hydro-blasting equipment is in the same range as the resonant frequency of the building, the impulse to generate the vibration is small. Note that our calculation on the subject (FM 7.2 Exhibit 5) agrees with the document provided by American Hydro (FM 7.2 Exhibit 7);
2. There are strong photographic indications that the crack was present very early in the hydro-blasting process (FM 7.2 Exhibit 14);
3. The ability of the water jet to vibrate and push the liner plate slightly in the radial direction is compatible with its inability to put a thick section of concrete in vibration.

Conclusion:

Vibration induced by hydro-blasting was not a factor in creating the delamination. It could have been a factor in the propagation of the delamination.

7.3 Inadequate pattern of de-tensioning of tendons (Y)
7.4 Inadequate de-tensioning scope(Y)



7.3 Inadequate Detensioning Scope and Sequence(contributing factors)(Includes FM 7.4)

Description:

This failure mode investigates the details of the tendon detensioning scope and sequence and the potential impact of the scope on building stresses.

During the 2009 Steam Generator Replacement (SGR) outage, 17 hoop tendons and 10 vertical tendons were detensioned in the containment structure panel 34 in order to prepare for cutting an access hole in the containment for the new steam generators. The horizontal tendons span two bays; so bays 23 and 45 were also partially detensioned. The details of the analysis performed for this opening are contained in Engineering Change package 63016 (EC 63016).

The tensioned hoop tendons in the upper and lower parts of bay 34 (those above and below the intended opening) lead to a bulging effect at the center part of the detensioned area. The extent of detensioning can therefore influence the extent of bulging and the shear, tensile, compression, and bending stresses present in the bay.

This failure mode investigates the detensioning scope and sequence applied to the CR3 containment wall prior to cutting the access opening, namely the extent to which hoop and vertical tendons were detensioned.

Data to be Collected and Analyzed:

1. Detensioning scope used during the 2009 CR3 outage (FM 7.3 Exhibit 1 lists the hoop (H) and vertical (V) tendons that were detensioned. FM 7.3 Exhibit 2 is a graphical representation of the tendons that were detensioned);
2. Work Order #1165095-06 for the field work on tendon detensioning as performed at CR3 during the 2009 SGR outage, with sign-offs and in process changes as the work was being performed (FM 7.3 Exhibit 3 is WO #1165095-06);
3. Detensioning sequence conducted for delamination repairs (FM 7.4 Exhibit 4)
4. PII computer simulation results showing showing building displacement and delamination result of the SGR de-tensioning. (FM 7.4 Exhibit 5).

Verified Supporting Evidence:

1. The Finite Element Models developed by PII were used on the CR3 containment walls to demonstrate that a larger extent of detensioning around the opening can significantly reduce stress gradients. This potential to reduce local stress concentrations has been studied extensively by PII as it closely relates to the CR3 delamination repair approach. The Finite Element models developed by PII with data and information available after the delamination of the CR3 containment wall show that detensioning in and around the opening could have reduce local stress concentrations during detensioning but it alone would not have prevented the delamination. .
2. The additional repair detensioning work that involved significantly more detensioning with a more symmetric sequence around entire containment structure did not produce additional delamination. This demonstrates that a more symmetrical sequence around the entire structure might have reduced the potential for delamination. (FM 7.3 Exhibit 4)

Verified Refuting Evidence:

None



7.3 Inadequate Detensioning Scope and Sequence(contributing factors)(Includes FM 7.4)

Discussion:

The stress gradient can be minimized when using a gradual uniform detensioning sequence of the post-tensioned structure. This can sometimes be done, for example, by skipping one or more tendons in the detensioning sequence. In that manner, a more gradual and uniform release of post-tensioning forces and associated change in the concrete structure can be achieved. The Finite Element Models developed by PII with data and information available after the delamination of the CR3 containment wall showed that a more uniform detensioning sequence alone would not have prevented the delamination. Furthermore, PII's investigation also showed that detensioning more tendons outside the opening would have made the stress bulging that caused the delamination worse, thus exacerbating the delamination. Understanding that tendon scope and sequence were key contributors to the delamination event, the PII analysis codes were used to validate the detensioning scope and sequence used in the March 2010 detensioning. (FM 7.5 Exhibit 4). Based on the PII modelling, the detensioning scope and sequence for the repair had to be modified significantly to prevent stresses that would have caused further damage to the containment. The final scope of detensioning was larger than the original detensioning plan by a factor of eight. In addition, the detensioning sequence was adjusted through numerous model iterations to arrive at the detensioning plan that successfully avoided delamination in the other bays (EC 75218).

Conclusion:

The detensioning sequence and scope used at CR3 are considered to have been contributing factors in the delamination.

7.5 Added stress due to removing tendons and concrete at opening (Y)



7.5 Added Stress Due to Removing Concrete at SGR Opening (Contributing Factor)

Description:

The process for creating the SGR opening had two steps. The first was to de-tension the tendons that would have to be removed. The second was to remove the concrete to make the SGR opening. This Failure Mode considers whether the concrete removal contributed to the delamination damage.

Data to be collected and Analyzed:

1. Finite Element Analysis evaluations to display the effects of de-tensioning and concrete removal (FM 7.5 Exhibits 2 and 3)
2. Photographs showing SGR opening conditions during the transition from de-tensioning and concrete removal.FM 7..5 Exhibit 1)
3. The SGR de-tensioning timeline (FM 7.5 Exhibit 1)

Verified Supporting Evidence:

1. Finite Element Analysis indicates continuing radial displacement as a result of concrete removal indicating that it contributed to the final outcome.

Verified Refuting Evidence:

None

Discussion:

Photographic evidence is inconclusive (FM 7.5 Exhibit 1) The photographic evidence documents the discovery of cracking, the appearance of water, and the discovery of delamination but in each case it is not possible to determine whether the effect was caused by concrete removal or exposed by concrete removal. Uncertainties in Finite Element Analysis prevent pinpointing the degree of delamination which existed when concrete removal became significant but that removal only assisted the delamination process.(FM 7.5 Exhibit 3)

Conclusion:

The concrete removal associated with the creating the SGR opening did contribute to delamination.

7.6 Vibrations due to cutting tendons under tension (R)



7.6 Vibrations due to cutting tendons under tension (piano effect)

Description:

The procedure used to remove the tendons from the sleeves that intersect the SGR opening is as follows, taken from FM 7.6 Exhibit 1 which contains excerpts of the Engineering Change package relating to tendon detensioning, and FM 7.6 Exhibit 2 which contains excerpts of the Precision Surveillance Corporation (PSC) field manual:

1. Degrease tendon sleeves;
2. Cut tendons using a plasma torch;
3. Pull tendons using a coiler machine.

An important point to note is that the tendon cutting is performed without releasing the tension. A plasma torch is slowly applied to the wire button-heads until the wire yields and snaps in a tensile fracture. The sudden release of energy has a "piano effect" in the containment that can result in additional stresses and/or vibrations in the concrete.

Data to be collected and Analyzed:

1. Tendon cutting procedure (FM 7.6 Exhibit 1 and FM 7.6 Exhibit 2);
2. Calculate amount of energy released by cutting one wire (FM 7.6 Exhibit 3 is a calculation of the energy released when plasma cutting 1 wire, 20 wires, and a whole tendon at once);
3. Finite Element Modelling (FEM) analysis to determine the vibration induced additional forces on the concrete (FM 7.6 Exhibit 4 is an Abaqus analysis of the vibration frequency and amplitude upon plasma cutting 20 wires at once).
4. De-tensioning sequence and procedure is provided in FM 7.6 Exhibit 7.

Verified Supporting Evidence:

None

Verified Refuting Evidence:

1. The FEM impact energy analysis determined that the excitation force due to the energy released by 20 wires plasma cut at once is not sufficient to delaminate the concrete (FM 7.6 Exhibit 3 and FM 7.6 Exhibit 4);
2. The operation of plasma cutting the tendons under load is now standard industry practice and has been used successfully in many Steam Generator Replacement (SGR) concrete containment opening jobs (FM 7.6 Exhibit 5 is an email from Paul Smith, PSC president and FM 7.6 Exhibit 6 is an interview with Gary Goetsch, PSC superintendent).

Discussion:

The consequence of cutting a wire is a shock vibration rather than a resonant vibration. The calculations performed by PII show that releasing 20 wires at once generates only a small additional stress in the concrete structure.

Conclusion:

The vibration induced by plasma cutting the tendons under tension (piano effect) did not generate the delamination.

7.7 Cracking due to pre-existing defects in this area (R)



7.7 Pre-Existing Delamination

Description:

Nuclear pre-stressed concrete structures are subject to multiple sources of design, construction and duty factors that can impact material properties and degradation:

1. Design and construction material specifications, conformance with those design and construction specifications (see FM series 1 and 2 for additional details on related subjects);
2. The concrete is subjected to large original pre-stresses when tensioning the hoop and vertical tendons. In the case of CR3, the hoop pre-stress is approximately 2,000 psi and the vertical pre-stress is approximately 1,100 psi;
3. The tendon plane, particularly the hoop tendon plane, is the most vulnerable location for delamination potential from a stress standpoint, as the tendons are exerting maximum compressive stress on the inner concrete ring and thus place a tensile stress on the outer concrete ring at this same interface plane. The large number of tendons also reduce the concrete load bearing area at this plane;
4. The concrete is subjected to aging through thermal stresses, daily, seasonally, and during outages (see FM 4.8 for additional details on the subject);
5. The concrete is subjected to aging through long term creep, time-dependant strain in the concrete under constant load (see 4.5 for additional details on the subject);
6. The concrete is subjected to aging through long term vibrations (see FM 1.7 for additional details on the subject).

Each of these factors provides potential for introducing defects that can take the form of localized cracks and/or distributed micro-cracks across the structure.

This FM investigates only the possibility of a large delamination in bay 34 being present for several years, i.e., pre-dating the SGR activities. Possible micro-scale degradation of the concrete material is analyzed in FM 7.1. Design and construction related issues are addressed in FM series 1 and 2 documents.

Data to be collected and Analyzed:

1. Carbonation studies of the fracture surfaces to determine the age of the crack (FM 7.7 Exhibit 2, FM 7.7 Exhibit 3, FM 7.7 Exhibit 4, and FM 7.7 Exhibit 5);
2. Literature review on the use of carbonation to date a fracture surface (FM 7.7 Exhibit 7, FM 7.7 Exhibit 8, FM 7.7 Exhibit 9, and FM 7.7 Exhibit 10);
3. Condition assessment of the CR3 containment and determination of the extent of the delamination (FM 7.7 Exhibit 6 is the CTL report describing the technical procedure and the extent of delamination).
4. Drawing of De-tensioned Tendon pattern for SGR de-tensioning compared to the delamination map. (FM 7.7 Exhibit 11, Slides 29 and 30 from NGG Presentation on 3/9/2010.)

Verified Supporting Evidence:

1. As hydro-demolition initially progressed and surface concrete was removed, large cracked sections were observed behind the rebar mat suggesting a degraded and damaged condition was being uncovered. It was unknown at this stage whether the observed condition was pre-existing the outage or pre-existing the hydro-demolition activity only, e.g., created during the detensioning activity (FM 7.7 Exhibit 1).

Verified Refuting Evidence:

1. Traditional petrographic analyses did not detect the presence of pre-existing defects in the concrete (FM 7.7 Exhibit 2, FM 7.7 Exhibit 3, FM 7.7 Exhibit 4, and FM 7.7 Exhibit 5);
2. The largest part of the observed fracture surface is found to be a new crack (FM 7.7 Exhibits 3 to 5);



7.7 Pre-Existing Delamination

3. The CTL work shows that the delamination is present only in bay 34, the panel where the SGR opening operations were performed, and not in any of the other five bays (FM 7.7 Exhibit 6).
4. The shape of the delaminated area of bay 34 corresponds exactly to the region of de-tensioned horizontal and vertical tendons, (See FM 7.7 Exhibit 9, Slide 8). The first tensioned tendon above the de-tensioned zone was 42H35 at elevation 210' 63/4" and the first tensioned tendon going down was at 181' 8 3/4" between the area that did not delaminate and the de-tensioned area that would be expected to inhibit delamination. The neck begins to narrow at 210' and 181' with a minimum width at 197'. The fit is exact. This indicates that the de-tensioning process influenced the delamination process which could not happen if the delamination occurred prior to the de-tensioning. The CTL Impulse Response information was independently confirmed by core samples in both the undamaged and delaminated areas (FM 7.7 Exhibit 6). Prior to the SGR outage there was nothing unique about the area around 197' which would have inhibited delamination in the neck area.

Discussion:

One common approach to determining the age of a fracture surface is the carbonation analysis (FM 7.7 Exhibit 7, FM 7.7 Exhibit 8, FM 7.7 Exhibit 9, and FM 7.7 Exhibit 10). This is based on the reaction between constituents in the concrete paste and the carbon dioxide in the air. Upon reaction, the pH of the concrete decreases and this can be observed using various pH tools.

The observation of cracking and concrete chunks in early stages of concrete removal makes it unlikely that delamination occurred later due to concrete removal.

Conclusion:

The subject delamination did not pre-exist the SGR opening operations.

7.8 Excessive water jet pressure (R)



7.8 Excessive Water Jet

Description:

During hydro-blasting, a high-pressure water jet impacts the concrete to be removed (FM 7.8 Exhibit 1 is a September 2004 International Concrete Repair Institute (ICRI) Technical Guideline "Guide for the Preparation of Concrete Surfaces for Repair Using Hydro-demolition Methods" and FM 7.8 Exhibit 2 is the ACI 546R-04 Concrete Repair Guide). The water jet pressure that is used is nominally 20,000 psi (FM 7.8 Exhibit 3 is the Work Plan agreed by Mac & Mac, the hydro-blasting company used for this project, and Progress Energy, the owner) although in practice it can vary somewhat (FM 7.8 Exhibit 4 is an interview with Dave McNeill, co-owner of Mac & Mac and FM 7.8 Exhibit 5 is an interview of Robert Nettinger, President of American Hydro). The pressure is obtained by means of a plunger positive displacement pump. The water nozzles rotate at 500 rpm. The jet flow rate per nozzle is around 50 gallons per minute. The intent of hydro-demolition as applied here is to damage and remove the concrete section of interest. This is indeed the point of using this technology in this particular application where concrete has to be removed. This FM is looking at if and how the hydro-pressure might cause damage beyond the application area via force or pressure build-up.

Damage to underlying or surrounding concrete (outside the targeted removal area) may occur if water jet pressure and flow is not maintained within a controllable range.

Note that issues associated with resonant frequency are analyzed separately in FM 7.2 and hydro blasting rate is addressed in FM 7.9.

Data to be collected and Analyzed:

1. Determine impulse force associated with the hydro-blasting technology (FM 7.8 Exhibit 7 is a PII calculation containing calculation of the force of the water on the wall, and FM 7.8 Exhibit 8 is an excerpt of a calculation performed by American Hydro);
2. Photograph of the hydro-blasting nozzles as used at CR3 (FM 7.8 Exhibit 13);
3. Calculation of the water pressure as a function of distance from the nozzle (FM 7.8 Exhibit 14);
4. Observations of phenomena that may be related to impact from the water jets (FM 7.8 Exhibit 9 describes observations made at the CR3 containment near the liner);
5. Review of the Turkey Point liner issues during its concrete containment opening (FM 7.8 Exhibit 10 is a report summary of the issues observed at Turkey Point during concrete containment hydro-blasting).

Note: Exhibit number 6 is not used in this FM.

Verified Supporting Evidence:

1. The hydro-blasting water jets appear to be responsible for some damage to the surrounding concrete close to the liner plate (FM 7.8 Exhibit 9). This occurred late in the hydro-blasting process when the thickness of concrete left in front of the liner plate was low.

Verified Refuting Evidence:

1. The force and pressure applied by the hydro-blasting water jet were within the expected range for the intended operation, and within a controllable range to prevent/limit unintended concrete removal or damage to surrounding concrete or structures (FM 7.8 Exhibit 7);
2. The PII calculation (FM 7.8 Exhibit 7) agrees with a calculation done by American Hydro (FM 7.8 Exhibit 8). They also conclude that the force from the water jet to the containment is minimal;
3. There is no indication that Mac & Mac operated the equipment at a higher pressure than expected (FM 7.8 Exhibit 3 and FM 7.8 Exhibit 4);
4. The first time the hydro-blasting equipment was turned on, a demonstration operation was performed.



7.8 Excessive Water Jet

This consisted of a small 8ft wide by 6ft high area, located at the lower right corner of the SGR opening, to be hydro-blasted about 10 inches deep. There are indications that the crack was present very early while this demonstration was being performed (FM 7.8 Exhibit 11 is a summary of observation of cracks very early in the hydro-blasting process). The cracks are observed on the side of the hydro-blasted area in Exhibit 11. This would indicate that the delamination may have been present before the hydro-blasting operation started;

5. There is no indication that Mac & Mac equipment and operation is fundamentally different from American Hydro equipment and operation.

Discussion:

Interviews with engineers at Mac & Mac and at American Hydro demonstrated that the two systems are mostly similar. PII calculations and American Hydro calculation confirm that in both cases the force from the water jet to the concrete is not sufficiently high to generate damage by itself. The principle of hydro-blasting confirms that hydro-blasting takes advantage of pre-existing cracks (FM 7.8 Exhibit 12 is chapter 5 "Waterjets in Civil Engineering Applications" from Professor David Summers book on water jets and their applications).

Note that there in the Mac & Mac interview (FM 7.8 Exhibit 4), the "force on the wall" was 100 pounds instead of psi.

We can also perform the calculation done in FM 7.8 Exhibit 8 by American Hydro using the slightly different water pressure of $P = 17,000$ psi and water flow of 40 gpm for Mac & Mac. The equations in FM 7.8 Exhibit 8 then lead to water velocity $v = 1,588$ ft/s, and mass flow $M = 0.166$ slugs/s. this gives a force on the concrete equal to $F = M * v = 263$ lbf. This is the force per nozzle. Our calculation FM 7.8 Exhibit 7, page 7 of 11 reports 1,252 lbf for 6 nozzles, for a force of 209 lbf per nozzle. The two values are in agreement. It should also be pointed out that this is the case for complete used of the water energy for hydro-demolition. The real energy would be somewhat lower.

American Hydro has performed eight SGR openings into post-tensioned reactor building containments (seven were performed when we started this investigation in October 2009 and one more was done since at TMI). All were successful, demonstrating capability and process effectiveness for hydro-blasting SGR openings without unacceptable collateral damage to surrounding concrete or structures.

Additionally, all the literature we found on comparing the various means to perform concrete removal agree that hydro-blasting is the least damaging to the underlying structure. Pressures and forces generated during hydro-blasting are limited by the equipment and water requirements. When providing sufficient control for confining concrete removal to the desired area and depth, no damage is expected to occur in adjacent areas. Also, hydro-blasting does not result in mechanical impact per-se, but rather in rapid erosion/disintegration of the paste/aggregate sub-components (FM 7.8 Exhibit 12).

The analysis of cracked features in the concrete on the outside of containment, close to the liner plate, concluded that the water jet had enough force to push the liner (FM 7.8 Exhibit 9). This can be explained because the water at that stage in the hydro-blasting is impacting on a thin (3/8 in) long (25 ft x 27 ft) plate of steel, loosely bonded on the four sides (mostly through mechanical locking due to the plate stiffeners).

The containment opening at Turkey Point also had issues with the hydro-demolition, due to pressurization between the concrete and the liner and pushing of the liner away from the concrete (FM 7.8 Exhibit 10)

Although the forces generated by the water jet are not sufficient to initiate the delamination, it is possible they could have been in a factor in propagating it. Once the crack started in the plane of the tendon sleeves, it is "active" because it is in an area of local tensile stresses. Therefore it can be propagated with minimal forces serving as an "activation energy" force just pushing the local tensile stress above the tensile strength of the concrete. It is important to note, however, that the available data does not prove or disprove a contribution from the water jet forces to the propagation of the delamination.



7.8 Excessive Water Jet

Conclusion:

Excessive water jet pressure was not a factor in creating the delamination.
It could have been a factor in the propagation of the delamination.

7.9 Inadequate hydro-blasting rate (R)



7.9 Inadequate Hydro-Blasting

Description:

During hydro-blasting, a high-pressure water jet impacts the concrete to be removed (FM 7.9 Exhibit 1 and FM 7.9 Exhibit 2). The water jet pressure that is used is nominally 20,000 psi (FM 7.9 Exhibit 3) although in practice it can vary somewhat (FM 7.9 Exhibit 4 and FM 7.9 Exhibit 5). Detailed discussion of the fundamentals of hydro-blasting is beyond the scope of this document, but a good reference can be found in the book by Professor David Summers, from Missouri Science & Technology University, Rolla, Missouri, in particular chapter 5, "Water jets in civil engineering applications" (FM 7.9 Exhibit 11). One parameter of interest is the movement speed of the water jet nozzles over the surface to be hydro-blasted.

The intent of hydro-demolition as applied here is to break-up and remove the concrete section of interest. This is indeed the point of using this technology in this particular application where concrete HAS to be removed. This FM is attempting to determine if and how the nozzle movement rate might cause damage beyond the application area via force or pressure build-up.

1. If the rate is too high (nozzles move fast over the concrete surface), the force may result in simply "banging" on the concrete wall without any time for the hydro-blasting process to really make a meaningful impact through the action of erosion and water pressurization within the pre-existing micro-cracks and pores in the structure;
2. If the rate is too low (nozzles move slowly over the concrete surface), the dwell time becomes higher and the depth removed per pass can become too high or the pressurized water can have time to go deeper into the structure, for example along tendon sleeves;
3. This failure mode also considers the effect of the nozzles possibly being too close to the containment wall, leading to a higher impact pressure and a deeper concrete removal per each pass (FM 7.9 Exhibit 11 Figure 5.44).

Note that issues associated with resonant frequency are analyzed separately in FM 7.2 and issues dealing directly with excessive impact force are analyzed separately in FM 7.8.

Data to be collected and Analyzed:

1. Determine the change in water jet force on the wall as a function of the distance of the nozzle to the containment concrete (FM 7.9 Exhibit 6, FM 7.9 Exhibit 7, and FM 7.9 Exhibit 8);
2. Examine the fundamentals of water jets technology, particularly as applied in civil engineering (FM 7.9 Exhibit 11);
3. Interview Mac & Mac employees regarding nozzle movement rates and nozzle distances used during the hydro-blasting process at CR3 (FM 7.9 Exhibit 4 and FM 7.9 Exhibit 5);
4. Interview Mac & Mac employees and American Hydro employees regarding usual nozzle movement rates and nozzle distances used during hydro-blasting of nuclear containments (FM 7.9 Exhibit 4 and FM 7.9 Exhibit 5);
5. Work order for Mac & Mac for 2009 CR3 SGR opening hydro-blasting job (FM 7.9 Exhibit 14);
6. Summary of the Turkey Point liner issues during their containment opening (FM 7.9 Exhibit 10).

Verified Supporting Evidence:

1. The force on the wall resulting from the hydro-blasting water jet increases as the distance between the nozzles and the wall decreases (FM 7.9 Exhibit 6 and FM 7.9 Exhibit 7). This makes the process sensitive to keeping a minimum distance. However, no such distance was prescribed in the work instructions (FM 7.9 Exhibit 3 and FM 7.9 Exhibit 14).



7.9 Inadequate Hydro-Blasting

Verified Refuting Evidence:

1. Both the PII calculations (FM 7.9 Exhibit 6 and FM 7.9 Exhibit 7) and the American Hydro calculation (FM 7.9 Exhibit 8) both conclude that the baseline force from the water jet to the containment wall is low (less than 600 lbf per nozzle);
2. There are no indications that Mac & Mac operated the equipment at a higher nozzle movement rate than prescribed and expected (FM 7.9 Exhibit 3 and FM 7.9 Exhibit 4). Note that actual operating records are not available;
3. There are also no indications that Mac & Mac operated the equipment at a lower nozzle movement rate than prescribed and expected (FM 7.9 Exhibit 3 and FM 7.9 Exhibit 4). Note that actual operating records are not available;
4. The possibility of high-pressure water moving deep in the concrete along tendon sleeves and generating the delamination was suggestive. One critical observation refuting this point is that the delamination was observed at the time of the initial hydro-blasting demonstration operation (FM 7.9 Exhibit 12). This would indicate that the delamination may have been present before the hydro-blasting operation started. See additional discussion below.

Discussion:

We can also perform the calculation done in FM 7.9 Exhibit 8 by American Hydro using the slightly different water pressure of $P = 17,000$ psi and water flow of 40 gpm for Mac & Mac. The equations in FM 7.9 Exhibit 8 then lead to water velocity $v = 1,588$ ft/s, and mass flow $M = 0.166$ slugs/s. This gives a force on the concrete equal to $F = M * v = 263$ lbf. This is the force per nozzle. Our calculation FM 7.9 Exhibit 7, page 7 of 11 reports 1,252 lbf for 6 nozzles, for a force of 209 lbf per nozzle. The two values are in agreement.

In FM 7.9 Exhibit 7, the maximum stress is generated at resonance bending vibration of the panel. The larger the vibration amplitude the larger the stress will be. The panel undergoes the largest deflection when the force is applied at the point which corresponds to the lowest structural stiffness. The lowest structural stiffness is as far away from the border of the panel as possible (i.e. the middle). This model is conservative and does not include the equipment access hatch since it would further stiffen the structure. The midpoint of the panel is below the SGR opening. Hence, the closest point to the middle of the panel where hydro blasting pressure was applied is at the midpoint of the bottom SGR opening edge.

Additionally, in FM 7.9 Exhibit 7, there are many mechanisms that are dissipating the energy in the structure (i.e. dampen the vibration) from the hydro blasting event. The exact damping is unknown and hard to determine. However, as an engineering rule, structures are typically damped between 2% to 10% of the critical damping. Reinforced concrete structures are normally damped at 4%. Since this analysis is conservative (worst case), the lowest possible value was used to investigate the response. Since the response does not show large stresses with artificially low damping, confidence that no large stresses can occur with more realistic damping is concluded.

Interviews with engineers at two of the leading hydro-demolition companies, Mac & Mac and at American Hydro, demonstrated that the two systems are mostly similar. Our calculations and American Hydro calculation confirm that in both cases the force from the water jet to the concrete is not high. The force on the wall does, however, increase as the nozzles get closer to the concrete wall. American Hydro has performed eight Steam Generator Replacement (SGR) openings into post-tensioned reactor building containments (seven were performed when we started this investigation in October 2009 and one more was done since at TMI). All were successful, demonstrating that it is possible to hydro-blast the SGR opening into a post-tensioned aged concrete containment without collateral damage to surrounding concrete or structures.

It should be repeated that the field observations were that chunks of concrete started to come off during



7.9 Inadequate Hydro-Blasting

the demonstration run of the hydro-blasting system. The attempted removal depth was only 4.5", exposing no hoop sleeve, and therefore creating no pathway for the water to follow to pop off the chunks of concrete observed in FM 7.9 Exhibit 9. However, this was not possible in practice because the concrete chunks started appearing with the back side in contact with the hoop sleeves. For example, in FM 7.9 Exhibit 14, items 75.6 and 75.7 on page 16 of 42 indicate that the hydro-blasting reached a depth of about 4 ½" on 9/30/2009, which was a hold point in the hydro-blasting operations. At 4 ½" depth, the hydro-blasting would not have reached a depth that would expose the hoop sleeves, which is approximately 7 ½". The photos in FM 7.9 Exhibit 12 are dated the morning of the same day that the hydro-blasting reached the 4 ½" depth hold point, and they show concrete in some areas removed to the depth of the centerline of the hoop sleeves, which is approximately 10".

Additionally, all the literature we found on comparing the various means to perform concrete removal agree that hydro-blasting is the least damaging to the underlying structure. The reference book from our reviewer Professor David Summers (FM 7.9 Exhibit 11) and discussions with the author confirmed that hydro-blasting at pressures above 15,000 psi is the favored approach to prepare a concrete surface before adding new concrete on top, through a texturing effect that favors a stronger bond. Note that a water pressure of 800 bars, as exemplified in Figure 5.46 of FM 7.9 Exhibit 11 corresponds to 12,000 psi. Therefore the hydro-blasting technique is used in nuclear containment with the "moderate pressure philosophy" as described in FM 7.9 Exhibit 11.

We found no indications that the water was just "banging" on the wall. On the contrary, an early sign that things were not right was the presence of large chunks of concrete falling from the hydro-blasted area. This is now taken as an indication that a delamination layer was present behind the hydro-blasted concrete (FM 7.9 Exhibit 9). Additionally, the water jet is rotating at 500 rpm and therefore the water is always moving very fast over the concrete surface. The main effect of the nozzle movement rate is then the depth of cut.

Note also that observation of FM 7.9 Exhibit 6 shows that the actual pressure at the nozzle (17,000 psi versus 22,000 psi) is not as important as the distance of the nozzle to the wall in terms of actual water pressure impacting the wall.

Although the forces generated by the water jet are not sufficient to initiate the delamination, it is possible they could have been in a factor in propagating it. Once the crack started in the plane of the tendon sleeves, it is "active" because it is in an area of local tensile stresses. Therefore it can be propagated with minimal forces serving as an "activation energy" force just pushing the local tensile stress above the tensile strength of the concrete. It is important to note, however, that the available data does not prove or disprove a contribution from the water jet forces to the propagation of the delamination.

Conclusion:

The rate of hydro-blasting was not a factor in creating the delamination.



7.10 Hydro-Blasting Induced Cracking

Description:

The process of hydro-blasting exploits the existence of micro-cracks, voids, capillaries and cracks to enable concrete demolition using high pressure water jets. This raises the question of potential damage to concrete in adjoining area through direct pressure, vibrations, or crack propagation.

This document is intended to determine if hydro-blasting can cause cracking and if any occurred at CR3. Note that issues of vibration induced by hydro-blasting are covered in depth in FM 7.2, issues of excessive water pressure are covered in FM 7.8, and issues of nozzles rate are covered in FM 7.9.

Data to be collected and Analyzed:

1. Review literature (FM 7.10 Exhibit 1 is a "Guide for the Preparation of Concrete Surfaces for Repair Using Hydrodemolition methods", FM 7.10 Exhibit 2 includes selected pages from ACI 546R-04 "Concrete Repair Guide", FM 7.10 Exhibit 6 includes selected pages from the book "Hydrodemolition of Concrete Surfaces and Reinforced Concrete" by Andreas Momber, FM 7.10 Exhibit 7 is a published article "Hydrodemolition for Removing Concrete", and FM 7.10 Exhibit 8 is a research report from Missouri Department of Transportation "Hydrodemolition and Repair of Bridge Decks");
2. Interview personnel involved in the Hydrodemolition at CR3 (FM 7.10 Exhibit 3 is a summary of interviews);
3. Review physical data collected from the structure (FM 7.10 Exhibit 5 are photos taken of areas impacted by the demolition process).

Verified Supporting Evidence:

1. Hydro-demolition works through the introduction of high pressure water into cracks (FM 7.10 Exhibit 6). If a delamination crack is encountered during demolition, the water will fill it and exert pressure internally, potentially accelerating propagation. Eyewitness report large volume of water exiting the wall through a moon-shaped crack that developed outside the demolition area (FM 7.10 Exhibit 5).

Verified Refuting Evidence:

1. Literature review shows a consensus that hydro-demolition does not cause significant damage to adjacent material (see highlighted sections of FM 7.10 Exhibits 1, 2, 7, and 8). Alternative mechanical and impact methods can damage the residual concrete that is to be repaired (see for example FM 7.2 Exhibit 1, pages 3 and 4 of 16);
2. Hydro-demolition removes concrete not by impact, but by introducing high-pressure water into existing voids (FM 7.10 Exhibit 6). The high internal pressure in these voids causes the concrete to fail, spalling the surface material;
3. Cores taken adjacent to the demolition area did not show degradation of strength properties (FM 7.10 Exhibit 4). Concrete cores were taken in the concrete that had been subjected to hydro-blasting. These cores were taken in the hoop direction, perpendicular to the side of the SGR opening (as observed on FM 7.10 Exhibit 9) and in the vertical direction, perpendicular to the bottom of the SGR opening. The average splitting tensile strength for these cores was 615 psi and the average compression strength was 7,390 psi. This compares to an average splitting tensile strength of 599 psi and an average compression strength of 7,385 psi for cores taken away from the hydro-blasted concrete in the radial direction (FM 7.10 Exhibit 11). These results confirm that there was no degradation to the concrete adjacent to the hydro-demolition area.



7.10 Hydro-Blasting Induced Cracking

Discussion:

Published information about the principles of hydro-demolition (FM 7.10 Exhibit 6, page 3 of 21) describes the three modes through which it removes the concrete (the goal of the process in the first place). These are water flow into cracks, creating stress at the tip of the crack, water flowing into capillaries, resulting in internal pressure amplification, and water flowing through open pore system, creating friction forces to the material grains. The FM 7.10 Exhibit 6 provides research information and formulas on the topic.

Note that there are some slight discrepancies in operating conditions (pressure, flow rate, and rpm) in the various interviews. We established that the numbers from Mac & Mac are the best estimates and actual field operating conditions are the ones quoted by Mac & Mac.

The area shown in FM 7.10 Exhibit 5 where water from the hydro-blasting process was seen flowing out of the containment wall was later confirmed to be at the edge of the delaminated concrete, on the lower right side.

Hydro-demolition is often not recommended for structures with unbonded tendons. For example, in FM 7.10 Exhibit 2, Section 2.2.10 in lines 11 through 13, ACI Committee 546: "Hydrodemolition should not be used in structures with unbonded tendons, except under the direct supervision of a structural engineer". Also, in FM 7.10 Exhibit 10, first paragraph of Answer section: "Hydrodemolition is not recommended for concrete removal if there is a possibility that unbonded post-tensioned systems are within the concrete removal zone."

However, careful reading of FM 7.10 Exhibit 10 shows that the concerns are not relevant to the CR3 task:

1. Quoting FM 7.10 Exhibit 10, line "Hydrodemolition of post-tensioned concrete elements can cause a safety problem. It is potentially dangerous because it can accidentally undercut embedded anchors and result in explosive release of pre-stressing forces". This point does not apply at CR3, and would not apply at other nuclear containment hydro-blasting jobs, because the tendons in the concrete removal area are de-tensioned prior to hydro-blasting;
2. "If any part of the tendon is exposed to high water pressure, water may penetrate into the tendon". This point also is not important for CR3 as the tendon sleeves were intended to be removed and replaced. In fact, damage to the tendon sleeves was expected for this job;
3. "The water pressure used in hydroremoval equipment can force slurry into the sheathing". Again, the tendon sleeves were planned to be removed and replaced in the hydro-blasting area.

Hydro-demolition is not sensitive to the strength of the aggregates because it exploits the existence of micro-cracks, voids, capillaries and cracks to enable concrete demolition. If anything, weaker aggregates and/or defective aggregates could be removed more easily and therefore offer less resistance to the water jet and lead to less damage to the surrounding material.

Conclusion:

Hydro-demolition did not cause cracking and degradation of the concrete adjacent to the demolition area.

7.11 Added stress from pulling tendons out of sleeves and grease after cutting (R)



7.11 Added stress from pulling tendons out of sleeves and grease after cutting

Description:

The procedure to remove the tendons from the sleeves that intersect the SGR opening is as follows (FM 7.11 Exhibit 3 is the Precision Surveillance Corporation (PSC) Field and Quality Control Procedure for Tendon Removal):

1. Degrease tendon sleeves;
2. Cut tendons (detensioning). This can for example be performed using a plasma torch;
3. Pull tendons using a coiler machine (FM 7.11 Exhibit 4 shows the typical tendon coiler system used by PSC).

The tendon coiler used is hydraulically driven. Its end attaches to one end of a tendon and it pulls and coils the tendon as it rotates. When used on vertical tendons, the coiler is positioned on the dome of containment. When used on hoop tendons, the coiler is located in a platform that comes down from the dome along the buttress. The platform motion is resisted by the containment wall and the buttress wall.

The force required to pull the tendons out of the sleeves can be high because:

1. The tendons and grease have been in place and pre-stressed for more than 30 years;
2. The grease has a high viscosity;
3. The degreasing operation is not thorough for the hoop tendons.

This can result in additional stresses in the concrete around the sleeves during the removal operation.

Data to be collected and Analyzed:

1. Tendon removal procedure (FM 7.11 Exhibit 1 is an excerpt of the Engineering Change package creating and repairing the opening in the containment building and FM 7.11 Exhibit 3);
 2. Description of the tendon coiler equipment (FM 7.11 Exhibit 4);
 3. Maximum pulling capacity of the coilers (FM 7.11 Exhibit 2 is an email exchange with PSC personnel to try and determine the pulling capacity of a PSC tendon coiler);
 4. Coiler operation details (FM 7.11 Exhibit 5 is an email exchange with PSC personnel on the topic);
- Comparison of the force of a tendon coiler with the typical forces involved in the post-tensioned system.

Verified Supporting Evidence:

None

Verified Refuting Evidence:

1. The maximum pulling capacity of the coilers is only 16,000 lbs (FM 7.11 Exhibit 2). This is small compared to the typical forces applied to the post-tensioned concrete, around 1.6 million lbs. See discussion below regarding the forces typically involved in this containment;
2. Coiler operates at a slow pulling rate of 30ft / min (FM 7.11 Exhibit 5 is an email exchange with PSC personnel to try and determine the pulling rate of a PSC coiler).

Discussion:

As a comparison point, a SINGLE tendon wire 7mm in diameter, stressed at 70% of 240ksi Ultimate Tensile Strength, generates a force of $0.7 \times \pi \times (3.5 / 25.4)^2 \times 240,000 \text{ lbs} \sim 10,000 \text{ lbs}$. And one tendon contains 163 such wires for a force per tendon around 1,600,000 lbs.

The forces at play in the post-tensioned containment, seen by the concrete in everyday operation, are



7.11 Added stress from pulling tendons out of sleeves and grease after cutting

much larger than the pulling capability of the PSC tendon coiler. Again, the reader can refer to FM 7.11 Exhibit 4 for a view of the machinery described here.

Note that tendons 34V12 and 34V13 were ram-detensioned and not plasma torched. CR3 wanted to ensure the length of the replacement tendons were right, as those are the two vertical tendons curving the most around the equipment hatch opening. After being ram-detensioned, 34V13 wires were saw cut and some burr was created. It made the pulling of the tendon (all 163 wires) through the anchor very difficult. The tendon was finally flame torched above the anchor head before being lifted out of the sleeve using the crane.

Note in FM 7.11 Exhibit 1 page 9 of 10 in the red addition "34V13 may be plasma cut directly above the lower anchor head" allowing for this as an EC modification.

Conclusion:

The force from removing the tendons out of the sleeves did not generate the delamination.

8.1 Prior spray event leading to low pressure inside containment (R)



8.1 Prior Spray event leading to Low Pressure inside Containment

Description:

The containment spray event of October 1992 resulted in an injection of about 9400 gallons of borated water into the reactor building (RB) atmosphere. The event resulted in a decrease in RB internal pressure.

Data to be collected and Analyzed:

1. Review problem report of October 16, 1992 and associated containment atmosphere pressure graph. (FM 8.1 Exhibit 1)
2. Review Design bases for containment, FSAR Chapter 5, paragraph 5.2.1. (FM 8.1 Exhibit 2)
3. Review current Petrographic Reports. (FM 8.1 Exhibits 3 and 4)
4. Review IR Data (FM 8.1 Exhibit 5)

Verified Supporting Evidence:

None

Verified Refuting Evidence:

1. A comparison of the containment pressure excursion from the 1992 containment spray event and the design bases for containment pressure show that excursion did not result in the containment pressure exceeding its negative design pressure of 2.5 psig below external pressure. (FM 8.1 Exhibits 1 and 2).
2. The results of the petrographic examinations (FM 8.1 Exhibits 3 and 4) indicate that the delamination of the containment wall appears to be recent. The Building Spray event occurred 17 years ago. Therefore, the delamination does not appear to have been caused by the Building Spray event.
3. In addition, pressure stresses induced by the inadvertent containment spray event would likely have affected all areas of the containment building. However, Impulse Response scanning and confirmatory core bores have revealed no delamination in any areas beyond the panel where the SGR construction opening was cut. (FM 8.1 Exhibits 5).

Conclusion:

The 1992 spray event did not contribute the delamination.



8.2 Thermal Stresses due to Containment Spray

Description:

The containment spray event of October 1992 resulted in an injection of about 9400 gallons of borated water into the reactor building (RB) atmosphere. The event resulted in a change to the average containment temperature.

Data to be collected and Analyzed:

1. Review containment temperature graph record for the 1992 containment spray event. (FM 8.2 Exhibit 1). The four temperature curves on the graph of interest are numbered 5,6,7, and 8 on pg 2 of 4. Those numbers are the "PT" numbers listed in pg 3 of 4 and are also identified as "Tag" numbers. The Tag numbers are shown on pg 4 of 4 to indicate the elevation of the temperature reading).
2. Review FSAR Chapter 5, Section 5.5.1.1 and 5.5.1.2. (FM 8.2 Exhibit 2)
3. Review current Petrographic Reports. (FM 8.2 Exhibits 3 and 4)
4. Review the Impulse Response data. (FM 8.2 Exhibit 5)

Verified Supporting Evidence:

None

Verified Refuting Evidence:

1. The design average containment temperature is not to exceed 130 degrees F and to remain above a minimum temperature of 60 degrees F during normal operations. (FM 8.2 Exhibit 2)
2. The temperature excursion during the 1992 spray event was less than 10 degrees F for each of the four individual points, and the temperature nearest the liner decreasing from about 148 degrees F to about 144 degrees F, and decreased about 2 degrees F during the event. Therefore, it is concluded that the containment internal average temperature remained within acceptable limits during the transient caused by the inadvertent spray. (FM 8.2 Exhibit 1)
3. The results of the petrographic examinations (FM 8.2 Exhibits 3 and 4) indicate that the delamination of the containment wall appears to be recent. The Building Spray event occurred 17 years ago. Therefore, the delamination does not appear to have been caused by the Building Spray event.
4. In addition, thermal stresses induced by the inadvertent containment spray event would likely have affected all areas of the containment building. However, Impulse Response scanning revealed no delamination in any areas beyond the panel where the SGR construction opening was cut. (FM 8.2 Exhibit 5)

Conclusion:

The containment spray event of October 1992 did not lead to exceeding either a containment design or Technical Specification temperature limit. Therefore, any thermal stresses that may be postulated by the spray event were bounded by the containment design bases and were of such short duration to have had an insignificant effect, therefore, did not contribute to the delamination.

8.3 Effect of faster pressurization/depressurization rates during last ILRT ([Return to list](#))

8.3 Pressurization/Depressurization Rates During Last ILRT

Description:

The procedure for conducting the containment Integrated Leak Rate Test (ILRT) (SP-178) was changed before the last ILRT, which was performed in 2005. That change included a provision to allow the rate of change in internal pressure to 15 psi/hr, a higher rate than was used in previous ILRTs.

Data to be collected and Analyzed:

1. ILRT procedure. (FM 8.3 Exhibit 1)
2. 10 CFR 50.59 Evaluation of the ILRT procedure change relative to the pressurization/depressurization rate of 15 psi/hr. (FM 8.3 Exhibit 2)
3. Engineering Disposition (ECED 62366R0) included an evaluation to depressurize containment at 15 psi/hr. (FM 8.3 Exhibit 3)
4. Review IR data. (FM 8.3 Exhibit 4)

Verified Supporting Evidence:

None

Verified Refuting Evidence:

1. The ILRT procedure was appropriately changed and evaluated in accordance with Progress Energy procedures and 10 CFR 50.59. (FM 8.3 Exhibits 1 and 2)
2. ECED 62366R0 evaluated the 15 psi/hr change of containment pressurization/depressurization and concluded that "From a structural standpoint, depressurizing (or pressurizing) the RB at 15 psi/hr is not challenging, as accident conditions are much more severe". Although other issues may result from this change (such as coatings damage), they are not considered relevant to the structural integrity of the containment and therefore not contributors to the delamination issue. (FM 8.3 Exhibit 3, pg 5 of 5)
3. In addition, pressure stresses induced by the recent ILRT would likely have affected all areas of the containment building. However, Impulse Response scanning revealed no delamination in any areas beyond the panel where the SGR construction opening was cut. (FM 8.3 Exhibit 4)

Conclusion:

There was no effect on the containment structure from changing the ILRT procedure that had not already been bounded by its design. Therefore, the last IRLT did not contribute to the delamination.

8.4 Inadequate concrete structure monitoring/maintenance (IWL) (R)



8.4 Inadequate Concrete Structure Monitoring/Maintenance (IWL)

Description:

Visual examinations contained within the ASME Section XI Subsection IWL are conducted to determine surface concrete deterioration and distress (IWL 2000). These containment surface monitoring inspections sometimes result in identification of and subsequent repair to the containment concrete surface. While not a true failure mode, a deficient IWL program could have missed identifying or properly evaluating indications that would have led to the identification and repair of a flaw before the delamination occurred.

Note: The IWL program includes both concrete and tendon surveillances. FM 8.4 only addresses the concrete aspects of the program. The tendon aspects are discussed in the FM 6 series, which addresses Concrete-Tendon-Liner-Interactions.

Data to be collected and Analyzed:

1. Review the IWL Section 2000 containment monitoring requirements. (FM 8.4 Exhibit 1) Note: The 1992 Addenda of ASME Section XI was the code year of record for the 2007 IWL inspection, while the 2001 Edition through 2003 Addenda was the code year of record for the 2009 inspection. For the purpose of this FM evaluation, the differences in the code years are insignificant.
2. Review the recent IWL monitoring results. (FM 8.4 Exhibits 2, 3a, 3b, 3c, and 4)
3. Review Impulse Response Data. (FM 8.4 Exhibit 5)

Verified Supporting Evidence:

None

Verified Refuting Evidence:

1. The most recent IWL concrete containment monitoring was conducted during the last refueling outage (RFO 15) in 2007. (For selected pages of the inspections relating to the area between buttresses 3 and 4 see FM 8.4 Exhibit 2). The inspection concluded that the containment structure as of November 2007 did not experience abnormal degradation. (FM 8.4 Exhibits 3c and 4).
2. The results of the 2009 Augmented IWL inspection revealed numerous indications of containment surface degradation in areas beyond the SGR construction opening although confined between the buttresses 3 and 4. (FM 8.4 Exhibit 3a & 3b Pages 8 and 9).
3. The 2007 IWL inspection was effective and thorough, as demonstrated by the detailed report provided in FM 8.4 Exhibit 2 & 3c. The numerous indications in the 2009 augmented IWL report would have easily been identified had they existed in 2007.
4. As confirmation of the delamination limited to the area between buttresses 3 and 4, Impulse Response scanning of the entire containment outer surface conducted after the SGR hole was cut (with the exception of minor inaccessible areas) revealed no delamination in any containment surface areas beyond the area between buttresses 3 and 4. (FM 8.4 Exhibit 5)

Discussion:

The purpose of the containment surface monitoring program is to "determine the general structural condition of concrete surfaces of containments by identifying areas of concrete deterioration and distress..." (FM 8.4 Exhibit 1). Augmented IWL Exams of the containment between buttresses 3 and 4



8.4 Inadequate Concrete Structure Monitoring/Maintenance (IWL)

were requested as part of the root cause investigation to compare the differences between now and the last Scheduled Examination for Credit (2007). (IWL Exams are required every 5 years; the last scheduled exam was 2007). NCR 370875 was generated to document the Augmented IWL Examination findings. (Selected pages of NCR 370875 are found in FM 8.4 Exhibit 3a). The change in containment concrete physical condition between 2007 and the augmented 2009 IWL showed the delamination occurred after the last (RFO 15) IWL.

Conclusion:

An extensive review of the last IWL visual examination conducted during RFO 15 (2007) showed no abnormal containment surface structure degradation and that the IWL containment concrete structure monitoring was implemented correctly. Therefore, the IWL monitoring program did not contribute to the delamination.

8.5 Containment depressurization due to inadequate purging operation (R)



8.5 Containment Depressurization due to Inadequate Purging Operation

Description:

It was reported by a former CR3 operator (Dave Jones) that an event occurred in the late 1980's or early 1990's, during which a purge exhaust fan was operating with the inlet valve closed. This resulted in a vacuum in the containment building.

Data to be collected and Analyzed:

1. Dave Jones (former CR3 operator) interview dated November 10, 2009 placed the event in the late 1980s to early 1990's. (FM 8.5 Exhibit 1)
2. No NCR to document the event has been found. CR3 self-evaluation unit has exhausted all databases in their document search. Estimate maximum vacuum achievable with purge fan operation. (FM 8.5 Exhibit 1)
3. Selected pages of Purge fan vender manual: VTMA231. (FM 8.5 Exhibit 2)
4. Make/model of the purge fan: Joy Manufacturing Model 36-26.5-1770 axial vane fan. (FM 8.5 Exhibit 2)
5. Review containment design bases, FSAR Chapter 5, Section 2. (FM 8.5 Exhibit 3)
6. Review current Petrographic reports (FM 8.5 Exhibits 4 and 5)
7. Review Impulse Response data. (FM 8.5 Exhibit 6)

Verified Supporting Evidence:

None

Verified Refuting Evidence:

1. A calculation of a postulated worse-case vacuum generated by the purge fan demonstrated that the maximum achievable vacuum is less than 1 psi, which is less than the design basis for containment. (FM 8.5 Exhibit 1)
2. The results of the petrographic examinations (FM 8.5 Exhibits 4 and 5) indicate that the delamination of the containment wall appears to be recent. The subject purge event occurred approximately 20 years ago. Therefore, the delamination does not appear to have been caused by the purge event.
3. In addition, stresses induced by the inadvertent purge fan event would likely have affected all areas of the containment building. However, Impulse Response scanning revealed no delamination in any areas beyond the panel where the SGR construction opening was cut. (FM 8.5 Exhibit 6)

Conclusion:

The late 1980's to early 1990's inappropriate purge operation did not contribute to the containment delamination.



9.1 Hurricanes or Tornados

Description:

External forces, with the potential to challenge the design bases of containment, can be applied to the containment structure if hurricanes or tornadoes enter the Crystal River site.

Data to be collected and Analyzed:

1. Search historical records for hurricanes and tornadoes entering the local area. (NOAA internet data base, NOAA.gov)
2. Review the design bases of the containment structure. (FSAR Chapter 5. Section 2.1)

Verified Supporting Evidence:

None

Verified Refuting Evidence:

1. Hurricanes – The strongest hurricane in the vicinity of Crystal River (within 65 miles) between 1976 and the present was Category 1 (sustained wind speeds 74-95 mph) (1995, 2000, and 2004) (NOAA internet data base, NOAA.gov). (FM 9.1 Exhibits 1, 2, and 3).
2. No recorded tornado of any significant size or strength approached the site area. (NOAA internet data base, NOAA.gov) (FM 9.1 Exhibits 4, 5 and 6).
3. None of the containment design parameters contained in the FSAR Chapter 5 Section 2.1 for winds or external pressure loading from hurricanes or tornadoes have either been approached or exceeded since initial construction. (FM 9.1 Exhibit 7).

Conclusion:

Potential external forces applied to the containment structure did not contribute to the delamination since no recorded local hurricane or tornado with sufficient strength entered into the CR3 site between 1976 and the present.



9.2 Seismic Events

Description:

A seismic event of sufficient magnitude causing ground motion of sufficient intensity could exceed the design bases of the containment for such events.

Data to be collected and Analyzed:

1. Review the ground motion design criteria in the FSAR for comparison to historical data. (FM 9.2 Exhibit 1)
2. Search historical data base for past seismic events in the Crystal River area. (USGS internet data base)
3. Review CR3 Installed Seismic Record Data. (FM 9.2 Exhibit 2)

Verified Supporting Evidence:

None

Verified Refuting Evidence:

1. The FSAR design basis for earthquakes for CR3 is 0.05g horizontal and 0.033g vertical. The seismic instrumentation actuation set point is 0.01g. (FM 9.2 Exhibit 1)
2. There have been no CR3 Seismic instrumentation actuations. (FM 9.2 Exhibit 2)
3. A comparison of the data reviewed above and the data obtained from the USGS web site search reveals that there have been no recorded earthquakes in Florida between 1979 and the present that could have approached the ground motion design bases for containment. (FM 9.2 Exhibits 1, 3, and 4)

Conclusion:

Seismic events were not a contributor to the delamination.



9.3 Ground Movement (sink holes or geo-sliding)

Description:

Ground movement caused by sink holes and/or dissolution of the limestone under the containment can result in lack of foundation support.

Data to be collected and Analyzed:

1. Geo-technical report – Gilbert Geotechnical Study Section 1.2.11.7 and 1.2.11.8 (1971) (FM 9.3 Exhibit 1)
2. FSAR Chapter 2 Section 2.5.7.2 (FM 9.3 Exhibit 2)
3. Memo from Glenn Pugh. (FM 9.3 Exhibit 3)
4. Buttress and Dome Survey Data (FM 9.3 Exhibit 4)

Verified Supporting Evidence:

None

Verified Refuting Evidence:

1. The limestone supporting the containment was cement grouted to assure the continuity and integrity of the material. (FM 9.3 Exhibit 1)
2. There is no record of an observation of building cracking or sinkhole consistent with FSAR conclusions. (FM 9.3 Exhibits 2 and 3)
3. The Buttress and dome survey data show that the containment structure remains plum and the containment has not settled. (FM 9.3 Exhibit 4) See FM 1.5 for a more detailed discussion.

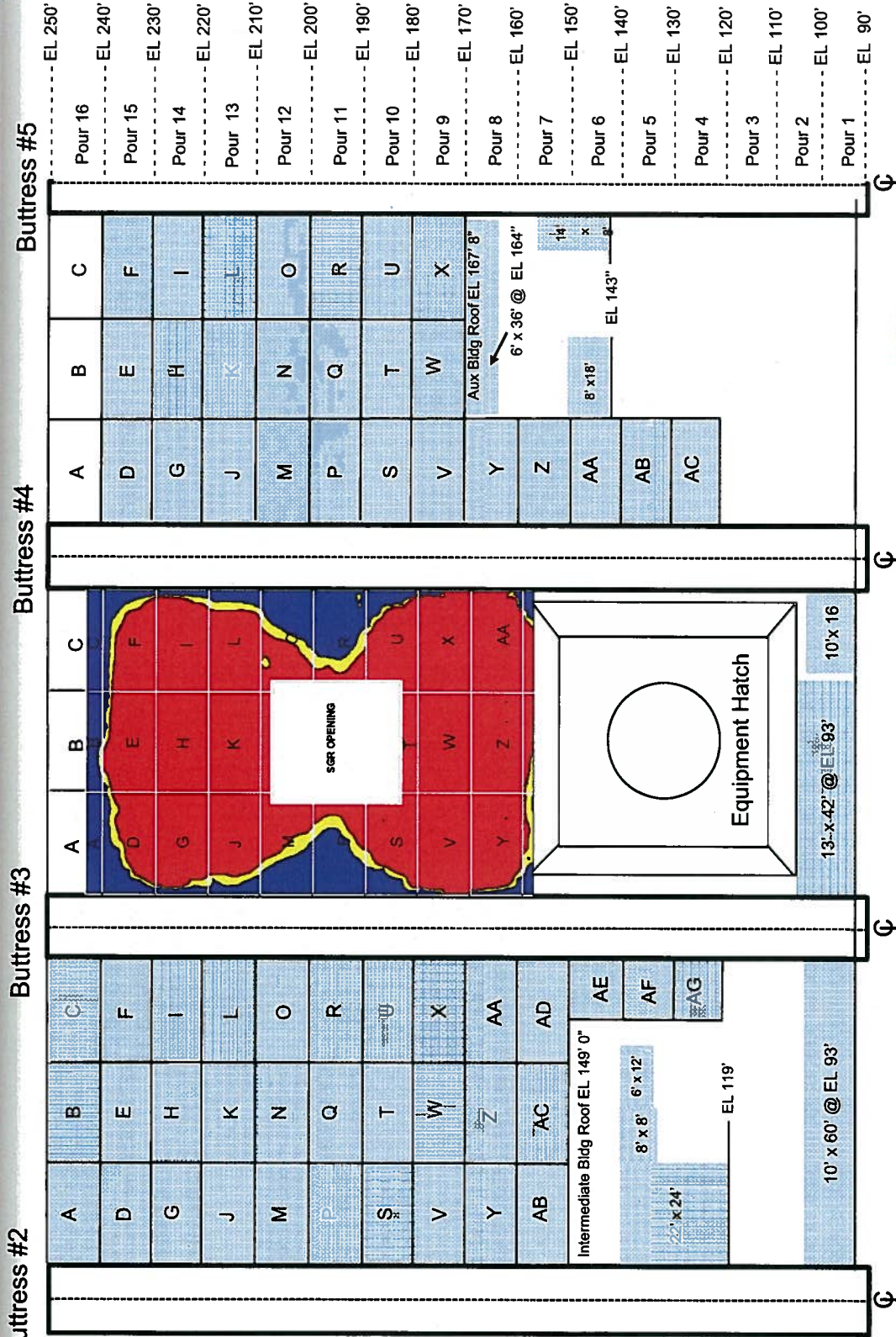
Conclusion:

There is no indication of containment settlement sufficient to cause added, asymmetrical stress in the containment.



Containment "Unfolded" – Buttriss 2 to 5

Mosaic IR Overlay scale is approximate



IR scans completed with no delamination
Blue = no delamination



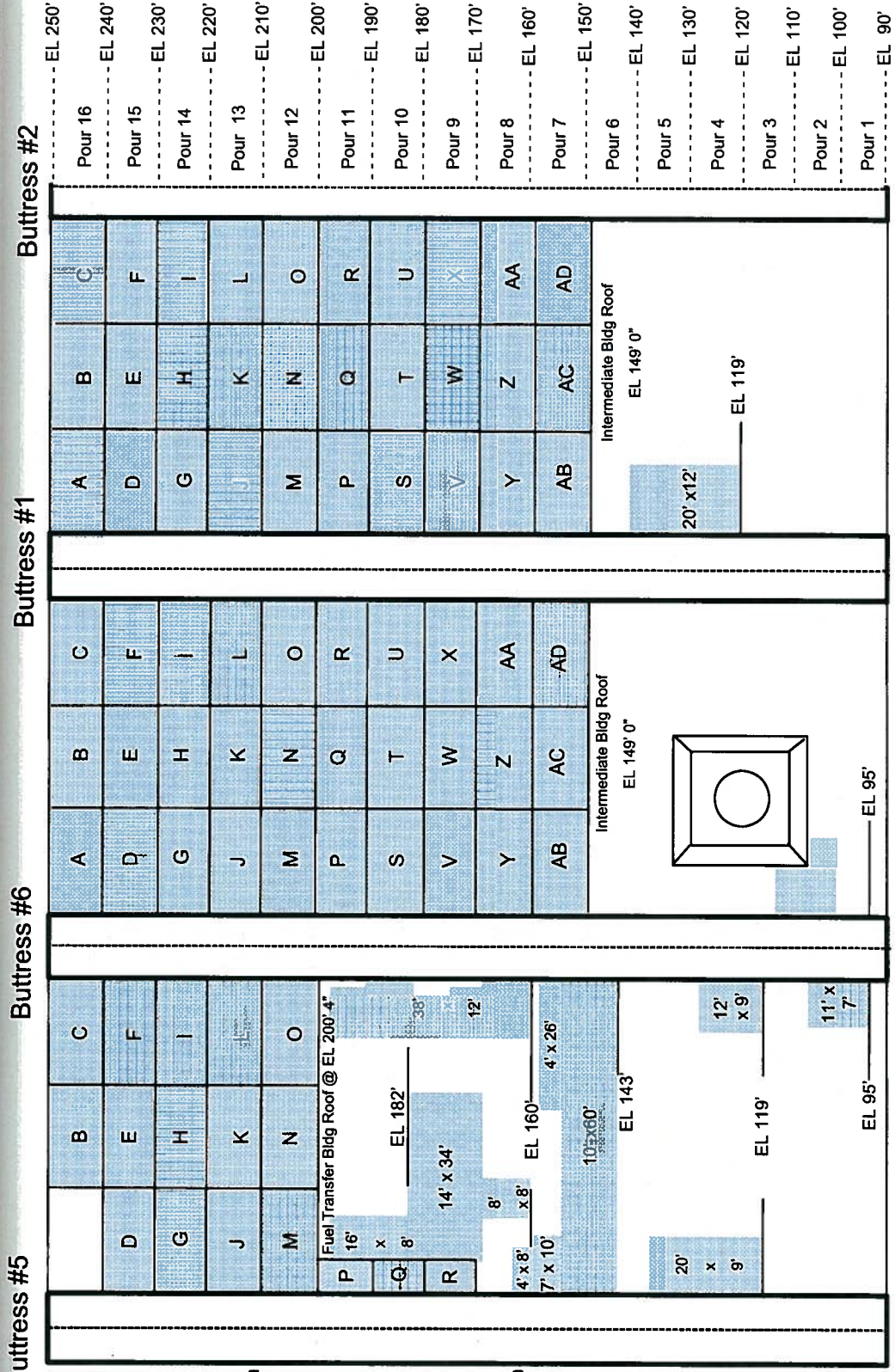
Actual IR scan output data:
Blue = no delamination
Yellow = transition
Red = delaminated

Drawing scale is not exact





Containment "Unfolded" – Buttress 5 to 2



IR scans completed with no delamination
Blue = no delamination



Actual IR scan output data:
Blue = no delamination
Yellow = transition
Red = delaminated

Drawing scale is not exact



